J-C THOMAS

ISSN 1240-1498
ISBN 2-905532-52-1

cinématique tertiaire et rotations de blocs dans l'ouest de l'Asie Centrale (Tien Shan Kirghiz et dépression Tadjik).

ETUDE STRUCTURALE ET PALEOMAGNETIQUE

MEMOIRES

1994

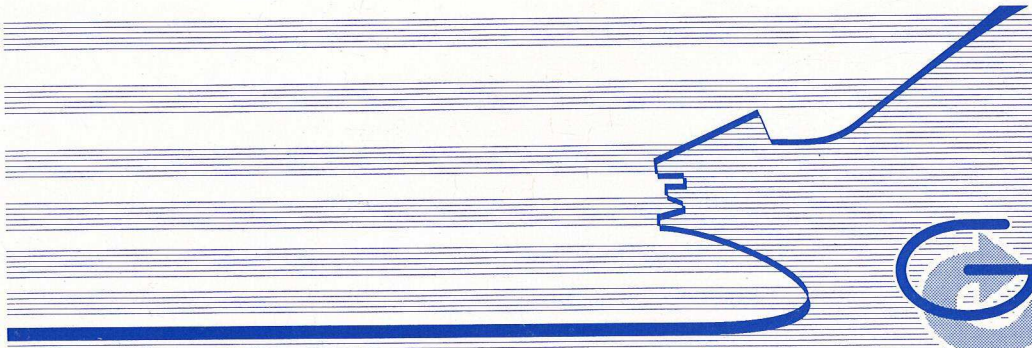

Géosciences Rennes

n° 53

MEMOIRES DE GEOSCIENCES - RENNES

n° 53

Jean-Charles THOMAS

Cinématique Tertiaire et Rotations de Blocs dans l'Ouest de l'Asie Centrale (Tien Shan Kirghiz et Dépression Tadjik)

Thèse de Doctorat de l'Université de Rennes I
soutenue le 10 Décembre 1993

Géosciences - Rennes
LP CNRS n°4661
Université de Rennes I
Campus de Beaulieu
F - 35042 - RENNES Cédex
(France)

1993

ISSN : 1240-1498

ISBN : 2-905532-52-1

1993

GEOSCIENCES RENNES
LP CNRS n°4661
Université de Rennes I - Campus de Beaulieu
F-35042-RENNES Cédex (France)

Jean Charles THOMAS

Cinématique tertiaire et rotations de blocs dans l'Ouest de l'Asie Centrale . (Tien Shan Kirghiz et Dépression Tadjik).

Mémoires de Géosciences Rennes, n° 53, 330 p.

D'après une théorie, le jour où quelqu'un découvrira exactement à quoi sert l'Univers et pourquoi il est là, ledit Univers disparaîtra sur-le-champ pour se voir remplacé par quelque chose de considérablement plus inexplicable et bizarre.

Selon une autre théorie, la chose se serait en fait déjà produite.

Douglas Adams, Le dernier restaurant avant la fin du monde (Le guide du routard galactique 2)

SOMMAIRE

AVANT-PROPOS

L'histoire de l'Asie, aussi bien culturelle et éthnologique que géologique, a toujours fasciné le monde Occidental. La reflexion d'Emile Argand (1924) sur la tectonique de l'Asie marque un tournant dans l'approche géologique de ce continent. Dès 1924, ce géologue à l'intuition visionnaire reconnaissait que la déformation Cénozoïque visible depuis l'Himalaya jusqu'en Arctique était liée à la convergence et à la collision de l'Inde avec l'Asie.

En effet, contrairement aux océans où la déformation est localisée sur des zones étroites, les continents sont caractérisés par une déformation distribuée sur une très grande surface.

Ces vingt dernières années ont été marquées par un extraordinaire apport de données et de modèles géologiques sur l'Asie tertiaire, dans une région où peu de littérature était disponible. Depuis l'interprétation cinématique globale de l'Asie proposée par Molnar et Tapponnier (1975), l'épaississement crustal et le déplacement de blocs le long de grands décrochements, ont été reconnus comme les deux mécanismes principaux accommodant la déformation Cénozoïque. Par ailleurs, de récentes évidences structurales (Cobbold et Davy, 1988) confirmées par le paléomagnétisme (cf. revue de Huang et Opdyke, 1993), ont montré que des rotations de blocs autour d'axes verticaux pouvaient être étroitement associées à la déformation, particulièrement autour des syntaxes Est et Ouest Himalayennes. Cependant, la quantification relative de ces différents mécanismes reste toujours difficile, de par l'imprécision des données et leur pauvreté dans de vastes régions d'accès difficile.

Nous avons eu la chance de pouvoir effectuer un travail de terrain dans le Tien-Shan Kirghiz et le Tadjikistan, deux pays faisant partie des anciennes républiques d'Asie Centrale de feu l'URSS, et maintenant indépendants. Ces régions situées au Nord et à l'Ouest de la syntaxe ouest-Himalayenne constituent la limite entre l'Asie déformée au Tertiaire et les cratons de Sibérie et du Kasakhstan de l'Asie stable. Nous verrons par la suite que l'épaississement, le décrochement et les rotations de blocs sont les trois mécanismes de déformation qui caractérisent cette région.

Le travail réalisé durant cette thèse est une contribution à l'étude cinématique de cette partie de l'Asie encore peu connue. Notre approche a été effectuée dans un souci de complémentarité en utilisant, d'une part, le paléomagnétisme comme outil de mesure de rotations, et d'autre part, les méthodes classiques de la géologie structurale.

Le chapitre I est un aperçu général de la cinématique Tertiaire de l'Asie et des problèmes qui s'y posent. La région de la syntaxe Est-Himalayenne qui est actuellement l'objet d'attention de nombreux géologues, y est plus précisément décrite. Elle présente en effet des caractéristiques cinématiques comparables dans bon nombre de cas à celles observées dans le Tien Shan et le Tadjikistan.

Le chapitre II est consacré au Tien-Shan Kirghiz. Il y est tout d'abord présenté une étude paléomagnétique effectuée dans les formations Tertiaires de bassins intramontagneux. La cinématique Cénozoïque du Tien-Shan et la structuration des bassins sont ensuite exposées.

Le chapitre III présente une interprétation cinématique de la déformation Cénozoïque de la dépression Tadjik à partir d'une étude paléomagnétique des sédiments Tertiaires et de données structurales (terrain, images satellites...). Une restauration manuelle de la dépression Tadjik est également proposée.

Enfin, dans le chapitre IV, nous intégrons sous forme de synthèse ces deux études régionales dans la cinématique de l'Asie Centrale de l'ouest.

Quelques réflexions sur les problèmes rencontrés lors des études paléomagnétiques sont présentées en annexe.

La plupart des résultats présentés dans les chapitres II et III de ce mémoire sont rédigés en Anglais sous forme d'articles ou projet d'article. Ces chapitres sont cependant constitués tous deux d'une première partie, rédigée en Français, où sont présentés le contexte géologique régional et les principaux résultats des études paléomagnétiques et structurales.

CHAPITRE I

Contexte tectonique et géodynamique de la déformation Cénozoïque en Asie

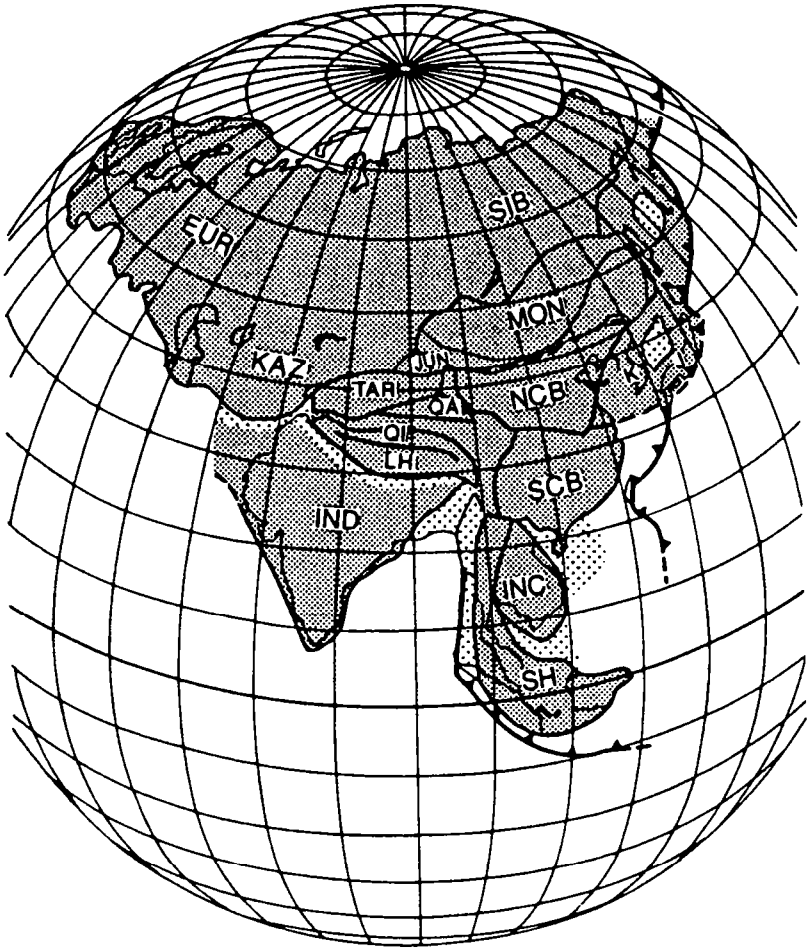

Figure I.1. Principaux blocs constituant l'Asie (D'après Enkin et al., 1992).
EUR: Europe ; INC : Indochine ; J : Japon; JUN : Junggar ; KAZ : Kazakhstan ; K : Corée ; LH : Lhassa ; MON : Mongolie ; NCB : Chine du Nord ; QA : Quaidam ; QI : Qiangtang ; SCB : Chine du Sud ; SH : Shan Thai ; SIB : Sibérie ; TAR : Tarim.

1. Introduction

Le continent asiatique est constitué d'une mosaïque de blocs (Figure I.1) dont l'assemblage s'est effectué depuis le Paléozoïque jusqu'au Tertiaire (Zonenshain et al., 1990). Grâce au paléomagnétisme, les grands traits chronologiques de la formation de l'Asie actuelle peuvent être tracés.

Les grands boucliers Sibérien et du Kasakhstan formant la partie Centrale et la partie Orientale de la Laurasia ont une histoire tectonique principalement Paléozoïque (Zonenshain et al., 1990; Sengör et al., 1993). Au Permien Supérieur, ces deux plaques formaient un ensemble commun avec le craton Européen (Khramov, 1981; Zhao et al., 1990), ainsi qu'avec les blocs du Tarim, du Junggar, de l'Hindou Kouch et de Turan (Boulin, 1988; Li, 1990). Du Trias au Crétacé Inférieur, tous les autres blocs constituant l'Asie Centrale et Orientale, à l'exception de l'Inde, se sont successivement accrétés sur la bordure sud de la plate-forme Asiatique (Enkin et al., 1992; Chen, 1992). On considère que la plupart de ces micro continents ont migré vers le Nord à la suite de la désagrégation progressive du supercontinent Gondwanien situé dans l'hémisphère Sud (Sengör, 1987). Ainsi, l'ensemble Mongolie - Chine du Nord - Chine du Sud - Indochine - Shan Thai s'est accrété à la bordure Sud-Sibérienne à la faveur de la fermeture de l'Océan Monghol-Okhotsk (Enkin et al., 1992). Les microblocs constituant le Tibet ainsi que l'Afghanistan et le Pakistan se sont assemblés quant à eux à la bordure sud Asiatique au cours de la fermeture de la Paléotethys, accomplie au Jurassique Inférieur, puis de la Tethys (Tapponnier et al., 1981 ; Sengör, 1987 ; Boulin, 1988, 1990)

C'est dans ce contexte géographique que s'est effectuée la collision de l'Inde avec l'Asie il y a environ 45 Ma, les différents âges proposés étant fonction des reconstructions cinématiques de l'Océan Indien (Patriat et Achache, 1984 ; Dewey et al., 1989). Cet âge coïncide avec une réorganisation notable de la cinématique des plaques de la région, probablement liée aux effets de la collision, à savoir :

- Une chute brutale de la vitesse de déplacement de l'Inde qui passe de 10 cm/an à environ 5 cm/an (Patriat et Achache, 1984). Cette vitesse est restée constante jusqu'à l'actuel.
- Un changement dans la direction de déplacement de l'Inde, subissant dès lors une rotation antihoraire qui atteint environ 30° actuellement (Dewey et al., 1989).

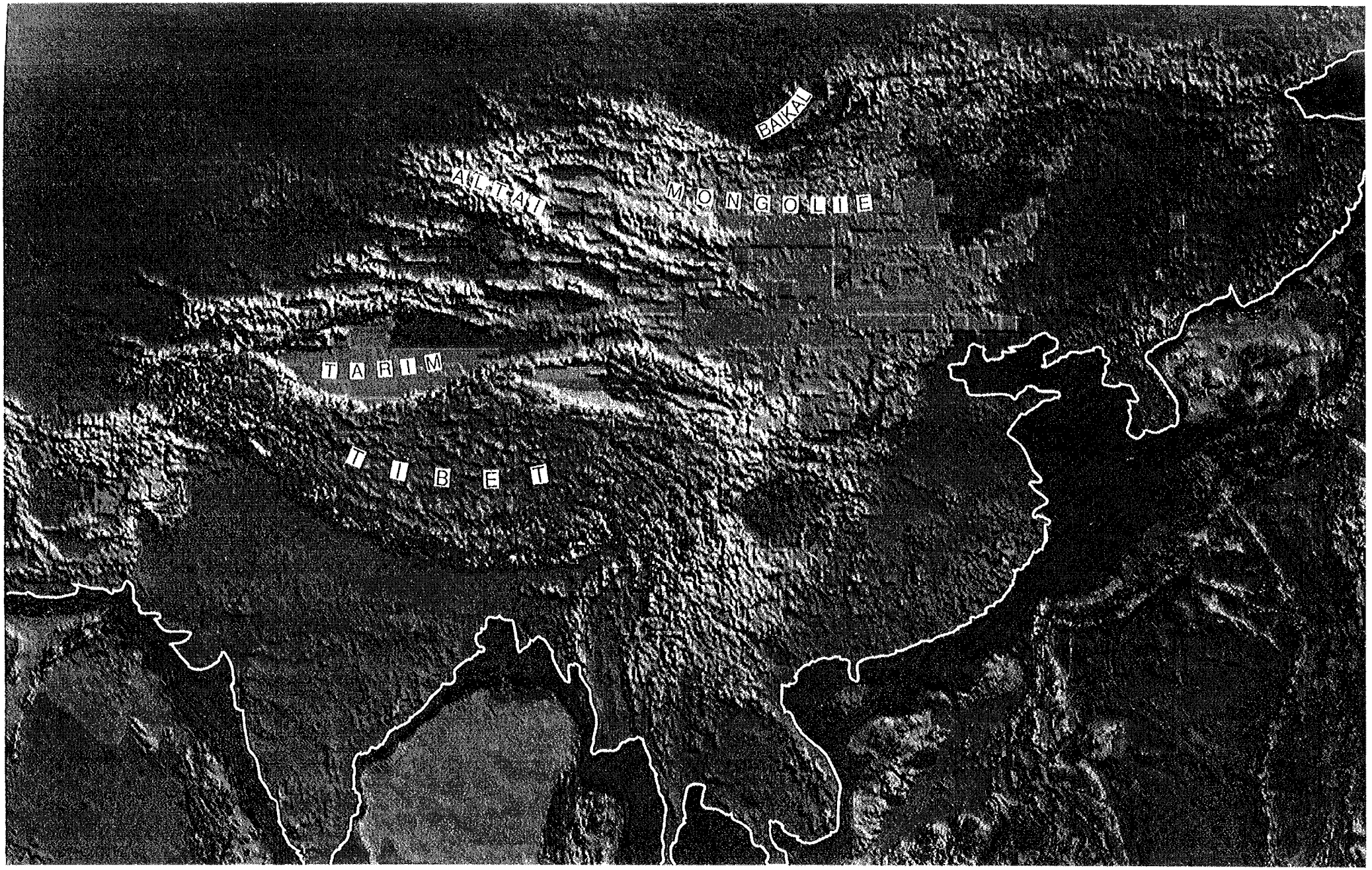

Figure I.2. Topographie de l'Asie.

2. Distribution de la déformation Cénozoïque

Depuis que l'Inde est entrée en contact avec l'Asie, la perte de surface totale entre les deux continents est de l'ordre de 7.10^6 km^2 pour un raccourcissement de 1850 km et 2600 km, respectivement à la hauteur des syntaxes ouest (Pakistan) et est (Assam) Himalayennes (Dewey et al., 1989 ; Le Pichon et al., 1992).

On considère que la topographie actuelle de l'Asie (Figure I.2) et l'épaississement crustal qui lui est associé, sont la conséquence directe de l'accommodation de cette convergence continentale (England, 1982). Le plateau du Tibet, large de plus de 1000 km, perché à près de 5000 m d'altitude et avec un Moho à une profondeur moyenne de 60 km (Hirn et al., 1984), en est l'exemple le plus spectaculaire (Argand, 1924). Ainsi, la zone de déformation Tertiaire (Figure I.3) définit un triangle de 4000 km de long sur 3000 km de large (Cobbold et Davy, 1988) dont la base est délimitée par la chaîne Himalayenne tandis que la bordure nord-ouest s'étend du Tien Shan au Baïkal ; le Pamir, la Chine du Sud-Ouest et la région du Baïkal en constituent les extrémités respectives.

Que ce soit la néotectonique ou le champ de failles Cénozoïques, tous deux montrent que les différents styles tectoniques sont présents en Asie (Figure I.3).

La compression et le chevauchement sont maximales dans la chaîne Himalayenne et dans le Pamir. Au Nord de l'Himalaya, le plateau du Tibet est actuellement en extension E-W, et ce depuis le Miocène moyen à supérieur (voir par exemple Mercier et al., 1987; Pecher et al., 1991). Les mécanismes qui ont procédé à sa surrection et son épaississement Oligo-Miocène restent encore mal compris (voir Harrison et al. (1992) pour une synthèse). Sur sa bordure nord-est et est, le plateau du Tibet présente des structures compressives (Quilian Shan, Bassin de Quaidam, Longmenshan) interprétées par certains auteurs comme témoins de l'extension actuelle du plateau vers le NE (Burchfiel et Royden, 1991 ; Tapponnier et al., 1990a). La faille de l'Altyn Tagh, décrochement sénestre majeur, constitue la bordure nord du plateau du Tibet.

Toujours vers le Nord, le bassin du Tarim qui présente peu de déformation interne peut, en première approximation, être considéré comme un bloc rigide. Son déplacement vers le nord, combiné à une rotation horaire par rapport à la Sibérie (Avouac et Tapponnier, 1992) est associé à la déformation Cénozoïque dans le Tien Shan. Dans cette chaîne d'orientation E-O, tout comme dans l'Altaï, au NE, la déformation est caractérisée par une combinaison de chevauchements et de décrochements.

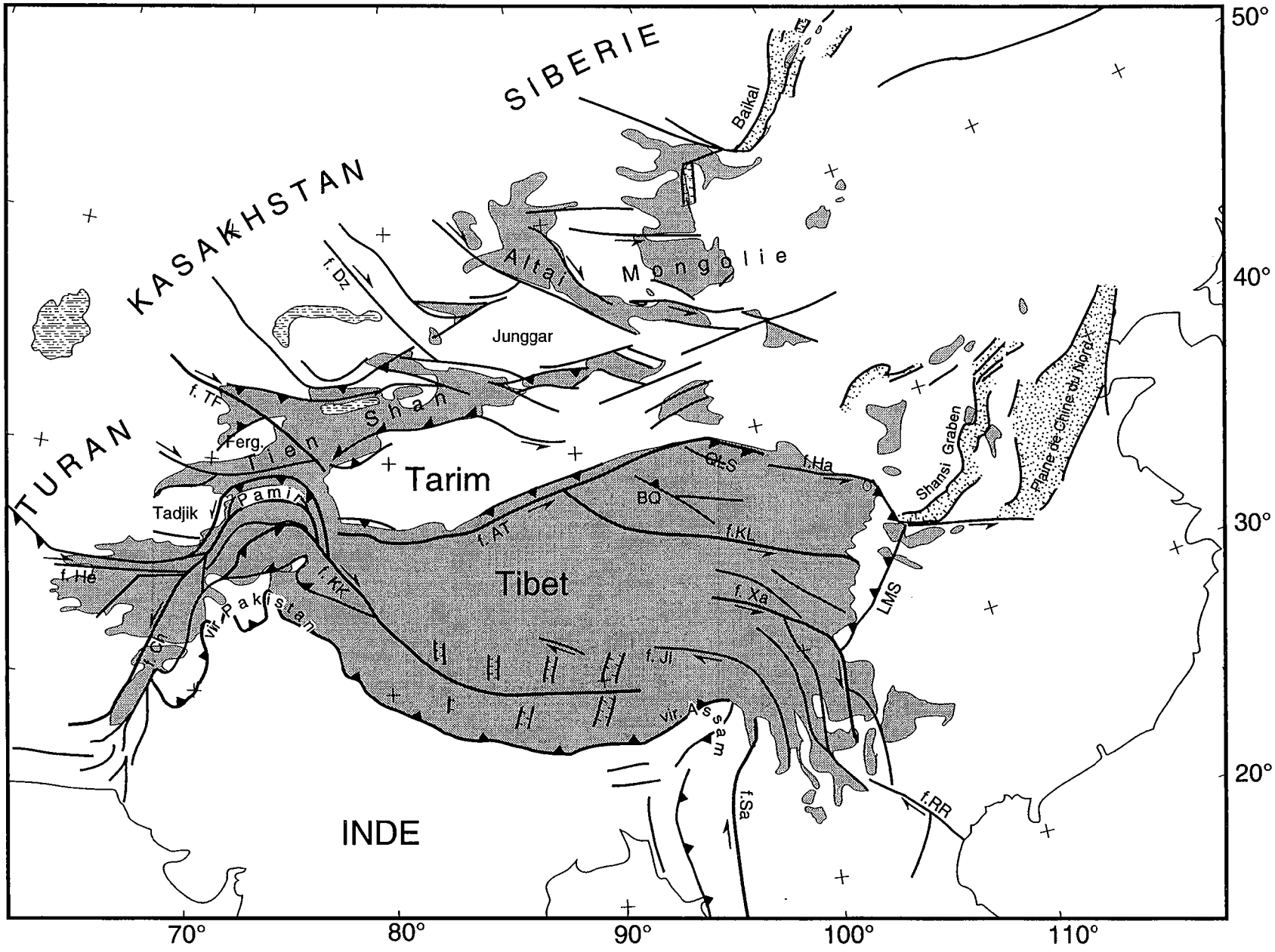

Figure I.3. Principaux traits tectoniques Cénozoïques de l'Asie (adapté d'après Cobbold et Davy, 1988).
Les altitudes supérieures à 2000 m sont représentées en grisé. Les bassins Cénozoïques sont en pointillés. QlS : Quilian Shan; LMS : Long Men Shan; Ferg. Fergana. Failles majeures: f. AT : Altyn Tagh; f. Ch : Chaman; f. Dz : Junggar; f. Ha : Haiyuan; f. He : Hérat; f. Ji : Jiali; f. KL : Kun Lun; f. Kk: Karakorum; f. RR : Rivière Rouge; f. TF : Talass-Fergana; f. Xa : Xanshuihe.

La déformation Cénozoïque de l'Asie Centrale dont nous venons d'avoir un rapide aperçu, s'est propagée de façon progressive dans le continent Asiatique depuis le début de la collision. Alors que l'épaississement dans l'Himalaya et dans le Tibet se fait à l'Oligocène et au Miocène (Harrison et al., 1992), il n'intervient principalement dans le Pamir, le Tien Shan et l'Altaï qu'à partir du Miocène Moyen (Mattauer, 1986 ; Avouac et al., 1993). Windley et al. (1990) considèrent que les principaux chevauchements sont localisés sur des structures préexistantes mésozoïques réactivées. A l'inverse, d'après Martinod (1991), la position des principaux chevauchements serait contrôlée par le flambage de la lithosphère asiatique associé aux premières phases de la déformation faisant suite à la collision de l'Inde.

Le domaine Est-asiatique est, quand à lui, en contexte général extensif (Baïkal, Shansi grabben, plaine de Chine du Nord). D'après Molnar et Tapponnier (1975, 1977), cette déformation est également contrôlée par la collision Inde-Asie. L'éloignement par rapport à la zone de poinçonnement et la présence de la marge Est-pacifique permet une modification du champ de contraintes qui passe progessivement de la compression à l'extension. Toutefois, la vision d'une déformation uniquement contrôlée par la collision Inde-Asie à travers toute l'Asie Centrale et Orientale (Molnar et Tapponnier, 1975, 1977) a été récemment remise en question. Ainsi, Windley et Allen (1993) ont proposé que l'extension en Mongolie et dans le Baïkal soit plutôt associée à la présence d'un point chaud. Plus au sud, en Chine du Sud et en Asie du Sud-Est, une part, sinon la totalité de l'extension, pourrait être uniquement liée à la présence de la marge active Est-pacifique (Burchfiel et Royden, 1991).

Une des caractéristiques majeures des conditions de la déformation en Asie est la présence, le long de la marge Est-asiatique, d'une zone de subduction océanique considérée comme une limite plus ou moins "libre de contraintes" compressives (Molnar et Tapponnier, 1977). A l'opposé, les boucliers peu déformables de Sibérie et du Kazakhstan constituent une bordure très confinée au Nord et à l'Ouest de la zone déformée. Molnar et Tapponnier (1975) ont montré l'influence majeure que pouvait avoir cette asymétrie des conditions aux limites sur le style et la propagation de la déformation. Nous verrons par la suite que ces conditions sont en partie responsables des controverses actuelles quant au mode de déformation Cénozoïque de l'Asie.

3. Champ de failles et cinématique

3.1. Modèles cinématiques de l'Asie

Bien qu'une incroyable somme de données de toute nature ait été collectée ces vingt dernières années, de nombreuses questions restent quant aux mécanismes de déformation et à la cinématique de l'Asie. Au centre des débats est la question du rapport entre épaississement et décrochement. Le problème est le suivant :

La déformation de l'Asie se fait elle principalement par épaississement crustal, ou bien par extrusion latérale le long de grands décrochements ?

La collision entre l'Inde et l'Asie peut être simplifiée en considérant le poinçonnement d'un bloc rigide (l'Inde) dans un milieu déformable (l'Asie). En partant de ce principe, l'approche numérique qui postule que la déformation s'effectue de façon homogène et continue (England et McKenzie, 1982 ; Vilotte et al., 1982 ; England et Houseman, 1986 ; Houseman et England, 1986), est en faveur d'une déformation principalement accommodée par de l'épaississement en avant du poinçon, même dans le cas d'une bordure est de l'Asie libre de contraintes (Houseman et England, 1993).

A l'opposé, Molnar et Tapponnier (1975) et par la suite Tapponnier et coll. (voir par exemple Tapponnier et al., 1986 ; Peltzer et Tapponnier, 1988 ; Armijo et al., 1989 ; Tapponnier et al., 1990 ; Avouac et Tapponnier, 1992) ont préféré une approche focalisée sur l'étude des failles majeures en Asie Centrale et l'estimation de leurs déplacements actuels et quaternaires. L'extrapolation de ces données aux derniers 45 Ma a permis à ces auteurs de proposer que jusqu'à 50% de la convergence entre l'Inde et l'Asie était accommodée par l'extrusion vers l'Est de blocs le longs de grands décrochements, extrusion favorisée par la bordure libre à l'Est, le reste étant accommodé par de l'épaississement.

Des positions intermédiaires ont été obtenues à partir d'approches différentes.

L'analyse de la topographie de l'Asie (et de l'épaississement crustal associé), ne rend compte que des 2/3 de la surface perdue par la convergence continentale entre l'Inde et l'Asie (Le Pichon et al., 1992). Selon ces auteurs, le reste est accommodé, soit par de l'extrusion, soit par l'éclogitisation de la croûte. Il est à noter que Dewey et al. (1989), en utilisant une approche

similaire, concluent à une convergence principalement accommodée par de l'épaississement.

La réalisation de modèles analogiques rhéologiquement dimensionnés (Davy et Cobbold, 1988) a montré un rapport extrusion/épaississement compris entre 1/3 et 2/5, proche de celui proposé par Le Pichon et al. (1992). Ces modèles ont par ailleurs mis en évidence une relation de type loi d'échelle, liant la longueur des failles et leurs déplacements cumulés (Davy et al., 1990). Ceci se caractérise, entre autre, par une déformation distribuée sur un grand nombre de petites failles en début de raccourcissement, puis se localisant progressivement pour n'être présente que sur quelques zones faillées majeures en fin d'expérimentation (Sornette et al., 1993). Cette observation peut être très importante lorsqu'il s'agit d'extrapoler à tout le Cénozoïque les mouvements actuels ou récents mesurés sur les failles.

Zhao et Morgan (1985) ont effectué une reconstrucion complète des déplacements CénozoÏques sur les failles majeures d'Asie. Ils concluent à une déformation accommodée par de l'extrusion et de l'épaississement. Une importante part de l'épaississement et du soulevement associé ne serait plus visible actuellement en raison d'une érosion rapide des reliefs himalayens.

Enfin, à partir d'une reconstruction du champ de déplacement sur les 10 derniers millions d'années, Cobbold et Davy, (1988) mettent en évidence une extrusion accommodant 20% à 40% de la convergence, le reste étant pris en compte par de l'épaississement. Ces auteurs montrent par ailleurs qu'au niveau de la syntaxe Est-himalayenne et dans une zone allant du Pamir au Baïkal, les mouvements décrochants sont associés à des rotations de blocs autour d'axes verticaux. Ce mécanisme, qui n'avait pas été pris en compte jusqu'alors, est également observé dans les expériences analogiques (Davy et Cobbold, 1988 ; Sornette et al., 1993 ; Fournier et al., en préparation).

La déformation en Asie Centrale apparaît comme une combinaison d'épaississement crustal, d'extrusion, et de rotations de blocs. Cependant, l'imprécision sur les données, et l'incertitude sur l'extrapolation de la néotectonique aux derniers 45 Ma, ne permettent que difficilement de définir les relations qualitatives et quantitatives entre ces trois mécanismes.

Deux zones, situées respectivement à la hauteur des syntaxes de l'Assam et du Pakistan, présentent un style de déformation combinant rotations, épaississement et décrochement (Cobbold and Davy, 1988) (Figure I.3). Ces régions apparaissent fondamentales pour l'étude de l'interaction entre les

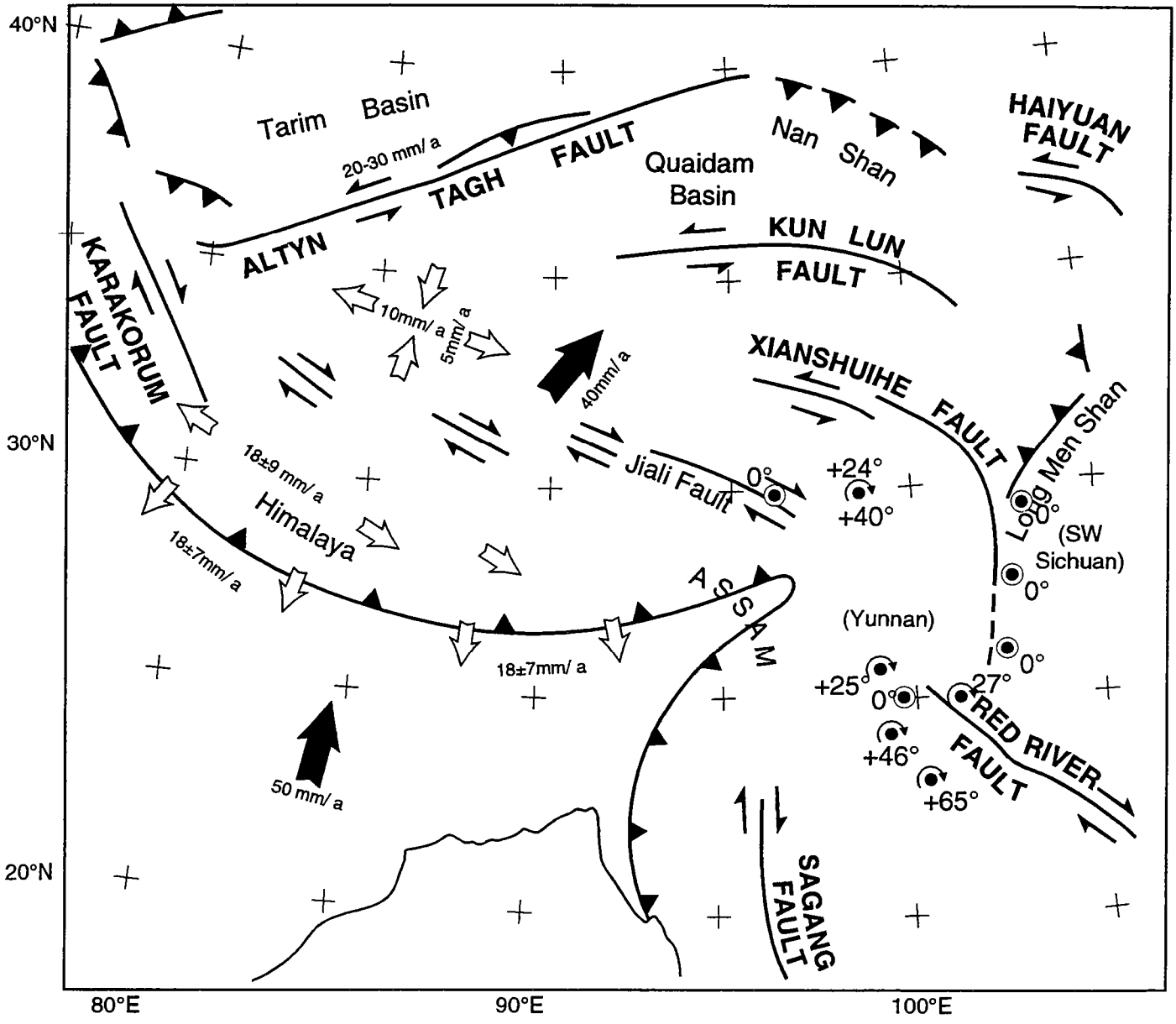

Figure I.4. Carte tectonique schématique du Tibet et de la Chine du Sud-Ouest (adaptée d'après Molnar et Lyon-Caen, 1988).

Les flèches noires indiquent les déplacements par rapport à la Sibérie, les flèches blanches les taux de déplacement pour le Quaternaire. Les cercles localisent les études paléomagnétiques. Les rotations indiquées ont été mesurées dans des sédiments Jurassique ou Crétacé. Deux mesures pour un même point correspondent à des rotations mesurées dans le Jurassique et dans le Crétacé respectivement (les rotations positives indiquent un sens horaire).

différents mécanismes de déformation, et, à fortiori, pour la compréhension de la cinématique de l'Asie.

A la hauteur de la syntaxe de l'Assam, la bordure est du plateau du Tibet et la Chine du Sud ont fait l'objet de nombreuses études tectoniques, sismotectoniques et paléomagnétiques. A l'inverse, au Nord et à l'Ouest de la syntaxe du Pakistan, dans les régions du Tien Shan et du Tadjikistan où mon étude a été réalisée, peu de données sont disponibles.

Dans la suite de ce chapitre, nous nous servons de l'exemple de la syntaxe de l'Assam pour illustrer le problème tectonique et cinématique de la région présentée dans ce mémoire.

3.2. La bordure Est-Tibet et le Sud-Ouest Sichuan: un exemple de déformation accommodée par de l'épaississement, du décrochement et des rotations de blocs

Le plateau du Tibet est bordé par deux zones décrochantes majeures (Figure I.3 et I.4) :

- la faille de l'Altyn Tagh au nord-ouest présente un déplacement sénestre à un taux actuel de 30±20 mm/an (Peltzer et al., 1989 ; Molnar et Deng, 1984) pour un déplacement cumulé Tertiaire estimé à plusieurs centaines de kilomètres.
- La zone décrochante dextre de Karakorum-Jiali qui s'étend depuis la bordure Est-Pamir jusqu'à la syntaxe de l'Assam.

Le mouvement général N-E du Tibet par rapport à la Sibérie se fait entre ces deux décrochements (Avouac et Tapponnier, 1992). L'extension récente E-O (depuis environ 6 Ma) est quand à elle étroitement associée au mouvement décrochant dextre le long de la faille du Karakorum-Jiali (Armijo et al., 1986 ; 1989).

Ce déplacement E-W est accommodé sur la bordure est du Tibet, par une série de décrochements sénestres actifs (Molnar et Deng, 1984) (Figure I.4).

La Faille de Xianshuihe présente un taux de déplacement actuel de 15±5 mm/a sur son segment NO, qui décroît à 5 mm/an sur son segment NS (Allen et al., 1991 ; Molnar et Deng, 1984). Le taux de déplacement sur la faille du Kunlun varie de 13 mm/a à 10 mm/a d'Ouest en Est (Kidd et Molnar, 1988). A l'extrémité NE du Tibet, la faille de Haiyaun présente quant à elle un taux de déplacement de 5 mm/a. Ces failles se courbent autour de la virgation Himalayenne, spécialement la faille de Xianshuihe qui passe d'une orientation

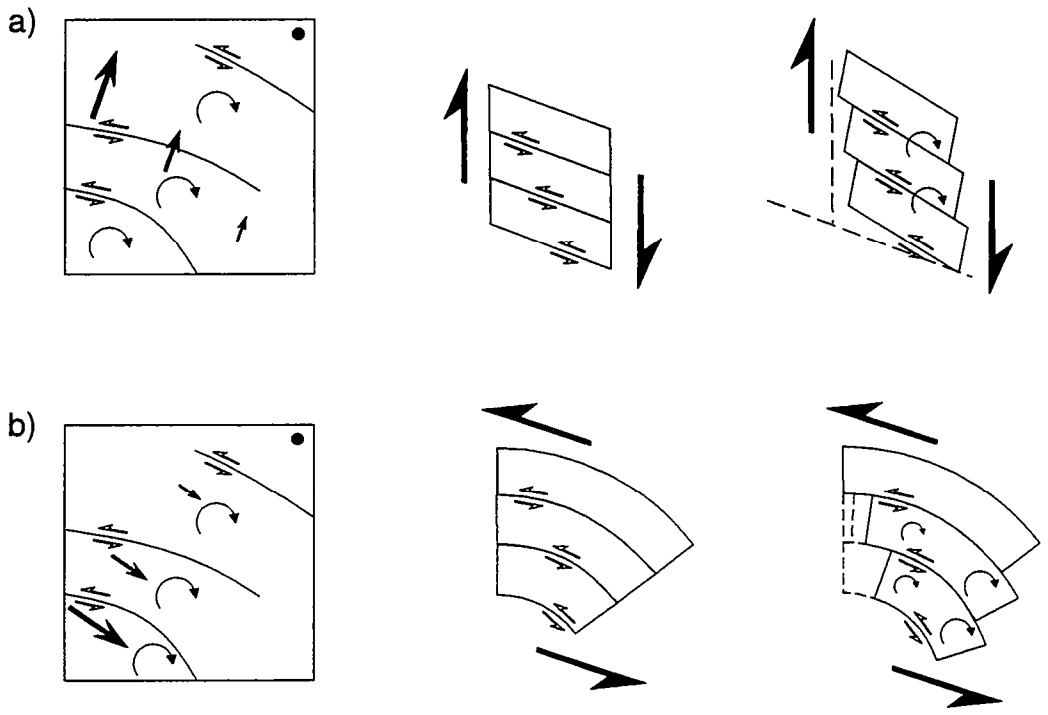

Figure I.5. Modèles de rotation de bloc proposés pour l'Est-Tibet (adapté d'après England et Molnar, 1990).

Pour a et b, le schéma de gauche représente de facon simplifiée les trois principales failles sénestres de l'Est-Tibet (cf Figure 4 et texte) et l'interprétation du champ de vitesses correspondant au modèle de rotation de blocs de gauche. Les vitesses sont représentées par rapport à un point fixe situé dans le coin supérieur gauche (rond noir). (a) La bordure Est de la région est considéré comme fixe et le mouvement sénestre sur les failles est associé à un cisaillement réginal N-S. La rotation horaire du domaine entraine un raccourcissement E-O et un étirement N-S. (b) La matière tourne entre les failles fixes et le mouvement E-O est transmis dans son intégralité à travers la zone. Les rotations finies des blocs augmentent vers l'Est.

ONO à une orientation presque NS. A partir des moments sismiques des séismes, Molnar et Deng (1984) ont montré que toute cette zone est en compression E-O et en extension N-S.

Cobbold et Davy (1988) et Dewey et al. (1989) ont proposé que ces décrochements sénestres ainsi que les blocs qu'ils délimitent, soient associés à des rotations autour d'axes verticaux de type domino (Jackson et McKenzie, 1983), dans un large domaine subissant un cisaillement dextre N-S (Figure I.5a). Ce cisaillement dextre sur la bordure Est du Tibet serait lié à l'indentation de l'Inde dans l'Asie et représenterait la continuation vers le nord du mouvement le long de la faille de Sagaing. L'analyse des taux de déformation actuels à partir de la sommation des tenseurs des moments sismiques (Holt et al., 1991 ; Holt et Haines, 1993) est en bon accord avec cette interprétation cinématique. En utilisant un tel modèle de rotation de blocs, England et Molnar (1990) ont montré que le taux de rotation actuel déduit des taux de déplacements sur les failles est compris entre 1° et 2°/Ma. Ce taux implique un raccourcissement E-O dans l'Est du Tibet compensant à peu près l'extension dans le Tibet.

La principale conséquence de ce modèle est que la plupart (voir la totalité) du déplacement du Tibet n'est pas transféré vers l'Est et donc qu'il y a peu ou pas d'extrusion de blocs en Chine du Sud.

A l'inverse, Molnar et Lyon Caen (1989) ont proposé un modèle (Figure I.5b) où l'extrusion vers l'Est du Tibet est accommodée sur sa bordure Est par glissement de matière le long des décrochements sénestres. La forme courbe des décrochements impose une rotation horaire de la matière mais pas nécessairement des failles limitant les blocs. Avouac et Tapponnier (1992), dans une interprétation de la cinématique active de l'Asie, reprennent un modèle proche et estiment que l'épaississement observé sur les bordures Nord-Est et Est du Tibet, à l'extrémité de la faille de l'Altyn Tagh (Quilian Shan, Quaidam) et dans le Lungmenshan, n'accommodent que partiellement le transfert de matière vers l'Est. Ainsi, ces auteurs proposent que le déplacement actuel vers le NE du Tibet (par rapport à la Sibérie) soit transféré en un mouvement SE à la Chine du Sud, à travers la bordure Est du Tibet. Ce mécanisme est en faveur de l'extrusion.

Des études paléomagnétiques récentes effectuées sur des sédiments d'âge Mésozoïque (Zhu et al., 1988 ; Otofuji et al., 1990 ; Enkin et al., 1991 ; Huang and Opdyke, 1992 ; Huang et al., 1992 ; Funahara et al., 1992, 1993 ; Huang and Opdyke, 1993) sont venues confirmer sans équivoque la présence d'importantes

rotations horaires dans cette région et dans le Yunnan (Figure I.4) ainsi que les prédictions réalisées à partir des tenseurs des moments sismiques. Les rotations horaires mesurées varient entre 25° et 60° au NO et au SO de la syntaxe, et deviennent nulles ou très faibles à l'Est de la faille de Xianshuihe. Cette distribution est en bon accord avec les prédictions des données sismiques sur les cents dernières années (Holt et Haines, 1993).

Le paléomagnétisme permet-il de trancher entre les différents modèles de rotation de blocs ? Le modèle de domino (Figure I.5a) implique des rotations uniformes au sein du domaine en cisaillement dextre et une rapide diminution des rotations sur ses bordures Est et Ouest. A l'inverse, le modèle de Molnar et Lyon-Caen (1989) implique des rotations faibles ou nulles aux abords des décrochements senestres et des rotations de plus en plus fortes vers l'est des blocs. Cependant, comme le montre la figure I.4, les données paléomagnétiques sont actuellement en trop petit nombre et la géométrie des blocs trop imprécise pour permettre une quelconque interprétation quand au mécanisme de rotation. Par ailleurs, la quantification de ces modèles est principalement basée sur l'extension dans le Tibet, phénomène récent par rapport à l'âge de la collision. Ils ne tiennent en effet pas compte d'une possible extrusion Oligo-Miocène de l'Indochine le long de la faille de la Rivière Rouge (Tapponnier et al., 1982, 1986), hypothèse récemment étayée par des données structurales (Tapponnier et al., 1990) et paléomagnétiques (Yang and Besse, 1993).

Indépendamment de toute interprétation, cet aperçu de la cinématique de l'Est-Tibet permet de juger de la complexité de la déformation dans cette zone. Les rotations de blocs apparaissent comme un mécanisme important, dont la compréhension est fondamentale pour l'interprétation de la cinématique régionale et des mécanismes qui gouvernent la déformation continentale.

3.3. De l'Afghanistan au Baïkal

La limite entre d'une part, les boucliers de la Sibérie et du Kasakhstan, et, d'autre part, l'Asie Centrale affectée par la déformation Cénozoïque, s'effectue le long d'une large bande allant de l'Afghanistan à la région du Baïkal en passant par le Tadjikistan, le Tien Shan et l'Altaï (Figure I.3).

Le style de la déformation évolue depuis, (1), un contexte principalement compressif et une composante de décrochement associée dans le Tien Shan, à (2), un contexte principalement décrochant dans l'Altaï et la Mongolie Occidentale, à (3), un contexte décrochant et extensif dans la région du Baïkal

(Molnar et Tapponnier, 1975 ; Tapponnier et Molnar, 1979). Une caractéristique particulière de cette zone est la disposition en échelon des principaux reliefs la composant. L'Hindou Kouch au Nord de l'Afghanistan, le Sud-Ouest Tien Shan, le Nord-Ouest Tien Shan, la bordure occidentale du bassin Junggar et l'Altaï sont autant de chaînes où l'altitude peut être supérieure à 5000 m et dont la disposition suggère un contexte régional décrochant sénestre (Cobbold et Davy, 1988). Ces linéaments sont en général soulignés par une série de décrochements dextres NO-SE. Les failles actives de Talass-Fergana et de Junggar de part et d'autre du Tien Shan en sont les deux exemples les plus spectaculaires (Tapponnier et Molnar, 1979).

A l'image du contexte cinématique de l'Est-Tibet décrit précédemment, Cobbold et Davy (1988) ont proposé que le jeu sur les décrochements dextres soit associé à des rotations antihoraires de blocs autour d'axes verticaux. Les modélisations analogiques (Cobbold et Davy, 1988 ; Sornette et al., 1993, Fournier et al., en préparation) suuggèrent que cette zone accommode partiellement le déplacement N-E de l'Asie Centrale déformée, par rapport à la Sibérie stable. Les rotations antihoraires de blocs qui y sont observées sont maximales (20° à 40°) aux abords du piston, dans une région qui correspondrait au Tien Shan et au Tadjikistan. A l'extrémité orientale de la zone, ces rotations seraient également associées à l'ouverture de la mer du Japon (Jolivet et al., 1990).

Le Tien Shan Kirghiz et la dépression Tadjik sont deux domaines situés respectivement au Nord et à l'Ouest du plateau du Pamir. L'Hindou Kouch et le Pamir sont tous deux caractérisés par une forte sismicité de profondeur intermédiaire (70-300 km), témoignant d'une ou plusieurs subductions lithosphériques dont les origines sont discutées (Molnar et al., 1977 ; Vinnik et al., 1977 ; Billington et al., 1977 ; Chatelain et al., 1980 ; Tapponnier et al., 1981, Mattauer, 1986). La répartition des séismes en profondeur permet de distinguer une subduction à plongement Nord sous l'Hindou kouch, d'une subduction à plongement Sud sous le Pamir Central. Les relations entre cette sismicité et la déformation de surface dans la dépression Tadjik et le Tien-Shan sont peu claires. La zone à pendage sud serait le résultat de la subuction sous le Pamir de la dépression Tadjik et du Tien shan (Tapponnier et al., 1981 ; Mattauer, 1986 ; Hamburger et al., 1992). Ceci est cependant difficilement compatible avec la zone à pendage nord qui serait le reflet de l'extrémité nord de la subduction de la lithosphère de l'Inde sous l'Asie (Billington et al., 1977 ; Tapponnier et al., 1981 ; Mattauer, 1986)

Dans l'Est-Tibet, une sismicité comparable n'est pas observée et les relations entre la déformation en profondeur et de surface apparaissent moins complexes. Une autre différence majeure réside dans la bordure confinée à l'Est de la zone Pamir-Baïkal contrastant avec la bordure plus "libre de contraintes" de la marge Pacifique. A travers les études effectuées dans la dépression Tadjik et dans le Tien Shan Kirghiz présentées dans ce mémoire, dont l'objet principal est de caractériser la cinématique de cette région, nous aborderons des problèmes proches de ceux observés pour la syntaxe Ouest-Himalyenne à savoir :

- Quelles sont les conditions aux limites qui contrôlent la déformation en surface et en profondeur ?

- Quelle est la part respective de la déformation accommodée par de l'épaississement et du décrochement ?

- Y a t'il des rotations de blocs ?

- Si des rotations sont présentes, quels en sont les mécanismes ?

4. Méthodes d'étude

Le paléomagnétisme est, à l'heure actuelle, une des méthode les plus efficaces pour mettre en évidence et quantifier des rotations finies de blocs autour d'axes verticaux. Les contraintes cinématiques apportées par le paléomagnétisme sont éloquentes dans des régions telles que la Californie (Luyendik, 1991), l'Israël (Ron et al., 1984) ou encore l'Arc Egéen (Kissel et Laj, 1988), où la plupart des modèles de rotation de blocs ont été définis (Freund, 1970 ; McKenzie et Jackson, 1983 ; Taymaz et al., 1991). Les différentes études paléomagnétiques effectuées sur ces régions ont cependant montré que les données nécessaires pour caractériser des mouvements rotationnels doivent être produite en grand nombre et localisées en fonction de la tectonique locale et régionale, afin de tenir compte du facteur d'échelle. Par ailleurs, les techniques et appareillages de mesure actuels ne permettent généralement de mettre en évidence de façon significative que des rotations supérieures ou égales à 10°.

L'interprétation des rotations mesurées ne peut se faire que par une bonne connaissance du terrain, de la géométrie des structures et de la cinématique sur les accidents. Le paléomagnétisme et la tectonique apparaissent comme deux méthodes complémentaires pour caractériser le style et les mécanismes de la déformation dans des régions où des rotations de blocs ont pu avoir lieu. Les travaux présentés dans ce mémoire ont été réalisés dans ce souci de complémentarité.

CHAPITRE II

Le Tien Shan Kirghiz : Paléomagnétisme et cinématique tertiaire

1. Introduction - résumé

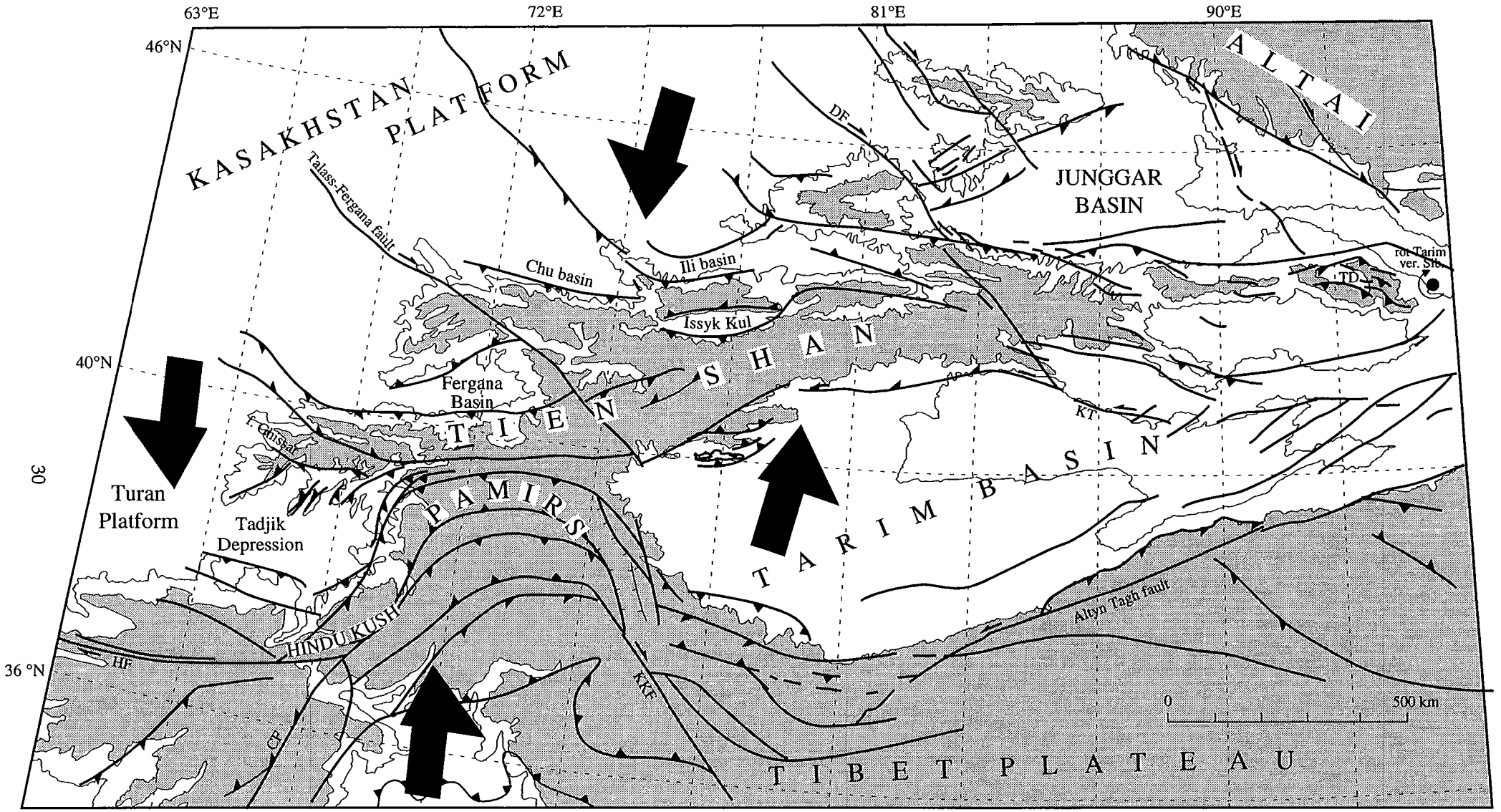

Figure II.1. Carte tectonique de l'Asie Centrale et contours topographiques à 1000 m et 2000 m (adaptée d'après Avouac et al., 1993).

Toutes les failles sont considérées comme ayant été actives à un moment ou à un autre au cours du Tertiaire. Les flèches noires représentent le contexte cinématique régional (Cobbold et Davy, 1988). CF : faille de Chaman ; DF : faille de Junggar ; HF : faille de l'Hérat ; KKF : faille du Karakorum ; KT : faille de Kurk-Tag ; TD : dépression de Turfan.

1.1. Contexte géologique

Le Tien Shan, qui s'étend d'Est en Ouest sur près de 2500 km avec des altitudes maximales avoisinant 7000 m, est une des chaînes de montagnes intracontinentales les plus remarquables (Figure II.1). Ce massif constitue la bordure nord-ouest de l'Asie Centrale déformée au Tertiaire. Il est limité au Sud par le bassin du Tarim et le plateau du Pamir, et au Nord par le bassin de la Junggarie et la plate-forme du Kasakhstan. La structuration du Tien Shan consiste en une succession de chaînes de socle, alternant avec des bassinsr Tertiaires intramontagneux.

Deux sutures Paléozoïques traversent le Tien Shan, signe d'une tectonique et structuration varisque et calédonienne trés marquée (Burtman, 1975) (Figure II.2). La suture Sud correspond à la fermeture de l'Océan Turkestan (Bakirov et Burtman, 1984) et à l'accrétion, au Dévonien supérieur et au Carbonifère, du bloc du Tarim (Windley et al., 1990 ; Allen et al., 1991) et de la plaque de Turan (Boulin, 1988) venant tous deux du Sud. La suture Nord est, quant à elle, d'âge Carbonifère supérieur (Windley et al., 1990 ; Allen et al., 1991). Au Permien Supérieur et Triassic inférieur, les données paléomagnétiques dans le Tien Shan Kirghiz montrent des rotations antihoraires pouvant être associées à un contexte tectonique régional décrochant (Audibert et Bazhenov, 1992 ; Bazhenov et al., 1993).

Le contexte tectonique régional du Tien Shan Kirghiz au cours du Mésozoïque est mal connu. Coté Chinois, la sédimentation Mésozoïque atteint plusieurs kilomètres d'épaisseur mais les interprétations quant au contexte tectonique diffèrent. Selon Allen et al. (1991), l'extension est le premier facteur qui contrôle la sédimentation jurassique dans le bassin Junggar, tandis que Graham et al. (1993) considèrent que les bassins adjacents au Tien Shan (Tarim, Turfan, Junggarie) se sont plutôt développés dans un contexte compressif lié à l'accrétion successive de microblocs sur la marge sud Asiatique. Dans le Tien Shan Kirghiz, les sédiments Mésozoïques sont présents dans le bassin de Fergana et, en faible quantité, dans le bassin d'Issyk-Kul. Des discordances stratigraphiques successives Mesozoïques sont clairement visibles dans le bassin de Fergana (Ministry of Geology of the USSR and the Tadjik Academy of Sciences, 1984). Par ailleurs, un bassin Jurassique est présent le long de

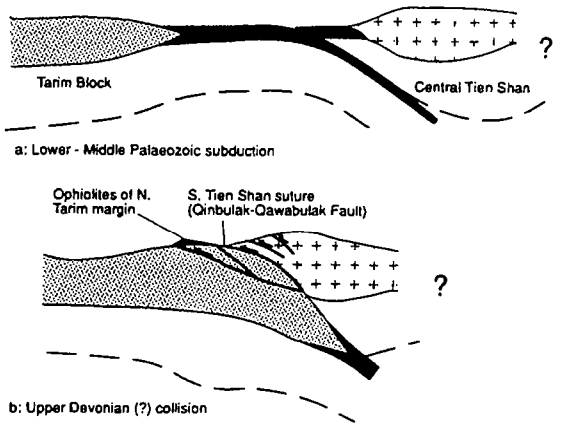

Fig. 9. Schematic diagram illustrating the tectonic evolution of the Southern Tien Shan collision.

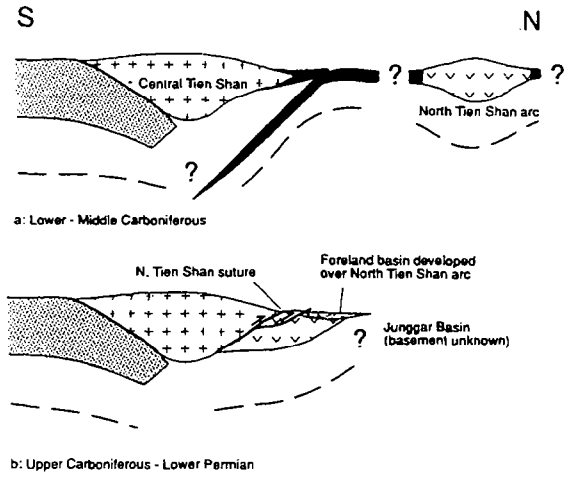

Fig. 13. Schematic diagram illustrating the tectonic evolution of the Northern Tien Shan collision.

Figure II.2. Histoire Paléozoïque du Tien Shan chinois (Allen et al., 1992).

l'extrémité sud-est de la faille de Talass-Fergana mais son contexte tectonique n'est pas expliqué.

Bon nombre des structures et accidents Paléozoïques ont été réactivés lors de l'orogénèse Tertiaire. L'analyse de la déformation à l'aide des images satellites (Tapponnier et Molnar, 1979) et les mécanismes au foyer des séismes (Ni, 1978 ; Nelson et al., 1987) indiquent une tectonique Quaternaire principalement compressive, particulièrement concentrée sur les bordures nord et sud du Tien Shan, et une direction de racourcissement globalement N-S. Le taux de racourcissement moyen actuel (probablement relativement constant depuis 20-30 Ma, Avouac et al., 1993) est de 13±7 mm/a (Molnar et Deng, 1984). Le moho atteint une profondeur de 50 km (Gubin, 1986 ; Burov et al., 1990), principalement suite à l'épaississement crustal Cénozoïque. En simplifiant, on peut considérer le Tien Shan comme un "pop-up" d'échelle crustale, chevauchant les bassins flexuraux, du Tarim au sud, de Junggar et d'Ili au Nord. La structuration et la sédimentation Cénozoïque de ces bassins de type foreland sont controlées par le développement des chevauchements nord et sud du Tien Shan (Windley et al., 1990 ; Allen et al., 1991, 1992 ; Avouac et al., 1993).

Cobbold et Davy (1988), à partir d'une reconstruction du champ de déplacement sur les dix derniers millions d'années, ont mis en évidence une rotation horaire Cénozoique du bloc du Tarim. L'élargissement progressif du Tien Shan de l'Est vers l'Ouest, visible sur la topographie (Figure II.1), serait ainsi lié à la rotation du Tarim, bloc rigide et peu déformable, par rapport à la plate-forme du Kasakhstan, selon un pôle situé à l'extrémité Est de la chaîne (Chen et al., 1991) (Figure II.1). Le gradiant de raccourcissement E-O correspondrait à une rotation horaire de 7°±2.5° du bassin du Tarim par rapport à la Sibérie (Avouac et al., 1993). Ceci implique un raccourcissement fini de l'ordre de 250 km à l'Est de la faille de Talass-Fergana, et de 150 km entre les bassins du Tarim et de la Junggarie (85°E).

Malgré une déformation compressive très marquée, de nombreux accidents témoignent d'une composante de décrochement régional. La faille NO-SE de Talass-Fergana qui traverse le Tien Shan occidental de part en part sur près de 400 km en est le plus bel exemple. Ce décrochement dextre, bien qu'asismique depuis le début du siècle, présente un taux de déplacement Holocène variant de 5 à 14 mm/a (Trifonov et al., 1992) dans sa partie centrale, pour un offset Quaternaire total de 10-14 km (Burtman, 1961 ; 1980 ; Wallace, 1976 ; Tapponnier et Molnar 1979 ; Trifonov et al., 1992). Le déplacement total depuis

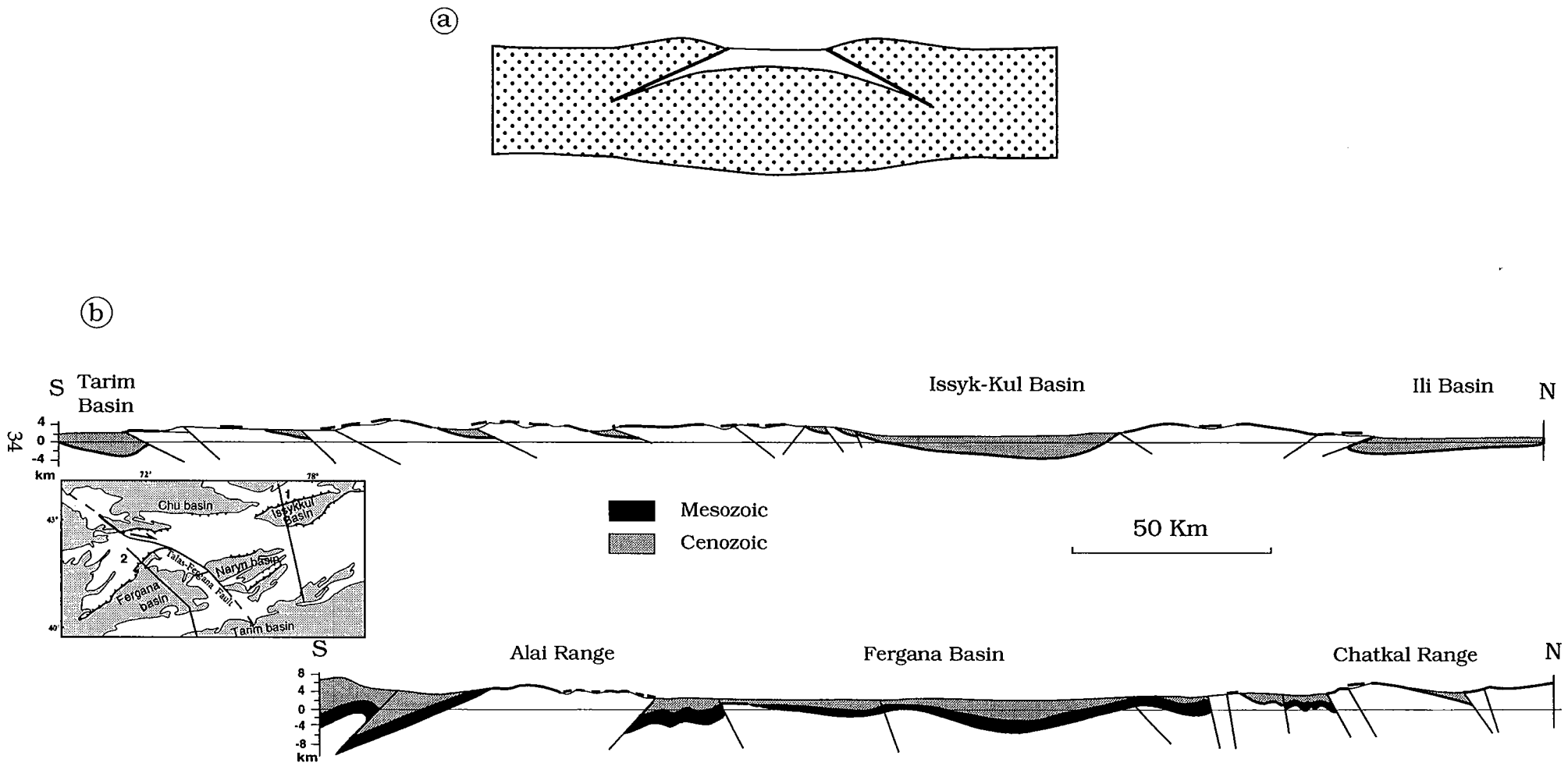

Figure II.3. a. Bassin de type ramp (Willis, 1928). b. Coupes simplifiées à travers le Tien Shan (Sadybakasov, 1991).

le Permien est de l'ordre de 200 km (Bakirov et Burtman, 1984), la majeure partie du mouvement ayant lieu durant le Cénozoïque (seconde partie de ce chapitre). En Chine, la faille de Junggar qui présente la même orientation est elle aussi un décrochement dextre majeur (Tapponnier et Molnar, 1979) tout comme la zone décrochante du Ghissar sur la bordure sud-ouest du Tien Shan (Chapitre III). Des déplacements sénestres sont également notables sur les failles de Kurk-Tag, sur la bordure sud-est du Tien Shan, ainsi qu'au Nord du bassin d'Issyk-Kul sur le système de failles de Chonkemin (Tapponnier et Molnar, 1979).

Une des particularités du Tien Shan est la présence de nombreux bassins Tertiaires intramontagneux (Fergana, Naryn, Issykkul, Susamyr...). Leur structuration (troisième partie de ce chapitre) est similaire à celle d'un bassin de type ramp (Willis, 1928 ; Cobbold et al., 1993) (Figure II.3a). En règle générale, des chevauchements à vergence opposée vers l'intérieur du bassin font reposer sur les bordures nord et sud, le socle sur les sédiments Tertiaires (Kalvoda, 1987 ; Sadybakasov, 1991) (Figure II.3b). La subsidence du bassin est controlée par (1) la flexuration liée aux chevauchements et (2) l'apport de sédiments depuis les chaînes limitrophes (Tondji Biyo, 1993).

Dans ces bassins intramontagneux et dans les bassins d'avant-pays au Nord et au Sud du Tien Shan, les dépôts Tertiaires sont marqués par un important apport de sédiments à partir du Miocène Moyen (Allen et al., 1991 ; Hendrix et al., 1992). Ceci marque la surrection des reliefs et la principale phase de déformation liée à la collision Inde-Asie au Sud. Cet âge est par ailleurs proche de celui déduit de la rotation finie du bloc du Tarim pour un taux de rotation constant pendant le Néogène (Avouac et al., 1993).

De l'analyse du champ de failles, Cobbold et Davy (1988) proposent un contexte tectonique régional compressif avec une composante décrochante sénestre. A plus grande échelle, le Tien Shan fait partie d'une zone orientée NE-SO allant d'Oman au Baïkal soumise à un décrochement sénestre où, selon Cobbold et Davy (1988), les décrochements dextres (Talass-Fergana, Junggar...) et les blocs qu'ils limitent subissent des rotations antihoraires.

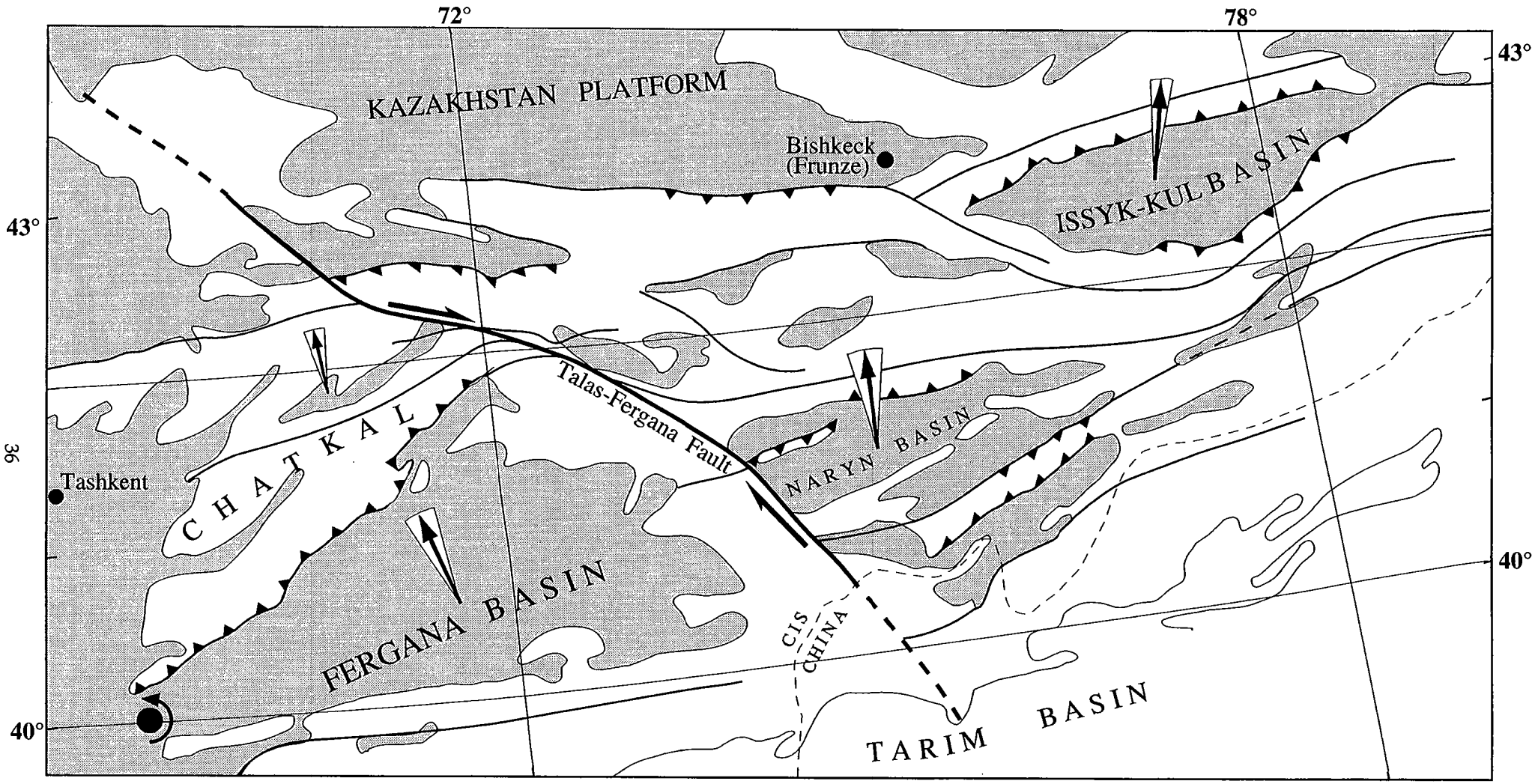

Figure II.4. Déclinaisons paléomagnétiques moyennes mesurées dans les bassins du Tien Shan Kirghiz .
Les bassins Tertiaires sont en grisé. La rotation antihoraire du bassin de Fergana se fait selon un pôle situé à son extrémité Sud-Ouest.

1. 2. Principaux résultats

Etude paléomagnétique

Les trois principaux bassins du Tien Shan Kirghiz ont été échantillonnés, à savoir, les bassins d'Issykkul, de Naryn et de Fergana (Figure II.4). Environ 500 échantillons ont été collectés, principalement dans des séries rouges continentales d'âge Paléogène. Quelques coulées basaltiques Paléocènes ont par ailleurs été prélevées sur la bordure nord du bassin d'Issyk-Kul. Pour la plupart des localités paléomagnétiques le test du pli est positif : l'aimantation isolée de haute température a donc été acquise avant le plissement.

Un résultat surprenant de l'étude paléomagnétique est la valeur de l'inclinaison magnétique mesurée. Celle-ci varie de 34° dans le bassin de Fergana, à 42° dans le Bassin d'Issyk-Kul. Les paléolatitude déduites de 18°N et 30°N respectivement à Fergana et à Issyk-Kul sont beaucoup plus basses que la paléolatitude de référence de 43°N calculée à partir de la récente courbe de dérive apparente du pôle (CDAP) de Besse et Courtillot (1990). Ceci impliquerait une migration vers le Nord d'au moins 2000 km depuis l'Oligocène quand seulement 200 à 300 km de déplacement N-S sont attendus dans le Tien Shan. Par ailleurs, les paléolatitudes mesurées à partir de sédiments Crétacés du bassin de Fergana sont en très bon accord avec la CDAP (Bazhenov, 1993). Il faudrait donc imaginer la combinaison improbable d'un déplacement vers le Sud fini-Crétacé début-Tertiaire, suivi d'un mouvement vers le Nord au Tertiaire.

La référence proposée par Besse et Courtillot (1991) a quant à elle été uniquement établie à partir de données d'Europe occidentale, en considérant l'Eurasie comme un ensemble rigide au Tertiaire. Des données provenant des zones stables de l'Asie seraient nécessaires afin d'obtenir une référence Tertiaire tout a fait fiable pour le Tien Shan.

Par ailleurs, les processus d'acquisition de l'aimantation ainsi que la déformation et la compaction peuvent avoir une influence notable sur l'inclinaison magnétique (voir Butler, 1992 pour une synthèse).

Une anomalie d'inclinaison similaire est également observée dans les sédiments Tertiaires de la dépression Tadjik (Chapitre III). Une anomalie de cette ampleur est, en tout état de cause, difficile à expliquer. Je propose en annexe 1 une réflexion plus approfondie sur la validité des différentes CDAP pour l'Asie, et les causes possibles d'anomalie d'inclinaison. Compte tenu des données actuelles, il me semble que l'origine de cette anomalie est plutôt à

rechercher dans les processus d'acquisition de l'aimantation, synchrones ou postérieurs au dépôt du sédiment.

La déclinaison magnétique mesurée ne semble pas affectée par cette anomalie, les rotations obtenues à partir de données Crétacées (Bazhenov, 1993) étant très similaires à celles obtenues sur le Tertiaire.

Les rotations déduites des déclinaisons magnétiques (Figure II.4) peuvent être regroupées en deux domaines distincts, de part et d'autre de la faille Talass-Fergana.

Le bassin de Fergana, à l'ouest de la faille, présente une rotation antihoraire de 20°±11° par rapport au bassin d'Issyk-Kul, situé à l'Est de la faille. Les rotations mesurées dans les sédiments Crétacés du bassin de Fergana (Bazhenov, 1993) sont en bon accord avec ce résultat. La cohérence des rotations à travers le bassin indique, au moins au premier ordre, un comportement rigide au cours de la déformation. Les rotations absolues des bassins d'Issyk-Kul et de Naryn par rapport l'Eurasie sont quant à elles faibles ou insignifiantes.

La chaîne du Chatkal qui sépare le bassin de Fergana de la plate-forme du Kasakhstan présente une forme topographique triangulaire (Figure II.1) suggérant une quantité croissante de raccourcissement depuis sont extrémité sud-ouest jusqu'à la faille de Talass-Fergana. Une rotation du bassin de Fergana par rapport à la plate-forme stable selon un pôle situé à son extrémité sud-ouest (figure II.4) permet de rendre compte aisément de cette observation. Dans un tel modèle, le déplacement dextre sur la faille de Talass-Fergana associé à une rotation antihoraire de 20°, est de l'ordre de 100 km, signifiant que le déplacement total estimé le long de cette faille est principalement Cénozoïque.

Etude structurale

Bien que la sismicité actuelle soit assez faible à l'intérieur du Tien Shan (Molnar et Chen, 1982), la carte des failles majeures Tertiaires (Figure II.5 et 3ième partie de ce chapitre) montre que la déformation est exprimée dans l'ensemble de la chaîne. A l'image du contexte compressif régional , les failles orientée E-O à ONO-ESE sont chevauchantes et principalement localisées sur les bordures des bassins. Ces failles présentent cependant assez fréquemment une composante décrochante sénestre (bordure sud des bassins de Naryn et d'Issyk-Kul par exemple).

Le chevauchement et le plissement sur les bordures des bassins est en général synchrone de la sédimentation. La carte des isopaques de la base du Tertiaire (3ième partie de ce chapitre) montre que le déplacement vertical relatif sur les bordures des bassins peut atteindre 14 km. Dans le bassin de Fergana en particulier, un déplacement vertical de 11 km est visible sur une distance d'au moins 20 km. Les interprétations des profils sismiques (Obukhov et al., 1991) sur les bordures nord et sud de ce bassin mettent en évidence des chevauchements localisés au dessus d'un niveau de décollement Silurien qui s'enracine probablement en profondeur sur des failles inverses d'échelle crustale.

Bien que les failles majeures soient préférentiellement situées sur les bordures des bassins, ceux-ci présentent une certaine déformation interne. Des failles décalant des sédiments ou des terrasses Quaternaires sont visibles dans le centre du bassin de Naryn et dans le bassin d'Issyk-Kul. Le bassin de Fergana présente lui aussi des évidences de déformation interne d'échelle cartographique bien visible sur les images satellites. Cette déformation témoigne probablement d'une tectonique de couverture.

Quelques données microtectoniques permettent de préciser l'évolution du style de la déformation dans le Tien Shan durant le Tertiaire. La plupart des stries observées sur des failles dans des sédiments Paléogènes présentent un mouvement décrochant dominant. A l'inverse, les stries dans les sédiments Néogènes sont majoritairement chevauchantes. Dans les deux cas, les failles sont compatibles avec une direction de racourcissement N-S. Ceci suggère que le style de la déformation était plutôt décrochant au Paléogène puis que la déformation compressive, migrant depuis les régions plus au sud, a affecté le

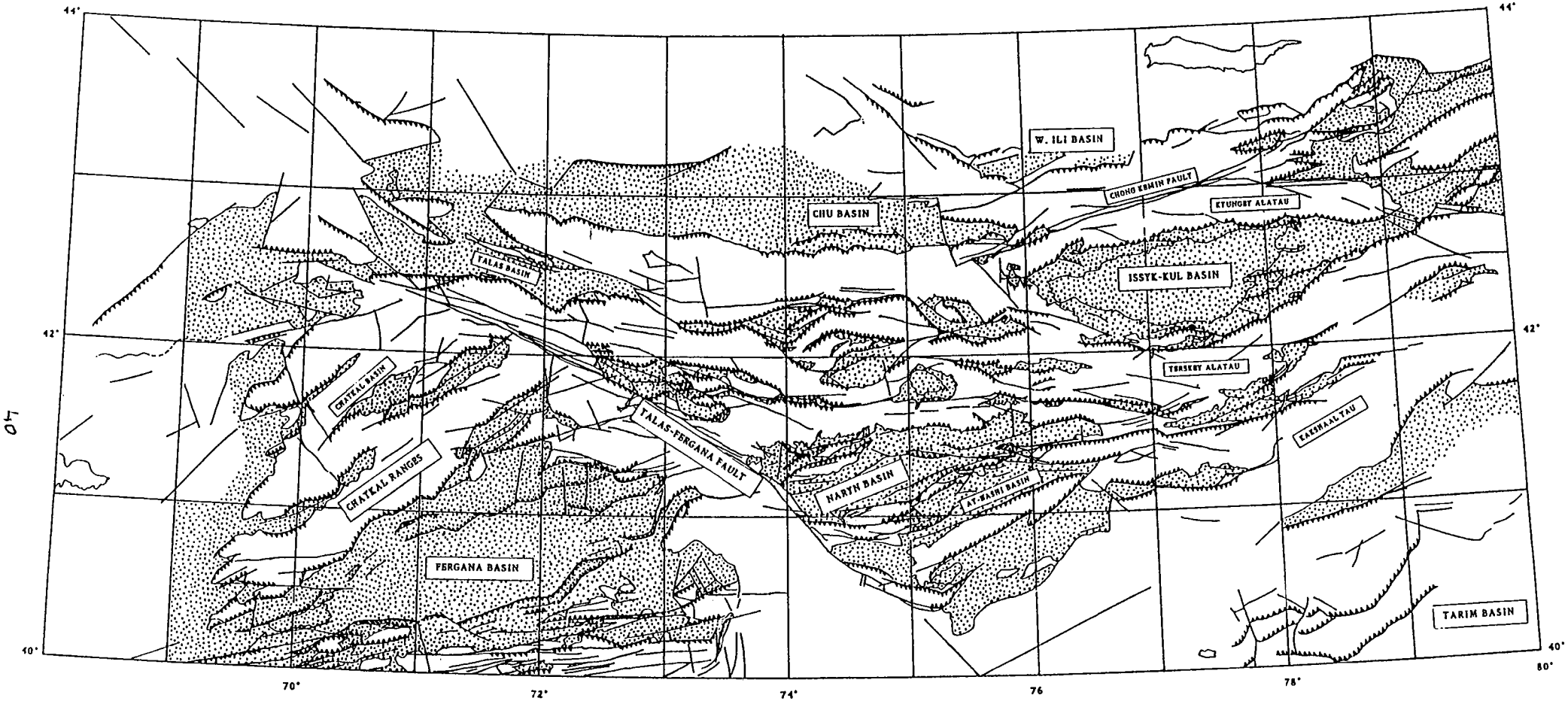

Figure II.5. Carte des failles et bassins Cénozoïques du Tien Shan Kirghiz.

Tien Shan à partir du Miocène. La zone décrochante aurait quant a elle été transférée dans l'Altaï et la Mongolie.

En résumé, le Tien Shan est affecté par la déformation durant tout le Cénozoïque. Les données structurales sont en faveur d'un faible développement des bassins compressifs au cours du Paléogène, avec une tectonique principalement décrochante, tandis que le Miocène marque un soulèvement général et des déplacements verticaux de plusieurs kilomètres sur les bordures des bassins. Le déplacement sur la faille de Talass-Fergana est accompagné par la rotation antihoraire du bassin de Fergana par rapport au bassin d'Issyk-Kul, les bassins situés à l'Est de la faille ne subissant qu'une faible rotation. Le poinçonnement du Pamir dans l'Asie stable est probablement étroitement associé au jeu dextre sur la faille de Talass-Fergana et à cette hétérogénéité des rotations. En accord avec la reconstruction cinématique de Cobbold et Davy (1988), le contexte tectonique général durant tout le Cénozoique apparaît comme transpressif sénestre au sein du Tien Shan Kirghiz.

2. Etude paléomagnétique des formations Tertiaires du Tien-Shan Kirghiz et implications tectoniques

A paleomagnetic study of Cenozoic formations from the Kyrgyz Tien-Shan and its tectonic implications

Article publié dans le "Journal of Geophysical Research", 98, 9571-9589, 1993.

JOURNAL OF GEOPHYSICAL RESEARCH, VOL. 98, NO. B6, PAGES 9571-9589, JUNE 10, 1993

A Paleomagnetic Study of Tertiary Formations From the Kyrgyz Tien-Shan and Its Tectonic Implications

J.-C. THOMAS,[1] H. PERROUD,[2] P. R. COBBOLD,[1] M. L. BAZHENOV,[3] V. S. BURTMAN,[3] A. CHAUVIN,[1] AND E. SADYBAKASOV[4]

As part of a general investigation of Cenozoic deformation in Central Asia, we studied the paleomagnetism of Tertiary red beds and lava flows from intermontane basins in the Tien-Shan region of Kyrgyzstan. We collected 532 cores and hand samples from 78 sites at 12 localities and progressively demagnetized them, thermally or with alternating fields. For most sites, there are magnetic components with unblocking temperatures higher than 600°C. We infer that the magnetic carriers are mainly hematite and magnetite. For most localities, the high-temperature component appears to predate tectonic folding. For all localities, mean inclinations are shallower than expected from apparent polar wander paths. Inclination anomalies range from 16°±5° for the Issyk-Kul basin, to 26°±7° for the Fergana basin. If due to changes in latitude, these anomalies imply at least 2000 km of northward displacement of the Tien-Shan during the Tertiary, for which there is no tectonic evidence. We thus consider that the paleomagnetic reference directions cannot be directly compared with our Tertiary data. We explored other possible reasons for this anomaly, which has also been reported from other parts of the Alpine belt, but we could not find a satisfactory explanation. Absolute rotations cannot be accurately determined, because of problems with the reference direction. Nevertheless, the mean declination for the Fergana basin lies counterclockwise by 20°±11° from the mean declination of the Issyk-Kul basin. This result is consistent with the counterclockwise rotation inferred for the Fergana basin from the pattern of Cenozoic faults and folds. It suggests a Cenozoic right-lateral displacement of 110±60 km on the Talas-Fergana fault.

INTRODUCTION

Argand [1924] compiled a tectonic map of Eurasia. He inferred that northward motion of India and its subsequent collision ("affrontement") with Asia were responsible for Cenozoic reactivation of earlier structures and for anomalous relief throughout much of Central Asia. Recent work has done much to confirm and quantify these ideas. Crustal shortening within Tibet was attributed to reactivation of earlier structures by *Dewey and Burke* [1973]. Seismicity and studies of fault traces on satellite imagery confirmed the extent of active deformation within Central Asia [*Molnar and Tapponnier*, 1975]. From magnetic anomalies in the Indian Ocean, India is estimated to have collided with Eurasia about 55 Ma ago [*Patriat and Achache*, 1984]. Since then, paleomagnetic and structural evidence suggests that there has been a further convergence of about 2000 km between India and Eurasia [*Achache et al.*, 1984; *Savostin et al.*, 1986].

Still not clear is the style of deformation within Central Asia over the last 55 Ma. *Molnar and Tapponnier* [1975] drew attention to the importance of strike-slip faulting. *Tapponnier et al.* [1982] suggested that strike-slip faulting could have led to significant eastwards extrusion of large blocks, with accompanying rotations. *Peltzer and Tapponnier* [1988] further suggested that eastward extrusion of Tibet accounts for about 50% of the convergence between India and Asia, the rest being taken up by crustal thickening. In contrast, *England* [1982], *Houseman and England* [1986] and *Dewey et al.* [1989] have argued that crustal thickening accounts for almost all of the convergence.

Davy and Cobbold [1988] and *Cobbold and Davy* [1988] compared analogue models of continental indentation with the pattern of Cenozoic faults in Central Asia (Figure 1a). They concluded that lateral extrusion accounts for somewhere between 20% and 45% of convergence, the rest being taken up by thickening. Such thickening must attenuate laterally across wrench zones, left-lateral in the west and right-lateral in the east. *Cobbold and Davy* [1988] found structural evidence for left-lateral wrenching, not only on the edges of thickened areas, but also in a long strip, running from the Gulf of Oman, through the Pamirs, to Lake Baikal and beyond. This belt, they argued, is responsible for some eastwards extrusion of Central Asia. On structural evidence, wrenching is partially accommodated by rotation of fault blocks and antithetic strike-slip faults, domino style. Rotations were inferred to be counterclockwise in the Gulf of Oman-Pamirs-Baikal wrench zone, clockwise in eastern Tibet. The Fergana basin in the Tien Shan was inferred to have rotated about 30° counterclockwise in the Cenozoic [*Cobbold and Davy*, 1988]. Bakirov [1960] had already made a rather similar suggestion, but he thought the rotation occurred during the Late Paleozoic.

Using the active velocity field, *England and Molnar* [1990] calculated that clockwise block rotation in eastern Tibet currenly accommodates nearly all the northeastward motion of Tibet and that no eastward or southeastward motion of China or Indonesia are necessary. *Jolivet et al.* [1990] suggested that the opening of the Japan Sea was a consequence of counterclockwise rotation of blocks at the northeastern end of the Gulf of Oman-Pamir-Baïkal wrench zone.

Paleomagnetism appears to be an excellent technique for measuring block rotations; but little work has been done so far to demonstrate Cenozoic rotations in Central Asia. Bazhenov

[1]Centre National de la Recherche Scientifique, Géosciences, Université de Rennes, Rennes, France.
[2]Département des Sciences de la Terre, Université de Pau, Pau, France.
[3]Geological Institute, Academy of Sciences, Moscow, Russia.
[4]Institute of Seismology, Kirghiz Academy of Sciences, Bishkeck, Kyrgyztan.

Paper number 92JB02912.
0148-0227/93/92JB-02912$05.00

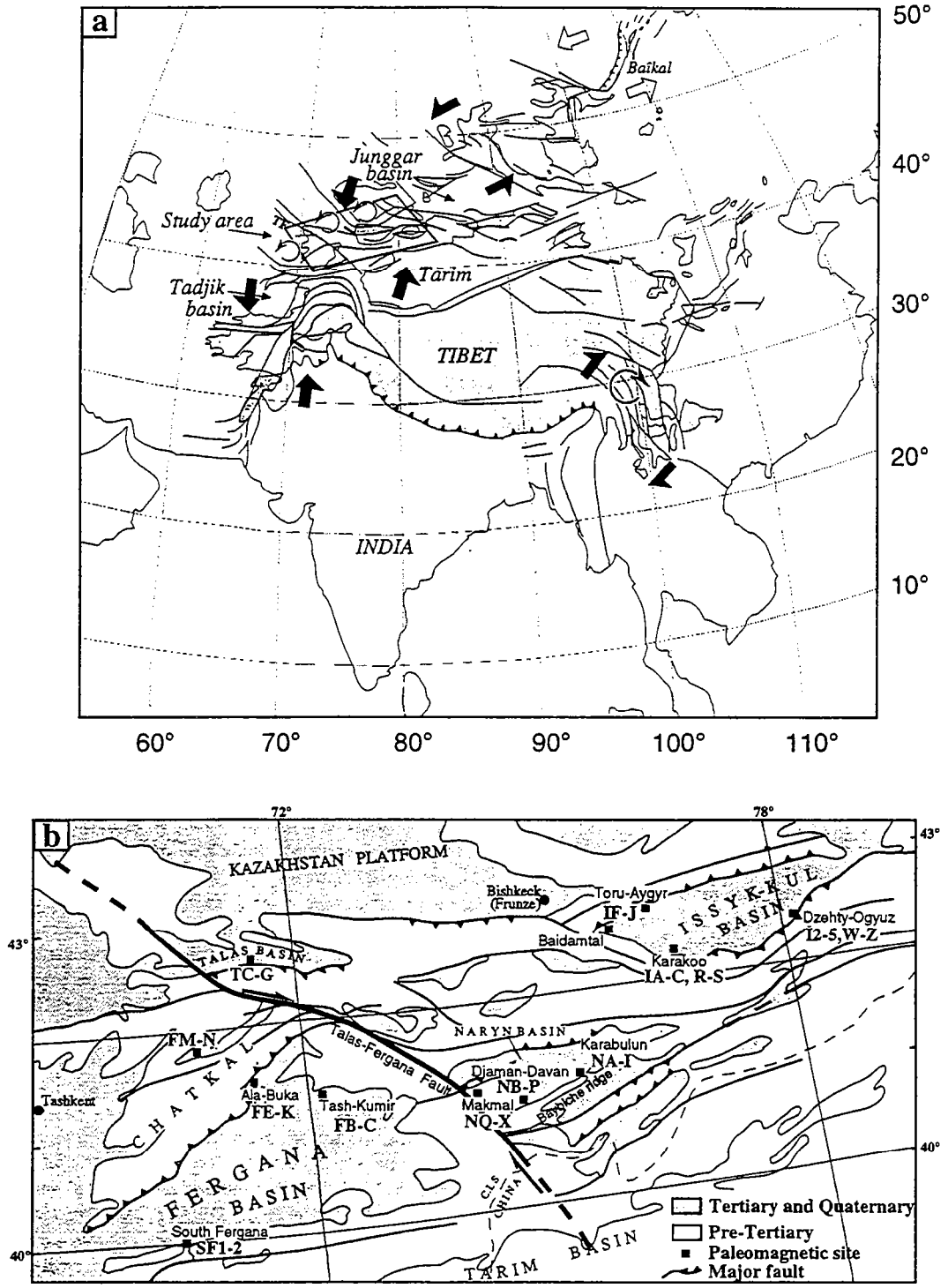

Fig. 1. (a) Cenozoic deformation in Central Asia [after *Cobbold and Davy*, 1988]. Map shows traces of major faults, areas with elevation greater than 2 km (hatched) and inferred Cenozoic displacement pattern. Pairs of arrows indicate horizontal displacement gradients (solid for contractional, open for extensional). solid half arrows indicate dominant wrenching in Altai and eastern Tibet; asymmetric solid arrows, convergent wrenching in Hindu-Kush and Tien-Shan; asymmetric open arrows, divergent wrenching in Baïkal; round arrows, rotations relative to stable Asia. (b) Structural map of the Kirghiz Tien-Shan, showing main faults, Tertiary basins and paleomagnetic sampling localities.

and *Burtman* [1986] were able to demonstrate rotations in the area of the Pamir-Punjab syntaxis; *Chen et al.* [1991] found paleomagnetic and structural evidence for small rotations of the Tarim and Junggar blocks in Western China; and *Pozzi and Feinberg* [1991] proposed a significant counterclockwise rotation of part of the northern Tadjik basin.

To study rotations throughout the Gulf of Oman-Pamirs-Baikal strip, a paleomagnetic project was set up between the Centre National de la Recherche Scientifique (CNRS) and the Geological Institute of the Academy of Sciences (Moscow). In the summer of 1989, Bazhenov, Burtman, Cobbold, Perroud and Sadybakasov took part in a 1-month expedition to the

Tien-Shan region of Kyrgyzstan. The objectives were to sample Tertiary red beds and lavas and to test for rotations between individual basins and even within them.

GEOLOGICAL SETTINGS

In the Tien-Shan region of Kyrgyzstan, mountain ranges several kilometers high alternate with intermontane basins (Figure 1b). Paleozoic and older rocks form the ranges whereas Mesozoic and Cenozoic sediments fill the basins. Mesozoic sediments are common throughout the large Fergana basin but are rare in the other basins. The Paleogene succession is continental and only a few hundred meters thick, to the north of the Talas-Fergana fault; but it is marine and more than 1 km thick, to the south of the fault. The Neogene succession is several kilometres thick in the major basins and is entirely continental. On the ranges, there are old erosion surfaces with remnants of Paleogene sediments. Erosion surfaces and sediments have been folded and faulted, as a result of Cenozoic tectonics [*Schulz*, 1948; *Sadybakasov*, 1972, 1991]. Anticlinal ranges are commonly thrusted over neighboring synclinal basins.

The general strike of the Tien-Shan ranges is East-West, but there are significant deviations, especially near the major Talas-Fergana fault, which separates the Western Tien-Shan from the Central and Eastern Tien-Shan (Figure 1b). This strike-slip fault originated in the Paleozoic and has been active in the Cenozoic [*Burtman*, 1961; *Wallace*, 1976; *Tapponnier and Molnar*, 1979]. Most of the displacement on it has been right-lateral. The Quaternary offset is more than 10 km. The total offset since the Permian is about 200 km [*Burtman*, 1980]; but so far it has not been possible to determine how much of this is Cenozoic and how much is older [*Tapponnier and Molnar*, 1979].

SAMPLING LOCALITY

We sampled Tertiary sediments and lavas in several basins throughout the Northern, Central and Western Tien-Shan. We collected a total of 408 cores and 124 hand samples at 78 sites (6-8 samples per site) from 12 localities within Eocene to Miocene rocks. Both solar and magnetic compasses were used for orientation; when both were present, calculated declinations differed from the present day-field declination by less than 1° or 2°.

As a base map, we used the 1:1,000,000 Operational Navigation Chart (sheet F6), published by the U.S. Defense Mapping Agency. For convenience, place names quoted in this paper have been taken from this map wherever possible. We used Landsat satellite images, geological maps at 1:200,000 and 1: 500,000 [*Ministry of Geology of the USSR and Kyrgyz Academy of Sciences*, 1978] and detailed topographic maps. We carefully recorded the attitudes of bedding, folds and other structures. From these data, we constructed geological sections. We used a portable navigational instrument (Magellan GPS NAV 1000^{TM}) to locate each paleomagnetic site on the ground with an accuracy of 30 m.

Northern Tien-Shan

Here we sampled Tertiary sediments and lavas on the edges of two east-west trending basins: Issyk-Kul and Talas (Figure 1b).

In the Issyk-Kul basin, we mainly sampled the Kokturpak formation (Eocene) and the Dzhety-Ogyuz formation (Oligocene-Miocene). At the northern edge of the basin (Toru-Aygyr locality), the Kokturpak formation consists of reddish sandy marls, sandstones and clays, of lacustrine and subaerial origin, resting upon a basalt flow (or flows) 12 m thick. Only a few meters above the basalt, the sediments have yielded mammalian and reptilian remains (*Depereteella* and *Prothyrecodon* sp.) attributed to the Middle to Late Eocene [*Turdukulov*, 1980]. The basalt has yielded a radiometric age of 55-Ma whole-rock K-Ar date [*Krilov*, 1960]. Underlying sandstones have been baked over a thickness of 1 m. We sampled four sites (IF to IJ) in the basalts and underlying sandstones. On average, the succession here dips gently southwestwards, but locally it is folded. Basalts and sediments of the Kokturpak formation were also sampled at four sites (IN to IQ) at the Baidamtal locality (western end of Issyk-Kul Basin), where the succession dips gently southwestward.

The Dzhety-Ogyuz Formation consists of red sandstones and conglomerates. Remnants of an Oligocene tortoise have been found at the type locality of Dzhety-Ogyuz [*Sidorenko*, 1972]. The formation is here more than 1000 m thick and the top may be Lower Miocene. The bedding dips gently to the NNW. We sampled 12 sites, seven near the base of the formation (IT to IZ) and five near the top (I1 to I5). Seven randomly oriented pebbles were sampled at one of the sites, in order to perform a conglomerate test.

At the Karakoo locality, on the southwestern edge of the Issyk-Kul basin, Paleogene sediments dip gently westward. We sampled two sites (IA, IB) in Paleogene red beds and three sites (IC, IR and IS) in Miocene grey to yellowish-grey sediments.

At the southern edge of the Talas basin (Talas locality), the bedding dips gently southward. We sampled seven sites (TA to TG) in red Paleogene detrital sediments of continental origin, similar to those of the Kokturpak Formation of Issyk-Kul basin.

Central Tien-Shan

The Tertiary stratigraphy of the Naryn basin is less well known. At all localities, we sampled red sandstones close to the underlying Paleozoic basement. The sandstones are similar to those of the Kokturpak Formation of the Issyk-Kul basin.

On the southern edge of the Naryn basin is the ENE-trending Baybiche ridge (Figure 1b). On geomorphological and stratigraphic evidence, this ridge was uplifted in the Quaternary [*Sadybakasov*, 1991]. Its Paleozoic core is overlain by Cenozoic sediments, dipping northwestwards on average. In detail, the Baybiche ridge is made up of en-echelon folds striking east. We sampled nine sites (NA to NI) in the Karabulun and Karabuk valleys (grouped as Karabulun locality) and seven sites (NJ to NP) at Djaman-Davan locality, where the Baybiche ridge locally trends EW. At both localities, the red sandstones are drape-folded, sometimes strongly, over underlying basement faults.

In the NW corner of the Naryn basin, at Makmal locality, we sampled eight sites (NQ to NX) on the slopes of the Ak-Shirak ridge. Here the red sandstones dip gently southeastward.

Western Tien-Shan

We investigated Paleogene sedimentary rocks on the northern and northwestern edges of the Fergana basin and in the Lower Chatkal basin.

On the northern edge of the Fergana basin, near the town of Tash-Kumyr, we sampled three sites (FA to FC) in mudstones and sandstones of the Massaget Formation, which has marine fauna of Oligocene age [*Sodorenko*, 1972]. The bedding at this locality dips steeply southward.

On the northwestern edge of the Fergana basin, in the foothills of the Chatkal ridge, is the Ala-Buka syncline, asymmetric and southeasterly verging. On its northwestern limb, where the bedding dips steeply southeastwards, we sampled four sites (FH to FK) in the Massaget Formation; and on the southeastern limb, where the bedding dips gently northwestward, we sampled another four sites (FD to FG) in pink marls of marine origin, attributed to the Eocene [*Sidorenko*, 1972].

The intermontane Chatkal basin is situated within the Chatkal ranges. This basin is an open syncline trending NE. We sampled six sites, four on one limb (FL to FO), two on the other (FP and FQ), all in continental Paleogene sediments (marls and sandstones).

Near the southern edge of the Fergana basin, pale-red calcareous siltstones were sampled from the basal member of the Massaget Formation (Late Oligocene to Miocene) on both limbs of an EW trending syncline (sites SF-1 and SF-2). Hand samples, oriented with a magnetic compass, were taken along sections across about 15 meters of true stratigraphic thickness, on each limb.

PALEOMAGNETIC STUDY

The samples were studied at Rennes paleomagnetic laboratory. Remanent magnetization was measured with either a cryogenic magnetometer (LETI) or a Schonstedt spinner flux gate magnetometer. We isolated characteristic directions of remanent magnetism after progressive thermal demagnetization or alternating field demagnetization, performed with Schonstedt equipment. In general, we found thermal cleaning to be more efficient for sediments. At each step in the demagnetization process, we measured bulk susceptibility. We determined paleomagnetic directions by principal component analysis, within a graphical interactive system [*Perroud*, 1985], and we used the statistics of *Fisher* [1953]. We studied one specimen from each core and two specimens from each hand sample. We considered as reliable any site which presented consistent magnetic behavior from at least three samples.

Fold tests were carried out in two ways, according to *McElhinny* [1964] and *McFadden and Jones* [1981]. For some localities, the number of sites which yielded acceptable results was rather limited and so we had to use sample directions. The algorithm, on which is based the test of *McFadden and Jones* [1981], was used in three different ways. First, we compared mean directions from different localities within a single basin, to see if the differences were statistically significant (the consistency test). To perform the fold test sensu stricto, we sorted the sampling sites into groups of similar bedding orientation, irrespective of location. Finally, the reversal test was carried out for data from each basin, again irrespective of site location.

Magnetic Mineralogy

For most sedimentary samples, natural remanent magnetization (NRM) intensities range from $5*10^{-4}$ to 10^{-2} A m^{-1}, whereas basalts and some sediments (sites IA, IB, IW, IF, IJ, I5 and FB), including those from zones of contact with basalts, have higher intensity of magnetization, from 10^{-2} to 5 A m^{-1} (Figure 2a). A similar difference is also observed in weak field susceptibility, with values between 10^{-5} and 10^{-3} SI units for most of the sediments and values between 10^{-3} and 10^{-2} SI units for the other sedimentary sites and the basalts (Figure 2b).

Isothermal remanent magnetization (IRM) was given in about 20 steps to one sample from each site. The most common progressive acquisition curves illustrate two stages (Figure 2c): first, for applied fields up to 200 mT, the IRM intensity increases rapidly; then, from 200 mT up to 1.2 T, the intensity increases more slowly, indicating that the sample did not reach saturation. For a few samples, IRM was acquired more gradually (Figure 2c) and saturation was still not reached at 1.2 T.

To further explore the magnetic mineralogy of our rocks, we conducted an additional experiment on seven samples, from sites IC, IR, IS, IY, IZ, I2 and I5, following a method suggested by *Lowrie* [1990], in which different coercivity fractions of IRM are magnetized in successively smaller fields, along three orthogonal directions, and then thermally demagnetized. The three-component IRMs were produced in fields of, first, 1.2 T along the *Z* axis; then, 0.15 T along the *X* axis; and finally, 0.05 T along the *Y* axis. These fields were chosen so as to evaluate the influence of hematite and goethite for the *Z* axis, single-domain magnetite for the *X* axis and low-coercivity magnetite for the Yaxis. In two samples (grey sandstones from sites IC and IR), the IRM appears to be dominated by magnetite (Figure 2d). In the other five samples, both hematite and magnetite are indicated in various proportions, with hematite usually prevailing (Figures 2e and 2f).

For the basalts, thermomagnetic curves, obtained with the automated vertical Curie balance at Rennes, show a clear inflection point at about 350°C (probably due to maghemite) and a Curie point at 580°C (due to magnetite, the main carrier of magnetization).

Anisotropy of Magnetic Susceptibility

To check for a possible bias in paleomagnetic directions, due to anisotropy of our samples, we measured the anisotropy of magnetic susceptibility (AMS) for all sites which gave paleomagnetic results, using the enhanced Digico apparatus at Rennes. The basalt samples reveal no anisotropy. Sediments from all basins, except Issyk-Kul, display randomly oriented ellipsoids and very low anisotropy ratios. For the Issyk-Kul basin, anisotropy ratios are also low, but AMS ellipsoids are either triaxial or prolate ($k_{int}/k_{min} > k_{max}/k_{int}$), with a vertical minor axis and a major axis along the trend of the Issyk-Kul basin (Figure 3). This AMS may be of purely sedimentary origin, or it may result from a combination of a sedimentary fabric and tectonic shortening in a NW-SE direction. Nevertheless, the degree of anisotropy is usually lower than 5%.

From the combined IRM experiments discussed above, for most red samples from the Issyk-Kul basin, we think that hematite is the main carrier of magnetization, even though magnetite is present in various amounts. The domination by hematite on the IRM suggests that it should also dominate the susceptibility. If so, we can infer that its anisotropy mainly reflects the distribution of hematite particles in our samples.

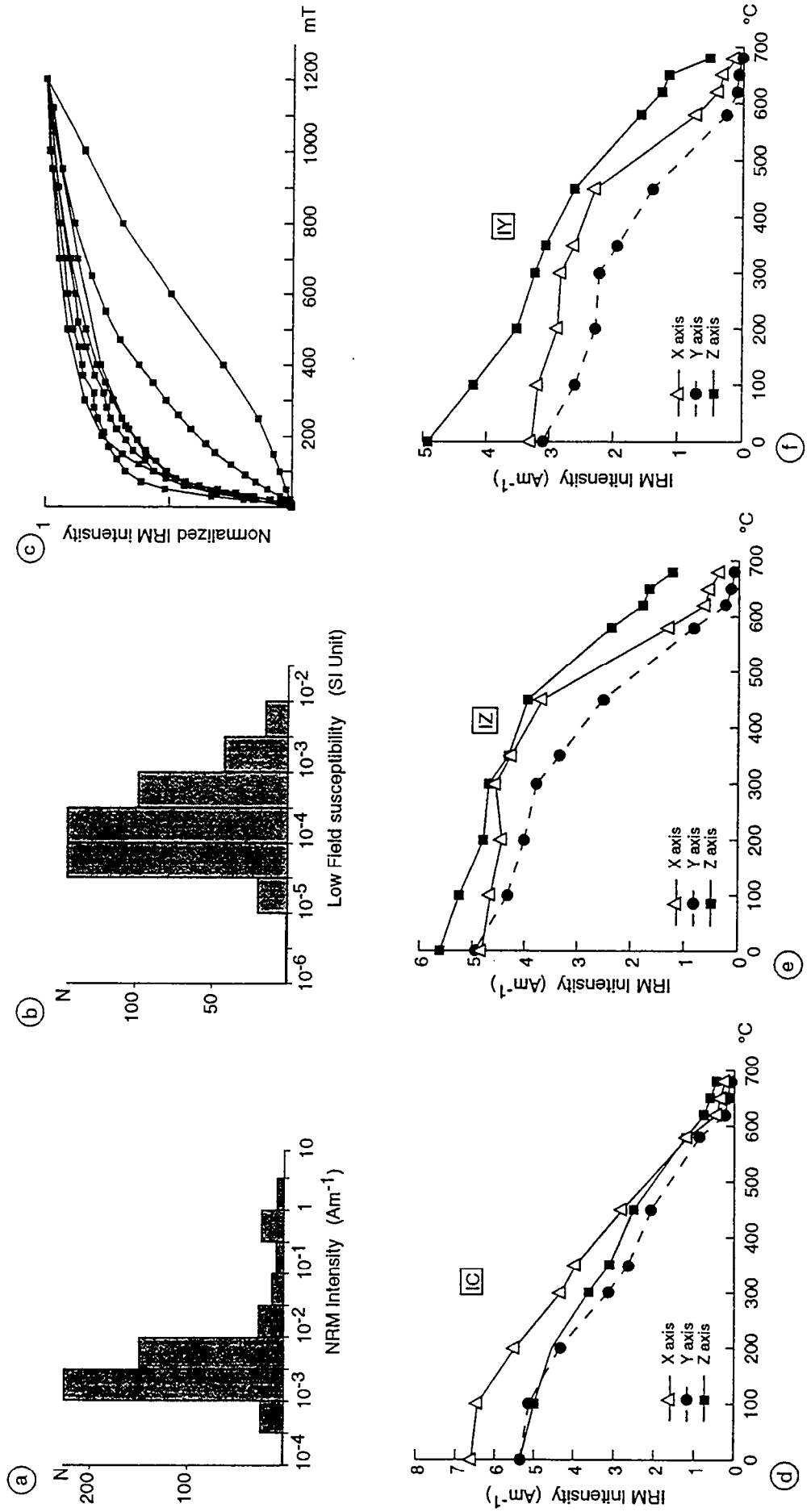

Fig. 2. Rock magnetic study. Histograms of (a) NRM intensity and (b) low field susceptibility for the entire collection; (c) representatives normalized IRM intensity curves for sediments. IRM demagnetization data after *Lowrie* (1990) (compare text): (d) gray sandstone, (e) and (f), red sandstones.

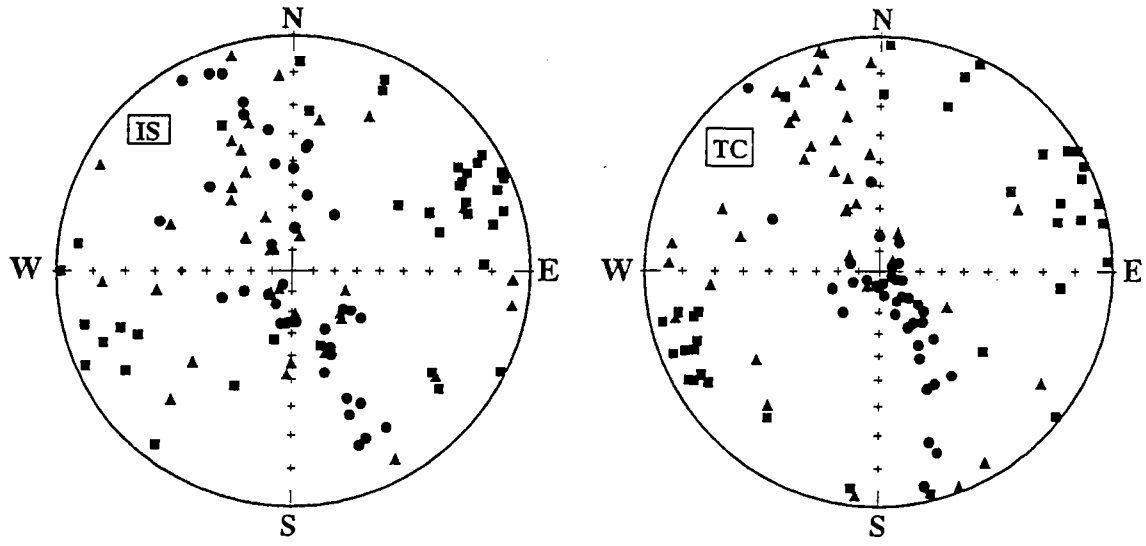

Fig. 3. AMS data for the Issyk-Kul basin. Stereographic projection shows attitude of maximum (squares), intermediate (triangles) and minimum (circles) principal axes of susceptibility. In stratigraphic coordinates, susceptibility ellipsoid is prolate with a vertical minor axis and a major axis along the trend of the Issyk-Kul basin.

Paleomagnetic Results

Issyk-Kul basin: Dzhety-Ogyuz. At six sites (I1, I3, I4, IT, IV and IX) where samples were the most coarse-grained, we were not able to isolate consistent paleomagnetic directions. During thermal demagnetization, samples from these sites had an erratic behaviour for temperatures higher than 350°-400°C. We had similar problems with a few samples from other sites too. However, on the remaining samples from five sites (I2, I5, IW, IY and IZ), thermal cleaning revealed two magnetic components (Figure 4). The first was usually removed below 350°C. In geographic coordinates, this low-temperature component (LTC) clusters well around the present-day magnetic field direction (I = 61°). This LTC is therefore interpreted as a recent overprint. Between 350°C and 680°C, a second component was isolated. This high-temperature component (HTC) exhibits both polarities (Table 1), and its in situ mean direction is far from the present-day dipole field. No fold test is possible here since the dip of the bedding ranges only from 33° to 41° northwards. The tilt-corrected HTC mean direction is D=0°, I=+44°, α_{95}=11°. From the conglomerate layer, five out of the seven pebbles display a well-defined magnetization, but their directions are randomly distributed, eliminating the possibility of blanket remagnetization of the whole sequence.

Issyk-Kul basin: Karakoo. Four sites (IA, IC, IR and IS), out of the five sampled, provided good results. The LTCs are rather scattered, especially for sites with reverse polarity; whereas the HTCs are rather well determined on all samples. In stratigraphic coordinates, both polarities are present, with nearly antipodal directions (Table 1). The dip of the bedding

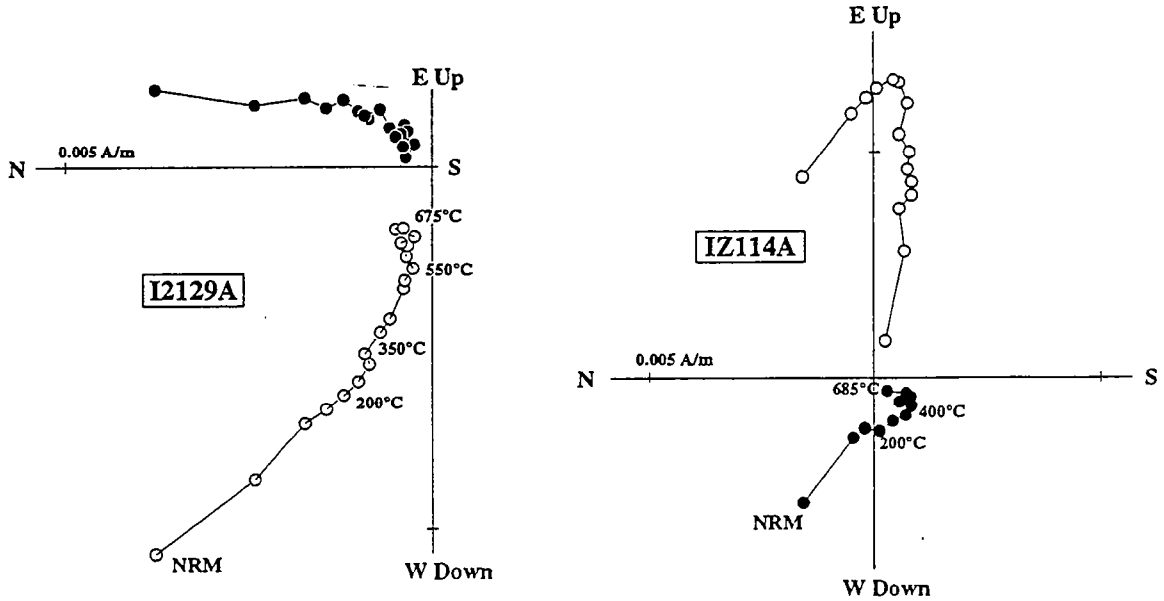

Fig. 4. Thermal demagnetization for two sites (I2 and IZ) from Issyk-Kul basin. Orthogonal vector projections in geographic coordinates show changes in magnetization with temperature, from initial attitude (NRM), toward full demagnetization at the origin. Solid (or open) symbols are in horizontal (or vertical) plane. Low-temperature components (LTC) are close to the present field (unblocking temperature around 350°C), whereas high-temperature components (HTC) are of both polarities.

TABLE 1. Paleomagnetic Data for Issyk-Kul basin

Site	Latitude, (°N)	Longitude, (°E)	Bedding	*n/N*	AF/TH	In Situ D	In Situ I	Tilt Corrected D	Tilt Corrected I	*k*	α_{95}	Litho	Age
						Dzhety-Oguyz							
IW	42.334	78.234	264/41	6/7	TH	078	78	11	46	58	9	S	Oligo-Miocene
IY	42.334	78.234	264/41	6/7	TH	356	80	354	39	35	12	S	Oligo-Miocene
IZ	42.344	78.231	256/37	7/7	TH	251	-88	169	-53	38	10	S	Oligo-Miocene
I2	42.356	78.225	241/33	4/7	TH	45	76	352	51	30	17	S	Oligo-Miocene
I5	42.357	78.224	261/33	6/7	TH	20	61	7	30	78	8	S	Oligo-Miocene
						Karakoo							
IA	42.183	76.725	206/14	6/6	TH	19	58	0	54	90	7	S	Paleocene
IC	42.203	76.675	088/53	6/6	AF/TH	176	-16	173	-68	19	16	S	Miocene
IR	42.200	76.670	337/11	4/4	TH	334	54	349	53	38	15	S	Miocene
IS	42.200	76.670	337/11	5/5	TH	165	-63	185	-59	33	13	S	Miocene
						Toru-Aygyr							
IF	42.621	76.385	135/10	16/16	AF+TH	209	-37	206	-47	45	6		
IG	42.625	76.389	215/10	6/7	AF+TH	190	-37	184	-32	506	3	B	Eocene
IH	42.625	76.389	259/03	7/7	AF+TH	192	-46	191	-43	312	3	B	Eocene
IJ	42.632	76.392	145/32	24/24	AF+TH	200	-26	178	-52	95	3		

Mean	*N*	In Situ D	In Situ I	Tilt Corrected D	Tilt Corrected I	*k*	α_{95}
Dzhety-Ogyuz	5	33	78			47	11
				0	44	50	11
Karakoo	4	354	49			11	29
				357	59	97	9
Toru-Aygyr	4	198	-36			50	10
				190	-49	48	10
All sites	13	12	57			10	12
				2	49	42	6

Top part of table gives localities, site numbers, site location, site stratification, number of samples used for statistics (*n*), number of samples measured (*N*), method of demagnetization (AF for alternating field, TH for thermal), mean declination (D) and mean inclination (I) for high-temperature component of samples, Fisher statistics (*k* for grouping parameter, α_{95} for radius of circle of confidence at 95% probability level), rock type (B for basalt, S for sediment) and approximate stratigraphic age. Bottom part of table gives number of data used for calculation (*N*), mean declination (D) and inclination (I) for each locality, and Fisher statistics for high-temperature component (HTC).

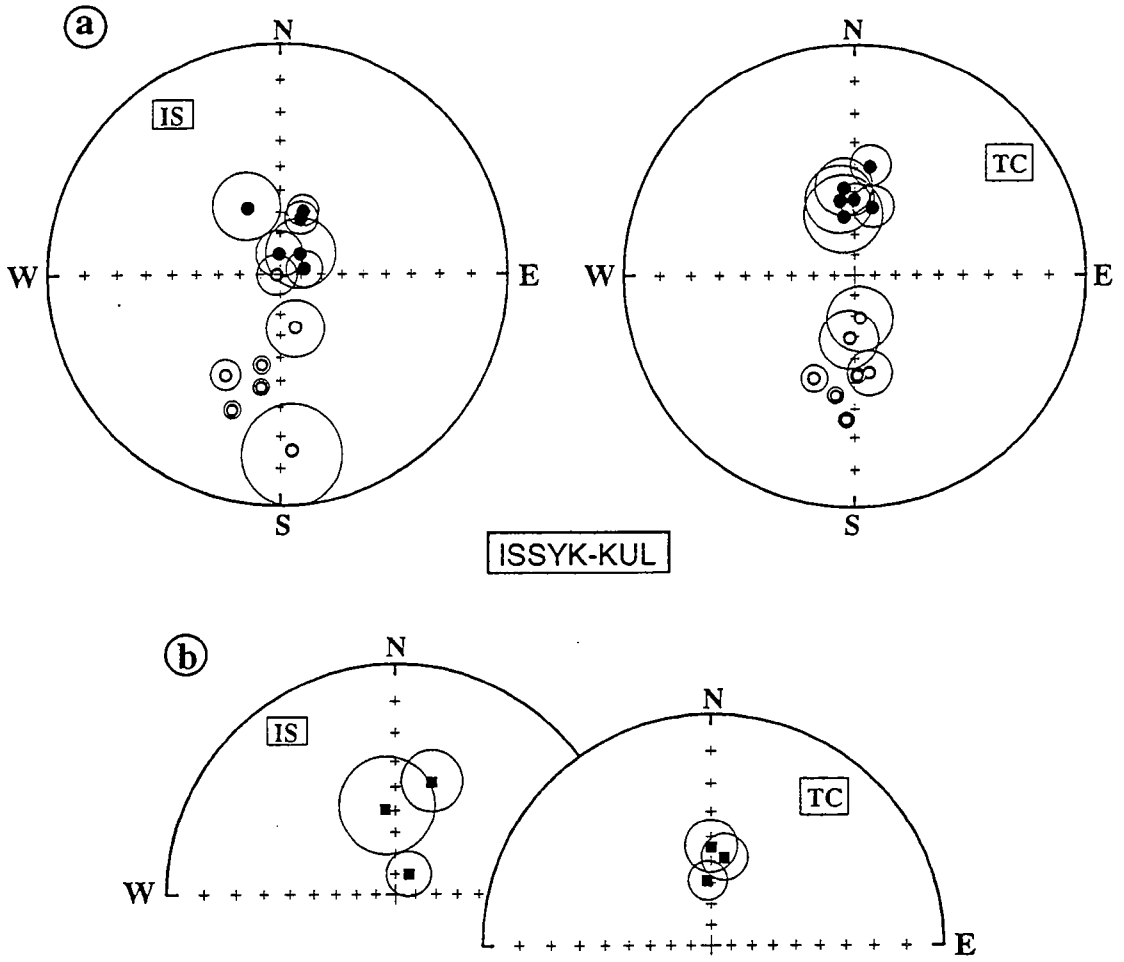

Fig. 5. (a) Stereographic projection of mean directions for sites from Issyk-Kul basin. (b) Stereographic projection of mean directions for the three localities of Issyk-Kul basin. Solid (or open) circles are projections in the lower (or upper) hemisphere. Coordinates are either geographic (IS) or stratigraphic (TC).

ranges from 11° to 53° and the fold test after *McElhinny* [1964] is positive at the 99% confidence level . The tilt-corrected mean direction is D=357°, I=+59°, $\alpha 95$=9°.

Issyk-Kul basin: Baidamtal. This locality provided good results only on the lava flow of site IQ, but the attitude of this flow could not be measured accurately. Thus we excluded this result from further analysis.

Issyk-Kul basin: Toru-Aygyr. For two of the four sites sampled in the basalts, we also collected underlying sediments in the contact zones (sites IF and IJ). As discussed previously, the intensity and susceptibility of these sediments are unusually high and their magnetization is dominated by magnetite. Furthermore, mean directions from sediments and volcanics are quite similar. From these magnetic properties, the sediments appear to have been totally remagnetized during lava emplacement. To determine the mean direction of these two sites, we therefore decided to combine the results for both sediments and volcanics. The four final site-mean directions (Table 1) are well clustered both before and after tilt correction, with a tilt-corrected mean at D= 190°, I=-49°, $\alpha 95$= 10°.

Issyk-Kul basin: Entire basin. The site mean directions for the entire Issyk-Kul basin are presented in Figure 5a, both before and after tilt correction. The dip of the bedding (Table 1) ranges through about 90°, from about 40° toward the north, to about 50° toward the south. For the consistency test (Table 2), the calculated F statistic slightly exceeds the critical value; but it is mainly due to the steeper bedding dip at Karakoo locality, where the rocks are slightly younger. However, the mean declinations from all three localities are statistically identical (Figure 5b). For all 13 site means from all localities, the fold test according to *McElhinny* [1964] is positive at the 99% confidence level. At the scale of the entire Issyk-Kul basin, the fold test according to *McFadden and Jones* [1981] is positive too (Table 2); however, two results (site IJ from Toru-Aygyr and site IC from Karakoo) have deviating bedding attitudes and cannot be incorporated into the test. Finally, for all 13 tilt-corrected site means, the reversal test is positive (Table 2). We conclude that the Issyk-Kul basin acquired its synformal structure later than its magnetization. The overall mean paleomagnetic direction for the Issyk Kul basin is D= 2°, I=+49°, $\alpha 95$= 6°.

Talas basin. A characteristic magnetization was isolated in samples from four sites out of the seven sampled. Both polarities are observed (Table 3). In geographic coordinates, the mean direction for the locality is far from that of the present field. A fold test is not significant , but the dip of the bedding ranges only from 25° to 39° southward. The tilt-corrected mean direction for the basin is D=343°, I=+54°, $\alpha 95$= 22°. Because the data set is of limited reliability, we

TABLE 2. Results of Field Test Application

Test	L	DF	CV	IS	TC
		Issyk-Kul Basin			
Consistency	site	4,20	2.9	8.7	3.3
Fold*	site	4,16	3.0	12.5	1.6
Reversal	site	2,22	3.4		0.7
		Naryn Basin			
Consistency	site	4,26	2.8	3.9	2.6
Fold	site	4,26	2.8	8.4	1.0
Reversal	site	2,28	3.3		0.8
		Ala-buka Locality			
Fold	sample	2,52	1.9	102.0	0.4
		Fergana Basin			
Consistency	sample	4,86	2.5	7.2	2.1
Fold	sample	8,82	2.1	56.0	1.9
Reversal	sample	2,88	3.1		1.5
		Fergana and Chatkal			
Consistency	sample	6,104	2.2	9.4	2.4

Consistency test is the comparison of locality mean directions; fold test is performed for the entire data set from a basin with bedding attitudes being regrouped irrespective of locality if necessary; reversal test is performed for tilt-corrected data for each basin separately with data being divided into polarity groups irrespective of locality and bedding attitudes; L is the level at which the tests are performed; DF is the number of degrees of freedom; CV is the 95% critical value, IS and TC are in situ and tilt-corrected calculated values of field statistics, respectively.

* Two sites with deviating beddings were not incorporated into any group.

decided not to consider it for the final tectonic interpretation.

Naryn basin. Three kinds of behavior were observed during demagnetization. Some samples had a single well-defined component, with unblocking temperature around 670°C (Figure 6a). Other samples had two magnetic components: an LTC near the present field direction, which we interpret as a partial recent overprint (Figure 6b and 6c), and an HTC with unblocking temperature higher than 655°C, showing both polarities. Finally, other samples had a single very well-defined component with unblocking temperature less than 570°C, whose direction was close to the present field (Figure 6d), suggesting complete recent remagnetization.

Naryn basin: Karabulun. This locality provided seven reliable sites out of nine (Table 4). All except NI have a reverse component of magnetization. However HTCs are rather scattered within three sites (ND, NC and NG), leading to rather large confidence circles around the mean directions. Although the dip of the bedding ranges from 33° SE to 25° NW, a fold test is not significant at the 95% level, according to *McElhinny* [1964]. The tilt-corrected mean direction is D=358°, I=+30°, α_{95}=14°.

Naryn basin: Djaman Davan. Six sites out of seven provided reliable results. One site (NN) shows a large degree of scatter, but the others do not. Most sites show normal polarity (Table 4). The mean directions are better clustered after tilt correction than in situ, but a fold test [*McElhinny*, 1964] is inconclusive. The tilt-corrected mean direction is D=26°, I=+46°, α_{95}=17°.

Naryn basin: Makmal. Out of eight sites, only five provided acceptable results and two of these (NW and NQ) show a large degree of scatter (Table 4). The fold test according to McElhinny [1964] is again inconclusive. The tilt-corrected mean direction is D=355°, I=+36°, α_{95}=31°.

Naryn basin: Entire basin. When the data are considered at the scale of the entire Naryn basin (Figure 7a), there is some within-site scatter, but site means are rather consistent, except for two sites (NO, Djaman Davan, and NW, Makmal) which

TABLE 3. Paleomagnetic Data for Talas Basin

Site	Latitude, (°N)	Longitude, (°E)	Bedding	*n/N*	AF/TH	In Situ D	In Situ I	Tilt Corrected D	Tilt Corrected I	*k*	α_{95}	Litho
TC	42.499	71.550	95/30	4/8	TH	180	-29	177	-59	13	26	S
TE	42.499	71.550	90/25	4/6	TH	155	-10	150	-33	12	27	S
TF	42.499	71.550	85/39	6/6	TH	166	-33	151	-71	62	9	S
TG	42.500	71.535	97/26	6/6	TH	359	34	354	59	44	10	S

	N	In Situ D	In Situ I	Tilt Corrected D	Tilt Corrected I	*k*	α_{95}
	4	350	27			27	18
				343	54	20	22

Same symbols as in Table 1. At all sites, sediments are of undifferentiated Paleogene age.

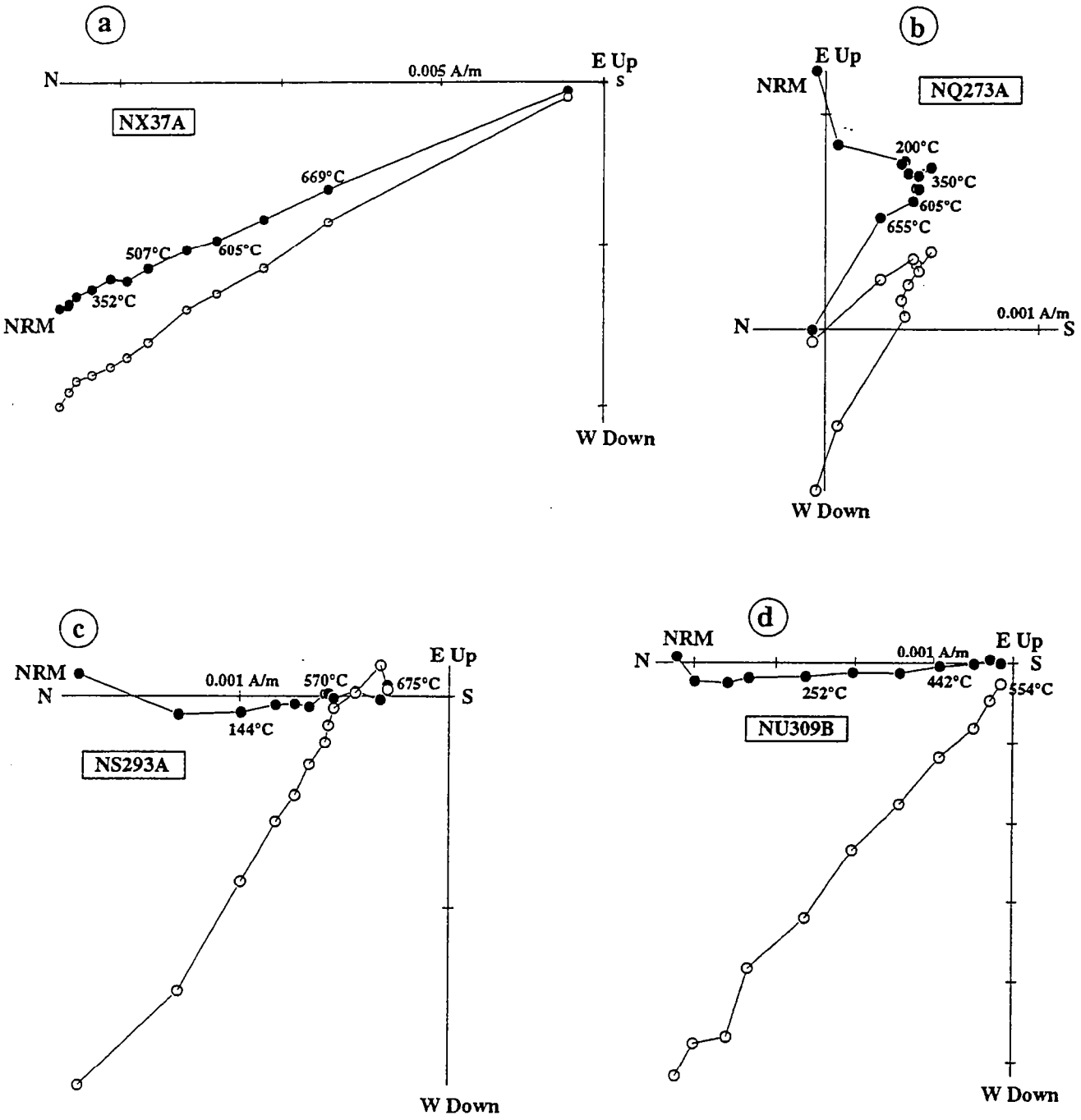

Fig. 6. Orthogonal vector projections of representative thermal demagnetizations for the Naryn basin. For site (a) NX, magnetization is carried by hematite. For sites (b) NQ and (c) NS, LTCs show unblocking temperatures around 350°C and are near the present field in geographic coordinates; whereas HTCs present both polarities, with unblocking temperature higher than 655°C. For site (d) NU, there is one component of magnetization, close to the present field in geographic coordinates and probably a complete overprint. Symbols and conventions are as for Figure 3.

deviate strongly (more than 40°) from the overall mean. After their omission, the three tilt-corrected locality means are statistically identical (Figure 7b) and the overall mean for the Naryn basin (D=5°, I=+37°, α_{95}=11°) agrees well with the mean direction for the Issyk-Kul basin. After data regrouping, although the fold test according to *McElhinny* [1964] is not conclusive due to large dispersion, the fold test according to *McFadden and Jones* [1981] is positive, as is the reversal test (Table 2).

Fergana basin. Most samples show two components of magnetization (Figure 8). The LTCs are rather close to the present field direction and have unblocking temperatures between 200°C and 350°-400°C. Unblocking temperatures for HTCs are generally around 680°C, except for site FH, where they are below 580°C, suggesting that magnetization could be carried by magnetite (Figure 8).

Fergana basin: Tash-Kumyr. Data from site FA are highly scattered and so we discarded them. For the remaining two sites

TABLE 4. Paleomagnetic Data for Naryn Basin

Site	Latitude, (°N)	Longitude, (°E)	Bedding	n/N	AF/TH	In Situ D	In Situ I	Tilt Corrected D	Tilt Corrected I	k	α_{95}	Litho
					Karabulun							
NA	41.280	75.373	66/33	4/6	TH	182	20	181	-10	23	19	S
NB	41.280	75.373	170/13	6/6	TH	201	-10	198	-17	38	11	S
NC	41.280	75.373	32/15	3/6	TH	176	-43	191	-51	28	23	S
ND	41.277	75.359	241/19	3/6	TH	176	-55	169	-37	11	40	S
NE	41.277	75.359	210/18	7/7	TH	167	-40	159	-27	26	14	S
NG	41.221	75.226	266/21	5/7	TH	186	-47	184	-26	12	23	S
NI	41.221	75.226	219/14	7/7	TH	351	47	344	36	17	16	S
					Djaman-Davan							
NJ	41.067	74.779	257/31	4/7	TH	47	68	14	44	60	12	S
NL	41.067	74.779	270/32	6/7	TH	73	75	23	51	44	10	S
NM	41.067	74.779	270/32	7/7	TH	222	-53	27	-26	26	12	S
NN	41.044	74.795	160/37	8/8	TH	45	3	39	36	8	35	S
NO*	41.047	74.791	143/50	6/7	TH	50	26	42	76	41	10	S
NP	41.047	74.791	143/50	5/7	TH	41	23	19	70	119	7	S
					Makmal							
NQ	41.224	74.077	31/25	5/8	TH	138	-20	143	-44	9	27	S
NS	41.224	74.077	31/25	3/6	TH	357	1	0	15	115	12	S
NT	41.233	74.096	63/25	5/7	TH	19	20	30	36	21	17	S
NW*	41.220	74.080	43/22	5/6	TH	315	-3	315	19	8	28	S
NX	41.230	74.100	50/21	6/6	TH	338	20	342	40	19	16	S

Mean	N	In Situ D	In Situ I	Tilt Corrected D	Tilt Corrected I	k	α_{95}
Karabulun	7	1	33			8	22
				358	30	19	14
Djaman-Davan	5	46	45			7	25
				26	46	21	17
Makmal	4	348	17			9	28
				355	36	10	31
All sites	16	10	34			6	16
				5	37	13	11

Same symbols as in Table1. At all sites, sediments are of undifferentiated Paleogene age.
* Theses two sites were not incorporated in the localities mean direction as basin mean direction (compare text).

(FB and FC, Table 5), statistics were calculated at sample level, giving a tilt-corrected mean direction of D=170°, I=-26°, α_{95}=13°. The bedding dips uniformly for both sites and so a fold test is not significant.

Fergana basin: Ala-Buka. Five sites out of eight provided reliable results. Demagnetization usually revealed two components. In geographic coordinates, HTCs are all far from the present field (Table 5). The bedding dips either steeply to the SE or gently to the NW. After tilt correction, both polarities are observed, with roughly antiparallel directions. The fold test according to *McElhinny* [1964] is positive at site level. So is the test according to *McFadden and Jones* [1981], but at sample level due to the small number of sites (Table 2). The tilt-corrected mean direction, calculated at site level, is D=337°, I=+36°, α_{95}=15°.

Fergana basin: South Fergana. Samples from the southern limb (SF-2) responded well to thermal cleaning and a characteristic (HTC) component was isolated above 350°. We found directions of both polarities and they are nearly antipodal. The data from the other limb (site SF-1) show more scatter and HTC directions were recovered from three samples only. For this locality, the fold test according to *McElhinny* [1964] is positive at the sample level. The mean direction is D=340°, I=+40°, α_{95}=10°.

Fergana basin: Entire basin. Recovered paleomagnetic directions for Fergana basin are presented in Figure 9a, both before and after tilt correction. At the scale of the entire basin, the fold test according to *McElhinny* [1964] is positive at site level. Because the number of accepted sites from each locality is limited, we performed other tests at sample level. For all three localities, the consistency test (Figure 9b), the fold test according to *McFadden and Jones* [1981] and the reversal test are all positive (Table 2). The mean direction for the basin is D=342°, I=+34°, α_{95}=9°.

Chatkal basin. Samples from three sites showed no stable endpoint demagnetization. For sites FM and FN only, where bedding dips gently to the NW, we determined HTC directions, showing both polarities of the Earth's magnetic field, roughly antiparallel in stratigraphic coordinates (Figure 10 and Table 5). The tilt-corrected mean direction, calculated at sample level, is D=352°, I=+42°, α_{95}=9°. Combining Chatkal and Fergana data sets led to calculated statistics somewhat larger than the critical values for the consistency test (Table 2).

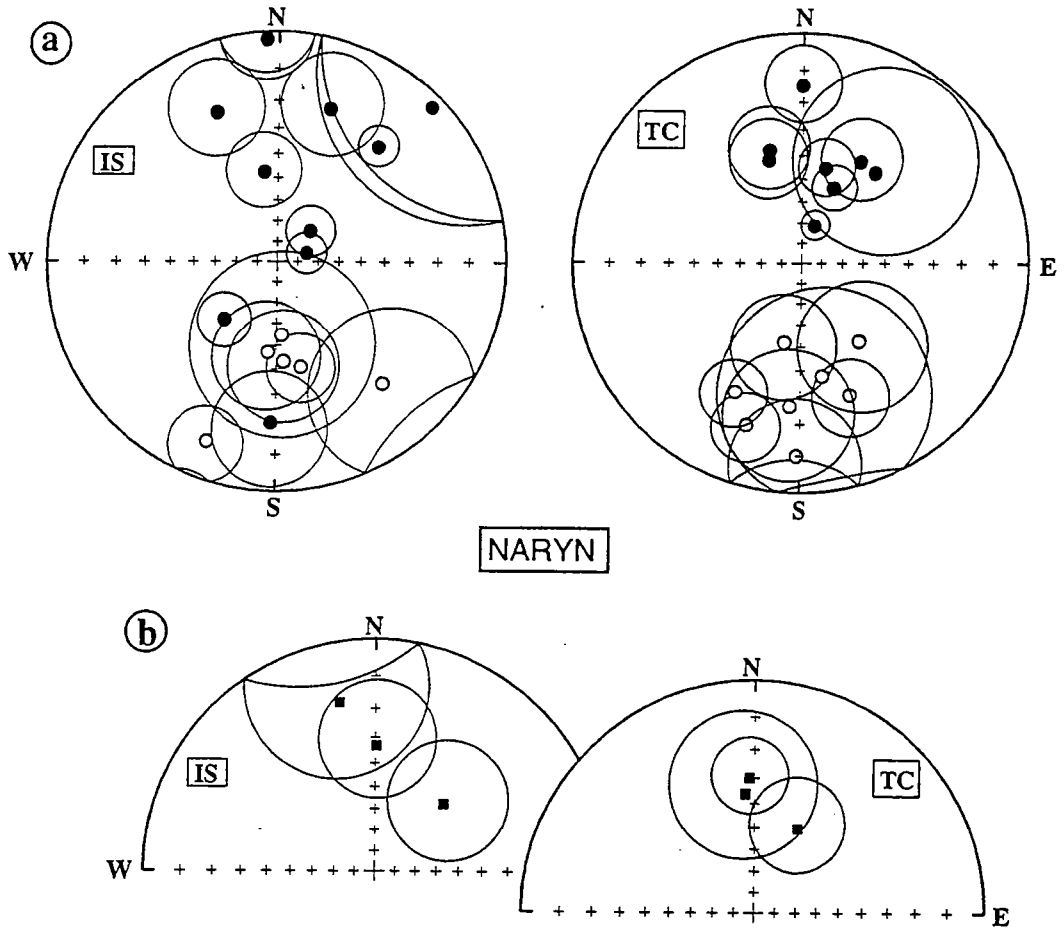

Fig. 7. (a) Stereographic projection of mean directions for sites from Naryn basin. (b) Stereographic projection of mean directions for the three localities of Naryn basin. Symbols and conventions as for Figure 4.

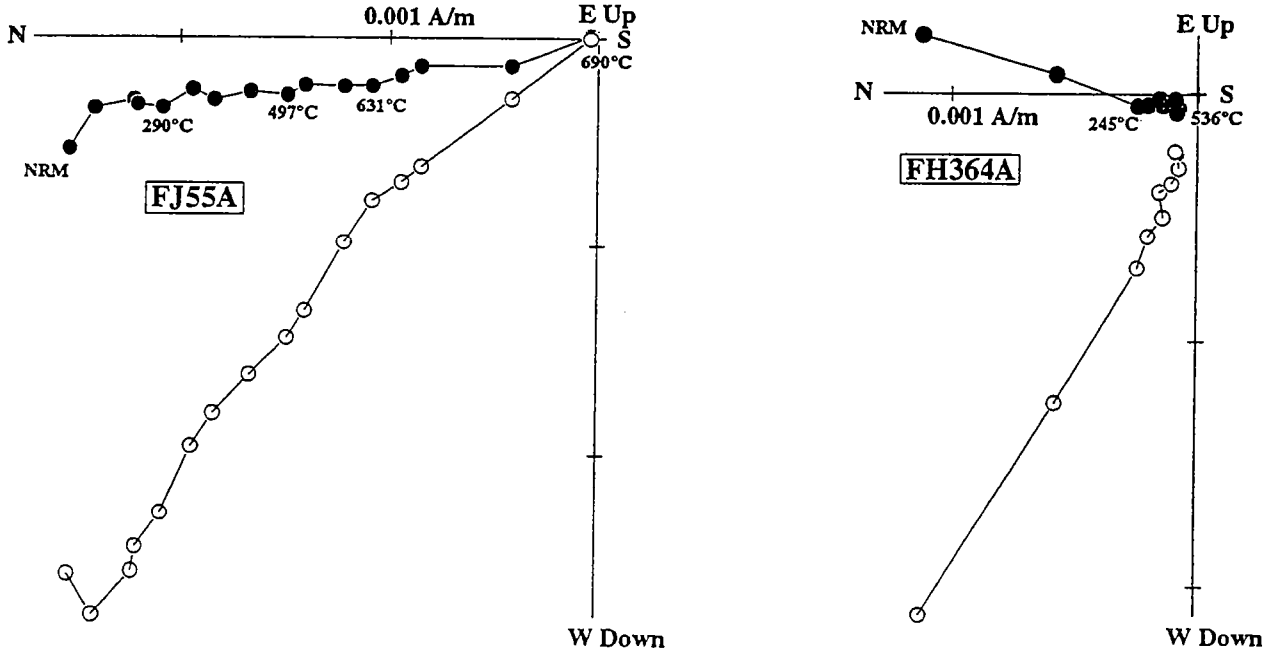

Fig. 8. Orthogonal vector projections of representative thermal demagnetizations for Fergana basin. There are two components of magnetization. For site (a) FJ, the HTC has an unblocking temperature of 690°C and is carried by hematite; whereas for site (b) FH, the HTC has an unblocking temperature of 570° and is probably carried by magnetite. Symbols and conventions are as for Figure 3.

TABLE 5. Paleomagnetic Data for Fergana and Chatkal Basins

Site	Latitude, (°N)	Longitude, (°E)	Bedding	*n/N*	AF/TH	In Situ D	In Situ I	Tilt Corrected D	Tilt Corrected I	*k*	α_{95}	Litho	Age
						Tash-Kumir							
FB	41.328	72.200	78/71	3/7	TH	343	-46	344	24	35	21	S	Oligocene
FC	41.328	72.200	79/71	6/7	TH	178	42	177	-29	18	16	S	Oligocene
						Ala-Buka							
FE	41.396	71.294	40/83	8/8	TH	162	42	158	-33	12	16	S	Paleogene
FG	41.396	71.294	44/81	5/6	TH	158	30	163	-44	15	20	S	Paleogene
FH	41.390	71.357	232/32	5/6	TH	347	69	333	38	27	15	S	Paleogene
FJ	41.390	71.357	218/24	4/6	TH	350	31	343	12	73	11	S	Paleogene
FK	41.390	71.357	208/23	6/7	TH	347	68	324	49	40	11	S	Paleogene
						South Fergana							
SF-1	40.0	70.1	91/45	3/6	TH	351	-17	351	28	31	15	S	Oligocene
SF-2	40.0	70.1	265/29	6/6	TH	305	70	333	46	46	9	S	Oligocene
						Chaktal							
FM	41.685	71.709	253/28	6/8	TH	3	64	354	37	22	15	S	Paleogene
FN	41.691	70.699	227/12	4/7	TH	180	-60	169	-51	47	14	S	Paleogene

Mean	*N*	In Situ D	In Situ I		Tilt Corrected D	Tilt Corrected I	*k*	α_{95}
Tash-Kumir	9*	173	44				21	11
					170	-26	18	13
Ala-Buka	5	74	86				3	45
					337	36	27	15
South Fergana	9*	332		47			4	50
					340	40	24	10
Entire Fergana basin	9	345	-14				3	-
					342	34	33	9
Chatkal	10*	2	62				31	8
					352	42	25	9

Mean direction for the Fergana basin is calculated at the site level. Same symbols as in Table 1.
* Statistics on sample level.

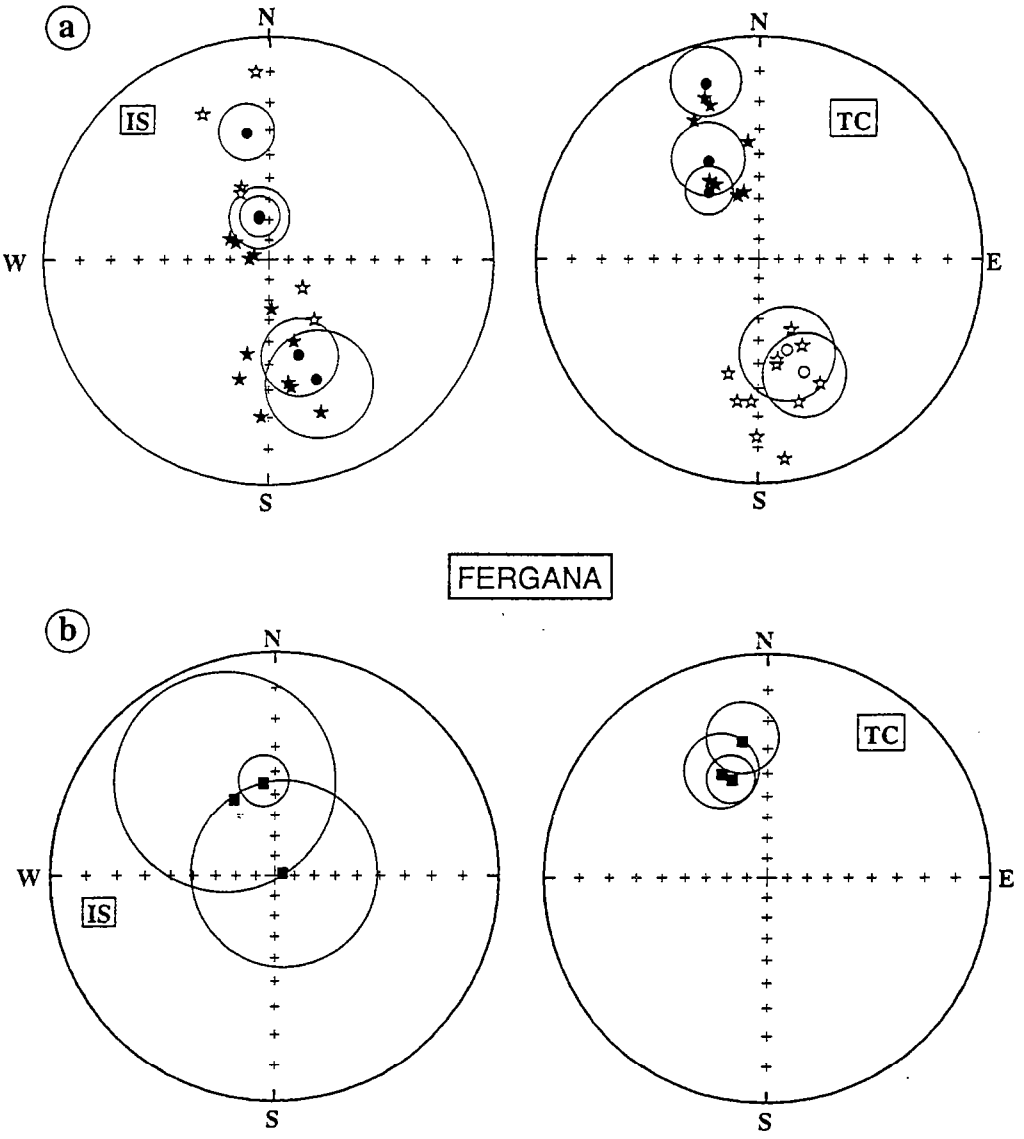

Fig. 9. (a) Stereographic projection of samples directions (stars) and sites mean directions (circles) from Fergana basin. (b) Stereographic projection of mean directions for the three localities of Fergana basin. Symbols and conventions as for Figure 4.

However, we cannot be sure that this discrepancy is significant, because of the small size of the Chatkal data set.

Discussion

Timing of Magnetization

For most of our samples, demagnetization provided well-determined HTCs, consistent at basin level.The reversal test is also positive for the three basins, as well as the conglomerate test at Dzhety-Ogyuz locality. Fold tests were positive for all localities where they could be applied. For every basin, a fold test was also positive. We therefore conclude that magnetization was acquired before folding.

For the Tien Shan as a whole, deformation started in the Paleogene, became more rapid in the Neogene and has continued to the present day [*Schulz*, 1948; *Sadybakasov*, 1991], the evidence being provided by crustal thickening, uplift, erosion of ranges and deposition of molasse sediments. Because the formations studied are Eocene to Oligocene (sometimes Early Miocene) and the various field tests are positive (Table 2), we conclude that the HTCs were acquired early in the rock history. We shall therefore consider them as the primary magnetizations in these rocks.

Interpretation

Inclination. In interpreting any anomaly in the direction of magnetization, one of the main considerations is to separate rock magnetic factors from tectonic factors. Apparent polar wander paths (APWPs) for the Eurasian plate have been calculated by *Irving and Irving* [1982] and by *Westphal et al.* [1986]. Recently, *Besse and Courtillot* [1991] have calculated a new APWP; however, its Cenozoic part does not differ significantly from those published earlier: the Eurasian pole is almost stable between 40 Ma and 10 Ma. Hence any interpretation is almost independent of the reference data and the age of magnetization. Under these conditions, we have chosen as a reference the pole at 40 Ma (latitude = 80°N, longitude = 145°E, A95 = 4°) according to *Besse and Courtillot* [1991].

Our paleomagnetic results show shallower inclinations

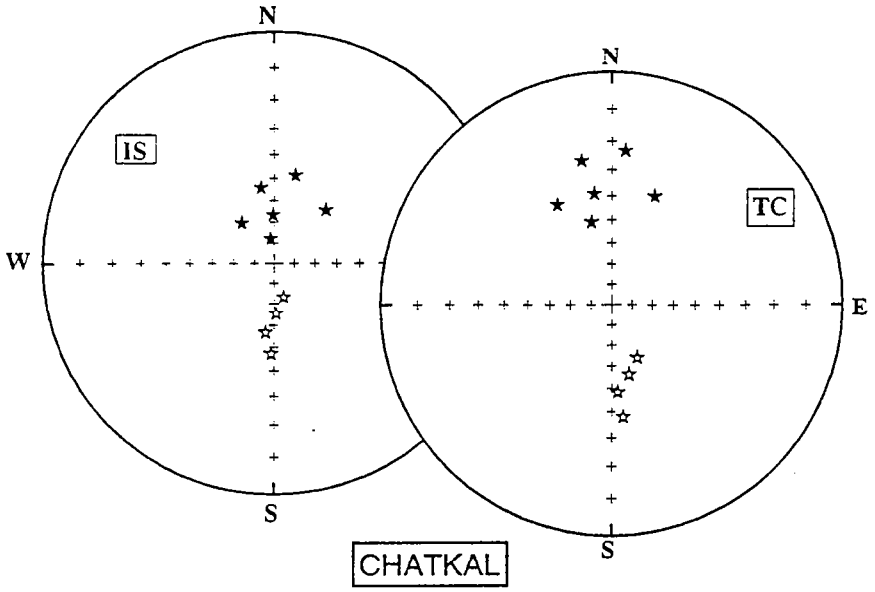

Fig. 10. Stereographic projection of mean direction for samples from the two sites of the Chatkal basin. Symbols and conventions are as for Figure 4.

than those predicted by the reference pole at 40 Ma (Figure 11), the differences ranging from 16°±5° for Issyk-Kul to 26°±7° for Fergana (Table 6). Furthermore, the inclination for Issyk-Kul is influenced by the steep vectors from the Karakoo locality where some data are from younger rocks; without this locality, this inclination difference for Issyk-Kul is still larger (20° ± 6°).

A long-term nondipole field may induce errors in reference data. Recently, *Schneider and Kent* [1990] have suggested that positive axial quadrupole terms, around 3% or 4% of the dipole term, have been present throughout the entire Tertiary. However, this leads to a negligible difference in inclination (1.5° at 40° latitude) in comparison with a pure dipole.

Very few paleomagnetic data apart from ours are available for Central Asia for the Cenozoic. *Bazhenov and Burtman* [1986] studied Paleogene sediments in the Northern Pamirs. Among five localities, inclinations range between 29° and 40°, with a mean value of 35°. These values are in good agreement with our own and such a coherence reinforces the suggestion that inclination was not modified by local deformation or by magnetic anisotropy. Unfortunately, other existing paleomagnetic results are of inadequate quality, mainly because of poor cleaning. Still more unfortunately, there are no data on volcanic rocks, usually regarded as more faithful recorders of geomagnetic field.

Tectonic deformation or compaction can modify the magnetic fabric and thus the paleomagnetic inclination. *Blow and Hamilton* [1978] have shown with analogue models that a 60% compaction of varved clays can induce a 15° shallowing of inclination. On this basis, if compaction reaches 50%, as it can indeed in some red beds, the inclination shallowing could be between 10° and 15°. Nevertheless, compaction experiments on red beds have yielded negligible inclination shallowing [*Stamatakos et al.*, 1989]. Except for two sedimentary sites from Baidamtal locality, which yielded no results, we found no evidence for strong compaction or penetrative deformation in our samples. Instead, the rocks are simply folded. Moreover, the main body of our data are from sandstones, which are not liable to noticeable compaction [e.g., *Meade*, 1966]. As shown above, anisotropy of susceptibility is lower than the 5% level required to alter significantly the paleomagnetic vector [*Nagata*, 1961].

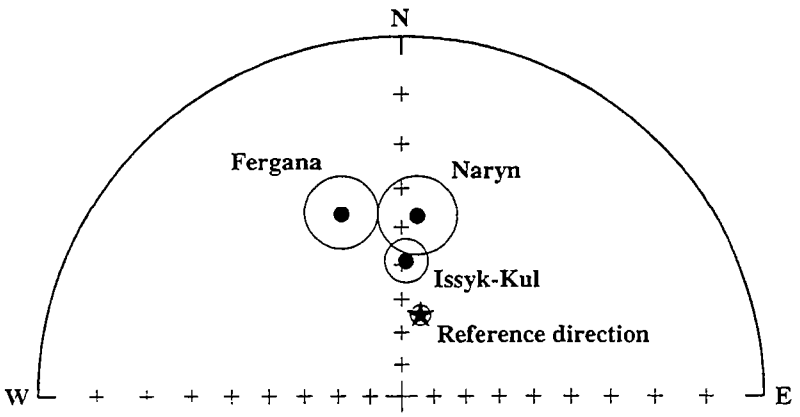

Fig. 11. Stereographic projection of mean paleomagnetic directions measured for the three main basins and reference direction computed from 40 m.y. mean pole of *Besse and Courtillot* [1991]. No significant inclination difference is observed between the basins, whereas the reference direction (star) is significantly steeper. Other symbols and conventions are as for Figures 3 and 4.

TABLE 6. Poles and Associated Paleomagnetic Directions for Eurasia at 40 Ma, Compared With Our Measured Data

Pole (40 Ma)	Latitude (°N)	Longitude (°E)	A95	Direction D	Direction I
Besse and Courtillot [1991]	80	145	3.8	13	62
Irving and Irving [1982]	78	159	6.0	16	60
Westphal et al. [1986]	83	136	9.0	9	63

	Flattening versus Besse and Courtillot Pole	Rotation Versus Besse and Courtillot Pole	Rotation Versus Issykkul Basin
Issyk-Kul	16°±5°	-11°±9°	-
Naryn	25°±8°	-8°±11°	-
Fergana	26°±7°	-31°±10°	-20°±11°
Chaktal	18°±10°	-22°°±11°	-10°±12°

Poles are taken from three apparent polar wander curves and directions calculated for a point located at 41°N 75°E (top part of table). Flattening and rotations are calculated according to *Beck* [1980] and *Demarest* [1983]. Symbol A95 is radius of circle of confidence at 95% probability level; other symbols as in Table 1.

Furthermore, no anisotropy was measurable, either in basalts, or in sediments from the Naryn and Fergana basins. We therefore conclude that neither compaction nor deformation can explain our regional inclination anomaly.

The studied rocks accumulated under continental conditions, many of them on alluvial fans. These may have primary tilts of 10° or more; but it is very unlikely that all tilts were in the same direction.

Finally, a large scatter of paleomagnetic directions was found at between-site level and, most important, at within-site level. A large dispersion of paleomagnetic data is known to lead to a somewhat shallower mean inclination [*Calderone and Butler*, 1991], but only by a few degrees.

Each of the factors discussed above could have modified the magnetic inclination for the entire collection by only a few degrees, compared with the reference data. To create the observed anomaly of about 20°, all factors should be additive, which is not a satisfactory explanation.

The mean inclination for Issyk-Kul, Naryn and Fergana basins indicates a paleolatitude of 24°N, whereas the expected paleolatitude is 45°N. The simplest interpretation is a northward displacement of Tien-Shan terranes by at least 2500 km. This is far larger than the 200-300 km estimated by *Molnar and Tapponnier* [1975] or the 200 km estimated by *Avouac* [1991], assuming a mechanism of crustal thickening alone. The only other possibility for accommodating the relative displacement is a strike-slip displacement of several thousand kilometers. So far there is no evidence for this. We therefore consider that a straightforward comparison of reference latitude and measured latitude is not valid here. As it happens, this is not the first sign of alarm for Paleogene paleomagnetic data from Eurasia. *Westphal et al.* [1986] found the same systematic shallowing of inclinations throughout a midlatitudinal band between Iberia and Central Asia and this was later confirmed by *Kissel et al.* [1987] and Huang and *Opdyke* [1992]. No adequate interpretation of this phenomenon has been proposed so far.

Declination. The above analysis of inclination data makes us cautious about the validity of a reference Eurasian declination. We therefore prefer to compare declinations from one basin to another.

The most suitable basin for a local reference appears to be Issyk Kul. No large faults are known to crosscut this basin [*Sadybakasov*, 1991]. Mean declinations are statistically identical for all localities and the fold and reversal tests show that the data are consistent. We therefore infer that Issyk-Kul behaved as a quasi-rigid block during the Cenozoic. Furthermore, Issyk-Kul is relatively near the undeformed foreland. Another area in a similar tectonic position is the Northern Chinese Tien Shan, where paleomagnetic results from Cretaceous and Tertiary rocks have revealed no rotations [*Chen et al.*, 1991]. In what follows, for ease of description, we will take as a regional reference direction the mean declination for Issyk-Kul (2°±9°).

Paleomagnetic data from the Naryn basin are rather scattered on all levels (Figure 12); nevertheless, all tests for the entire basin are positive. The mean direction for Naryn agrees with that for Issyk Kul, implying no relative rotation between the two basins. This conclusion can probably be extended to the entire area north-east of the Talas-Fergana fault. Nevertheless, the large observed scatter might be hiding some rotations at local scale. Indeed, the basin is known to be crosscut by faults [*Sadybakasov*, 1991]. Our structural studies have shown that many such faults have strike-slip displacements, especially within the Paleogene succession, and these could be associated with variable rotations. More paleomagnetic data are necessary for a definite conclusion.

The mean declinations for Issyk Kul and Naryn basins are slightly westward of the Eurasian reference declination for 40 Ma (Table 6), the difference being marginally significant for the former and insignificant for the latter. Considering the quality of our data as well as the questionable validity of the Eurasian reference data, we cannot attribute any tectonic significance to these differences.

For the Fergana basin, the tests point to uniformity of paleomagnetic data from the three localities. We infer that the basin rotated in a quasi-uniform manner during the Cenozoic. Several large faults are known to crosscut the basin [*Sadybakasov*, 1991] and so it may be that internal blocks underwent similar rotations, in domino style. With reference to Issyk-Kul, the Fergana basin has rotated on average 20°±11° counterclockwise. Chatkal data slightly differ from

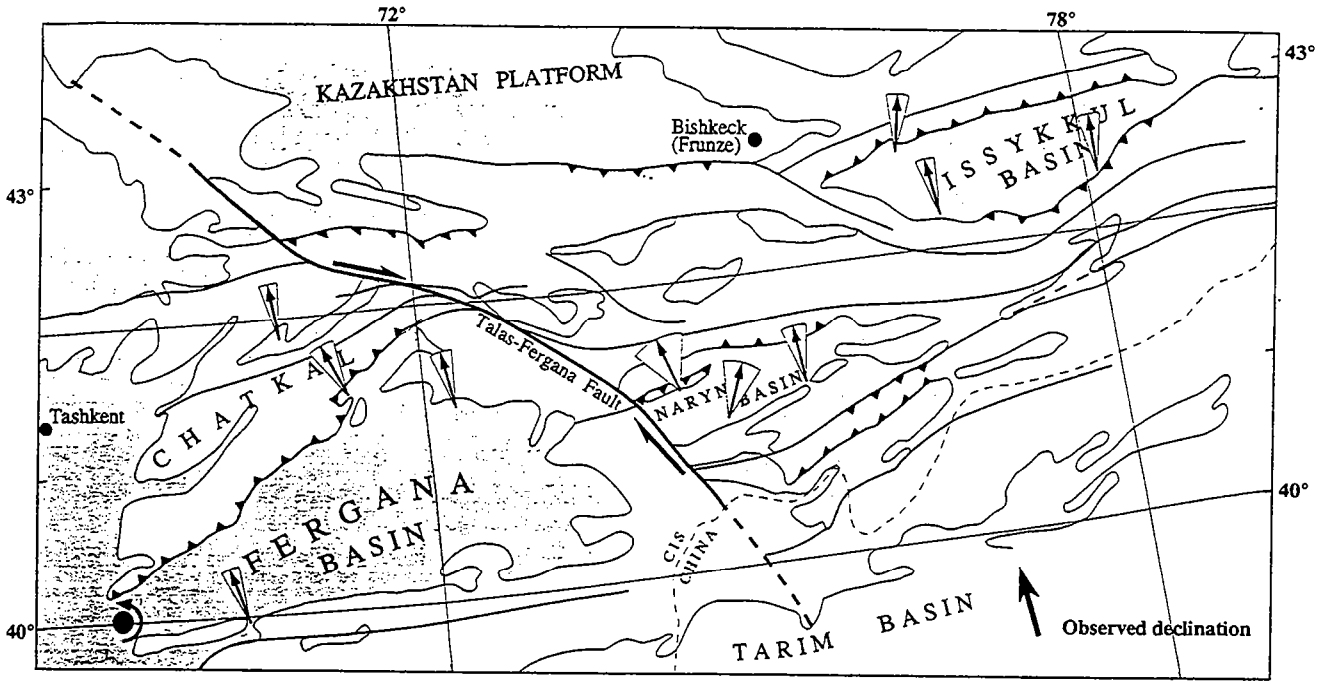

Fig. 12. Observed paleomagnetic declinations, superimposed on a simplified structural map of the Kirghiz Tien-Shan. Solid circle in the western Fergana basin indicates assumed pole of relative counterclockwise rotation between Fergana basin and Kazakhstan platform. Rotation of the Fergana basin relative to the Issyk-Kul basin is 20°±11° counterclockwise. The rotation mode implies a Cenozoic left-lateral displacement of 110±60 km on the Talas-Fergana fault. Symbols and conventions are as for Figure 1 .

Fergana data. The apparently smaller angle of rotation for Chatkal (Table 6) is in agreement with predictions from structural data [*Cobbold and Davy*, 1988]. Unfortunately, the reliability of this conclusion is hindered by the scarcity of data from the Chatkal basin.

Our result for the Fergana basin is in good agreement with rotations inferred from the structure of the basin and adjacent areas. The Chatkal ranges form a triangular area on a map, with the apex in the SW (Figure 12). The altitude increases progressively northeastwards, as far as the Talas-Fergana fault. Our structural studies indicate that the direction of shortening across the ranges is NW-SE and that the amount of shortening increases toward the NE. This implies a counterclockwise rotation of the Fergana basin, with respect to the Kazakhstan paltform [*Cobbold and Davy*, 1988]. Assume a pole at the apex of the ranges. For a rotation of 20°±11°, the amount of shortening across the Chatkal ranges then increases toward the NE, from zero to a value of 110±60 km. The corresponding strike-slip displacement along the Talas-Fergana fault is right-lateral, with a value of 110±60 km. If the pole of rotation were further to the SW, this value would be greater. Even the minimum value is compatible with the 200-km offset of Permian and older structures observed by *Burtman* [1980]. It suggests that much, if not all, of the total offset on the Talas-Fergana fault is Cenozoic.

A counterclockwise rotation of the Fergana basin has also been inferred from a recent paleomagnetic study of Cretaceous sediments [*Bazhenov*, 1993]. Out of a total of 15 localities, 14 secondary prefolding directions were inferred to be Late Cretaceous. The mean directions for these localities show a counterclockwise rotation of 25°±7° compared with the Late Cretaceous reference direction. For seven localities, a bipolar prefolding component, presumably primary and lower Creatceous, was also isolated. A counterclockwise rotation of 21°±10° is inferred from this component. Such results are in very good agreement with our own Tertiary data.

In Mesozoic sediments of the eastern Tadjik depression (Figure 1), *Bazhenov and Burtman* [1981, 1986] and *Pozzi and Feinberg* [1991] determined counterclockwise rotations relative to stable Asia. These data and our results from the Fergana basin are in good agreement with the block rotations inferred by *Cobbold and Davy* [1988] from the Cenozoic fault pattern.

Thus the paleomagnetic results show that Cenozoic deformation has been heterogeneous at the scale of Kyrgyzia. The Talas-Fergana fault appears to be a major lithospheric discontinuity, separating domains with differing amounts of block rotation. Counterclockwise rotations to the west of the fault may be associated with indentation and emplacement of the Pamir thrust sheets.

CONCLUSIONS

Our study of Cenozoic formations from the Tien-Shan shows that bipolar remanent magnetizations were acquired before folding and are probably of primary origin. From the paleomagnetic inclinations, we infer paleolatitudes between 20°N and 30°N. These are small in comparison with paleolatitudes predicted by APWPs of Eurasia. Our inferred paleolatitudes are also incompatible with the kinematics of Central Asia as we understand them today. We thus consider that the APWPs for Eurasia are not directly applicable to the Kyrgyz Tien-Shan and that the measured inclinations are affected by factors not yet well understood.

From our measured declinations, we infer that the Fergana basin has rotated 20°±11° counterclockwise relative to the Issyk-Kul basin since the Paleogene. This is compatible with the rotation inferred by *Cobbold and Davy* [1988] from the

Cenozoic fault pattern. It implies a right-lateral displacement of at least 110±60 km on the Talas-Fergana fault. This is compatible with the 200-km offset of Permian and older markers observed by *Burtman* [1980], suggesting that most, if not all, of the displacement on the fault is Cenozoic.

Acknowledgments. Our highly successful 1989 expedition to the Kyrgyz Tien-Shan was organized by V.S. Burtman and M. Bazhenov, under the terms of an international agreement for scientific cooperation between the CNRS (International Division) and the Academy of Sciences (ex-URSS). We thank the Director of the Geological Institute, A. Knipper, for his support. Landsat tapes were acquired with funds from the Programme National de Télédétection Spatiale, France. Jean Letouzey, of the Institut Français du Pétrole, kindly provided color prints of the Landsat images. We also thank Guy Aubert, Assistant Director of the Institut National des Sciences de l'Univers, for providing funds to acquire the Magellan positioning instrument. For his visit to France (1991-1992), M. Bazhenov acknowledges financial support from the Ministère de la Recherche et de la Technologie, the Université de Rennes and the Université de Pau.

REFERENCES

Achache, J., and V. Courtillot, Paleogegraphic and tectonic evolution c southern Tibet since middle Cretaceous time: New paleomagnetic data and synthesis, *J. Geophys. Res., 89*, 10,311-10,339, 1984.

Argand, E., *La tectonique de l'Asie*, Belgique, Premier fascicule, 171-371, 1924.

Avouac, J. P., Application des méthodes de morphologie quantitative à la néotectonique. Modèle cinématique des déformations en Asie Centrale, thèse, Univ. de Paris VII, 1991.

Bakirov, A., On the mode of the late plaleozoic tectonic movements within the ranges adjacent to the Fergana basin, in *Tectonics of the Western Part of the North Tien-Shan*, edited by M. M. Adyshev, pp. 35-46, Ilim, Frunze, Kirghyz, 1960.

Bazhenov, M. L., Creataceous paleomagnetism of the Fergana basin and adjacent ranges: Tectonic implications, *Tectonophysics,* in press, 1993.

Bazhenov, M. L., and V. S. Burtman, Formation of the Pamir-Punjab syntaxis: Implications from paleomagnetic investigations of Lower Cretaceous and Paleogene rocks of the Pamirs, in *Contemporary Geoscientific Researches in Himalaya*, edited by A. K. Sinha, pp. 71-81, Bishen Singh Mahendra Pal Singh, Derha Dun, India, 1981.

Bazhenov, M. L., and V. S. Burtman, Tectonics and paleomagnetism of structurals arcs of the Pamir-Punjab syntaxis, *J. Geodyn., 5*, 383-396, 1986.

Beck, M. E., Paleomagnetic record of plate margin. Tectonic processes along the western edge of North America, *Jour. Geophys. Res., 85*, 7115-7131, 1980.

Besse, J., and V. Courtillot, Revised and synthetic apparent polar wander paths of the African, Eurasian, North American and Indian plates, and true polar wander paths since 200 Ma, *J. Geophys. Res., 96*, 4029-4050, 1991.

Blow, R. A., and N. Hamilton, Effect of compaction of a detrital remanent of magnetization in fine grained sediments, *Geophys. J. R. Astron. Soc., 52*, 13-23, 1978.

Burtman, V. S., On the Talasso-Fergana strike-slip fault, *Bull. Acad. Sci. USSR Geol. Soc., 12*, 37-48, 1961.

Burtman, V. S., Faults of Middle Asia, *Am. J. Sci., 280*, 725-744, 1980.

Calderone, G. J., and R. F. Butler, The effect of noise due to random undetected tilts and paleosecular variationson regional paleomagnetic directions, *J. Geophys. Res., 93*, 3973-3977, 1991.

Cobbold, P. R., and P. Davy, Indentation tectonics in nature and experiments, 2, Central Asia, *Bull. Geol. Inst. Univ. Uppsala, 14*, 1988.

Davy, P., and P. R. Cobbold, Indentation tectonics in nature and experiments, 1, Experiments scaled for gravity, *Bull. Geol. Inst Univ. Uppsala, 14*, 129-141, 1988.

Demarest, H. H., Error analysis for the determination of tectonic rotation from paleomagnetic data, *J. Geophys. Res., 88*, 4321-4328, 1983.

Dewey, J. F., and K. C. A. Burke, Tibetan, Variscan, and Precambrian reactivation: Products of continental collision, *J. Geol., 81*, 683-692, 1973.

Dewey, F. D., S. Cande, and W. C. Pitman, Tectonic evolution of India/Eurasia collision zone, *Eclogae Geol. Helv., 82*(3), 717-734, 1989.

England, P., Some numerical investigations of large scale continental deformation, in *Mountain Building Processes*, edited by K. Hsü, pp. 129-139, Academic, San Diego, Calif., 1982.

England, P., and P. Molnar, Right lateral shear and rotation as an explaination for strike-slip faulting in Eastern Tibet, *Nature, 344*, 140-142, 1990.

Fisher, R., Dispersion on a sphere, *Proc. R. Soc. London, Ser. A, 217*, 295-305, 1953.

Housemann, G., and P. England, Finite strain calculations of continental deformation, 1., Method and general results for convergent zones, *J. Geophys. Res., 91*, 3651-3663, 1986.

Huang, K., and N. D. Opdike, Paleomagnetism of Cretaceous to Lower Tertiary rocks from southwestern Sichuan: A revisit, *Earth Planet. Sci. Lett., 112*, 29-40, 1992.

Irving, E., and G. A. Irving, Apparent polar wander paths carboniferous through Cenozoic and the assembly of Gondwana, *Geophys. Surv., 6*, 141-187, 1982.

Jolivet, L., P. Davy, and P. R. Cobbold, Right-lateral shear along the Northwest pacific margin and the India-Eurasia collision, *Tectonics, 9*, 1409-1419, 1990.

Kissel, C., C. Laj, A. M. C. Sengor, and A. Poisson, Paleomagnetic evidence for rotation in opposite senses of adjacent blocks in northeastern Aegea and western Anatolia, *Geophys. Res. Lett., 14*, 907-910, 1987.

Krilov, A. Y., Absolute age of the rocks of the Central Tien-Shan and application of Argon methods to metamorphic and sedimentary sediments, in *Determination of the Absolute Age of Pre-Quaternary Formations*, edited by I. E. Starik, pp. 222-224, Nedra, Moscow, 1960.

Lowrie, W., Identification of ferromagnetic minerals by coercivity and unblocking temperatures properties, *Geophys. Res. Lett., 17*, 159-162, 1990.

Mc Elhinny, M. W., Statistical significance of the fold test in paleomagnetism, *Geophys. J. R. Astron. Soc., 8*, 338-340, 1964.

McFadden, P. L., and D. L. Jones, The fold test in paleomagnetism, *Geophys. J. R. Astron. Soc., 67*, 53-58, 1981.

Meade, R. H., Factors influencing the early stages of the compaction of clays and sands; A review, *J. Sediment. Petrol., 36*, 391-408, 1966.

Ministry of Geology of the USSR and the Kyrghyz Academy of Sciences, Geological map of the Kyrgyzstan, scale 1:500 000, six sheets, Frunze, 1978.

Molnar, P., and P. Tapponnier, Cenozoic tectonics of Asia: Effects of a continental collision, *Science, 189*, 419-426, 1975.

Nagata, T., *Rock Magnetism*, 350 pp., Mazuren, Tokyo, 1961.

Patriat, P., and J. Achache, India-Eurasia collision chronology has implication for crustal shortenning and driving mechanism of plates, *Nature, 311*, 615-621, 1984.

Peltzer, G., and P. Tapponier, Formation and evolution of strike-slip faults, rifts and basins during the India-Eurasia collision: An experimental approach, *J. Geophys. Res., 93*, 15,085-15,117, 1988.

Perroud, H., Paléomagnétisme dans l'arc Ibéro-Armoricain et l'orogénèse varisque en Europe occidentale, thèse, Univ. de Rennes, 1985.

Sadybakasov, E., *Neotectonics of the Central Tien-Shan* (in Russian), 117 pp., Ilim, Frunze, Kirghyz, 1972.

Sadybakasov, E., *Neotectonics of the High Asia* (in Russian), 117 pp., Ilim, Frunze, Kirghyz, 1991.

Savostin, L. A., J.-C. Sibuet, L. P. Zonenshain, X. Le Pichon, and M.-J. Roulet, Kinematics evolution of the Tethys belt from the Atlantic ocean to the Pamirs since the Triassic, *Tectonophysic, 123*, 1-35, 1986.

Schneider, D. A., and D. V. Kent, Testing models of the Tertiary paleomagnetic field, *Earth Planet. Sci. Lett., 101*, 260-271, 1990.

Schulz, S. S., *Analysis of Neotectonics and Relief of the Tien-Shan* (in Russian), 222 pp., Geografgiz, Moscow, 1948.

Sidorenko, A. V., *Geology of the USSR*, 280 pp., Nedra, Moscow, 1972.

Stamatakos, J. A., K. P. Kodama, L. F. Vittorio, and T. L. Pavlis, Paleomagnetism of Cretaceous and palocene sedimentary rocks acroos the castle mountain fault, South Central Alaska, in *Deep Structures and Past Kinematics of Accreted Terranes.*, edited by J. W. Hillhouse, pp. 151-177, Washington, AGU,1989.

Tapponnier, P., G. Peltzer, A. Y. Le Dain, R. Armijo, and P. R. Cobbold, Propagating extrusing in Asia: New insights from simple experiments with plasticine, *Geology, 10*, 611-616, 1982.

Turdukulov, A. T., *Geology of the Paleogene and Neogene of North Kyrgyzia* (in Russian), 264 pp., Ilim, Frunze, 1980.

Wallace, R. E., The Talas-Fergana fault, Kirghizia and Kasakhstan, *Earthquake Info. Bull., 8*, 4-13, 1976.

Westhphal, M., M. L. Bazhenov, J. P. Lauer, D. M. Pechersky, and J. C. Sibuet, Paleomagnetic implications on the evolution of the Tethys belt from the Atlantic Ocean to the Pamirs since the Triassic, *Tectonophysics, 123*, 37-82, 1986.

M. L.Bazhenov and V.S. Burtman, Geological Institute, Academy of Sciences, 109017 Moscow, Russia.

A. Chauvin, P.R. Cobbold and J.-Ch.Thomas, Géosciences (CNRS), Université de Rennes, 35042 Rennes Cédex, France.

H. Perroud, Département des Sciences de la Terre, Université de Pau, 64000 Pau Cédex, France.

E. Sadybakasov, Institute of Seismology, Kirghiz Academy of Sciences, 720060 Bishkeck, Kyrgyzstan.

(Received April 15, 1992;
revised November 3, 1992;
accepted November 29, 1992.)

3. Transpression Cénozoique et développement de bassins dans le Tien-Shan Kirghiz, Asie Centrale

Cenozoic transpression and basin development, Kyrghyz Tien-Shan, Central Asia

Article sous presse dans "Géodynamic evolution of sedimentary basins", édité par F. Roure, éditions Technip, Paris.

Fergana) are bounded on both sides by thrust zones with basinward vergences. In plan, many basins are rhombohedral or elliptical, as a result of strike-slip faulting.

We have measured fault-slip data for minor faults at 7 sites. Faults in Paleogene rocks are dominantly strike-slip. The principal direction of shortening varies, from NW in Fergana to NE in Naryn. After restoration of Neogene block rotations, revealed by paleomagnetism, the direction of shortening becomes nearer N-S. Thus these faults may have formed in the Paleogene. Faults in Neogene rocks are dominantly reverse. For them, the principal direction of shortening is N-S, as it is today.

Introduction

In August 1989, two of us (P.R.C. and E.S.) took part in a one-month paleomagnetic sampling expedition throughout the Kyrghyz Tien Shan. The object was to test for Cenozoic block rotations about vertical axes. Samples came from Tertiary redbeds and lavas within major Cenozoic basins. In July 1991, J.C.T. and E.S. took part in a shorter expedition, to check structural interpretations. During these expeditions, neither the manpower nor the time were sufficient for detailed structural mapping, let alone for sedimentological observations. The region is vast. Nevertheless, we have obtained enough data, from our joint field work, paleomagnetic studies and interpretation of satellite images, as well as from previous work (Sadybakasov, 1991) and an abundant literature (mostly in Russian), to write a summary of the Cenozoic basins and their tectonic history.

There are two main reasons why the subject may be scientifically interesting for an international audience. One is the current controversy surrounding the style of Cenozoic deformation in Central Asia as a whole and its relationship with the collision of India and Eurasia. The other is the increasing interest in sedimentary basins developed in contexts of crustal thickening or transpression.

In this paper, we first describe the controversy surrounding the style of Cenozoic deformation in Central Asia. Then we briefly review the tectonic history of the Tien-Shan. The main part of the paper is nevertheless devoted to new data from the Tien-Shan and especially from the basins: maps, figures, photographs and data, to a large extent self-explanatory. We believe that there is convincing evidence for synchronous sedimentation and crustal thickening in Kyrghyzia during the Neogene. What is more, they seem to have prevailed over much of Central Asia, not only during the Cenozoic, but also during earlier periods.

Deformation in Central Asia, following collision with India

Argand (1924) compiled the first tectonic map of Eurasia. He documented Cenozoic compression, reactivation of earlier structures, crustal thickening and anomalous relief throughout much of Central Asia. He inferred that all this was due to collision ("affrontement") of India, after its northwards drift from an initial position near Madagascar. Recent work has done much to quantify these ideas and little to change them. Dewey and Burke (1973) described crustal shortening within Tibet, by reactivation of earlier structures. Molnar and Tapponnier (1975) dramatically

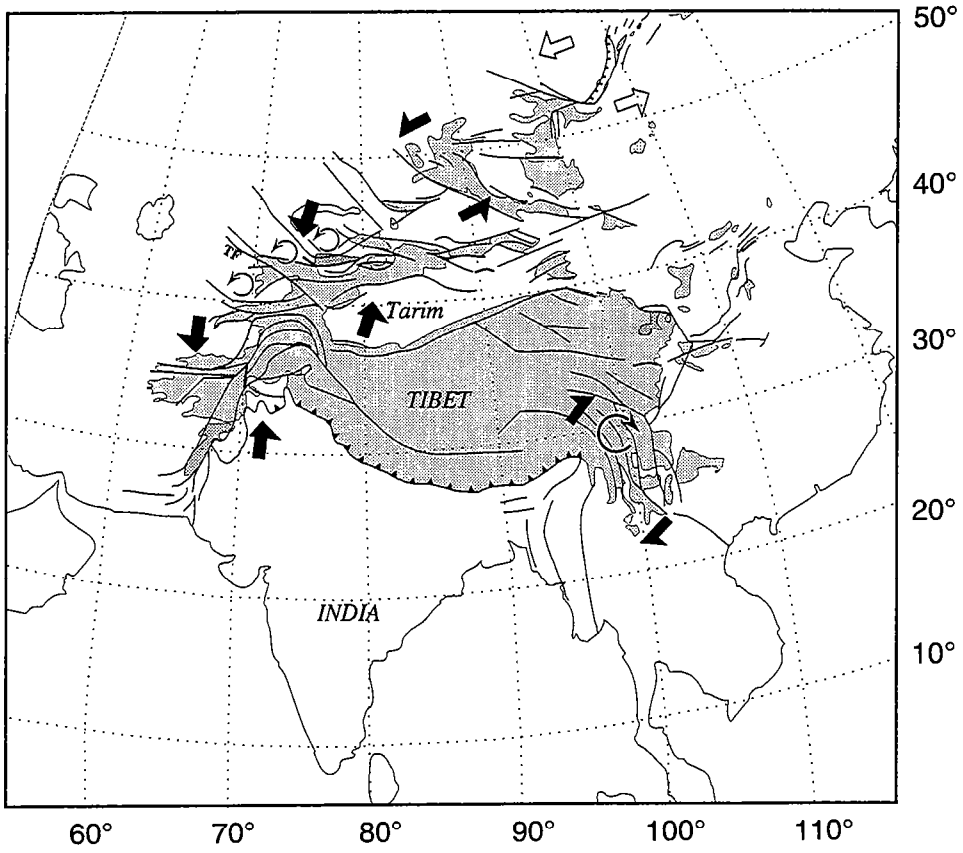

Fig. 1. Cenozoic tectonics of Central Asia (after Cobbold and Davy, 1988).

Map shows traces of major Cenozoic fault zones (thick lines) and areas with altitudes over 2000 m (grey). Faults range in style from reverse in Himalaya (triangles pointing in direction of underthrusting), through strike-slip, to normal in the NE (ticks on downdropped side). Wrench zones (solid black arrows when convergent, empty white arrows when divergent) and block rotations (circular arrows) were inferred by Cobbold and Davy (1988) from structural data.

illustrated the extent of active deformation within Central Asia, by studies of seismicity and satellite imagery. From magnetic anomalies in the Indian Ocean, Patriat and Achache (1984) estimated that India collided with Eurasia about 55 Ma ago. Since then, there has been a further convergence of about 2000 km, according to paleomagnetic and other evidence (Achache et al., 1984).

In spite of this progress, there is still controversy over the style of Cenozoic deformation in Central Asia. Some authors favour crustal thickening; whereas others favour strike-slip faulting and lateral extrusion. Molnar and Tapponnier (1975) first drew attention to the importance of strike-slip faulting. Tapponnier et al (1982) suggested that it could have led to significant eastwards extrusion of large continental blocks, with accompanying rotations about vertical axes. Peltzer and Tapponnier (1988) estimated that eastwards extrusion of Tibet accounts for about 50% of the convergence between India and Asia, the rest being taken up by crustal thickening. In contrast, England (1982), Houseman and England (1986) and Dewey et al (1989) have persistently argued that crustal thickening accounts for almost all of the convergence.

Davy and Cobbold (1988) and Cobbold and Davy (1988) compared analogue models of continental indentation with the pattern of Cenozoic faults in Central Asia. They concluded that lateral extrusion accounts for somewhere between 20% and 45% of convergence, the rest being taken up by thickening. Such thickening must attenuate laterally across wrench zones, left-lateral in the west and right-lateral in the east (Cobbold and Davy, 1988; Dewey et al., 1989) (Fig. 1). There is structural evidence for left-lateral wrenching, not only on the edges of thickened areas, but also in a long strip, running from the Gulf of Oman, through the Pamirs, Kyrghyzia, Lake Baikal and beyond (Cobbold and Davy, 1988). This belt may have allowed some eastwards extrusion of Central Asia. On structural evidence, wrenching should be partially accommodated by rotation of fault blocks and antithetic strike-slip faults about vertical axes, in domino style. Rotations are inferred to be counterclockwise in the Gulf of Oman-Baykal wrench zone, clockwise in eastern Tibet. Recent paleomagnetic work in the Tien-Shan has indeed provided evidence for Cenozoic counterclockwise rotations, both in the Fergana basin (Thomas et al., 1993a; Bazhenov, 1993) and in the Tajik basin (Thomas et al., work in progress).

Tectonic setting of the Kyrghyz Tien-Shan

General structure

In the Tien-Shan region of Kyrghyzstan, mountain ranges several kilometers high alternate with intermontane basins (Fig. 2). On geophysical evidence, the Moho

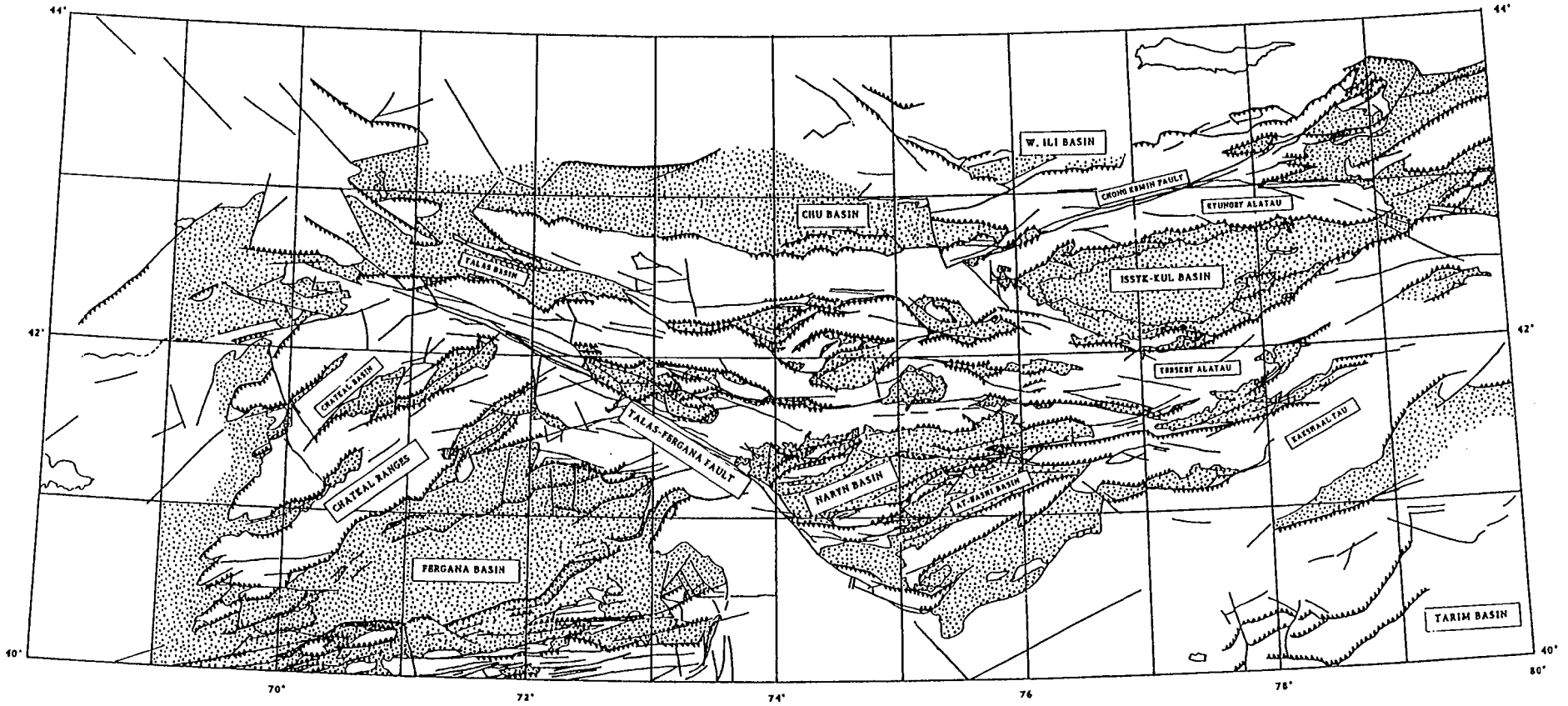

Fig. 2. Cenozoic faults and basins of the Kyrghyz Tien-Shan.
Map compiled by PRC in 1990. Topographic base and geographical coordinates are from Operational Navigation Chart (sheet ONC F-6, scale 1:1 000 000, Lambert conformal conic projection), published by Defense Mapping Agency, St. Louis, Miss., USA. Geological boundaries and fault traces are from Landsat MSS colour images and 1:500 000 geological map (Ministry of Geology of the USSR and Kyrghyz Academy of Sciences, 1978). Cenozoic basins (stippled) alternate with mountain ranges (blank). Both are frequently bounded by faults with reverse components (triangles pointing in direction of underthrusting).

currently reaches depths of up to 50 km beneath the Tien-Shan (Gubin, 1986; Burov et al., 1990). Paleozoic and older rocks form the ranges; whereas Mesozoic and Cenozoic sediments fill the basins. The general strike of the Tien-Shan ranges is ENE, but there are significant deviations, especially near the major Talas-Fergana fault (Fig. 2).

A striking feature of the region is the large number of basins containing Cenozoic rocks (Fig. 2). Prominent is the intermontane Fergana basin in the southwest. This contains up to 8 km of Cenozoic sediments. Other major intermontane basins are Issyk-Kul in the east and Naryn in the south. On the edges of the Tien-Shan, there are foreland basins with Cenozoic sediments several km thick. Prominent are the Chu and West Ili basins in the N.

Cenozoic tectonics

The present morphology and structure of the Tien Shan are very largely due to Cenozoic tectonics.

The Tien Shan ranges are amongst the most active in the world (Tapponier and Molnar 1979). Sharp fault traces and offset topographic features are visible on satellite images. Most focal mechanisms of earthquakes indicate thrusting on faults trending E-W; but some indicate strike-slip motions, left-lateral on faults trending ENE and right-lateral on faults trending NW. Over most of the region, the inferred direction of maximum shortening is approximately N-S. Thus the current tectonic context is one of transpression.

Cenozoic basins, both intermontane and of foreland type, are often bounded by major thrusts. These have been active at various times during the Cenozoic (Sadybakasov, 1991). Several major strike-slip faults have been active as well. A striking example is the Talas-Fergana fault (Fig. 2), for which the Quaternary offset is about 10 km and the total offset since the Paleozoic is about 200 km (Burtman, 1980). Recent paleomagnetic studies suggest that much, if not all, of this total offset is Cenozoic (Thomas et al., 1993a; Bazhenov, 1993).

Mesozoic tectonics and sedimentation

In contrast with the Chinese Tien-Shan, where up to 7 km of continental Mesozoic sediments accumulated in basins of foreland type (Hendrix et al., 1992), little is known about the tectonic context of Kyrghyzia during the Mesozoic.

In the Issyk-Kul and Fergana basins, Jurassic sandstones and coal-bearing shales of continental origin unconformably overlie Carboniferous and older rocks. In Issyk-Kul, the sequence is only a few hundred meters thick and consists mainly of quartzitic sandstones. In Fergana, it is less than 1 km thick. To our knowledge, no

synsedimentary faults have been described. Along the Talas-Fergana fault, there are continental Jurassic sequences up to several kilometres thick, restricted to narrow basins, but their tectonic context is not known.

Lower Cretaceous continental redbeds (from conglomerates to mudstones) are widespread in Fergana, but not in the other basins. From studies in coal mines, there is a small angular unconformity (up to 10°) between the Cretaceous and the Jurassic.

A branch of the Cretaceous Tethyan Seaway left a marine depositional record in the Fergana basin, as it did simultaneously in the Tajik basin to the south and in the western part of the Tarim basin in China (Fig. 2). In the Fergana basin, marine clastic sediments of Albian age pass upwards into deeper water platform sediments (limestones, marls and siltstones) of Cenomanian-Turonian age. Nevertheless, the entire Mesozoic sequence in Fergana is no more than 1 km thick. The tectonic context is not known.

Paleozoic tectonics

Paleozoic tectonics have been responsible for crustal thickening and strike-slip faulting in the Tien-Shan (Burtman, 1975, 1980, 1984). The evidence is multiple. First, many basement faults are unconformably overlain by unfaulted Mesozoic or Paleogene platform sediments. Second, Paleozoic rocks often show metamorphism, whereas later sediments do not. Third, Paleozoic granites of crustal origin are widespread. Fourth, metamorphosed ophiolites mark the suture of the Paleozoic Turkestan ocean. This suture runs along the southern edge of the Naryn basin and is offset right-laterally by the Talas-Fergana fault. It then runs along the southern edge of the Fergana basin, before veering northwards towards the Aral Sea and the Urals.

From structural studies, there have been two major Paleozoic episodes of crustal thickening, one labelled Variscan, the other Caledonian. In the Naryn basin, Variscan thrusts cut Carboniferous limestones and Devonian red sandstones, but stop at a Paleogene unconformity. The Carboniferous and Devonian have undergone burial metamorphism. The Devonian is unconformable on Silurian slates, showing greenschist-facies metamorphism. Unfortunately, such geological relationships are not always clear. Geochronological data are lacking and there is no concensus on the relative intensities of Cenozoic and Paleozoic deformation.

Judging from metamorphic grades and the occurrence of Permian syntectonic granites, Variscan deformation was most intense in the Southern Tien-Shan (south of the Fergana basin).

Precambrian tectonics

Five cycles of tectonic and metamorphic activity have been postulated to occur, for the period between 2500 and 600 Ma. (Bakirov and Burtman, 1984).

Cenozoic sediments

Paleogene

Paleogene sediments crop out around the margins of major basins and within minor basins perched up in the ranges. In the major basins, Paleogene rocks are also known from boreholes and from the seismic record (Sadybakasov, 1991). Everywhere to the NE of the Talas-Fergana fault, the Paleogene consists of reddish continental redbeds, a few hundred meters thick. In general, the colour grades upwards, from deep wine red at the base, to vermilion at the top. In contrast, in the Fergana basin, the Paleogene is marine and more than one kilometer thick.

Continental Paleogene sediments are best known from the Issyk-Kul basin. Near the northwestern margin, at Toru-Aygyr, the lowermost Paleogene (Kokturpak Fm.) consists of reddish sandy marls, sandstones and clays, of lacustrine and meandering-fluvial origin. An intercalated basalt flow (or flows), 12 m thick, has yielded a radiometric age of 55 Ma, by K-Ar on whole rock (Krilov, 1960). Only a few meters above the basalt, sediments have yielded mammalian and reptilian remains (*Deperetella* and *Prothyrecodon*), attributed to the Middle to Late Eocene (Turdukulov, 1987). At Dzhety-Ogyuz, near the southeastern margin of the Issyk-Kul basin, the lowermost Paleogene (Chonkurshak Fm.), consists mainly of red shales. The overlying Dzhety-Ogyuz Fm. consists of deep red alluvial conglomerates and sandstones, more than 1000 m thick. The conglomerates are moderately to poorly imbricated, with basinward current directions. Remnants of an Oligocene tortoise have been found near the top of the Dzhety-Ogyuz Fm. (Sidorenko, 1972).

In the Naryn basin, up to 100 m of continental red conglomerates, sandstones and mudstones unconformably overlie Paleozoic basement. Neither radiometric ages nor vertebrate remains have been reported, but the sequence is attributed to the Paleogene (Sadybakasov, 1991), because it is lithologically similar to the Kokturpak Fm. of Issyk-Kul basin.

In the Fergana basin, the Paleogene succession is marine. The Paleocene Buchara beds are evaporitic, shallow-water bioclastic limestones, formed in a lagoonal environment. Attributed to the Eocene (Sidorenko, 1972) are overlying pink marls of shallow-marine origin, with oyster beds. Overlying them in turn are mudstones and

sandstones of the Massaget Fm. The base of this has marine fauna of Oligocene age (Sidorenko, 1972); but the rocks coarsen upwards into Neogene sandstones of continental origin.

Neogene

Throughout all the basins, Neogene sediments are of continental origin (Sadybakasov, 1991). In general, their colour grades upwards, from yellow to brown for the Miocene, through pale yellow for the Pliocene, to grey for the Pleistocene. The rocks have been dated using mammalian and reptilian remains, as well as pollen analysis.

Alluvial conglomerates alternate with sandstones and siltstones of braided-fluvial origin, or sandstones, siltstones and mudstones of meandering-fluvial and lacustrine origins. Clastic pulses do not always correlate from one major basin to the next, nor are they always homogeneous within any one basin. Nevertheless, Upper Pliocene conglomerates are abundant in most basins, suggesting rapid rates of erosion throughout the region at that time.

In foreland basins to the NW of the Tien-Shan, especially the Chu basin (Fig. 2), sediments are asymmetrically distributed. From seismic and well data, conglomerates are more abundant near the Tien Shan ranges. In intermontane basins, distributions are more symmetric, as one might expect.

Major Cenozoic faults

We have drawn a tectonic map of Kyrghyzia, showing major faults that have been active at one time or another during the Cenozoic (Fig. 2).

As a base map, we used the 1: 1 000 000 Operational Navigation Chart (sheet ONC-F6), published by the US Defense Mapping Agency. To locate fault traces, we used Landsat satellite images and geological maps at 1: 500 000 (Ministry of Geology of the USSR and Kyrghyz Academy of Sciences, 1978). Other information has been taken from the works of Sadybakasov (1991) and Chedia (1986). A certain number of localities we were able to visit during our 1989 and 1991 expeditions.

We used two criteria for classifying faults as Cenozoic. First, we included all currently active faults, showing seismic activity, or characteristic surface breaks on Landsat images or on the ground. Second, we included all faults that offset Cenozoic beds or cause variations in sediment thicknesses or facies. Some examples of the relationships between faults and sedimentation are given in the following section.

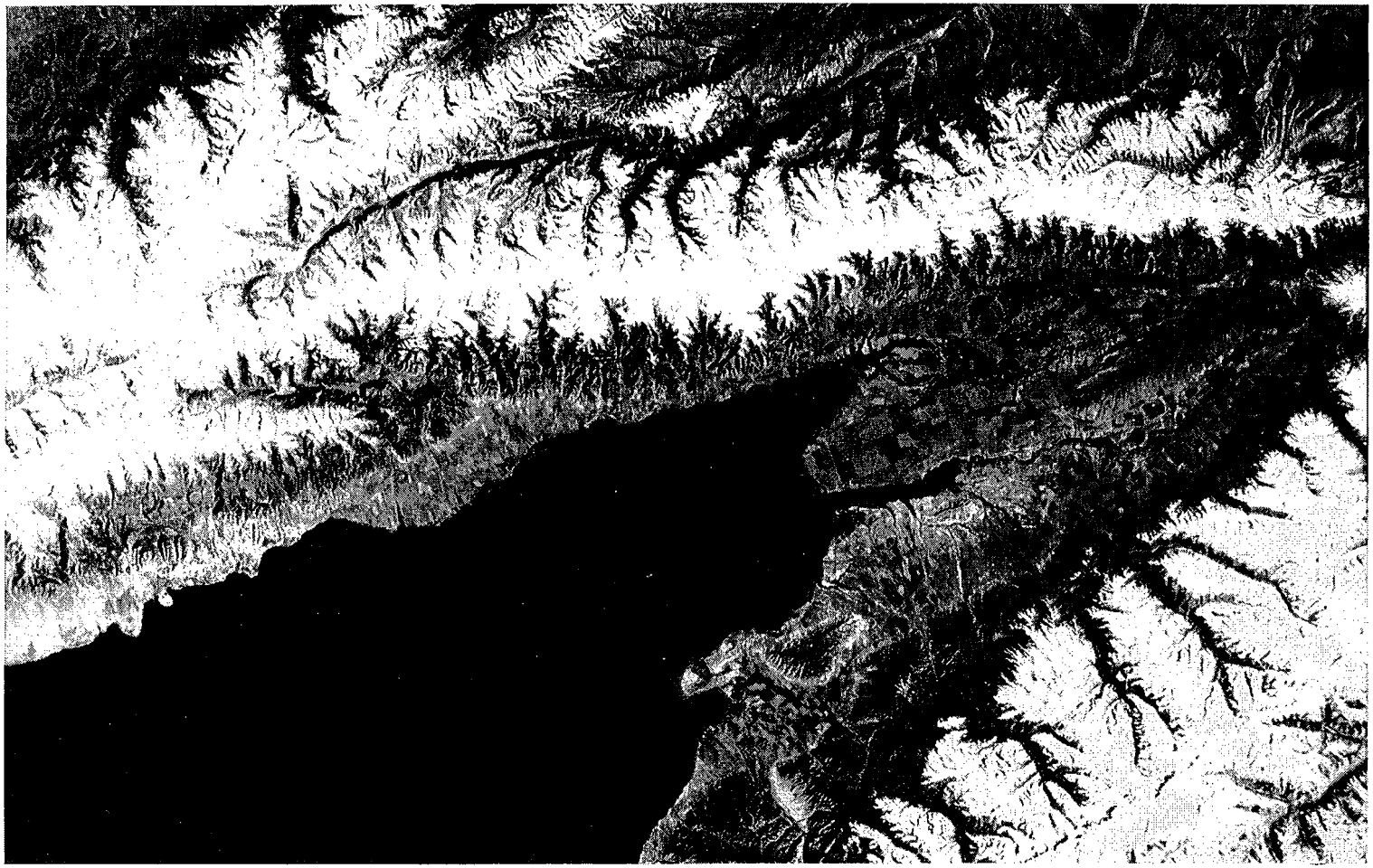

Fig. 3. Issyk-Kul basin.
Landsat MSS image shows Issyk-Kul lake (bottom left) at 1800 m, surrounded by snow-covered ranges, Kyungey Alatau to N (reaching 4800 m) and Terskei Alatau to SE (5000 m). For location and interpretation, see Fig. 2. Ranges are made of Paleozoic sediments, granites and Precambrian metamorphic rocks. Lake and depression are underlain by Cenozoic sediments, up to 4 km thick. For a cross-section, see Fig. 4. Basin is broadly synclinal, but contains folds, such as large anticlinal hinge visible at eastern end. A series of arcuate thrusts, currently active, form the sharp northern margin to the basin. At its southeastern margin, the Paleogene succession, resting unconformably on basement, forms northward-dipping flat-irons (see Fig. 5). To NE of Kyungey Alatau, active faults with strike-slip and reverse components intersect obliquely, separating basement ridges from small rhombohedral basins. North of Issyk-Kul, Chon Kemin strike-slip fault zone occupies narrow valley, trending ENE and separating two parallel ranges of Kyungey Alatau.

According to our map, faults with dominantly reverse motions are the most common. Most mountain ranges and most Cenozoic basins are bounded, on one side or another, by reverse faults. To illustrate this, a good area is the Issyk-Kul basin (Fig. 3). Issyk-Kul lake, at 1800 m, is surrounded by snow-covered ranges, Kyungey Alatau to the north (4800 m) and Terskei Alatau to the south (5000 m). These ranges are made of Paleozoic sediments, granites and Precambrian metamorphic rocks. From wells and seismic surveys, Issyk-Kul basin is known to contain Cenozoic sediments up to 4 km thick (Sadybakasov, 1972, 1991). The basin is broadly synclinal. At its southeastern edge, the Paleogene succession, resting unconformably on the basement, forms northward-dipping flat-irons. A series of arcuate thrusts, currently active, mark the sharp northern edge of the basin. The basin also contains folds, such as the large anticlinal hinge, visible at its eastern end.

Summarizing many years of field work, Sadybakasov (1972, 1991) has produced a series of structural sections through the Tien-Shan. We have redrawn two of these sections, simplifying them and using equal horizontal and vertical scales (Fig. 4). The sections illustrate well the intensity of reverse faulting in the Tien-Shan and its control on the development of sedimentary basins.

Although thrusting has been dominant thoughout the Kyrghyz Tien-Shan, there are also major strike-slip faults. Prominent is the Talas-Fergana system of right-lateral strike-slip faults, trending NW-SE (Fig. 2). This system is currently active, producing spectacular topographic features (Burtman, 1961, 1980; Wallace, 1976; Tapponier and Molnar, 1979). The Quaternary offset is more than 10 km. The total offset since the Permian is about 200 km (Burtman, 1980) and much of this may be Cenozoic, according to recent paleomagnetic work (Thomas et al., 1993).

There are also major left-lateral faults, trending NE-SW, slightly oblique to the mountain ranges. Prominent is the Chon Kemin (or Chonkemina) fault system, in the core of the Kyungey Alatau range, north of Issyk-Kul lake (Figs. 2 and 3). Here is the surface break of the 1911 Kebin earthquake (Tapponier and Molnar, 1979), showing reverse and left-lateral faulting. During field studies at the western end of the Chon Kemin system, we also documented reverse and left-lateral faulting, of undifferentiated post-Paleogene age.

Faults with strike-slip components are especially common in the foreland of the Tien-Shan. Northeast of Issyk-Kul, active faults with strike-slip and reverse components intersect obliquely, separating basement ridges from small rhomohedral basins (Fig. 3).

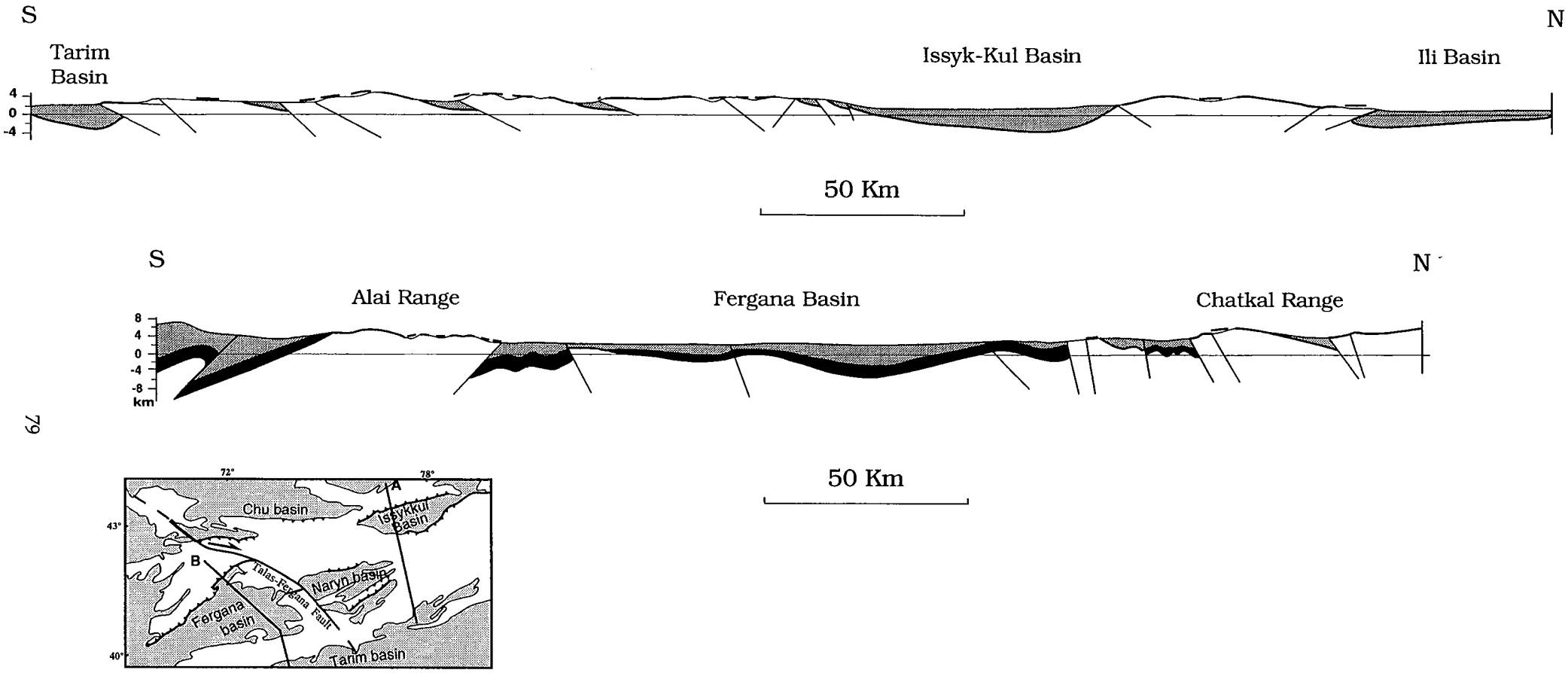

Fig. 4. Two representative structural sections through the Kyrghyz Tien Shan, one on each side of the Talas-Fergana strike-slip fault (after Sadybakasov, 1991).

Inset map (bottom left) shows location of section lines (A and B). Vertical and horizontal scales are identical for both sections. Geological details of the basement (white) have been omitted, for clarity. Overlying it are Mesozoic sediments (black, section B only) and Cenozoic sediments (stippled). In basins, data are from seismic lines and from wells. In mountain ranges, base of Tertiary (dashed line) is inferred from perched erosion surfaces (see text). Base of Tertiary is offset across major reverse faults (thin lines). Fault dips are known at the surface from field mapping, but are little constrained at depth. Notice foreland style of Ili and northern Tarim basins (section A), compared with more symmetric styles of Issyk-Kul basin (section A) and Fergana basin (section B).

Relationship of major faults to sedimentation

Schulz (1948) recognized that Neogene sedimentation in the basins of the Tien-Shan was synchronous with North-South compression and crustal thickening. He pointed out that intramontane basins are usually synclinal and bounded by reverse faults. He recognized that, on many a section, older strata (Paleogene) are more steeply dipping than younger strata (Neogene). Illustrated in the abundant Russian literature are many examples of such relationships (see Schulz, 1948; Sadybakasov, 1972, 1991; Chedia, 1986).

Here we document relationships between reverse faulting and sedimentation at 5 localities, one in Issyk-Kul, two in Naryn and two in Fergana.

1. *Dzhety-Ogyuz valley, southern edge of Issyk-Kul basin (Fig. 5).*

On the southeastern edge of the Issyk-Kul basin, the Dzhety-Ogyuz river has cut a gorge through the entire Tertiary succession (Fig. 5). Mostly, the strata dip towards the NNW; but the angle of dip increases progressively southwards, from horizontal for the Quaternary, through about 15° for the Pliocene and 25° for the Miocene, to 50° for the Oligocene. Thus the dip increases as one goes from younger to older formations (Schultz, 1948). The dips also increase downwards. In fact, all Tertiary formations onlap a hangingwall anticline above a southward-verging thrust. The anticline exposes an inlier of basement (granite and amphibolites), capped by Carboniferous sediments. A thin layer of Jurassic quartzite and shales overlies the Carboniferous with a small (15°) angular unconformity. Further to the south is a major, northward-verging, basin-bounding thrust. Between both thrusts is a small basin containing Eocene shales (Chonkurchak Fm.), up to 1 km thick.

From these relationships, we infer that folding and thrusting at Dzhety-Ogyuz has been synchronous with sedimentation, from the Eocene to the Present. In the Oligocene, rapid erosion resulted in alluvial conglomerates (Dzhety-Ogyuz Fm.), several hundred metres thick. The conglomerates show slight imbrication, with basinward current directions. Most of the infill of the Issyk-Kul basin is, however, Neogene.

2. *Naryn river, central Naryn basin (Fig. 6).*

At Dzhan-Bulak, on the northern bank of the Naryn river, an active thrust has put Pliocene sandstones on top of Quaternary gravels. In the hangingwall, the gravels rest unconformably upon tilted and eroded Pliocene strata; whereas, in the footwall, the gravels fill a depocentre. Even the toposoil is folded and faulted. The thrust dips

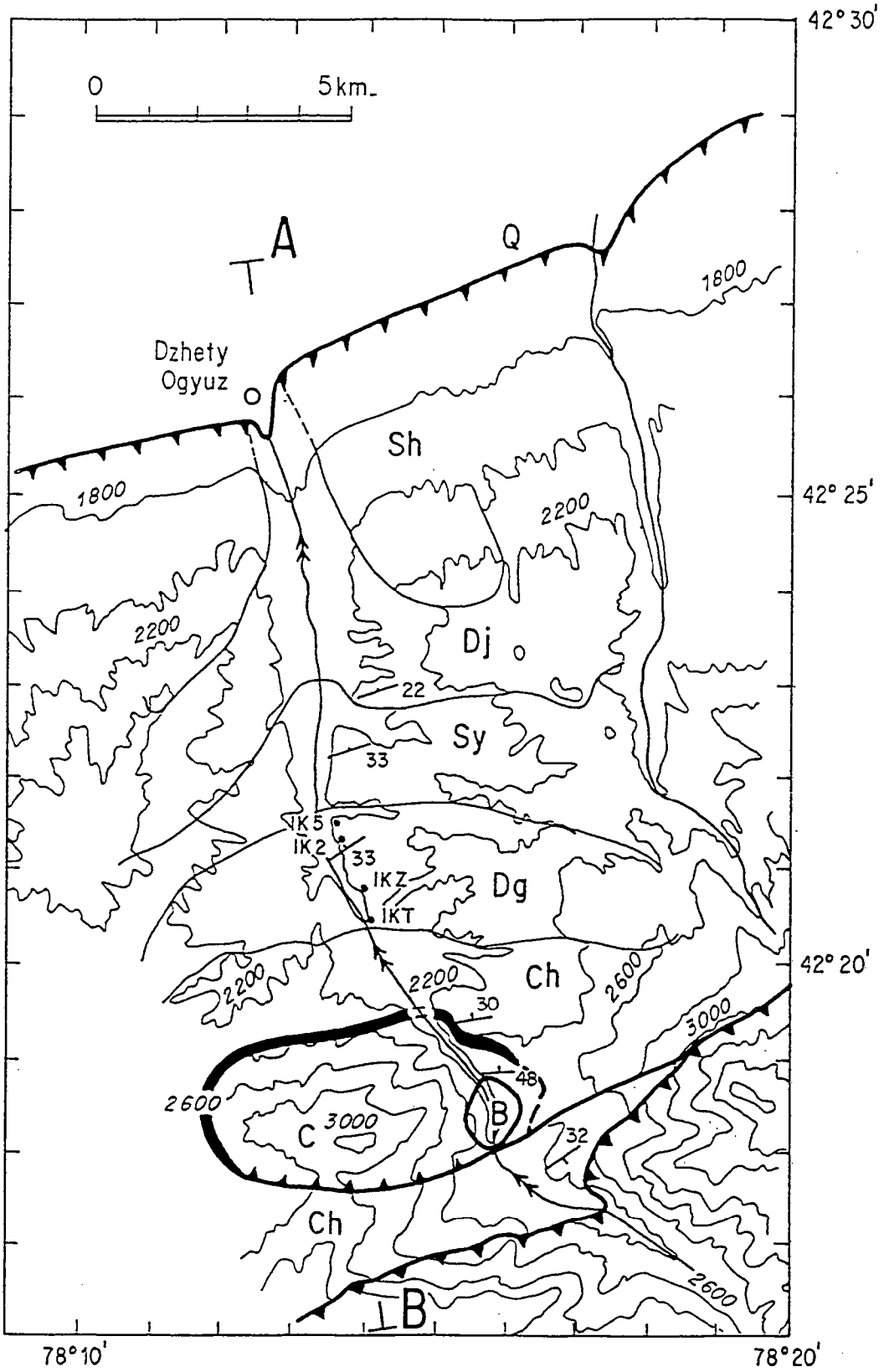

Fig. 5. Cenozoic thrusting and sedimentation, Dzhety-Ogyuz, southeastern margin of Issyk-Kul basin.

Geological map (a) and accurate section (b) were compiled in the field by PRC in August 1989. Base for map (a) is 1:100 000 topographic sheet, with contours in metres. Dip symbols, measured in the field, refer to bedding. Numbers with IK prefixes indicate paleomagnetic sampling sites (Thomas et al., 1993a). Line of section is A-B.

Section (b) shows topographic profile (thin line) and geological information, projected onto section along strike-lines from ridges on both sides of Dzhety-Ogyuz valley.

Basement (B) includes paleozoic granites and metamorphic rocks (amphibolites) of unknown age. Carboniferous sediments (C) are overlain unconformably by Jurassic quartzites (thin black layer). Tertiary formations, from Eocene to Pliocene, are Chonkurchak (Ch), Dzhety-Ogyuz (Dg), Soguty (Sy), Djunky (Dj) and Sharpildak (Sh). Village of Dzhety-Ogyuz is built on Quaternary river gravels (Q), in footwall of active thrust. Dzhety-Ogyuz river has cut deep gorge, exposing ramp anticline and basement inlier. Tertiary sequence onlaps ramp anticline. We infer synsedimentary thrusting, from Eocene to Quaternary.

5b

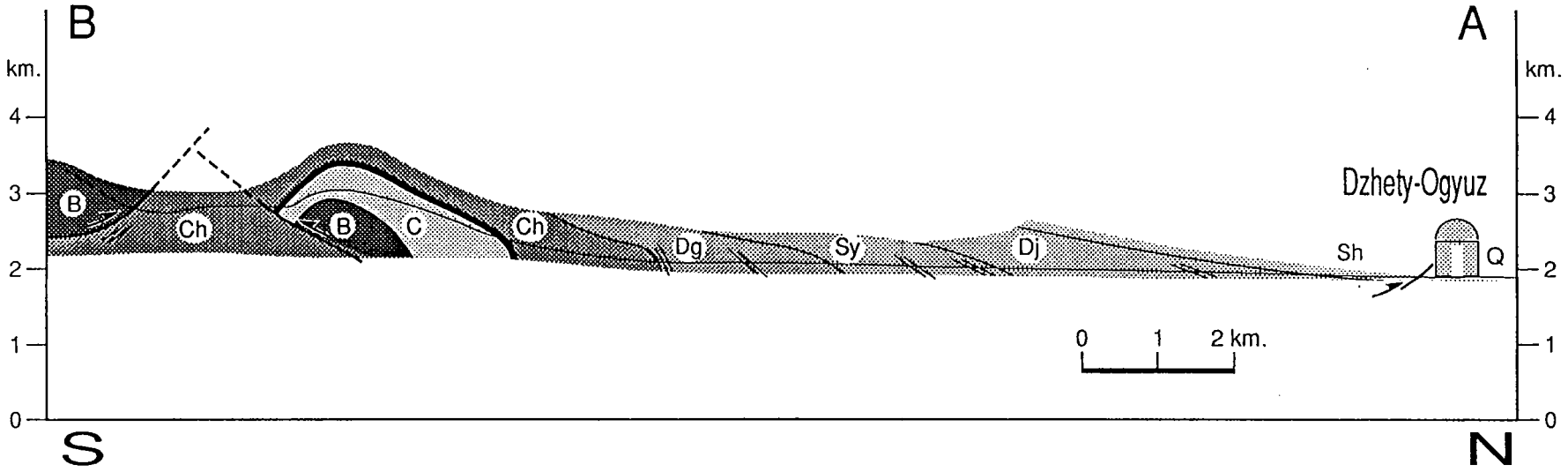

about 30° N and the Quaternary offset is about 10 m. We infer that thrusting here has been coeval with Quaternary sedimentation.

3. *Djaman-Davan gorge, Baybiche ridge, southern edge of Naryn basin (Fig. 7).*

The anticlinal Baybiche ridge strikes ENE, separating the Naryn basin to the north, from the At-Bashi basin to the south (Fig. 2). Its Paleozoic core is unconformably overlain by a thin veneer (about 100 m) of Paleogene redbeds (Fig. 7). Neogene sediments onlap the ridge from the north and the south. In detail, the ridge is made up of en-echelon reverse faults that cut basement and strike E-W. This suggests a component of left-lateral wrenching. The dominant vergence of the reverse faults is southwards. The overlying Tertiary sediments are drape-folded over the faults (Fig. 7). Several rivers flowing northwards have cut gorges through the ridge, indicating recent uplift. Along the Djaman-Davan river, there are spectacular exposures of the Paleozoic core and its Paleogene veneer, thrust southwards over Neogene sediments, here more than 1000 m thick (Fig. 7). The fault surface dips almost due N and carries downdip striae, developed in Neogene sediments. From the stratigraphic record, we infer that thrusting was continuous throughout most of the Neogene. Offset river terraces show that the thrust is still active today.

4. *Northern and southern margins of Fergana basin (Fig. 8).*

All four margins of the Fergana basin are fault zones with reverse components (Sadybakasov, 1972, 1991; Kalvoda et al., 1987, Yablonskaya, 1989; Khain et al., 1991). At the edge of the Chatkal range, an outcropping major fault with downdip striae puts crystalline basement directly on top of Neogene sediments (Fig. 2). In other places, there are thin-skinned thrust belts.

The Isbaskent and Rishtan thrust belts are both in Kyrghyzstan, one on the northern margin of the Fergana basin and the other on the southern margin (Fig. 2). They have been studied during exploration for oil and gas (Obukhov et al. 1991). The basement here consists of Paleozoic sediments (Silurian to Permian), cut by Hercynian thrusts. It is unconformably overlain by platform sediments (Jurassic to Paleocene) of nearly uniform thickness (1 to 2 km). Infilling the basin are continental Tertiary

Fig. 6. Active thrust, Naryn basin.

Locality is Dzhan-Bulak, on northern bank of Naryn river, about 10 km west of Naryn town (41° 26' N, 75° 50' E). Photograph (view towards ENE) shows river bank, about 10 m high, exposing Pliocene sandstones (bottom), unconformably overlain by Quaternary river gravels (top) and thin layer of topsoil. Entire sequence is offset and folded across thrust fault dipping about 30° N. From thickness variations, we infer that thrusting has been coeval with Quaternary sedimentation.

Fig. 7. Neogene thrusting and sedimentation, Naryn area.

Locality is gorge of Djaman-Davan river, Baybiche basement ridge, southern edge of Naryn basin (41° 03' N, 74° 48' E). Photograph (view towards WNW) shows about 1000 m of relief on west bank of river (for scale, see huts at bottom right). Large thrust in centre (dipping 39° due North) separates Baybiche basement ridge (right), from Neogene sediments (left). Basement consists of Silurian slates (grey), faulted against unmetamorphosed Devonian sandstones (red). It is overlain unconformably by veneer of Paleogene redbeds. Neogene sediments (left) range from Miocene (yellow-brown), through Pliocene (pale yellow), to Quaternary (light grey).

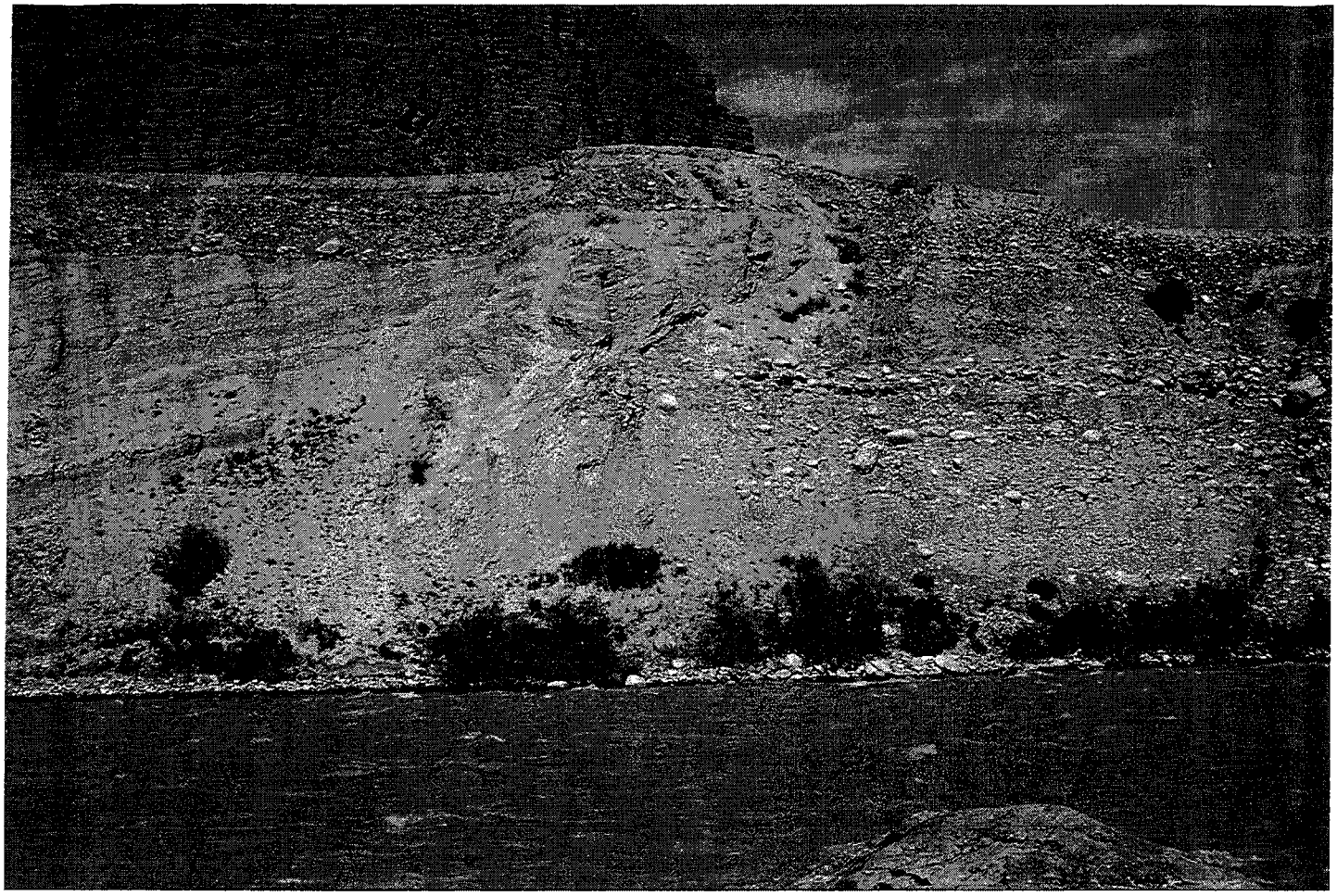

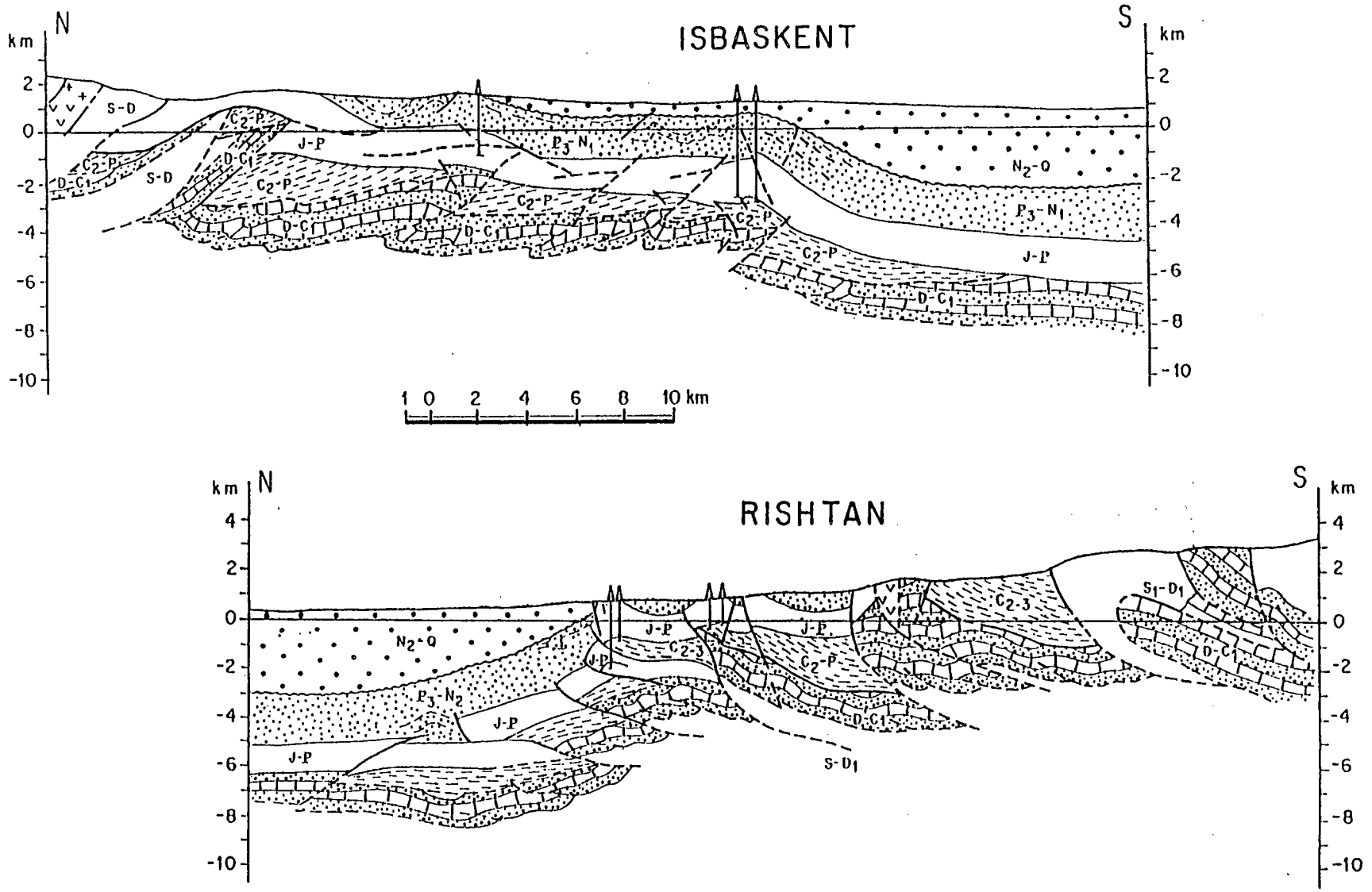

Fig. 8. Cenozoic thrusting and sedimentation at edges of Fergana basin, Kyrghyzstan (after Obukhov et al., 1990, with deep interpretation omitted).

Sections (approximately N-S) cross Isbaskent field (40° 59'N, 71° 12'E), at northern edge of basin (top), and Rishtan field (40° 22'N, 71° 16'E), at southern edge (bottom). Central part of basin is not shown. Sections are based on surface geology, wells (indicated) and seismic lines. Vertical scale equals horizontal scale. Sequences are Silurian to Devonian (S - D1), Devonian to Carboniferous (D - C1), Carboniferous (C2-3), Carboniferous to Permian (C2 - P), Jurassic to Paleocene (J - P), Eocene to Oligocene (P3 - N2) and Miocene to Quaternary (N22 - Q). Basin is bounded by thin-skinned thrust belts (above a Lower Paleozoic detachment), rooting into thick-skinned thrusts (not illustrated).

sediments, separated for convenience into two units, one of highly variable thickness (Pliocene to Recent), the other of less variable thickness (Massaget Fm., Oligocene-Miocene). On one of the seismic sections published by Obukhov et al. (1991), Neogene and even Paleogene reflectors may be seen to onlap the southern edge of the Fergana basin near Rishtan. A small basin formed in the Paleogene, between reverse faults of opposite vergence; then the structure became inactive and buried in the Neogene (Fig. 8). On stratigraphic evidence, folding and thrusting became more intense in the Pliocene. New active thrusts, marking the onlapping margin of the basin, appeared successively, by hangingwall propagation (overstacking), rather than by the more conventional piggy-back propagation (understacking). The Isbaskent and Rishtan fields are situated above Neogene thrust fronts, where hangingwall anticlines bring the Paleogene and even the Mesozoic to the surface.

Thin-skinned thrusting has occurred above a décollement surface in Silurian shales. Obukhov et al. (1991) have attributed the thrust belts to gravitational gliding, off the shoulders of rift valleys. We argue instead that they are due to crustal thickening. We suggest that, on each margin of the basin, the thin-skinned thrusts root into a major thick-skinned reverse fault, verging basinward and offsetting crystalline basement (not visible in Fig. 8).

At Tash-Kumyr, near the Isbaskent field, we recorded right-lateral strike-slip components, on faults trending east-west. On Landsat images of the southern margin of the Fergana basin, we have also seen evidence for right-lateral strike-slip. We therefore suspect that some of the faults visible in the sections (Fig. 8) may have right-lateral strike-slip components.

Structure-contour map on base of Tertiary

Because of its arid climate and numerous Cenozoic basins, Central Asia is probably one of the few regions of crustal thickening on Earth, where it is possible to draw a structure-contour map on the base of the Tertiary. We have drawn one for Kyrghyzia (Fig. 9). As a topographic base, we used the 1: 1 000 000 Operational Navigation Chart (sheet ONC-F6), published by the US Defense Mapping Agency. Fault traces we took from Fig. 2.

Our map is most accurate over the major basins, where there are boreholes and seismic data, supplemented by other geophysical data. In the Fergana basin, we took as a reference level the base of the marine Buchara beds (Paleocene). In Issyk-Kul, we used the base of either the Kokturpak or the Chonkurchak Fm. (Eocene). In Naryn, we used the base of the redbeds, supposedly Paleogene. Data are from Sadybakasov

Fig. 9. Structure-contour map on base of Tertiary, Kyrghyz Tien Shan.

Map compiled at Rennes by E.S. and P.R.C in 1991. Topographic base and geographical coordinates are from Operational Navigation Chart (sheet ONC F-6, scale 1:1 000 000, Lambert conformal conic projection), published by Defense Mapping Agency, St. Louis, Miss., USA. For locations and gridlines, see Fig. 2. Fault traces are from Fig. 2, simplified. Faults with reverse components have triangles pointing in direction of underthrusting. Contours are for altitude of base of Tertiary (Paleocene limestone in Fergana basin, Eocene shales in Issyk-Kul basin, base of Paleogene redbeds in Naryn basin, perched erosion surfaces in mountain ranges). Depths below -4000 m (dark grey) occur mainly in Fergana and Tarim basins, but also in Issyk-Kul, Naryn and Chu basins. Heights above 4000 m (light grey) occur on most ranges, but especially in the SE, next to Tarim basin.

(1991), Chedia (1986) and references therein, supplemented or modified by our own observations.

In the ranges, we first located all known outcrops of the base of the Tertiary. Then we identified old erosion surfaces, using field data from Sadybakasov (1991) and Chedia (1986), supplemented by Landsat images. These erosion surfaces are ubiquitous throughout the Tien-Shan and much of Central Asia. They are relatively smooth enveloping surfaces, cutting across Paleozoic structures, but broadly concordant with Paleogene and Mesozoic outliers (Fig. 10). Frequently, the surfaces have been tilted, folded or faulted. Locally, the old erosion surfaces are often highly dissected, as a result of late fluvial or glacial erosion; but they neverthless tend to be well preserved in areas of gentle relief. Small Tertiary basins, associated with minor reverse faults, are sometimes perched at altitudes of up to 4000 m. We do not claim that the old erosion surfaces are well dated. They may be of any age between Triassic and Paleogene. Nevertheless, the Paleogene succession lies concordantly on them with only small thickness variations.

From our structure-contour map, we infer that there have been differential vertical motions of up to 14 km during the Cenozoic. To some extent, these vertical motions are distributed in wavelike form, indicating flexure or buckling of the upper crust, possibly of the entire lithosphere. However, there are also sharp breaks across faults. At the southern edge of the Chu foreland basin, near Bishkek (Frunze), the vertical throw across the basin-bounding thrust zone is at least 6 km. On the northwestern edge of the Fergana basin, a vertical displacement of 11 km is distributed over a horizontal distance of at most 20 km and this spans at least one major basin-bounding thrust. Unfortunately, our data and our map do not always provide enough resolution for measuring vertical offsets across individual faults. Nevertheless, it is clear from the sedimentary record that these vertical offsets are mostly Neogene.

To estimate horizontal throws across thrust faults is an even bigger task, because fault dips are seldom constrained at depth. For this reason, we have not yet attempted to calculate crustal shortening and thickening, leaving the exercise for a future paper. Nevertheless, from our structure-contour map, Cenozoic shortening and thickening are distributed throughout the Tien-Shan in a rather penetrative way. Even though the rocks have not deformed in ductile fashion, faults are closely spaced at the scale of the area. Many of the faults are probably reactivated structures, Paleozoic or older.

Structure contours are sharply interrupted across the Talas-Fergana fault, confirming that this is indeed a major strike-slip fault. From rough estimates of shortening on each side, the Talas-Fergana fault has a right-lateral Cenozoic offset of a hundred kilometres or more, as suggested independently by paleomagnetic studies

Fig. 10. Tilting of Pre-Tertiary erosion surfaces, Naryn basin.

Locality is Karabulun valley, Baybiche basement ridge, southern edge of Naryn basin (41° 15' N, 75° 23' E).

Top photograph (view towards SW) shows planar erosion surface through Carboniferous limestones. Surface is now tilted about 30° SSE, as a result of Cenozoic tectonics. Such surfaces can be mapped on Landsat images. Road follows a deep but narrow gorge, cut through Baybiche basement ridge by Karabulun river.

Bottom photograph (view towards SW) shows basal Paleogene redbeds, dipping about 20° NW and resting on tilted erosion surface through Carboniferous limestones.

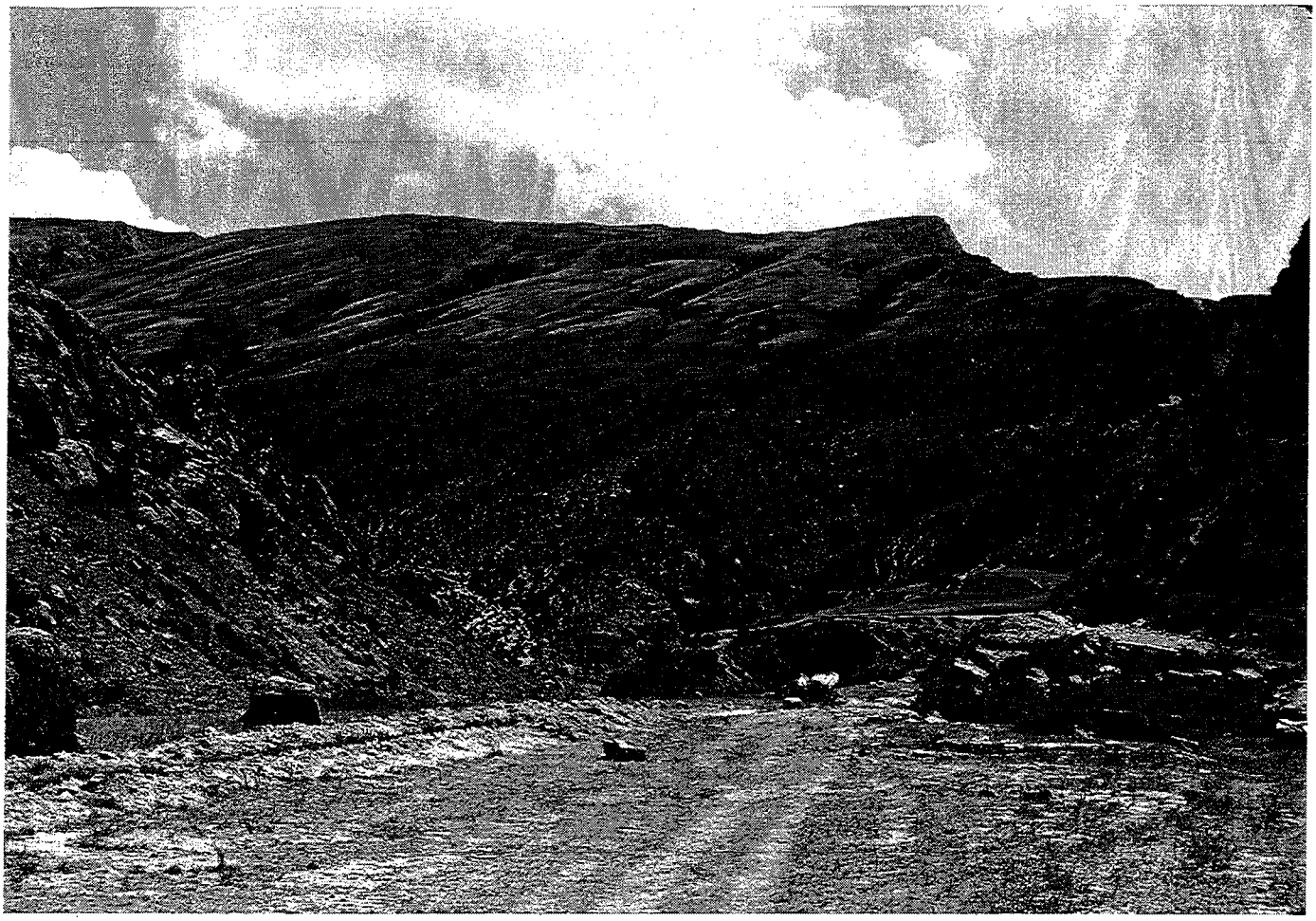


MJC 715

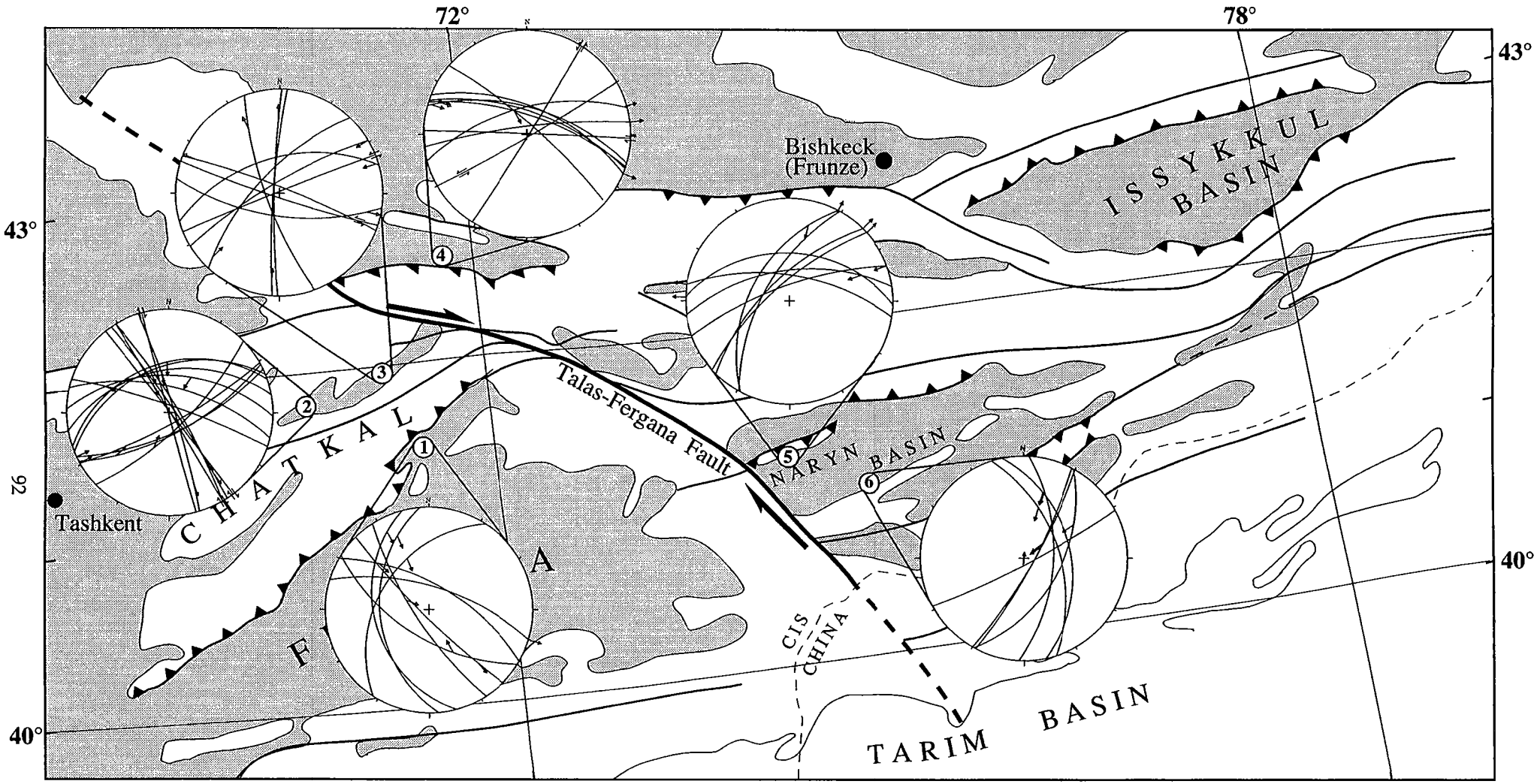

Fig. 11. Minor faults at 6 sites in Paleogene redbeds.
Background map shows main Cenozoic faults and basins (grey). Superimposed stereograms (lower hemisphere projection) show attitudes of faults (great circles) and striae (arrows indicating motion of hangingwall).

(Thomas et al., 1993a). Other strike-slip faults, especially left-lateral ones trending NE, seem to have little expression on our structure-contour map.

Styles of Cenozoic basins

During the Neogene, basins in the Kyrghyz Tien-Shan all appear to have developed in a context of transpression. Nevertheless, they have a variety of styles, both in section and in plan.

In section, basins lying on the edges of the Tien-Shan mountains are strongly asymmetric, being bounded on one side by major thrusts. They appear as typical foreland basins. Good examples are the Chu basin, around Bishkek (Frunze), and the West Ili basin, around Alma-Ata (Fig. 2). Intermontane basins tend to be more symmetric, some being bounded by reverse faults of opposite (basinward) vergences. Where the basins are narrow (less than 200 km or so), the thrust motions interfere. Flexure within the basin floor is inhibited, but subsidence is encouraged. This leads to narrow, deep, symmetric basins. In the Kyrghyz Tien-Shan, major basins of this style are Issyk-Kul and Fergana; but there are also many minor basins scattered throughout the region. Similar basins occur in neighbouring parts of Central Asia, especially Tajikistan (Thomas et al., 1993b) and the Chinese Tien-Shan (Windley et al., 1990). In general, we believe that such basins are common in a tectonic context of crustal shortening and thickening, be it due to continental collision, or to convergence of Andean type (Cobbold et al., 1993).

In plan, many basins in the Kyrghyz Tien-Shan have characteristically rhombohedral shapes. They seem to be due to basin-bounding faults with oblique motions (right-lateral reverse or left-lateral reverse). Clearly rhombohedral are Fergana and some of the minor basins lying along the Talas-Fergana fault. Other basins, like Issyk-Kul, are more elliptical. We believe that these rhombohedral and elliptical basins are characteristic of transpression.

Because of the limited exposure and thicknesses of Paleogene rocks, we know little about basin style during the Paleogene.

Minor Cenozoic faults

During our 1989 expedition, we measured fault-slip data for a total of 64 minor faults at 6 paleomagnetic sampling sites in Paleogene redbeds (Figs. 11 and 12) and 5 faults at one site in Neogene conglomerates (Fig. 13). The sites are from Fergana, Chatkal, Talas and Naryn basins. We were particularly careful to record data only for

those faults where the striae and the sense of slip were perfectly clear. All the striae were in fact imbricate crystal fibres, usually of calcite. None of the measured faults could be dated using stratigraphic criteria and all of them appeared to have formed after lithification. Despite the small number of faults and sampling sites, the data provide some insights into the tectonic history of the region. To our knowledge, no other comparable fault-slip data have been published for Kyrghyzia.

We were surprised to discover that most of the minor faults we observed in Paleogene redbeds were dominantly strike-slip. In contrast, most major faults offsetting the Paleogene sequence are dominantly reverse and dominantly Neogene, according to stratigraphic criteria. The 5 minor faults measured in Neogene conglomerates (site 4B, Fig. 13) are also dominantly reverse. Although our data are not numerous, they are sufficient for estimating principal directions of shortening, by the method of overlapping right-dihedra (Pfiffner and Burkhard, 1987). We have also used the method of Etchécopar et al. (1981) to estimate paleostresses. For one site in Paleogene redbeds (site 2, Fig. 12), we separated the 16 faults into two classes, dominantly strike-slip (11 faults), or dominantly reverse (5 faults).

From both methods of analysis, fault-slip data are mutually compatible at each site, yielding relatively well-constrained directions of maximum and minimum shortening (or compression). For all sites in Paleogene redbeds, the directions of maximum and minimum shortening, estimated by the method of right dihedra, are horizontal, showing that strike-slip faulting is dominant (Fig. 12). The direction of maximum shortening varies, from NW (for Fergana and eastern Talas basins), through N (western Chatkal basin) to NE (eastern Chatkal and western Naryn basins). Such a variation may result from (1) a heterogeneous stress field in the Paleogene; (2) rotations of faults and fault blocks about vertical axes since the Paleogene; or (3) a combination of both. These alternatives we discuss in the next section, in the light of paleomagnetic results.

For reverse faults in either Paleogene or Neogene sediments, the principal direction of shortening is nearer N-S (Fig. 13). This is compatible with the directions of thrusting measured or inferred for major Neogene faults (Fig. 2). It is also compatible with the current N-S direction of compressive stress, as deduced from seismicity and from surface breaks of active faults (Tapponier and Molnar, 1979).

Neither true normal faults, nor oblique-slip faults with normal components, appear to be common in the Kyrghyz Tien-Shan. Along the Talas-Fergana fault system, there are a few small Quaternary pull-apart basins, compatible with right-lateral wrenching (Burtman, 1961). At Toru-Aygyr, on the northwestern margin of Issyk-Kul basin, we observed a few small normal faults, dipping about 50° to the SSE. These are in sediments underlying unfaulted basalt flows of early Eocene age. We infer that the normal faults were active at this locality during the Eocene, but we do

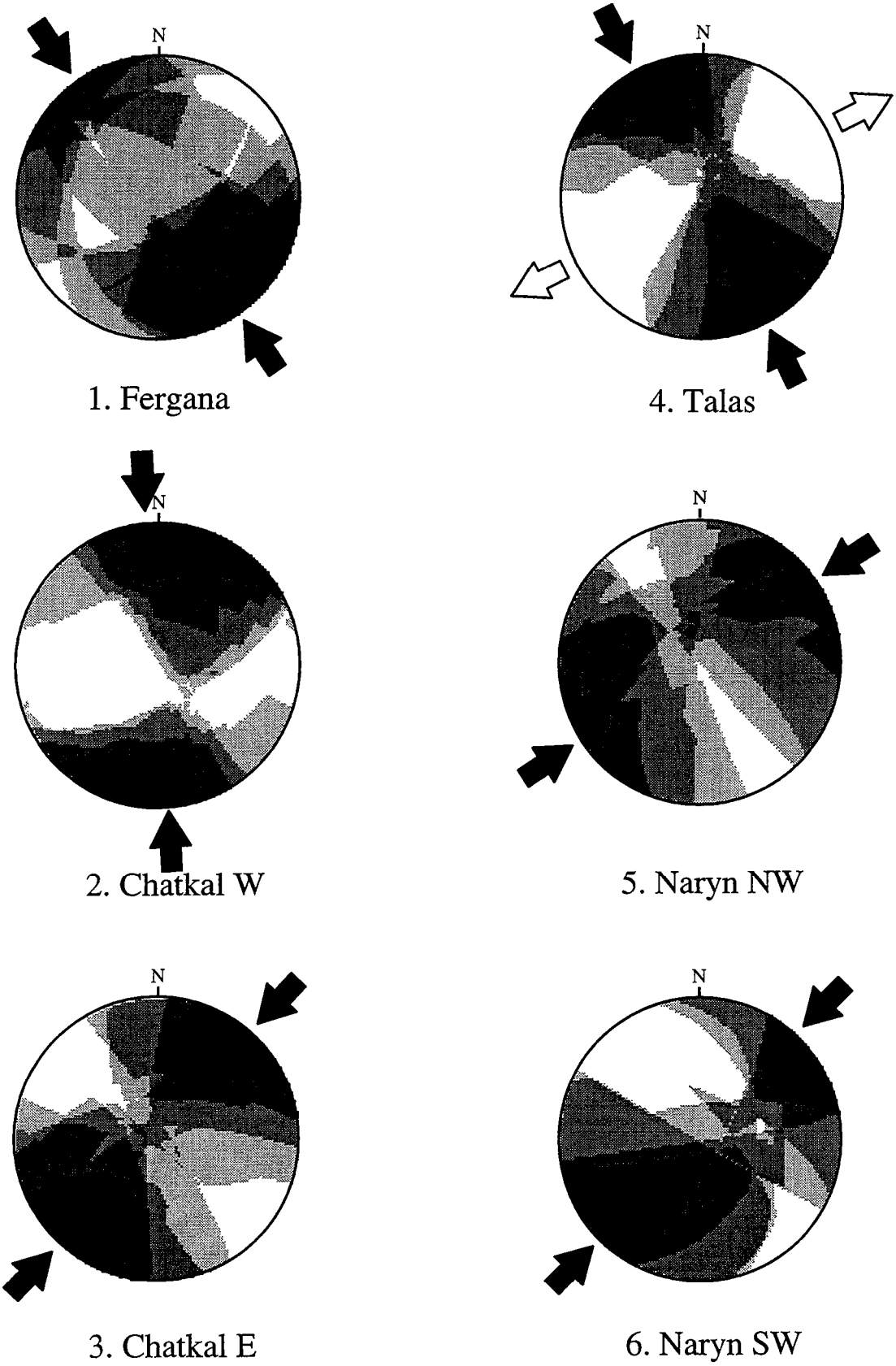

Fig. 12. Analysis of minor faults at 6 sites in Paleogene redbeds.
Stereograms (lower hemisphere projection) show right-dihedra of shortening, one for each fault, superimposed according to method of Pfiffner and Burkhard (1987). Shades of grey indicate number of superimpositions, coded in five classes, between all faults (black) and no faults (white). Principal directions of compression (black arrows) are from method of Etchécopar et al. (1981).

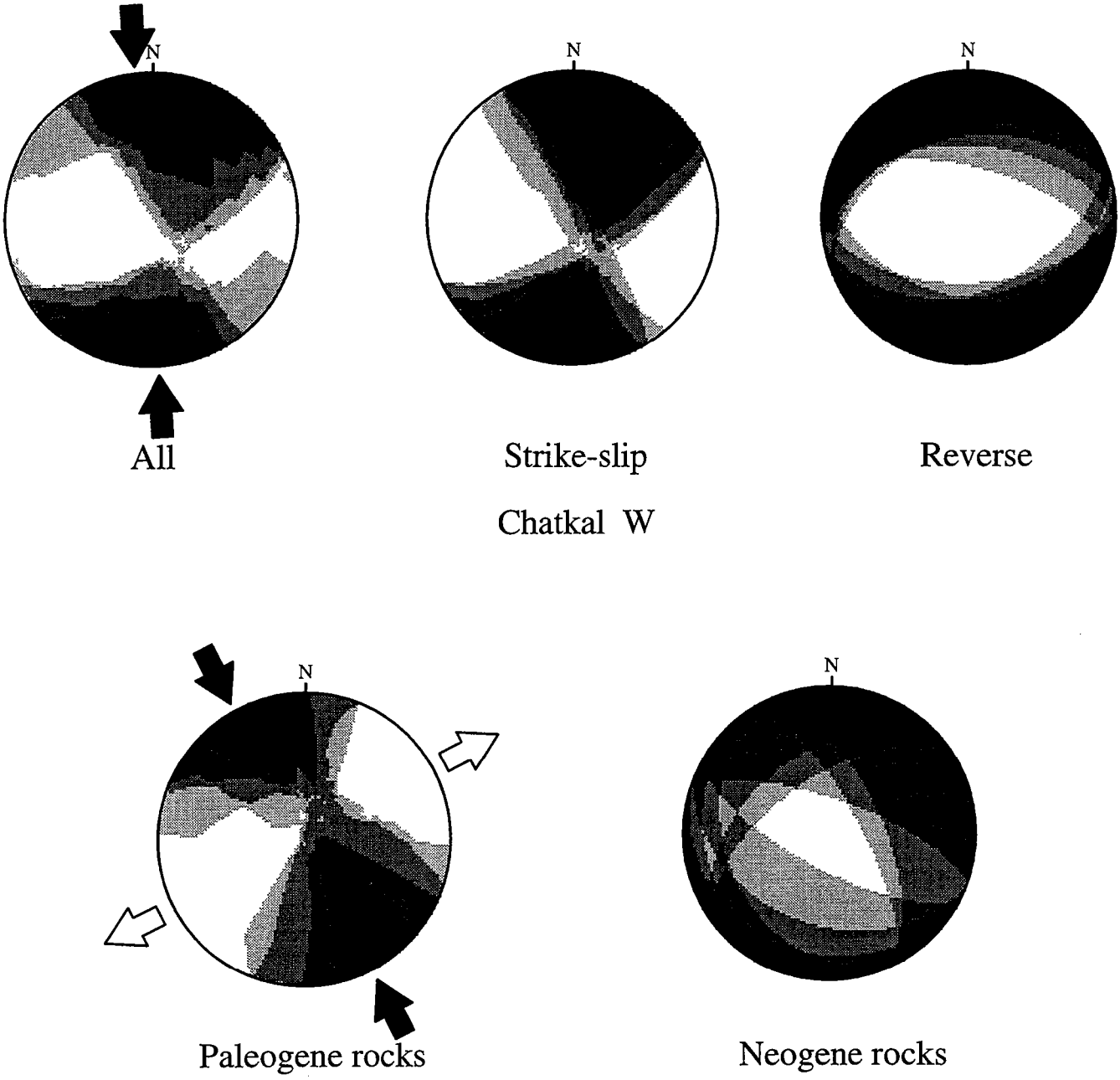

Fig. 13. Analysis of minor faults, classified as strike-slip or reverse
Stereograms (lower hemisphere projection) show right-dihedra of shortening, one for each fault, superimposed according to method of Pfiffner and Burkhard (1987). Shades of grey indicate number of superimpositions, coded in five classes, between all faults (black) and no faults (white). Principal directions of compression (black arrows) are from method of Etchécopar et al. (1981).
For site 2 (Chatkal W) in Paleogene redbeds (top), results for all faults (left) should be compared with results for strike-slip faults only (centre) or for reverse faults only (right).
Results for site 4 (Talas) in Paleogene redbeds (bottom left) should be compared with results for site 4B in Neogene sediments (bottom right).

not know if they reflect regional and thick-skinned extension, or purely local and thin-skinned extension.

Block rotations at various scales

From a recent paleomagnetic study of Paleogene sediments in the Kyrghyz Tien-Shan, Thomas et al. (1993a) concluded that remanant magnetism was acquired in the Oligocene and that since then there have been rotations about vertical axes at the scale of major basins.

In paleomagnetic studies of this kind, the sampling scale is of great importance. Let a basin vector be the mean of paleomagnetic vectors for all localities within that basin. A locality vector is the mean of paleomagnetic vectors from all sites for that locality (generally 6 or 7 sites per locality). Finally, a site vector is the mean of paleomagnetic vectors from all samples for that site (generally 6 or 7 samples per site).

For both Issyk-Kul and Fergana basins, locality vectors and sample vectors show acceptable degrees of scatter (Fig. 14). Hence it is possible to compare basin vectors. On that basis, the Fergana basin has rotated by a significant amount (20° ± 11° counterclockwise) with respect to the Issyk-Kul basin, since the Oligocene. From the triangular shape of the Chatkal range, we infer that a pole of relative rotation, between the Fergana basin and the Kazakhstan platform, lies at the southern tip of the range. On this basis, the shortening across the Chatkal range increases from zero in the S. to 110 ± 60 km in the N. The latter value is also a good estimate for the left-lateral strike-slip displacement on the Talas-Fergana fault (Thomas et al., 1993a).

For the Naryn basin, there is considerable scatter amongst locality vectors (Fig. 14). Hence the Naryn basin does not appear to have behaved as a single rigid block and no conclusions can be drawn as to its overall rotation. Furthermore, for two localities in the Naryn basin, there is considerable scatter amongst site vectors, even though, for each site, sample vectors show acceptable scatter. One interpretation for scatter of this kind is that it is of magnetic origin, due for example to secular variation. Another interpretation is that scatter is due to differing amounts of block rotation about vertical axes. This may occur at basin scale, or even conceivably at locality scale.

In the Kyrghyz Tien-Shan, we measured fault-slip data wherever possible at the scale of paleomagnetic sites. For the 5 sites where fault-slip data and reliable paleomagnetic data are simultaneously available, the azimuths of compression directions, calculated by the method of Etchécopar et al. (1981), seem to correlate with the azimuths of paleomagnetic site vectors (Fig. 15). In particular, where one is clockwise (or anticlockwise), so is the other. It is therefore possible that strike-slip faults formed in the Paleogene, together with the paleomagnetism, and that they both

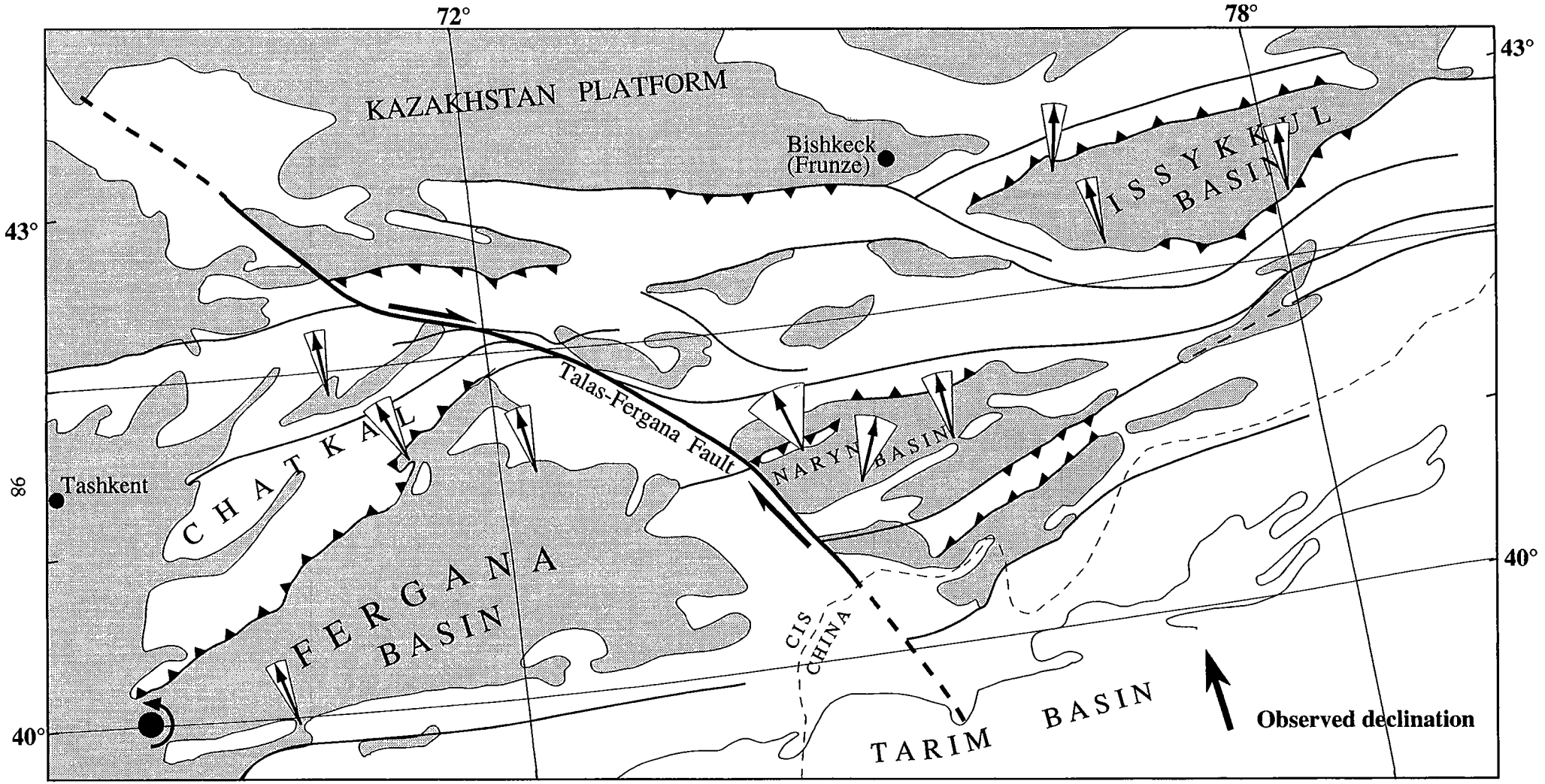

Fig. 14. Paleomagnetic results on Tertiary formations (after Thomas et al., 1993a).
Background map shows main Cenozoic faults and basins (grey). Superimposed are mean declinations (arrows) and confidence limits (white sectors) of paleomagnetic vectors for 10 localities in Paleogene redbeds or lavas, after thermal and AC cleaning. For both Fergana and Issyk-Kul basins, locality vectors show little scatter. Fergana basin is therefore inferred to have rotated 20° ± 11° counterclockwise, with respect to Issyk-Kul basin. From structural data, pole of relative rotation is inferred to be at southern tip of Chatkal range (black dot with circular arrow). For Naryn basin, locality vectors show much more scatter. Hence rotation of Naryn basin, relative to Issyk-Kul basin, cannot be estimated with confidence.

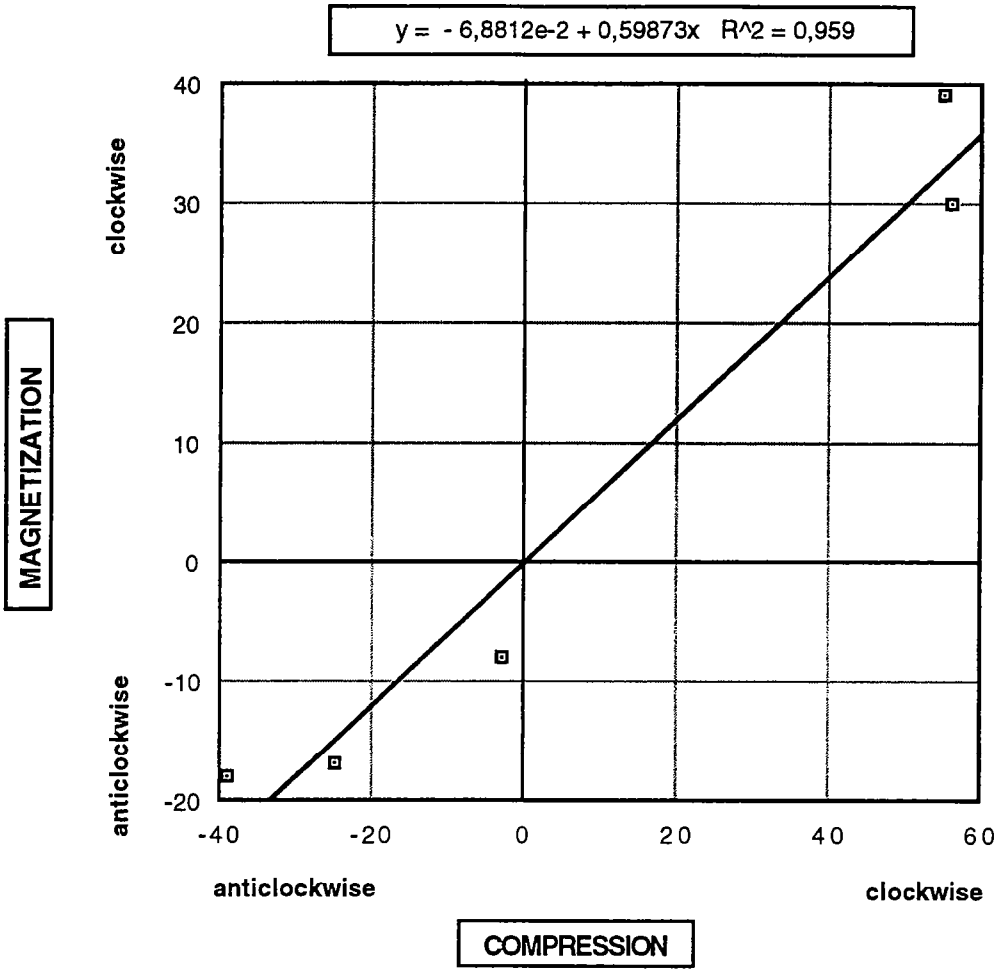

Fig. 15. Azimuth of magnetization vector (in degrees) versus azimuth of principal direction of compression (in degrees), for 5 sites in Paleogene redbeds.

Compression direction was calculated from fault-slip data by method of Etchécopar (see Fig. 13). Magnetization vectors are from Thomas et al. (1993a). Sites are Fergana (1, FE, FG), Chatkal W (2, FM, FN), Talas (4, TC, TE, TF, TG), Naryn NW (5, NT) and Naryn SW (6, NN), where the numbers in the brackets refer to the fault-slip sites of Fig. 11 and the letters refer to the paleomagnetic sites of Thomas et al. (1993a, tables 3, 4 and 5).

This plot raises the possibility that the minor faults formed in the Paleogene and became rotated about vertical axes (see text).

rotated during the Neogene. If so, the compression axes are, in fact, paleocompression axes, no longer in their original orientations.

Assuming that paleomagnetic declinations are reliable for each site, we can rotate them into parallelism with the reference direction (that of Issyk-Kul basin), thus restoring the azimuths of the paleocompression axes. The restored compression directions become more uniform and more nearly N-S. This makes them comparable with Neogene and current compression directions.

Because of the limited numbers of sites and of faults, we do not claim to have proved, either rotation of strike-slip faults in Paleogene redbeds, or the Paleogene ages of such faults. Nevertheless, these must be considered serious possibilities, to be verified if possible in the future. As for the technique of correlating fault-slip data and paleomagnetism, it may be worth testing in other regions as well, if enough data are available; but, for this, the sampling scales should be carefully monitored.

Cenozoic history of deformation

From our studies of major faults, minor faults and sedimentary thicknesses, we infer that thrusting and crustal thickening were dominant in the Neogene, as they are today. Nevertheless, there was also significant wrenching, in response to transpression. This tectonic context appears to have been responsible for the rombohedral or elliptical shapes of many basins. The shortening direction was nearly N-S. The component of wrenching was left-lateral along the Kyrghyz Tien-Shan, accounting perhaps for the counterclockwise rotation of the Fergana basin.

Stratigraphic thicknesses and vertical offsets on major faults are much smaller for the Paleogene than they are for the Neogene. Nevertheless, small reverse faults have been inferred from seismic data (Fig. 8). Minor faults observed in Paleogene rocks are mostly strike-slip. There is a possibility that they underwent rotations about vertical axes, together with Paleogene paleomagnetic vectors. If so, wrenching may have been more dominant in the Paleogene. The principal direction of shortening may have been nearly N-S, as it was later.

Northwestern China and western Mongolia are currently areas of active strike-slip tectonics with little associated crustal thickening (Tapponier and Molnar, 1979). From focal mechanisms of earthquakes, the shortening direction is NNE. This raises an intriguing possibility: that the Tien-Shan was in a similar strike-slip context during the Paleogene, but that since then it has been overtaken by crustal thickening. The new tectonic context may have migrated northeastwards through the region, together with an indenting India. Such a migration of deformational styles through an indented

medium has indeed been observed in experiments with physical models (Davy and Cobbold, 1988).

Conclusions

From our studies, we draw the following conclusions on the history of deformation and basin development in the Kyrghyz Tien-Shan.

1. Cenozoic deformation is pervasive throughout the Kyrghyz Tien-Shan. It has resulted in many basins, both major and minor.

2. During the Paleogene, vertical displacements nowhere exceeded about ±1 km. Continental redbeds accumulated in shallow basins. Reverse faulting occurred, but strike-slip faulting may have dominated, with a principal direction of shortening oriented nearly N-S.

3. During the Neogene, reverse faulting, folding and crustal thickening dominated. The principal direction of shortening was nearly N-S. Vertical displacements attained as much as ±7 km. Rates of erosion increased. Basins became infilled with large thicknesses of alluvial and lacustrine sediments. Strike-slip faulting on the Talas-Fergana fault was accompanied by counterclockwise rotation of the Fergana basin, relative to Issyk-Kul. The overall tectonic context was one of left-lateral transpression across the Kyrghyz Tien-Shan.

4. Neogene basins are commonly bounded by reverse faults. Foreland basins (such as Chu) are asymmetric in section, being bounded by one major fault. Intermontane basins (such as Issyk-Kul, Naryn and Fergana) are more symmetric, being bounded by faults of opposite (basinward) vergences.

5. In plan, some basins have rhombohedral shapes, probably as a result of oblique-slip (strike-slip and reverse) motions on boundary faults.

Acknowledgements.- The memorable 1989 expedition to the Kyrghyz Tien-Shan was organized by V.S. Burtman and M.L. Bazhenov. It was part of a paleomagnetic project, jointly financed by the Academy of Sciences (ex-USSR) and the CNRS (International Division). The 1991 expedition was jointly financed by the Kyrghyz Academy of Sciences and Géosciences Rennes. E.S. acknowledges further support from Géosciences Rennes for a 5-month visit there in 1990. The Programme National de Télédétection Spatiale (CNRS) provided funds for Landsat tapes. Jean Letouzey kindly arranged for the Institut Français du Pétrole to provide coloured Landsat prints. We have benefitted from discussions with B. Coletta (Institut Français du Pétrole), Professor V.E. Khain (Lomonosov State University, Moscow), Dr. A.N. Obukhov (IGIRGI, Moscow), Dr. R.H. Graham (BP) and A. Wright (BP).

References

Achache, J., Courtillot, V and Zhou, Y.X. 1984. Paleogeographic and tectonic evolution of southern Tibet since middle Cretaceous time: new paleomagnetic data and synthesis. *Journal of Geophysical Research*, 89, B12, 10311-10339.

Argand, E. 1924. La tectonique de l'Asie. *Congrès Géologique International, Comptes Rendus de la XIII Session, Belgique, 1922*, 1, 171-371.

Bakirov, A.B. and Burtman, V.S. (compilers). 1984. *International Geological Congress, 27th Session, Moscow, Guidebook for Excursion 032: Tectonics of the Tien Shan Variscides.* Kyrghyzstan Publishing House, Frunze (Bishkek), Kyrghyzstan, 74 pp.

Bazhenov, M.L., 1993. Cretaceous paleomagnetism of the Fergana basin and adjacent ranges: tectonic implications. *Tectonophysics* (submitted).

Burov, E.V., Kogan, M.G., Lyon-Caen, H. and Molnar, P. 1990. Gravity anomalies, the deep structure and dynamic processes beneath the Tien Shan. *Earth and Planetary Science Letters*, 96, 367-383.

Burtman, V.S. 1961. On the Talasso-Fergana strike-slip fault (in Russian). *Bulletin of the Academy of Sciences of the USSR, Geology Section*, 12, 37-48.

Burtman, V.S. 1975. The structural geology of the Variscan Tien Shan, USSR. *American Journal of Science*, 275-A, 157-186.

Burtman, V.S. 1980. Faults of Middle Asia. *American Journal of Science*, 280, 725-744.

Chedia, O.K. 1986. *Morphology and neotectonics of the Tien-Shan* (in Russian). Ilim Publications, Frunze (Bishkek), Kyrghyzstan, 313 pp.

Cobbold, P.R., and Davy, P. 1988. Indentation tectonics in nature and experiment. 2. Central Asia. *Bulletin of the Geological Institutions of the University of Uppsala*, N.S. 14, 143-162.

Cobbold, P.R., Gapais, D., Lecorre, C., Rossello, E.A., Thomas, J.C., Tondji Biyo, J.J. and de Urreiztieta, M. 1993. Sedimentary basins and crustal thickening. *Sedimentary Geology* (in press).

Davy, P., and Cobbold, P.R. 1988. Indentation tectonics in nature and experiment. 1. Experiments scaled for gravity. *Bulletin of the Geological Institutions of the University of Uppsala*, N.S. 14, 129-141.

Dewey, J.F. and Burke, K.C.A. 1973. Tibetan, Variscan and Precambrian reactivation: Products of continental collision. *Journal of Geology*, 81, 683-692.

Dewey, J.F., Cande, S. and Pitman, W.C. 1989. Tectonic evolution of the India/Eurasia collision zone. *Eclogea Geologicae Helv*eticae, 82 (3), 717-734.

England, P.C. 1982. Some numerical investigations of large-scale continental deformation. In: *Mountain Building Processes (edited by K. Hsu)*, Academic Press, Orlando, Florida, 129-139.

England, P., and Molnar, P. 1990. Right-lateral shear and rotation as the explanation for strike-slip faulting in eastern Tibet. *Nature*, 344, 140-142.

Etchécopar, A., Vasseur, G. and Daignières, M. 1981. An inverse problem in microtectonics for the determination of stress tensors from fault striation analysis. *Journal of Structural Geology*, 3, 51-65.

Gubin, I.E. (editor) 1986. *The lithosphere of the Tien-Shan* (in Russian). Nauka, Moscow, 155 pp.

Hendrix, M.S., Graham, S.A., Carroll, A.R., Sobel, E.R., McKnight, C.L., Schulein, B.J. and Wang, Z. 1992. Sedimentary record and climatic implications of recurrent deformation in the Tian Shan: Evidence from Mesozoic strata of the North Tarim, south Junggar, and Turpan basins, northwest China. *Geological Society of America Bulletin*, 104, 53-79.

Houseman, G and England, P. 1986. Finite strain calculation of continental deformation 1. Method and general results for convergent zones. *Journal of Geophysical Research*, 91, 3651-3663.

Kalvoda, J., Leonov, Yu.G. and Nikonov, A.A. 1987. Main features of the neotectonic evolution of the Pamirs-Thyan Shan and the Karakoram-Himalayas mountain ranges. *Acta Montana*, 77, 65-84.

Khain, V.E., Sokolov, B.A., Kleshchev, K.A. and Shein, V.S. 1991. Tectonic and geodynamic setting of oil and gas basins of the Soviet Union. *American Association of Petroleum Geologists Bulletin*, 75 (2), 313-325.

Krilov, A.Y. 1960. Absoulte ages of rocks from the Central Tien Shan and application of Argon methods to metamorphic and sedimentary rocks (in Russian). In: *Determination of the absolute ages of Pre-Quaternary formations* (edited by I.E.Starik), Moscow, 222-224.

Ministry of Geology of the USSR and Kyrghyz Academy of Sciences. 1978. *Geological map of the Kyrghyz SSR*. Scale: 1: 500 000. Six sheets.

Molnar, P., and Tapponnier, P. 1975. Cenozoic tectonics of Asia: effects of a continental collision. *Science*, 189, 419-426.

Obukhov, A.N., Shedaldin, B.P., Gorshenin, E.B., Musaev, C.I. and Silits, A.M. 1991. A rifting origin for the intermontane basins of the Central Asian orogenic belt (in Russian). Name of journal not known.

Patriat, P. and Achache, J. 1984. India-Asia collision chronology has implications for crustal shortening and driving mechanism of plates. *Nature*, 311, 615-621.

Peltzer, G. and Tapponnier, P. 1988. Formation and evolution of strike-slip faults, rifts and basins during India-Asia collision: an experimental approach. *Journal of Geophysical Research,* 93, B12, 15085-15117.

Pfiffner, O.A. and Burkhard, M. 1987. Determination of paleo-stress orientation from fault, twin and earthquake data. *Annales Tectonicae,* 1, 48-57.

Sadybakasov, E. 1972. *Neotectonics of the central Tien-Shan* (in Russian). Ilim Publications, Frunze (Bishkek), Kyrghyzstan, 117 pp.

Sadybakasov, E. 1991. *Neotectonics of High Asia* (in Russian, with English abstract). Nauka, Moscow, 181 pp.

Schulz, S.S. 1948. *Analysis of the neotectonics and relief of the Tien Shan* (in Russian). Geografgiz, Moscow, 222 pp.

Sidorenko, A.V. (editor). 1972 *Geology of the USSR* (in Russian). Nedra Publications, Moscow, 85 (1), 280 pp.

Tapponier, P., Peltzer, G., Le Dain, A.Y., Armĭjo, R., and Cobbold, P.R. 1982. Propagating extrusion tectonics in Asia : new insights from simple experiments with plasticine. *Geology,* 10, 611-616.

Tapponnier, P. and Molnar, P. 1979. Active faulting and Cenozoic tectonics of the Tien-Shan, Mongolia and Baykal regions. *Journal of Geophysical Research,* 84, B7, 3425-3459.

Thomas, J.C., Perroud, H., Cobbold, P.R., Bazhenov, M.L., Burtman, V.S., Chauvin, A. and Sadybakasov, E. 1993a. A paleomagnetic study of Tertiary formations from the Kyrghyz Tien-Shan and its tectonic implications. *Journal of Geophysical Research* (in press).

Thomas, J.C., Gapais, D., Cobbold, P.R., Meyer, V. & Burtman, V.S. 1993b. Tertiary kinematics of the Tadjik depression: inferences from fault and fold patterns. In: *Geodynamic evolution of sedimentary basins* (edited by F. Roure), Editions Technip, Paris (in press).

Turdukulov, A.T. 1987. *Geology of the Paleogene and Neogene of North Kyrghyzia* (in Russian). Ilim Publications, Frunze (Bishkek), Kyrghyzstan, 264 pp.

Wallace, R.E. 1976. The Talas-Fergana fault, Kirghizia and Kazakhstan. *Earthquake Information Bulletin,* 8 (4), 4-13.

Windley, B.F., Allen, M.B., Zhang, C., Zhao, Z-Y and Wang, G-R. 1990. Paleozoic accretion and Cenozoic redeformation of the Chinese Tien Shan range, central Asia. *Geology,* 18, 128-131.

Yablonskaya, N.A. 1989. Tectonic structure of the southern Tien Shan and stages of its formation (in Russian). *Geotektonika,* 1, 61-71.

CHAPITRE III

la dépression Tadjik : Paléomagnétisme et cinématique tertiaire

1. Introduction - résumé

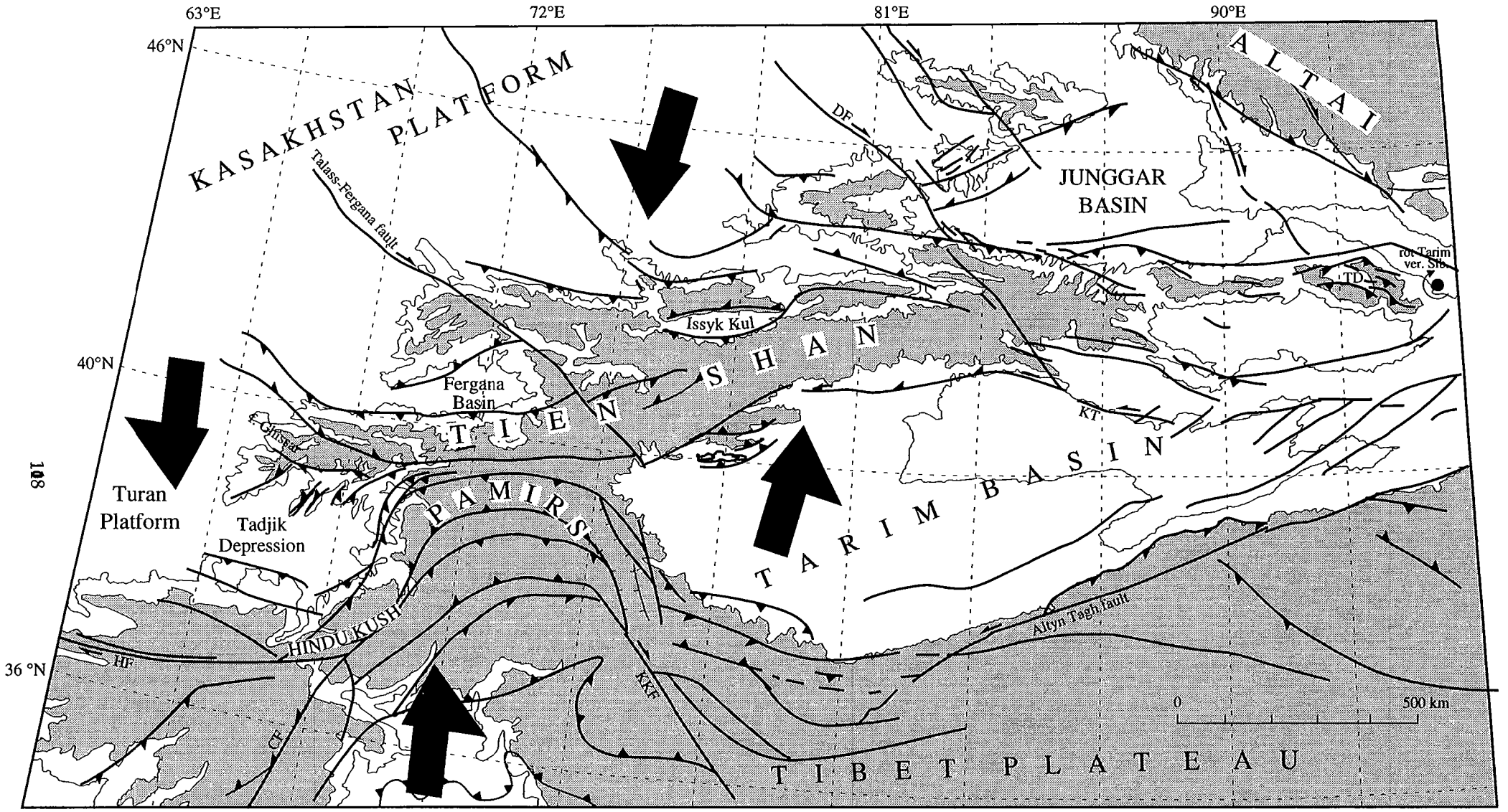

Figure III.1. Carte tectonique de l'Asie Centrale et contours topographiques à 1000 m et 2000 m (adaptée d'après Avouac et al., 1993).

Toutes les failles sont considérées comme ayant été actives à un moment ou à un autre au cours du Tertiaire. Les flèches noires représentent le contexte cinématique régional (Cobbold et Davy, 1988). CF : faille de Chaman ; DF : faille de Junggar; HF : faille de l'Hérat ; KKF : faille du Karakorum ; KT : faille de Kurk-Tag ; TD : dépression de Turfan.

Dans cette partie, je présente les données régionales nécessaires pour la compréhension de la structuration et de la cinématique Tertiaire de la dépression Tadjik. Un contexte géologique complet est proposé dans la quatrième partie de ce chapitre.

1.1. Contexte géologique de la déformation Cénozoïque

La dépression Tadjik est un large bassin intramontagneux rempli d'une épaisse série sédimentaire Méso-Cénozoïque et traversé par une succession de chaînons anticlinaux concentriques (Figures III.1 et III.2a). La structuration, d'âge Cénozoïque, est étroitement associée aux zones faillées qui limitent la dépression, à savoir, le Pamir et l'Hindou Koush à l'Est, le Ghissar au Nord, le S-O Ghissar à l'Ouest et la faille de l'Alburz au Sud. Voyons tout d'abord leurs principales caractéristiques.

Contrairement au Tien Shan qui est un chaîne linéaire, les massifs du Pamir et de l'Hindou Koush, situés au Nord de la syntaxe du Pakistan, présentent une forme générale courbe, probablement acquise au cours du Tertiaire suite au poinçonnement de l'Inde dans l'Asie (Tapponnier et al., 1981 ; Bazhenov et Burtman, 1986). D'après les mécanismes au foyer des séismes (Billington et al., 1977 ; Chatelain et al., 1980 ; Roecker et al., 1980) et la cinématique globale (De Mets et al., 1990), la direction de raccourcissement régionale actuelle est N-S à NNO-SSE. Cette région est caractérisée par une intense activité sismique de profondeur intermédiaire (70-300 km de profondeur) définissant deux zones à plongements respectifs opposés vers le Nord et vers le Sud (Billington et al., 1977). Son origine, bien que controversée, pourrait refléter l'extrémité Nord de la subduction lithosphérique de l'Inde sous l'Asie, ainsi que la néosubduction vers le sud, de la dépression Tadjik et du Tien Shan sous le Pamir (Tapponnier et al., 1981 ; Mattauer, 1986 ; Hamburger et al., 1992). On considère que le plateau du Pamir a subi un raccourcissement Cénozoïque total d'au moins 200 km (Peive et al., 1964 ; Burtman and Molnar, 1992) et un épaississement crustal associé amenant le Moho à une profondeur moyenne de 60 km. Le déplacement N-S du Pamir par rapport à la Sibérie a été accommodé sur ses bordures par la faille décrochante dextre du Karakorum à l'Est, et le décro-chevauchement sénestre de Darvaz-Karakul à l'Ouest. Cette dernière faille, qui constitue la limite Est de la dépression Tadjik, devient principalement chevauchante sur la bordure nord du Pamir. Elle est également considérée comme l'extension Nord de la faille de Chaman (Trifonov, 1978) (Figure III.1) qui accommode en

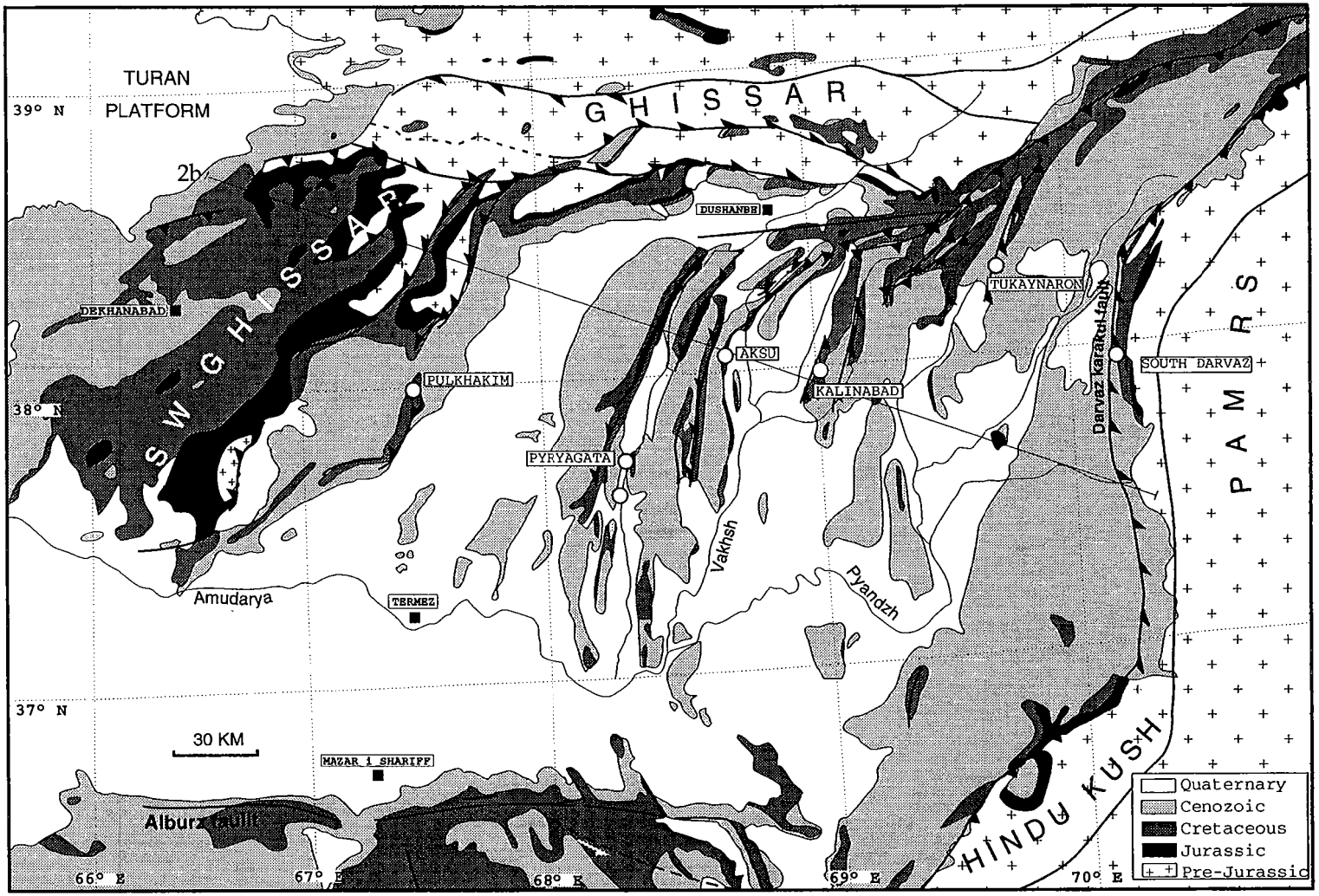

Figure III.2a. Carte géologique de la dépression Tadjik et des régions adjacentes.
Les cercles blancs situent les localités paléomagnétiques Tertiaires (cf. Etude paléomagnétique).

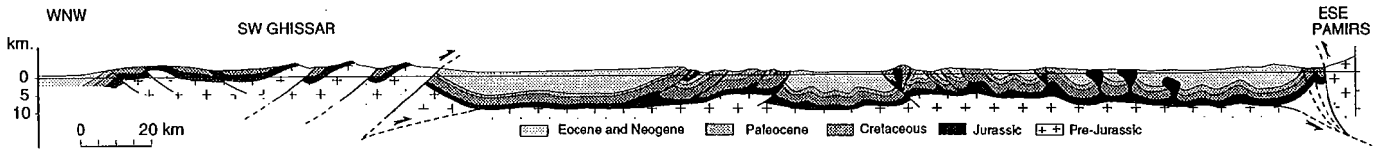

Figure III.2b. Coupe géologique à travers la dépression Tadjik (d'après Zakharov 1958, 1/500.000 geological map of Tadjikistan et observations de terrain).
Localisation sur la figure III.2a

Afghanistan et au Pakistan l'indentation de l'Inde dans l'Asie. Le jeu transpressif sur la faille de Darvaz-Karakul fait chevaucher le Pamir et l'Hindou Koush sur les sédiments Tertiaires de la dépression Tadjik.

Le Ghissar, au Nord de la dépression Tadjik, marque l'extrémité sud-ouest du Tien Shan et constitue une zone décro-chevauchante dextre majeure. Ce mouvement est synthétique de la faille de Talass-Fergana (Figures III.1 et I.3) et s'inscrit dans la continuité des décrochements dextres de la zone Pamir Baïkal (Cobbold et Davy, 1988). La composante chevauchante est responsable d'un mouvement vertical relatif par rapport à la dépression Tadjik de 7 à 8 km et d'un épaississement crustal mettant le Moho à 45-50 km de profondeur (Burov et al., 1990).

Le Sud-Ouest Ghissar qui sépare la dépression Tadjik de la plate-forme stable de Turan présente une tectonique principalement compressive. Dans le secteur Nord-Est (Figure III.2a), une série de chevauchements à vergence Est fait reposer le socle Paléozoïque cristallin sur les sédiments Tertiaires de la dépression. Un seul chevauchement de ce type se prolonge dans le secteur Sud, révélateur d'une augmentation du raccourcissement E-O à travers le Sud-Ouest Ghissar, depuis son extrémité sud jusqu'à sa jonction avec le Ghissar.

Enfin, la dépression Tadjik est bordée au Sud par la faille de l'Alburz qui marque le début du Turkestan Afghan s'étendant jusqu'à la faille de l'Hérat. La faille de l'Alburz est probablement une faille normale d'âge triasique, réactivée au cours du Tertiaire (Boulin, 1988). Un mouvement principalement chevauchant vers le Nord apparaît sur la carte géologique (Ministry of Geology of the USSR and Tadjik Academy of Sciences, 1984). De plus, l'orientation NNO-SSE de quelques plis qui se branchent sur sa partie est (Figure III.2a), et une série de plis en échelon directement au Sud suggèrent également une composante décrochante sénestre.

A l'intérieur de la dépression Tadjik, la déformation est intense dans la zone de convergence entre le Pamir et le Tien Shan où se situent les chaînes de Peter the First et de Vaksh (Leith et Alvarez, 1985; Leith et Simpson, 1986 ; Hamburger et al., 1992), et distribuée sur de larges plis plus espacés dans la partie centrale de la dépression (Figure III.2a). En règle générale, ces plis sont faillés sur un flanc et chevauchent les bassins qu'ils limitent (Figure III.2b). La couverture sédimentaire Méso-Cénozoïque est d'épaisseur maximale au centre de la dépression ainsi que le long du Pamir et du Sud-Ouest Ghissar où elle peut atteindre 10 à 12 km. Ces deux derniers dépocentres sont typiques d'une flexuration liée aux chevauchements du socle du Pamir et du S-O Ghissar vers l'intérieur de la dépression.

Deux domaines structuraux caractérisent la dépression Tadjik :

- Les chevauchements de la partie Ouest de la dépression sont à vergence Est, synthétiques des chevauchements du Sud-Ouest Ghissar.

- Les chevauchements de la partie Est de la dépression sont à vergence Ouest, synthétiques de la faille de Darvaz-Karakul (Figure III.2b).

Le centre de la dépression forme une structure en "pop-down". les chevauchements s'enracinent dans un niveau de décollement évaporitique majeur d'âge Jurassique supérieur (Leith et Alvarez, 1985). La sismicité, principalememt localisée au dessus de 10 km de profondeur (Leith et Simpson, 1986) montre clairement que la plus grande partie de la déformation dans la dépression est localisée au dessus de ce niveau de décollement. La nature du socle ant-jurassique de la dépression Tadjik est encore inconnue.

Tout comme pour le Tien Shan, le Miocène est marquée par un important apport de sédiments d'origine continentale soulignant le début de la phase majeure de déformation Tertiaire et la surrection des reliefs avoisinants.

1.2. Principaux résultats

1.2.1. Etude paléomagnétique

Environ 500 carottes ont été prélevées depuis le bord du Pamir jusqu'au Sud-Ouest Ghissar dans 6 localités constituées de grès rouges d'âge Miocène inférieur (Figure III.2). Cinq localités ont fournis de bons résultats, où l'aimantation de haute température mesurée a été acquise avant le plissement. Un échantillonnage des séries rouges d'âge Crétacé réalisé de façon conjointe fait l'objet d'une autre étude (annexe 2, Bazhenov et al., soumis).

Les inclinaisons mesurées présentent une anomalie comparable à celle observée dans le Tien Shan Kirghiz. Elles sont en moyennes 30° plus faibles que celles déduites de la courbe de dérive apparente du pôle de Besse et Courtillot (1991). Nous avons par ailleurs prélevé des sédiments Miocènes à Dekhanabad, sur la bordure Ouest du Sud-Ouest Ghissar, en marge de la plate forme stable de Turan (Chauvin et al., 1992). Cette zone est très peu déformée et les données paléomagnétiques obtenues sur des échantillons Crétacé de la même région ne montrent pas de rotation significative. La direction moyenne mesurée à Dekhanabad, qui présente une anomalie d'inclinaison identique à celle observée dans la dépression, a donc été choisie comme référence

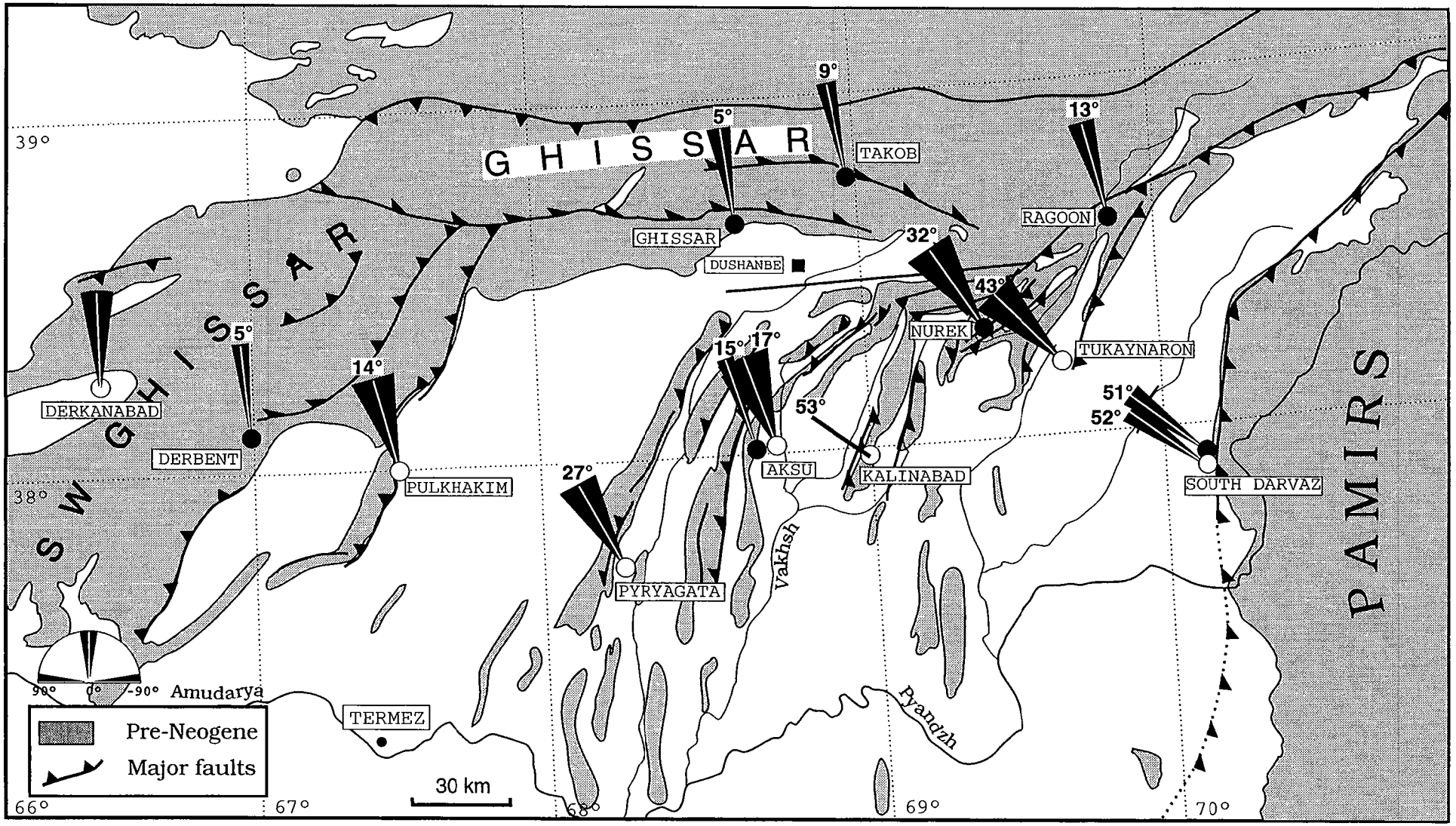

Figure III.3. Compilation des rotations paléomagnétiques pour la dépression Tadjik.
Les cercles blancs indiquent les rotations mesurées dans les sédiments Tertiaires (2nd partie de ce chapitre), les cercles noirs, les rotations dans les sédiments Crétacés. Les rotations (la valeur exacte est indiquée) et leur incertitude sont toutes représentées par rapport à une direction de référence N-S.

paléomagnétique locale (cette donnée ainsi que la discussion du problème de l'inclinaison sont présentés en détail en annexe 1).

Dans la dépression, les rotations paléomagnétiques Tertiaires calculées par rapport à Dekhanabad apparaissent toutes antihoraires mais leur intensité est très variable d'une localité à l'autre (Figure III.3). Deux domaines géographiques peuvent être distingués :

1. Dans la partie Est de la dépression, aux localités de Tukaynaron, Kalinabad et South Darvaz, les rotations paléomagnétiques antihoraires sont fortes (46°±14°, 54° et 52°±13°, respectivement).

2. Dans la partie Ouest, aux localités d' Aksu, Pulkhakim et Pyryagata, les rotations antihoraires sont plus faibles (17°±16°, 14°±15° et 27°±14° respectivement)

Les données paléomagnétiques Crétacées de la bibliographie (Pozzi et Feinberg, 1991) et acquises dans le cadre de cette étude (Bazhenov et al., annexe 2) permettent de préciser et de compléter ces observations, particulièrement pour les domaines en bordure de la dépression. En effet, aux localités de South Darvaz et Aksu, les rotations Tertiaires obtenues dans les sédiments Crétacés sont très proches de celles obtenues dans les sédiments Tertiaires. De plus, les rotations paléomagnétiques apparaissent faibles à nulles dans le Sud-Ouest Ghissar (5°±5°) et dans le Ghissar (5°±5° à Ghissar, 9°±6° à Takob).

Plusieurs conclusions peuvent d'ores et déjà être tirées:

- La similitude des rotations dans le Crétacé et le Tertiaire implique qu'il n'y a pas eu de rotations significatives entre le Crétacé Supérieur et le Miocène Inférieur. Les rotations sont donc principalement associées à la phase de déformation majeure Néogène.
- Les domaines géographiques de rotations paléomagnétiques correspondent aux domaines structuraux Est et Ouest de la dépression identifiés à partir de la vergence des chevauchements.
- La diminution importante des rotations de l'Est vers l'Ouest souligne l'influence majeure du poinçonnement du Pamir dans l'Asie sur la déformation dans la dépression.
- Les rotations faibles ou nulles mesurées dans le Ghissar et le Sud-Ouest Ghissar suggèrent que ces deux régions sont restées fixes en orientation au cours de la déformation.

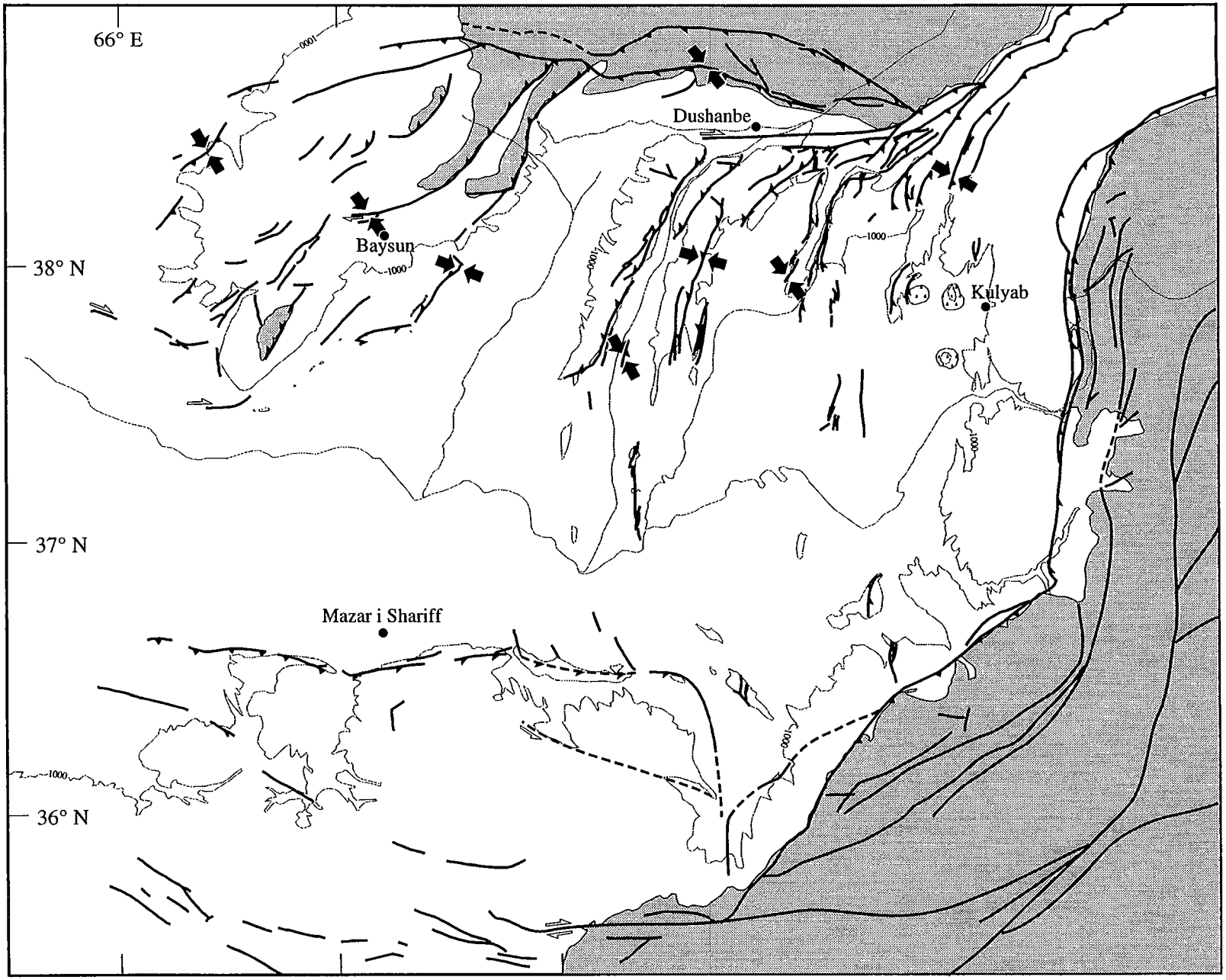

Figure III.4. Carte des failles majeures Cénozoïques de la dépression Tadjik et des régions avoisinantes.

Les fléches noires représentent les directions de raccourcissement déduites de l'analyse microtectonique. Le socle pré-Mesozoique est en grisé. Des dômes de sel jurassique sont visibles près de la ville de Kulyab (triangles noirs).

1.2.2. Etude structurale

L'étude structurale a été effectuée dans un souci de compréhension de la cinématique globale de la dépression Tadjik et des rotations paléomagnétiques.

Une carte des failles majeures Cenozoïques (Figure III.4) a été réalisée a partir de l'analyse d'images satellites, des données de terrain et de la bibliographie existante.

Des données microtectoniques (troisième partie de ce chapitre et annexe 4) ont été recueillies au niveau des localités paléomagnétiques (Figure III.4), le long des accidents qui bordent les bassins. Les directions principales de la déformation ont été déterminées par la méthode des Dièdres Droits (Angelier et Mechler, 1977). En règle générale, la direction de raccourcissement est sub-horizonthale et orientée N90° à N150°. Les directions intermédiaires et d'extension sont souvent moins bien définies, dessinant un plan perpendiculaire à la direction de raccourcissement. De plus, les directions de raccourcissement sont pour la plupart obliques par rapport à la direction des accidents. Ceci suggère un tenseur de déformation de type aplatissement et une composante de décrochement associée au chevauchement.

Ainsi, à l'échelle de la dépression Tadjik, les failles d'orientation sub-méridienne présentent une composante de décrochement sénestre combinée au chevauchement, tandis que les failles E-O présentent une composante décrochante dextre (mise à part la bordure Sud de la dépression). Ce contexte régional décrochant sénestre est étroitement associé au mouvement du Pamir vers le Nord par rapport à l'Asie stable.

Les relations entre la sismicité et le champ de failles sont assez révélatrices du style de la déformation dans la dépression Tadjik. Les épicentres des séismes (pour la plupart compris entre 0 et 10 km de profondeur) soulignent les zones où la couverture sédimentaire est intensément déformée, telles que les chaînes de Peter the First et de Vaksh, ainsi que les failles bordant la dépression. Ces dernières failles qui sont, nous l'avons vu, des accidents de socle néoformés ou réactivés au Cénozoïque, sont également marquées par une sismicité de profondeur crustale (Leith et Simpson, 1986, et ce chapitre). A l'intérieur de la dépression, la sismicité diminue très rapidement en s'éloignant du Pamir sans regroupement préférentiel le long des accidents, bien que de nombreux indices de déformation active soient visibles sur le terrain (Trifonov, 1978, 1987). Ainsi, la déformation de socle qui caractérise les bordures de la dépression est soulignée par la sismicité, tandis que la déformation de couverture localisée au

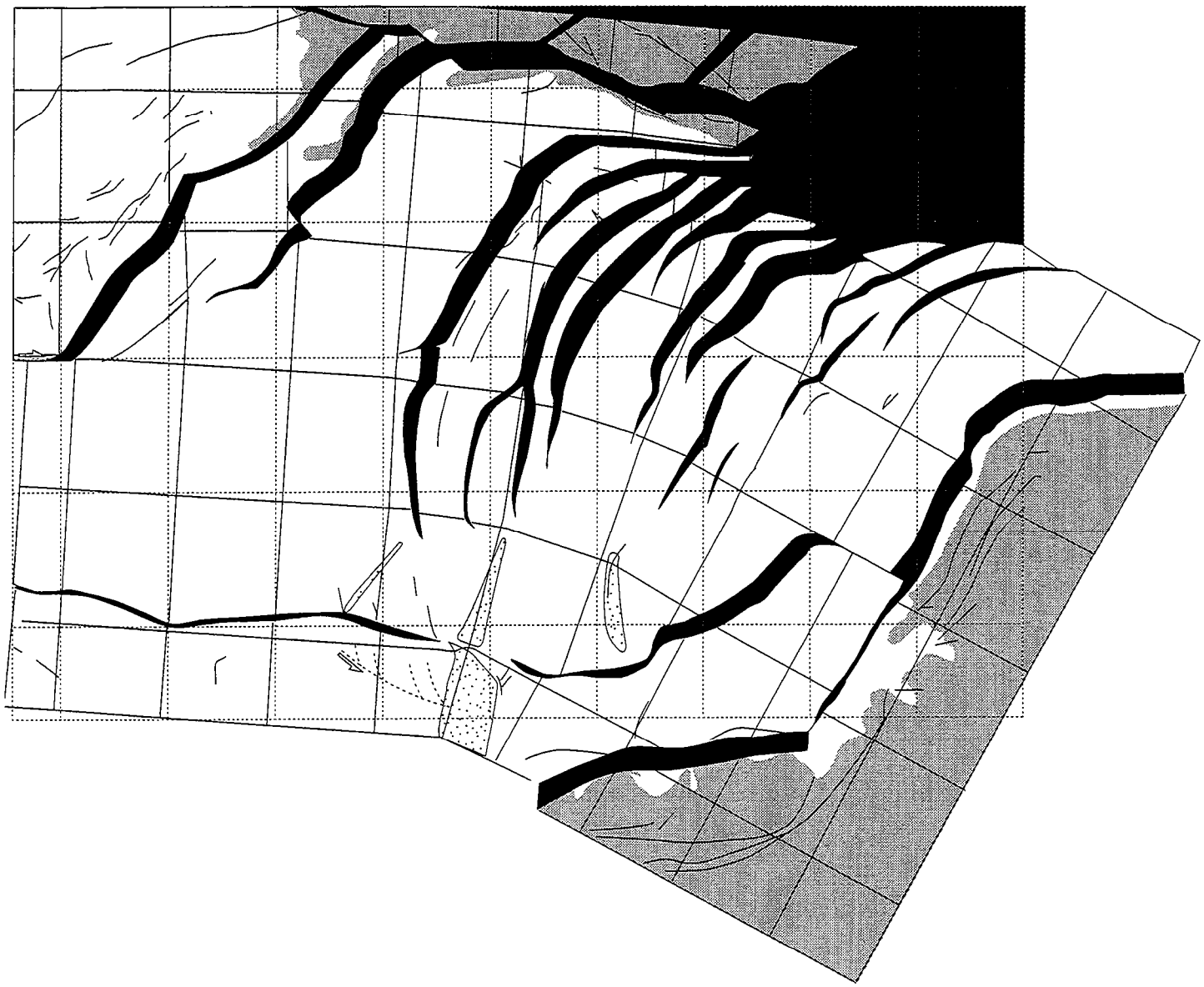

Figure III.5. Restauration manuelle de la dépression Tadjik.
La carte de départ est l'état déformé actuel (Figure III.4). Les lignes de longitude et latitude ont été considérées comme des lignes matérielles (lignes actuelles en pointillé, déformées en trait plein). La restauration des chevauchements crée des vides (en noir) entre les failles. Les domaines en pointillés correspondent aux recouvrements ponctuels du papier. Une restauration tenant compte d'un mouvement senestre au sud-est de la dépression (faille en pointillés) devrait permettre d'annuler cet effet de recouvrement.

dessus du niveau de décollement évaporitique se fait de façon globalement asismique (excepté dans la zones de déformation intense au N-O de la dépression et autour de dômes de sel actifs).

La réalisation d'une carte isopaque de la base du Tertiaire m'a permis d'effectuer une restauration manuelle de la dépression Tadjik (Figure III.5), en estimant le déplacement horizontal sur les accidents de la carte tectonique (Figure III.4 et 4^{ième} partie de ce chapitre).

L'état restauré de la dépression Tadjik met en évidence l'augmentation progressive vers le Nord du raccourcissement le long des chevauchements. Le raccourcissement augmente brutalement dans la partie N-E de la dépression, au niveau des chaînes de Peter the First et de Vaksh. Au centre de la dépression, le raccourcissement est de l'ordre de 20% entre le Sud-Ouest Ghissar et le Pamir, tandis qu'il passe à 60% dans la zone de convergence entre le Tien Shan et le Pamir. Cette dernière valeur est en bon accord avec celle déduite d'une coupe équilibrée effectuée dans la chaîne de Peter the First (Hamburger et al., 1992) en considérant la dépression Tadjik comme un bassin de type foreland au Mesozoïque plutôt qu'une marge passive amincie (Leith, 1985).

La restauration met également en évidence des rotations antihoraires. La présence de ces rotations distribuées sous forme d'éventail est directement liée au gradient de raccourcissement N-S. Elles passent de 5°-15° dans la partie Ouest de la dépression, à 25°-30° dans la partie Est. Cette répartition des rotations est tout à fait comparable à celle déduite de l'étude paléomagnétique bien que les valeurs soient légèrement plus faibles dans la restauration.

La restauration suggère par ailleurs que la partie sud de la dépression ait été en extension. Ceci n'a probablement pas ou peu de signification géologique et est plutôt lié au manque de données précises pour cette région située en Afghanistan. En effet, cette "extension" devrait être facilement accommodée dans le processus de restauration en tenant compte d'un déplacement senestre sur les accidents du Sud de la dépression (extrémité Est de la faille de l'Alburz et faille NO-SE au Sud). On remarquera ici une des intérêts de la restauration qui permet indirectement de préciser le déplacement sur des accidents mal contraints.

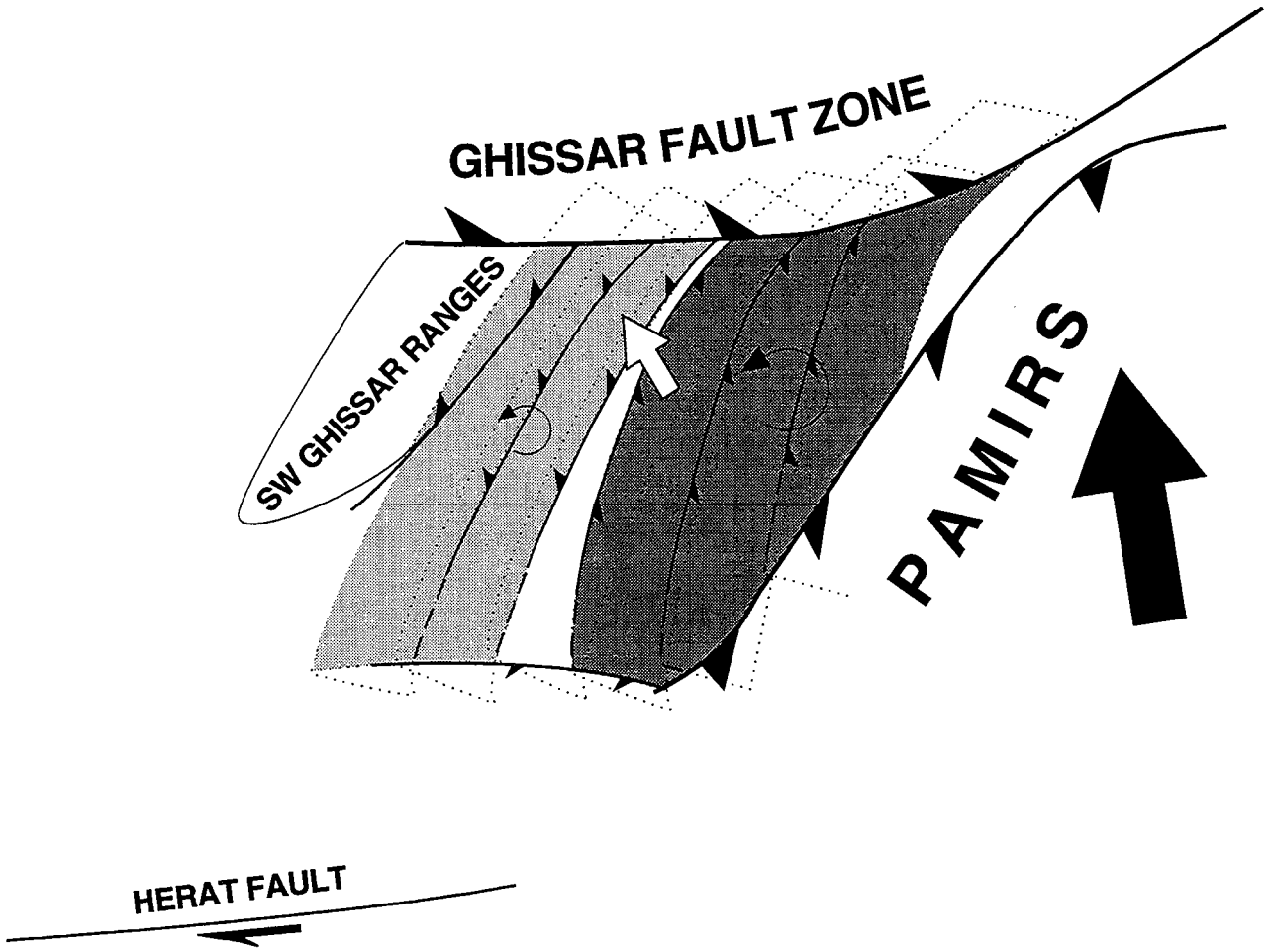

Figure III.6. Modèle cinématique Cénozoïque proposé pour la dépression Tadjik.

La déformation est considérée comme étant principalement associée au poinçonnement du Pamir. La rotation de la dépression est accompagnée par son extrusion vers le NO (flèche blanche) entre la zone décrochevauchante du Ghissar au Nord et la zone décrochante sénestre mineure au S-O. Les rotations antihoraires sont fortes dans le secteur Est (domaine gris fonçé), plus faibles dans le secteur Ouest (domaine gris clair). Le domaine central (blanc) est un bassin en "pop-down". Le déplacement relatif entre les blocs est transpressif sénestre, les bordures pointillées des blocs représentant les portions chevauchées.

Ainsi, les décro-chevauchements dextres du Ghissar au Nord, et sénestre de l'Alburz au Sud, accommodent l'extrusion vers le N-O et la rotation antihoraire de la dépression Tadjik (Figure III.6). La rotation s'effectue dans un contexte tectonique régional présentant une composante décrochante sénestre visible sur les failles limitant les blocs constituant la dépression.

Le Sud-Ouest Ghissar accommode le déplacement de la dépression Tadjik principalement par chevauchement. Le gradient croissant de raccourcissement du Sud vers le Nord suggère par ailleurs un pôle de rotation moyen pour la dépression situé dans sa partie sud.

Le Ghissar, qui ne montre pas de rotation paléomagnétique semble être resté fixe entre deux domaines ayant subi une rotation antihoraire : la dépression Tadjik et le bassin de Fergana. Cette observation met l'accent sur la relation entre les rotations observées en surface et la déformation crustale. En effet, quelle est la continuité en profondeur du domaine de la croûte affecté par les rotations ?

La dépression Tadjik présente un niveau de décollement majeur entre 10 et 12 km de profondeur. Quelle est la part de rotation affectant la couverture sédimentaire et transmise dans le socle sous-jacent ? La rotation du socle de la dépression pourrait être idéalement obtenue en restaurant ce niveau de la même façon que la base du Tertiaire. Nous avons vu que les accidents affectant le socle sont pour la plupart localisés sur les bordures de la dépression. De même, Les rotations déduites de la restauration manuelle sont principalement associées aux chevauchements qui, dans la dépression, n'affectent pas ou peu le socle. Cependant, les rotations de la restauration sont plus faibles que celles déduites du paléomagnétisme. Une rotation du socle reste donc possible mais est, en tout état de cause, plus faible que celle de la couverture sus-jacente décollée sur le niveau évaporitique.

Par ailleurs, Le Ghissar qui limite la dépression Tadjik au nord présente un épaississement crustal notable avec un Moho à une profondeur de 45-50 km (Burov et al., 1990). La zone décro-chevauchante qui le traverse est probablement crustale et une rotation du Ghissar devrait logiquement se faire à cette échelle. On peut raisonnablement considérer que la rotation de la couverture de la dépression Tadjik est plus facile que la rotation de la zone faillée crustale du Ghissar, ce qui rendrait compte des rotations faibles à nulles qui y sont observé. La composante chevauchante dans le Ghissar est compatible avec une rotation relative entre cette zone et les bassins adjacents.

La déformation de la dépression Tadjik et des massifs environnants, qui combine épaississement crustal, décrochement et rotations de blocs, apparaît

donc relativement complexe. Tout comme pour le Tien-Shan Kirghiz, le poiçonnement du Pamir dans l'Asie est étroitement associé à la déformation et au contexte tectonique régional transpressif sénestre. Ce contexte permet l'extrusion vers le Nord-Ouest et la rotation antihoraire de la dépression. La présence d'un niveau de décollement majeur suggère cependant que les rotations affectent principalement la couverture sédimentaire.

2. Evidences paléomagnétiques pour des rotations de blocs Cénozoiques dans la dépression Tadjik, Asie Centrale

Paléomagnetic evidence for Cenozoic block rotations in the Tadjik depression, Central Asia

Article soumis à publication dans le "Journal of Geophysical Research".

Paleomagnetic Evidence for Cenozoic Block Rotations in the Tadjik Depression (Central Asia)

J.-Ch Thomas[1], A. Chauvin[1], D. Gapais[1], M. L. Bazhenov[2], H. Perroud[3], P. R. Cobbold[1], and V. S. Burtman[2]

[1] Géosciences Rennes (CNRS), Université de Rennes I, 35042 Rennes Cedex, France

[2] Geological Institute, Academy of Sciences of Russia, Pyzhevsky Lane, 7, Moscow

[3] Département des Sciences de la Terre, Université de Pau, 64000 Pau Cedex, France

ABSTRACT

This paper presents results of a paleomagnetic study of Oligo-Miocene red beds of the Tadjik depression in Central Asia. We sampled about 530 cores at six localities across the depression and along the western border of the Pamirs. Samples were thermally demagnetized and high-temperature components appear to predate folding. Throughout the depression, paleomagnetic inclinations are consistent with those observed on the stable Turan platform, at the Western margin of the depression. However, they are shallower by about 30° than the inclination predicted from the reference APWP. This appears to indicate a 23° difference in latitude, which is incompatible with paleogeographic reconstructions for the Tertiary. A sound interpretation of this anomaly would require a better-constrained Tertiary paleomagnetic reference for Asia. Inside the Tadjik depression, paleomagnetic declinations are all significantly rotated counterclockwise with respect to those measured on the Turan platform. The eastern part of the depression is a domain of large rotation (52°±13° to 46±15°), whereas smaller amounts of rotation have occurred in the western part (27°±14° to 14°±15°). The similarity between Tertiary and Cretaceous data available for the area shows that rotations have occurred since the Miocene. Little or no paleomagnetic rotations are observed in the ranges bordering the Northern and Western parts of the depression. Paleomagnetic and structural data suggest that block rotations in the Tadjik depression are associated with indentation of the Pamirs into stable Asia. At a larger scale,

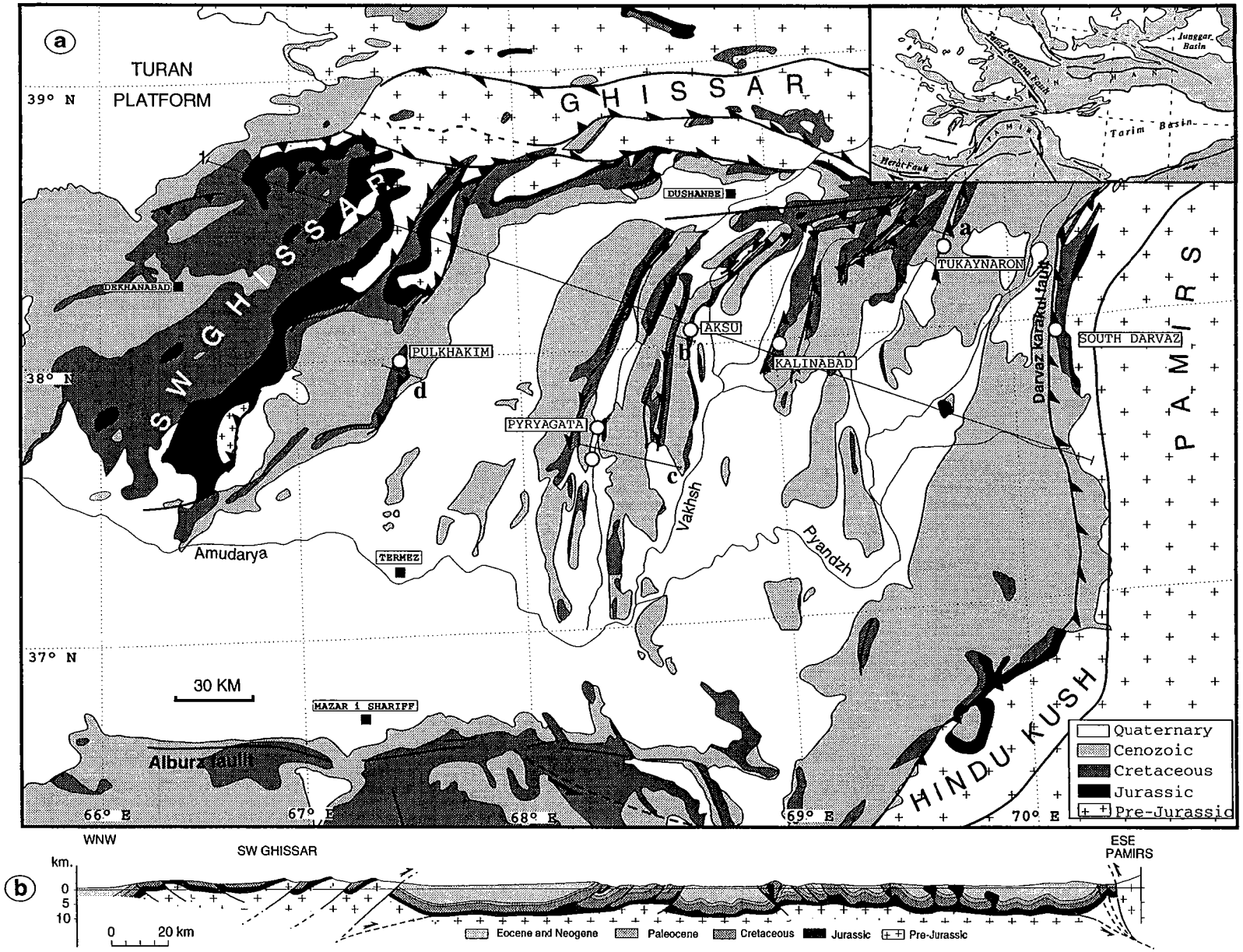

Fig. 1. (a) Simplified geological map of the Tadjik depression.
Open circles are paleomagnetic localities. Lines 1b, a, b, c, and d correspond to cross sections of Figures 1b and 3a to 3d, respectively. Oblique triangles on faults point in direction of underthrusting. Inset map shows main tectonic features of Central Asia (shaded areas are Mesozoic and older units). (b) Cross section through the Tadjik depression. Data are from Zakharov [1962], Ministry of Geology of the USSR and the Tadjik Academy of Sciences, [1989], and own observations.

observed rotations are compatible with a model of regional sinistral wrenching along a strip running from the Gulf of Oman to Lake Baikal.

INTRODUCTION

Central Asia provides a remarkable example of large-scale active intracontinental deformation. For the last 55 Ma [*Patriat and Achache*, 1984], regional tectonics are considered to result from the indentation of India into Asia [*Argand*, 1924; *Molnar and Tapponnier*, 1975], with a bulk NS shortening of about 2000 km [*Achache and Courtillot*, 1984; *Savostin et al.*, 1986]. Amongst the various kinematic models [see for example *Dewey and Burke*, 1973; *Achache and Courtillot*, 1984; *Houseman and England*, 1986, 1993; *Cobbold and Davy*, 1988; *Davy and Cobbold*, 1988; *Dewey et al.*, 1989; *Avouac and Tapponnier*, 1992; *Le Pichon et al.*, 1992] a key point, but a controversial one, is the partitioning between thickening and strike slip motions along major faults. Furthermore, the relative amount of convergence accommodated by eastward escape of large continental blocks is still debated [*Tapponnier et al.*, 1986; *England and Molnar*, 1990; *Houseman and England*, 1993].

The existence, the nature, the regional distribution and the amount of block rotation about vertical axes are critical features for constraining the way bulk shortening has been accommodated throughout Asia [see *England and Molnar*, 1990]. From an analysis of the regional fault pattern, *Cobbold and Davy* [1988] inferred block rotations, clockwise in the eastern Himalayan syntaxis, counterclockwise in the western syntaxis and along a wide strip of sinistral wrenching running from the Gulf of Oman to Lake Baikal. Recent paleomagnetic studies have consistently revealed clockwise rotations of up to 40° in Cretaceous rocks from eastern Tibet and Southwest China [*Otofuji et al.*, 1990; *Huang and Opdike*, 1992, *Funahara et al.*, 1993], and counterclockwise rotations of up to 20° in Cretaceous and Paleogene rocks of intermontane basins of the Tien-Shan [*Thomas et al.*, 1993a; *Bazhenov*, 1993].

The Tadjik depression, which lies South of the Tien-Shan and West of the Pamirs (Figure 1), is part of the Oman-Baikal sinistral wrench zone [*Cobbold and Davy*, 1988]. A few earlier paleomagnetic studies [*Abdullaev and Rzhevsky*, 1973; *Pozzi and Feinberg*, 1991], as well as field observations [*Thomas et al.*, 1993b] have provided evidence for counterclockwise rotations in the Tadjik depression. We have undertaken a paleomagnetic sampling of Cenozoic and Cretaceous red beds in the depression and adjacent ranges in order to provide better constraints on the kinematic history of the area. This paper describes the

paleomagnetic results for Tertiary samples. Results for the Cretaceous are described in detail elsewhere [Bazhenov et al., submitted].

GEOLOGICAL SETTING

Tectonics

At regional scale, the Tadjik depression appears as an intermontane pushed-down basin, bounded by crustal-scale fault zones with thrust and wrench components (Figure 1).

In the East, the Darvaz-Karakul fault zone marks the boundary between the Pamirs and the depression. The relative motion of the Pamir wedge with respect to Asia is currently in a NS to NNW-SSE direction [*Minster and Jordan*, 1978; *De Mets et al.*, 1990]. Seismological and geological data [*Hamburger et al.*, 1992] further suggest that the northeastern part of the Tadjik depression has been subducted under the Pamirs, a substantial part of the displacements being accommodated by westward thrusting and sinistral wrenching along the Darvaz-Karakul fault zone (Figure 1a) [*Peive et al.*, 1964; *Burtman and Molnar*, 1992]. The Ghissar range of the Southwestern Tien-Shan forms the northern margin of the depression. It consists of Hercynian basement, reactivated during the Tertiary [*Burtman*, 1975] and is considered a major and still active right-lateral wrench zone [*Trifonov, 1978; Thomas et al.*, 1993b], with a component of southward thrusting [*Ministry of Geology of the USSR and Tadjik Academy of Sciences*, 1984]. To the West, the SW Ghissar ranges separate the Tadjik depression from the Turan platform. Here, eastward thrusting is dominant (Figure 1b). Local thrusting of basement rocks over the Tertiary sediments of the depression suggests thick-skin tectonics. South of the Amudarya river, the East-West striking Alburz fault separates Quaternary deposits of the Tadjik basin from Tertiary and Mesozoic sediments of Northern Afghanistan. Seismological data show that this fault is currently active [*Heuckroth and Karim*, 1973, *Shareq*, 1981]. From geological maps [*Ministry of Geology of the USSR and Tadjik Academy of Sciences*, 1984] and unpublished subsurface data, there is a component of northward directed thrusting. The occurence of en echelon folds located in the vicinity of the eastern termination of the Alburz fault [Ministry of Geology of the USSR and Tadjik Academy of Sciences, 1984] suggests that thrusting is combined with a component of sinistral wrenching. Further South, the Herat fault is considered to be a Mesozoic suture, reactivated as a dextral strike-slip fault during the India-Eurasia collision [*Tapponnier et al.*, 1981].

The Tadjik depression itself is a succession of alternating basins and ranges, striking nearly North-South (Figure 1). Basins are generally bounded by thrusts

and asymmetric faulted folds with oblique-slip components [*Thomas et al.*, 1993b]. Thrusting is partly thin-skinned, above a décollement level of Upper Jurassic evaporites [*Leith and Simpson*, 1986; *Thomas et al.*, 1993b] (Figures 1a and 1b). Thrusts are of westward vergence in the eastern part of the depression (synthetic to the Darvaz-Karakul fault, eastern depression boundary) and of eastward vergence in the western part (synthetic to thrusting along the SW Ghissar ranges) (Figure 1).

Deformation in the depression and uplift of surrounding ranges mainly occurred during late Miocene to Quaternary times, as indicated by an increasing supply of continental sediments during this period. Shallow seismic activity is widespread in the eastern part of the depression, especially in the strongly deformed area between the Pamirs and the South Tien Shan (Peter the First range) [*Leith and Simpson*, 1986; *Hamburger et al.*, 1992]. Quartenary faulting is also common throughout the depression [*Trifonov*, 1978].

Sedimentology

Sediments in the Tadjik depression and SW Ghissar area range in age from Lower Jurassic to Quaternary. The total thickness of the cover can reach 10 km. Neogene and Quaternary deposits constitute roughly half of this. They are particulary thick in the center of the depression and towards its eastern and western margins (Figure 1b).

The Jurassic sequence consists of Hettangian to Kimmeridgian limestones, overlain by late Jurassic evaporites which provide a major décollement level. The thickness reaches up to 2.5 km in the SW Ghissar ranges. Overlying Cretaceous deposits are about 2 km thick and changes gradually from continental to shallow marine.

Paleogene rocks are generally conformable on the Upper Cretaceous; but slight angular unconformities occur locally. The whole Paleogene sequence is commonly several hundred meters thick. However, considerable lateral changes in facies and thickness are observed. A change from shallow marine to continental environment occurs during the Oligocene.

The overlying Baljuan Series, of Miocene age (and perhaps Upper Oligocene) consist of intercalated red sandstones and conglomerates. They are overlain by Pliocene to Quaternary alluvial sandstones and conglomerates.

Our paleomagnetic study was mainly performed on Oligo-Miocene red beds, especially sandstones and siltstones.

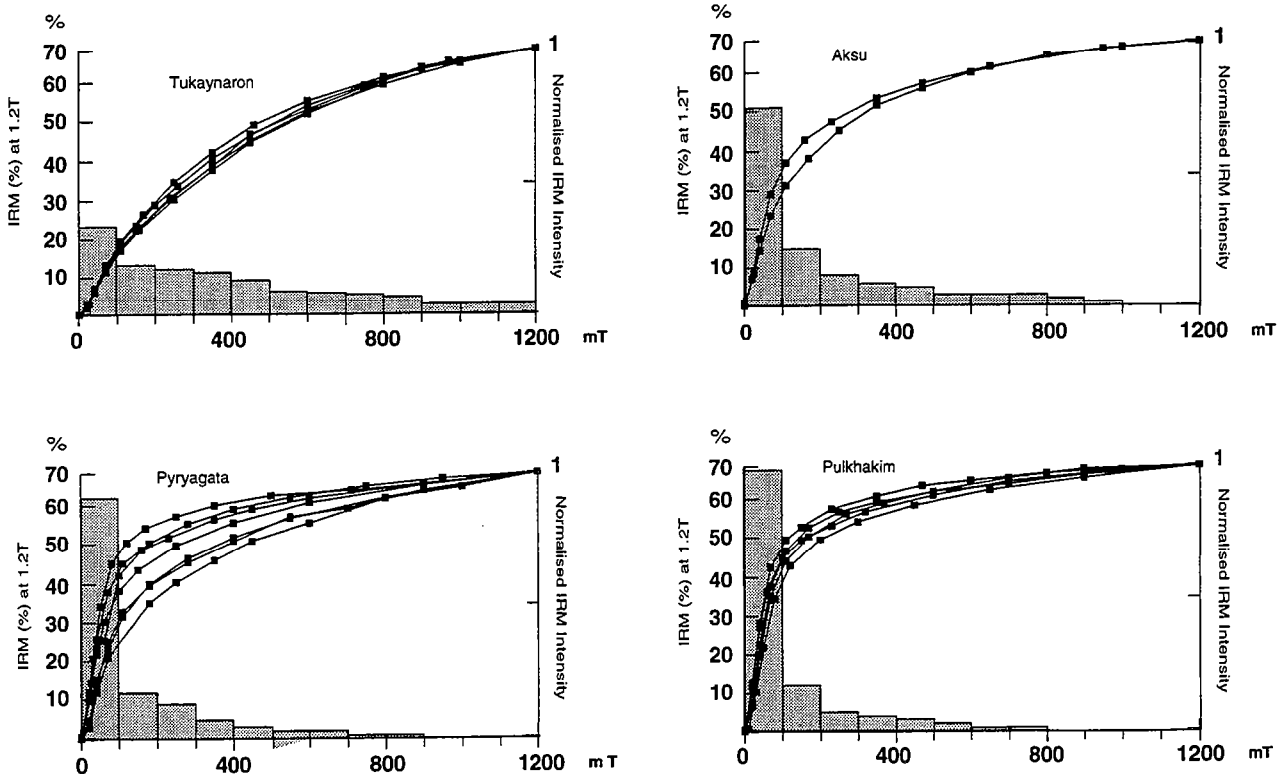

Fig 2. Normalised isothermal remanent magnetization curves and coercivity spectra (in grey) for representative samples from various localities.
Scale on left hand side of diagrams show % of IRM at 1.2 T. Hematite is dominant for Tukaynaron locality, whereas both hematite and magnetite are present for other localities.

PALEOMAGNETIC ANALYSIS

We collected 530 cores at five localities across the depression, between the Pamirs and the South-West Ghissar ranges (Figure 1a). Each locality consisted of several sites where seven to nine cores were collected in two or three adjacent beds. Both solar and magnetic compasses were used for orientation. Sites were located precisely with a portable satellite positioner (GPS).

Remanent magnetization was measured with a cryogenic magnetometer (LETI). We isolated characteristic directions of remanent magnetism after progressive thermal demagnetization. Alternating field demagnetization was found to be less efficient. The bulk susceptibility was measured at each step during demagnetization. Characteristic paleomagnetic directions were determined by principal component analysis. A complete reinterpretation of data from the outskirts of the Pamirs (South Darvaz locality), previously published by *Bazhenov and Burtman* [1986], is also included in this study.

Lithology and Magnetic Mineralogy

Natural remanent magnetization (NRM) was found to range in intensity between 10^{-3} A/m and 10^{-2} A/m for the overall collection. All samples which showed stable demagnetization presented unblocking temperatures higher than 600°C. Isothermal remanent magnetization (IRM) was given to representative samples from each locality (Figure 2). Magnetization never reached saturation for an applied field of 1.2 T. Curves for Tukaynaron locality (Figure 2a) indicate magnetic minerals with high coercivity, probably hematite. For the other localities, curves show two stages. First, for fields smaller than 0.2 T, IRM intensity increases rapidly; then intensity increases much more slowly, but does not reach saturation. We infer two magnetic phases, magnetite and hematite. From both unblocking temperatures and IRM curves, the high-temperature component of our samples is carried mainly by hematite, even for samples where the proportion of magnetite is significant. For Tukaynaron locality, where hematite is clearly dominant on IRM curves, samples are fine-grained reddish sandstones. For the other localities, samples are more brownish to pink in color and the grain size is larger. Representative polished sections from all localities, observed under a reflected-light microscope, show that samples consist of clast-supported sandstones and siltstones essentially made of quartz. Clasts are angular and their size varies from about 60 mm in sandstones to less than 10 mm in siltstones. Spaces between quartz grains are filled with a reddish matrix, at least partly composed of hematite pigment

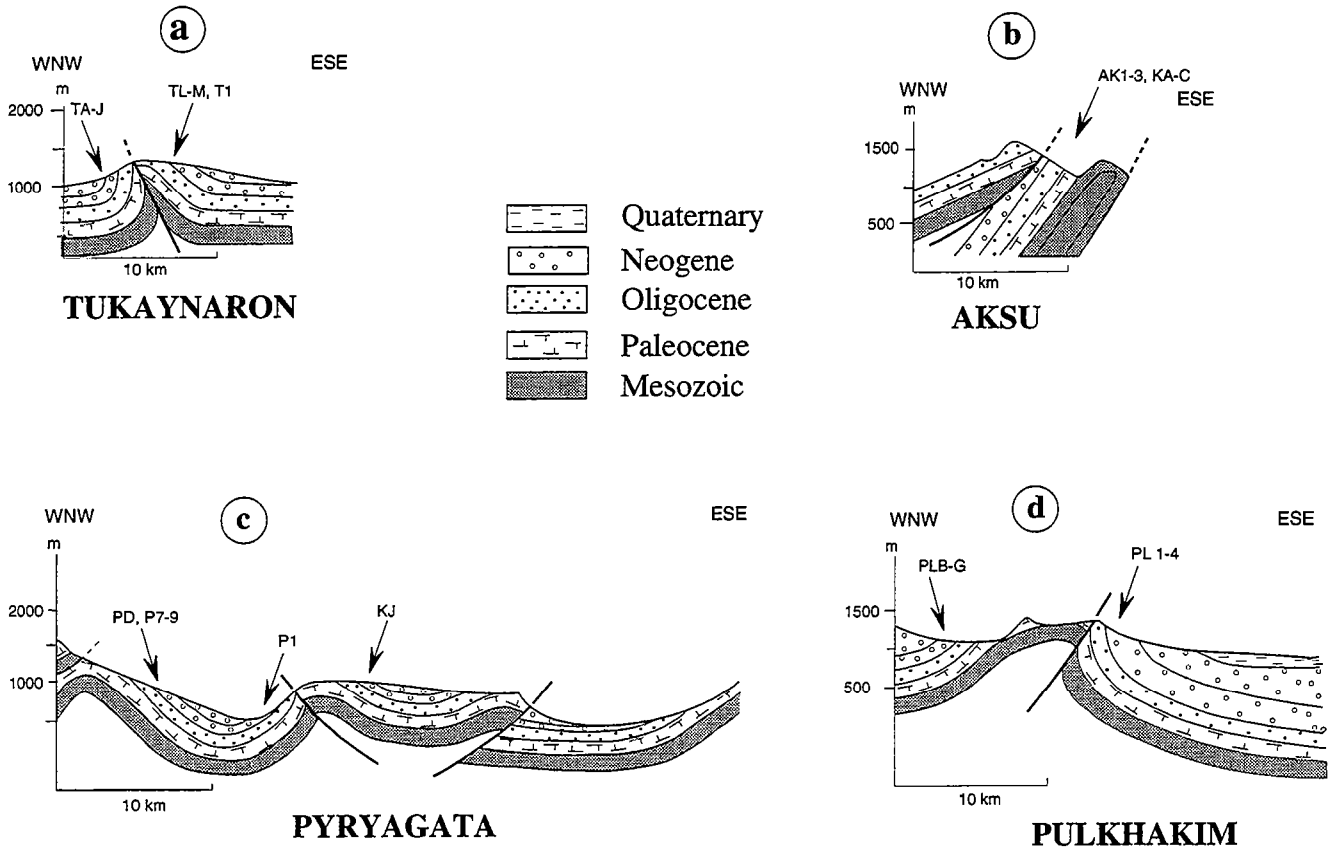

Fig 3. Schematic cross sections located on Figure 1 for 4 out of 6 localities.
Arrows indicate locations of sampling sites.

which probably carries most of the NRM. Large specular hematite grains are locally observed.

Paleomagnetic Results

Tukaynaron

Tukaynaron locality is located in the North Eastern part of the Tadjik depression, at the termination of an anticline. On both limbs of the fold (Figure 3a), we sampled fine-grained reddish sandstones of Upper Oligocene to Lower Miocene age. Most samples yielded two components of magnetization after thermal demagnetization (Figures 4a and 4b). The low-temperature component, removed around 350°C to 500°C, is close to the current dipole field direction. The high-temperature component has an unblocking temperature between 650°C and 680°C. Both polarities of the earth's magnetic field are observed. As the axis of the studied fold plunges 42° towards 192°, we corrected data both for tilt and for fold axis orientation (Table 1). Both fold test and reversal test are positive at the 99% level [*Mc Elhinny*, 1964] (Figure 4c).

Kalinabad

At Kalinabad locality, a syncline is exposed along the Vakhsh river. Ten sites were sampled on both limbs. Unfortunately, only two sites provided results with clear characteristic components (Figure 5a). Other sites showed erratic or unstable behavior during thermal demagnetization. This we attribute to the magnetic mineralogy and to recent weathering of sediments. Indeed, on polished sections, the rock is strongly altered. Intergranular spaces are filled with a grey matrix replacing the original pink matrix which contained the hematite. In tilt-corrected coordinates, the two sites revealed antipodal paleomagnetic directions (Figure 5b and Table 2).

Aksu

At Aksu locality, in the center of the depression, six sites were sampled on one limb of an anticline (Figure 3b). Three sites (AK1 to AK3) were collected in Lower Miocene fine-grained reddish sandstones; the three other sites (KA to KC), a few kilometers to the south, in pale brownish sandstones. Thermal demagnetization (Figure 6a and 6b) revealed two components: a low-temperature component with a direction close to the present field and an unblocking temperature around 300°C to 450°C; and a high-temperature component, usually very stable and completely removed around 680°C. These two components can have antipodal directions (e.g. Figure 6a), and the high-

Site	Latitude, (°N)	Longitude, (°E)	Bedding	n/N	In Situ D	In Situ I	Tilt Corrected D	Tilt Corrected I	Unfolded D	Unfolded I	k	α_{95}	Age
TA	38.338	69.640	186/66	5/8	32	47	324	34	297	34	48	11	Up. Oligocene
TB	38.338	69.640	184/71	7/8	15	7	1	12	332	12	36	8	Up. Oligocene
TC	38.338	69.640	183/74	7/8	28	39	327	29	298	29	12	18	Up. Oligocene
TD	38.338	69.640	179/76	8/8	204	1	186	-24	157	-24	14	16	Up. Oligocene
TE	38.338	69.640	181/79	7/7	216	-36	145	-35	113	-35	41	10	Up. Oligocene
TI	39.333	69.633	188/73	8/8	60	35	332	52	302	52	18	13	Up. Oligocene
TJ	39.333	69.633	184/62	7/8	33	41	332	39	308	39	30	11	Up. Oligocene
TL	39.333	69.633	116/40	4/7	171	-9	158	-39	156	-39	10	30	Lw. Miocene
TM	39.333	69.633	89/35	7/7	341	2	337	35	341	35	8	22	Lw. Miocene
T1	38.300	69.648	45/63	6/9	123	27	122	-35	143	-35	70	8	Lw. Miocene

Mean	N	In Situ D	In Situ I	Tilt Corrected D	Tilt Corrected I	Unfolded D	Unfolded I	k	α_{95}
	10	17	18					4	25
				335	30			19	11
						317	33.5	19	11

Table 1. Paleomagnetic data for Tukaynaron locality.

Upper part of table gives site label, site location, bedding attitude, number of samples used for statistics versus number of samples measured (n/N), mean declination (D) and mean inclination (I) for high-temperature components in In Situ, tilt-corrected and unfolded coordinates, Fisher statistics (k for dispersion parameter, a_{95} for radius of circle of confidence at 95% probability level), and approximate stratigraphic age. Unfolded data are corrected for both bedding tilt and inclination of the fold axis. Lower part of table gives number of data used for calculation of mean locality direction (N), mean declination (D) and inclination (I) for each locality, and Fisher statistics for high-temperature components.

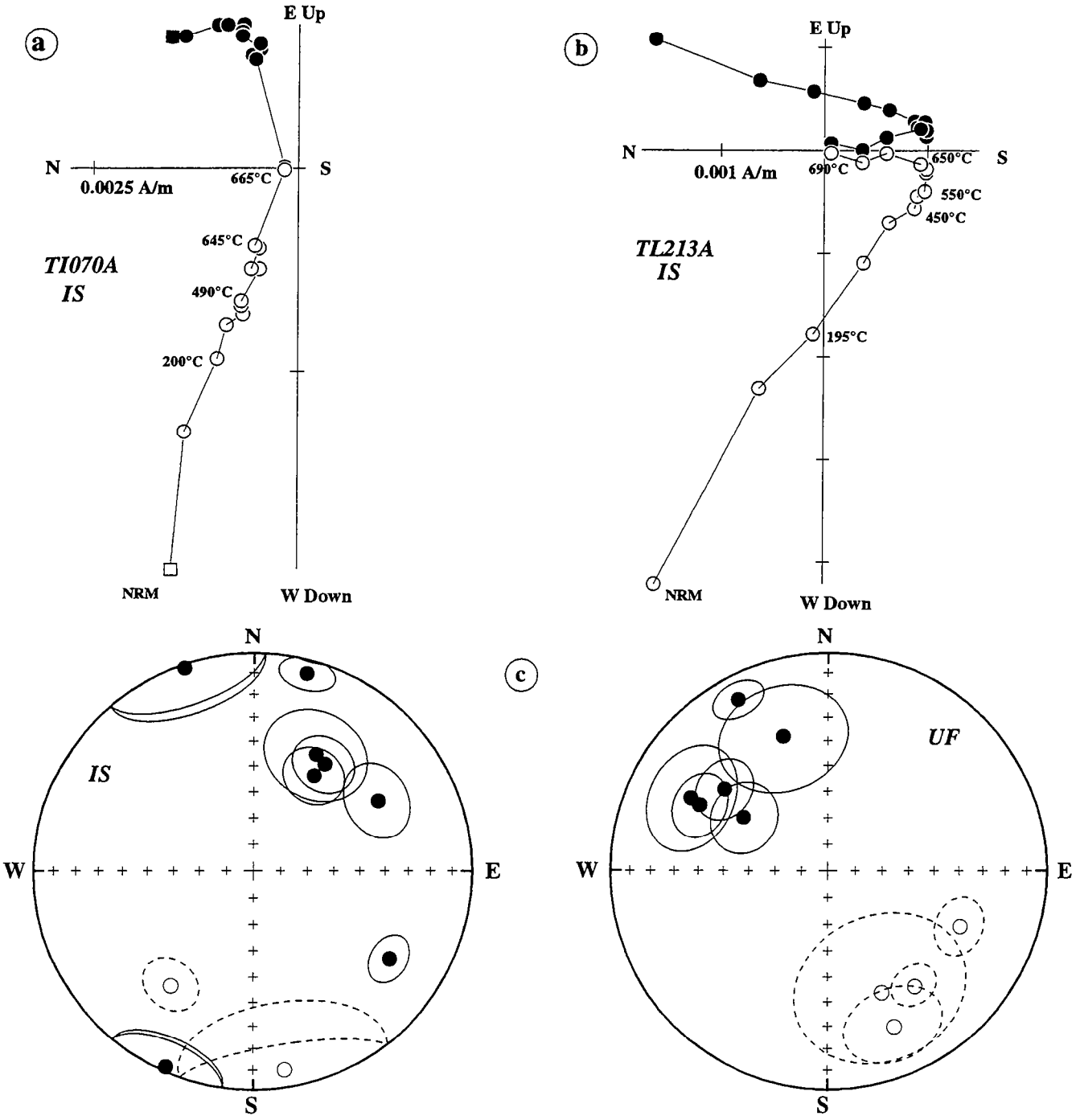

Fig 4. Paleomagnetic data for Tukaynaron locality.
(a) and (b), Representative demagnetization curves. Solid and open symbols are in horizontal and vertical plane respectively. (c), Equal-area projections of mean site directions (IS, in situ coodinates; UF, unfolded coordinates). Solid and open circles are projections in the lower and upper hemisphere respectively.

Site	Latitude, (°N)	Longitude, (°E)	Bedding	n/N	In Situ D	In Situ I	Tilt Corrected D	Tilt Corrected I	k	α_{95}
KG	37.967	69.011	189/55	6/8	354	60	311	23	76	7
K1	37.964	68.996	26/37	7/7	125	-3	128	-39	20	14

Mean	N	In Situ D	In Situ I	Tilt Corrected D	Tilt Corrected I	k	α_{95}
	13	320	34			5	20
				310	33	25	9

Table 2. Paleomagnetic data for Kalinabad locality.

Due to small number of sites, statistics are calculated at sample level. Ages are Lower Miocene. Other comments as for Table 1.

Site	Latitude, (°N)	Longitude, (°E)	Bedding	n/N	In Situ D	In Situ I	Tilt Corrected D	Tilt Corrected I	Unfolded D	Unfolded I	k	α_{95}
KA	37.961	68.549	170/24	6/8	182	-48	155	-48			36	11
KB*	37.961	68.549	194/26	4/8	34	29	18	35			19	21
KC	37.961	68.549	198/24	8/8	180	-56	155	-43			19	13
AK1	38.105	68.608	197/70	7/8	212	-36	165	-23	180	-23	20	15
AK2	38.105	68.608	197/75	7/8	219	-37	162	-26	179	-26	32	11
AK3	38.105	68.608	198/71	4/8	212	-55	143	-23	160	-23	14	25

Mean	N	In Situ D	In Situ I	Tilt corrected D	Tilt corrected I	Unfolded D	Unfolded I	k	α_{95}
	5	22	48					25	16
				336	33			33	13
						347	33	26	15

*Rejected site

Table 3. Paleomagnetic data for Aksu locality.

Ages are Lower Miocene. Other comments as for Table 1.

Site	Latitude, (°N)	Longitude, (°E)	Bedding	n/N	In Situ D	In Situ I	Tilt Corrected D	Tilt Corrected I	k	α_{95}
P1	37.830	68.230	197/72	4/8	211	-42	158	-22	31	17
P7	37.507	68.031	214/45	8/8	24	62	334	34	37	9
P8	37.715	68.150	1/45	6/8	314	4	326	35	8	25
P9	37.715	68.150	6/45	6/7	330	-5	335	20	12	20
PD	37.531	68.029	197/75	7/8	330	32	333	53	30	12
KJ	38.105	68.608	198/71	6/8	168	-37	167	-17	49	10

Mean	N	In Situ D	In Situ I	Tilt Corrected D	Tilt Corrected I	k	α_{95}
	6	343	32			5	32
				336	30	30	12

Table 4. Paleomagnetic data for the Pyryagata locality.

Ages are Lower Miocene. Other comments as for Table 1.

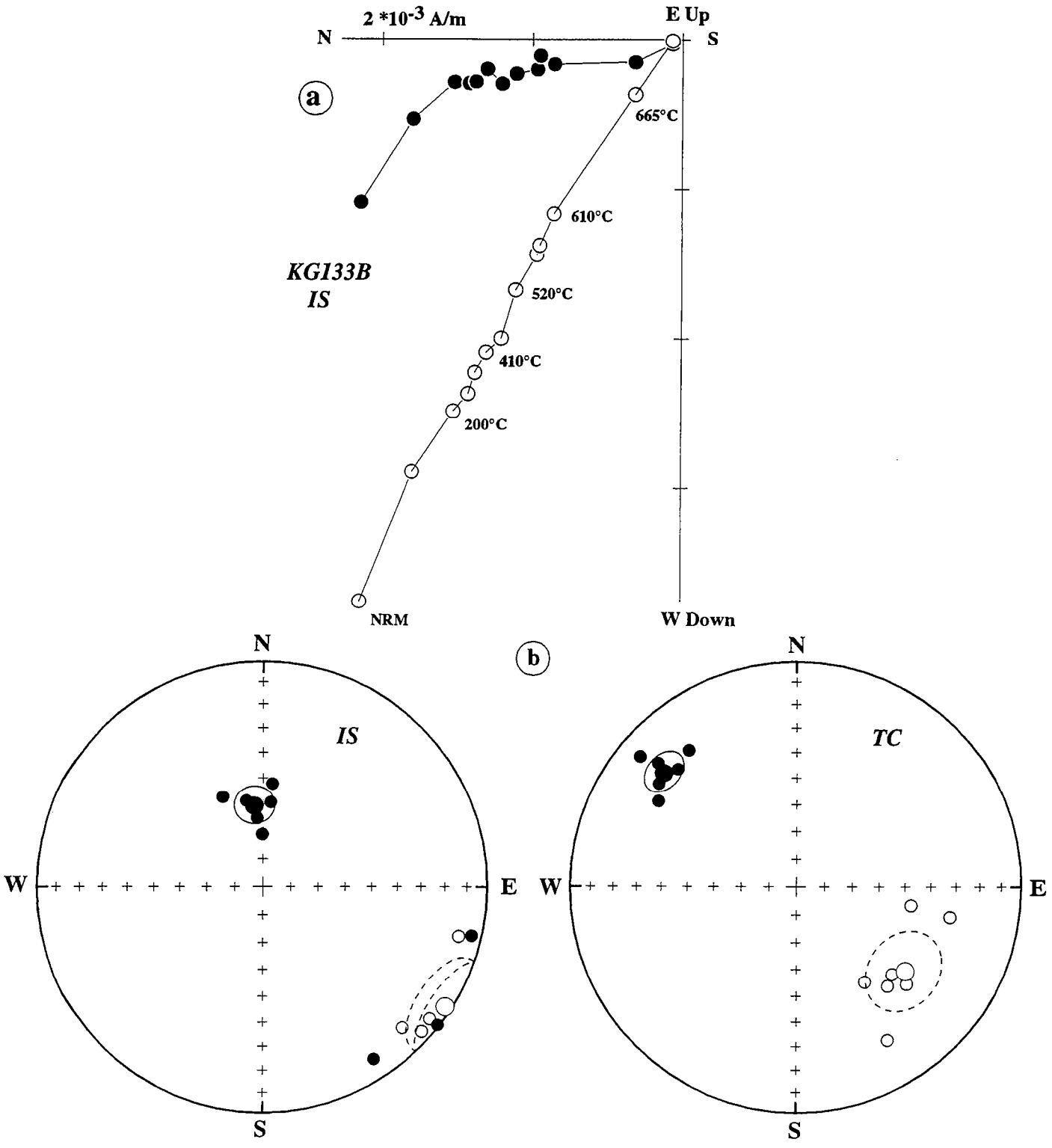

Fig 5. Paleomagnetic data for Kalinabad locality.
Projections show both sample and site mean directions; TC is for tilt-corrected coordinates; other comments as on Figure 4.

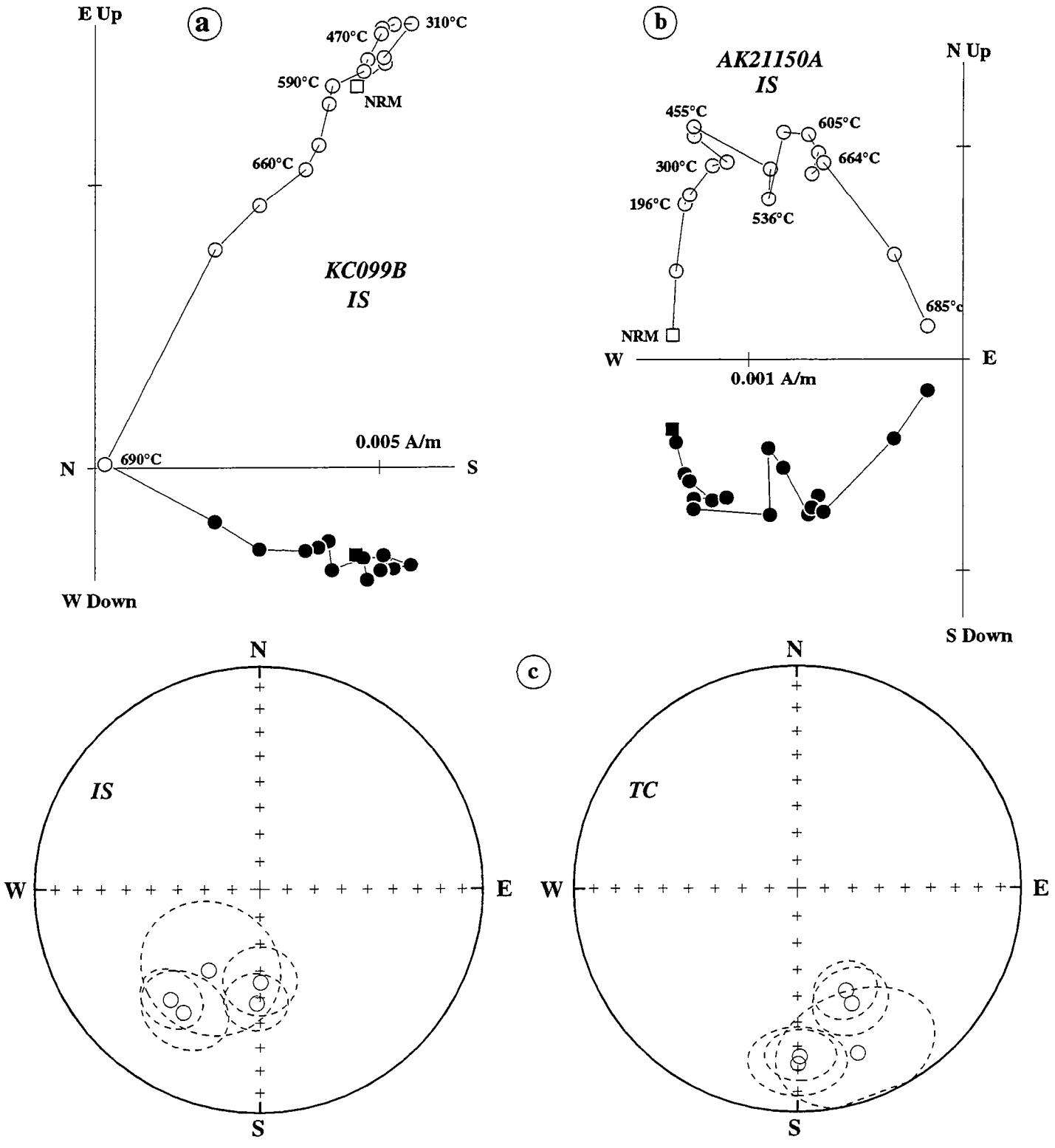

Fig 6. Paleomagnetic data for Aksu locality.
Same comments as for Figure 4.

temperature component is always of reverse polarity. Unfortunately, bedding dips do not vary enough to perform a fold test (Figure 6c and Table 3). Structural observations show that sites AK1 to AK3 are located on a fold with an axis plunging 22° toward N7°. Cretaceous samples were collected on both limbs of this fold. Corresponding paleomagnetic directions showed better clustering after unfolding than after simple tilt correction [*Bazhenov et al.*, submitted]. In-situ directions for sites AK1 to AK3 were therefore unfolded.

Pyryagata

At Pyryagata locality, in the South Central part of the depression, 19 sites were sampled in Lower Miocene rocks on three limbs of a syncline-anticline pair (Figure 3c). As for Kalinabad locality, many samples proved unstable during thermal demagnetization. These samples were often coarse-grained with a pale-brownish color, probably induced by weathering. Nevertheless, six sites provided reliable results. Two types of behavior were observed: one set of samples showed a unique component (Figure 7a) which is very stable, with unblocking temperatures distributed between 100°C and 680°C. For the other samples (Figure 7b), a low-temperature component was always removed after 550°C and a high-temperature component was usually removed after 650°C; this latter component is not so well defined as for the first set of samples. Despite the relatively small number of sites, both polarities are observed (Figure 7c and Table 4) and a fold test is positive at the 99% level [*Mc Elhinny*, 1964].

Pulkhakim

Pulkhakim locality is on the western margin of the depression. We sampled 12 sites on both limbs of a faulted box-fold (Figure 3d), within reddish to brownish sandstones of Lower Miocene age. During thermal demagnetization, most samples showed a well-defined characteristic component. As for Pyryagata locality, two types of behavior are observed during thermal demagnetization. Figure 8a shows an example with a unique characteristic component converging towards the origin and with an unblocking temperature around 680°C. Figure 8b shows more complex behavior. Up to 600°C, no clear component can be isolated. This is probably due to simultaneous removal of two components carried by magnetic minerals with overlapping spectra of unblocking temperatures. Between 620°C and 680°C, a high temperature component can be isolated. At the scale of the locality (Figure 8c and Table 5), this component presents both polarities of the earth magnetic field. A reversal test is positive; so is a fold test at the 99% level [*Mc Elhinny*, 1964].

Site	Latitude, (°N)	Longitude, (°E)	Bedding	*n/N*	In Situ D	In Situ I	Tilt Corrected D	Tilt Corrected I	*k*	α_{95}
PLB	38.091	67.426	213/12	8/8	31	41	20	39	15	15
PLC	38.091	67.426	219/32	5/6	37	42	12	34	22	17
PLD	38.091	67.426	219/32	3/6	197	-37	181	-21	23	26
PLE	38.091	67.426	224/22	7/8	343	54	334	30	36	10
PLF	38.091	67.426	214/26	3/9	2	63	336	44	34	21
PLG	38.091	67.426	214/25	7/8	4	73	329	54	30	11
PL1	38.060	67.475	20/83	6/8	334	-11	359	42	20	15
PL2	38.060	67.475	18/94	5/6	170	21	176	-28	28	15
PL3	38.060	67.475	17/93	5/6	167	38	154	-22	83	8
PL4	38.060	67.475	4/118	8/9	166	56	134	-33	21	12

Mean	*N*	In Situ D	In Situ I	Tilt Corrected D	Tilt Corrected I	*k*	α_{95}
	10	0	22			3	34
				349	35	16	13

Table 5. Paleomagnetic data for the Pulkhakim locality.
Ages are Lower Miocene. Other comments as for Table 1.

Site	Latitude, (°N)	Longitude, (°E)	*n/N*	In Situ D	In Situ I	k	α_{95}	Tilt Corrected D	Tilt Corrected I	*k*	α_{95}
S1	37.830	68.230	13/19	74	51	5	20	291	37	9	15
S2	37.507	68.031	9/9	46	24	3	38	311	20	6	24
S3	37.715	68.150	6/12	65	24	5	31	310	37	7	26

Mean	*n/N*	In Situ D	In Situ I	Tilt Corrected D	Tilt Corrected I	*k*	α_{95}
	28/40	62	37			4	16
				312	32	7	11

Table 6. Paleomagnetic data for the South Darvaz locality.
Statistics are calculated at sample level. See text for ages. Other comments as for Table 1.

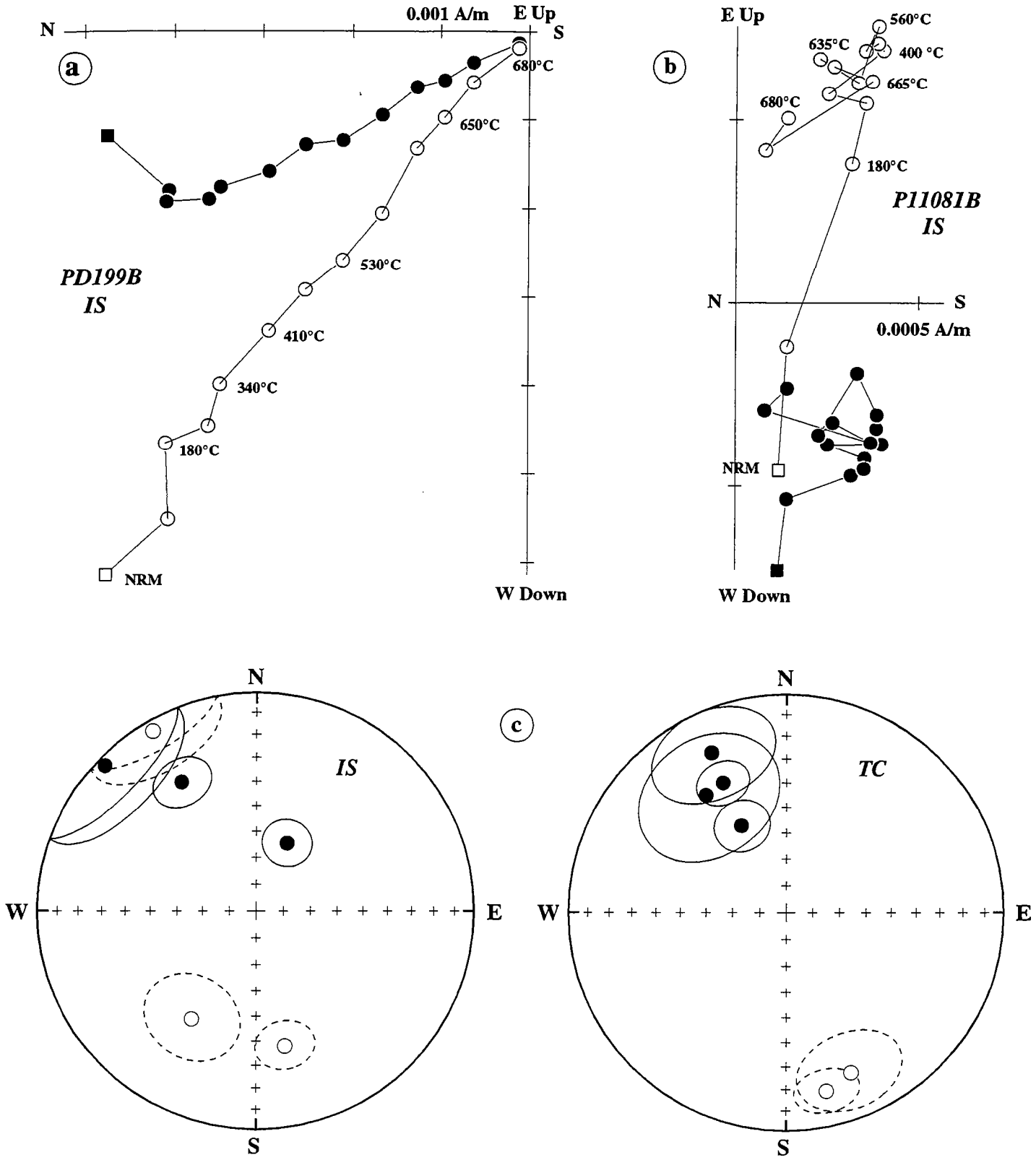

Fig 7. Paleomagnetic data for Pyryagata locality.
Same comments as for Figure 4.

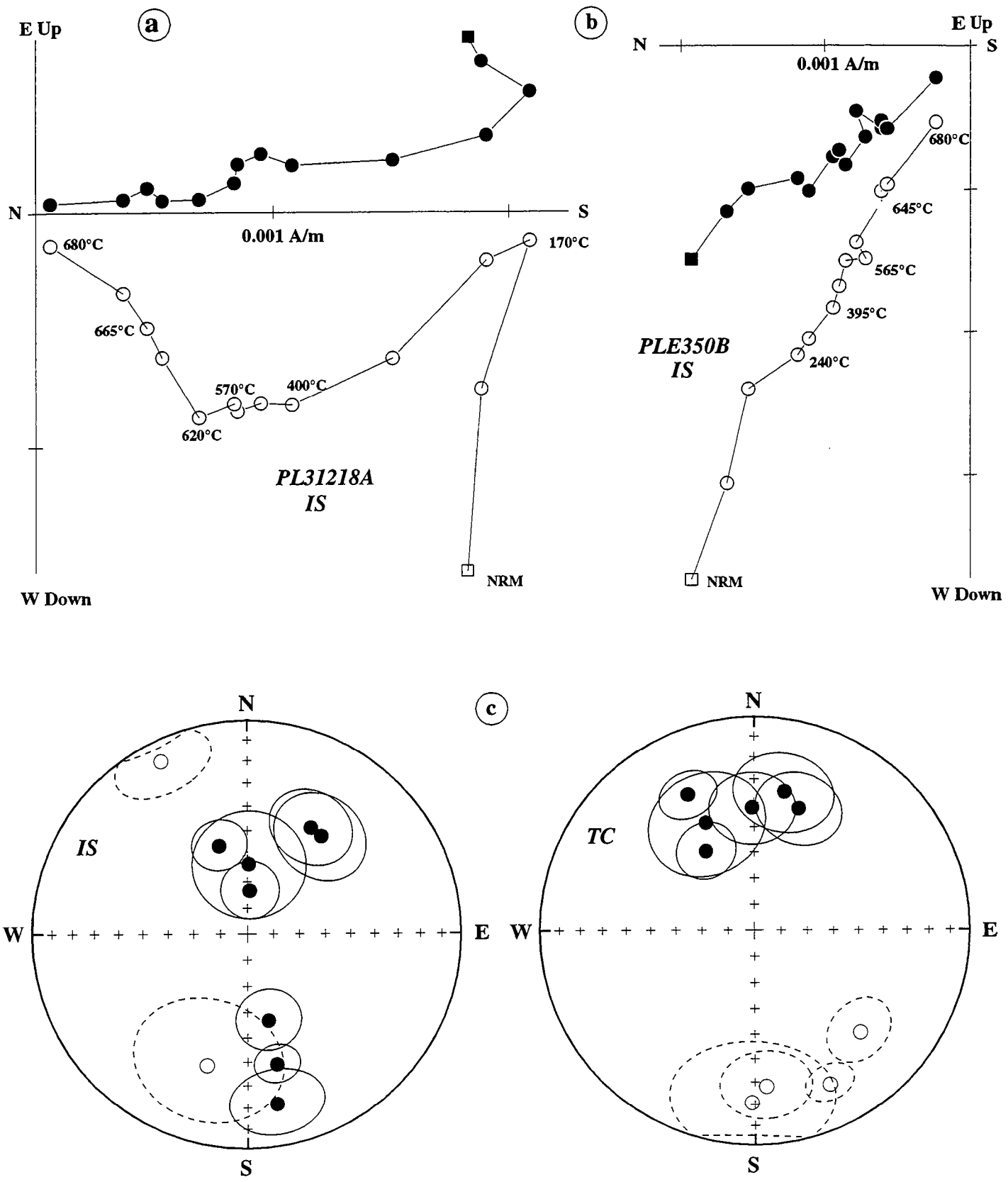

Fig 8. Paleomagnetic data for Pulkhakim locality.
Same comments as for Figure 4.

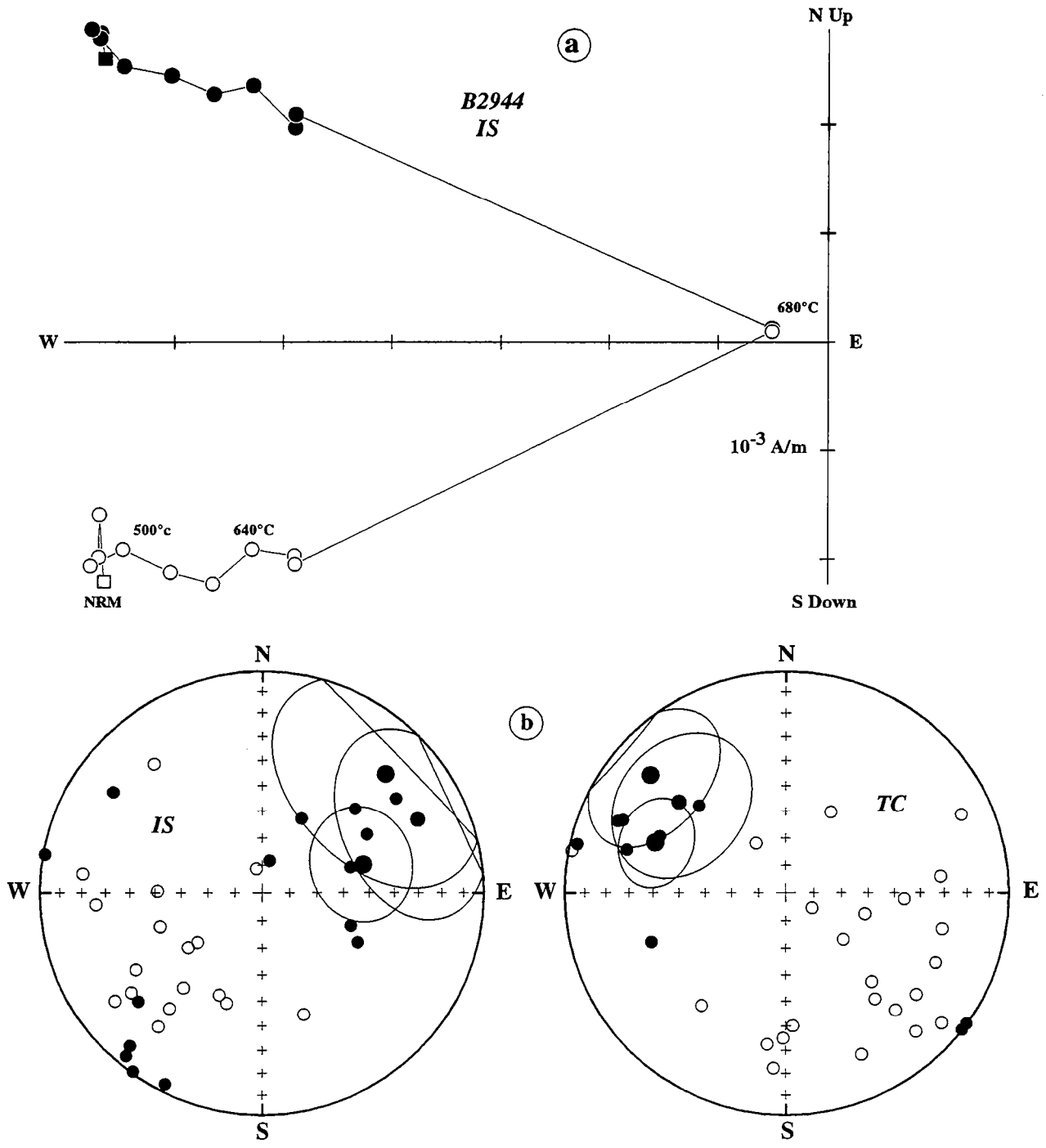

Fig 9. Paleomagnetic data for South Darvaz locality.
Same comments as for Figure 5.

	Latitude (°N)	Longitude (°E)	A95
Besse and Courtillot [1991]			
Pole (100 Ma)	76.7	197.1	5.0
Pole (30 Ma)	81	132.8	2.7
[*Chauvin et al.*, 1992]			
Dekhanabad (Lw. Mio)	68	239	9

	Inclination difference		Rotation	
	versus Besse and Courtillot Pole	versus Dekhanabad Locality Pole	versus Besse and Courtillot APWP	versus Dekhanabad Locality
			Oligo- Miocene (this study)	
South Darvaz	+28°±09°	+2°±15°	-59°±10°	-52°±13°
Tukaynaron	+25°±9°	+5°±11°	-54°±12°	-46°±14°
Kalinabad	+29°	-1°	-62°	-54°
Aksu	+27°±12°	+3°±17°	-24°±15°	-17°±16°
Pyryagata	+30°±10°	0°±12°	-35°±12°	-27°±14°
Pulkhakim	+24°±11°	+5°±16°	-21°±13°	-14°±15°
			Up. Cretaceous *Bazhenov et al.*, [1993]	
South Darvaz	-7°±6°		-51±7°	
Aksu	+1°±5°		-15°±5°	
Derbent	+1°±3°		-05°±5°	
Takob	+4°±6°		-09°±6°	
			Up. Cretaceous *Pozzi and Feinberg*, [1991]	
Nurek	+7°±8°		-32°±15°	
Guissar	-4°±5°		-05°±7°	
Ragoon	-12°±4°		-13°±8°	

Table 7. Poles and associated reference paleomagnetic directions for Eurasia at 30 Ma and 100 Ma (Upper part of table), and their comparison with available data in the Tadjik depression (lower part of table).

Differences in inclination and declination (rotation) between reference and measured data are calculated according to *Beck* [1980] and *Demarest* [1983]. Positive rotations are clockwise rotations. Positive inclination differences are for inclinations lower than expected. A95 is radius of circle of confidence at 95% probability level.

South Darvaz

South Darvaz locality is on the Eastern border of the Tadjik depression, along the Pamir boundary. We sampled siltsones and grey or brownish-red sandstones along a section through steeply-dipping beds of Paleocene to Early Miocene age. Additional hand samples were collected along three sections, about two kilometers apart: the first section (S1, 19 samples) is through Eocene to lower Miocene beds; the other two (S2, 9 samples; S3, 12 samples) through Oligocene to lower Miocene rocks. This collection was previously studied by *Bazhenov and Burtman* [1986] but with only partial demagnetization (up to 400°C). Demagnetization was completed at Rennes in 1992. Most demagnetization curves show a single-vector component from 100°-200°C to 680°C (Figure 9a). Despite a well-defined component for most samples, paleomagnetic directions are rather scattered (Figure 9b and Table 6). Both polarities are observed (Figure 9b) and a reversal test is positive. No fold test could be performed, because bedding dips almost uniformly at this locality.

DISCUSSION ON PALEOMAGNETIC DATA

Quality and Reliability of Data

At two localities (Tukaynaron, Pulkhakim), despite positive fold tests, data are still rather scattered at the between-site level after tilt correction (k=12 and k=16). For these localities, k increases continuously during unfolding. Thus, the observed scattering in tilt-corrected coordinates cannot be due to magnetization acquired on tilted beds. *Butler* [1992] suggested that the magnetization of red beds, similar to those from Tukaynaron and Pulkhakim, is a chemical remanent magnetization (CRM) acquired between 10^2 and 10^5 years after sedimentation. If the CRM is acquired before 10^3 years, then the between-site scattering can be explained by an acquisition of remanence faster than the time necessary to satisfactorily average the secular variation of the geomagnetic field. Nevertheless, at Tukaynaron and Pulkhakim localities, a substantial number of sites (10) have mean directions of overall good quality. We thus consider that the bulk mean directions for these localitites are reliable.

For Kalinabad and Pyryagata localities, we rejected a large number of sites for which it was impossible to obtain well-defined high-temperature components. This probably reflects the poor quality of the outcrops. In some areas, we had great difficulty in finding red beds suitable for paleomagnetic study. Weathering, coarse-grained sediments and prolonged CRM (more than 10^5 years after sedimentation) are possible reasons for the poor quality of the

remanence. However, for Pyryagata locality, the six remaining sites show antipodal directions and a good clustering after tilt correction. We therefore consider the mean direction to be reliable. At Kalinabad locality, only two sites yielded a reliable mean direction. Given that only few Tertiary paleomagnetic data exist for the Tadjik depression, we have not rejected this locality, keeping in mind that corresponding data must be interpreted with caution.

In general, fold tests are positive. For two localities (Aksu and South Darvaz), fold tests could not be done. However, positive fold tests were already obtained on Cretaceous rocks from the same regional structures (Table 7) [*Bazhenov et al.*, submitted], but with a steeper mean direction. The good consistency of tilt-corrected results between all localities suggests that magnetization was acquired before folding.

Paleomagnetic reference

Discussion and interpretation of paleomagnetic data require a reliable reference, established for undeformed areas. Over the last ten years, several authors have calculated apparent polar wander paths (APWPs) for Eurasia [*Irving and Irving*, 1982; *Westhphal, et al.*, 1986; *Besse and Courtillot*, 1991]. However, some paleomagnetic studies of Tertiary sediments from Asia [*Westphal et al.*, 1986; *Bazhenov and Burtman*, 1986; *Huang and Opdike*, 1992; *Thomas et al.*, 1993a] have revealed major differences between observed directions and those expected from APWPs, especially for inclinations. Furthermore, most APWPs for the Cenozoic are based only on data from Western Europe, very few or none on data from stable Asia.

To obtain a more reliable regional reference, we sampled Tertiary rocks on the stable Turan platform adjacent to the Tadjik basin. We collected Lower Miocene rocks on the western margin of the SW Ghissar ranges, near Dekhanabad city (Figure 1a). There, sediments of the platform are only slightly tilted. Cretaceous rocks were also sampled in the SW Ghissar ranges. For these rocks, *Chauvin et al.* [1992] and *Bazhenov et al.* [submitted] show that there are no significant paleomagnetic differences in inclination and in declination between the measured Cretaceous direction and the direction predicted by the APWP of *Besse and Courtillot* [1991] at 100 Ma. Dekhanabad locality, which belongs to the same structural unit, can thus be considered as a stable area since the late Cretaceous. We therefore consider the mean paleomagnetic direction of this locality as a local Tertiary reference for the Tadjik basin and adjacent areas. The mean pole for the locality is: Lat 68°N, Long 239°E [*Chauvin et al.*, 1992]. Compared with the APWP curve of *Besse and Courtillot* [1991] at 30 Ma (Lat:

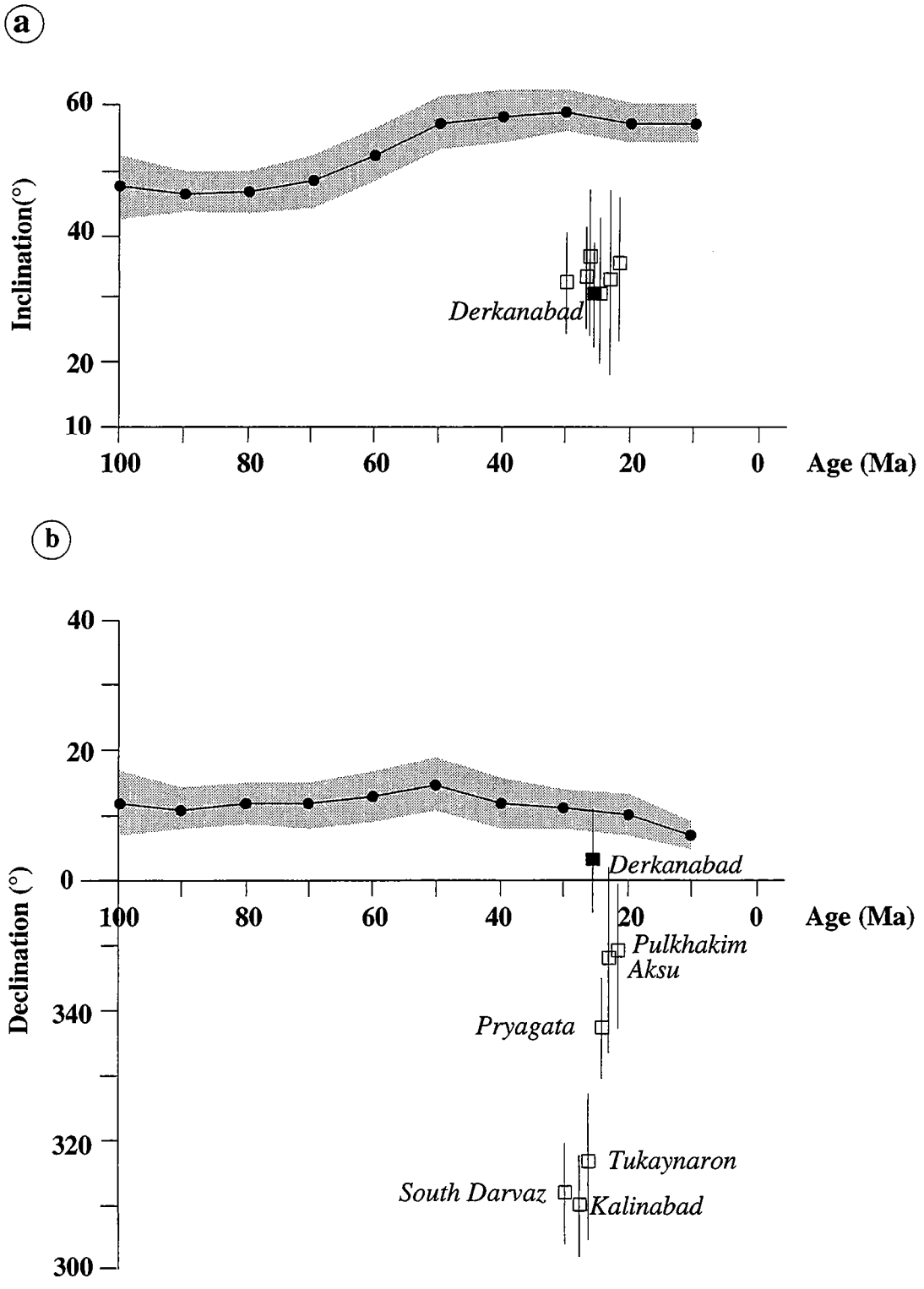

Fig 10. Observed paleomagnetic directions compared with the Besse and Courtillot [1990] APWP curve (95% confidence interval is shaded).

a), inclination versus age; (b), declination versus age. Filled square is Dekhanabad reference locality [Chauvin et al., 1992]. Inclinations are very consistent and are about 30° shallower than expected. Declinations are strongly heterogeneous, varying from -54° to -14° with respect to Dekhanabad.

81°N, Long: 132°E, Table 7), there is no significant difference in declination; but the inclination at Dekhanabad is 30°±7° lower than expected. This anomaly will be discussed in the following section.

Inclination

In Figure 10a and Table 7, inclinations observed on Tertiary rocks within the Tadjik depression and along its margins are compared with the APWP of *Besse and Courtillot* [1991]. The most remarkable feature is the very good consistency between localities, including the reference locality of Dekhanabad. Inclinations range from 30°±12° to 35°±13°. This emphazises that Tertiary inclinations are actually lower by about 30°±10° than those predicted by the APWP (61°). Comparable inclination anomalies have already been described, not only for various parts of Central Asia [*Bazhenov and Burtman,* 1986; *Huang and Opdyke,* 1991; *Thomas et al.,* 1993a; *Chauvin et al.,* 1992], but also at the scale of Eurasia as a whole [*Westphal et al.,* 1986; *Westphal,* 1993]. These anomalies are discussed by *Thomas et al.* [1993a] and *Chauvin et al.* [1992].

Processes usually invoked to account for inclination shallowing in rocks are compaction, deformation and magnetization acquisition. However, these can hardly explain anomalies of 30°, unless all factors contribute in the same sense.

If due to a change in latitude, the observed inclination anomaly would require at least 2500 km of N-S displacement, whereas no more than a few hundreds of kilometers are readily accounted for by Cenozoic deformation North of the Tadjik depression, in the Tien-Shan ranges [*Avouac and Tapponnier,* 1992; *Avouac et al.,* 1993; *Thomas et al.,* 1993a]. Moreover, the Late Cretaceous inclination is 30° steeper than the Tertiary inclination, which would further imply a 1500 km southward motion before the hypothetic Tertiary northward displacement.

Recently, *Westphal* [1993] has suggested that, during the Eocene, the earth's magnetic field was not that of an axial dipole but had an axis inclined at 18° to the earth's rotation axis. This interpretation is based on data from the Eurasian Tethyan belt. We do not favour it for several reasons. First, our sediments are mainly Lower Miocene in age, which would imply an abnormal behavior of the geomagnetic field during at least 40 Ma. Second, the data selected by *Westphal* [1993] are not always convincing. In particular, ages are not all precisely constrained (see discussion below on the data of *Pozzi and Feinberg* [1990] in the Tadjik depression). Third, corresponding inclination anomalies would be expected in other parts of the world, but have not been observed so far. Hence, we decided to use the Dekhanabad pole as a local reference for our study.

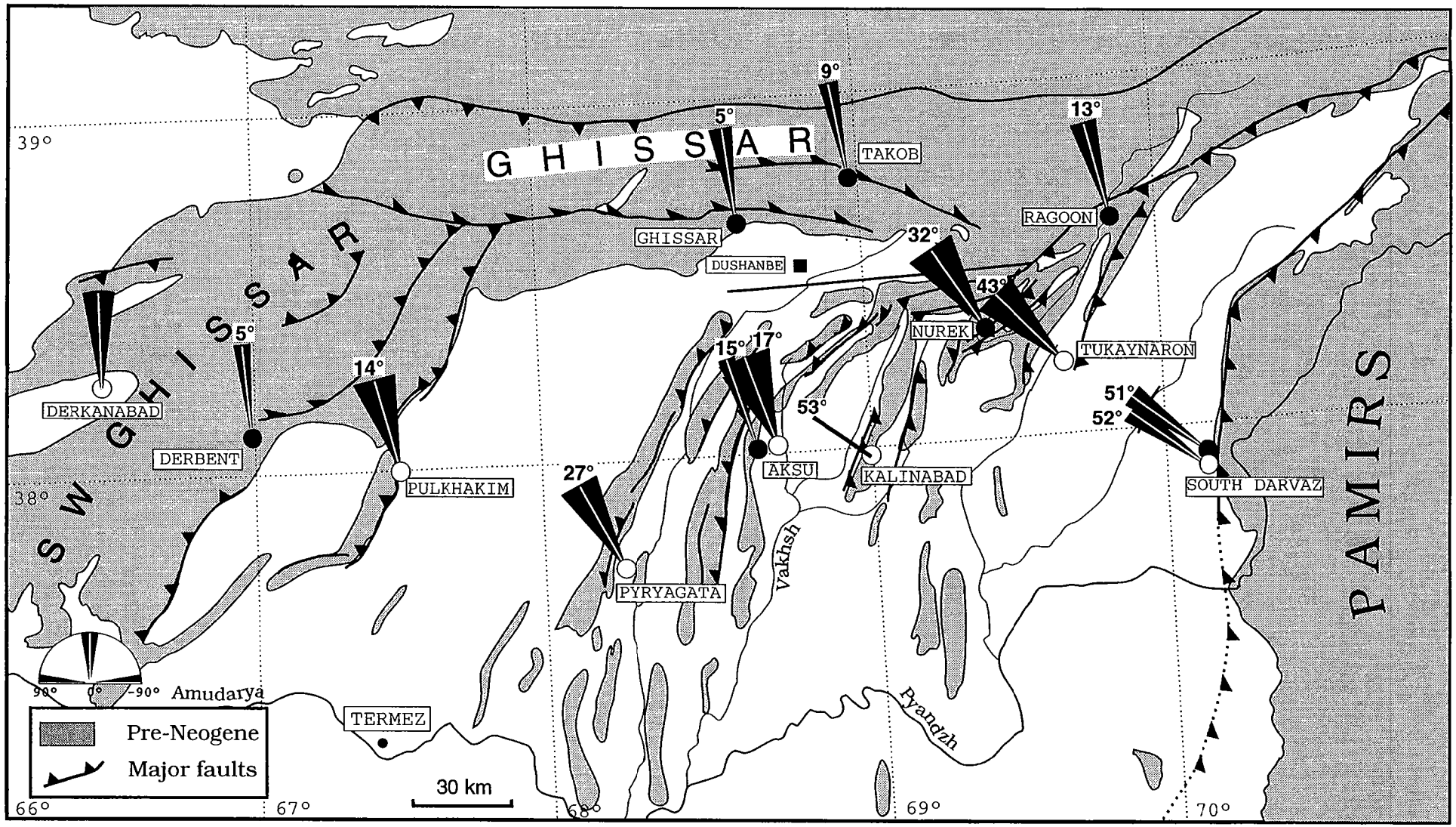

Fig 11. Compilation of paleomagnetic rotations for the Tadjik depression.
Rotations are calculated using Besse and Courtillot [1990] pole at 100 Ma for Cretaceous data (black circles), and using Dekhanabad locality [Chauvin et al., 1992] for Tertiary data (open circles). Rotations (absolute values are given) and attached uncertainties are shown with respect to a N-S reference direction. Rotations are all counterclockwise, larger in the eastern part of the depression than in the western part of the depression. No or little rotation is measured in the Ghissar and SW Ghissar ranges.

The consistency of measured inclinations across the Tadjik depression shows that there have been no significant changes in latitude between the eastern margin of the Tadjik depression and the Turan platform since the Tertiary.

Declination

In contrast with inclinations, measured declinations are strongly variable across the Tadjik depression (Figure 10b and Table 7). Compared with the Dekhanabad reference (which has undergone no rotation), two geographic domains of declination can be distinguished (Figure 11).

1. In the Eastern part of the depression, Tukaynaron, Kalinabad and South Darvaz localities show large counterclockwise paleomagnetic rotations (46°±14°, 54° and 52°±13°, respectively).

2. In the West, Aksu, Pulkhakim and Pyryagata localities show smaller counterclockwise rotations (17°±16°, 14°±15° and 27°±14° respectively). Uncertainities are large for Aksu and Pulkhakim localities. However, at Aksu locality, Cretaceous rocks sampled by *Bazhenov et al.* [submitted] show a significant counterclockwise rotation of 15°±5° (Figure 11 and Table 7) with respect to the *Besse and Courtillot* [1991] APWP (Table 7). Thus, with two independent references, Cretaceous and Tertiary samples from the same fold have yielded very similar paleomagnetic rotations. We assume that rotations for Tertiary and Cretaceous rocks have the same tectonic origin. If so, the rotation recorded at Pulkhakim may also be significant.

Table 7 shows the amounts of rotation calculated with respect to the APWP of *Besse and Courtillot* [1990] at 30 Ma. At Aksu and South Darvaz localities, this leads to rotations which are larger for Tertiary rocks than for Cretaceous rocks. This rather unexpected result strengthens our choice of Dekhanabad locality as a convenient reference for our study.

Other data

Figure 11 (see also Table 7) shows all reliable paleomagnetic data on Mesozoic and Cenozoic rocks in the Tadjik depression [*Pozzi and Feinberg*, 1991; *Bazhenov et al.*, submitted; *Chauvin et al.*, 1992; this study]. *Pozzi and Feinberg* [1991] studied Cretaceous sediments from three localities in the northwestern part of the depression. They interpreted the mean direction as a Tertiary overprint linked to the Alpine-Himalayan orogenesis. However, *Bazhenov et al.* [submitted] studied equivalent formations and showed that the overprint is more probably Upper Cretaceous. We therefore choose an Upper Cretaceous

reference to reinterpret data of *Pozzi and Feinberg* [1991]. Corresponding directions must be interpreted with care, because of the small number of samples per locality.

The Cretaceous data confirm and complete the Tertiary data, especially in the northern and western parts of the study area. In the Ghissar and SW Ghissar ranges, small to insignificant paleomagnetic rotations are observed (5°±5° for Ghissar, 9°±6° for Takob, 5°±5° for the SW Ghissar).

TECTONIC INTERPRETATION

The major inferences from the declination data are as follows.

1. Tertiary and Cretaceous rotations are very similar. Thus, we infer that no significant rotations occurred between the Upper Cretaceous and the Lower Miocene.

2. Significant counterclockwise rotations occurred within the Tadjik depression. Rotations were larger in the eastern part than in the western part.

3. Little or no rotation occurred in the SW Ghissar ranges and in the Ghissar range.

Tapponnier et al. [1981] suggested that the current geometry of the depression, with its arcuate fold traces, results from westward extrusion induced by the Pamirs. If so, one would expect clockwise rotations in the northern part of the depression, counterclockwise rotations in the southern part, and no rotations in the central part. No paleomagnetic data are available for the southern part of the depression; however, in the northern and central parts, rotations are all counterclockwise. A simple symmetric extrusion model cannot explain this rotation pattern.

We prefer a model where the Tadjik depression is a lozenge-shaped basin bounded by thrust-wrench zones (Figure 12).

In their interpretation of the rotation pattern observed in intermontane basins of the Western Tien-Shan, *Thomas et al.* [1993a] and *Bazhenov* [1993] have suggested that regional kinematics were strongly associated with the indentation of the Pamirs into Asia. Current plate motions indicate a NNW to NS movement of the Pamirs [*Minster and Jordan*, 1978; *De Mets et al.*, 1990]. In the Tadjik depression, structural analysis [*Thomas et al.*, 1993b] has revealed that thrusting is combined with a regional component of sinistral wrenching, synthetic to the relative motion of the Pamirs with respect to the Turan Platform. Paleomagnetic data presented above show that this sinistral wrenching is accompanied by counterclockwise rotations about vertical axes.

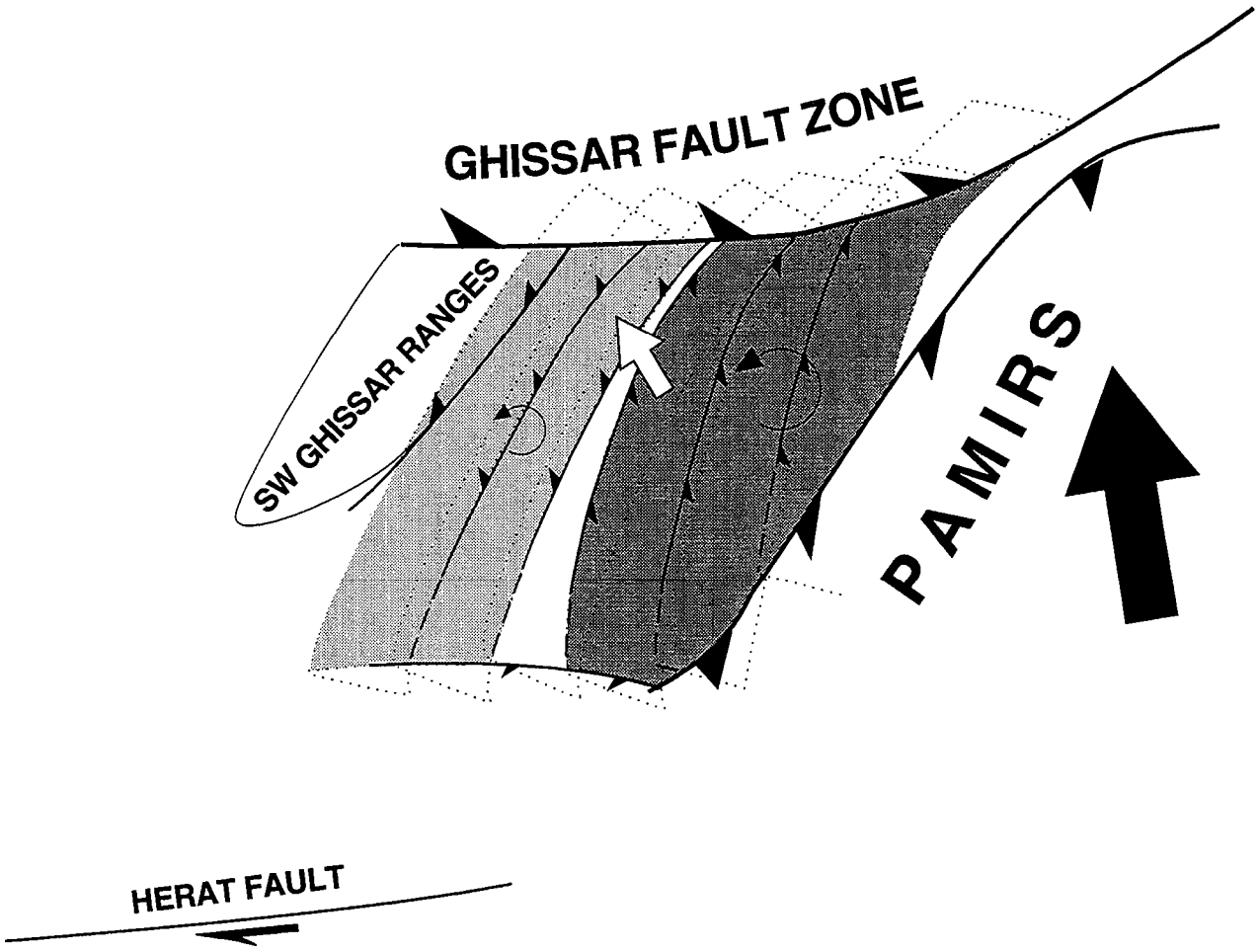

Fig 12. Inferred Cenozoic kinematics of the Tadjik depression.
Deformation is assumed to be essentially associated with motion of the Pamirs (thick arrow). Relative displacement between blocks is taken up by oblique-slip thrusting, dashed boundaries of blocks representing underthrust edges. In the eastern part of the depression (dark-grey domain), counterclockwise rotations are large; they are smaller in the western part (light-grey domain). Central domain (white) is a pop-down basin .

Both counterclockwise rotations and NS to NE-SW sinistral wrenching fit the regional model of Tertiary kinematics proposed by *Cobbold and Davy* [1988] for the area.

The Tadjik depression has two paleomagnetic domains, with large rotations near the Pamirs, and smaller rotations near the SW Ghissar ranges (Figure 12). These also appear to be major structural domains of the depression (Figures 1b and 12): the eastern part of the depression shows westward directed thrusts; whereas the western part shows eastward directed thrusts. A pop-down (full ramp) basin occurs between these two domains. The occurence of opposite senses of strike-slip components along the northern and southern boundaries of the depression (Figure 12) suggests that the rotation of the depression was accompanied by northwestward extrusion. Thick-skinned deformation occurs at the margins of the Tadjik depression (Ghissar, SW Ghissar, Pamirs). The deformation inside the depression, especially in its central part, also involves basement (Figure 1b). From this, we infer that rotations observed in the cover reflect probably block rotations throughout the brittle crust. The importance of the Upper Jurassic décollement level remains however unknown.

In the SW Ghissar ranges, no significant paleomagnetic rotations have been found. Except in the northermost part of these ranges, deformation decreases gradually toward the stable Turan platform. We therefore infer that the SW Ghissar ranges remained relatively fixed during the deformation, with respect to the Tadjik depression and the Turan platform. Thrusts involving basement are much more developed in the northern part of the SW Ghissar ranges than in their southern part (Figure 1a). Topographic maps show that the uplifted area has a triangular shape, with the apex to the South. These two features suggest that the amount of horizontal convergence between the Tadjik depression and the Turan platform decreases southward (Figure 12). This in turn indicates that the mean pole of counterclockwise rotation of the depression is located somewhere in its southwestern part.

North of the Tadjik depression, the E-W striking Ghissar are a major uplifted fault zone which curves counterclockwise, from NW-SE in the vicinity of the stable platform, to WSW-ENE North of the Pamirs (see Figure 1). This change in orientation coincides with increasing regional deformation. Counterclockwise rotations have occurred in areas North and South of the Ghissar range and neighbouring mountain belts, in the Fergana basin and in the Tadjik depression respectively. These features suggest that substantial counterclockwise rotations could have affected the Ghissar range. In contrast, our paleomagnetic study reveals minor to negligible counterclockwise rotations of this domain. Two end-members hypotheses can be invoked. (1) Regional

counterclockwise rotations have been partly compensated by local clockwise rotations. This could for instance have been achieved by rotation of second-order antithetic dominoes within the Ghissar dextral wrench zone. (2) The Ghissar range is a relatively fixed domain, uplifted between two rotated domains. This hypothesis implies substantial amounts of underthusting of blocks North and South of the ranges. Indeed, structural data show that substantial thrusting has accompanied dextral wrenching throughout the Ghissar range and at the northern boundary of the Tadjik depression. Other features are in favor of limited rotation of the Ghissar range compared with the Tadjik depression. First, maps [*Ministry of Geology of the USSR and the Tadjik Academy of Sciences,* 1984] show that the Ghissar range is associated with a single set of numerous major thrust-wrench faults parallel to the belt and probably of lithospheric scale; but they do not show evidence for well-developed sets of antithetic dominoes. Second, the major crustal thickening expected in this area is likely to limit its ability to rotate, compared with the less thickened crust beneath the Tadjik depression. Third, faults and fold axes within the Tadjik depression strike about NS in the center of the depression, and curve to become at a low angle to the strike of the Ghissar range in its vicinity (Figure 1). This curvature is compatible with dextral wrenching along the Ghissar range; but it is also compatible with a jump in the amount of rotation between blocks of the Tadjik depression and the Ghissar range. Sandbox experiments [*Gapais et al.*, 1991] have indeed shown that bending of faults can accommodate jumps in rigid rotation across incoherent boudaries between domains of conjugate fault sets.

Acknowledgements

Data presented in this paper were collected in 1990 during a one-month field expedition, under the terms of an international agreement between the Academy of Sciences, Moscow, and the CNRS (international division).

REFERENCES

Abdullaev, K. A., and Y. S. Rzhevsky, *Lower Cretaceous paleomagnetism of the Tadjik basin*, 104 pp., Donish, Tashkent, 1973.

Achache, J., and V. Courtillot, Paleogeographic and tectonic evolution of southern Tibet since middle Cretaceous time: New paleomagnetic data and synthesis, *J. Geophys. Res., 89*, 10311-10339, 1984.

Argand, E., La tectonique de l'Asie, *Congrès géologique international, Comptes-Rendus de la XIII session*, Belgique, premier fascicule, 171-371, 1924.

Avouac, J. P., and P. Tapponnier, Cinématique des déformations actives en Asie Centrale, *C. R. Acad. Sci. Paris, 315*, 1791-1798, 1992.

Avouac, J. P., P. Tapponnier, M. Bai, H. You, and G. Wang, Active thrusting and folding along the Northern Tien Shan and late Cenozoic rotation of the Tarim relative to Dzungaria and Kasakhstan, *J. Geophys. Res., 98*, 6755-6804, 1993.

Bazhenov, M. L., Cretaceous paleomagnetism of the Fergana basin and the adjacent ranges: tectonic implications, *Teconophysics*, 221, 251-267, 1993.

Bazhenov, M. L., and V. S. Burtman, Tectonics and paleomagnetism of structurals arcs of the Pamir-Punjab syntaxis, *J. Geodyn., 5*, 383-396, 1986.

Bazhenov, M. L., H. Perroud, A. Chauvin, and V. S. Burtman, Paleomagnetism of Cretaceous red beds from the Tadjikistan and Cenozoic deformations related to the India-Eurasia collision, *Earth Planet. Sci. Lett.*, submitted.

Beck, M. E., Paleomagnetic record of plate margin tectonic processes along the western edge of North America, *J. Geophys. Res., 85*, 7115-7131, 1980.

Besse, J., and V. Courtillot, Revised and synthetic apparent polar wander paths of the African, Eurasian, North American and Indian plates, and true polar wander paths since 200 Ma, *J. Geophys. Res., 96*, 4029-4050, 1991.

Burtman, V. S., Structural geology of the Variscan Tien-Shan, *Am. Jour. Sci., 275A*, 157-186, 1975.

Burtman, V. S., and P. Molnar, Geological and geophysical evidence for the subduction of continental crust beneath the Pamir, Inter. sym. on the Karakorum and Kunlun mountains abstracts, Kashi, China, 30, 1992.

Butler, R. F., *Paleomagnetism*, Blackwell, Cambridge, 319 pp., 1992.

Chauvin, A., M. L. Bazhenov, and H. Perroud, Low inclinations from Tertiary sediments of Central Asia, *EOS, 73*, 148, 1992.

Cobbold, P. R., and P. Davy, Indentation tectonics in nature and experiments. 2. Central Asia, *Bull. Geol. Inst. Univ. Uppsala, 14*, 143-162, 1988.

Demarest, H. H., Error analysis for the determination of tectonic rotation from paleomagnetic data, *J. Geophys. Res., 88*, 4321-4328, 1983.

De Mets, C., R. G. Gordon, D. F. Argus, and S. Stein, Current plate motion, *Geophys. Jour. Int., 101*, 425-478, 1990.

Dewey, J. F., and K. C. A. Burke, Tibetan, Variscan, and Precambrian reactivation: Products of continental collision, *J. Geol., 81*, 683-692, 1973.

England, P., and P. Molnar, Right lateral shear and rotation as an explanation for strike-slip faulting in Eastern Tibet, *Nature, 344*, 140-142, 1990.

Funahara, S., N. Nishiwaki, F. Murata, Y. Otofugi, and Y. Z. Wang, Clockwise rotation of the Red River fault inferred from paleomagnetic study of Cretaceous rocks in the Shan-Thai-Malay block of western Yunnan, China, *Earth Planet. Sci. Lett., 117*, 29-42, 1993.

Gapais, D., G. Fiquet, and P. R. Cobbold, Slip system domains - 3 - New insights in fault kinematics from plane-strain sandbox experiments, *Tectonophysics, 188*, 143-157, 1991.

Hamburger, M. W., D. R. Sarewitz, T. L. Pavlis, and G. A. Papandopulo, Structural and seismic evidence for intracontinental subduction in the Peter The First Range, Central Asia., *Geol. Soc. Amer. Bull., 104*, 397-408, 1992.

Heuckroth, L. E., and R. A. Karim, Afghan seismotectonics, *Phil. Trans. R. Soc. Lond., 274*, 389-395, 1973.

Houseman, G., and P. England, Finite strain calculations of continental deformation 1. Method and general results for convergent zones, *J. Geophys. Res., 91*, 3651-3663, 1986.

Houseman, G., and P. England, Crustal thickening versus lateral expulsion in the Indian-Asian continental collision, *J. Geophys. Res., 98* , 12233-12249, 1993.

Huang, K., and N. D. Opdike, Paleomagnetism of Cretaceous to Lower Tertiary rocks from southwestern Sichuan: A revisit, *Earth. Planet. Sci. Lett., 112*, 29-40, 1992.

Irving, E., and G. A. Irving, Apparent polar wander paths from carboniferous through Cenozoic and the assembly of Gondwana, *Geophys. Surv., 6*, 141-187, 1982.

Leith, W.and D. W. Simpson, Seismic domains within the Ghissar-Kokshal seismic zone, Soviet Central Asia, *J. Geophys. Res., 91*, 689-699, 1986.

Le Pichon, X., M. Fournier, and L. Jolivet, Kinematics, topography, shortening, and extrusion in the India-Eurasia collision, *Tectonics, 11*, 1085-1098, 1992.

Mc Elhinny, M. W., Statistical significance of the fold test in paleomagnetism, *Geophys. J. R. Astron. Soc., 8*, 338-340, 1964.

Ministry of Geology of the USSR and the Tadjik Academy of Sciences, Geological map of the Tadjikistan, scale 1/500 000, 4 sheets, Dushanbe, 1984.

Minster, J. B., and T. H. Jordan, Present-day plate motions, *J. Geophys. Res., 83*, 5331-5354, 1978.

Molnar, P., and P. Tapponnier, Cenozoic tectonics of Asia: Effects of a continental collision, *Science, 189*, 419-426, 1975.

Otofuji, Y., Y. Inoue, S. Funahara, F. Murat, and X. Zheng, Paleomagnetic study of eastern Tibet. Deformation of the Three Rivers region, *Geophys. J. Int., 103*, 85-94, 1990.

Patriat, P., and J. Achache, India-Eurasia collision chronology has implications for crustal shortening and driving mechanism of plates, *Nature, 311*, 615-621, 1984.

Peive, A. V., V. S. Burtman, S. V. Rhuzentsev, and A. I. Suvorov, Tectonics of the Pamirs Himalayan sector of Asia, Rep. 22nd Sess. Int. Geol. Congr., New Delhi, Part XI: Himalayas and Alpine orogeny, 441-462, 1964.

Pozzi, J. P., and H. Feinberg, Paleomagnetism in the Tadjikistan: continental shortening of Eurasian margin in the Pamirs during the Indian-Eurasian collision, *Earth Planet. Sci. Lett., 103*, 365-378, 1991.

Savostin, L. A., J.-C. Sibuet, L. P. Zonenshain, X. Le Pichon, and M.-J. Roulet, Kinematic evolution of the Tethys belt from the Atlantic ocean to the Pamirs since the Triassic, *Tectonophysics, 123*, 1-35, 1986.

Shareq, A., Geological observations and geophysical investigations carried out in Afghanistan over the period of 1972-1979, in *Zagros, Hindu Kush, Himalaya, geodynamic evolution*, edited by H. K. Gupta, 75-86, AGU, Washington, 1981.

Tapponnier, P., M. Mattauer, F. Proust, and C. Cassaigneau, Mesozoic ophiolites, sutures and large scale movements in Afghanistan, *Earth. Planet. Sci. Lett., 52*, 355-371, 1981.

Tapponnier, P., G. Peltzer, and R. Armijo, On the mechanics of the collision between India and Asia, in *Collision tectonics*, edited by M. P. Coward and A. C. Ries, *Geol. Soc. London Spec. Pub.*, 115-157, 1986.

Thomas, J. C., H. Perroud, P. Cobbold, M. L. Bazhenov, V. S. Burtman, A. Chauvin, and E. Sadybakasov, A paleomagnetic study of Tertiary formations of the Kirghiz Tien-Shan and its tectonic implications, *J. Geophys. Res., 98*, 9571-9589, 1993a.

Thomas, J. C., D. Gapais, P. R. Cobbold, and V. S. Burtman, Tertiary kinematics of the Tadjik depression inferred from fault and fold patterns, in *Geodynamic*

evolution of sedimentary basins, edited by F. Roure, Technip, Paris, 1993b, in press.

Trifonov, V. G., Late Quaternary movements of western and central Asia, *Geol. Soc. Amer. Bull., 89*, 1059-1072, 1978.

Westphal, M., Did a large departure from the geocentric axial dipole hypothesis occur during the Eocene? Evidence from the magnetic polar wander path of Eurasia, *Earth Planet. Sci. Lett., 117*, 15-28, 1993.

Westhphal, M., M. L. Bazhenov, J. P. Lauer, D. M. Pechersky, and J. C. Sibuet, Paleomagnetic implications on the evolution of the Tethys belt from the Atlantic Ocean to the Pamirs since the Triassic, *Tectonophysics, 123*, 37-82, 1986.

Zakharov, S. A., Tectonic provinces and structural map of Tadjikian depression, *Trans. Geol. Acad. Sci. Tadjikistan Republic, 5*, 1962.

3. Cinématique Tertiaire de la dépression Tadjik (Asie Centrale) à partir d'une étude micro et macro-tectonique

Tertiary kinematics of the Tadjik depression (Central Asia): inferences from fault and fold patterns

Article sous presse dans "Géodynamic evolution of sedimentary basins", édité par F. Roure, éditions Technip, Paris.

TERTIARY KINEMATICS OF THE TADJIK DEPRESSION (CENTRAL ASIA): INFERENCES FROM FAULT AND FOLD PATTERNS

J.C. THOMAS[1], D. GAPAIS[1], P.R. COBBOLD[1], V. MEYER[1] AND V.S. BURTMAN[2]

ABSTRACT

The Tadjik depression, situated West of the Pamirs (Central Asia), is a wide intermontane compressive basin. Its overall structure is that of a fold-and-thrust belt, made of alternating basins and ranges striking N-S to NE-SW. Basins are filled with Cenozoic and Quaternary sediments up to 6 km thick. Major reverse fault zones verge westwards and eastwards in the eastern and western parts of the depression, respectively, the central domain forming a pop-down basin. From fold and fault patterns throughout the area, (1) the direction of regional shortening is subhorizontal or gently plunging and trends NW-SE to WNW-ESE, (2) thrusting is generally accompanied by significant wrenching along the ranges and (3) the sense of shear is sinistral in the depression and dextral at its EW striking northern boundary (Ghissar range). Inferred kinematics are consistent with the northward displacement of the Pamirs with respect to Asia during Himalayan tectonics. At a larger scale, they are consistent with NE-SW directed sinistral wrenching along the Pamirs-Baikal zone, as a result of the India-Asia collision. Our observations are further compatible with the occurrence of counterclockwise block rotations throughout the Tadjik depression, as revealed by paleomagnetic studies.

1. Laboratoires de Tectonique et Tectonophysique, Géosciences Rennes, Université de Rennes, 35042 Rennes cedex, France.

2. Geological Institute, Academy of Sciences, 109017, Moscow, Russia.

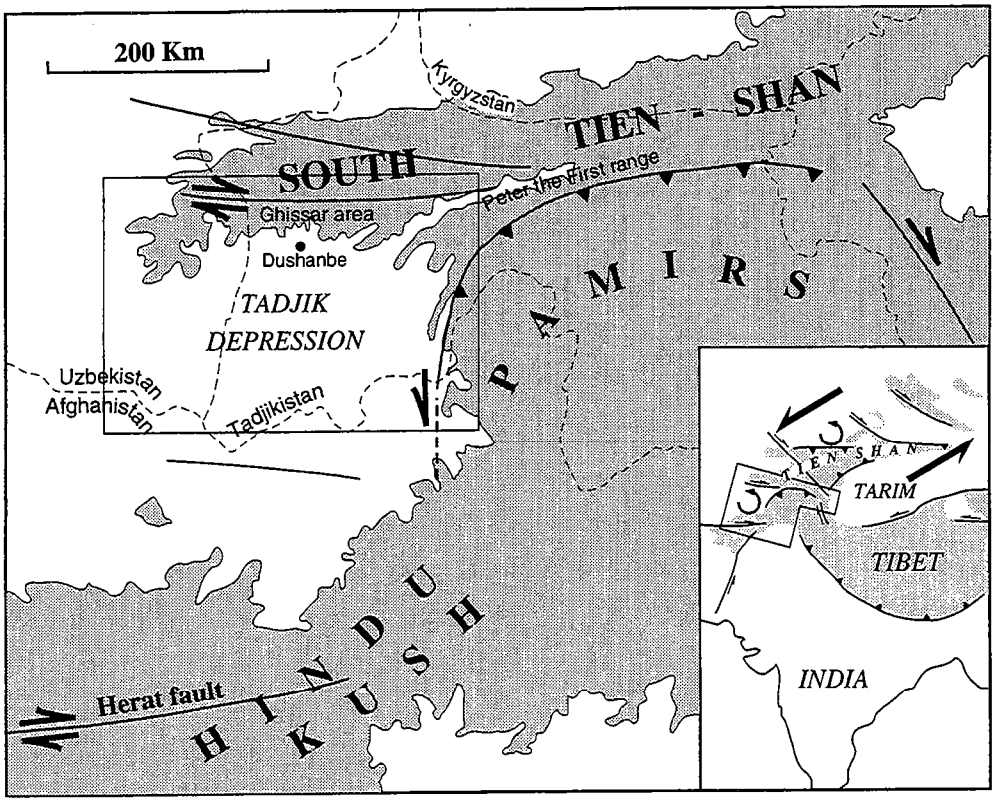

Fig. 1. Simplified map of the Pamirs and adjacent areas (adapted from Leith, 1985).
Shaded areas are above 2000 meters.

INTRODUCTION

For the last 55 Ma, Asia has been deforming, as a result of collision and indentation by India. Crustal thickening occurs in the Himalayas, Tibet, Tien Shan and Altai, while major strike slip displacements are accommodated along the Altyn Tagh, Red River or Talas-Fergana faults. The way indentation is distributed throughout Asia is somewhat controversial. Tapponnier et al., (1986) and Peltzer and Tapponnier (1988) have suggested that about 50% of convergence has been accommodated by eastwards extrusion of continental blocks. Tapponnier et al., (1990) and Avouac and Tapponnier (1992), have believed that Indochina was extruded towards the South East during the Tertiary. In contrast, England (1982) and Dewey et al., (1989) consider that most part of the convergence has been accommodated by crustal thickening. Cobbold and Davy (1988) have suggested that crustal thickening in the Himalayas attenuates laterally across wrench zones, left-lateral in the western Himalayan syntaxis and right lateral in the eastern one. They also argued that a SW-NE band, from the Pamirs through the Tien-Shan and Alai ranges to the Baikal area, has undergone left-lateral wrenching, partially accommodated by a set of NW-SE dextral antithetic faults (Fig. 1). They inferred that wrenching is accompanied by block rotations.

The Tadjik depression is located in the southern part of the Pamirs-Baikal band (Fig.1). It is bounded to the East by the Pamirs and to the North by the South Tien-Shan range. There are various models for the formation of the depression. Leith (1985) suggested that it was a Mesozoic passive margin, reactivated during Cenozoic compression. Tapponnier et al., (1981) considered that it was a Mesozoic marginal basin, which became a foreland basin after the India-Asia collision. Finally, Hamburger et al., (1992) used balanced cross-sections in the North-Western part of the depression to infer that it has been a foreland basin since the Mesozoic. In this paper, we desribe faults and other structure developed in Tertiary rocks and we infer principal directions of strain throughout the depression.

Hamburger et al., 1992). Depths of hypocenters are almost always less than 10 km in the Peter the First range, whereas they can reach up to 70 km in the Northern Pamirs. In the Central Pamirs, another zone of intense seismic activity is present, but at depths between 70 km and 250 km. This pattern of seismicity is attributed to intracontinental subduction of the Tadjik depression beneath the Pamirs (Roecker et al., 1980; Mattauer, 1986; Hamburger et al., 1992). As in the Peter the First range, seismicity within the Tadjik depression is limited to shallow depths, mainly above 10 km, which is the maximum depth of the Jurassic evaporite horizon (Leith and Simpson, 1986). Fault plane solutions are rather consistent throughout the area, with compressive stress axes clustered around a NNW-SSE direction (Roecker et al.; 1980, Prévot et al., 1980; Leith and Simpson, 1986).

MAJOR STRUCTURES

The overall structure of the Tadjik depression is that of a wide fold-and-thrust belt. Basins alternate with anticlinal ranges where Mesozoic series are often exposed (Figs. 2a, 3 and 4a). A regional cross-section (Fig. 2b) shows that the Jurassic evaporites have provided major décollement, especially in the eastern part of the depression, where some salt diapirs crop out. These are associated with significant seismic activity (Leith and Simpson, 1986). The depression is bounded by two main thrust zones of opposite vergences, the western boundary of the Pamirs to the East, and the eastern boundary of the SW Ghissar range to the West. The overall deformation pattern in the depression itself appears strongly controlled by the boundary conditions: major reverse faults verge dominantly westwardly and eastwardly in the eastern and western parts of the depression respectively, the central domain defining a large pop-down structure (ramp basin, see Cobbold et al., in press). Thus, the Tadjik depression appears as an intermontane compressive basin.

The strike of regional folds changes gradually from N-S in the center of the depression, to nearly E-W along the Northern Ghissar range (Fig. 2a). Where exposed, the tips of individual ranges are generally rather symmetric anticlinal hinges, with moderately plunging axes (commonly around 30°-40°) (Fig. 4b). The degree of deformation varies strongly along the ranges. With increasing deformation, asymmetric box folds become strongly asymmetric folds with steep to reverse short limbs defining basin margins (Fig. 4c), then high-angle thrust zones bringing Mesozoic rocks or Paleocene limestones over steeply dipping to inverted Neogene strata (Fig. 4d). From such changes in the

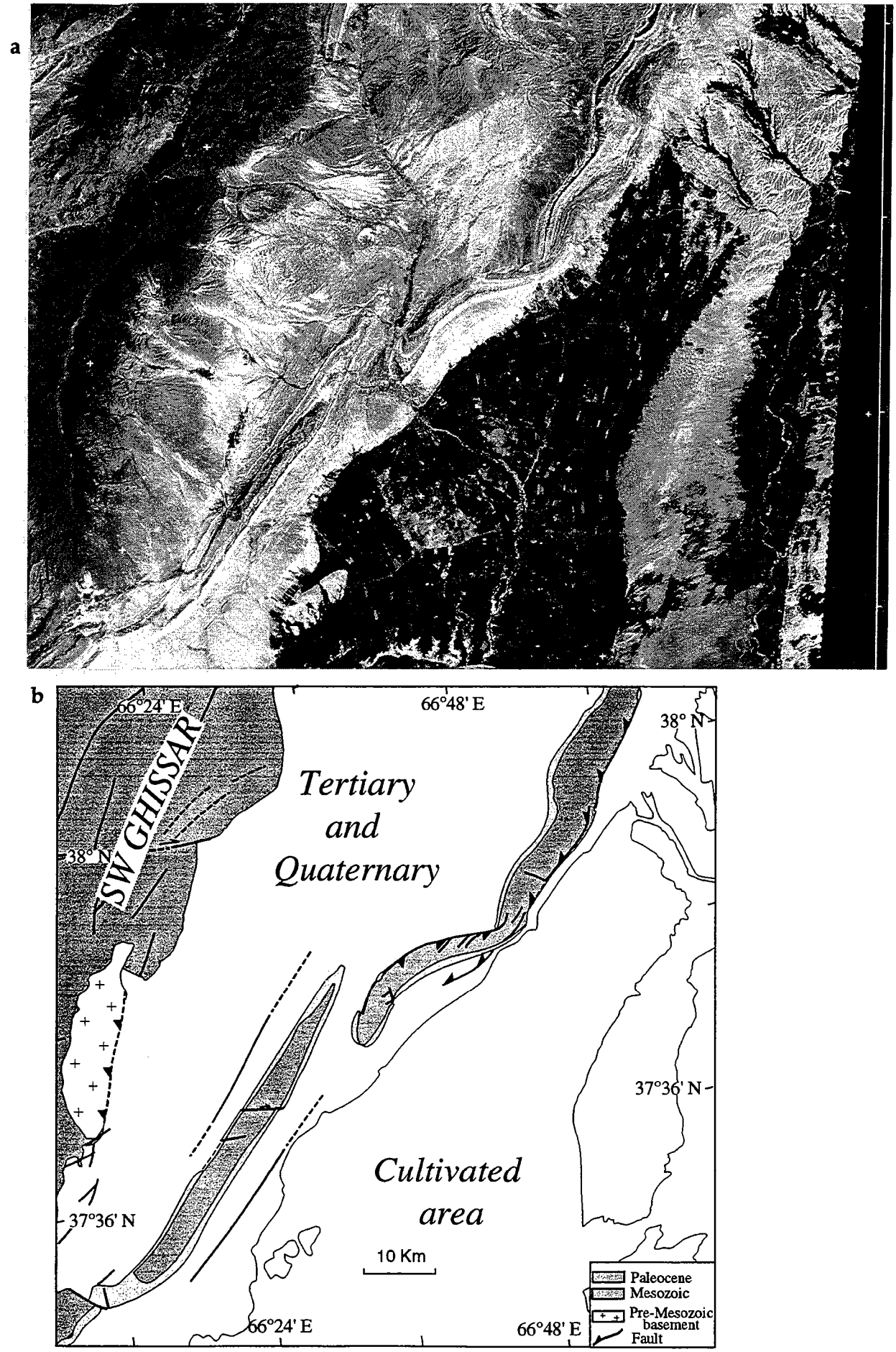

Fig. 3. Landsat TM image of the western boundary of the Tadjik depression (a) and its schematic structural interpretation (b).

Oblique triangles on faults point in direction of underthrusting. Total image width is about 80 km. see location on Fig. 2a.

ENE a WSW

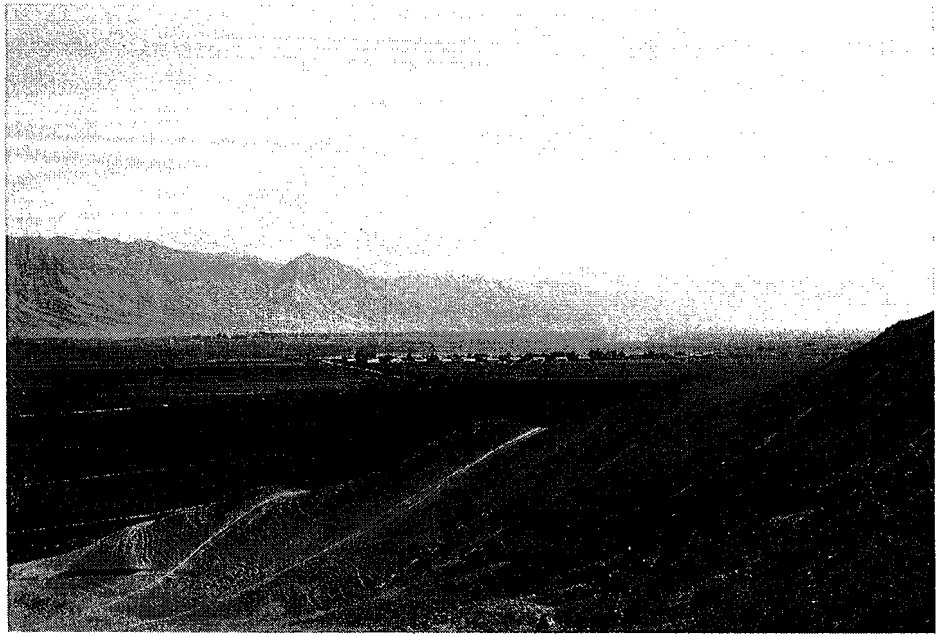

SW b NW

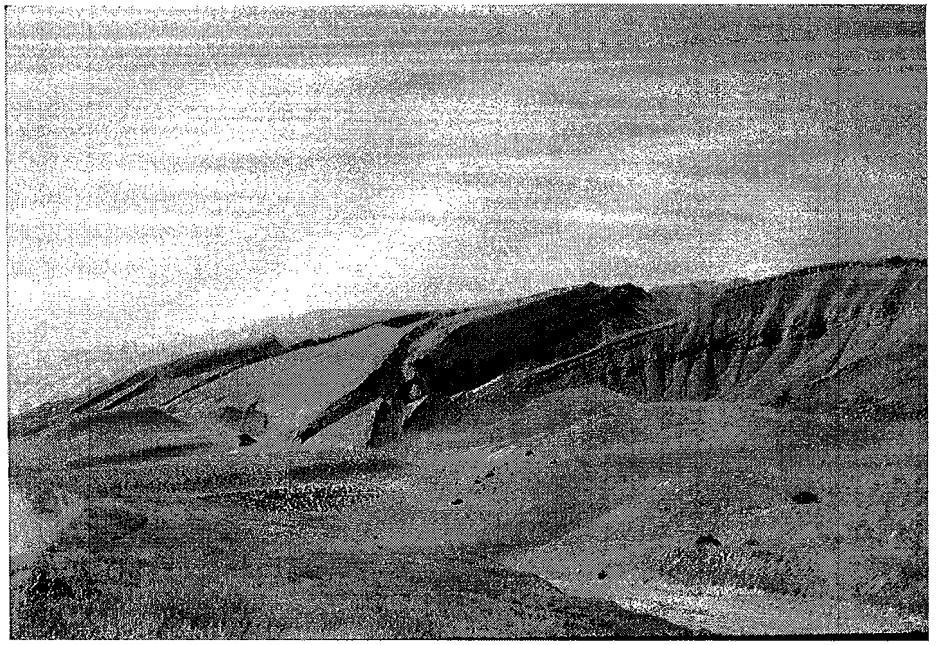

SSE c NNW

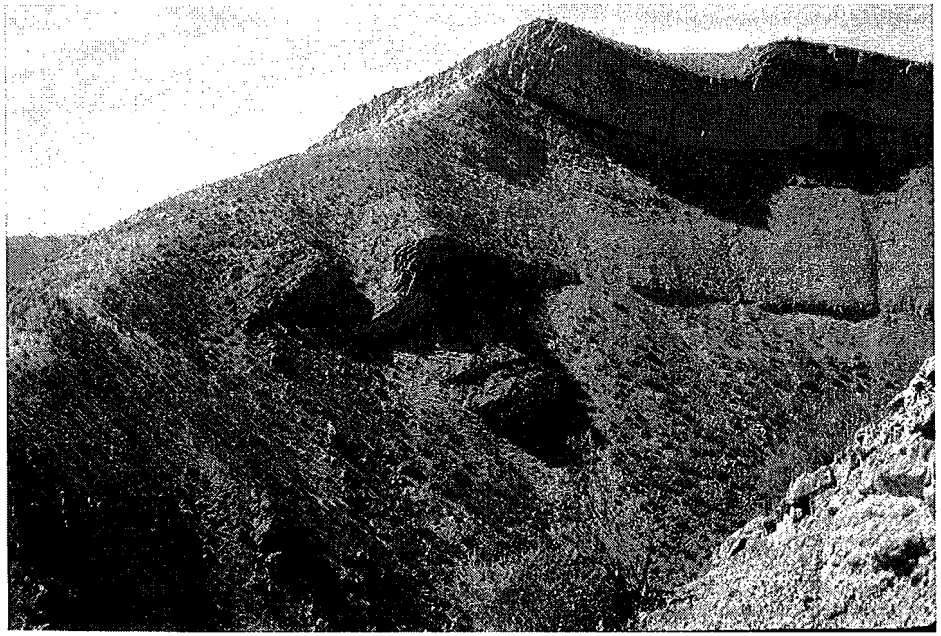

WSW d ENE

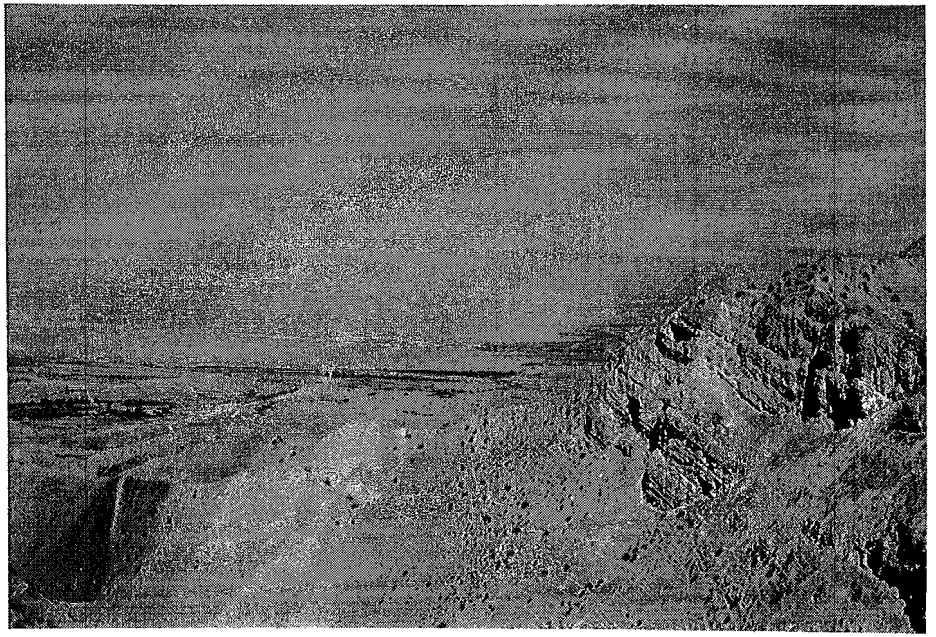

a. Aksu area. N-S basin intercalated between ranges.

b. Kafirnigan area. Plunging anticline at tip of range.

c. Pulkhakim area. Asymmetric fold above thrust.

d. Kafirnigan area. faulted fold with gently dipping Paleocene limestones (right) thrust over subvertical Oligocene series (left).

Fig. 4. Photographs showing the general basin-and-range topography of the area and various structural patterns observed at basin margins (For approximate locations, see Fig. 7).

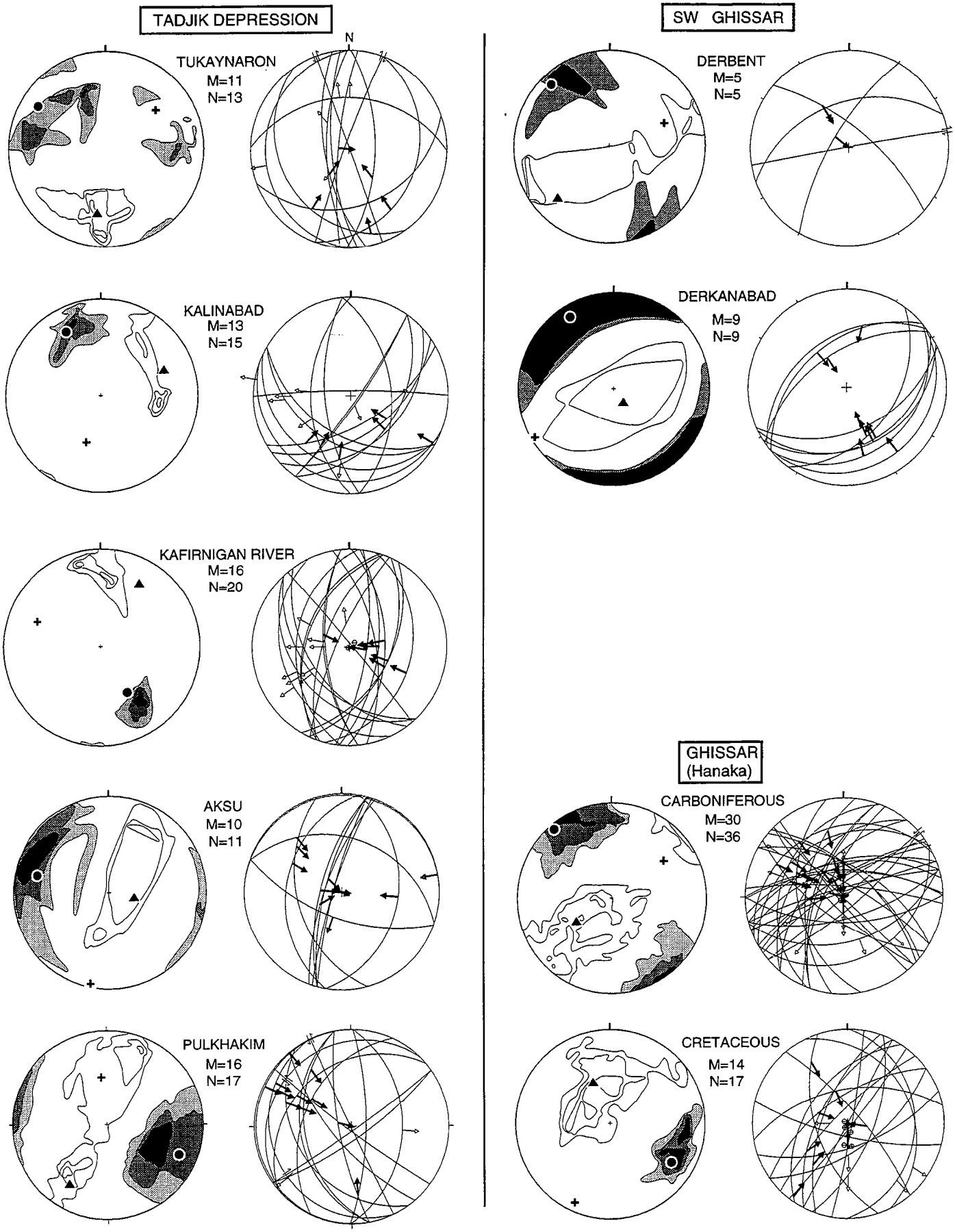

Fig. 5. Equal area stereographic projections (lower hemisphere) of fault-slip data.
For each locality, right-hand diagram shows measured fault planes and associated striations. Arrows (bold for reverse faults, thin for normal faults) indicate azimuths of striations. Left-hand diagrams show results of kinematic analysis (method of right-dihedra). Contours are percentages of faults for which shortening dihedra (shaded) and stretching dihedra (white) are compatible. Analysis yields principal directions: shortening (dot), extension (triangle) and intermediate (cross). N is the number of measured faults; M, the number of faults defining a maximum.

amount of thrusting along strike, we infer strike-slip components. In fact, folds and thrusts are locally en échelon (Fig. 3) (Leith and Alvarez1985).

SLIP DATA FOR MINOR FAULTS

To better constrain the regional kinematics, we have measured populations of small-scale striated faults at several localities along faulted basin margins (see Fig. 7 for locations). Measurements were mainly made in Paleocene limestones, except for two localities. At the westernmost locality (Derkanabad), is a fault zone within upper-Cretaceous sandstones. At Hanaka locality, located at the southern margin of the Ghissar range, North of Dushanbe (see Fig. 7), Carboniferous rocks are thrusted over Cretaceous limestones along a fault striking 70°N and dipping steeply northward. Fault measurements were made in both Carboniferous and Cretaceous sediments.

For each locality, we used the method of overlapping right dihedra (Angelier and Mechler, 1977; Pfiffner and Burkhard, 1987) to infer bulk kinematics. For a single fault, two compressional and two extensional right dihedra can be defined. Superposition of dihedra for a given fault population allows us (1) to check the kinematic compatibility between faults, (2) to define the overall shape of bulk extension and shortening fields, and (3) to determine principal kinematic axes (best shortening, extension and intermediate axes). This latter calculation involves the diagonalisation of the Scheidegger orientation tensor (Scheidegger, 1965) for strain fields deduced from the right dihedra method (Meyer et al., 1991).

Except for three localities (Tukaynaron, Kalinabad, and Kafirnigan River), results are mostly consistent, despite the locally limited amount of data (Fig. 5). The main features are as follows.

The direction of principal shortening is generally subhorizontal or gently plunging, and lies between 90°N and 150°N. In contrast, the attitude of the principal stretching direction is much more variable. For several sites (e.g. Aksu, Pulkhakim, Derbent) the extension field defines a great circle, normal to a well-defined shortening direction. For these localities, we infer bulk flattening strains, a feature which suggests that deformation differs from pure thrusting. This is confirmed by (1) the highly variable pitch of striations on fault planes with reverse components (Figs. 5 and 6), and (2) the locally subhorizontal or gently dipping attitude of the principal extension direction (e.g. Aksu, Pulkhakim, or Hanaka Carboniferous localities).

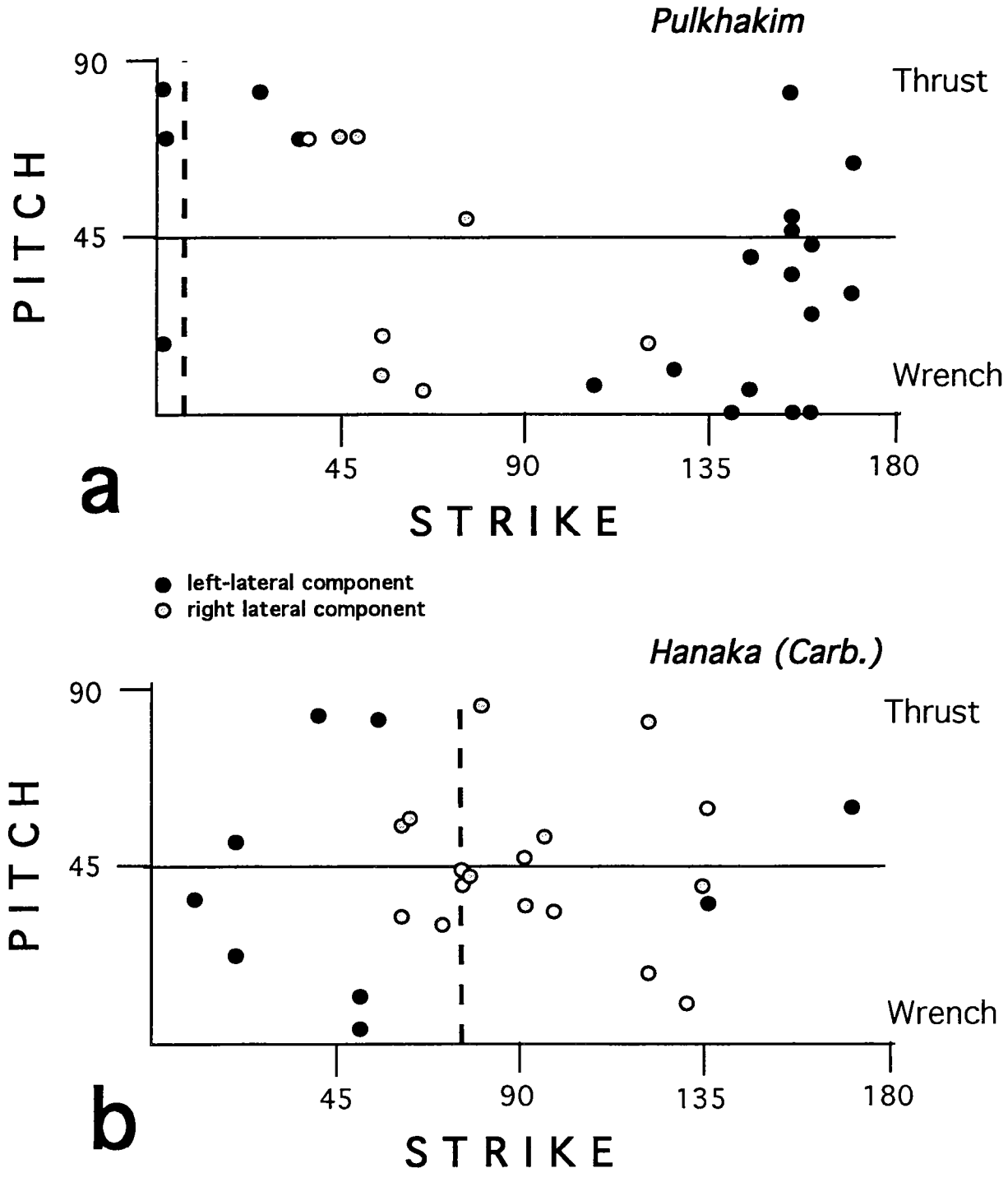

Fig. 6. Pitch of striations versus strike of fault plane for strike-slip faults and faults with reverse components at Pulkhakim (a) and Ghissar (b).
Black and grey dots represent faults with sinistral or dextral strike-slip components, respectively. Dashed line shows mean local structural trend. For further explanation, see text.

At Tukaynaron, Kalinabad and Kafirnigan River, maxima within extension and shortening fields are not orthogonal (Fig. 5). There are problems of compatibility between some faults at these localities. Nevertheless, there is a satisfying agreement between the calculated principal directions and the overall attitude of individual fault planes and striations (fig. 5). Furthermore, calculated best directions of principal shortening are consistent with those observed at other localities.

For two representative localities, plots of pitch of striations versus strike of individual strike-slip faults and faults with reverse components provide further insight into the regional kinematics (Fig. 6). Many faults show substantial strike-slip components, sinistral or dextral on faults striking N-S to N30 or N70 to N120, respectively. Quasi-parallel faults can be either thrusts or strike-slip faults, a feature which suggests strong partitioning of displacements; but we have no reliable information about possible changes of local kinematics with time. At Pulkhakim (Fig. 6a, see also Fig. 5), the dominant shear sense is sinistral, at a low angle to the local structural strike (about 10°N); whereas it is dextral at Hanaka (Fig. 6b), where structures strike 70°N. In fact, three types of fault patterns are found along basin boundaries, depending on the local structural strike. Thus, sinistral thrust-wrench faults, indicating substantial amounts of bulk sinistral strike-slip along strike, are frequent at sites located within the depression, where regional structures strike NNE-SSW to N-S (e.g. Aksu and Pulkhakim, Figs. 5 and 6a). In contrast, fault populations along fault zones striking more E-W (Hanaka and Derbent, Fig. 5 and 6b) indicate components of dextral strike-slip. An intermediate situation is observed at Derkanabad, where the local structural trend is NE-SW, all faults being nearly pure thrusts (Fig. 5).

Figure 7 shows relationships between regional structures and principal shortening directions deduced from local fault patterns. Most localities show significant obliquity between shortening directions and trends of regional structures. These obliquities are consistent with regional sinistral wrenching throughout the Tadjik depression and with dextral wrenching along the northern Ghissar boundary.

DISCUSSION AND CONCLUSIONS

According to Cobbold and Davy (1988), the Tadjik depression is part of the Pamir-Baikal sinistral wrench zone. In their interpretation, NNE-SSW sinistral wrenching along the stable Eurasian plateform involved antithetic

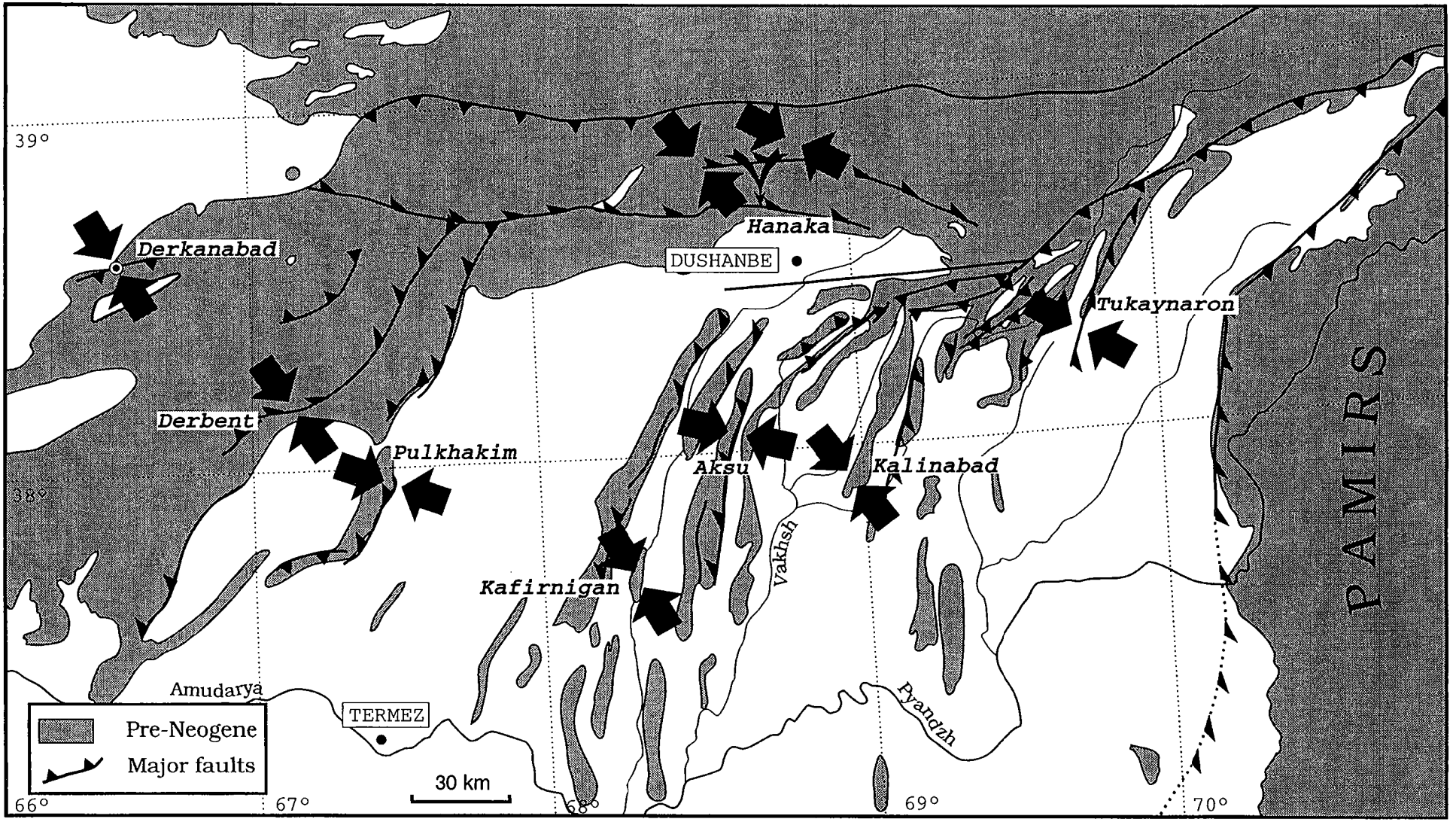

Fig. 7. Relationship between regional structures and principal shortening directions inferred from the analysis of fault populations.

For most localities, the shortening direction is oblique to the regional structures, indicating strike-slip components. For further explanation, see text.

dextral slip along NW-SE faults (e.g. Talas-Fergana fault), with associated anticlockwise block rotations (see Fig. 1). Dextral slip along NW-SE striking faults is well documented throughout the whole area (Burtman, 1975; Cobbold and Davy, 1988; Cobbold et al., this issue). Our structural analysis reveals dextral wrenching along the northern margin of the Tadjik depression, whereas the depression itself shows a regional component of NNE-SSW sinistral wrenching (Fig. 7).

Available paleomagnetic data for the area further attest to Tertiary rotations about vertical axes. Bazhenov and Burtman (1986) report up to 60° counterclockwise rotations in the easternmost part of the depression, along the Pamir boundary. Within the depression itself, two main domains are observed. Counterclockwise rotations of about 50° affect the eastern part of the depression; whereas up to about 20° rotation affects the western part (Abdullaev and Rzhevsky, 1973; Pozzi and Feinberg, 1990; Bazhenov et al., 1993; Thomas et al., submitted). Our analysis also support these observations. Thus, the two paleomagnetic domains found in the depression correspond most probably to the two structural domains which bound the central pop-down. In the the western part, eastward verging faults dominate, and westward verging faults dominate in the eastern part (Figs. 2b, 7 and 8). In addition, the strong changes in the amount of thrusting observed along major faults are consistent with rotations around vertical axes during sinistral wrenching.

The orientation of the principal shortening direction deduced from fault analysis, which varies between NNW and WNW (Fig. 7) is further consistent with counterclockwise rotations. Indeed, they are parallel or show apparent counterclockwise rotation with respect to the inferred direction of convergence of the Pamirs, which varies between NS and NNW-SSE according to the chosen boundary conditions (Minster and Jordan, 1978; Dewey et al., 1988; DeMets et al., 1990). Rotations reported by paleomagnetic studies probably involve basement blocks beneath the décollement level of Jurassic evaporites. Indeed, (1) the basement is largely involved in the deformation along western, northern, and eastern boundaries of the depression, and (2) the general structural pattern indicates that some major faults within the depression offset the basement (Fig. 2) (Zakharov, 1962).

In summary, the Tadjik depression appears as a wide lozenge-shaped compressive basin, bounded by conjugate thrust-wrench faults, and made of three main domains affected by combined sinistral wrenching and counterclockwise rotations during the Tertiary indentation of the Pamirs

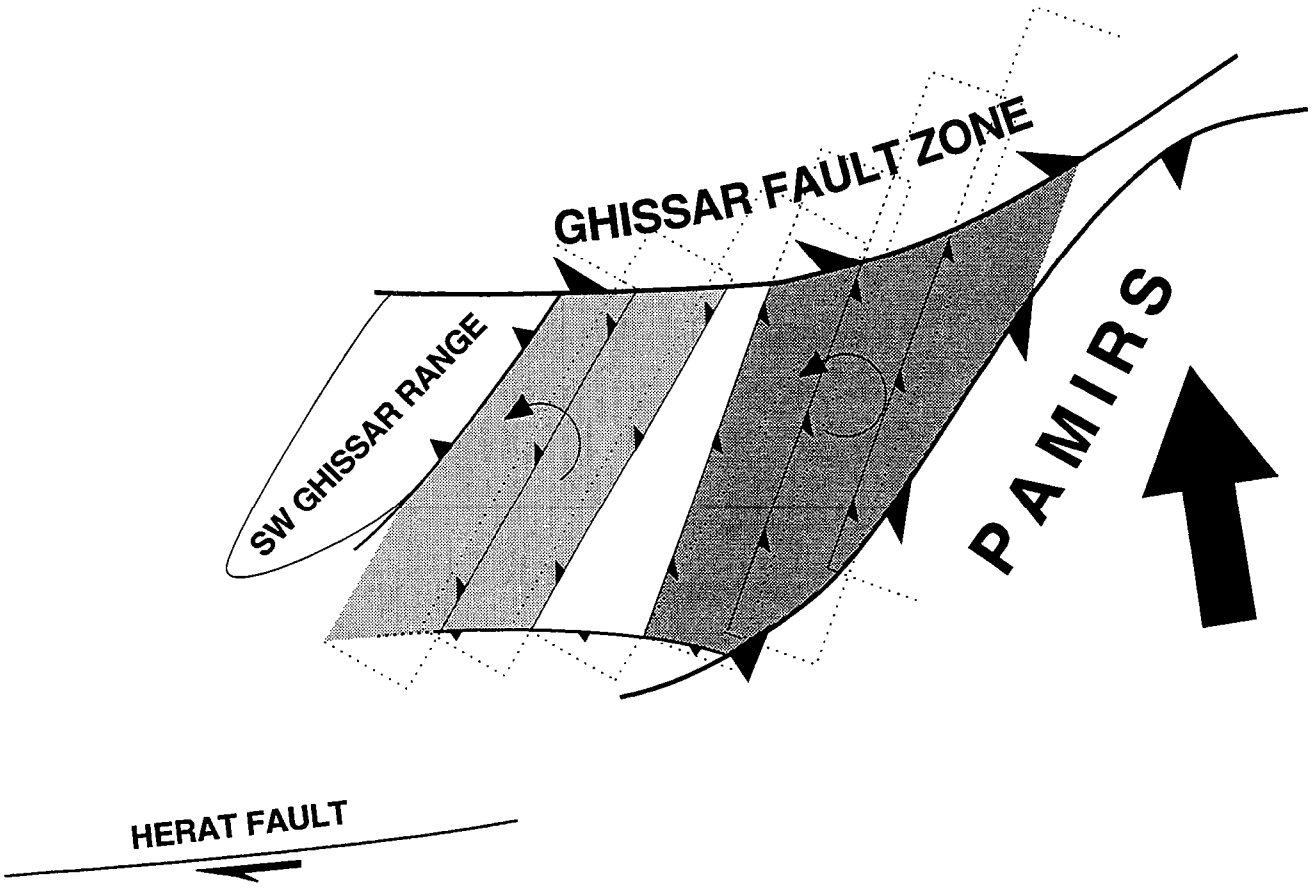

Fig. 8. Inferred Cenozoic kinematics of Tadjik depression due to India-Asia collision. Indentation by the Pamirs (arrow) is assumed to control the deformation. Relative displacement between blocks is taken up by oblique-slip thrusting, dashed boundaries of blocks representing underthrust edges. In the eastern part of the depression (dark domain), there are large counterclockwise rotations; whereas smaller counterclockwise rotations occur in the western part (light-grey domain). Central domain is a pop down basin (white).

(Fig. 8). The triangular topographic shape of the South-West Ghissar range, which widens northward (Figs. 2a and 8), suggests that the amount of basin underthrusting increases toward the North along its western margin ( ). This in turn suggests rotations around an axis located somewhere to the SW of the depression. The above kinematic interpretation implies that the Tertiary deformation of the Tadjik depression has been accompanied by substantial crustal thickening.

ACKNOWLEDGEMENTS

Data presented in this paper were mainly collected in 1990 during a one-month field expedition devoted to paleomagnetic sampling throughout the Tadjik depression, under the terms of an international agreement between the Academy of Sciences, Moscow, and the CNRS (international division). M. Bazhenov, A. Chauvin and H. Perroud are kindly thanked for their scientific contribution during the field work. Data at Derkanabad were collected by P.R. Cobbold in 1991, during a short field trip to SW Ghissar, organized by British Petroleum and the University of St. Petersburg. The computer program for extracting principal directions from right-dihedra analysis was implemented by V. Meyer, on the basis of programs kindly provided by M. Burkhard.

REFERENCES

Abdullaev, K.A, and Rzhevsky, Y.S., 1973. Lower Cretaceous paleomagnetism of the Tadjik basin. *Donish*, Tashkent, 104 pp. in Russian.

Angelier, J., and Mechler, P., 1977. Sur une méthode graphique de recherche des contraintes principales également utilisable en tectonique et en sismologie. La méthode des dièdres droits. *Bull. Soc. Geol. Fr.*, 7: 1309-1318.

Avouac, J. P. and Tapponnier, P., 1992. Cinématique des déformations actives en Asie Centrale, *C. R. Acad. Sci. Paris*, 315: 1791-1798.

Bazhenov, M.L., and Burtman, V.S., 1986. Tectonics and paleomagnetism of structural arcs of the Pamir-Punjab syntaxis. *Jour. Geodynamics*, 5: 383-396.

Bazhenov, M.L., Perroud, H., Chauvin, A., and Burtman V.S. ,1993. Paleomagnetism of Cretaceous red beds from the Tadjikistan and Cenozoic deformations related to the India-Eurasia collision, *Earth. Planet. Sci. Lett*, submitted.

Burtman, V.S., 1975. Structural geology of the Variscan Tien-Shan. *Am. Jour. Sci.*, 275A: 157-186.

Cobbold, P.R., and Davy, P., 1988. Indentation tectonics in nature and experiment. 2. Central Asia. *Bull. Geol. Inst. Univ. Uppsala*, 14, 143-162

Cobbold, P.R., Davy, P., Gapais, D., Rossello, E.A., Sadybakasov, E., Thomas, J.C., Tondji Biyo, J.J., and de Ureiztieta, M.,1993, Sedimentary basins and crustal thickening, *Sed. Geol.*, in press.

Cobbold, P.R., Sadybakasov, E. and Thomas, J.C., 1993. Cenozoic transpression and basin development, Kyrghyz Tien-Shan, Central Asia. *this issue.*

DeMets, C., Gordon, R.G., Argus, and D.F., Stein, S., 1990. Current plate motions. *Geoph. J. Int.*, 101: 425-478.

Dewey, F.D., Cande, S., and Pitman, W.C., 1989. Tectonic evolution of India/Eurasia collision zone. *Eclogae Geol. Helv.*, 82/3: 717-734.

England, P. 1982. Finite strain calculations of continental deformation 2: comparison with India-Eurasia collision zone. *J. Geophys. Res.*, 91: 3664-3676.

Hamburger, M.W., Sarewitz, D.R., Pavlis, T.L., and Papandopulo, G.A., 1992. Structural and seismic evidence for intracontinental subduction in the Peter The First Range, Central Asia. *Geol. Soc. Am. Bull.*, 104: 397-408.

Keith, C.M., Simpson, D.W., and Soboleva, O.V., 1982. Induced seismicity and style of deformation at Nurek reservoir, Tadjik SSR. *J. Geophys. Res*, 87: 4609-4624.

Kristy, M.J., and Simpson, D.W., 1980. Seismicity changes preceding two recent earthquakes, Central Asia. *J. Geophys. Res.*, 85, 4829-4837.

Leith, W., 1985. A mid-Mesozoic extension across Central Asia?, *Nature*, 313: 567-570.

Leith, W., Simpson, D.W., 1986. Seismic domains within the Ghissar-Kokshal seismic zone Soviet Central Asia. *J. Geophys. Res.*, 91: 689-699.

Leith, W., and Alvarez., W., 1985. Structures of the Vakhsh fold and thrust belt, Tadjik SSR: geologic mapping on a Landsat image base. *Geol. Soc. Amer. Bull.*, 96: 875-885.

Mattauer, M., 1986. Les subductions intracontinentales des chaînes tertiaires d'Asie; leurs relations avec les décrochements, *Bull. Soc. Geol. Fr.*, 8: 143-157.

Meyer, V., Gapais, D., Cobbold, P.R., and Marquer, D., 1991. Interpretation of fault sets in terms of bulk deformation. 2. Some practical aspects from brittle to ductile environnements. *in "the geometry of naturally deformed rocks", Mitt. aus den Geol. inst. ETH Zürich, Neue Folge,,* 239b: 191 (abstract).

Minster, J.B., and Jordan, T.H., 1978. Present day plate motions. *J. Geophys. Res.*, 83: 5331-5354.

Peltzer, G., and Tapponnier, P., 1988. Formation and evolution of strike slip faults, rifts and basins during the India-Eurasia collision: an experimental appraoch. *J. Geophys. Res.*, 93, B13, 15085-15117.

Pfiffner, O.A., and Burkhard, M., 1987. Determination of paleo-stress axes orientation from fault, twin and earthquakes data. *Annales Tectonicae.* 1,1,48-57.

Pozzi, J.P., and Feinberg, H., 1991. Paleomagnetism in the Tadjikistan: continental shortening of Eurasian margin in the Pamirs during the Indian-Eurasian collision. *Earth planet. Sci. Let.*, 103: 365-378.

Prévot, R., Hatzfeld, D., Roecker, S.W., and Molnar, P., 1980. Shallow earthquakes and active tectonics in Eastern Afghanistan. *J. Geophys. Res*, 85: 1347-1357.

Roecker, S.W., Soboleva, O.V., Nieresov, I.L., Lukk, A.A., Hatzfield, D., Chatelain, J.L., and Molnar, P., 1980. Seismicity and fault plane solutions of intermediate depth earthquakes in the Pamir HinduKush region. *J. Geophys. Res.*, 85, 1358-1364.

4. Tectonique Tertiaire et rotations de blocs dans la dépression Tadjik, Asie Centrale

Tertiary tectonics and block rotations in the Tadjik depression, Central Asia

TERTIARY TECTONICS AND BLOCK ROTATIONS IN THE TADJIK DEPRESSION, CENTRAL ASIA

J. C. Thomas[1], P. R. Cobbold[1], A. Wright[2] and D. Gapais[1]

1. Géosciences Rennes (CNRS), Université de Rennes I, 35042 Rennes Cedex, France
2. B P Exploration, 4/5 Long Walk, Stockley Park, Uxbridge, Middlesex, UB11 1 BP, England

ABSTRACT

The Tadjik depression, situated West of the Pamirs and South of the Tien-Shan, is a wide intermontane basin filled by a thick Mesozoic to Cenozoic sedimentary sequence. Its overall structure is that of wide a fold and thrust belt, made of alternating basins and ranges striking N-S to NE-SW. At its boundaries, the Tadjik depression is limited by major crustal scale thrust-wrench zones while, inside of it, deformation occurs mainly above a décollement level of Upper Jurassic evaporites. Seismicity is in close relation with the style of the deformation. Earthquakes underline the boundaries of the depression which consist of basement faults while active deformation inside the depression appears often aseismic. Kinematics on faults combine thrusting and strike-slip motions. Along the E-W Alburz fault, at the southern boundary of the depression, thrusting is combined with sinistral strike-slip motion. In the South West Ghissar ranges and inside the depression, thrusting is combined with sinistral strike-slip on roughly N-S faults while a component of dextral strike-slip occurs on roughly E-W faults. Differential vertical motions between the depression and adjacent ranges can reach 10 km. The pre-deformed state of the Tadjik depression has been obtained from the restoration of the base of the Tertiary level. Large counterclockwise block rotations are evidenced to the east, smaller to the west. This is fully rotations revealed by paleomagnetism. Shortening is at least of 20% in the center of the depression and at least of 60% in the Northeastern part, between the Pamirs and the Tien-Shan. During the Tertiary, the Tadjik depression appears to have undergone counterclockwise rotation and Northwestward extrusion in a thrust-wrench tectonic context closely associated with the Northward motion of the Pamirs relative to Asia. Most of the displacements have been probably restricted to the sedimentary cover above the evaporitic décollement level.

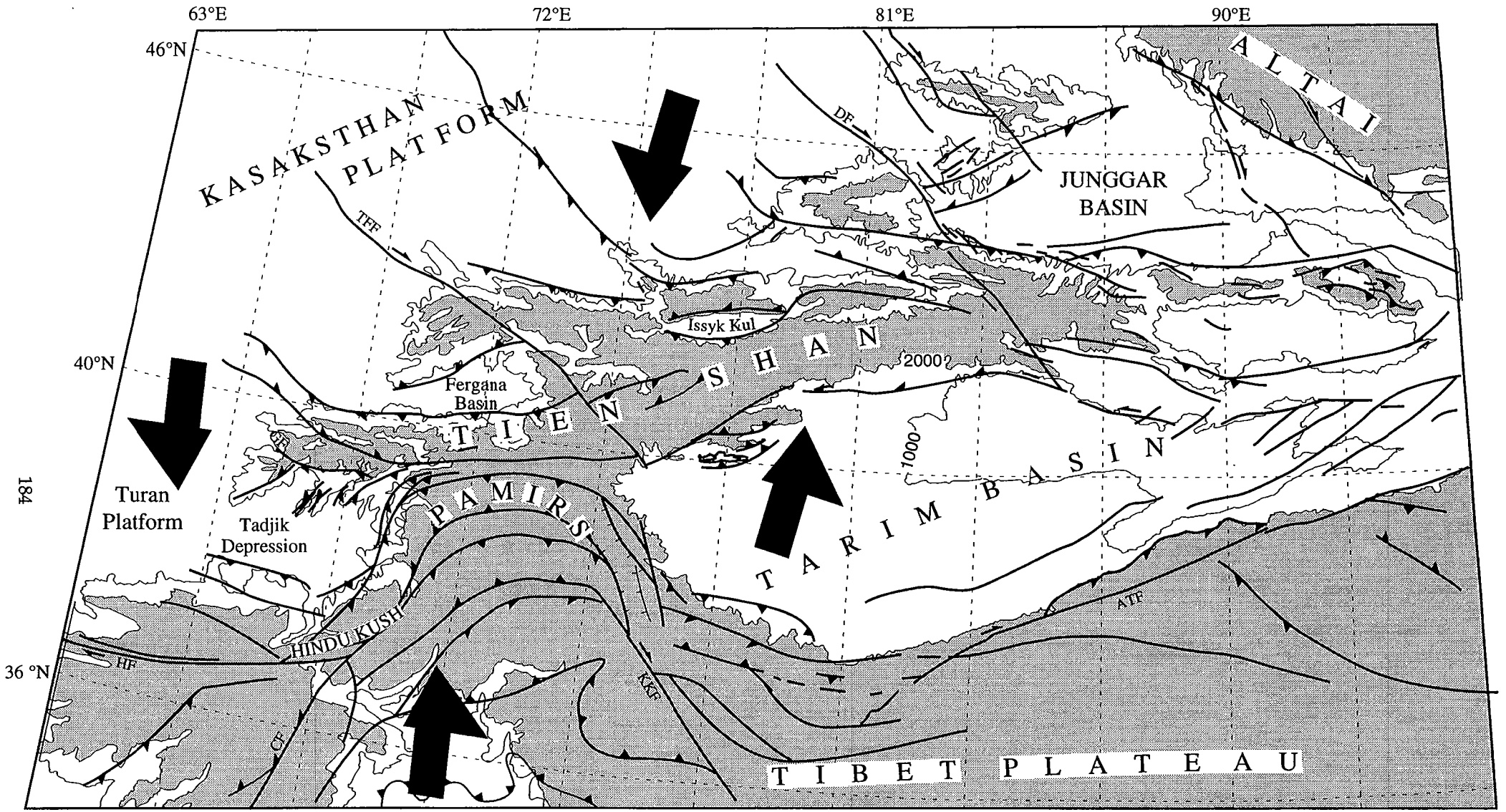

Figure 1. Cenozoic Tectonic map of Central Asia with topography in background (adapted from Avouac et al., 1993).
Fault pattern is from Cobbold and Davy (1988), Cobbold et al., (1993b) and Avouac et al, (1993) and our own fieldwork. All faults are inferred to have been active at one time or another during the Cenozoic. Black arrows summarize the regional Cenozoic kinematics (Cobbold and Davy, 1988). ATF: Altyn Tagh fault CF: Chaman fault; D : Junggar fault; GF: Ghissar fault; HF: Hérat fault; KKF: Karakorum fault; TFF: Talass-Fergana fault.

INTRODUCTION

Throughout the Asian continent, the Cenozoic deformation is distributed over the all Central, Eastern an Southeastern Asia. It has been now recognized that much of this deformation is related to the collision between India and Asia (Argand, 1924; Molnar and Tapponnier, 1975) which occurred about 55 Ma ago (Patriat and Achache, 1984). From paleomagnetism and plate kinematics, a minimum of 2000 km of shortening (Achache and Courtillot, 1984; Savostin et al., 1986; Dewey et al., 1989; Le Pichon et al., 1992) have occurred between the two continents. This shortening has been accommodated in various ways by intense intracontinental deformation, as evidenced by the high plateau and mountains ranges and also by the numerous large scale Cenozoic faults. Among the various kinematic interpretations (Dewey and Burke, 1973; Molnar and Tapponnier, 1975; Achache and Courtillot, 1984; Houseman and England, 1986, 1993; Cobbold and Davy, 1988; Davy and Cobbold, 1988; Dewey et al., 1989; Avouac and Tapponnier, 1992; Le Pichon et al., 1992), a key point is the relative amount of convergence accommodated by thickening and by eastward escape of large continental blocks. Peltzer and Tapponnier (1988) suggested that eastward extrusion of Tibet accounts for about 50% of the convergence. In contrast, Houseman and England (1993) and Dewey et al. (1989) infer no more than 10% of lateral escape, the rest being taken up by thickening.

From a reconstruction of the displacement field for the last 10 Ma, Cobbold and Davy (1988) have inferred that about 20% of the convergence has been accommodated by lateral extrusion, the rest being taken up by crustal thickening and block rotations about vertical axes. They infer clockwise rotations in eastern Tibet and counterclockwise rotations in a left-lateral wrench zone running from the Gulf of Oman to Lake Baikal. The existence, the nature, the regional distribution and amounts of block rotations around vertical axes, are critical features to discuss the way bulk shortening has been accommodated throughout Asia (England and Molnar, 1990).

The Tadjik depression lies South of the Tien-Shan and West of the Pamirs (Figure 1), within the Oman-Baikal sinistral wrench zone of Cobbold and Davy (1988). It is an intermontane basin filled by a thick Mesozoic to Cenozoic sedimentary sequence. The Tertiary deformation of the Tadjik depression is associated with major fault zones of crustal scale at its boundaries, in a regional wrench-thrust tectonic context. In this area, the convergence between India and Asia has been accommodated in a complex way. It is therefore a particularly interesting place for the study of intracontinental deformation and, more especially, for testing the models of Tertiary kinematics of Western Central

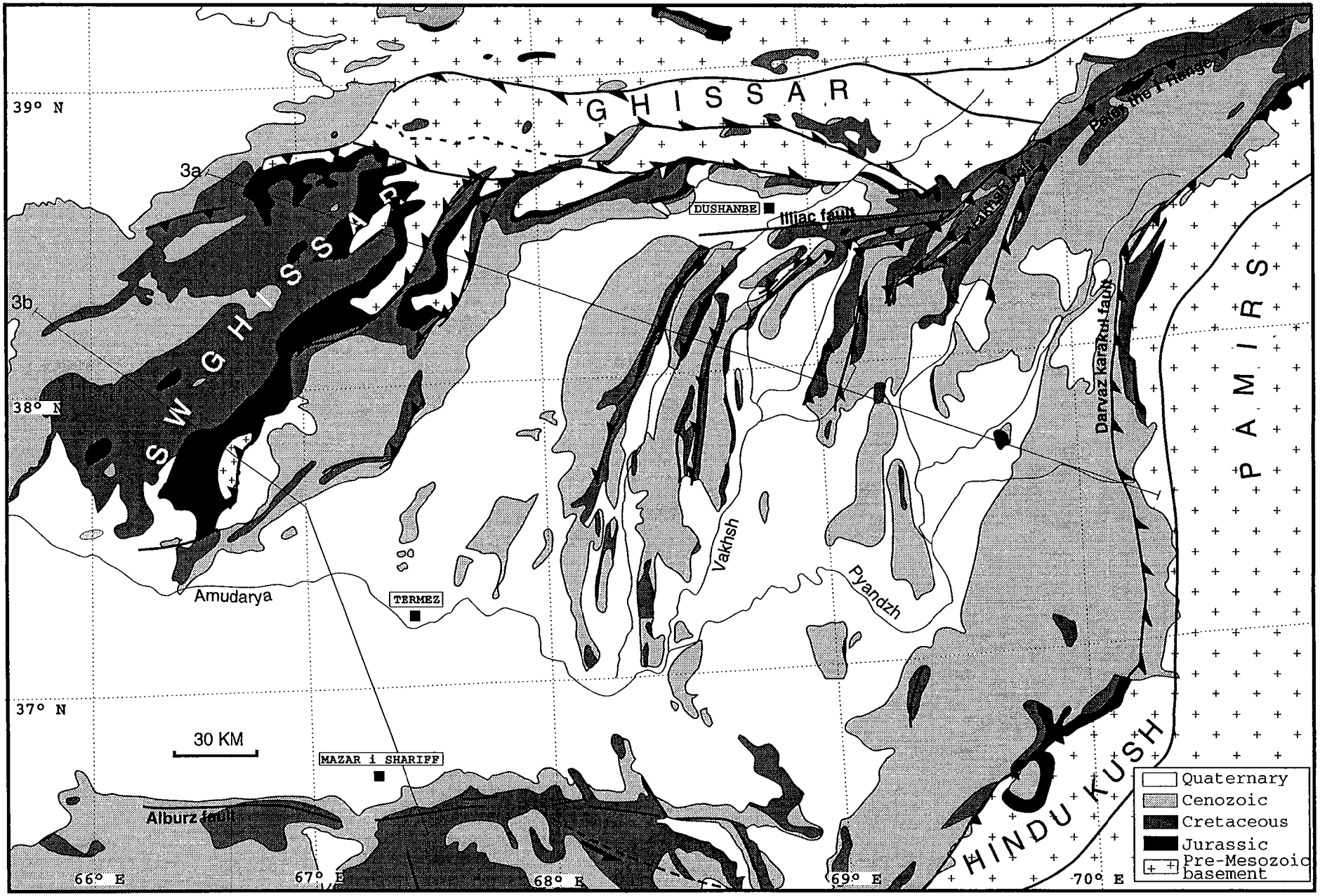

Figure 2. Simplified geological map of the Tadjik depression and surrounding areas.
Oblique triangles on faults point in direction of underthrusting. The depression is bounded by three major faulted zones: the Darvaz-Karakul fault to the East, the Ghissar dextral wrench-thrust zone to the north and the South West Ghissar thrusts to the West. Numbers of cross sections refers to number of the figures.

Asia. Following on previous works (Thomas et al., 1993, submitted, Bazhenov et al., submitted), we discuss new tectonic, seismotectonic and isopach data for the Tadjik depression and surrounding areas. We then attempt a restoration of the displacement field, showing that the regional kinematics have been dominated by thickening, strike-slip motion and block rotations about vertical axis.

GEOLOGICAL SETTING

The Tadjik depression is a wide fold-and-thrust belt bounded by three major tectonic and topographic features (Figure 2). The Pamirs and the Hindu Kush, the South Tien Shan and the South West Ghissar ranges constitute the Eastern, Northern and Western respectives boundaries. The Alburz fault, of less importance, constitutes the southern boundary. Inside the depression, basins alternate with anticlinal ranges, where Mesozoic series are exposed (Figure 2). We have drawn a geological section across the Tadjik depression (Figure 3) using the data of the literature (Zakharov, 1958), the geological map of Tadjikistan (Ministry of Geology of the USSR and the Tadjik Academy of Sciences, 1984) and our field observations. The geology is rather well constrained in the sedimentary cover by seismic and drill data. However, very little information is currently available for the nature and the deformation of the basement underlying the depression. The cross-section (Figure 3a) shows that the Upper Jurassic evaporites have provided major décollement, especially in the eastern part of the depression, where some salt diapirs crop out. For some salt domes, diapirism is currently active and is associated with a significant seismic activity (Leith and Simpson, 1986a). The strike of regional folds changes gradually from N-S in the center of the depression, to nearly E-W along the Ghissar range. Where exposed, the tips of individual ranges tend to be symmetric anticlinal hinges, with moderately plunging axes (commonly around 30°-40°). The degree of deformation varies strongly along the ranges. This was described in a previous work (Thomas et al., 1993), and is interpreted to be the result of a strike slip component combined with the thrusting. Toward the NE, the Tadjik depression narrows between the South Tien-Shan and the Pamirs. Folds tighten and shortening strongly increases in the Vaksh belt and the Peter the First range (Tapponnier et al., 1981; Hamburger et al., 1992).

Two major thrust zones of opposite vergence bound the Tadjik depression (Figures 2 and 3). To the East, the Pamirs overthrust westwardly the depression along the Darvaz-Karakul fault (Peive et al., 1964) while to the West, the South

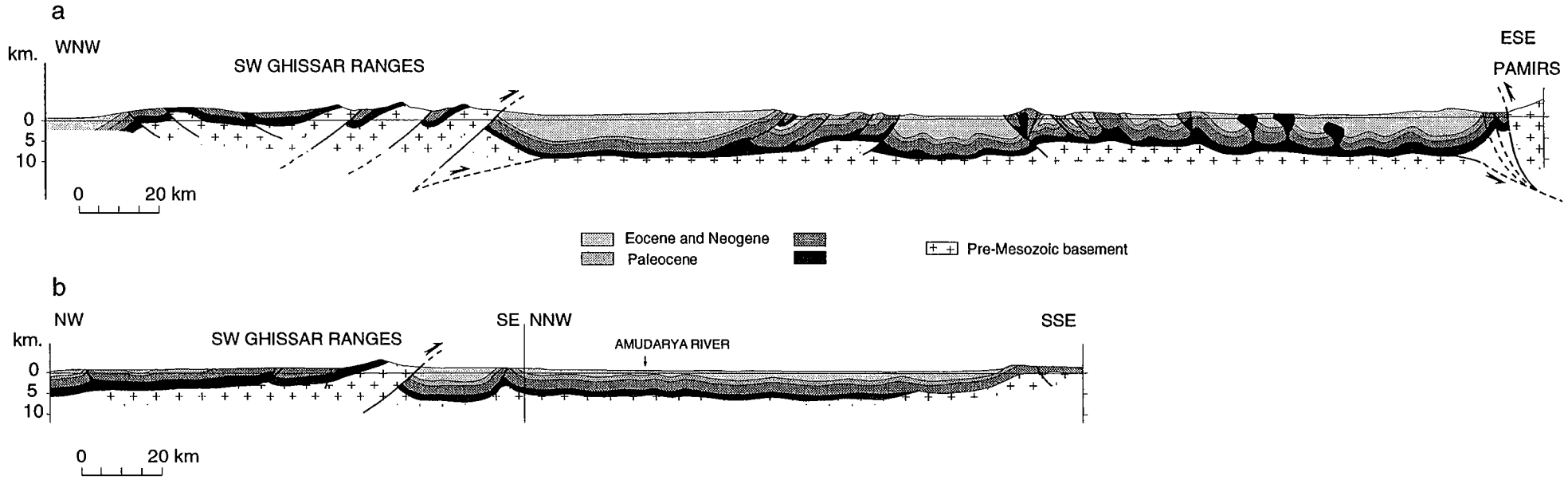

Figure 3. Geological sections across the Tadjik depression (data from Zakharov 1958, 1/500000 geological map of Tadjikistan, and our own observations) (For section lines, see Fig. 2).

The overall structure of the Tadjik depression is that of a compressive intermontane basin. Two basement thrusts of opposite vergence bound the depression to the East and to the West. Within the depression, deformation occurs above a décollement level of Jurassic salt, except on both sides of the pop-down basin in the center where basement thrusting may occurs. Salt diapirism with associated seismicity occurs in the eastern part of the depression. To the South the Alburz fault separates the Tadjik depression of the Afghan Turkestan.

West Ghissar ranges overthrust eastwardly the western margin of the depression. Inside the depression, faulting in the sedimentary cover is closely related to these two boundary conditions. Thrust faults verge dominantly westwardly and eastwardly in the eastern and western parts of the depression respectively, the central domain defining a ramp basin (Cobbold et al., 1993a). Therefore, the depression appears as a large intermontane compressive basin (Cobbold et al., 1993a) filled by up to 10-12 km of Mesozoic to Cenozoic sediments.

Thus, it already appears that the Tertiary deformation of the depression is closely associated with the tectonics units on its boundaries. These units are described below.

The Pamirs

The Tadjik depression is limited to the East by the Pamirs and the Western Hindu Kush. this area consist of a mosaic of microblocs with a complex tectonic history. Northern Pamirs and Western Hindu Kush are the Southern part of the Hercynian orogen (Boulin, 1988). They are separated from the Central and the South Pamirs by a major suture corresponding to the closure of the PaleoTethys ocean (Boulin, 1988; Zonenshain et al., 1990) achieved between the Triassic and the Lower Jurassic, during the Eocimmerian orogen (Boulin, 1988). Nowadays, strong seismicity occurs in the Hindu-Kush and Central Pamirs. Most of the earthquakes are deeper than 70 km and define a contorted Benioff zone (Billington et al., 1977). This has been interpreted as an intracontinental subduction, dipping to the north in the Hindu Kush and to the South in the Pamirs. Some authors have inferred that, in the Hindu Kush, Indian plate has been subducted towards the North under the Asian plate, whereas the Tadjik depression and the Asian plate have been subducted towards the South under the Pamirs since more recent time (Tapponnier et al., 1981; Mattauer, 1986; Hamburger et al., 1992). However, the significance of this double vergence is a matter of debate (see Chatelain et al., 1980; Roecker et al., 1980). According to paleomagnetic evidences, the arcuate shape of the Pamirs was probably acquired in the Tertiary during the indentation of India into Asia (Bazhenov and Burtman, 1986). Northward displacement of the Pamirs relative to Asia is inferred to be at least 200 km (Peive et al., 1964; Burtman and Molnar, 1992). The Darvaz-Karakul fault, which separates the Tadjik depression from the Pamirs, has partly accommodated by sinistral wrenching this motion of the Pamirs.

The Ghissar

The Tadjik depression is bounded to the North by the Ghissar of the Southwestern Tien-Shan. The South Tien-Shan which was strongly affected by the Hercynian deformation, was accreted to the Central Tien-Shan during the Carboniferous, after the closure of the Turkestan ocean (Burtman, 1975; Bakirov and Burtman, 1984; Boulin, 1988; Windley et al., 1990). Hercynian structures have been strongly reactivated in the Tertiary, and E-W faults are major and still active thrust wrench zones with a dextral strike slip component (Trifonov, 1978; Thomas et al., 1993). Reverse motion on these faults is apparently responsible for much of the uplift of the Ghissar range (Leith and Simpson, 1986b). Remnants of Mesozoic formations including Cretaceous are present within the Ghissar range while same formations are at 3-4 km deep South of Dushanbe. This implies a relative vertical displacement of about 8 km between the Tadjik depression and the Ghissar range, mainly during the Tertiary.

The South West Ghissar

The Tadjik depression is separated from the Turan platform to the West by the South West Ghissar ranges. Along the Tadjik depression, basement thrusts with eastward vergence dominate, while faulting and folding gradually decreases toward the Turan platform. Strike slip faulting, often combined with thrusting motion on faults , is also a significant feature of the area. We present a detailed tectonic study of the area in a latter section.

Afghan Turkestan

South of the Amu-Darya river, the East-West Alburz fault separates Quaternary deposits of the Tadjik depression from Tertiary and Mesozoic sediments of northern Afghanistan (Figure 2 and 3b). Geological mapping suggests northward thrusting on this fault (Ministry of Geology of the USSR and the Tadjik Academy of Sciences, 1984). Furthermore, the occurrence of NNW-SSE folds branching on the eastern segment of the Alburz fault and en échelon folds at its vicinity suggest a component of sinistral wrenching (Figure 2). The Alburz fault also marks a regional rising of the basement of about 3 km. On the Afghan-Turkestan plateau which extends until the Herat fault to the South, E-W to WNW-ESE faults are present (Figures 1 and 2). Boulin (1990) has interpreted these faults (as well as the Alburz fault) as borders of blocks, tilted during Triassic extension, and reactivated in the Tertiary. The Herat fault is the Western continuation of the Paleotethys suture (Boulin, 1988) and was reactivated as a dextral strike slip fault in the Cenozoic (Tapponnier et al., 1981).

Mesozoic to Cenozoic geodynamic setting of the Tadjik depression

Little is know about the tectonic context of the Tadjik depression during the Mesozoic. During the Triassic, the Paleotethys was subducted under the southern margin of Asia (Sengör, 1987). Some Authors (Tapponnier et al., 1981; Boulin, 1988) have inferred that, at that time, extension related to the opening of a marginal basin occurred in Tadjikistan and Northern Afghanistan. However, Triassic formations are very scarce in the area and the nature of the basement under the depression is still unknown.

The closure of the Paleotethys occurred in the Lower Jurassic, together with the accretion of the Farad block along the Herat suture zone (Tapponnier et al., 1981; Boulin, 1988). According to Leith (1985) and Boulin (1990), marginal basin extension occurred in the Tadjikistan during all the mid-Jurassic and Cretaceous time, in response to the subduction of the Neotethys farther to the South. Leith (1985) used tectonic subsidence curves for the E and NE parts of the depression to infer that extension caused half thinning of the Tadjik depression during that time. In contrast, Hamburger et al. (1992) have inferred that the increasing thickness of Mesozoic sediments in the depression observed by Leith (1985) from the Ghissar to the Pamirs, was better explained within the framework of an intracontinental foreland basin rather than by extension on a passive margin.

The Tadjik depression acquired its current configuration during the Tertiary. It already appears that, the convergence between the Tien Shan and the Pamirs (ultimately Asia), and the reactivation of older basement structures, are the two main conditions associated with the deformation of the depression. In the following section, we describe new tectonic data for the Tadjik depression and the relations with adjacent ranges.

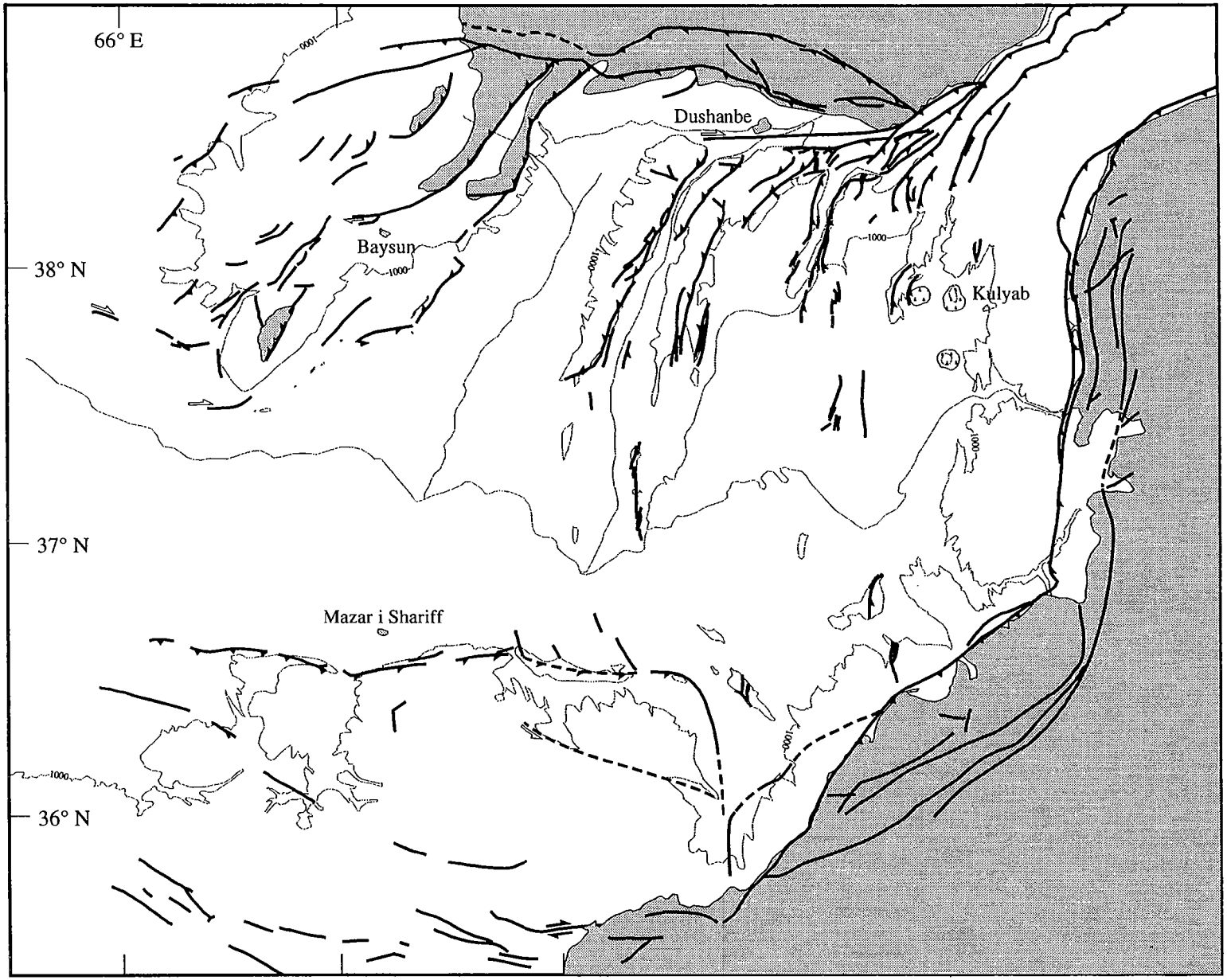

Figure 4. Major Cenozoic faults of the Tadjik depression and surrounding areas.
For the SW Ghissar ranges, fault pattern is simplified from the detailed tectonic map of the Figure 5. Shaded area represent pre-Mesozoic basement. Thrusting is dominant but in most cases, combined with strike slip motion. Dextral strike-slip motion occurs on roughly E-W faults whereas senestral strike-slip motion occurs on N-S to NE-SW faults. Note large salt domes (black triangles) near Kulyab city.

CENOZOIC FAULT MAP OF THE TADJIK DEPRESSION AND ADJACENT AREAS

Few data are currently available for the Tadjik depression. We thus have drawn a map of the major Cenozoic faults, as a base for further kinematics interpretation (Figure 4). We compiled the available literature and our own field observations (partly described in Thomas et al., 1993). We also used satellite images for specific areas. Our main source of data was the geological map the Tadjikistan at the 1/500.000 scale (Ministry of Geology of the USSR and the Tadjik Academy of Sciences, 1984). The eastern and northeastern parts of the depression have been studied by Leith and Alvarez (1985), Leith and Simpson (1986b), and Hamburger et al. (1992). In contrast, the SW Ghissar ranges, which constitute a major feature between the depression and the Turan platform, are appear to have receive less attention. We thus made a detailed study of this area (next section). We also describe the southern part of the depression using the available literature.

The South West Ghissar ranges

We have drawn a detailed map of the major faults of the South West Ghissar ranges (SWGR) using Landsat TM satellite images and data collected on the field (Figure 5). As a topographic base, we used a 1/500.000 Tactical Pilot Chart (sheets TPC G-6A and TPC G-6B, US Defense Mapping Agency). Satellite images at the 1/250.000 scale were used for mapping. The various rock facies and the absence of vegetation in the area were favorable conditions for an accurate identification of faults. However, we were very careful for mapping, and kinematic interpretations on faults were made with field support or in the most obvious situations on the images.

On the Figure 5, The SWGR are between latitudes 37°30'N and 39°00'N and connect to the North to the South Western Tien-Shan. The 1000 meters elevation contour marks roughly the boundaries with the Tadjik depression and with the Turan platform.

Thrust faults

Our mapping show that faults are mainly NNE-SSW oriented, following the general trend of the SWGR, and that thrusting is dominant. Major basement thrusting with dominant Eastward vergence, occurs in the Central and Eastern parts of the area. Vertical offset of the Mesozoic series on the thrust bounding the Tadjik depression (North of Baysun) is at least of 4 km. Thrusts of Westward vergence, of less importance (except in the Northern most part),

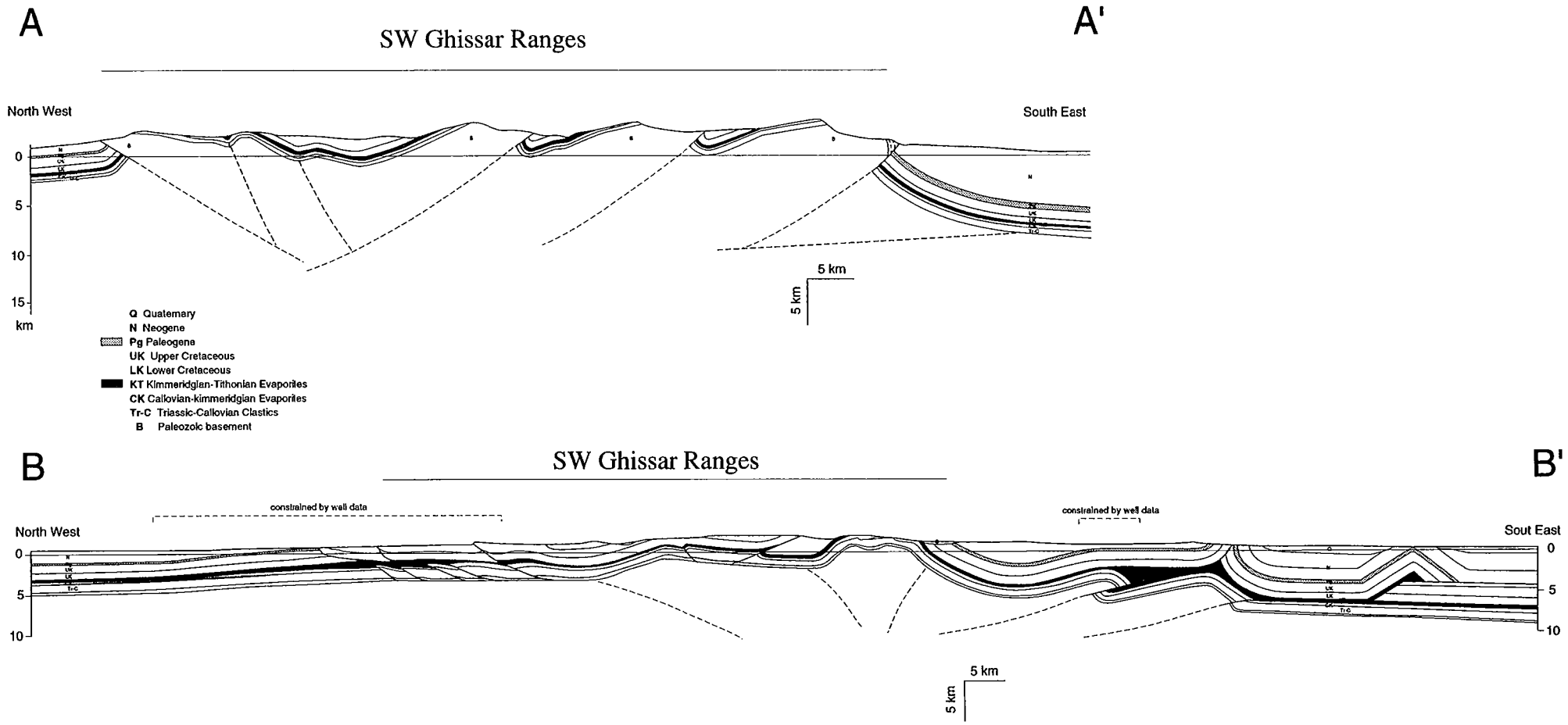

Figure 6. Cross sections through the SW Ghissar ranges (data from the 1/500000 geological map of Tadjikistan, seismic lines and our own observations).

The SW Ghissar ranges appears as an asymmetric pop-up structure with major eastward thrusts and antithetic minor westward thrusts. Deformation mainly involves the basement in the SWGR and is thin-skin in the Tadjik depression.

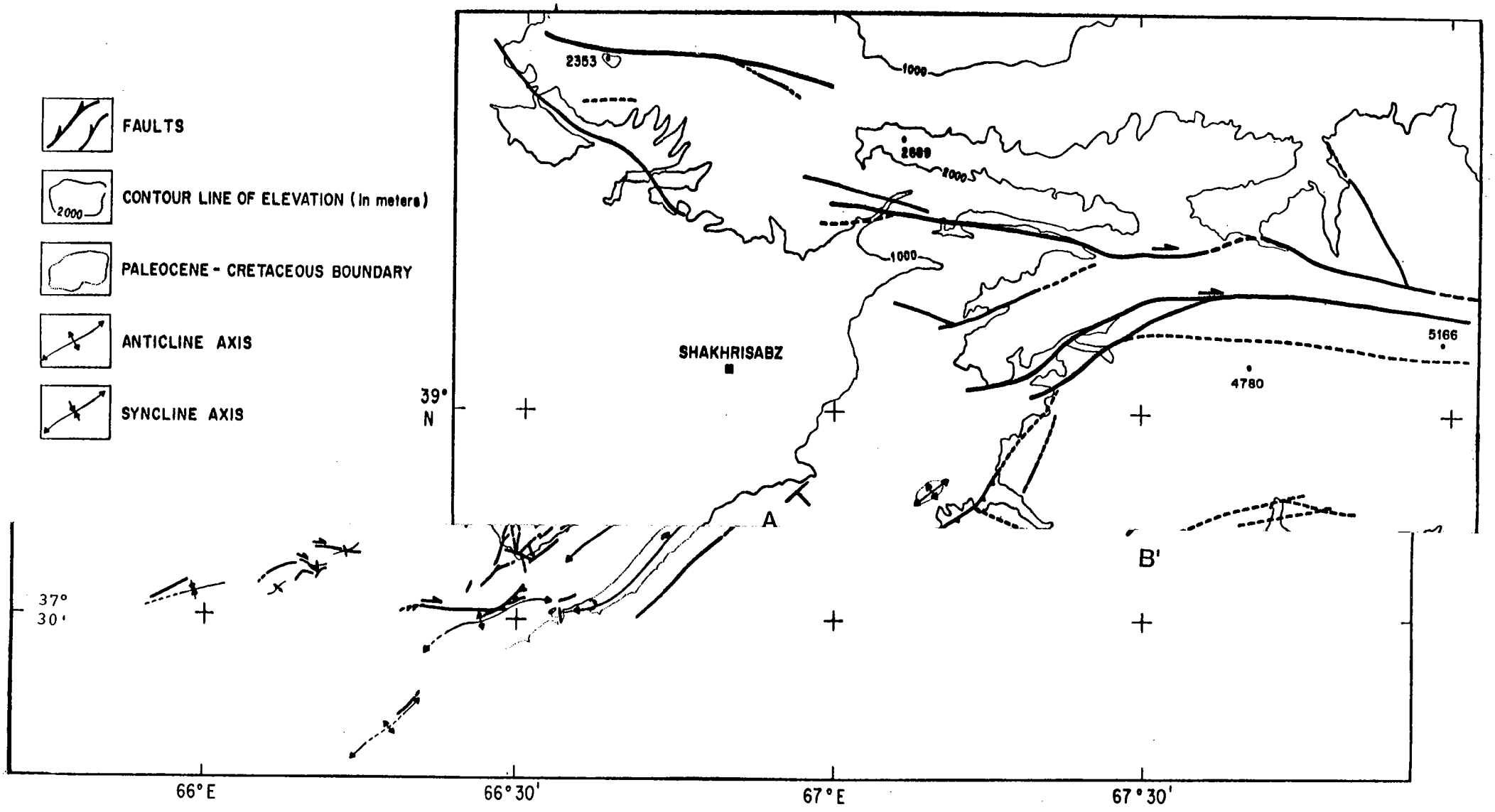

Figure 5. Major faults of the SW Ghissar ranges.
The 1000 m elevation contour roughly corresponds to the boundary with the Turan platform to the West, and with the Tadjik depression to the East. Major thrusts are of eastward vergence on the eastern margin of the domain. Intensity of faulting and folding increases from South to North and from West to East. Letters of cross sections refers to the Figure 6.

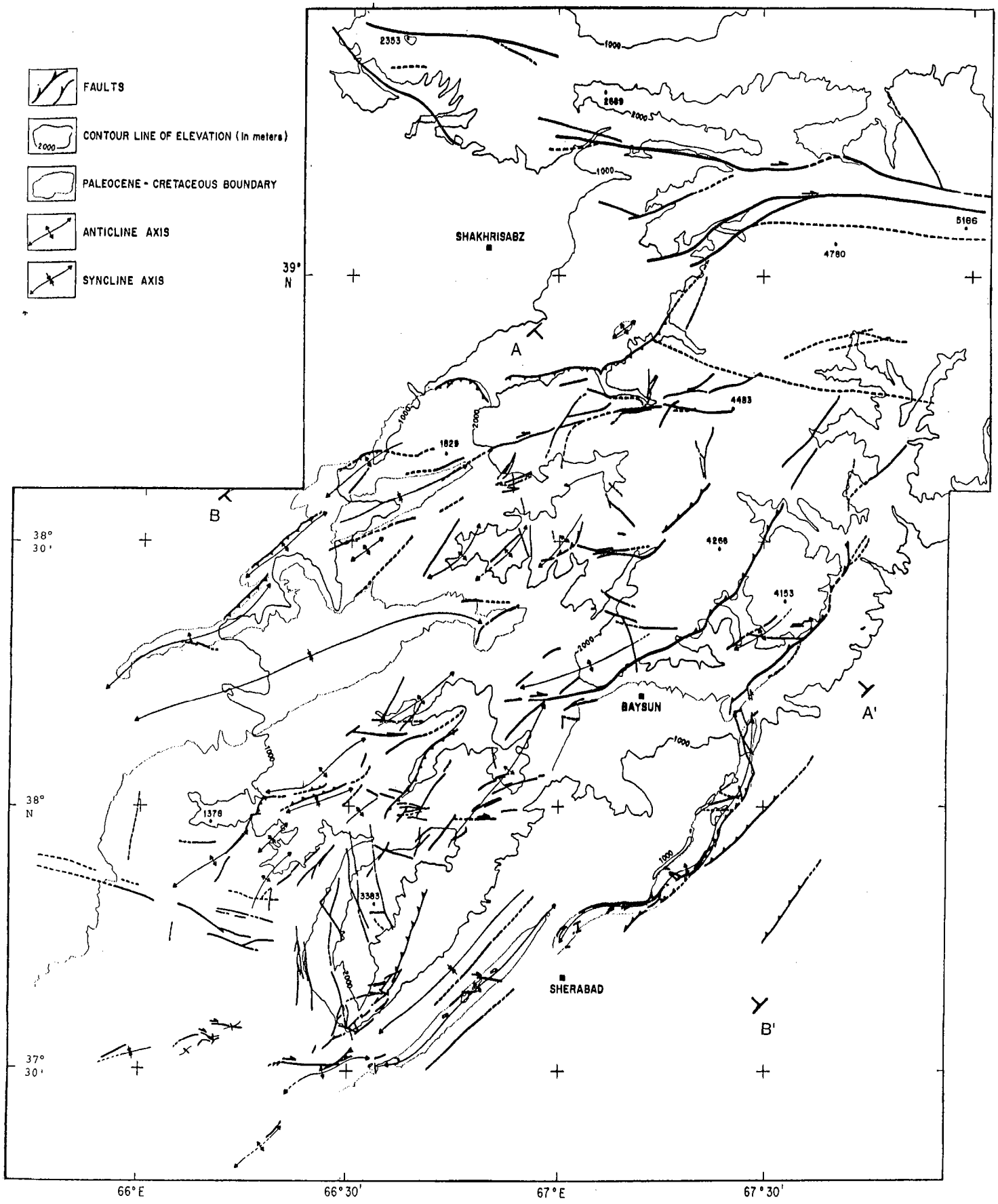

Figure 5. Major faults of the SW Ghissar ranges.
The 1000 m elevation contour roughly corresponds to the boundary with the Turan platform to the West, and with the Tadjik depression to the East. Major thrusts are of eastward vergence on the eastern margin of the domain. Intensity of faulting and folding increases from South to North and from West to East. Letters of cross sections refers to the Figure 6.

bound the Western margin of the domain. Elevations are maximum in the Eastern part of the SWGR (up to 4300m) and gradually decrease until 1000 m toward the Turan platform.

Intensity of faulting and folding varies along the trend of the range. North of the Baysun city (38°10'N of latitude), deformation is distributed over an area about 100 km wide, faults are numerous and elevation is mostly greater than 2000 m. South of Baysun city, faults are present in a narrower area and elevation decreases. This suggests that shortening increases from south to north and reaches a maximum against the Ghissar range. Note that the two folds north and East of Sherabad town are within the Tadjik depression.

Cross sections throughout the SWGR (Figures 3 and 6) illustrate the degree of the deformation which increases from South to North and from West to East. The Eastward vergence thrusts of the SWGR appears associated with the depocenter of Tertiary sediments of the western Tadjik depression. In fact, the SWGR appears as a pop up asymmetric structure with major Eastward thrusts to the East and antithetic minor Westward thrusts to the West. Basement is involved in the deformation, especially in the Eastern part of the area while the deformation in the Tadjik depression mainly occurs above a décollement level of Upper Jurassic evaporites (Figure 6b).

Strike-slip motion

Although thrusting is dominant, many indicators of strike slip motion are present. Major dextral wrenching occurs at the Western termination of the Ghissar against which faults of the SWGR abruptly stop. In the SWGR, most of the roughly E-W oriented faults show a dextral srike slip component. This is especially the case to the West of Baysun at the southwestern termination of a basement thrust. Dextral wrenching is indicated by "en echelon" folds at the latitude 38°30' N, in the center of the SWGR, along a roughly E-W direction (Figure 7). Dextral strike-slip faulting also occurs at the apex of the SWGR. Although strike slip displacements doesn't seem important in this last area, we will see below that it is necessary for a good kinematic interpretation (Figure 8).

Sinistral strike slip motion is also visible. In general, it is combined with thrusting on NE-SW faults (Thomas et al, 1993a), especially in the Eastern part of the SWGR. Recent sinistral strike-slip movement associated with the major thrust bordering the Tadjik depression (NE of Baysun) has been reported (Trifonov, 1978). Sinistral wrenching is also suggested by the "en echelon" folds and thrusts along the western margin of the SWGR.

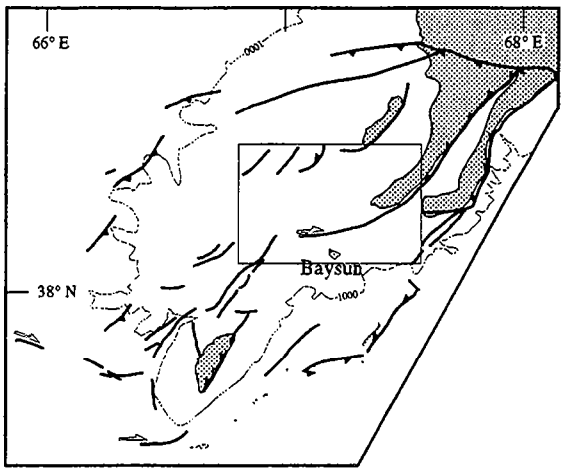

Figure 7. Landsat TM image of the central part of the SW Ghissar ranges (see location above).

Dextral wrenching is illustrated by "en échelon" faulted folds (axes in white) in the upper right quadrant, and at the termination of a major thrust (pointed by white arrows) Northwest of Baysun city. West of Baysun city, two plunging anticlines of Jurassic (in purple red) are seen. The overlying Jurassic salt (in light blue) is thicker into the synclinal part of the folds and into the plunging fold axis. This suggests either that salt has flowed after the deformation, or that the Jurassic anticlinal structure was partly acquired prior to the deposition of Kimmeridgian to Tithonian evaporites.

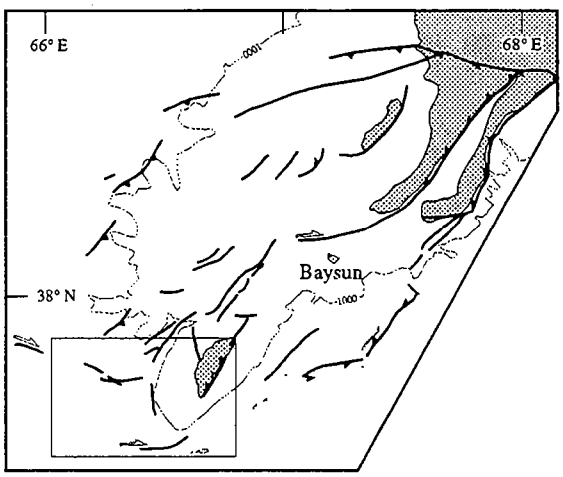

Figure 8. Landsat TM image of the southern prong of the SW Ghissar ranges (see location above).

Dextral strike-slip motion occurs at the southern termination of the Jurassic anticline (in purple red) and also along roughly E-W lineament in the center of the image. The Upper Jurassic limestones exposed on the anticlinal are crossed by kink folds and faults which do not continues into the overlying Cretaceous and Tertiary series. Theses structures present a NNW-SSE orientation, strongly deviant from the general trend of the Cenozoic structures. They may be therefore of Mesozoic age.

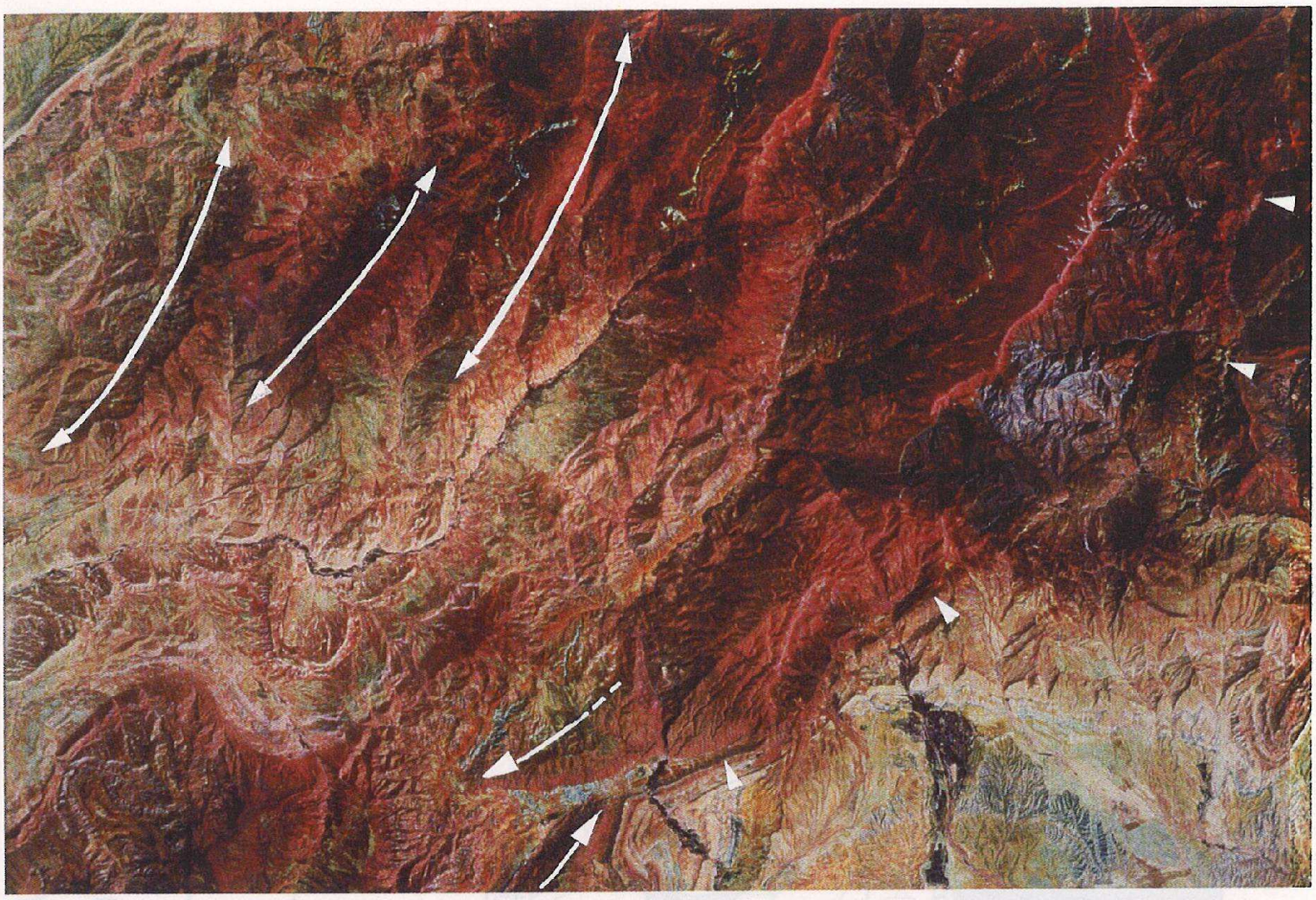

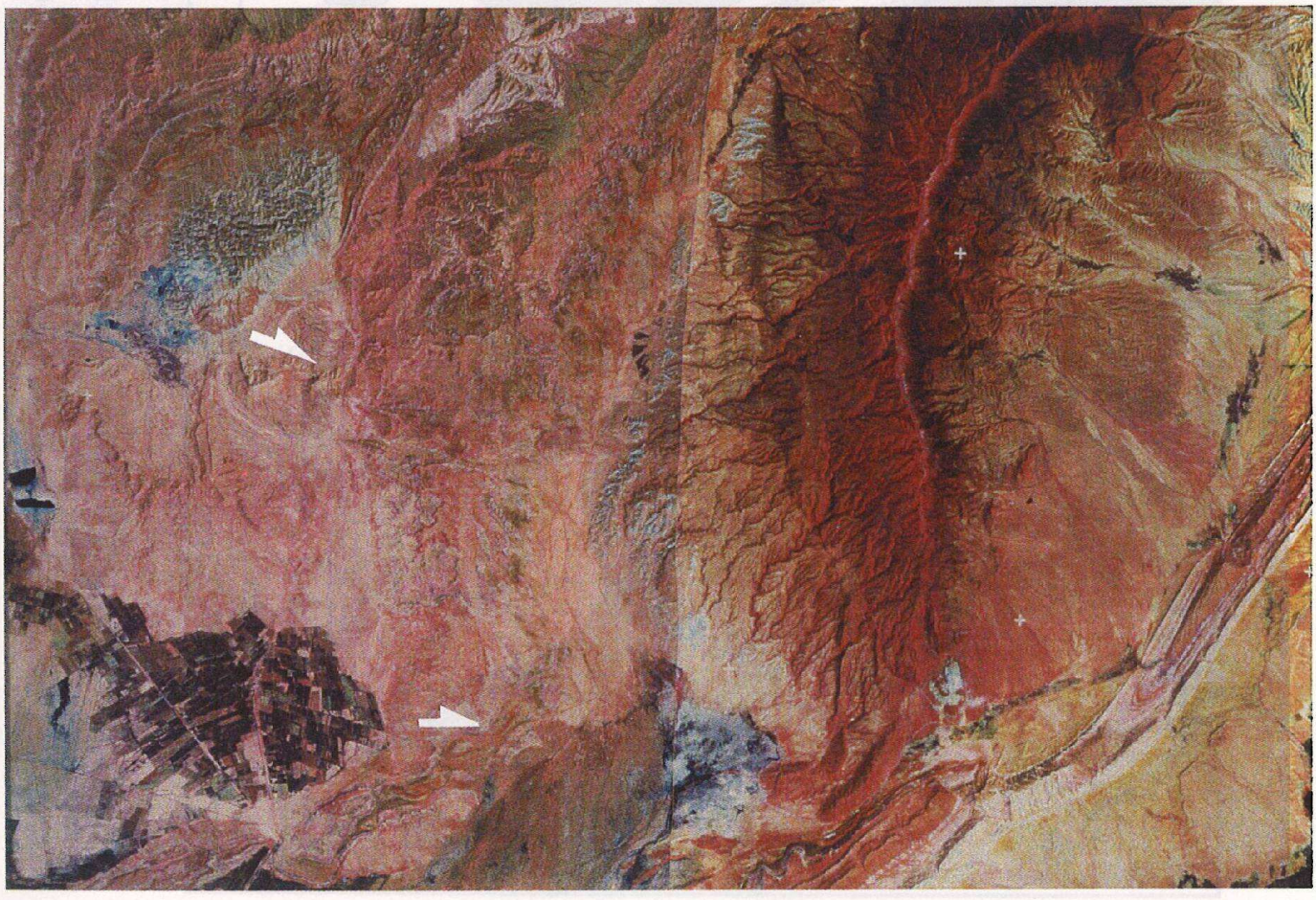

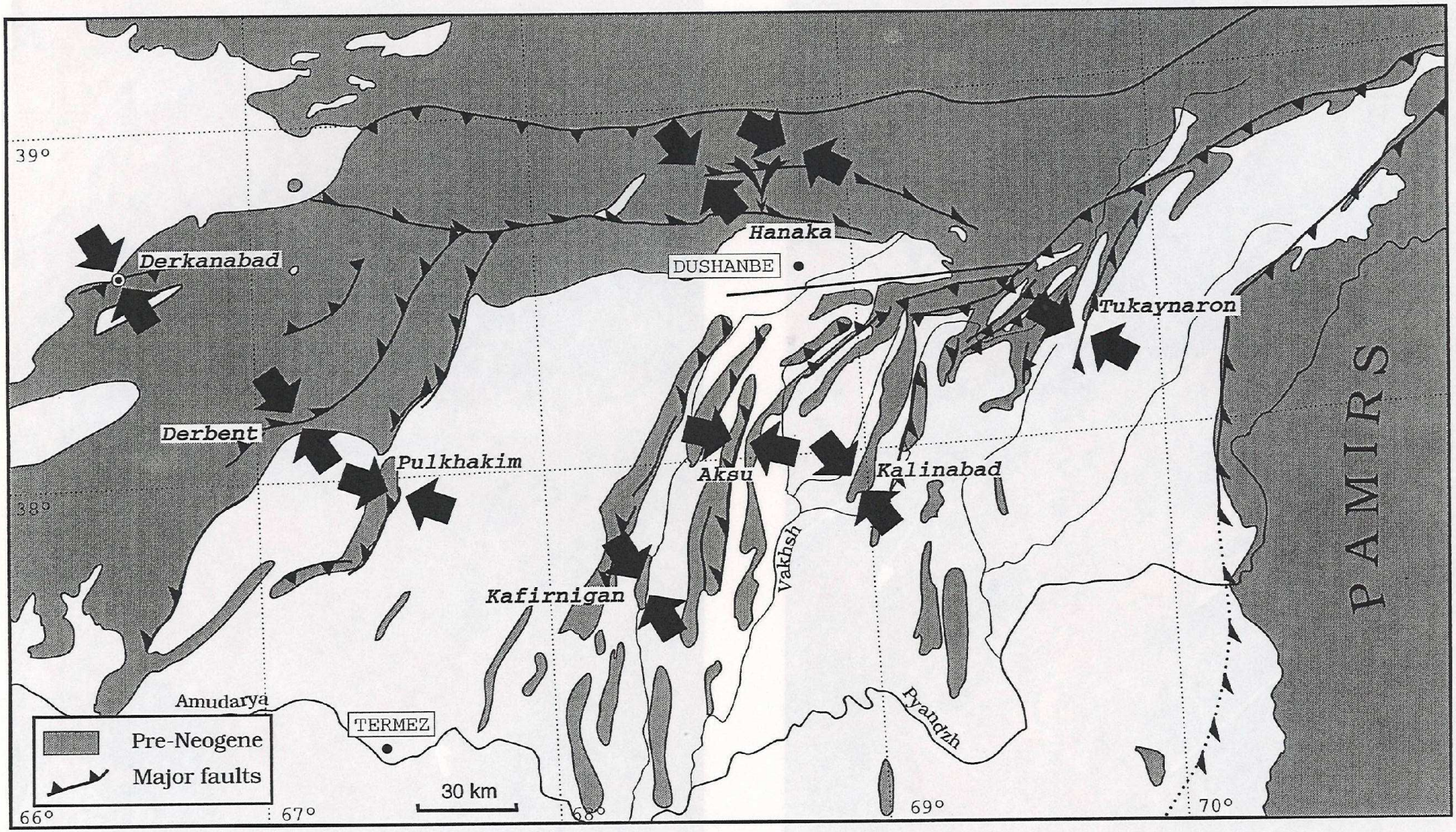

Figure 9. Relationship between regional structures and principal shortening directions inferred from the analysis of fault populations (from Thomas et al., 1993).

For most localities, the shortening direction is oblique to the regional structures, indicating strike-slip components.

All the faults previously described affect the Cenozoic formation. Thus, they were or have been active during the Tertiary. However in few areas, some structures suggest Mesozoic tectonics. We describe two of them in the following paragraph.

(1) Southwest of the Baysun city, two plunging anticlines of Jurassic limestone are seen (Figure 7). The overlying Jurassic salt is thicker into the synclinal part of the fold and into the plunging fold axis. This suggest either that salt has flowed after the folding, or that the Jurassic anticlinal structure was partly acquired prior to deposition of Kimmeridgian to Tithonian evaporites.

(2) In the Southern part of the SWGR, Upper Jurassic limestones are exposed on an anticlinal thrusted over the Tadjik depression (Figure 8). Kink folds and faults cross this formation but do not apparently continue into the Cretaceous or Tertiary series. Furthermore, these structures NNW-SSE oriented are strongly deviant from the general trend of the Cenozoic structures described above. Therefore, such faults could be of Jurassic age.

Mesozoic deformation may be related to the active continental margin, south of the Asian continent (Boulin, 1990), but data are too scarce for further kinematic interpretation.

Southern edge of the Tadjik depression, Afghanistan

We compiled data from various origin for the mapping of the Cenozoic faults of the South Tadjik depression (Weippert et al., 1964; Shareq, 1981; Ministry of Geology of the USSR and the Tadjik Academy of Sciences, 1984; Boulin, 1990) (Figure 4). However, in this area, kinematics are poorly constrained, especially for strike-slip components on faults. According to Boulin (1990), most of the discontinuities trending N-E to WNW-ESE are extensional faults of Triassic age reactivated in the Tertiary (Boulin, 1990). Theses faults are roughly parallel to the Ghissar and Herat dextral wrench zone, which suggest that Cenozoic dextral strike slip component may occur on them. Dextral strike slip motion has been also documented at the Western termination of the Hindu Kush (Tapponnier et al., 1981).

Sinistral strike slip motion may have also occurred. Southeast of the Alburz fault, "en echelon" folds suggest sinistral wrenching along a NE trending structure (Figure 5).

At the southeastern boundary of the depression, along the Hindu Kush, few cross sections (Hinze et al., 1964) show the Tertiary overturned, suggesting northwestward thrusting. Active thrusting has also been reported from the analysis of satellite images (Avouac, 1991).

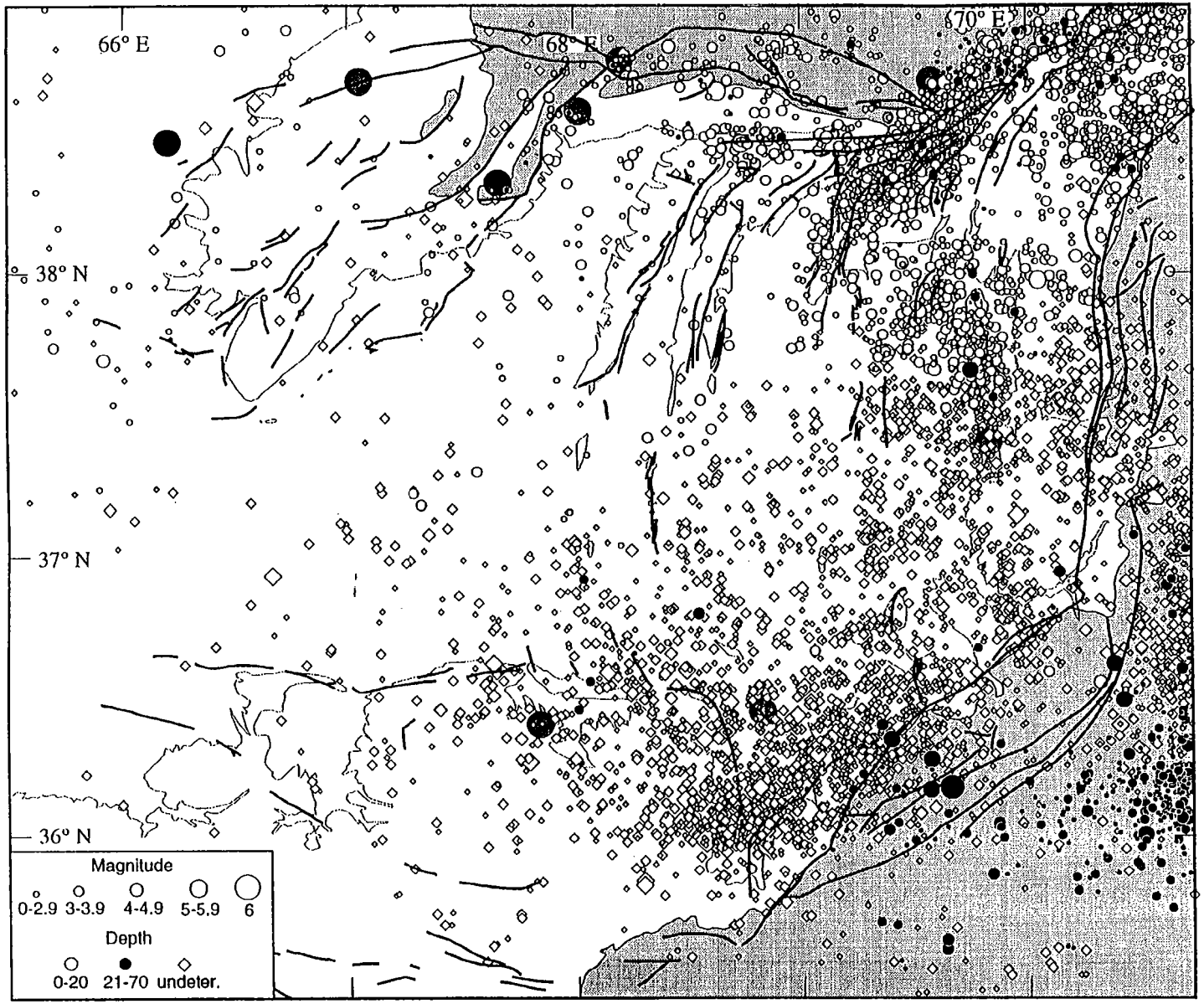

Figure 9. Seismotectonic map of the Tadjik depression and adjacent ranges.
Seismicity is strongly associated to the boundaries of the depression and reactivation of older basement faults. In the depression, seismicity induced by salt doming occurs near the Kulyab city and along inferred basement faults bordering the central pop-down structure. Elsewhere, deformation is partly creep and distributed. Data are from the Central Asia regional network from 1964 to 1985. We have arbitrarily "randomized" by ±0.05° the coordinates of poorly located events on the margins of the seismic network, to avoid the apparent gridding of epicenters. Historical events (shded circles) are from Leith and Simpson (1986) and Nikonov (1976). Other symbols as for Figure 4.

Our general fault pattern for the Tadjik depression (Figure 5), obviously show that thrusting is dominant inside and along its margins. However, Strike-slip motion appears to be a significant feature of the regional kinematics. This motion is observed from active tectonics (Trifonov, 1978) but also on main of the faults of the depression as shown by microtectonic data (Thomas et al., 1993 and Figure 9). In general, roughly E-W faults show a dextral strike slip component whereas N-S to NNE-SSW faults show a sinistral strike slip component, associated with the Northward motion of the Pamirs.

RELATIONSHIP OF FAULTS TO NEOTECTONICS AND SEISMICITY

The Northern Hindu kush and central Pamirs are amongst the most seismically active intracontinental mountains in the world. Most of the earthquakes occurs at intermediate depths, between 70 km and 300 km. In contrast, seismicity in the Tadjik depression is restricted to shallow depth, mainly in the first 10 km, in other words, within the Mesozoic to Cenozoic sedimentary cover.

The regional earthquake catalog for Central Asia between 1964 and 1985 (Academy of Science of the USSR, 1964-1985) lists more than 15000 events for the study area (Figure 10). The catalog has been described by Simpson and Kappel (1984), Leith and Simpson (1986b), Eneva and Hamburger (1989) and Pavlis and Hamburger (1991). On the representation of the Figure 10, we have distinguished the earthquakes undetermined in depths. These events are mostly south of the latitude 37°N which is the margin of the Soviet seismic network, explaining that they are less accurately located. Most of them occurred in the Tadjik depression, along the Northern Hindu kush, where seimicity is shallow (Heuckroth and Karim, 1973; Chatelain et al., 1980; Shareq, 1981). We thus consider that most of these earthquakes are directly related to deformation of the Tadjik depression, rather than to deeper processes occurring in the Hindu Kush.

Most of the earthquakes in the Tadjik depression are located at shallow depths, in the first tenth kilometers (Leith and Simpson, 1986b). This roughly coincides with the depth of the Jurassic décollement level and confirms that deformation in the depression is mainly restricted to the sedimentary cover. Inside the depression, density of earthquakes gradually decreases from East to West. In fact, as described below, seismicity is strongly related to the major structures bounding the depression.

South Tien-Shan margin

The Peter the First range (PFR) is the area of the depression (Leith and Simpson, 1986b) where earthquakes are the most numerous. Using a balanced cross section, Hamburger et al. (1992) interpret this activity to be associated with the subduction of the Tadjik depression under the Pamirs. South West of the PFR, the seismicity follows the Vaksh fold and thrust belt (Leith and Simpson, 1986b) and continues in the depression toward the south in a zone of complex imbricated thrusts around Nurek. A significant number of deeper earthquakes also occurs along the Ghissar boundary due to the reactivation of basement faults (Leith, 1985; Leith and Simpson, 1986b).

A striking feature is the concentration of earthquakes along the Illiac fault, south of Dushanbe, which joins the Vaksh fold and thrust belt to the East. This fault shows evidence of dextral strike slip motion (Trifonov, 1978) and probably involves basement (Leith and Simpson, 1986b). South of the western end of the Illiac fault, earthquakes underline NE-SW thrusts. In contrast, very few earthquakes occurs in the area which separates these thrusts from the Vaksh belt. This suggest that the Illiac fault is an active transfer zone between the Vaksh belt and the thrusts of the center of the depression.

Parallel to the Illiac fault are the dextral strike slip faults of the Ghissar range, north of Dushanbe. Although less dense, the seismic activity follows the line of these faults as far as the margin of the Turan platform.

South West Ghissar ranges

In the South West Ghissar ranges, most of the earthquakes are concentrated along the two major eastward verging thrusts of the Eastern border. a few historical earthquakes have been reported for these thrusts. Elsewhere, seismicity is lower, although few moderates ($m \geq 4$) and historical earthquakes have occurred along the thrusts of the Western margin. Significant microseismicity is also present in the southern part of the domain where dextral faulting occurs.

Pamir and Hindu Kush margins

On the Eastern border of the depression, the Darvaz-Karakul fault along the northern Pamirs show strong seismic activity. However, its southward continuation is associated with more diffusive seismicity. Further to the South, along the Hindu Kush, seismicity is again very active. Focal mechanism solutions indicate pure thrusting for two shallow earthquakes ($\approx$20km depth) located in the Hindu Kush and in the depression (Abers et al., 1988). This is in agreement with the change of orientation of the fault limiting the basement.

Indeed, From a N-S orientation (Darvaz-Karakul part) with a strike slip motion, the fault curves to a NE-SW orientation, roughly perpendicular to the regional compressive direction inferred from the focal mechanisms (Chatelain et al., 1980, Prevot et al., 1980, Leith and Simpson, 1986b) and current plate motion (Minster and Jordan, 1978; De Mets et al., 1990). However, in the depression, there is no clear field evidence of faulting in the area of strong seismicity. Abers et al. (1988) attribute this seismicity to the reactivation of basement normal faults of Triassic age. Such reactivation occurs along the southern boundary of the depression on the Alburz fault (Figure 10). Some local network have revealed that seimic activity extends until the western extremity of this fault (Shareq, 1981).

Inside the Tadjik depression, seismicity is clustered around salt domes of Jurassic evaporite (see figures 2 et 3a) in the region of Kulyab, with the occurrence of moderate (m>5) earthquakes. Most of these events are restricted above the décollement level. Salt is generally too weak to lead to moderate size earthquakes; thus, this seismicity may reflect fracturing country rock above or adjacent to the diapirs (Leith and Simpson, 1986a).

Hence, earthquakes are mostly concentrated on the boundaries of the Tadjik depression along reactivated basement faults. Inside the depression, seismicity underline strongly deformed areas, basement faults as the thrusts limiting both sides of the pop-down structure, and salt domes. Elsewhere, seismicity is comparatively very low, although numerous field observations of active faulting have been reported in the overall depression (Trifonov, 1978). Thus, we infer that inside the depression, the deformation is partly creep and distributed, on and above the salt décollement level.

CONTOUR-MAP ON BASE OF THE TERTIARY

We have drawn a structure-contour map on the base of the Tertiary for the Tadjik depression and adjacent ranges (Figure 11). For the main part of the depression, we used the data of Zhakharov (1958) which are rather well constrained by boreholes and seismic data. In the ranges, we identified old erosion surfaces of Mesozoic age using Landsat images (Cobbold et al., 1993b).

We infer that the differential vertical motions visible on the map are of Cenozoic age. Vertical motion along the faults is maximum along those involving basement which bound the Tadjik depression to the East and to the

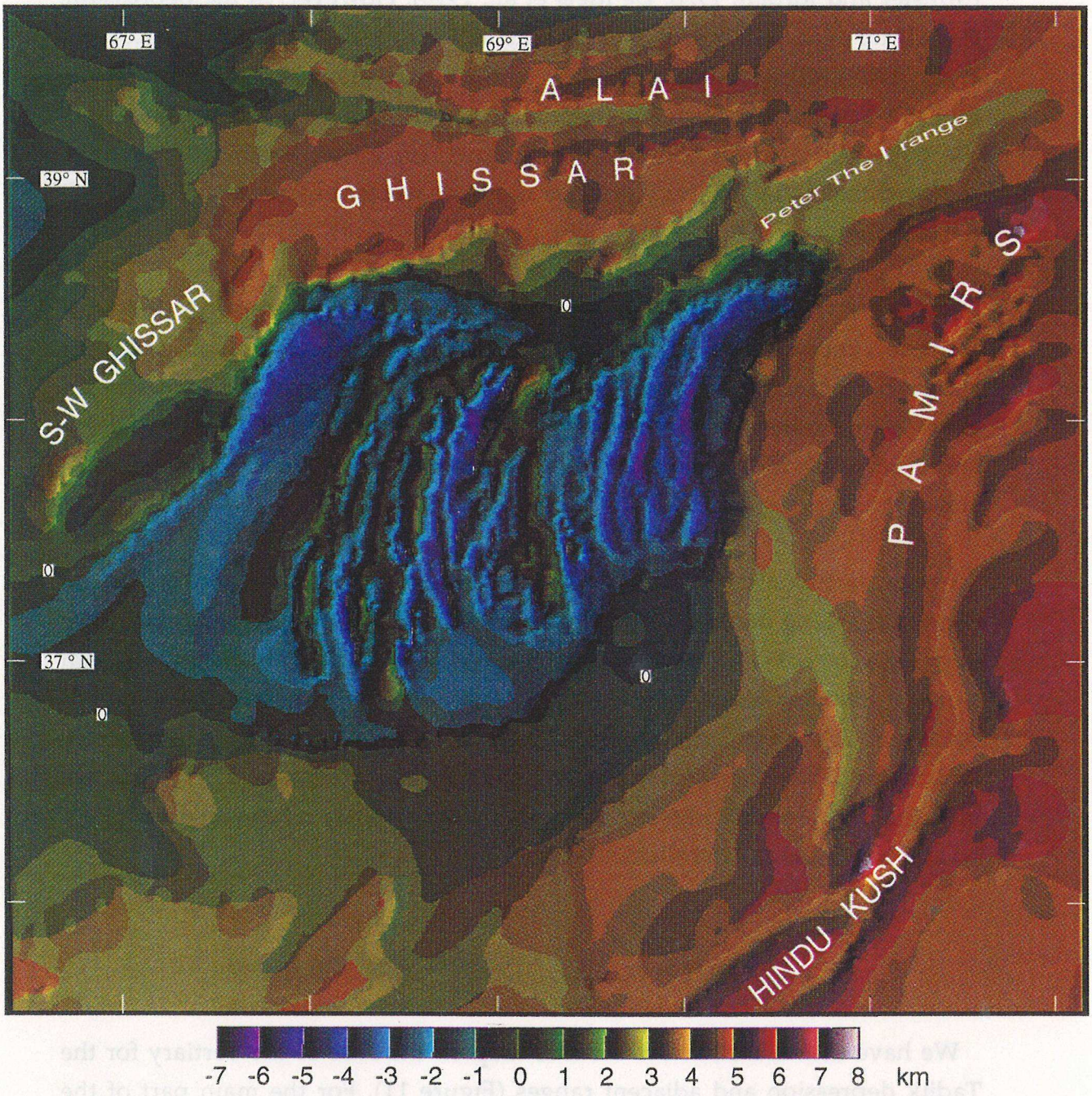

Figure 11. Coutour-map on base of the Tertiary inside and around the tadjik depression. The most accurate area is the Tadjik depression. Relative vertical motion along the Pamir boundary is at least 10 km, and 7 km along the SW Ghissar ranges. Two main depocenters lie along the Eastern and Western margins of the depression, a smaller one in the center.

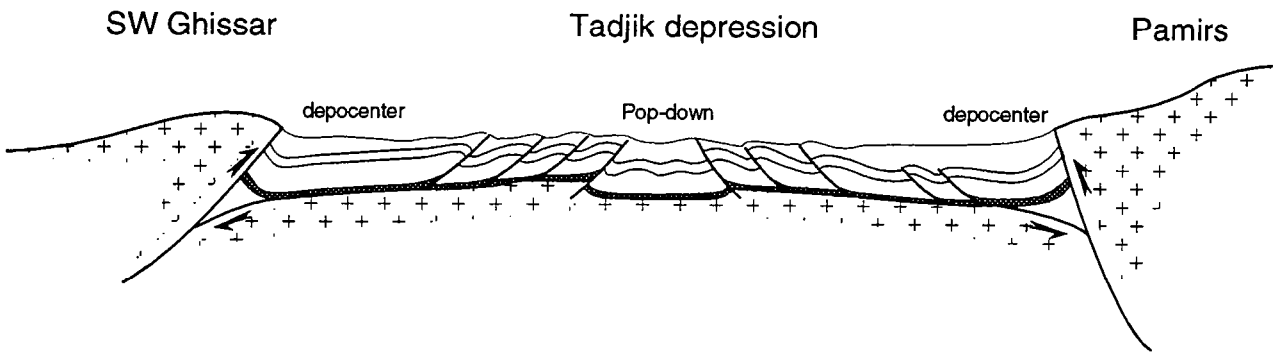

Figure 12. Schematic section across the Tadjik depression. the overall structure is very close to a ramp basin (Cobbold et al., 1993). The flexuration of the basement occurs in response to the thrust loading on both sides of the depression. The basement is deepest along the margins of the depression and shallows toward its center. Upper Jurassic salt décollement level is in black. (scale is not respected).

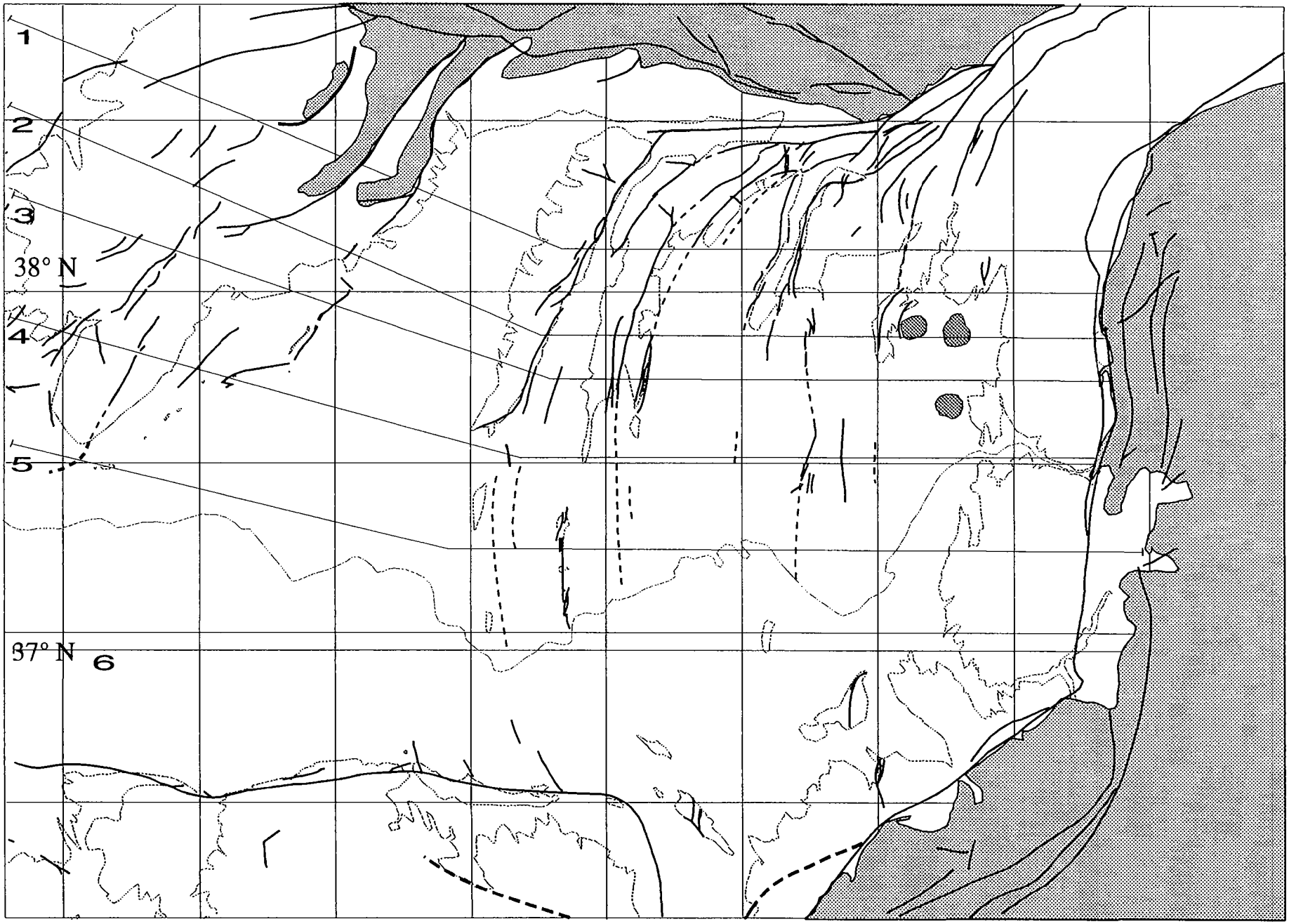

Figure 13a. Base map used for the restoration and location of the cross sections for the base of the Tertiary level. Symbols as for figure 4. Dashed faults have been added to take into account the deformation accommodated by folding.

West. Along the Pamirs and the SW Ghissar ranges it is up to 10 km and 7 km, respectively. In the center of the depression where basement thrusting probably occurs, differential vertical motion on faults is about five kilometers.

Our map clearly illustrates the structure of the Tadjik depression. It is a ramp basin (Willis, 1928; Cobbold et al., 1993a), with major thrusts and associated depocenters, along both Eastern and Western margins (Figure 12). Thin-skinned fold and thrust belts of opposite vergence have developed on both sides of the depression. We infer that the wide distribution of the deformation in the sedimentary cover which occurs as far as 150 km from the basement thrust is a consequence of the salt décollement level (Davis and Engender, 1985).

RESTORATION IN PLANE OF THE DEFORMATION

One of the main interest of the contour map on base of the Tertiary is that it can be used to restore the Tadjik depression to its pre-Tertiary shape.

Firstly, we estimate the heaves from the dips of major thrusts. Inside the depression, from borehole and seismic data, thrusts dip at about 45°. In the SW Ghissar and along the Pamirs, dips of faults are much less constrained at depth. From our interpretations on cross section (see Figures 3 and 6), we estimate the mean dips of thrusts in the SW Ghissar ranges to be between 45° and 55°. More problematic is the sinistral South Darvaz fault along the Pamirs. The strike-slip component is maximum when the fault is NS oriented and then gradually decreases toward the North when the fault trends NE-SW. A 10° pitch on the N-S part of the Darvaz-Karakul fault is enough to create the observed 10 km differential vertical motion (for 50 km of total northward displacement). We thus assume that the Darvaz-Karakul fault has a mean dip of 70° along its NS part and 50° in front of the Peter the First range. In general, dips of thrusts appear to be rather steep. We infer that this is a consequence of the regional sinistral wrenching suffered by the Tadjik depression during the Cenozoic (Thomas et al., 1993, and below).

We have drawn six serial sections showing the base of the Tertiary across the Tadjik depression (Figure 13) using the structure-contour map and our tectonic map. For simplification, we have drawn the faults with uniform dips inside the depression and in the SW Ghissar ranges respectively. We assume that the bending of bedding on both sides of the thrusts is a local effect associated with the faulting. The horizonthal displacement on each fault was then estimated by the addition of the unfolding of the fold bending along the fault, with the

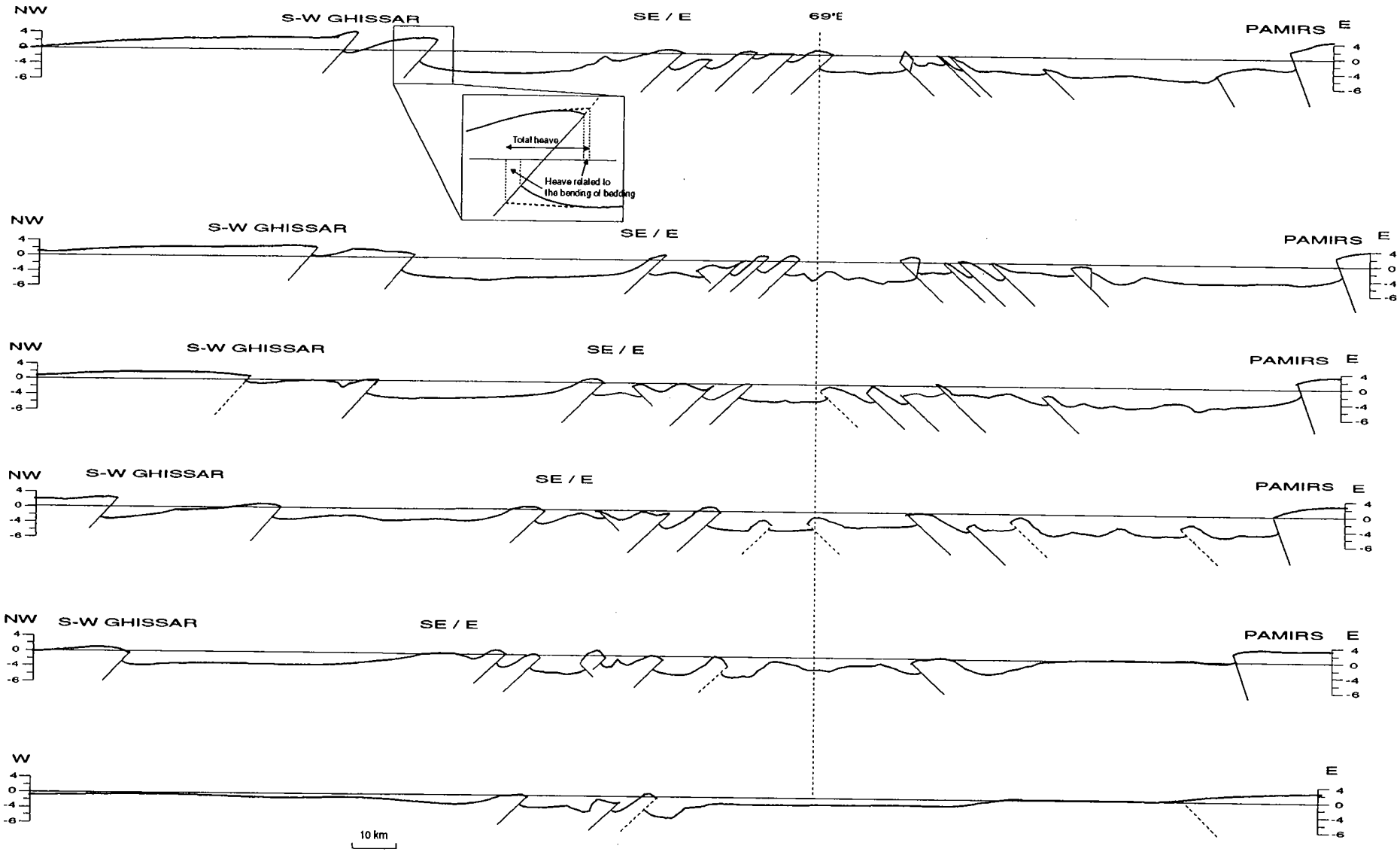

Figure 13b. Serial cross sections for the base of the Tertiary level.
Dips of faults are uniform in the depression and in the SW Ghissar ranges respectively. Dashed faults have been added to take into account the deformation accommodated by folding. Inset explains the estimation of the horizonthal displacement on faults (see text).

horizontal projection of the fault heave (see inset on Figure 13b). In order to take into account the shortening accommodated by folding without faulting, we have drawn artificial faults on major folds and on strong steps of the stratigraphic level. However, we are aware that we do not consider all the horizontal deformation and the estimation of horizontal motion for the overall depression is a minimum value. In the area between the Pamirs and the Tien-Shan, horizontal motion is poorly constrained. Nevertheless, we will see later that the deformation of this region can be deduced from the restoration of the rest of the depression.

The pattern of the depression after manual restoration is represented on figure 14. To obtain this, we assume fixed the Northeastern part of the area. We first cut the paper along the Ghissar fault, to allow strike slip movements, and along the Peter the First range, to allow differential motion between the Pamirs and the Tien-Shan. Then we progressively restore the horizontal movements, from West to East, by cutting along each fault trace and pulling the paper. We assume the Pamirs to be a rigid block, which is an oversimplification, as discussed below. However, this has no influence on the restored pattern inside the depression. We made several reconstructions, for various amounts of horizontal movement on faults, ranging between extreme values. All restored patterns were nevertheless similar.

Reconstruction pattern

Our reconstruction shows that the amount of Tertiary shortening in the central part of the Tadjik depression increases gradually from South to North. Toward the NE, the area of convergence between the Pamirs and the Tien-Shan (in the Vaksh belt and the Peter the First range) show a large jump in the amount of shortening. Note that this shortening, despite the lack of data in this area, is fully constrained by the restoration of the center of the depression. The change of orientation of the South Tien-Shan margin, from E-W north of Dushanbe, to NW-SE toward the East (nearly perpendicular to the regional shortening direction) is partly responsible for this large amount of shortening. A simple calculation, comparing lengths between the current and restored states shows that shortening is at least 20% between the SW Ghissar ranges and the Pamirs, through the center of the depression. Between the South Tien-Shan and the Pamirs, across the Peter the First range, the shortening is of 60%. This value could be slightly modified by a possible northward movement of the South Tien-Shan during the deformation, as shown in the restored pattern. Indeed, paleomagnetic data suggest that, during the Cenozoic, the South Tien

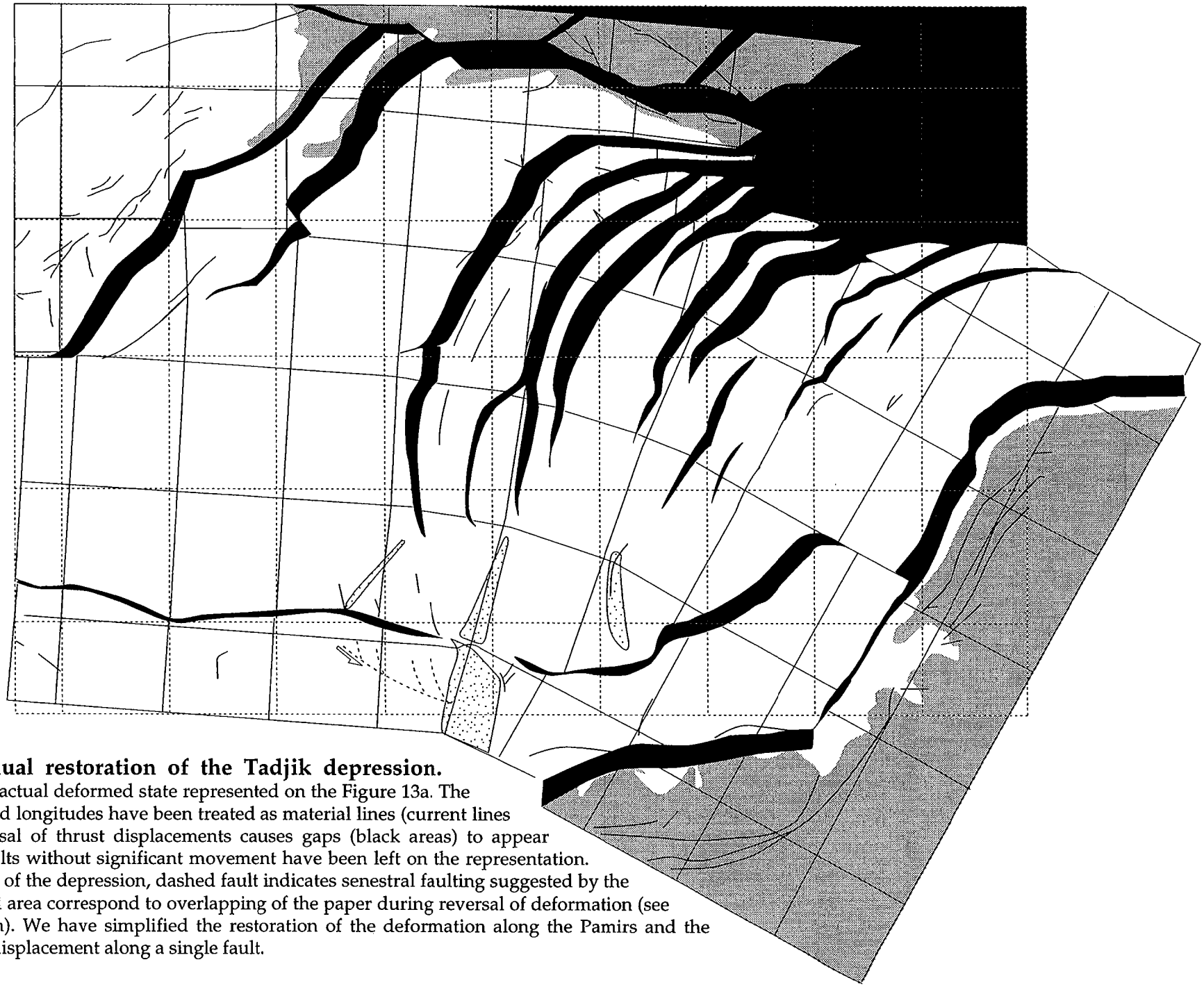

Figure 14. Manual restoration of the Tadjik depression.
Starting map is the actual deformed state represented on the Figure 13a. The lines of latitudes and longitudes have been treated as material lines (current lines are dashed). Reversal of thrust displacements causes gaps (black areas) to appear between faults. Faults without significant movement have been left on the representation. At the southen part of the depression, dashed fault indicates senestral faulting suggested by the fold pattern. Dotted area correspond to overlapping of the paper during reversal of deformation (see text for explanation). We have simplified the restoration of the deformation along the Pamirs and the Ghissar ranges by displacement along a single fault.

shan did not undergo large rotations relative to the Tadjik depression at the vicinity of the Ghissar ranges (Thomas et al., submitted), but suffered counterclockwise rotations toward the East, in the Alai range (Bazhenov, 1993). However, independently, a minimal 55% shortening for the Peter the First range has been obtained from balanced cross sections (Hamburger et al., 1992). We thus feel that our estimate of horizontal motion on faults is acceptable.

Another major consequence of the N-S gradient of shortening in the south the Tadjik depression, are the occurrence of counterclockwise block rotations. Rotations are small in the western part of the depression (6° to 10°), and increase in the Eastern part, reaching 30° along the Pamirs. This abrupt increase of counterclockwise rotations is clearly illustrated by the finite displacement field (Figure 14). A similar rotation pattern was independently inferred from paleomagnetic studies (Thomas et al., submitted) (Figure 15).

Because we assume that blocks between faults are rigid, rotations occur about poles located south of the depression, and near the southern terminations of thrusts. As a consequence, some bending and overlapping of the paper is inevitable (Figure 14). This would imply that some extension occurred in the southern part of the Tadjik depression (arrows in the displacement field with a Westward component). N-S normal faults affecting the Tertiary are documented South of the Alburz fault (Weippert et al., 1964), and may indeed accommodate some of the extension induced by the counterclockwise rotation of the Tadjik depression.However, in our restoration, we assume that blocks rotate rigidly. Consequently, the amount of rotation does not change from North to South. It seems however sensible to assume that rotations are stronger in the Northern part of the depression where the deformation is maximum, and decrease gradually toward the South. Therefore, overlapping of the paper in the South of the depression would be much more limited than it appears. Furthermore, our reconstruction does not take into account the area between the Alburz fault and the Herat fault (Afghan Turkestan), for which few data are available. "En echelon" NNE trending folds south of the Alburz fault suggest sinistral strike slip motion along a NW trend (see Figures 4 and 13). If we were to include this folding in the reconstruction, it would create gaps roughly compensating the overlapping of the paper.

Dextral strike-slip motion, combined with shortening, is mainly concentrated along the Ghissar fault. It also occurs along the Illiac fault. During the restoration, to maintain continuity and avoid unwarranted gaps and overlaps, we found it necessary to allow dextral strike slip movement at the southern border of the SW Ghissar ranges. This condition, suspected from the tectonic

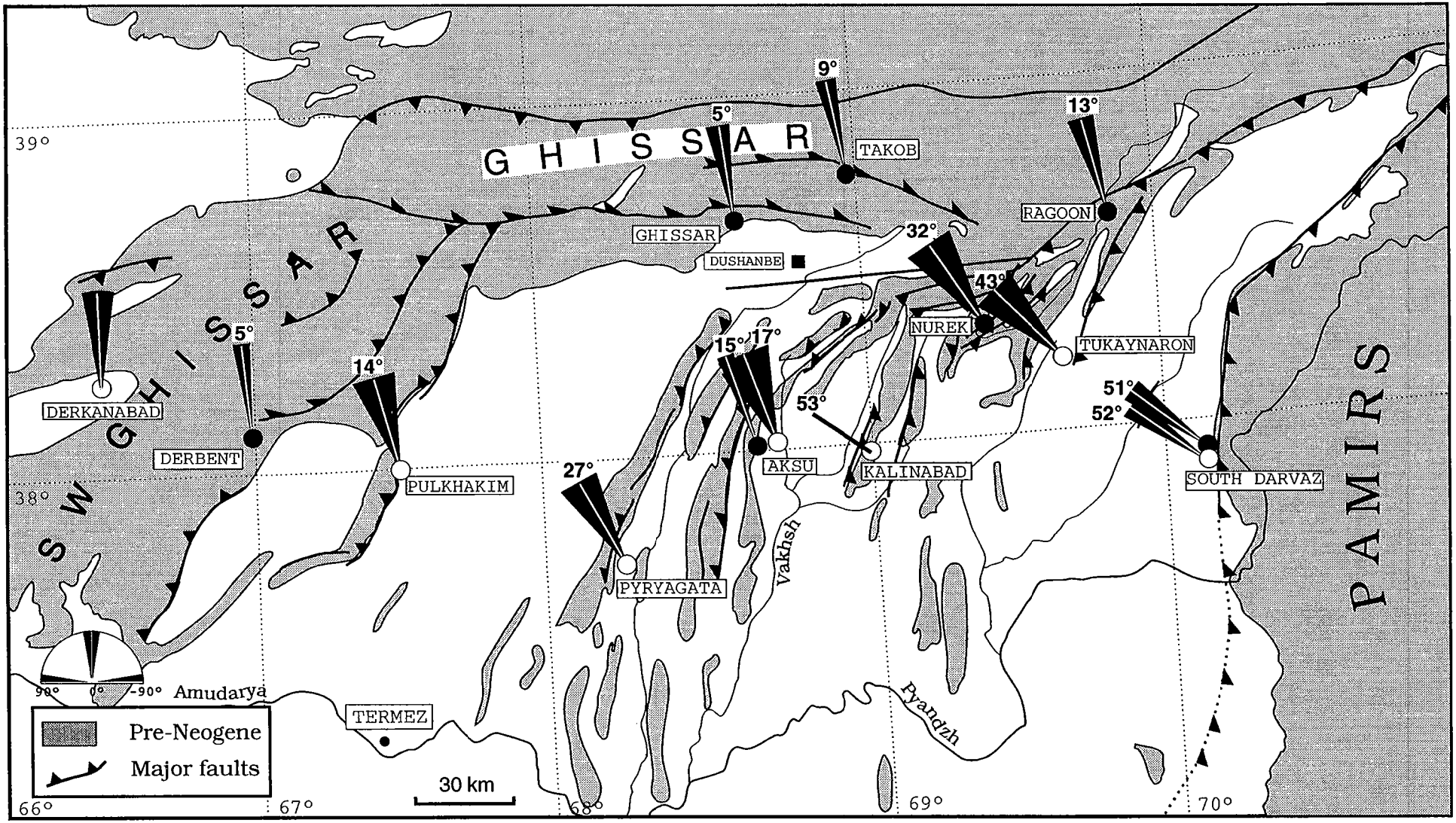

Fig 15. Compilation of paleomagnetic rotations for the Tadjik depression (from Thomas et al., submitted).
Rotations (absolute values are given) and attached uncertainties are shown with respect to a N-S reference direction. Rotations are all counterclockwise, larger in the eastern part of the depression than in the western part of the depression. No or little rotation is measured in the Ghissar and SW Ghissar ranges.

mapping of the area (see below), appears to be essential for an accurate restoration.

DISCUSSION AND CONCLUSION

The Cenozoic kinematic evolution deduced from our reconstruction provides quantification for shortening and block rotations for the Tadjik depression. Independent paleomagnetic and structural data are in agreement with the restoration.

- Paleomagnetic counterclockwise rotations measured on Cretaceous and Tertiary rocks (Pozzi and Feinberg, 1991; Bazhenov et al., submitted; Thomas et al., submitted) are large in the Eastern part of the depression (≈50°) and smaller in the Western part (≈20°) (Figure 15). The rotations are generally greater than those obtained from restoration. However, we made a minimal estimation of the deformation in the depression and, consequently, of the rotations. The displacement field (Figure 16) implies rotations about mean poles situated to the South of the depression. Although these poles are partly constrained by the technique of the manual reconstruction, their locations are in agreement with the increasing gradient of shortening from South to North in the SW Ghissar ranges.

- Restored balanced cross section in the Peter the first range (Hamburger et al., 1992), assuming that the Tadjik depression is a foreland basin during the Mesozoic, implies shortening in agreement with our restoration.

The less well constrained part of the reconstruction is the southern part of the Tadjik depression. In this area, thrusting and sinistral strike slip displacement might have occurred, in roughly parallel direction but opposite in sense to the Ghissar Dextral shear zone to the north. The uncertainty on the tectonics of the southern part of the depression did not allowed us to satisfactorily take into account a strike slip component on the oblique slip thrusts crossing N-S the Tadjik depression. Indeed, microtectonic data show that thrusting is generally accompanied by sinistral wrenching along the N-S to NE-SW faults of the depression (Thomas et al., 1993) (Figure 9). This motion is consistent with the northward displacement of the Pamirs with respect to Asia during the Tertiary. However, strike-slip displacement is probably small, compared to the thrusting component and it may not change noticeably the final pattern of the reconstruction.

We assumed the Pamirs as a rigid block for simplification, since it has no influence on the restoration of the overall depression. Hence, we did not

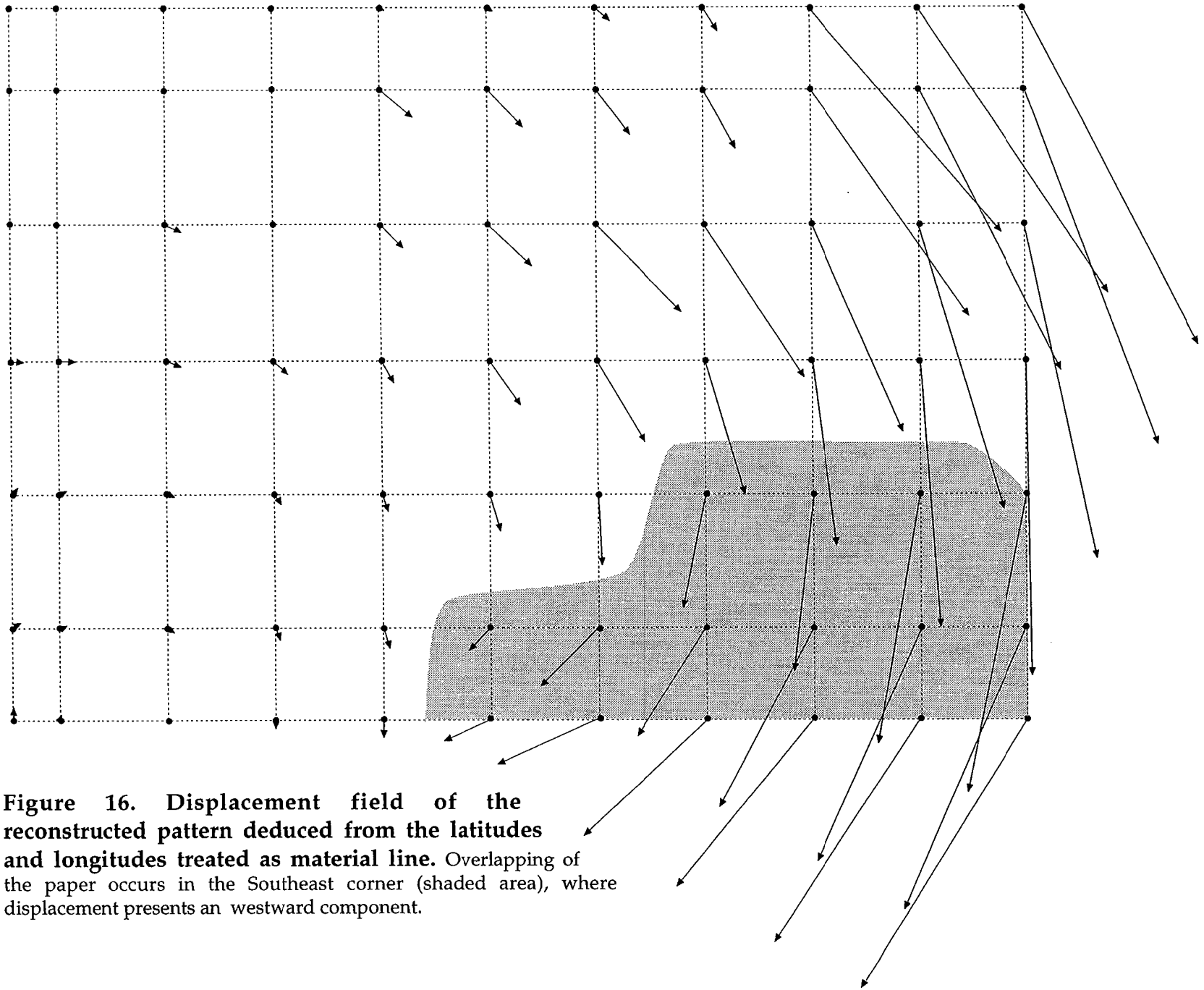

Figure 16. Displacement field of the reconstructed pattern deduced from the latitudes and longitudes treated as material line. Overlapping of the paper occurs in the Southeast corner (shaded area), where displacement presents an westward component.

restored the arcuate shape of the Pamirs which may have been acquired during its indentation into Asia (Bazhenov and Burtman, 1986). However, since its collision with Eurasia, India has rotated counterclockwise by about 25° (Dewey et al, 1989) and Pamir has probably also undergone counterclockwise rotation. We thus infer that the counterclockwise rotation of the Pamirs observed on the reconstruction has, at least partly, a geological significance.

Earlier models for the Tertiary development of the Tadjik depression are based on westward extrusion, associated with indentation of the Pamir wedge (Legler and Przhiyalgovskaya, 1979; Tapponnier et al., 1981). Tectonic data described here allow us to specify the kinematic pattern of the area and confirms our previous preliminary model (figure 12 in Thomas et al., submitted).

The Tadjik depression is a wide lozenge-shaped compressive basin (Figure 14), bounded by three major currently active thrust-wrench zones: the Darvaz-Karakul fault, the Ghissar fault zone and the SW Ghissar uplift. Strike slip motion may have also occurred at the southern boundary of the depression. From these boundaries conditions, we infer that the Tadjik depression accommodated the convergence between India and Asia by counterclockwise rotation and Northwestward extrusion.

- Counterclockwise rotations affect The N-S elongated domains constituting the depression and decrease from the Pamirs toward the Turan platform.

- Northwestward extrusion is accommodated by two roughly paralllel fault zones, to the North the Dextral shear zone of the Ghissar, and to the South the senestral displacement along the Alburz fault.

Displacements and rotations are compatibles with the Cenozoic regional kinematics pattern inferred by Cobbold and Davy (1988) (Figure 1).

Minimum shortening of 50 km occurred in the center of the depression. Between the Pamirs and the Tien-Shan, shortening is at least of 90 km, mainly accommodated in the Peter the First range. This shortening is fully in agreement with the one inferred by Hamburger et al. (1992), under the assumption that the Tadjik depression was a foreland basin rather than a rifted-margin during the mid-Mesozoic (Leith, 1985). Moreover, we infer from our data that main, if not all, shortening measured by Hamburger et al. (1992), occurred during the Tertiary, as a consequence of the India-Asia Collision.

The Upper Jurassic evaporites are of great importance in the style of the deformation in the depression. They provide a major décollement level above which main part of the deformation occurs. In fact, although boundary conditions of the deformation consist of crustal scale faults, rotations and extrusion inside the depression are probably mainly restricted to the

sedimentary cover. The style of deformation in the basement underlying the depression could be specified by a restoration similar to the one made for the Tertiary level.

Acknowledgements

The earthquakes data were kindly provided by M. Hamburger and D. Simpson. B.P Exploration provided technical support and Landsat images.

REFERENCES

Abers, G., Carol, B., 1988. Thrusting of the Indu-Kush over the Southeastern Tadjik basin, Afghanistan: evidence from two large earthquakes. Tectonics, 7: 41-56.

Achache, J., Courtillot, V., Zhou, X.Y., 1984. Paleogegraphic and tectonic evolution of southern Tibet since middle Cretaceous time: New paleomagnetic data and synthesis. J. Geophys. Res., 89: 10311-10339.

Argand, E., 1924. La tectonique de l'Asie. Comptes rendus du XIII Cong. Geol. Int, Belgique, pp. 171-371.

Avouac, J.P., 1991. Application des méthodes de morphologie quantitative à la néotectonique. Modèle cinématique des déformations en Asie Centrale. Thèses de l'Université Paris VII. 156 pp.

Avouac, J.P., Tapponnier, P., 1992. Cinématique des déformations actives en Asie Centrale. C. R. Acad. Sci. Paris, 315: 1791-1798.

Bakirov, A.B., Burtman, V.S., 1984. Tectonics of the Tien-Shan Variscides. in Bakirov, A.B., Burtman, V.S., Int. Geol. Congr., 27th, Guide Excursion 032, Moscow, 74 pp..

Bazhenov, M.L., 1993. Cretaceous paleomagnetism of the Fergana basin and adjacent ranges: tectonic implications. Tectonophysics, 221: 251-267.

Bazhenov, M.L., Burtman, V.S., 1986. Tectonics and paleomagnetism of structural arcs of the Pamir-Punjab syntaxis. J. Geodyn., 5: 383-396.

Bazhenov, M.L., Perroud, H., Chauvin, A., Burtman, V.S., Thomas, J.C., Paleomagnetism of Cretaceous red beds from the Tadjikistan and Cenozoic deformations related to the India-Eurasia collision. submitted to Earth. Planet. Sci. Lett.

Billington, S., Isacks, B.L., Barazangi, M., 1977. Spatial distribution and focal mechanism of mantle earthquakes in the Hindu Kush-Pamir region: a contorted Benioff zone. Geology, 5: 699-704.

Boulin, J., 1988. Hercynian and Eocimmerian events in Afghanistan and adjoining regions. Tectonophysics, 148: 253-278.

Boulin, J., 1990. Neocimmerian events in central and western Afghanistan. Tectonophysics, 175: 285-315.

Burtman, V.S., 1975. Structural geology of the Variscan Tien-Shan. Am. Jour. Sci., 275A: 157-186.

Burtman, V.S., Molnar, P., 1992. Geological and geophysical evidence for the subduction of continental crust beneath the Pamir. Inter. symp. on the Karakorum and Kunlun mountains, Kashi, China, 30.

Chatelain, J.L., Roecker, S.W., Hatzfield, D., Molnar, P., 1980. Microearthquake seismicity and fault plane solutions in the Hindu-Kush region and their tectonic implications. J. Geophys. Res., 85: 1365-1387.

Cobbold, P.R., Davy, P., 1988. Indentation tectonics in nature and experiment. 2. Central Asia. Bull. Geol. Inst. Univ. Uppsala, 14: 143-162.

Cobbold, P.R., Davy, P., Gapais, D., Rossello, E.A., Sadybakasov, E., Thomas, J.C., Tondji Biyo, J.J., de Urreiztieta, M., 1993. Sedimentary basins and crustal thickenning. Sed. Geol., 86: 77-89.

Cobbold, P.R., Sadybakasov, E., Thomas, J.C., 1993. Cenozoic basins and crustal thickenning in the Kirghiz Tien-Shan, Central Asia. In: F. Roure (Eds), Technip, Paris,

Davis, D.M., Engelder, T., 1985. The role of salt in fold-and-thrust belts. Tectonophysics, 119: 67-88.

Davy, P., Cobbold, P.R., 1988. Indentation tectonics in nature and experiments.1. Experiments scaled for gravity. Bull. Geol. Inst Univ. Uppsala, 14: 129-141.

De Mets, C., Gordon, R.G., Argus, D.F., Stein, S., 1990. Current plate motion. Geophys. Jour. Int., 101: 425-478.

Dewey, F.D., Cande, S., Pitman, W.C., 1989. Tectonic evolution of India/Eurasia collision zone. Eclogae Geol. Helv., 82(3): 717-734.

Dewey, J.F., Burke, K.C.A., 1973. Tibetan, Variscan, and Precambrian reactivation: Products of continental collision. J. Geol., 81: 683-692.

Eneva, M., Hamburger, M.W., 1989. Spatial and temporal patterns of earthquakes distribution in Soviet Central Asia: application of pair analysis statistics. Bull. Seismol. Soc. Am., 79: 1439-1456.

England, P., Molnar, P., 1990. Right lateral shear and rotation as an explanation for strike-slip faulting in Eastern Tibet. Nature, 344: 140-142.

Hamburger, M.W., Sarewitz, D.R., Pavlis, T.L., Papandopulo, G.A., 1992. Structural and seismic evidence for intracontinental subduction in the Peter The First Range, Central Asia. Geol. Soc. Am. Bull., 104: 397-408.

Heuckroth, L.E., Karim, R.A., 1973. Afghan seismotectonics. Phil. Trans. R. Soc. Lond., 274: 389-395.

Hinze, C., 1964. Die geologische entwicklung der östlichen Hindukush-Nordflanke (nord Afghanistan). Geol. Jahrb., Beih., 70: 19-75.

Houseman, G., England, P., 1986. Finite strain calculations of continental deformation 1. Method and general results for convergent zones. J. Geophys. Res., 91: 3651-3663.

Houseman, G., England, P., 1993. Crustal thickening versus lateral expulsion in the Indian-Asian continental collision. J. Geophys. Res., 98: 12233-12249.

Le Pichon, X., Fournier, M., Jolivet, L., 1992. Kinematics, topography, shortening, and extrusion in the India-Eurasia collision. Tectonics, 11: 1085-1098.

Legler, V.A., Przhiyalgovskaya, I.A., 1979. Interaction of the Indian and Asiatic plates and tectonics of the Tadjik depression. In: L. P. Zonenshain, O. G. Sorokthin (Eds), Lithospheric Plate Structure. Plate Interaction and Formation of Crustal Structures (in Russian). Inst. Oceanol. USSR Acad. Sci., Moscow, 125-188.

Leith, W., 1985. A mid-Mesozoic extension across Central Asia ? Nature, 313: 567-570.

Leith, W., Simpson, D.W., 1986. Earthquakes related to active salt doming near Kulyab, Tadjikistan, USSR. Geophys. Res. Lett., 1019-1022:

Leith, W., Simpson, D.W., 1986. Seismic domains within the Ghissar-Kokshal seismic zone Soviet Central Asia. J. Geophys. Res., 91: 689-699.

Mattauer, M., 1986. Les subductions intracontinentales des chaînes tertiaires d'Asie; leurs relations avec les décrochements. Bull. Soc. Geol. Fr., 8: 143-157.

Minster, J.B., Jordan, T.H., 1978. Present-day plate motions. J. Geophys. Res., 83: 5331-5354.

Molnar, P., Tapponnier, P., 1975. Cenozoic tectonics of Asia: Effects of a continental collision. Science, 189: 419-426.

Patriat, P., Achache, J., 1984. India-Eurasia collision chronology has implication for crustal shortening and driving mechanism of plates. Nature, 311: 615-621.

Pavlis, G.L., Hamburger, M.W., 1991. Aftershock sequences of intermediate-depth earthquakes in the Pamir-Hindu Kuush seismic zone. J. Geophys. Res, 96: 18107-18117.

Peive, A.V., Burtman, V.S., Rhuzentsev, S.V., Suvorov, A.I., 1964. Tectonics of the Pamirs Himalayan sector of Asia. Rep. 22nd Sess. Int. Geol. Congr, New Delhi, 441-462.

Peltzer, G., Tapponier, P., 1988. Formation and evolution of strike-slip faults, rifts and basins during the India-Eurasia collision: An experimental approach. J. Geophys. Res., 93: 15085-15117.

Pozzi, J.P., Feinberg, H., 1991. Paleomagnetism in the Tadjikistan: continental shortenning of Eurasian margin in the Pamirs during the Indian-Eurasian collision. Earth planet. Sci. Let., 103: 365-378.

Prevot, R., Hatzfeld, D., Roecker, S.W., Molnar, P., 1980. Shallow earthquakes and active tectonics in Eastern Afghanistan. J. Geophys. Res, 85: 1347-1357.

Roecker, S.W., Soboleva, O.V., Nersesov, I.L., Lukk, A.A., Hatzfeld, D., Chatelain, J.L., Molnar, P., 1980. Seismicity and fault plane solutions of intermediate depth earthquakes in the Pamir Hindu-Kush region. J. Geophys. Res, 85: 1358-1364.

Savostin, L.A., Sibuet, J.-C., Zonenshain, L.P., Le Pichon, X., Roulet, M.-J., 1986. Kinematic evolution of the Tethys belt from the Atlantic ocean to the Pamirs since the Triassic. Tectonophysics, 123: 1-35.

Sengör, A.M.C., 1987. Tectonics of the Tethysides: orogenic collage development in a collisional setting. Ann. Rev. Earth. Planet. Sci., 15: 213-244.

Shareq, A., 1981. Geological observations and geophysical investigations carried out in Afghanistan over the period of 1972-1979. In: H. K. Gupta (Eds), Zagros, Hindu Kush, Himalaya, geodynamic evolution. AGU, Washington, 75-86.

Tapponnier, P., Mattauer, M., Proust, F., Cassaigneau, C., 1981. Mesozoic ophiolites, sutures and large scale movements in Afghanistan. Earth. Planet. Sci. Let., 52: 355-371.

Thomas, J.C., Perroud, H., Cobbold, P., Bazhenov, M.L., Burtman, V.S., Chauvin, A., Sadybakasov, E., 1993. A paleomagnetic study of Tertiary formation of the Kirghiz Tien-Shan and its tectonic implications. J. Geophys. Res., 98: 9571-9589.

Thomas, J.C., Gapais, D., Cobbold, P.R., Burtman, V.S., 1993. Tertiary kinematics of the Tadjik depression infered from fault and fold patterns. In: F. Roure (Eds), Geodynamic evolution of sedimentary basins. Technip, Paris, in press.

Thomas, J.C., Chauvin, A., Gapais, D., Cobbold, P.R., Bazhenov, M.L., Perroud, H., Burtman, V.S., Paleomagnetic evidence for Cenozoic block rotation in the Tadjik depression (Central Asia). Submitted to J. Geophys. Res.

Trifonov, V.G., 1978. Late Quaternary movements of western and central Asia. Geol. Soc. Amer. Bull., 89: 1059-1072.

Weippert, D., 1964. Zuir Geologie des Gebietes Doab-Sayghan-Hajar (Nord Afghanistan). Geol. Jahrb., Beih., 70: 153-183.

Willis, B., 1928. Dead sea problem: rift valley or ramp valley? Geol. Soc. Am. Bull., 39: 490-542.

Windley, B.F., B., A.M., Zhang, C., Zhao, Z.Y., Wang, G.R., 1990. Paleozoic accretion and cenozoic redeformation of the Chinese Tien-Shan range, Central Asia. Geology, 18: 128-131.

Zakharov, S.A., 1958. Stratostructures of Mesozoic and Cenozoic rocks in the Tadjik basin. Geol. Inst. Tadjikistan. Sci. Acad, Dushanbe, 228 pp.

Zonenshain, L.P., Kuzmin, M., Natapov, L.M., 1990. Geology of the USSR: a plate-tectonic synthesis. Geodynamics Series, Page B.M. (Eds), AGU, Washington, 21, 242 pp.

CHAPITRE IV

Synthèse

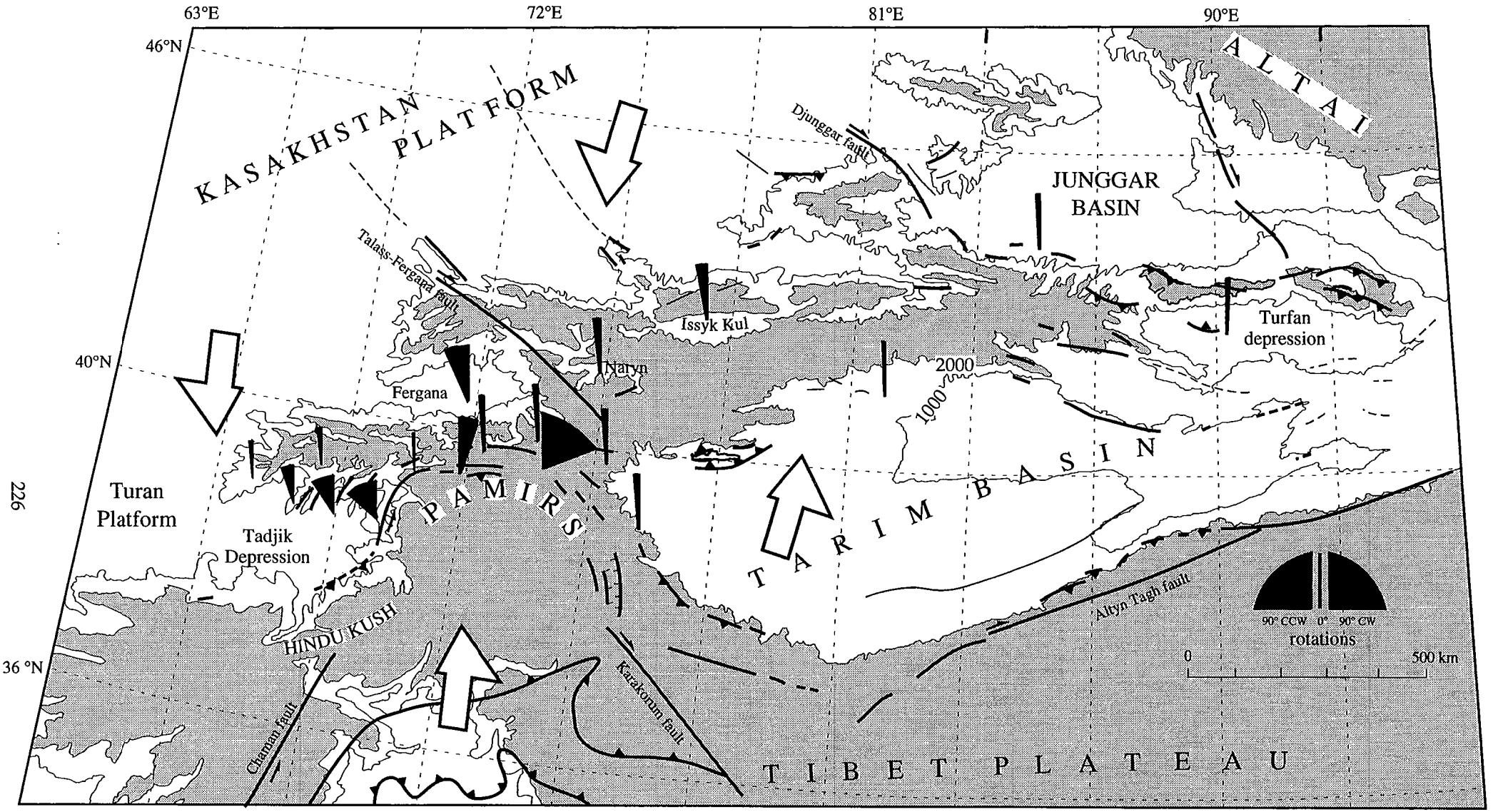

Figure IV.1. Failles actives, rotations paléomagnétiques et topographie de l'Asie Centrale (adaptée d'après Avouac et al., 1993).
Les rotations ont été mesurées dans des sédiments Jurassique supérieur, Crétacé et Cénozoïque et calculées par rappot à l'Asie stable. Elles sont représentées par rapport à une référence verticale. Dans le dépression Tadjik et le Bassin de Fergana, les rotations obtenues par différentes études ont été été moyennées. Références : dépression Tadjik : chapitre II, annexe 2 et Pozzi et Feinberg 1991; Nord-Pamir : Bazhenov et Burtman, 1986; Sud-Fergana : Bazhenov, 1993; bassin de Fergana : Thomas et al., 1993 et Bazhenov 1993; Bassins de Naryn et Issyk-Kul : Thomas et al., 1993; Ouest-Tarim : Chen et al., 1993; Nord-Tarim : Li et al., 1988; bassin Junggar : Chen et al., 1991; dépression de Turfan : Cogné et al., 1993. Les flèches noires représentent le contexte cinématique régional (Cobbold et Davy, 1988). Les rotations horaires sur la bordure Nord du Pamir sont liées à l'acquisition de la courbure oroclinale lors de son indentation dans l'Asie (Bazhenov et Burtman, 1986). La chaîne de l'Alaï, dans le Tien Shan, directement au nord du Pamir n'a pas subit cet effet tectonique et ne présente que de faibles rotations.

Les données structurales et paléomagnétiques présentées dans ce travail apportent de nouvelles contraintes quant à l'évolution tectonique et la cinématique Tertiaire de l'Asie Centrale de l'Ouest.

1. Les données cinématiques

La déformation dans le Tien Shan et la dépression Tadjik s'effectue dans un contexte transpressif sénestre. La composante chevauchante est généralement dominante et à l'origine des principaux reliefs. La composante de décrochement sénestre apparaît aussi bien à l'échelle très régionale (dans la topographie par exemple) que localement sur le terrain. Les décrochements antithétiques dextres (Faille de Talass-Fergana, du Ghissar ...) participent au décrochement sénestre régional.

Les relations entre mouvements décrochants et chevauchants évoluent dans l'espace et dans le temps :

- Les observations de terrain en Kirghizie suggèrent une évolution temporelle du style de la déformation depuis un contexte principalement décrochant à l'Oligocène, devenant principalement compressif au cours du Miocène et marquant la phase tectonique majeure et la surrection des reliefs. Cette évolution temporelle reflète la migration vers le Nord de la déformation compressive liée à la collision Inde-Asie qui n'affecte les régions du Tien Shan, du Pamir, du Kunlun et du Quilian Shan qu'à partir du Tertiaire Supérieur (Mattauer, 1986).

- La déformation finie observable sur le terrain montre également une composante décrochante bien plus exprimée dans la dépression Tadjik que dans le Tien Shan Kirghiz. La situation de la dépression, sur la bordure latérale du poinçon du Pamir, comparée à la position plus frontale du Tien Shan explique aisément cette variation spatiale de la déformation, en accord avec l'interprétation cinématique à grande échelle de Cobbold et Davy (1988) (Figure IV.1).

2. Les Rotations

D'importantes rotations de blocs autour d'axes verticaux peuvent être associées à la déformation. Dans ce sens, deux domaines bien distincts apparaissent (Figure IV.1) :

- A l'Est de la faille de Talass-Fergana les rotations antihoraires sont faibles ou insignifiantes dans les bassin de Naryn et Issyk-Kul, mais également à l'extrémité Est du Tien Shan, dans le bassin de la Junggarie (Chen et al., 1991).
- A l'inverse, les régions mitoyennes du Pamir et à l'Ouest de la faille de Talass-Fergana présentent des rotations antihoraires de 20° à 25° dans le bassin de Fergana et de 15° à 50° dans la dépression Tadjik.

Nous avons vu que les rotations sont souvent associées à des mouvements décro-chevauchant de couverture aux limites de blocs comme dans la dépression Tadjik, et d'échelle crustale sur les failles majeures qui bordent les domaines comme dans le Ghissar. Par ailleurs, les données paléomagnétiques et structurales suggèrent que :

- la rotation de la dépression Tadjik et du bassin de Fergana se fait par rapport à un pôle moyen situé respectivement dans la partie sud et sud-ouest de chaque domaine ;
- la zone faillée crustale dextre du Ghissar, qui limite ces deux domaines, présente une rotation antihoraire faible à nulle.

Ces conditions aux limites complexes rendent la comparaison avec les modèles classiques de rotations de blocs difficile (Freund, 1970; McKenzie et Jackson, 1983).

L'importance majeure des niveaux de décollement sur la déformation dans les bassins et donc sur les rotations doit cependant être soulignée. Dans la dépression Tadjik, la couverture sédimentaire, décollée sur les évaporites jurassiques, subit une déformation et une rotation dont une grande partie n'affectent pas le socle. Dans le bassin de Fergana, la sismique suggère également un niveau de décollement dans les séries argileuses Siluriennes. Par ailleurs, un découplement général des mouvements rotationels au niveau de la transition crustale fragile-ductile (≈15 km de profondeur) est probable (Garfunkel, 1989). En tout état de cause, il semble que les rotations observées en surface ne reflètent pas la rotation de la croûte profonde (Garfunkel, 1989).

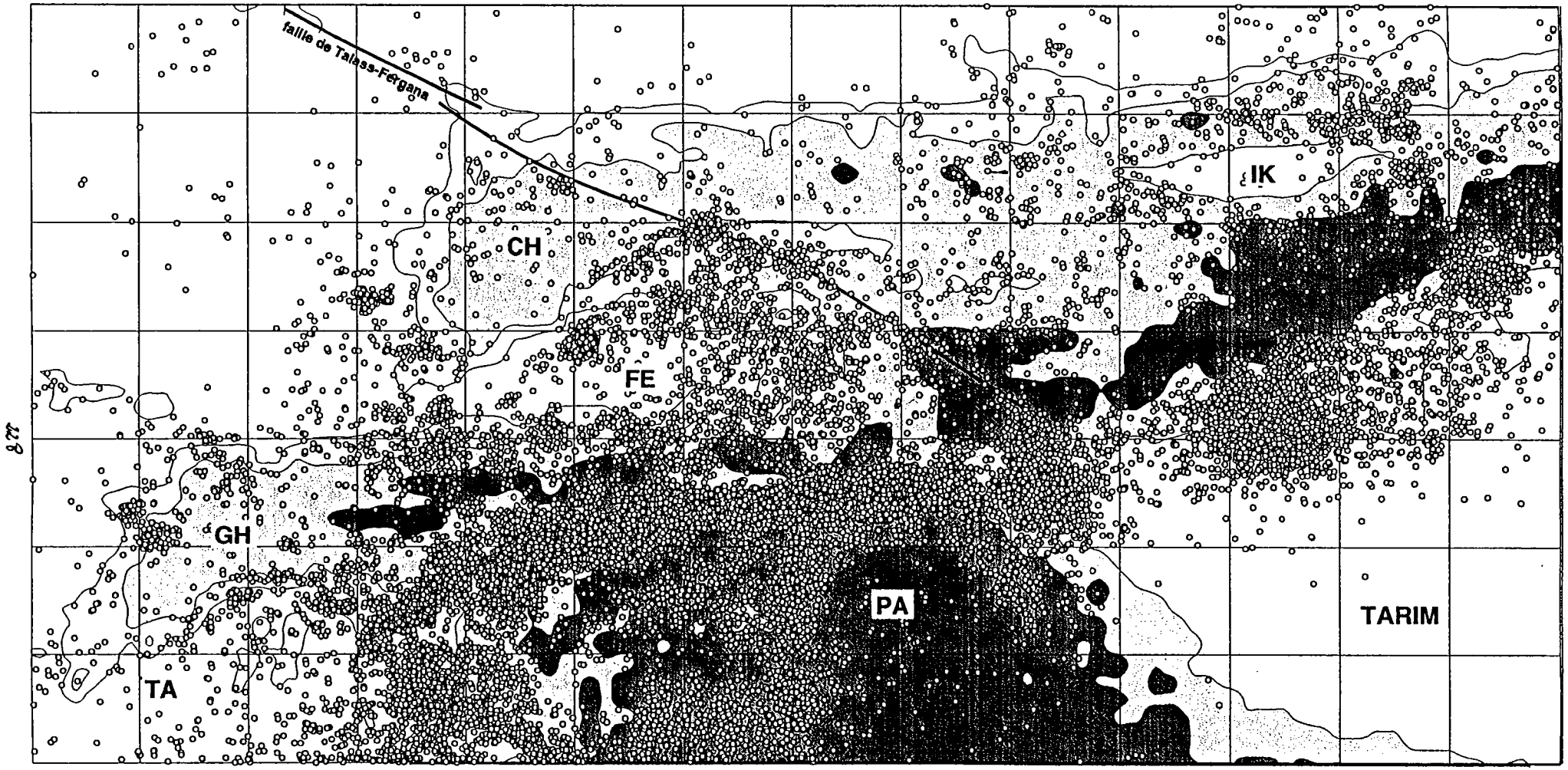

Figure IV.2. Carte des séismes compris entre 0 et 70 km de profondeur, enregistrés dans le Tien Shan Kirghiz, la dépression Tadjik et le Nord Pamir.

Données issues du réseau régional d'Asie Centrale de 1964 à 1982. CH : Chaîne du Chatkal ; FE : Bassin de Fergana ; GH : Chaîne du Ghissar ; IK : bassin d'Issyk-Kul ; PA : Pamir. Les contours topographiques correspondent aux altitudes 1000, 2000 et 3500 m.

A l'inverse, nous verrons dans le paragraphe suivant que la faille de Talass-Fergana est une discontinuité d'échelle crustale si ce n'est lithosphérique. De même, la chaîne du Ghissar présente un épaississement crustal associé au fonctionnement de la zone faillée décro-chevauchante qui la traverse.

Ainsi, les rotations qui affectent les bassins ont une continuité en profondeur beaucoup plus faible que les zones faillées qui les limitent. La rotation de ces deux structures liée à la cinématique régionale n'est donc probablement pas homogène. En d'autres termes, la rotation des bassins n'implique pas nécessairement la rotations des zones faillées qui les limitent. De nouvelles données paléomagnétiques et structurales le long des décrochements du Ghissar et Talass-Fergana seraient nécessaires pour mieux contraindre les relations de ces accidents vis à vis des domaines adjacents.

3. Importance de la faille de Talass-Fergana et proposition de synthèse cinématique

L'analyse structurale et les données paléomagnétiques montrent que le poinçonnement du Pamir et la faille de Talass-Fergana jouent un rôle majeur dans la déformation de l'Asie, au nord de la syntaxe Ouest-Himalayenne.

La faille de Talass-Fergana est une discontinuité Paléozoïque (Burtman, 1975) réactivée au cours de l'orogenèse Tertiaire. Elle traverse le Tien Shan de part en part selon une direction NO-SE et sa signature morphologique sur les images satellite (Tapponnier et Molnar, 1979) en fait une discontinuité majeure. Son jeu dextre est associé à la rotation du bassin de Fergana et, nous le verrons, au poinçonnement du Pamir dans l'Asie. Plusieurs types de données ajoutées aux rotations paléomagnétiques viennent confirmer la présence de deux domaines géologiquement bien distincts de part et d'autre de la faille de Talass-Fergana.

Séismes

Sur la figure IV.2 sont représentés les séismes compris entre 0 et 70 km de profondeur enregistrés par le réseau régional d'Asie Centrale (cf. chapitre III) dans le Tien Shan Kirghiz et au Tadjikistan. La sismicité apparaît maximale dans l'étroite zone de convergence intensément plissée entre le Pamir et le Tien Shan. Les principales failles qui structurent la région sont également soulignées, particulièrement celles correspondant aux bordures nord et sud du bassin de Fergana et aux limites nord et est de la dépression Tadjik. La faille de

Talass-Fergana est elle aussi très clairement marquée bien qu'aucun séisme de forte magnitude n'y ait été enregistré au cours de ce siècle (Tapponnier et Molnar, 1979). On remarquera que c'est le segment Sud de la faille et plus particulièrement son transect mitoyen du bassin de Fergana qui est le plus actif, en accord avec les observations des déplacements quaternaires (Tapponnier et Molnar, 1979 ; Trifonov, 1992) L'extrémité sud-est de la faille de Talass-Fergana est également marquée par une forte sismicité, localisée au niveau d'une série de chevauchements sur lesquels est transféré le mouvement décrochant de la faille.

A l'Est de la faille de Talass-Fergana, la sismicité est principalement présente sur la bordure nord du Tarim et autour du bassin d'Issyk-Kul tandis qu'elle est faible à l'intérieur du Tien-Shan.

La déformation active, principalement compressive comme le montrent les mécanismes au foyer des séismes (Ni, 1978 ; Tapponnier et Molnar, 1979; Nelson et al., 1987), semble donc plus intense dans le Tien Shan de l'Ouest.

Sismologie

l'Analyse de la propagation des ondes sismiques fait également ressortir deux domaines de comportement différents séparés par la faille de Talass-Fergana. Les faibles vitesses de propagation des ondes enregistrées dans le Manteau supérieur, à l'Est de la faille, sont interprétées comme reflétant une faible densité et une activité thermique mantellique anormalement élevée (Vinnik et Saipbekova, 1984; Kosarev et al., 1993). Ainsi, les reliefs du Tien Shan, classiquement associés à l'unique épaississement crustal, seraient également liés, à l'Est de la faille de Talass-Fergana, à la compensation isostatique d'une lithosphère mantellique réchauffée. A nouveau, ceci suggère un raccourcissement plus important dans le Tien Shan de l'Ouest.

Les données structurales vont dans ce sens. Tapponnier et Molnar (1979), remarquant que les sédiments au Nord du Pamir sont plus intensément plissés que dans la zone de Kashgar du Nord-Ouest Tarim, concluent à un mouvement relatif vers le Nord du Tien Shan de l'Ouest par rapport au Tien Shan de l'Est.

Le déplacement cénozoïque le long de la faille de Talass-Fergana résulte donc probablement de l'addition de la rotation antihoraire du bassin de Fergana (cf. chapitre II), et du déplacement vers le Nord du Tien Shan de l'Ouest par rapport au Tien Shan de l'Est en réponse au poinçonnement du

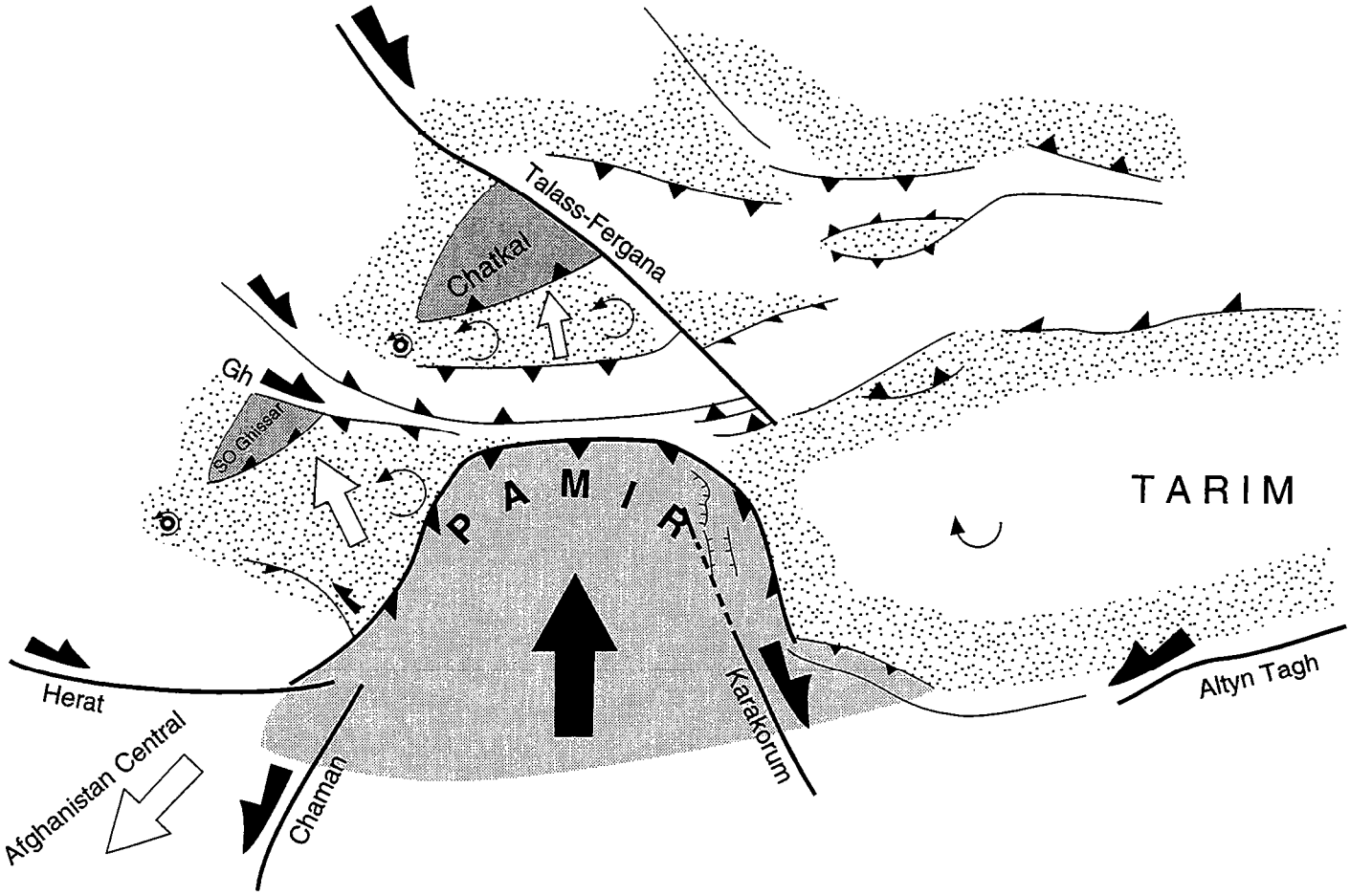

Figure IV.3. Cinématique Tertiaire de l'Asie Centrale Occidentale.
L'indentation du Pamir dans l'Asie (flèche noire)est accommodée à l'Est par le système de décrochements dextres du Karakorum et de Talass-Fergana. A l'Ouest de ce système, le mouvement du Pamir par rapport à l'Asie stable induit une composante décrochante sénestre importante; Le bassin de Fergana et la dépression Tadjik subissent des rotations antihoraires combinée à de l'extrusion (flèche blanche). L'Afghanistan Central est extrudé vers le Sud-Ouest. A l'Est de la faille de Talass-Fergana, le déplacement régional décrochant sénestre n'est pas suffisant pour créer des rotations antihoraires mesurables par le paléomagnétisme. La rotation horaire du Tarim par rapport à la Sibérie s'effectue selon un pôle situé à l'extrémité Est du Tien Shan (Avouac et Tapponnier, 1992).

Pamir. Nous l'avons vu, l'influence du Pamir est également fondamentale sur la déformation de la dépression Tadjik et du Sud-Ouest Ghissar, à l'Ouest. A l'inverse à l'Est, le bassin du Tarim, chevauché par le Pamir (Tapponnier et al., 1993), ne présente pas sur sa bordure ouest de déformation ni de rotations paléomagnétiques (Chen et al., 1993) comparables à celles observées dans la dépression Tadjik.

La Faille de Talass-Fergana apparaît donc clairement comme le segment Nord d'un système de décrochements dextres bordant le Karakorum et l'Est Pamir (Peive et al., 1964; Tapponnier et Molnar, 1979) et séparant deux domaines de structuration distinctes. Aux extrémités des différents segments décrochants, le déplacement relatif dextre peut être transféré en chevauchement comme à l'extrémité sud de la faille de Talass-Fergana ou encore sur des failles normales limitant des bassins en échelon à l'extrémité nord de la faille du Karakorum (Mustagh Ata graben) (Figure IV.3). Ce système constitue une zone de découplage accommodant le mouvement relatif vers le Nord du Pamir par rapport au Tibet et au Tarim. La présence d'importantes rotations antihoraires uniquement localisées à l'Ouest de ce système et plus généralement, le style de la déformation autour de la syntaxe Ouest-Himalayenne apparaît associé a ces conditions aux limites.

Tapponnier et al. (1981) ont proposé un modèle d'évolution par extrusion des domaines situés à l'Ouest de la syntaxe du Pakistan, en Afghanistan. Je propose qu'un tel modèle, combinant extrusion et rotation autour du Pamir, s'applique à l'ensemble du système de blocs à l'Ouest de la faille de Talass-Fergana (Figure IV.3). L'extrusion qui s'effectue le long de la série de décrochements dextres est maximale pour le bloc Central-Afghan et modérée à l'Ouest et au Nord du Pamir ou le raccourcissement interne est important. Au Sud, l'Afghanistan central est extrudé vers le Sud-Ouest entre les failles de Chaman et de l'Hérat; à l'Ouest du Pamir, la dépression Tadjik est extrudée vers le Nord-Ouest entre les failles du Ghissar et de l'Alburz, tout en subissant une rotation antihoraire; au Nord du Pamir, l'Ouest Tien-Shan est extrudé vers le NNO le long de la faille de Talass-Fergana tout en subissant lui aussi une rotation antihoraire. L'extrusion et la rotation de ces deux derniers domaines sont compensées respectivement dans la plate-forme asiatique par de l'épaississement dans le Sud-Ouest Ghissar et dans le Chatkal.

Le contexte décrochant sénestre dans cette zone est lié au mouvement relatif vers le nord du Pamir et de l'ouest de l'Inde par rapport à l'Asie. En l'occurrence, le mouvement vers le Nord du Pamir par rapport à l'Asie est d'au

moins 300 km (Burtman et Molnar, 1992). A l'opposé, à l'est de la faille de Talass-Fergana et jusqu'au Baïkal, les expériences analogiques (Davy et Cobbold, 1988; Sornette et al., 1993; Fournier et al., en préparation) suggèrent que la composante régionale décrochante sénestre (Cobbold et Davy, 1988) est plutôt associée à un mouvement global vers l'Est de toute l'Asie déformée par rapport à l'Asie stable. Le déplacement sénestre fini le long de cette zone doit cependant être modéré au vu de la cinématique active (Avouac, 1991; Avouac et Tapponnier, 1992) et des faibles (ou nulles) rotations antihoraires mesurées par le paléomagnétisme dans le Tien Shan Central (bassins d'Issyk-Kul et de Naryn), dans le bassin Junggar (Chen et al., 1991) et en Mongolie (Pruner, 1987).

Bibliographie générale

Allen, C.R., Zhuoli, L., Hong, Q., Xueze, W., Huawei, Z., Weishi, H.., 1991. Field study of a highly active fault zone: the Xanshuihe fault of southwestern China. Geol. Soc. Amer. Bull., 103: 1178-1199.

Allen, M.B., Windley, B.F., Zhang, C., Zhao, Z.Y., Wang, G.R., 1991. Basin evolution within and adjacent to the Tien-Shan Range, NW China. J. Geol. Soc., 148: 369-378.

Allen, M.B., Windley, B.F., Chi, Z., 1992. Paleozoic collisional tectonics and magmatism of the Chinese Tien Shan, Central Asia. Tectonophysics, 220: 89-115.

Angelier, J., Mechler, P., 1977. Sur une méthode graphique de recherche des contraintes principales également utilisable en tectonique et en sismologie. La méthode des dièdres droits. Bull. Soc. Geol. Fr., 7: 1309-1318.

Argand, E., 1924. La tectonique de l'Asie. Comptes rendus du XIII Cong. Geol. Int., Belgique, 171-371.

Armijo, R., Tapponnier, P., Mercier, J.L., Tonglin, H., 1986. Quaternary extension in southern Tibet: field observation and tectonic implication. J. Geophys. Res., 91: 13803-13972.

Armijo, R., Tapponnier, P., Tonglin, H., 1989. Late Cenozoic right-lateral strike-slip faulting in southern Tibet. J. Geophys. Res., 94: 2787-2838.

Audibert , M., Bazhenov, M.L., 1992. Permian paleomagnetism of the northern Tien Shan and its tectonic implications. Tectonics, 11: 1057-1070.

Avouac, J.P., Tapponnier, P., 1992. Cinématique des déformations actives en Asie Centrale. C. R. Acad. Sci. Paris, 315: 1791-1798.

Avouac, J.P., Tapponnier, P., Bai, M., You, H., Wang, G., 1993. Active thrusting and folding along the Northern Tien Shan and late Cenozoic rotation of the Tarim relative to Dzungaria and Kasakhstan. J. Geophys. Res., 98: 6755-6804.

Bakirov, A.B., Burtman, V.S., 1984. Tectonics of the Tien-Shan Variscides. in Bakirov, A.B., Burtman, V.S., Int. Geol. Congr., 27th, Guide Excursion 032, Moscow, 74 pp.

Bazhenov, M.L., 1993. Cretaceous paleomagnetism of the Fergana basin and adjacent ranges: tectonic implications. Tectonophysics, 221: 251-267.

Bazhenov, M.L., Burtman, V.S., 1986. Tectonics and paleomagnetism of structural arcs of the Pamir-Punjab syntaxis. J. Geodyn., 5: 383-396.

Bazhenov, M.L., Chauvin, A., Audibert, M., Levashova, N.M., 1993. Permian and Triassic paleomagnetism of the southwestern Tien Shan: timing and mode of tectonic rotations. Earth. Planet. Sci. Lett., 118: 195-212.

Bazhenov, M.L., Perroud, H., Chauvin, A., Burtman, V.S., Paleomagnetism of Cretaceous red beds from the Tadjikistan and Cenozoic deformations related to the India-Eurasia collision. submitted to Earth. Planet. Sci. Lett.

Besse, J., Courtillot, V., 1991. Revised and synthetic apparent polar wander paths of the African, Eurasian, North American and Indian plates, and true polar wander paths since 200 Ma. J. Geophys. Res., 96: 4029-4050.

Billington, S., Isacks, B.L., Barazangi, M., 1977. Spatial distribution and focal mechanism of mantle earthquakes in the Hindu Kush-Pamir region: a contorted Benioff zone. Geology, 5: 699-704.

Boulin, J., 1988. Hercynian and Eocimmerian events in Afghanistan and adjoining regions. Tectonophysics, 148: 253-278.

Boulin, J., 1990. Neocimmerian events in central and western Afghanistan. Tectonophysics, 175: 285-315.

Burchfiel, B.C., Royden, L.H., 1991. Tectonics of Asia 55 years after the death of Emile Argand. Eclogae Geol. Helv., 84/3: 599-629.

Burov, E.V., Kogan, M.G., Lyon-Caen, H., Molnar, P., 1990. Gravity anomalies, deep structures, and dynamic processes beneath the Tien-Shan. Earth Planet. Sci. Let., 96: 367-383.

Burtman, V.S., 1961. On the Talasso-Fergana strike-slip fault. Bull. Acad. Sci. USSR Geol. Soc., 12: 37-48.

Burtman, V.S., 1975. Structural geology of the Variscan Tien-Shan. Am. J. Sci., 275A: 157-186.

Burtman, V.S., 1980. Faults of Middle Asia. Am. J. Sci., 280: 725-744.

Burtman, V.S., Molnar, P., 1992. Geological and geophysical evidence for the subduction of continental crust beneath the Pamir. Inter. symp. on the Karakorum and Kunlun mountains, Kashi, China, 30.

Chatelain, J.L., Roecker, S.W., Hatzfield, D., Molnar, P., 1980. Microearthquake seismicity and fault plane solutions in the Hindu-Kush region and their tectonic implications. J. Geophys. Res., 85: 1365-1387.

Chauvin, A., Bazhenov, M.L., Perroud, H., 1992. Low inclinations from Tertiary sediments of Central Asia. EOS, 73: 148.

Chen, Y., 1992. Evolution tectonique le long d'une transversle entre Inde et Sibérie. Thèse de l'Université de Paris VII, 306 pp.

Chen, Y., Cogné, J.P., Courtillot, V., Avouac, J. P., Tapponnier, P., Wang, G., Bai, M., You, H., Li, M., Wei, C., Buffetaut, E. 1991. Paleomagnetic study of Mesozoic continental sediments along the northern Tien-Shan (China) and heterogeneous strain in Central Asia. J. Geophys. Res., 96: 4065-4082.

Chen, Y., Cogné, J.P., Courtillot, V., 1993. New Cretaceous paleomagnetic poles from the Tarim basin, Northwestern China. Earth Planet. Sci. Lett., 114: 17-38.

Cobbold, P.R., Davy, P., 1988. Indentation tectonics in nature and experiment. 2. Central Asia. Bull. Geol. Inst. Univ. Uppsala, 14: 143-162.

Cobbold, P.R. Davy, P., Gapais, D., Rossello, E. A., Sadybakasov, E., Thomas, J. C., Tondji Biyo, J. J., de Urreiztieta, M., 1993. Sedimentary basins and crustal thickenning. Sed. Geol., 86: 77-89.

Cogné, J.P., Rocher, F., Chen, Y., Courtillot, V., 1993. Préliminary paléomagnetic results from the Turfan basin, NW China. Terra abstracts, 5: 256.

Davy, P., Cobbold, P.R., 1988. Indentation tectonics in nature and experiments.1. Experiments scaled for gravity. Bull. Geol. Inst Univ. Uppsala, 14: 129-141.

Davy, P., Sornette, A., Sornette, D., 1990. Some consequences of a proposed fractal nature of continental faulting. Nature, 348: 56-58.

De Mets, C., Gordon, R.G., Argus, D.F., Stein, S., 1990. Current plate motion. Geophys. Jour. Int., 101: 425-478.

Dewey, F.D., Cande, S., Pitman, W.C., 1989. Tectonic evolution of India/Eurasia collision zone. Eclogae Geol. Helv., 82(3): 717-734.

England, P., 1982. Some numerical investigations of large scale continental deformation. In: K. Hsü (Eds), Mountain building processes. Academic, San Diego, Calif., 129-139.

England, P., MCkenzie, D.P., 1982. A thin viscous sheet model for continental deformation. Geophys. J. R. Astron. Soc., 70: 295-321.

England, P., Houseman, G., 1986. Finite strain calculations of continental deformation 2: comparison with India-Eurasia collision zone. J. Geophys. Res., 91: 3664-3676.

England, P., Molnar, P., 1990. Right lateral shear and rotation as an explanation for strike-slip faulting in Eastern Tibet. Nature, 344: 140-142.

Enkin, R.J. Chen, Y., Courtillot, V., Besse, J., Xing, L., Zhang, Z., Zhuang, Z., Zhang, J., 1991. A Cretaceous pole from South China and the Mesozoic hairpin turn of the Eurasian apparent polar wander path. J. Geophys. Res., 96:

Enkin, R.J., Yang, Z., Chen, Y., Courtillot, V., 1992. Paleomagnetic constraints on the geodynamic history of the major blocks of China from the Permian to the Present. J. Geophys. Res., 97: 13953-13989.

Fournier, M., Thomas, J.-C., Jolivet, L., Davy, P., Indentation, gravitational spreading, and subduction-related extension: an analogic approach of continental deformation. in preparation.

Freund, R., 1970. Rotation of strike-slip faults in Sistan, Southeast Iran. Jour. Geology, 78: 188-200.

Funahara, S., Nishiwaki, N., Miki, M., Murata, F., Otofugi, Y., Wang, Y. Z., 1992. Paleomagnetic study of Cretaceous rocks from the Yangtze block, Central Yunnan, China: implications for the India-Asia collision. Earth. Planet. Sci. Lett., 113: 77-91.

Funahara, S., Nishiwaki, N., Murata, F., Otofugi, Y., Wang, Y.Z., 1993. Clockwise rotation of the Red River fault inferred from paleomagnetic study of Cretaceous rocks in the Shan-Thai-Malay block of western Yunnan, China. Earth Planet. Sci. Lett., 117: 29-42.

Garfunkel, Z., 1989. Regional deformation by bloc translation or rotation. In: C. &. L. Kissel C. (Eds), Paleomagnetic rotations and continental deformation. Academic Publishers, 181-208.

Graham, S.A., Hendrix, M.S., Wang, L.B., Caroll, A.R., 1993. Collisional successor basins of western China: impact of inheritance on sand composition. Geol. Soc. Amer. Bull., 105: 323-344.

Gubin, I.E., 1986. The lithosphere of the Tien-Shan (in Russian). Nauka, Moscow, 155 pp.

Hamburger, M.W., Sarewitz, D.R., Pavlis, T.L., Papandopulo, G.A., 1992. Structural and seismic evidence for intracontinental subduction in the Peter The First Range, Central Asia. Geol. Soc. Amer. Bull., 104: 397-408.

Harrison, M.T., Copeland, P., Kidd, W.S.F., Yin, A., 1992. Raising Tibet. Science, 255: 1663-1670.

Hendrix, M.S. Graham, S.A., Caroll, A.R., Sobel, E.R., McKnight, C.L., Schulein, B.J., Wang, Z., 1992. Sedimentary record and climatic implications of recurrent deformation in the Tien-Shan : Evidence from Mesozoic strata of the north Tarim, south Junggar and Turpan basin, northwest China. Geol. Soc. Amer. Bull., 104: 53-79.

Hirn, A. Nercessian, A., Sapin, M., Jobert, G., Xu, J. X., Gao, E. Y., Lu, D. Y., Teng, J. W., 1984. Lhasa block and bordering suture: a continuation of a 500 km Moho traverse through Tibet. Nature, 307: 25-27.

Holt, W.E., Ni, J.F., Wallace, T.C., Haines, A., 1991. The active tectonics of the eastern Himalayan syntaxis and surrounding regions. J. Geophys. Res., 96: 14.595-14.632.

Holt, W.E., Haines, A.J., 1993. Velocity fields in deforming Asia from the inversion of earthquakes-released strains. Tectonics, 12: 1-20.

Houseman, G., England, P., 1986. Finite strain calculations of continental deformation 1. Method and general results for convergent zones. J. Geophys. Res., 91: 3651-3663.

Houseman, G., England, P., 1993. Crustal thickening versus lateral expulsion in the Indian-Asian continental collision. J. Geophys. Res., 98: 12233-12249.

Huang, K., Opdike, N.D., 1992. Paleomagnetism of Cretaceous to Lower Tertiary rocks from southwestern Sichuan: A revisit. Earth. Planet. Sci. Lett., 112: 29-40.

Huang, K., Opdyke, N.D., Peng, X., Li, J., 1992. Paleomagnetism of Cretaceous rocks from Eastern Quiangtang terrane of Tibet. J. Geophys. Res., 97: 1789-1799.

Huang, K., Opdyke, N., 1993. Paleomagnetic results from Cretaceous and Jurassic rocks of South and Southwest Yunnan: evidence for large clockwise rotations in the Indochina and Shan-Tai Malay terranes. Earth Planet. Sci. Lett., 117: 507-524.

Jackson, J., McKenzie, D., 1983. The geometrical evolution of normal fault system. Jour. Struct. Geol., 5: 471-482.

Jolivet, L., Davy, P., Cobbold, P.R., 1990. Right-lateral shear along the Northwest pacific margin and the India-Eurasia collision. Tectonics, 9: 1409-1419.

Kalvoda, J., Leonov, Y.G., Nikonov, A.A., 1987. Main features of the neotectonic evolution of the Pamirs-Thyan-Shan and the Karakorum hymalayas mountain ranges. Acta Montana, 77: 65-84.

Khramov, A.N., Petrova, G.N., Perchesky, D.M., 1981. Paleomagnetism of the Soviet Union. In: M. W. McElhinny (Eds), Paleooreconstruction of the continents. AGU, Washington, D. C, pp. 177-194.

Kidd, W.S.F., Molnar, P., 1988. Quaternary and active faulting observed on the 1985 Academia-Sinica Royal Society Geotraverse of Tibet. Phil. Trans. R. Soc. Lon., A327: 337-363.

Kissel, C., Laj, C., 1988. The Tertiary geodynamical evolution of the Aegean arc: a paleomagnetic reconstruction. Tectonophysics, 146: 183-201.

Kosarev, G.L., Petersen, L.V., Vinnik, L.P., Roecker, S.W., 1993. Receiver fonctions for the Tien Shan analog broadband network: contrasts in the evolution of structures across the Talasso-Fergana fault. J. Geophys. Res., 98: 4437-4448.

Le Pichon, X., Fournier, M., Jolivet, L., 1992. Kinematics, topography, shortening, and extrusion in the India-Eurasia collision. Tectonics, 11: 1085-1098.

Leith, W., 1985. A mid-Mesozoic extension across Central Asia ? Nature, 313: 567-570.

Leith, W., Alvarez, W., 1985. Structure of the Vakhsh fold and thrust belt, Tadjik SSR: geologic mapping on a Landsat image base. Geol. Soc. Amer. Bull., 96: 875-885.

Leith, W., Simpson, D.W., 1986. Seismic domains within the Ghissar-Kokshal seismic zone Soviet Central Asia. J. Geophys. Res., 91: 689-699.

Li, Y., 1990. An apparent polar wander path from the Tarim block, China. Tectonophysics, 181: 31-41.

Li, Y., Zhang, Z. K., McWilliams, M., Sharps, R., Zhai, Y. J., Li, Y. A., Li, Q., Cox, A., 1988. Mesozoic paleomagnetic results of the Tarim craton: Tertiary relative motion between China and Siberia ? Geophys. Res. Lett., 15: 217-220.

Luyendik, B.P., 1991. A model for Neogene crustal rotations, transtension and transpression in southern California. Geol. Soc. Amer. Bull., 103: 1528-1536.

Martinod, J., 1991. Instabilités périodiques de la lithosphère (flambage, boudinage) en compression et en extension. Thèse de l'Université de Rennes, 170 pp.

Mattauer, M., 1986. Les subductions intracontinentales des chaînes tertiaires d'Asie; leurs relations avec les décrochements. Bull. Soc. Geol. Fr., 8: 143-157.

McKenzie, D. ., Jackson, J., 1983. The relationship between strain rates, crustal thickenning, paleomagnetism, finite strain and fault movement within a deformation zone. Earth Planet. Sci. Let., 65: 182-202.

Mercier, J.L., Armijo, R., Tapponnier, P., Carey-Gailhardis, E., Lin, H.T., 1987. Change from late Tertiary compression to Quaternary extension in southern Tibet during the India-Asia collision. Tectonics, 6: 275-304.

Ministry of Geology of the USSR and the Tadjik Academy of Sciences, Geological map of the Tadjikistan, scale 1/500 000, 4 sheets, Dushanbe, 1984.

Molnar, P., 1984. Structure and tectonics of the Himalaya. Constraints and implications of geophysical data. Ann. Rev. Earth. Planet. Sci., 12: 489-518.

Molnar, P., Tapponnier, P., 1975. Cenozoic tectonics of Asia: Effects of a continental collision. Science, 189: 419-426.

Molnar, P., Tapponnier, P., 1977. Relations of the tectonics of Eastern China to the India-Eurasia collison : an application of the slip line field theory to large scale continental tectonics. Geology, 5: 212-216.

Molnar, P., Deng, Q., 1984. Faulting associated with large earthquakes and the average rate of deformation in Central and Eastern Asia. J. Geophys. Res., 89: 6203-6227.

Molnar, P., Lyon-Caen, H., 1988. Some simple physical aspect of the support, structure and the evolution of mountains belts. geol. Soc. Amer. Spec. Pap., 218: 179-207.

Nelson, M.R., McCaffrey, R., Molnar, P., 1987. Source parameters for 11 earthquakes in the Tien-Shan, Central Asia, determined by P and SH waveform inversion. J. Geophys. Res, 92: 12629-12648.

Ni, J., 1978. Contemporary tectonics in the Tien-Shan regions. Earth Planet. Sci. Let., 41: 347-354.

Obukhov, A.N., Shedaldin, B.P., Gorshenin, E.B., Musaev, C.I., Silits, A.M., 1991. A rifting origin for the intermontane basins of the Central Asian orogenic belt (in Russian). Name of journal not known.

Otofuji, Y., Inoue, Y., Funahara, S., Murat, F., Zheng, X., 1990. Paleomagnetic study of eastern Tibet. Deformation of the Three Rivers region. Geophys. J. Int., 103: 85-94.

Patriat, P., Achache, J., 1984. India-Eurasia collision chronology has implication for crustal shortening and driving mechanism of plates. Nature, 311: 615-621.

Pêcher, A., Bouchez, J.L., Le Fort, P., 1991. Miocene dextral shearing between Himalaya and Tibet. Geology, 19: 683-685.

Peive, A.V., Burtman, V.S., Rhuzentsev, S.V., Suvorov, A.I., 1964. Tectonics of the Pamirs Himalayan sector of Asia. Rep. 22nd Sess. Int. Geol. Congr, New Delhi, 441-462.

Peltzer, G., Tapponier, P., 1988. Formation and evolution of strike-slip faults, rifts and basins during the India-Eurasia collision: An experimental approach. J. Geophys. Res., 93: 15085-15117.

Peltzer, G., Tapponnier, P., Armijo, R., 1989. Magnitude of late quaternary left-lateral displacement along the north edge of Tibet. Science, 246: 1285-1289.

Pozzi, J.P., Feinberg, H., 1991. Paleomagnetism in the Tadjikistan: continental shortenning of Eurasian margin in the Pamirs during the Indian-Eurasian collision. Earth planet. Sci. Let., 103: 365-378.

Pruner, P., 1987. Paleomagneitsm and paleogeography of Mongolia in the Cretaceous, Permian and Carboniferous-Preliminary data. Tectonophysics, 139: 155-167.

Roecker, S.W., Soboleva, O.V., Nersesov, I.L., Lukk, A.A., Hatzfeld, D., Chatelain, J.L., Molnar, P., 1980. Seismicity and fault plane solutions of intermediate depth earthquakes in the Pamir Hindu-Kush region. J. Geophys. Res, 85: 1358-1364.

Ron, H., Freund, R., Garfunkel, Z., Nur, A., 1984. Block rotation by strike-slip faulting: structural and paleomagnetic evidence. J. Geophys. Res., 89: 6256-6270.

Sadybakasov, E., 1991. Neotectonics of the High Asia (in Russian). Ilim, Frunze, 117 pp.

Sengör, A.M.C., 1987. Tectonics of the Tethysides: orogenic collage development in a collisional setting. Ann. Rev. Earth. Planet. Sci., 15: 213-244.

Sengör, A.M.C., Natal'in, B.A., Burtman, V.S., 1993. Evolution of the Altaid tectonic collage and Paleozoic crustal Growth in Eurasia. Nature, 364: 229-306.

Sornette, A., Davy, P., Sornette, D., 1993. Fault growth in brittle-ductile experiments and the mechanics of continental collisions. J. Geophys. Res., 98: 12111-12139.

Tapponnier, P., Molnar, P., 1979. Active faulting and cenozoic tectonics of the Tien-Shan, Mongolia and Baïkal region. J. Geophys. Res., 82: 2905-2930.

Tapponnier, P., Peltzer, G., Le Dain, A.Y., Armijo, R., Cobbold, P.R., 1982. Propagating extrusing in Asia: New insights from simple experiments with plasticine. Geology, 10: 611-616.

Tapponnier, P., Mattauer, M., Proust, F., Cassaigneau, C., 1981. Mesozoic ophiolites, sutures and large scale movements in Afghanistan. Earth. Planet. Sci. Let., 52: 355-371.

Tapponnier, P., Peltzer, G., Armijo, R., 1986. On the mechanics of the collision between India and Asia. In: M. P. Coward, A. C. Ries (Eds), Collision tectonics. Geol. Soc. Spec. Pub., pp. 115-157.

Tapponnier, P., Lacassin, R., Leloup, P. H., Schärer, U., Dalai, Z., Haiwei, W., Xiaohan, L., Shaocheng, J., Lianshang, Z., Jiayou, Z., 1990. The Aliao Shan/Red river metamorphic belt: Tertiary left lateral shear between Indochina and south China. Nature, 343: 431-437.

Tapponnier, P., Meyer, B., Avouac, J. P., Peltzer, G., Gaudemer, Y., Shunmin, G., Hongfa, X., Kelun, Y., Zhitai, C., Shuahua, C., Huagang, D., 1990. Active thrusting and folding in the Quilian Shan and decoupling between between upper crust and mantle in northwestern Tibet. Earth Planet. Sci. Lett., 97: 382-403.

Tapponnier, P., Armijo, R., Avouac, J.P., Liu, Q., 1992. Subuction, Crustal folding, and slip partitioning along the edges of the Tibet. Inter. symp. on the Karakorum and Kunlun mountains, Kashi, China, 8.

Taymaz, T., Jackson, J., McKenzie, D., 1991. Active tectonics of the north and central Aegean sea. Geophys. J. Int., 106: 433-490.

Thomas, J.C., Perroud, H., Cobbold, P.R., Bazhenov, M.L., Burtman, V.S., Chauvin, A., Sadybakasov, E., 1993. A paleomagnetic study of Tertiary formation of the Kirghiz Tien-Shan and its tectonic implications. J. Geophys. Res., 98: 9571-9589.

Tondji Biyo, J.J., 1993. Chevauchements et bassins compressifs. Infleunce de la sédimentation et de l'érosion. Modélisation analogique et exemples naturels. Thèse de l'Université de Rennes.

Trifonov, V.G., 1978. Late Quaternary movements of western and central Asia. Geol. Soc. Amer. Bull., 89: 1059-1072.

Trifonov, V.G., 1987. Map of active faults of the U.S.S.R and adjacent areas. scale 1:8,000,000. Explanatory notes. Acad. Sci. U.S.S.R., Moscow, 48 pp.

Trifonov, V.G., Makarov, V.I., Skobelev, S.F., 1992. The Talas-Fergana active right-lateral fault. Annales Tectonicae, Supplement to vol. VI: 224-237.

Vilotte, J.P., Daignaires, M., Madariaga, R., 1982. Numerical modelling of intraplate deformation: simple mechanical modes of continental collision. J. Geophys. Res., 87: 10709-10728.

Vinnik, L.P., Lukk, A.A., Neresov, I.L., 1977. Nature of the intermediate-depth seismic zone in the mantle of Pamirs-Hindu-Kush. Tectonophysics, 38: T9-T14.

Vinnik, L.P., Saipbekova, M., 1984. Structure of the lithosphere and the asthenosphere of the Tien-Shan. Ann. Geophys., 2: 621-626.

Wallace, R.E., 1976. The Talas-Fergana fault, Kirghizia and Kasakhstan. Earthquake info. Bull., 8: 4-13.

Willis, B., 1928. Dead sea problem: rift valley or ramp valley? Geol. Soc. Amer. Bull., 39: 490-542.

Windley, B.F., B., A.M., Zhang, C., Zhao, Z.Y., Wang, G.R., 1990. Paleozoic accretion and cenozoic redeformation of the Chinese Tien-Shan range, Central Asia. Geology, 18: 128-131.

Windley, B.F., Allen, M.B., 1993. Mongolian plateau: evidence for a late Cenozoic mantle plume under Central Asia. Geology, 21: 295-298.

Yang , Z., Besse, J., 1993. Paleomagnetic study of Permian and Mesozoic sedimentary rocks from Northern Thailand supports the extrusion model for Indochina. Earth. Planet. Sci. Lett., 117: 525-552.

Zakharov, S.A., 1958. Stratostructures of Mesozoic and Cenozoic rocks in the Tadjik basin. Geol. Inst. Tadjikistan. Sci. Acad, Dushanbe, 228 pp.

Zhao, W.L., J., M., 1985. Uplift of Tibetan plateau. Tectonics, 4: 359-369.

Zhao, X., Coe, R.S., Zhou, Y., Wu, H., Wang, J., 1990. New paleomagnetic results from northern China: collision and suturing with Siberia and Kazakhstan. Tectonophysics, 181: 43-81.

Zhu, Z.W., Hao, T., Zhao, H., 1988. Paleomagnetic study on the tectonic motion of Pan-Xi block and adjacent area during the Yinzhi-Yanshan period. Acta Geophys. Sin., 31: 420-431.

Zonenshain, L.P., Kuzmin, M., Natapov, L.M., 1990. Geology of the USSR: a plate-tectonic synthesis. Geodynamics Series, Page B.M. (Eds), AGU, Washington, 21, 242 pp.

ANNEXE I

Anomalie d'inclinaison magnétique dans les sédiments Tertiaires de Kirghizie et du Tadjikistan

1. Introduction

Les études paléomagnétiques effectuées sur les sédiments Tertiaires de la dépression Tadjik et du Tien Shan Kirghiz (chapitres II et III) montrent une importante anomalie d'inclinaison magnétique par rapport aux courbes apparentes de dérive du pôle (CDAP). L'inclinaison mesurée est systématiquement plus faible de 20° à 30° par rapport à l'inclinaison attendue d'après les CDAP. A l'opposé, les inclinaisons mesurées sur les sédiments Crétacés sont en très bon accord avec les CDAP, que ce soit dans la dépression Tadjik (annexe 2) ou dans le bassin de Fergana dans le Tien Shan (Bazhenov, 1993).

Dans les régions de déformation à grande échelle telle l'Asie, une différence entre l'inclinaison magnétique théorique et l'inclinaison magnétique mesurée est classiquement reliée à un déplacement en latitude. Cependant, l'anomalie d'inclinaison Tertiaire observée est difficilement compatible avec les reconstructions paléogéographiques (Enkin et al., 1992; Chen et al., 1992).

D'autres mécanismes peuvent également contribuer à modifier l'inclinaison magnétique tels, un comportement anormal du champ magnétique terrestre ou, à plus petite échelle, la compaction, la déformation ou les processus d'acquisition de l'aimantation.

Une anomalie d'inclinaison Tertiaire de cette ampleur, par sa valeur et son extension géographique, soulève plusieurs interrogations:

- Quelle est la validité des différentes CDAP proposées pour l'Eurasie au Tertiaire ?
- Quelle est l'extension géographique et temporelle de cette erreur d'inclinaison ?
- Quels sont les différents processus susceptibles d'entraîner une erreur d'inclinaison dans les sédiments ?
- Quelle est l'influence de ces processus sur la déclinaison magnétique ?

La discussion de ce "problème de l'anomalie d'inclinaison" apparaît fondamentale. En effet, des questions soulevées précédemment, dépend la validité des interprétations tectoniques et paléogéographiques issues des données paléomagnétiques.

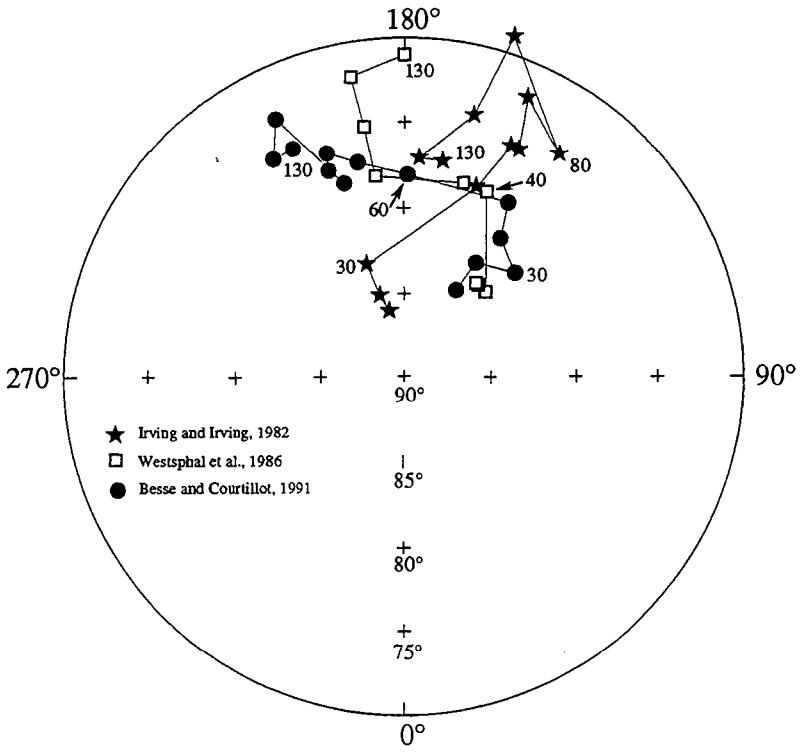

Figure A1. 1. Courbes de dérive apparente du pôle pour l'Eurasie pendant le Crétacé et le Tertiaire. Chaque point représente 10 Ma.

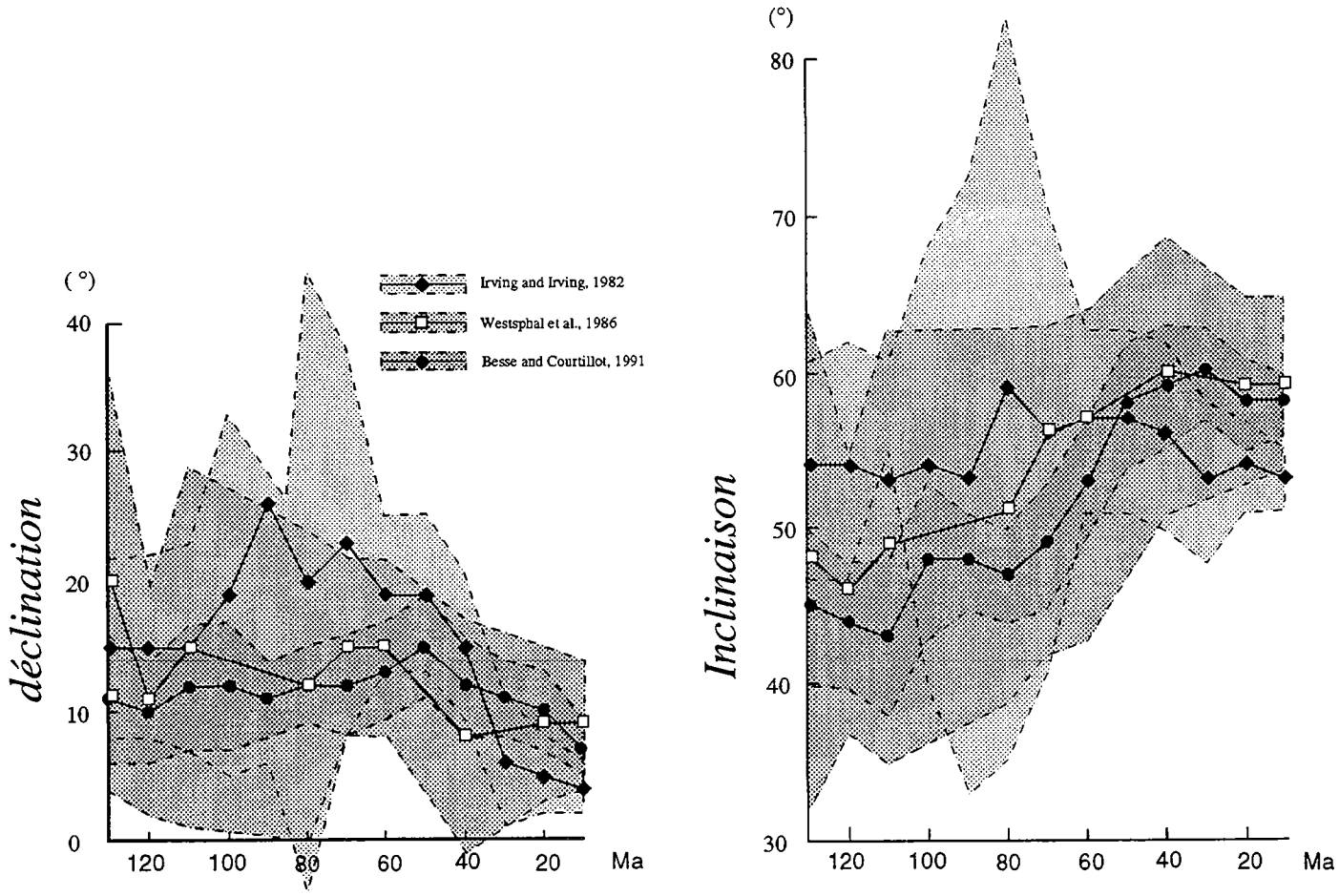

Figure A1.2. Evolution de la déclinaison et de l'inclinaison en fonction du temps, calculée à partir des différents CDAP, pour un point situé à 38°N, 69°E.

2. Données de référence pour le continent Eurasiatique

Les CDAP actuellement proposées pour le Mésozoïque et le Cénozoïque de l'Eurasie sont représentées sur la figure A1.1 (Irving et Irving, 1982; Westphal et al., 1986; Besse et Courtillot, 1991). Toutes considèrent a priori l'Eurasie comme un bloc rigide dans son ensemble depuis le Jurassique. La courbe calculée par Irving et Irving (1982) présente des variations notables par rapport aux deux autres. Ceci est du aux différences dans les jeux de données qui ont permis d'établir les CDAP.

La CDAP proposée par Irving et Irving (1982) est établie à partir de pôles répartis sur toute la plate-forme Eurasiatique. De ce fait, les auteurs ont introduit des données de la CEI qui sont souvent de faible qualité et obtenues à partir des désaimantations partielles (cf. base de données paléomagnétiques de McElhinny et Lock, 1990). Elles sont par ailleurs parfois localisées dans des zones où la déformation Tertiaire est importante, telles le Tien Shan, la dépression Tadjik ou le Caucase (≈15% du jeu de données). Westphal et al., (1986) et Besse et Courtillot (1991) ont respectivement proposé une CDAP établie exclusivement sur des pôles paléomagnétiques d'Eurasie stable (non déformée). En raison d'une sélection plus rigoureuse sur la qualité, les données Tertiaires sont situées en Europe occidentale (France, Allemagne, Royaume-Uni). Besse et Courtillot (1991) ont par ailleurs transféré dans un système de référence commun les CDAP calculées pour chacun des continents (Eurasie, Afrique, Amérique du Nord, Inde). La bonne corrélation entre les différentes courbes leur permet de proposer une CDAP synthétique avec un faible intrevalle de confiance. Deux remarques peuvent être faites au vus des CDAP de Westphal et al., (1986) et Besse et Courtillot (1991). Les pôles d'âge Oligocène et Miocène Supérieur sont établis sur très peu de données ; ceci est une conséquence directe de la sélection plus exigeante des données. De plus, l'hypothèse a priori d'une Eurasie rigide dans son ensemble ne tient pas compte d'un éventuel déplacement relatif Tertiaire entre l'Europe et l'Asie (ou une partie de l'Asie).

L'évolution, depuis le Crétacé, de l'inclinaison et de la déclinaison magnétique, calculée à partir des CDAP pour un point situé arbitrairement à 38°N et 69°E est représentée sur la figure A1.2. Les différences importantes entre les trois courbes soulignent l'importance du choix de la référence et ses conséquences lors des interprétations paléogéographiques ou tectoniques.

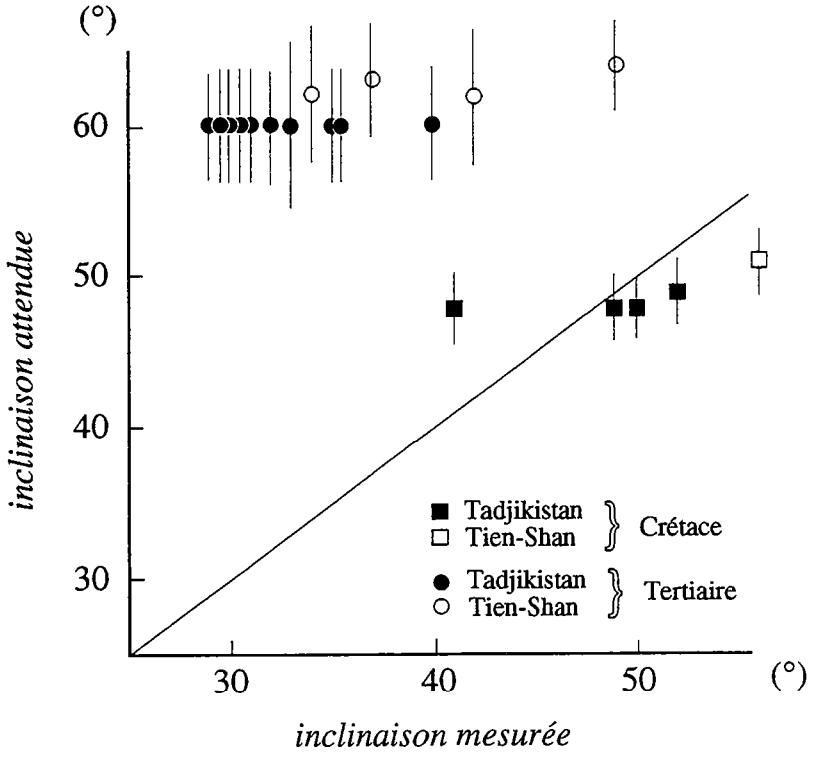

Figure A1.3. Représentation de l'inclinaison mesurée, en fonction de l'inclinaison attendue à partir de la CDAP de Besse et Courtillot (1991).

L'adéquation parfaite entre la référence et la mesure est représentée par la droite de pente 1.

A l'heure actuelle, la CDAP de Besse et Courtillot semble la mieux contrainte, tant par le choix des données que par les faibles incertitudes sur les pôles synthétiques. Il est probable que de nouvelles données provenant du Craton sibérien permettront de préciser cette CDAP sans pour autant la remettre fondamentalement en cause.

3. Inclinaison magnétique Tertiaire en Asie Centrale

Peu d'études paléomagnétiques ont été effectuées sur les formations Cénozoïques d'Asie Centrale en comparaison du nombre maintenant substantiel de données d'âge Mésozoïque (voir Huang et Opdyke, 1993 pour une revue des données Mésozoïques). Grâce au projet de base de données paléomagnetique (McElhinny et Lock, 1990), de nombreuses études réalisées en CEI sont maintenant accessibles. Cependant, leur faible qualité ne permet que rarement de les prendre en compte.

Je présente ici de façon sommaire les études paléomagnétiques effectuées sur des formations Tertiaires en Asie Centrale et dans les régions avoisinantes. Seules sont exposées les données de qualité et bien documentées.

3.1. Données dans les zones déformées

Kirghizie et Tadjikistan (Chapitres II et III). La figure A1.3 illustre l'anomalie d'inclinaison observée sur les sédiments Tertiaires qui ont été prélevés en Kirghizie et au Tadjikistan. Les données de Bazhenov et Burtman (1986) sur la dépression Tadjik sont également reportées. A titre de comparaison, j'ai représenté les inclinaisons mesurées dans les sédiments Crétacés de la dépression Tadjik (cf. annexe) et du bassin de Fergana (Bazhenov, 1993). L'anomalie d'inclinaison moyenne Tertiaire est de 21° dans le Tien Shan et 27° dans la dépression Tadjik tandis que les inclinaisons Crétacées sont en bon accord avec la CDAP. Le faciès sédimentaire des séries Crétacées diffère sensiblement de celui des séries Tertiaires. Les grès Crétacés présentent une couleur rouge pourpre et un grain moyen à fin. L'aimantation rémanente naturelle (ARN) est portée principalement par de l'hématite. Les grès Tertiaires sont généralement brun clair à rose avec un grain moyen à grossier. L'ARN est portée en diverses proportions par de la magnétite et de l'hématite.

Pakistan. Des séries Tertiaires ont été échantillonées dans la Salt Range, située dans la syntaxe Ouest-Himalayenne, au sud de la zone de suture Tertiaire entre l'Inde et l'Asie. Les sédiments calcaires d'âge Paléocène

(Klootwijk et al., 1986) présentent une inclinaison impliquant une paléolatitude proche de l'équateur, en bon accord avec la position de l'Inde à cette époque. Des grès rouges Mio-Pliocène ont également fourni une inclinaison très homogène de 35° (Opdyke et al., 1982, Tauxe et Opdyke, 1982). A l'inverse, la paléolatitude déduite, de 19°N, est bien plus faible que celle prédite de 29°N, proche de la position actuelle. Cette anomalie d'inclinaison de près de 20° dans les sédiments tertiaires est interprétée par les auteurs comme étant due a la compaction.

Chine du Sud-Ouest. Des grès rouges Crétacés et Paléogènes (Paléocène et Eocène) du sud-ouest de la province de Sichuan, à l'Est du Tibet, ont été échantillonnés (Huang et Opdyke, 1992). Alors que les inclinaisons d'âge Crétacé sont en accord avec la CDAP, les directions mesurées sur les grès rouges Tertiaires présentent une anomalie de faible inclinaison de près de 40°!

Chine du Nord. Deux études ont été réalisées en Chine du Nord sur des basaltes Miocènes de Mongolie Centrale (Zhao et al., 1990; Zheng et al., 1991). Dans les deux cas, les tests du pli sont positifs et la variation séculaire du champ magnétique est moyennée de façon satisfaisante. Zheng et al. (1991) proposent un pôle moyen pour la région, calculé à partir des deux études. Ce pôle est en très bon accord avec la référence de Besse et Courtillot (1991). La différence entre l'inclinaison mesurée et l'inclinaison attendue n'est pas significative.

Tibet. Dans le bloc de Lhassa du Sud-Tibet, des séries volcaniques Paléogène (60-45 Ma) ont été échantillonnées conjointement à des séries rouges Crétacées moyen (Achache et al. 1984). Les deux formations présentent des paléolatitudes très homogènes, de l'ordre de 13°N. Ceci implique un raccourcissement N-S Tertiaire de 2000±800 km au nord du bloc de Lhassa ce qui, compte tenu de la marge d'erreur, est en accord avec les données tectoniques (Dewey et al., 1989).

Iran. Les études paléomagnétiques effectuées en Iran ont été principalement réalisées sur des formations plutoniques et volcano-sédimentaires d'âge Eocène (Soffel et Forster, 1980; Conrad et al., 1981; Bina et al., 1986). Le nombre d'échantillons mesuré par localité est relativement faible. L'inclinaison magnétique observée est en général proche de celle attendue.

3.2. Nouvelles données sur la plate-forme stable de Turan

Afin de quantifier l'effet de la tectonique régionale et d'un éventuel déplacement en latitude sur l'anomalie d'inclinaison, nous avons échantillonné des sédiments Tertiaires, situés sur la bordure ouest de la chaîne du Sud-Ouest Ghissar, près de la ville de Dekhanabad (Chauvin et al., 1992) (Figure 1 p. 130).

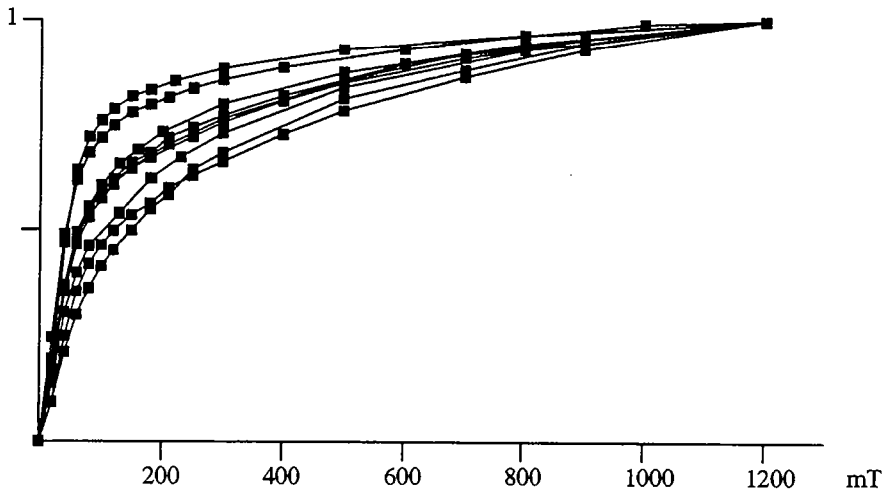

Figure A1.4. Courbes d'ARI normalisées, représentatives de la localité de Derkhanabad.

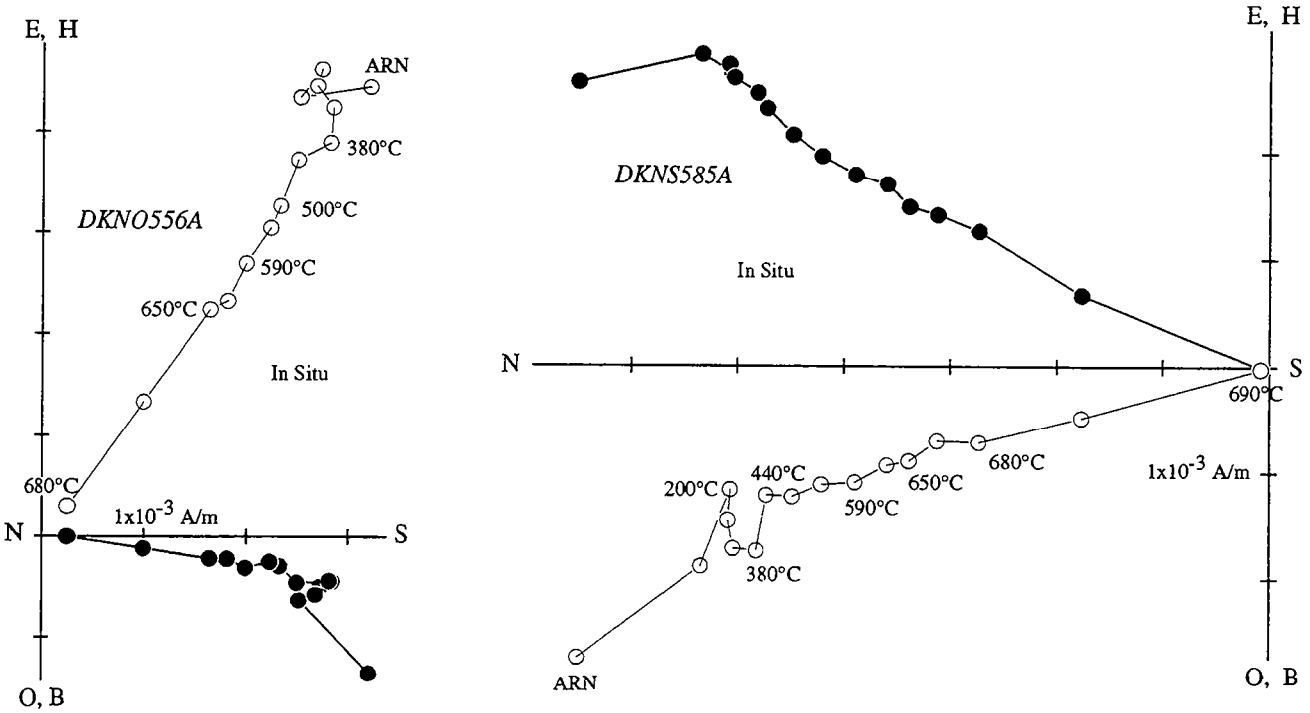

Figure A1. 5. Diagrammes orthogonaux représentatifs de la localité de Derkhanabad

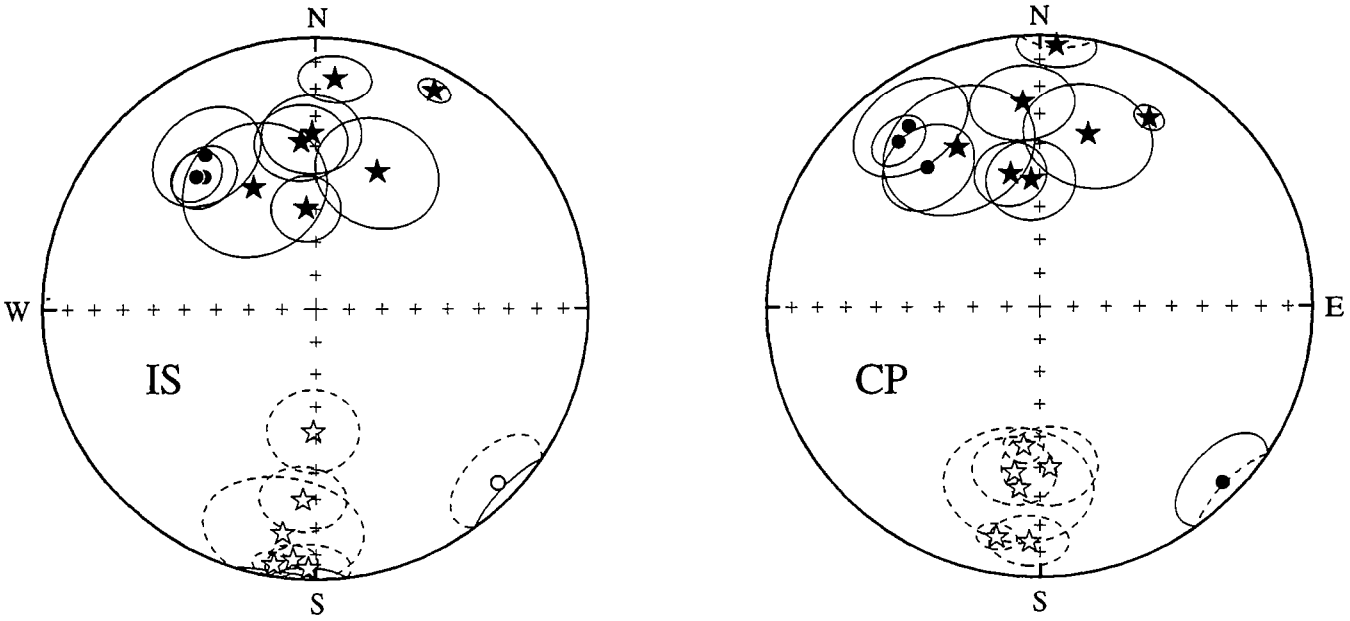

Figure A1.6. Projection de Schmitt des directions moyennées par sites pour la localité de Dekhanabad.
Les étoiles correspondent aux sites utilisés pour le calcul de la direction moyenne; les cercles noirs sont les sites présentant des directions de transition (coordonnées IS : in situ, CP : correction de pendage).

Cette zone constitue l'extrémité sud-ouest du Tien Shan et sépare la dépression Tadjik de la plate-forme de Turan. La direction mesurée dans des sédiments Crétacés de la partie centrale de la chaîne est en très bon accord avec la CDAP, ce qui confirme que cette région peut-être considérée comme un référence paléomagnétique locale Crétacé-Tertiaire.

19 sites ont été échantillonnés sur les deux flancs d'un synclinal où les pendages n'excèdent pas 20°. Les séries échantillonnées sont d'âge Oligo-Miocène et sont constituées de sédiments rouges silteux à grains moyen à fin. Les courbes d'aimantation rémanente isotherme (ARI) suggèrent que l'aimantation rémanente naturelle est portée par de la magnétite et de l'hématite (Figure A1.4). Les désaimantations thermiques des échantillons montrent en général la présence d'une composante unique d'aimantation (Figure A1.5). Cette composante est progressivement éliminée entre 200°C et 680°C. Un site (DKNQ) n' a pas fourni de désaimantation stable au dessus de 300°C. Les autres présentent une direction moyenne souvent bien définie ainsi que les deux polarités du champ magnétique (Figure A1.6). Malgré une faible correction de pendage, le test du pli est positif (McFadden et Jones, 1981), ainsi que le test de renversement. La direction moyenne obtenue après correction de pendage est : D=3°, I=30°, k=19, a_{95}=9°.

On remarquera que la dispersion des sites est relativement importante. Quatre sites présentant des directions de transition n'ont d'ailleurs pas été inclus dans le calcul de la direction moyenne. En général, un site correspond à un banc sédimentaire de la séquence stratigraphique. La dispersion des directions par site peut donc être attribuée à une acquisition rapide de l'aimantation ($<10^{-2}$ ans) où la variation séculaire du champ magnétique n'est pas parfaitement moyennée. Ceci est en faveur d'une aimantation d'origine détritique.

La direction obtenue ne présente pas de différence significative de déclinaison par rapport à la CDAP de Besse et Courtillot (1991). A l'opposé l'inclinaison mesurée est de 29°±8° plus faible que celle attendue.

Cette différence est du même ordre de grandeur que dans la dépression Tadjik. Le raccourcissement Tertiaire, accumulé dans la plate forme de Turan et le bloc Kasakh, est au maximum de l'ordre de la centaine de kilomètres. Il permet donc de ne prendre en compte qu'une très faible part de l'erreur d'inclinaison.

A partir des quelques données présentées ci-dessus, nous pouvons faire trois constatations :

- Une importante anomalie d'inclinaison, souvent incompatible avec la tectonique, peut être observée sur des sédiments Tertiaires d'Asie Centrale.

- Cette anomalie est observée sur des sédiments d'âge Paléogène et Néogène.

- Cette anomalie n'est pas observée sur les basaltes Miocènes de la Chine du Nord, du bloc de Lhassa et sur les formations plutoniques Eocène d'Iran.

On ne peut donc conclure à un caractère systématique de l'anomalie d'inclinaison en Asie Centrale, pendant le Paléogène ou le Néogène. Il faut cependant se garder de toute généralisation, le nombre de données étant faible.

4. Processus susceptibles d'entraîner une anomalie d'inclinaison

Nous entrons là dans un domaine où peu de réponses peuvent être apportées car il reste encore de nombreuses inconnues quand à la compréhension, de l'erreur d'inclinaison dans les sédiments (Butler, 1992, p.187), et des processus d'acquisition d'aimantation dans les grès rouge (Butler, 1992, p.202). Notre but n'est donc pas de faire une revue exhaustive mais plutôt de présenter des alternatives.

Je séparerai ici les processus "externes", agissant à grande échelle (tectonique de plaques, champ non dipôle...), des processus "internes" entraînant une erreur d'inclinaison (compaction, déformation...).

4.1. Processus externes

D'ores et déjà, il a été montré que l'anomalie d'inclinaison observée en Kirghizie et au Tadjikistan est indépendante d'un déplacement latitudinal de blocs par rapport à l'Eurasie stable.

Un champ magnétique terrestre non dipôle peut avoir une influence sur l'inclinaison magnétique (Schneider et Kent, 1990). Une erreur d'inclinaison de 20° nécessiterait une anomalie très développée, en intensité, dans l'espace (à l'échelle de l'Asie Centrale), et surtout dans le temps (pendant tout le Tertiaire). Cette anomalie devrait par ailleurs n'influer que sur la composante verticale de l'aimantation, les déclinaisons mesurées sur les zones stables (cf. Dekhanabad) étant cohérentes vis a vis de la CDAP. Une telle hypothèse semble improbable (Westphal, 1993).

A partir d'une compilation de données Paléogènes, sur la zone de déformation Alpine Eurasiatique, Westphal (1993) montre l'existence d'une anomalie d'inclinaison à l'échelle de l'Eurasie qu'il explique par la présence d'un champ magnétique terrestre dipôle mais non axial à l'Eocène. Les données paléomagnétiques actuellement disponibles semblent cependant difficilement supporter une telle hypothèse, pour les raisons suivantes :

- Les données sélectionnées par Westphal (1993) ne sont pas toujours clairement contraintes en âge (Ibérie, Italie, dépression Tadjik) ou en qualité (Afghanistan). De plus, le choix des données est parfois orienté vers celles qui présentent effectivement une erreur d'inclinaison (Iran).
- Le nouveau pôle proposé pour l'Eocène n'est pas compatible avec les données de l'Europe stable, en particulier celles de la British Tertiary Igneous Province (Ada-Hall et al., 1972; Wilson et al., 1972; Wilson et al., 1974; Hall et al., 1977). Il faudrait donc envisager, selon Westphal (1993), une oscillation du Champ magnétique pendant l'Eocène, entre une position stable axiale et une position inclinée à 18° par rapport à l'axe de rotation de la terre.
- Les données paléomagnétiques Tertiaires sur la dépression Tadjik présentées dans ce mémoire sont d'âge Miocène inférieur. L'anomalie d'inclinaison y étant observée, le comportement anormal du champ magnétique s'étendrait sur un période d'au moins 45 Ma, ce qui semble improbable.
- Enfin, un tel comportement du champ magnétique devrait être visible sur les données paléomagnétiques acquises dans d'autres parties du globe (Amérique du Nord en particulier) ce qui n'a pas été vérifié jusqu'à maintenant (voir par exemple Besse et Courtillot, 1991).

L'origine géomagnétique de l'anomalie d'inclinaison semble donc peu probable. Les séries volcaniques de Chine du Nord, du bloc de Lhassa et d'Iran qui ne présentent pas d'anomalie d'inclinaison constituent un argument dans ce sens.

4.2. Processus internes

Les processus internes agissant sur l'erreur d'inclinaison magnétique sont étroitement liés aux caractéristiques des porteurs magnétiques et au mode d'acquisition de l'aimantation.

Erreur d'inclinaison d'origine détritique. Dans le cas d'une aimantation d'origine détritique, des expériences de redéposition (King et Rees, 1966; Tauxe et Kent, 1984) ont montré une relation entre l'inclinaison du champ magnétique

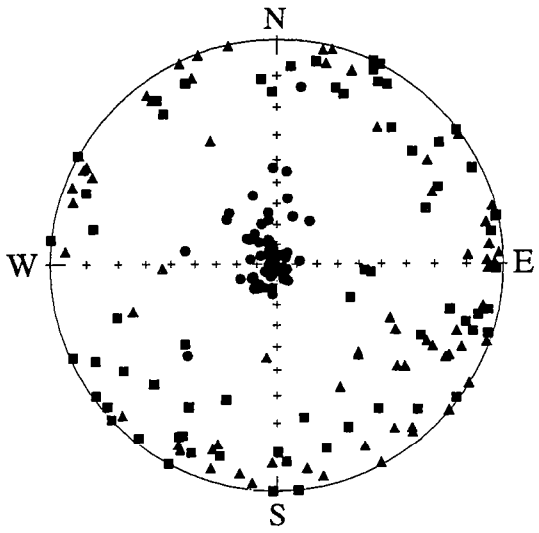

Dekhanabad

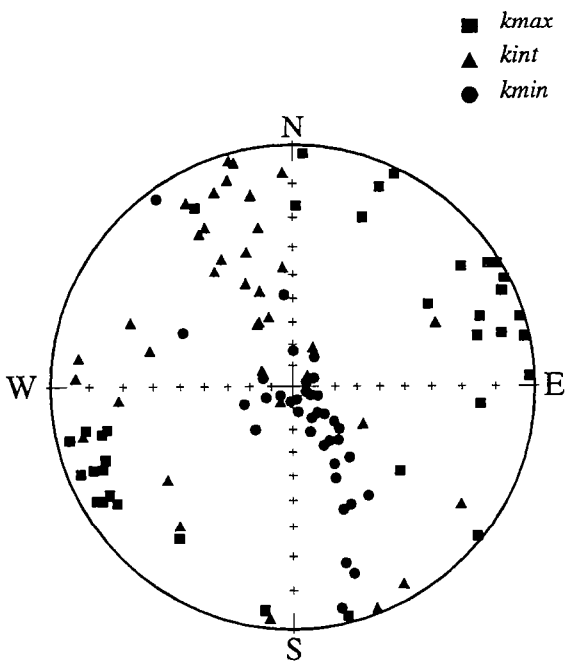

Bassin d'Issyk-Kul, Kirghizie

Figure A1.7. Tenseur d'ASM .
Représentation stéréographique en coordonées stratigraphiques

au moment du dépôt (I_H) et l'inclinaison mesurée (I_O) de type: $\tan(I_O)=f\tan(I_H)$. La valeur du facteur f dépend principalement de la nature du sédiment et des particules magnétiques. Pour des sédiments naturels de type grès rouges où l'hématite est le porteur de l'aimantation, Tauxe et Kent (1984) observent un f=0.55. Ainsi, pour un champ I_H=55°, l'erreur d'inclinaison est de l'ordre de 17°. Bien que l'aimantation dans les grès rouges soit plutôt considérée comme d'origine chimique (Butler, 1992), la contribution de l'hématite d'origine détritique sur l'ARN est toujours discutée (Turner, 1979; Butler, 1992). Des sections polies des grès rouges du Tadjikistan montrent une minéralogie composée de grains de quartz, d'une matrice rose contenant de l'hématite pigmentaire d'origine chimique, et, en faible proportion, de grains d'hématite spéculaire d'origine probablement détritique. Si cette hématite spéculaire porte une part de l'ARN, cela peut contribuer à diminuer significativement l'inclinaison magnétique. On notera qu'à Dekhanabad où l'anomalie d'inclinaison est également observée, l'origine détritique de l'hématite porteuse de l'aimantation est suggérée par la dispersion des directions moyennes des sites (cf. paragraphe précédent).

Déformation. La déformation pénétrative peut entraîner une erreur d'inclinaison. La mesure de l'anisotropie de susceptibilité magnétique (ASM) permet de tester l'influence de la déformation sur l'aimantation (Hrouda, 1981; Cogné, 1987). Le tenseur de susceptibilité magnétique mesuré dans les échantillons de Kirghizie et de Dekhanabad présente un axe minimum (k1) vertical, probablement lié à la compaction (Figure A1.7). Le facteur d'anisotropie (k3/k1) ne dépasse cependant généralement pas 5% ce qui est insuffisant pour entraîner une déviation significative de l'aimantation (Nagata, 1961).

Compaction. De nombreuses études ont été réalisées afin de tester l'influence de la compaction sur l'inclinaison magnétique (King, 1955; Griffiths et al., 1960; Blow and Hamilton, 1978; Anson and Kodama, 1987; Arason et Levi, 1990b). En règle générale, il est convenu que plus le sédiment est fin, plus la compaction est importante et plus la rotation des particules magnétiques est favorisée vers une inclinaison plus faible. Par ailleurs, la compaction croît avec la proportion de minéraux argileux (Füchtbauer, 1974 ; Figure A1.8). Des erreurs d'inclinaison de 10 à 15°, liées à la compaction, ont été mises en évidences sur des sédiments profonds du Nord-Ouest Pacifique (Arason et Levi, 1990a). Dans les séries rouges continentales, la compaction, bien que probablement significative (Turner, 1980) est difficile à évaluer. Füchtbauer (1974) présente

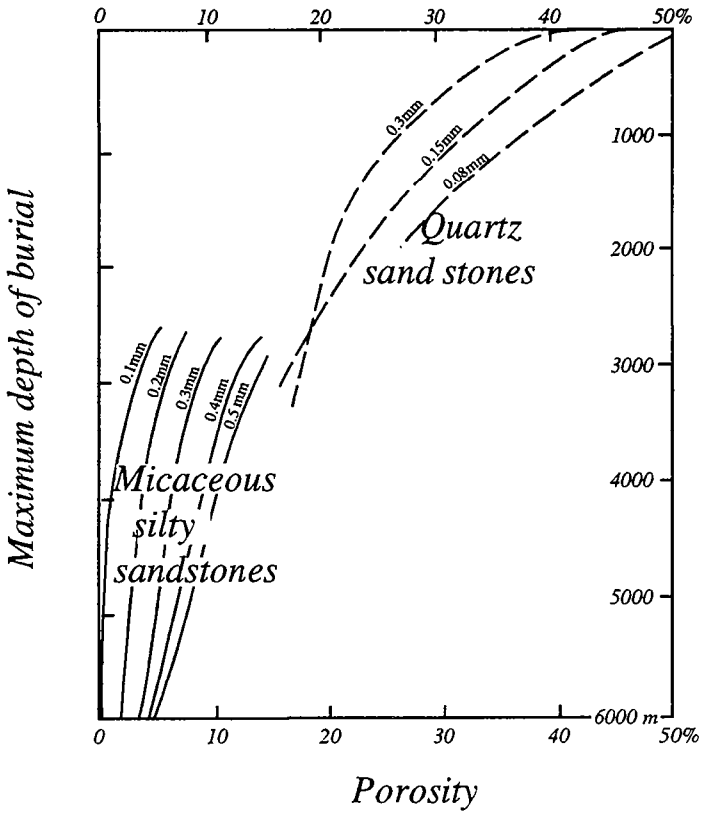

Figure A1.8. Evolution de la porosité dans les grès en fonction de l'enfouissement pour différentes tailles de grains et proportions de minéraux argileux (d'après Füchtbauer, 1974).

des résultats sur des sédiments gréseux, naturels, et compactés en laboratoire (Figure A1.8).

Une porosité initiale de 50% pour un sédiment non compacté devient inférieure à 20% après un enfouissement à 3000m de profondeur (ou équivalent). En section polie, certains échantillons du Tadjikistan présentent des grains jointifs et très peu de matrice, indice d'une compaction significative. La profondeur maximale des séries Miocènes dans la dépression Tadjik est de l'ordre de 4 à 5 km. La compaction est donc probablement significative et peut avoir une influence non négligeable sur l'inclinaison magnétique.

Les trois processus discutés ci-dessus sont ceux qui peuvent avoir l'influence la plus importante sur l'inclinaison. Néanmoins, d'autres mécanismes, moins significatifs, peuvent être également invoqués :

- Arason et Levi (1990b) montrent que, lors de la compaction, la dispersion de l'alignement des particules peut accroître l'erreur d'inclinaison. Les sédiments Tertiaires du Tien Shan et du Tadjikistan présentent une dispersion intra-site des directions magnétiques souvent significative, qui peut être représentative d'une dispersion interne des particules magnétiques porteuses de l'aimantation.

Une mauvaise séparation des composantes, dans le cas d'une composante de basse température proche du champ actuel, aura également tendance à diminuer les inclinaisons de polarité inverse.

- la plupart des processus internes agissent à différentes étapes de l'évolution du sédiment sans qu'il soit possible de proposer une chronologie. Mis à part le rôle joué par la déformation, tous ces processus jouent dans le même sens et peuvent, en s'accumulant, contribuer à diminuer significativement l'inclinaison magnétique.

Dans le cas des sédiments de Kirghizie et du Tadjikistan, les processus décrit précédemment n'ont a priori pas (ou peu) d'influence sur la déclinaison magnétique mesurée. En effet, les rotations mesurées dans les sédiments Crétacés de la dépression Tadjik sont en très bon accord avec celles mesurées dans les séries Tertiaires en utilisant la référence de Dekhanabad (cf. chapitre III). L'utilisation de la déclinaison dans le cadre d'une interprétation tectonique est donc possible

En résumé, l'origine "interne" de l'anomalie d'inclinaison (processus de dépôt et/ou postérieur au dépôt), observée sur les sédiments de Kirghizie et du Tadjikistan, me semble la plus probable. De nouvelles données sur des séries volcaniques Tertiaires sont cependant nécessaires pour le confirmer.

Une étude détaillée, **au cas par cas**, apparaît indispensable pour caractériser l'anomalie d'inclinaison dans les grès rouges. Ceci implique:

- une détermination précise de la minéralogie magnétique et de son origine.
- la quantification de la contribution de chaque phase magnétique sur l'ARN.
- la caractérisation et la quantification de la compaction.

Bibliographie

Achache, J., Courtillot, V., Zhou, X.Y., 1984. Paleogegraphic and tectonic evolution of southern Tibet since middle Cretaceous time: New paleomagnetic data and synthesis. J. Geophys. Res., 89: 10311-10339.

Ade-Hall, J.M., Dagley, P., Wilson, R.L., Evans, A., Riding, A., Smith, P.J., Skelhorne, R., Sloan, T., 1972. A paleomagnetic study of the Mull regional dyke swarm. Geophys. J. R. Astron. Soc., 27: 517-545.

Anson, G.L., Kodama, K.P., 1987. Compaction-induced shallowng of the post-depositional remanent magnetization in a synthetic sediment. Geophys. J. R. Astron. Soc., 88: 673-692.

Arason, P., Levi, S., 1990a. Compaction and inclination shallowing in deep-sea sediments from the Pacific ocean. J. Geophys. Res., 95: 4501-4510.

Arason, P., Levi, S., 1990b. Models of inclination shallowing during sediment compaction. J. Geophys. Res., 95: 4481-4499.

Bazhenov, M.L., 1993. Cretaceous paleomagnetism of the Fergana basin and adjacent ranges: tectonic implications. Tectonophysics, 221:

Bazhenov, M.L., Burtman, V.S., 1986. Tectonics and paleomagnetism of structural arcs of the Pamir-Punjab syntaxis. J. Geodyn., 5: 383-396.

Besse, J., Courtillot, V., 1991. Revised and synthetic apparent polar wander paths of the African, Eurasian, North American and Indian plates, and true polar wander paths since 200 Ma. J. Geophys. Res., 96: 4029-4050.

Bina, M.M., Bucur, I., Prevot, M., Meyerfeld, Y., Daly, L., Cantagrel, J.M., Mergoil, J., 1986. Paleomagnetism, petrology and geochronology of tertiary magmatic and sedimentary units from Iran. Tectonophysics, 121: 303-329.

Blow, R.A., Hamilton, N., 1978. Effect of compaction of a detrital remanent of magnetization in fine grained sediments. Gephys. J. Roy. Astron. Soc., 52: 13-23.

Butler, R.F., 1992. Paleomagnetism. Blackwell, Cambridge, 319 pp.

Chauvin, A., Bazhenov, M.L., Perroud, H., 1992. Low inclinations from Tertiary sediments of Central Asia. EOS, 73: 148.

Chen, Y., 1992. Evolution tectonique le long d'une transversle entre Inde et Sibérie. Thèse de l'Université Paris VII. 245 pp.

Cogné, J.P., 1987. Contribution à l'étude paléomagnétique des roches déformées. Mem. Doc. Caess 17, Rennes, 204 pp.

Conrad, G., Montigny, R., Thuizat, R., Westphal, M., 1981. Tertiary and Quaternary geodynamics of southern Lut (Iran) as deduced from paleomagnetic, isotopic and structural data. Tectonophysics, 75: T11-T17.

Dewey, F.D., Cande, S., Pitman, W.C., 1989. Tectonic evolution of India/Eurasia collision zone. Eclogae Geol. Helv., 82(3): 717-734.

Enkin, R.J., Yang, Z., Chen, Y., Courtillot, V., 1992. Paleomagnetic constraints on the geodynamic history of the major blocks of China from the Permian to the Present. J. Geophys. Res., 97: 13953-13989.

Füchtbauer, H., 1974. Sediments and sedimentary rocks 1. Halsted Press Div., Stuttgart, 464 pp.

Griffiths, D.H., King, R.F., Rees, A.I., Wright, A.E., 1960. Remanent magnetization of some recent varved sediments. Proc. R. Soc. London Ser. A., 256: 359-383.

Hall, J.M., Wilson, R.L., Dagley, P., 1977. A paleomagnetic study of the Mull lava succession. Geophys. J. R. Astron. Soc., 49: 499-514.

Hrouda, F., 1981. Magnetic anisotropy of rocks and its application in geology and geophysics. Geophysical Surveys., 5: 37-82.

Huang, K., Opdyke, N., 1993. Paleomagnetic results from Cretaceous and Jurassic rocks of South and Southwest Yunnan: evidence for large clockwise rotations in the Indochina and Shan-Tai Malay terranes. Earth Planet. Sci. Lett., 117: 507-524.

Irving, E., Irving, G.A., 1982. Apparent polar wander paths carboniferous through Cenozoic and the assembly of Gondwana. Geophys. Surv., 6: 141-187.

King, R.F., 1955. Remanent magnetism of some artificially deposited sediments. Mon. Not. R. Astron. Soc. Geophys. Suppl., 7: 115-134.

King, R.F., Rees, A.I., 1966. Detrital magnetism in sediments. An examination of some theoretical models. Jour. Geophys. Res., 71: 561-571.

Klootwijk, C.T., Nazirullah, R., de Jong, K.A., 1986. Paleomagnetic constraints on formation of the Mianwali reentrant, Trans-Indus and western Salt Range, Pakistan. Earth Planet. Sci. Lett., 80: 394-414.

McElhinny, M.W., Lock, J., 1990. Global paleomagnetic database project. Phys. Earth. Planet. Int., 63: 1-6.

McFadden, P.L., Jones, D.L., 1981. The fold test in paleomagnetism. Geophys. J. R. Astron. Soc., 67: 53-58.

Nagata, T., 1961. Rock magnetism. Mazuren, Tokyo, 350 pp.

Opdyke, N.D., Johnson, N.M., Lindsay, E.H., Tahirkheli, R.A.K., 1982. Paleomagnetism of the Middle Siwalik formations of northern Pakistan and rotation of the Salt Range decollement. Paleogeogr. Paleoclimatol. Paleoecol., 37: 1-15.

Schneider, D.A., Kent, D.V., 1990. Testing models of the Tertiary paleomagnetic field. Earth. Planet. Sci. Lett., 101: 260-271.

Soffel, H., Forster, H.G., 1980. Apparent polar wander path of Central Iran and its geotectonic interpretation. J. Geomagn. Geoelectr., 32(suppl. III): 117-135.

Tauxe, L., Kent, D.V., 1984. Properties of a detrital remanence carried by hematite from study of modern river deposits and laboratory redeposition experiments. Geophys. J. R. astr. Soc., 77: 543-561.

Tauxe, L., Opdyke, N.D., 1982. A time framework based on magnetostratigraphy for the Siwalik sediments of the Khaur area, Northern Pakistan. Paleogeogr. Paleoclimatol. Paleoecol., 37: 43-61.

Turner, P., 1979. The paleomagnetic evolution of continental red beds. Geol. Mag., 116: 289-301.

Turner, P., 1980. Continental red beds. Elsevier, Amsterdam, 562 pp.

Westphal, M., 1993. Did a large departure from the geocentric axial dipole hypothesis occur during the Eocene? Evidence from the magnetic polar wander path of Eurasia. Earth Planet. Sci. Lett., 117: 15-28.

Westphal, M., Bazhenov, M.L., Lauer, J.P., Pechersky, D.M., Sibuet, J.C., 1986. Paleomagnetic implications on the evolution of the Tethys belt from the Atlantic Ocean to the Pamirs since the Triassic. Tectonophysics, 123: 37-82.

Wilson, R.L., Ade-Hall, J.M., Skelhorn, R.R., Speight, J.M., Dagley, P., 1974. The British Tertiary Igneous Province: paleomagnetism of the Vaternish dyke swarm on north Skye, Scotland. Geophys. J. R. Astron. Soc, 37: 23-30.

Wilson, R.L., Dagley, P., Ade-Hall, J.M., 1972. Paleomagnetism of the British Tertiary Igneous Province: the Skye lavas. Geophys. J. R. Astron. Soc., 28: 285-293.

Zhao, X., Coe, R.S., Zhou, Y., Wu, H., Wang, J., 1990. New paleomagnetic results from northern China: collision and suturing with Siberia and Kazakhstan. Tectonophysics, 181: 43-81.

Zheng, Z., Kono, M., Tsunakawa, H., Kimura, G., Wei, Q., Zhu, X., Hao, T., 1991. The apparent, polar wander path for the North China Block since the Jurassic. Geophys. J. Int., 104: 29-40.

ANNEXE II

Paleomagnetism of Cretaceous redbeds from Tajikistan and Cenozoic deformations due to India-Eurasia collision

article accepté à "Earth and Planetary Sciences Letters".

Paleomagnetism of Cretaceous redbeds from Tajikistan and Cenozoic deformations due to India-Eurasia collision.

M. Bazhenov[1, 3], H. Perroud[2], A. Chauvin[3], V. Burtman[1], J. C. Thomas[3]

1 Geological Institute, Academy of Sciences, Moscow, Russia.
2 Département des Sciences de la Terre, Université de Pau, 64000 Pau, France
3 Géosciences Rennes, CNRS, Université de Rennes I, 35042 Rennes Cedex, France

Abstract.

To study the main features of Alpine tectonics in the Tajik depression, structural and paleomagnetic studies were carried out. About 340 cores from 43 sites of Lower Cretaceous red beds were sampled from 4 different localities in the basin itself and in adjacent ranges. A well defined component of magnetization (labelled A) of normal polarity with high unblocking temperatures (up to 650-670°C) was recognized on all sites. A second component of magnetization (named B) with unblocking temperatures between 650° to 680°C was isolated on only 15 sites. The B component shows the two polarities of the Earth's magnetic field. Positive fold test is obtained for the both components. Acquisition of the component A was situated during the long normal Cretaceous quiet interval and only this magnetization is used for tectonic interpretation. Comparison with Eurasian reference data shows reliable counterclockwise rotations on two localities: close to the Pamir wedge (R = 51 ± 5°) and in the inner part of the basin (R = 15°± 5°). On the two other localities at the periphery of the Tajik basin, no significant rotations are observed.

Introduction.

Fold belts are usually attributed to collision of lithospheric plates. The Alpine belt is thought to result from Cenozoic collision of the African plate in the west, or the Indian plate in the east, with the Eurasia landmass. Indentation of Eurasia by the rigid Indian wedge led to formation of mountain chains like the Himalayas, Tibet, Hindukush and Pamirs. It is also becoming clear that collision-related deformation has affected a very large area outside the Alpine belt sensu stricto and can be recognized as far as South China in the east or the Baykal rift system in the north [1, 2]. However, while some general agreement has already been reached concerning the relation of the Central Asia tectonics and the Eurasia-India collision, the mode and scale of tectonic processes remains unclear.

Key area is the Tien Shan belt and the deep sedimentary basins which surround the Pamir wedge (Fig. 1). The Tajik depression just to the west of this wedge is a basin filled with thick Mesozoic and Cenozoic sediments, folded and thrust in the Pliocene-Quaternary. Though the general structural pattern follows rather closely the outline of the Pamirs wedge, many features of the depression tectonics are still debatable, in particular, the estimation of horizontal movements and associated rotations about vertical axis.

Paleomagnetic data may be of great importance for that purpose. Indeed, Cretaceous and Paleogene rocks from the Tajik depression, the southern part of the Tien Shan (the Ghissar range) and the westernmost Pamirs have been studied by several authors. However, the main body of data from the depression and the Ghissar range is based on time-cleaning techniques only [e.g., 3] and thus cannot be considered reliable. One result from the western border of the Pamirs is based on thermal cleaning at 400°C, with a positive fold test [4]. Recently, Pozzi and Feinberg [5] presented fully demagnetizated data from the north-east of the Tajik basin, but from a limited number of samples.

To study the main features of Alpine tectonics in both the TienShan and Tajik depressions, structural and paleomagnetic studies were carried out by French-Soviet expeditions to the territories of Kirghizia and Tajikistan during 1989-1990 field seasons. In Tajikistan both Oligocene-Lower Miocene and Cretaceous rocks were sampled at a number of localities. This paper covers results obtained from Cretaceous samples.

Geological setting and sampling.

The Tajik basin (depression) is a diamond-shaped deep basin, bounded by the ranges of the Pamirs (the Darvaz and Peter the First ranges) in the east, the Ghissar and South-West Ghissar in the north and west and the mountain chains of Northern Afghanistan in the south (Fig. 1). The basement of the basin has not been reached by the deepest boreholes and has been studied only by geophysical methods; it is thought to be heterogeneous and made of strongly deformed Precambrian, Paleozoic and possibly Triassic complexes. The depression is filled with sediments up to 10-kilometers thick. The oldest sediments are Lower-Middle Jurassic terrigenous, sometimes coal-bearing. UpperJurassic marine limestones are overlain by Uppermost Jurassic evaporites. Lower Cretaceous red beds about 1,000-meter thick are covered by both marine and continental Upper Cretaceous to Paleogene sediments. Close to the Oligocene-Miocene boundary, an accumulation of several kilometers of thick conglomerates has started and still continued nowdays. In adjacent Tien Shan ranges, the Mesozoic and lower Tertiary parts of the section are represented by similar formations but with

several-fold reduced thicknesses, whereas the Upper Tertiary sequence is still greater reduced or absent at all.

The main deformation took place in the Pliocene-Quaternary, but weaker unconformities have been recognized in the Lower Miocene [6] and close to the Late Cretaceous-Paleocene boundary (P.R.Cobbold, personnal communication). The present geometry and tectonic structure of the depression is thought to result from Alpine deformation. In the east, the shortening of the strongly folded Mesozoic-Cenozoic sedimentary cover in the Peter the First and Transalay ranges occurs between the Pamirs and Tien Shan. Westward, the depression widens and is characterized by arcuate folds and faults of westward vergence. The magnitude of horizontal displacements is several kilometers at least but may be much larger. The Upper Jurassic evaporites are most probably the main decollement surface accounting for large discrepancies in the tectonic patterns above and below them.

We sampled Lower Cretaceous red beds, mainly Valanginian to Aptian or Albian in age [7, 8], at three localities in the basin it self and in adjacent ranges (Fig. 1):

1) Derbent locality is situated to the west of theTajik basin, in the NE-SW trending system of folds of the South-West Ghissar range, about 20 km westward from Baysun town. 14 sites were drilled in four sections with various bedding attitudes.

2) Aksu locality is situated on the eastern slope of the Esamol ridge in the north-central part of the depression, about 50 km south of Dushanbe town. Seven, six and three sites were sampled at the western and eastern limbs of the large anticline and its axial part, respectively. In addition, a large block was taken from a layer of intraformational conglomerate on the western limb. This rock contains dark-red sandstone pebbles, several millimeters wide, with clearly defined margins, immersed in a paler sandy matrix.

3) Takob locality is situated to the north of the depression on the southern slope of the Ghissar range, about 30 km north of Dushanbe town. Valanginian to Aptian sediments form a syncline with gentle southern and steep northern limbs. 11 sites were drilled on the southern limb. The same rocks were also sampled along two sections (12 and 13 hand-samples) on the two limbs of the syncline. The main part of this collection consists of redbeds, but several grey sandstone layers were sampled too.

Finally, we also re-studied 14 hand samples from the southern termination of the Darvaz range, about two kilometers to the west of the Paleozoic Pamir domain. These Cretaceous redbeds came from a N-S striking structure with

overturned bedding; the previously published result from this locality was based on incomplete demagnetization [4].

In general, a site covers a layer of apparently uniform lithology up to 5 meters along the strike and up to one meter cross-section. Six to nine cores, oriented with solar and magnetic compasses, were drilled at each site. When sampling along sections, hand-samples oriented with magnetic compass only were spaced by several meters cross-section.

Measurements and procedures.

One specimen from each core and two specimens from each hand-sample were heated in 15 steps up to 680° using the Schonstedt TSD-1 demagnetizer; six specimens from the conglomerate block were also demagnetized. Measurements were made either with a Schonstedt fluxgate magnetometer or with a LETI cryogenic magnetometer. All data were analyzed with stereonets and orthogonal plots, and interpreted with principal component analysis, coupled with a graphical interactive system [9]. All specimen directions from a site or a hand sample were averaged to obtain site or sample means. Since either a site or a hand-sample represents an independent record of the magnetic field, (though, of course, the latter is not as precisely defined), it was decided to give an equal weight to each mean vector.

Wherever possible, the McFadden and Jones [10] fold test (referred to here the M test) was performed for each locality separately; otherwise, the usual McElhinny [11] fold test (refered here as the PP test) was used. During tectonic interpretation, flattening F and rotation R, and their confidence limits were computed, following Demarest [12].

Results of paleomagnetic analysis.

Overview.

Intensities of natural remanent magnetization (NRM) usually range between 10^{-2} to 10^{-3} A/m. NRM directions concentrate in the northern half of the lower hemisphere, and already display a better grouping after tilt correction than In Situ. An unstable component of magnetization was usually removed by heating to 200° or 250°. Above that temperature, all samples revealed a well-defined component (labelled A) of normal polarity which persisted up to as high as 670° (Fig. 2). The unblocking temperature spectrum of this component is more or less uniform over the heating range and it was reliably isolated from most specimens. It is even the only component which can be recognized in many samples. Its directions clusters well within each site or hand sample.

Orthogonal plots often do not decay straight to the origin, and another linear trajectory can be recognized, thus implying the presence of a second component (Fig. 2a, 2b, 2d). This component (labelled B) can be isolated over a narrow temperature interval (650-680°C) and when present, accounted for 10 to 20% of the NRM intensity. In some samples, component B could not be accurately determined, even if its presence is attested to by demagnetization trajectories overshooting the origin.

Unbloking temperatures observed and isothermal remanent magnetization acquisitions (Fig. 2f) indicate that hematite is the dominant carrier of magnetization.

Derbent locality.

Component A was reliably isolated from all 14 sites (Table1). Component B, adequately resolved from 9 sites, is also of normal polarity. However, the polarity of component B is reversed at one site (DERH), but it could not be well isolated there (Fig. 2b, 2c).

As attested by the 99% positive PP test, the clustering of site-means after tilt-correction is much better than In Situ for both components (Table 1, 2, Fig. 3). However, the M test for component A yielded F statistics values larger than the critical ones. A closer inspection of the data showed that the results from one of the limbs (sites DERA to DERC) differ both in declination and inclination from all others, although these sites are quite similar to the other in all respects. If we omit these three sites, the F statistics value after tilt correction decreases from 14.8 to 4, with a considerable improvement of the grouping of data (k increases from 52 to 193). The F value is still slightly larger than the corresponding critical value (Table 1), but this is probably due to the limited number of sites. We assume therefore a prefolding age for the component A and we shall use the mean direction based on 11 sites only. The same problem arises for component B, and we shall use also sites DERD to DERN only, to compute its mean direction.

Aksu locality.

Component A was reliably isolated from all 16 sites (Table3). Component B, adequately resolved from 6 sites, is bipolar (Table 4). Usually, component B is rather poorly defined, but the general consistency of results is reasonable. Six specimens from the conglomerate yielded well-clustered directions close to component A mean direction (Table 3).

As for Derbent locality, the PP test is 99% positive but the M test is negative for component A (Table 3, Fig. 4). However, a fine analysis of bedding attitudes shows that the fold axis of the anticline plunges about 20° northward, tendering incorrect a simple tilt correction. When using a two-stage unfolding algorithm

[9], taking into account this plunge, we obtain an excellent agreement of component A mean vectors from the three limbs, and a positive M test. The grouping of component B directions is also improved when using the two-stage unfolding algorithm (Table 4, Fig. 5).

Takob locality.

Redbeds from this locality behaved like those sampled at Derbent and Aksu. The only difference is that all reliably isolated components have normal polarity (Fig. 6). However, component B was adequately resolved from a few specimens only and will not be used further. Grey-colored sandstones were very weakly magnetized and yielded no meaningful results. Both fold tests point to a prefolding age of component A (Table 5).

South Darvaz locality.

Only component A, of normal polarity, was isolated from 11 samples, and its tilt-corrected mean direction is very similar to the previously reported result (Table 5, Fig. 7). Orthogonal plots for some samples slightly miss or bypass the origin, indicating the possible existence of a second unresolved (B?) component. The PP fold testis not significant for this set of samples (Table 5), but earlier, these redbeds were shown to have a prefolding magnetization.

For several specimens of redbeds from this locality, chemical leaching in hydrochloric acid, revealed the same well-defined component A as did thermal demagnetization (Fig. 8). After removal of this component, paleomagnetic directions became erratic. Some leached and unleached specimens were isothermally magnetized in fields up to 600 mT and then thermally demagnetized (Fig. 8). The IRM acquisition curves show that the leaching has dissolved the high coercivity minerals, which were carrying component A. The high unblocking temperatures (up to 680°C) indicate that hematite is the carrier of component A. In the leached specimens, IRM is saturating in low fields, and unblocking temperatures are below 600°C. Magnetite can therefore be present in small proportions, and could carry the residual chaotic magnetization found at the end of chemical demagnetization.

Discussion.

Component A, which always has normal polarity, constitutes usually 80 to 90% of the NRM. Judging by orthogonal plots which often overshoot the origin, vector paths on stereonets, and the negative conglomerate test, this component is probably a secondary magnetization. As indicated by the leaching experiments, it seems to be carried by hematitic pigment, which can appear in redbeds long after deposition [9]. A similar conclusion was reached by Pozzi and Feinberg [5] for the same Lower Cretaceous redbeds, sampled in the north and north-east of

the depression. Moreover, Lower Cretaceous redbeds are widespread in the South Tien Shan and the Fergana basin, and a similar overprint of normal polarity was found there too [13].

Pozzi and Feinberg [5] identified a reverse high-temperature component, but failed to isolate it. We were more lucky, mainly because we had a much larger collection, but still the component B was often isolated in one or two specimens per site. In total, the high temperature bipolar component B has been found in less than fifty percent of the collection. Its rather high within-site scatter is probably due to the difficulty of isolating it accuratley from the short final parts of the orthogonal plots. It may also be contaminated by the largercomponent A. In spite of this scatter, component B has consistently lowerinclinations than component A, again in agreement with the Fergana results [13].

The main deformation in this region is Late Miocene or younger. Close to the Oligocene-Miocene boundary, conglomerates up to several kilometers thick started accumulating in the basin, thus indicating range-and-basin relief and therefore some tectonic activity. This is confirmed by Lower Miocene angular unconformities [6]. Also, angular unconformities of 10° to 15° between Upper Cretaceous and Paleocene strata have recently been reported (P.R.Cobbold, personnal communication). The problem is the regional significance of pre-Late Miocene unconformities, which usually are considered local. The excellent agreement of the component A mean directions from different fold limbs at Aksu and Takob localities, to lesser degree at Derbent locality (Tables 1, 3, 5), let us to state that this remanence was acquired prior to any folding in the region. For component B which presents a larger dispersion, we can only state that the magnetization predates the main folding.

Though showing some lateral variability, Lower Cretaceous rocks are essentially the same from Amudarya River in the south to the Tashkent area in the north and to the easternmost part the Fergana basin. Paleomagnetic properties of Lower Cretaceous rocks are also similar all over this region: they reveal a large secondary magnetization of normal polarity (component A), associated with a much weaker and less common high-temperature bipolar magnetization (component B). It seems improbable that the overprinting of component A could have occurred in the Cenozoic, because this era is characterized by frequent changes of polarity. For this reason, we disagree with the Pozzi andFeinberg [5] hypothesis of a 40 Ma age. Instead, we infer acquisition of normal polarity magnetization during the long normal Cretaceous quiet interval, which lasted from the Aptian to the Santonian. An approximate age of 100 Ma was assigned to component A.

In our study, the bipolar nature of component B agrees with the rock age (mainly pre-Aptian) and it may therefore be primary. But the systematically shallowed inclinations, both in the Tajik and Fergana basins, have to be explained, perhaps by an inclination error or an early diagenetic compaction. At the same time, we can compared component B to the results we have obtained on Oligocene-Lower Miocene redbeds from the Aksu locality, and which revealed a dual-polarity characteristic magnetization with the same low inclination (D = 347°, I = 33°, a_{95} = 15°, N = 5 sites [14a,b]). Moreover, anomalously low inclinations in Eocene to Lower Miocene rocks were reported from Kirghizia [15] and peri-Pamir area [4], as well as other parts of the Alpine belt [for review, see Westphal et al, 1986]. In this state of art, we cannot rule out the possibility of a Cenozoic age for component B and prefer to not use these results for the tectonicinterpretation.

Interpretation and Conclusion

Observed paleomagnetic inclinations and declinations from Tajikistan were compared with the Eurasian reference data (Fig. 9). Any tectonic interpretation is crucially dependent on this reference. Several propositions for the mean Cretaceous paleomagnetic pole appeared during the last decade, based on Eurasian data. Khramov et al. [16] reported a mean pole for extra-Alpine Eurasia (within the former Soviet Union) for the whole Cretaceous. Since the main body of data came from sediments, an Early Cretaceous pole for Eurasia was calculated by Bazhenov and Shipunov [17] as an intersection of paleomeridians, in order to take into account a possible shallowing of inclinations. Early and Late Cretaceous poles have been recomputed for Eurasia by Westphal et al.[18]. The latest version appeared in a new compilation of paleomagnetic data for Europe and North America [19]. All these poles were computed after application of different selection criteria. As a result, only two Early Cretaceous and three Late Cretaceous poles were left in the latest data set. In spite of this, all these mean poles (further on referred to as EA data) are rather similar and they predict for our area an inclination of about 55° and a declination of about 20° (Fig.9).

The reliability of the Eurasian Cretaceous data set has recently been questioned, and an alternative apparent polar wander path (APWP) suggested [20]. For its Cretaceous part, just one Early Cretaceous and one Late Cretaceous poles from Europe were left and three new ones from China and Korea were added. A global APWP was constructed by combining data from North America, Africa, Eurasia and India and transferring to each continent. The reference directions for our area, deduced from this APWP (further on referred

to as BC data), display systematically lower inclinations and more northerly declinations than those calculated from the EA poles (Fig. 9).

The internal consistency of our inclination data for component A is very good: the Aksu, Derbent and Takob mean inclinations fall within three degrees. The South Darvaz result is several degrees shallower but it is displaced in the correct sense if to take into account a possible northward push of this locality during the Pamirs indentation into the Eurasian landmass, and oroclinal bending of the External Pamirs tectonic zone [4]. With respect to the EA reference inclinations, our results are systematically shallower, but the exact value of displacement depends upon which EA pole is used. In contrast, our data match well the BC expected inclinations, none of the measured flattening values being statistically significant. Some shortening certainly took place in the Tien Shan during Alpine deformation, but it could hardly be more than 200 km [21].

Unless a new major revision of the Eurasian APWP appears, declinations which are significantly below the BC reference declination curve (Fig. 9) are certainly from counterclockwise rotated localities (any rotations established with respect to BC data are conservative estimates). South Darvaz locality is clearly rotated counterclockwise (R = 51°± 5°), most probably in relation with the oroclinal bending of the Pamirs arc. The result from the inner part oft he Tajik basin (Aksu) is also clearly rotated, in the same sense, but through a much lesser angle (with respect to 100 Ma BC, R = 15°± 5°). This finding is in accord to earlier results from the basin [3 and 5]. Mean declinations from the two localities at the periphery of the Tajik basin and Southern Tien Shan, Derbent and Takob, significantly differ from the EA poles and less from the BC data (Fig. 9). With respect to the 100 Ma BC direction, R values are 5°±5° and 9°±6°, respectively. Unless disprooved by new data, we cautiously consider Derbent locality as an unrotated part of Eurasia. For Takob locality, R value is statistically significant, but the amount of rotation is at the limit of paleomagnetically detectable rotations.

The pattern of paleomagnetic declinations of Cretaceous and younger rocks from the western part of the Tien Shan is shown in Figure 10. Both Cretaceous [this paper and 13] and Paleogene [15] declinations west of the Talas-Fergana fault are systematically rotated counterclockwise, with the exception of a limited area close tot he southern termination of the Talas-Fergana fault, where no rotations were found [13 and 22]. In contrast,the Issyk Kul and Naryn basins seems to be unrotated [15]. Further to the east, unrotated declinations were reported from Cretaceous and Tertiary rocks at the South Junggar basin-North Tien Shan boundary [23]. Finally, declinations in Upper Jurassic-Lower

Cretaceous and Upper Cretaceous rocks from Northern Tarim [24] agree well with the BC data (R values are 7°±11° and 2°±10° with respect to 130 Ma and 90 Ma BC poles, respectively). Though some local movements may be found in the future, there has been probably no regional rotation east of the Talas-Fergana fault.

Westerly declinations in the Fergana basin and adjacent Tien Shan ranges have been attributed to 25° counterclockwise rotation of the "Fergana block" around an Euler pole at c.40°N and 69°E [13 and 15]. This choice was based on an analysis of the Alpine deformation pattern; in addition, it was the only permissible pole not leading to disruption of the Paleozoic tectonic zonation in the region. This Euler pole is not suitable for the new data from the Tajik basin, since it would imply a movement towards the Pamir wedge. We therefore consider that the two basins, Fergana and Tajik, were separate blocks during the Alpine deformation.

Most geologists agree that Cenozoic deformation in Central Asia started in the Late Oligocene-Early Miocene, its main part being of the Pliocene age. This Neogene tectonic activity is usually connected to the India-Eurasia collision. Our results show that the rotation is certainly post-Cretaceous in age. This conclusion is also confirmed by westerly declinations which we found in Oligocene-Miocene rocks from Aksu locality, and the data of the same age reported from the South Darvaz area [13]. In general, the rotations deduced from paleomagnetic results in the western part of the Tien Shan and Tajik basin are close to the kinematic pattern as deduced from the structural and seismological data [1].

Acknowledgments.

Thanks are due to Academy of Sciences Moscow and CNRS Paris for financial support, the Ministère des Affaires Etrangères of France, the University of Rennes and the University of Pau for their grants to M B. We gratefully acknowledge F. Calza for assistance in the laboratory, S. V. Shipunov for permission to use his programs and P.R. Cobbold for organizing the project.

REFERENCES.

[1] Cobbold, P.R. and P.Davy, 1988, Indentation tectonics in nature and experiment: 2. Central Asia. Bull. Geol. Inst. Univ. Uppcala, N.S. 14, 143-162.

[2] Tapponnier, P. and P.Molnar, 1979, Active faulting and Cenozoic tectonics of the Tien Shan, Mongolia andBaykal region. J. Geophys. Res., 84, 3425-3459.

[3] Abdullaev, Kh.A., and Yu.S.Rzhevsky, 1973, Lower Cretaceous paleomagnetism of the Tajik basin. FAN, Tashkent, 104 p., (in Russian).

[4] Bazhenov, M.L. and V.S. Burtman, 1990, The structural arcs of the Alpine belt (the Carpathians, Caucuses,P amirs). Nauka, Moscow, 168 pp (in Russian).

[5] Pozzi, J.-P., and H.Feinberg, 1991, Paleomagnetism in the Tajikistan: continental shortening of the European margin in the Pamirs during Indian Eurasian collision, Earth and Planet. Sci. Lett., 103, 365-378.

[6] Belsky, V.A, 1978, Recenttectonics of the boundary between the North Pamirs and Tajik basin. Donish, Dushanbe, 256 p., (in [7] Akramkhojaev,A.M et al., 1971,.Lithology, stratigraphy and oil prospecting of southern and south-western Uzbekistan, FAN, Tashkent, (in Russian).

[8] Baratov, P.B.(Editor), 1982, Stratified and intrusive formations of Tajikistan, Donish, Dushanbe, p. (in Russian).

[9] Perroud H., 1985, Paléomagnétisme dans l'arc Ibéro-Armoricain et l' orogénèse varisque en Europe occidentale, thèse, Univ. de Rennes, 1985.

[10] McFadden, P.L. and Jones, D.L., 1981. The fold test in palaeomagnetism,Geophys. J.Roy. Astron. Soc., 67, 53-58.

[11] McElhinny, M.W., 1964. Statistical significance of the fold test in palaeomagnetism,Geophys. J.R. Astron. Soc., 8, 338-340.

[12] Demarest, H.H.,jr., 1983. Error analysis for the determination of tectonic rotation from paleomagnetic data. J. Geophys. Res., 88, 4321-4328.

[13] Bazhenov, M.L.,1992,Cretaceous paleomagnetism of the Fergana basin and adjacent ranges:tectonic implications. Tectonophysics, (submitted for publication).

[14a] Thomas, J.C., M. Bazhenov, V. Burtman, A. Chauvin, P. Cobbold, D. Gapais and H. Perroud, 1993, Paleomagnetic study of Tertiary and Cretaceous formations from the Tadjik depression, Central Asia, Terra Nova, 5, 270, EUG VII, Strasbourg.

[14b] Thomas J.C., A. Chauvin, D. Gapais, M.L. Bazhenov, P.R. Cobbold, H. Perroud and V.S. Burtman, 1993, A block rotation model for the Tadjik depression (Central Asia) during the Tertiary: paleomagnetic evidence, in preparation.

[15] Thomas, J.C., H. Perroud, P.R. Cobbold, M.L. Bazhenov, V.S. Burtman, A. Chauvin and E. Sadybakasov, 1993. "A paleomagnetic study of Tertiary formations from the Khirghiz Tien-Shan and its tectonic implications, J. Geophys. Res. (in press).

[16] Khramov, A.N., G.I. Goncharov, R.A. Komissarova, S.A. Pisarevsky, I.A. Pogarskaya, Yu.S. Rzhevsky, V.P. Rodionovand I.P. Slautsitais, 1982, Paleomagnitology, Nedra, Leningrad, 312 p.

[17] Bazhenov, M.L. and S.V.Shipunov, 1985, Paleomagnetism of Cretaceous rocks from Northern Eurasia: new results and analysis. Izv. Akad.Nauk SSSR, ser. Fizika Zemli, no.6, 88-100.

[18] Westphal, M., M.L. Bazhenov, J.P. Lauer, D.M. Pechersky and J.C. Sibuet, 1986, Paleomagneticimplications on the evolution of the Tethys belt from the Atlantic ocean tothe Pamirs from the Triassic, Tectonophysics, 123, 37-82.

[19] Van derVoo, R., 1990, Phanerozoic paleomagnetic poles from Europe and North America andcomparisons with continentalreconstructions. Rev. Geophys., v.28, 167-206.
[20] Besse, J. and Courtillot, V., 1990. Revised and synthetic Apparent Polar Wander Paths of the African, Eurasian, North American and Indian Plates and True Polar Wander Paths since 200 Ma. J. Geophys. Res., 96, 4029-4050.
[21] Molnar, P. and P.Tapponnier, 1975, .Cenozoic tectonics of Asia: effects of a continental collision, Science, 189, 419-426.
[22] Chen. Y., J.-P. Cogne and V. Courtillot, 1992, New Cretaceous paleomagnetic poles from the Tarim basin, NW of China. Earth Planet. Sci. Lett., 114, 17-38.
[23] Chen, Y., J.-P.Cogne,V.Courtillot, J.-Ph.Avouac, P.Tapponnier, G.Wang, M.Bai, H.You, M.Li, C Wei C and E. Buffetaut, 1991, Paleomagnetic study of Mesozoic continental sediments along the NorthernTien Shan (China) and heterogeneous strain in Central Asia. J. Geophys.Res., 96, B3, 4065-4082.
[24] Li Y.P., Z.K. Zhang, M. McWilliams, R. Sharps, Y.J. Zhai, Y.A. Li, Q. Li and A. Cox, 1988, Mesozoic paleomagnetic results of the Tarim craton: Tertiary relative motion between China andSiberia?, Geophys. Res. Lett., 15, 217-220.

FIGURE CAPTIONS

Figure 1. A. General location map showing traces of major faults and areas with elevations greater than 2km(shaded) simplified after Cobbold and Davy [1988]; B. Schematic geological map of the Tajik Basin, Souther Tien Shan and Pamirs Our sampling localities are shown as solid dots and those from Pozzi and Feinberg [1991] as open dots.

Figure 2. Representative orthogonal plots (a-e) for Lower Cretaceous red beds from different localities. Dashed lines denote isolated components labeled A and B as in the text. Data are plotted in stratigraphic coordinates (TC). Full (open) dots represent vector endpoints projected onto the horizontal (vertical) plane. Steps are in degrees Celsius for thermal demagnetization; f) Isothermal remanent magnetization acquisition curves

Figure 3. Equal-area projection of site-means of the component A (a,b) and component B (c,d) from Derbent locality in situ (a,c) and after tilt correction (b,d). Solid (open) symbols and solid (dashed) lines are projected onto lower (upper) hemisphere.

Figure 4. Equal-area projection of site-means (dots) of the component A from Aksu locality in situ (a), after simple tilt correction (b) and two-stage tilt correction as explained in the text (c). A dot with vertical tail denotes the mean direction from a large block of conglomerate. Blow-up (d) shows mean directions together with associated confidence circles for each limb after simple tectonic correction (triangles and dotted lines) and two-stage correction (inverted triangles and solid lines. All symbols are projected onto lower hemisphere.

Figure 5. Equal-area projection of site-means (dots) of the component B from Aksu locality in situ (a), after simple tilt correction (b) and two-stage tilt correction as explained in the text (c). Solid (open) symbols and solid (dashed) lines are projected onto lower (upper) hemisphere.

Figure 6. Equal-area projection of site-means (dots) and sample-means (stars) of the component A from Takob locality in situ (a) and after tilt correction (b). Solid (open) symbols and solid lines are projected onto lower (upper) hemisphere.

Figure 7. Equal-area projection of sample-means (stars) from South Darvaz locality in situ (a) and after tilt correction (b).Triangle is the mean direction of the component A isolated from the completely demagnetized subset (see text) and square is the mean direction of the whole collection afterheating to 400°C [Bazhenov, Burtman, 1990]. Solid (open) symbols and solid lines are projected onto lower (upper) hemisphere.

Figure 8. a) and b) are orthogonal plots for two specimens from the same hand-sample subjected to chemical leaching and thermal demagnetization, respectively. Solid (open) dots are projections onto horizontal (vertical) plane. Data are in stratigraphic coordinates. Steps are labeled in days (a) and degrees Celcius (b). c are isothermal magnetization curves for leached spesimen (open dots) and unleached one from the same hand-sample. Dashed line is a would-be magnetization curve for magnetic phase removed by leaching (obtained by subtraction of two previous curves). d is thermal gemagnetization of IRM for leached specimen.

Figure 9. Plots of inclination (a) and declination (b) versus age for Cretaceous data. Solid dots and encircled dot are our results (A, Aksu; D, Derbent; T, Takob; SD, South Darvaz) and overall mean from Pozzi and Feinberg [1991], respectively, together with error bars as solid lines. For clarity, our results are slightly displaced with respect to their presumedage (95 Ma). Open dots are reference values from Besse and Courtillot [1990] with associated confidence band (shaded). Square, triangle, inverted triangle and stars are Eurasian Cretaceous mean pole from Khramov et al., [1982], Eurasian Early Cretaceouspole from Bazhenov and Shipunov [1985], Eurasian Early Cretaceous pole fromWestphal et al., [1986], and European Early and Late Cretaceous poles from Van der Voo [1990], respectively. For reference date, error bars are shown as thin dashed lines(for the data from Van der Voo [1990] error bars are not shown due to limited number of poles used).Thick vertical dashed line marks the upper boundary of the Cretaceous quiet interval. Reference data are given the same ages as in the cited papers.

Figure 10. Distribution of paleomagnetic declinations over the Pamirs (inclined lines) and the western part of the Tien Shan (shaded). Thick arrows with black heads are measured directions together with confidence areas shown as unfilled angles (it is not our fault that the confidence areas for well-defined directions are difficult to see!). Solid dots are our data (A, Aksu; D, Derbent; T, Takob;SD, South Darvaz). Squares are Cretaceous data from the Fergana basin and adjacent ranges numbered as in Bazhenov [1992]. Triangles are Cretaceous data from Chen et al.,[1992](U, Uytak area; W, Wuqia area; Y, Yingjisha area). Stars are Lower Cretaceous data from the external Pamir tectonic zone (PF, Peter the Firstrange; WT, western Transalay range; eastern Transalay range) [Bazhenov, Burtman, 1990]. Open dots are Paleogene data (IB, Issyk Kul basin, AL, Alabuka, SF, South Fergana) [Thomas et al., 1993]. Thin arrows with white heads are reference datare calculated from Besse and Courtillot [1990]. Thick dashed line is theTalas-Fergana fault (TFF) and thin dashed lines are major faults of the Southern Tien Shan (SGF, South Ghissar fault). The major basins are labeled as TB, Tajik basin; FB, Fergana basin; NB, Naryn basin; IB, Issyk Kul basin. Encircled large crossand full solid dot are the poles of rotation for Fergana and "Tajik"blocks, respectively.

Table 1. Paleomagnetic directions of the component A from Derbent locality.

Site	n/n_0	INSITU				TILT CORRECTED			
		D	I	k	a_{95}	D	I	k	a_{95}
DERA	8/6	11	-11			33	58	149	6
DERB	7/6	1	-1			28	70	63	9
DERC	7/7	3	-11			33	73	253	4
DERD	8/8	323	6			14	52	238	4
DERE	7/7	332	12			3	50	274	4
DERF	8/8	328	20			6	53	81	6
DERG	9/9	26	71			358	50	297	3
DERH	9/9	33	66			4	47	159	4
DERI	9/9	19	56			358	46	469	2
DERJ	8/8	22	58			2	53	214	4
DERK	8/7	24	58			3	53	282	4
DERL	8/8	336	67			2	46	233	4
DERM	8/8	340	70			11	46	262	3
DERN	8/7	353	61			18	41	288	4
MEANS*									
DERA-C	3	5	-8	112	8	32	67	102	8
DERD-F	3	328	13	95	8	8	52	443	4
DERG-K	5	24	62	141	5	1	50	465	3
DERL-N	3	344	66	153	7	11	44	158	6
ALL	14	356	40	5	17	9	53	52	5
F(26,26)=1.9								ktc/kis = 10.4	
F(6,20)= 2.6				f = 95				f = 14.8	
DERD-N	11	351	53	8	15	6	49	193	3
F(20,20)= 2.1								ktc/kis = 24.8	
F(4,16)= 3.0				f = 74				f = 4.0	

* statistics on the site-meanslevel.
Legend: n/n_0 is the number of specimens studied/used; D is declination, I inclination; k is Fischer precision parameter; a_{95} is radius of 95-percent confidence circle; F is the 95% critical value of F distribution for the number of degrees of freedom in brackets; ktc/kis is the ratio of precision parameters after/before tilt correction; f is the calculated values of F statistics.

Table 2. Paleomagnetic directions of component B from Derbent locality.

Site	n/n_0	IN SITU				TILT CORRECTED			
		D	I	k	a_{95}	D	I	k	a_{95}
DERA	8/6	28	-14			47	44	40	11
DERB	7/5	5	-21			14	51	70	10
DERD	7/6	330	-1			5	44	21	15
DERE	7/7	338	-1			354	37	57	8
DERF	8/4	342	15			10	38	45	14
DERI	9/9	10	55			352	43	49	7
DERJ	8/8	16	43			4	37	42	9
DERM	8/6	7	56			17	28	91	7
DERN	8/7	357	50			14	31	62	8
MEANS*									
DERA-B	2	17	-18	-	-	32	49	-	-
DERD-F	3	334	4	53	11	3	40	119	7
DERI-K	2	13	49	-	-	358	40	-	-
DERM-N	2	2	53	-	-	16	29	-	-
ALL	9	358	21	5	20	10	40	34	8
F(16,16)= 2.3								ktc/kis = 6.4	
DERD-N	7	351	32	8	19	6	37	72	6
F(12,12)= 2.7								ktc/kis = 9.0	

* statistics on the site-means level.
Legend: see Table 1 for explanations.

Table 3. Paleomagnetic directions of component A from Aksu locality.

Site	n/n_0	IN SITU				TILT CORRECTED				UNFOLDED			
		D	I	k	a_{95}	D	I	k	a_{95}	D	I	k	a_{95}
AKS4	8/7	73	34			343	53			0	53	166	5
AKS5	7/7	72	38			339	53			355	53	252	4
AKS6	7/7	72	33			344	51			2	51	186	4
AKS7	6/6	68	38			345	49			1	49	320	4
AKS8	6/6	59	39			334	44			351	44	953	2
AKS9	7/7	70	37			343	48			359	48	432	3
AKSZ	7/7	67	41			338	47			352	45	603	2
CONGL*	6/6	74	44			330	50			345	50	528	3
AKSA	7/7	308	46			21	52			10	52	44	9
AKSB	9/9	308	37			7	51			356	51	120	5
AKSC	7/7	306	37			5	53			354	53	191	4
AKSD	7/7	302	35			355	45			345	45	225	4
AKSE	9/9	307	33			355	41			346	41	263	3
AKSF	8/8	305	33			3	53			351	53	261	3
AKSG	7/7	359	65			2	52			2	52	257	4
AKSH	8/7	350	64			0	50			359	50	124	5
AKSI	7/7	352	62			0	48			0	48	459	3
MEANS**													
AKS4-9,Z	7	69	37	287	3	340	49	292	3	357	49	311	3
AKSA-F	6	306	37	235	4	4	49	102	6	353	49	106	6
AKSG-I	3	354	63	986	4	1	50	1408	2	0	50	1309	2
ALL	16	10	52	3		353	50	75	4	356	49	199	3
F(4,26) = 2.7				f = 489					f = 11.7			f = 0.7	

* result from conglomerate was not used for calculation of the mean. ** statistics on the site-means level.
Legend: see Table 1 for explanations.

Table 4. Paleomagnetic directions of the component B from Aksu locality.

Site	n/n_0	IN SITU				TILT CORRECTED				UNFOLDED			
		D	I	k	a_{95}	D	I	k	a_{95}	D	I	k	a_{95}
AKS-5	7/5	62	35			347	46			3	46	27	15
AKS-9	7/7	188	-48			152	-3			168	-3	13	17
AKS-Z	7/5	192	-51			148	-7			165	-7	49	11
AKS-C	7/7	154	-35			193	-30			182	-30	16	16
AKS-F	8/4	162	-19			182	-17			171	-17	122	8
AKS-I	7/5	14	50			15	35			15	35	278	5
MEAN*	6	7	44	9	24	352	24	11		356	23	17	14

F(10,10) = 1.9 ktc/kis =1.2 kuf/kis = 2.

* all directions inverted to normal polarity.
Legend: see Table 1 for explanations.

Table 5 Paleomagnetic directions of component A from Takob and South Darvaz localities.

Site	n/n_0	IN SITU				TILT CORRECTED			
		D	I	k	a_{95}	D	I	k	a_{95}
TAKOB									
TAK1	6/6	350	45			353	48	21	15
TAK2	6/6	341	44			344	48	41	11
TAK3	7/7	342	38			344	43	46	9
TAK4	6/6	348	50			352	54	25	14
TAK5	7/7	349	48			356	46	1008	2
TAK6	6/6	348	50			356	48	167	5
TAK7	7/7	348	55			353	47	281	4
TAK8	6/6	352	54			355	46	57	9
TAK9	6/5	6	42			14	39	17	19
TAK10	6/6	354	55			6	54	289	4
TAK11	6/5	4	63			20	59	219	5
HS-SL	12/10	350	57	59	6	9	52	72	5
HS-NL	13/6	357	-14	49	8	0	56	52	8
MEAN*	27	352	40	8	10	2	52	60	4
F(4,48) = 2.6				f = 92				f = 1.0	
SOUTH DARVAZ									
MEAN	14/11	56	7	33	7	321	41	69	5
F(20,20) = 2.1								ktc/kis =2.1	
MEAN**	14/34					314	44	54	3
F(4,62) = 2.5				f = 8.5				f = 0.6	

* the same weight given to site-means and sample-means.
** the result and related statistics are from Bazhenov and Burtman [1990].
Legend: HS-SL, HS-NL: hand-samplesfrom the southern and northern fold limbs, respectively. see Table 1 for other explanations.

A

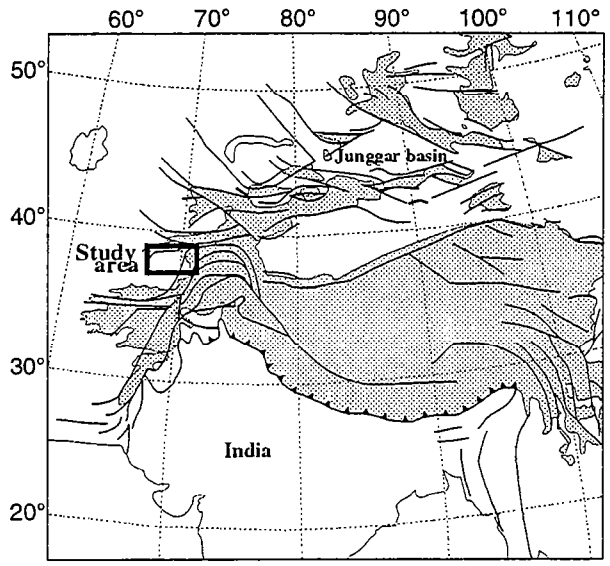

B

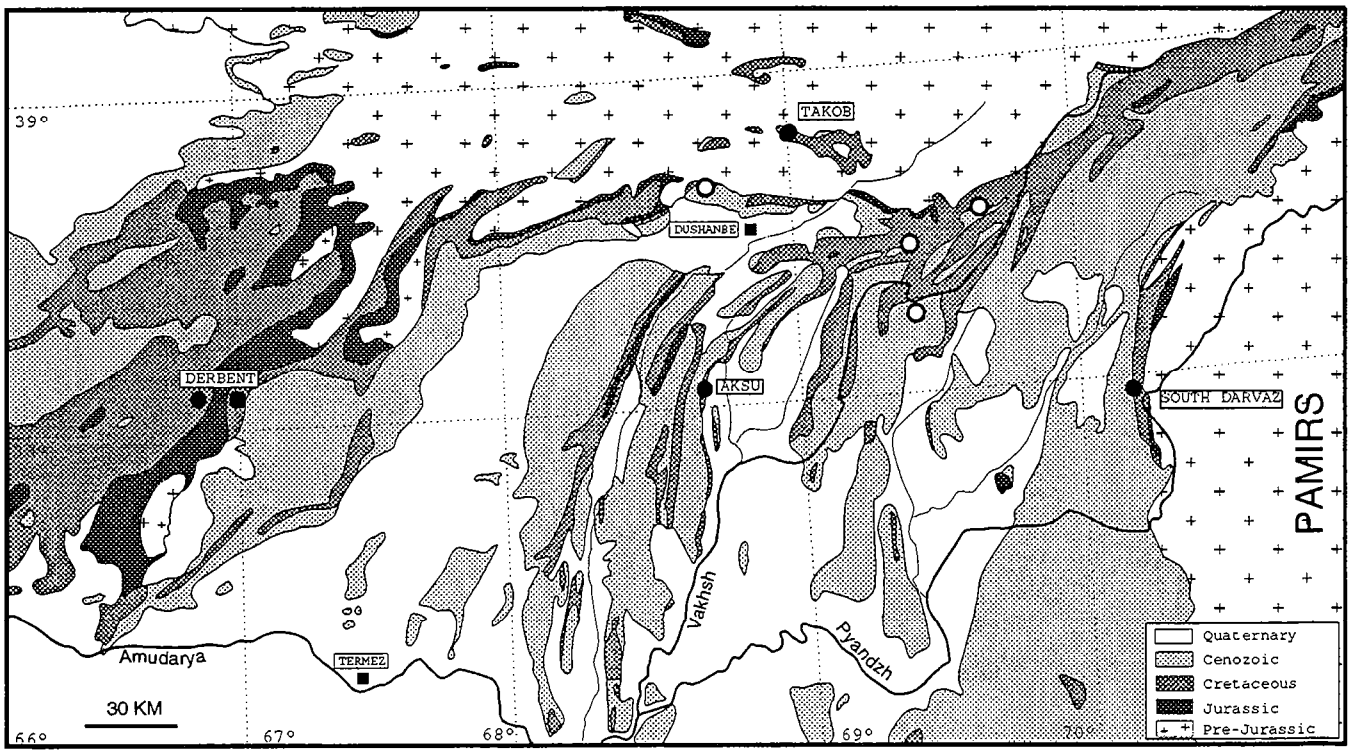

FIGURE 1. Cretaceous paleomagnetism of Tajikistan

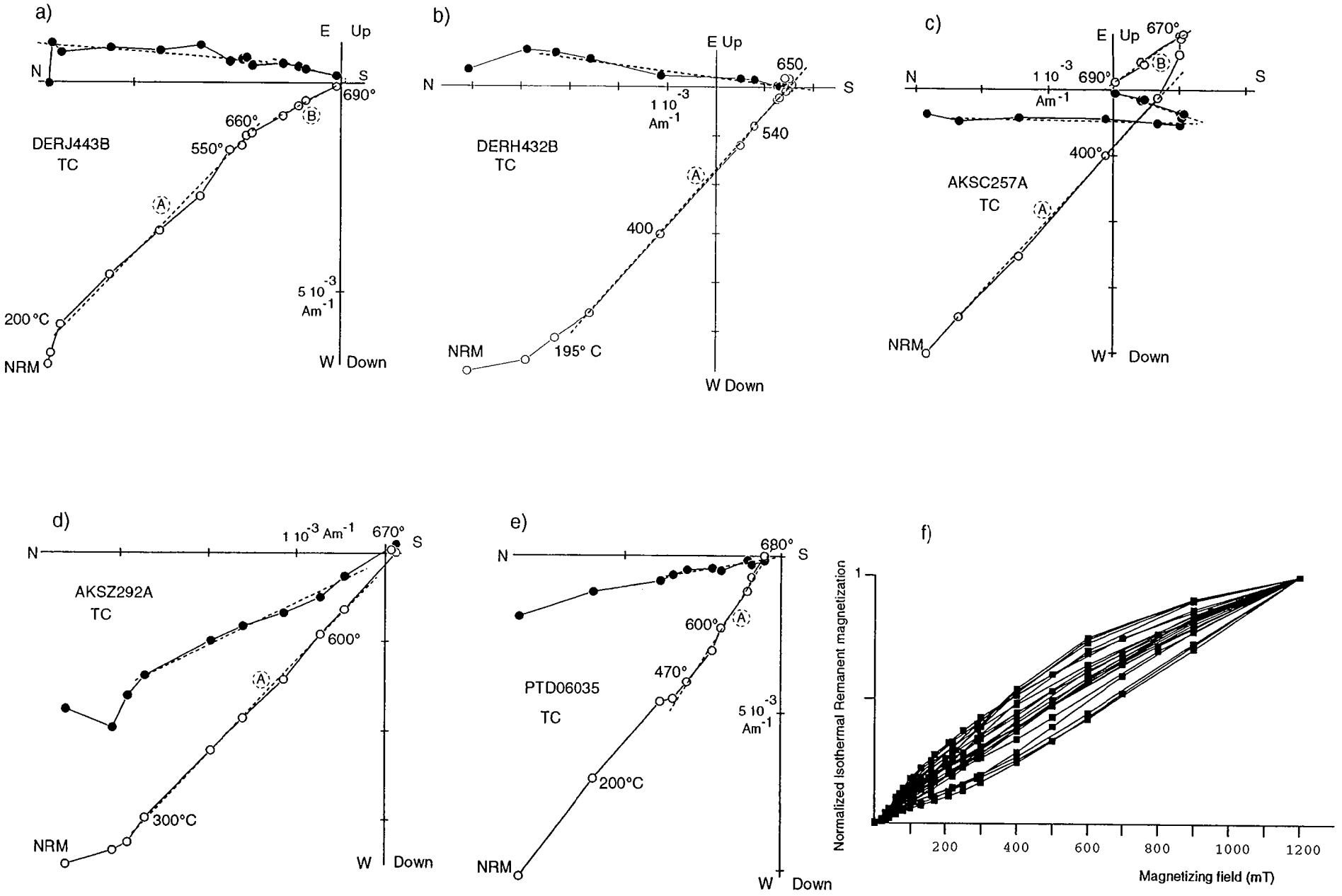

Figure 2. Cretaceous paleomagnetism of Tajikistan

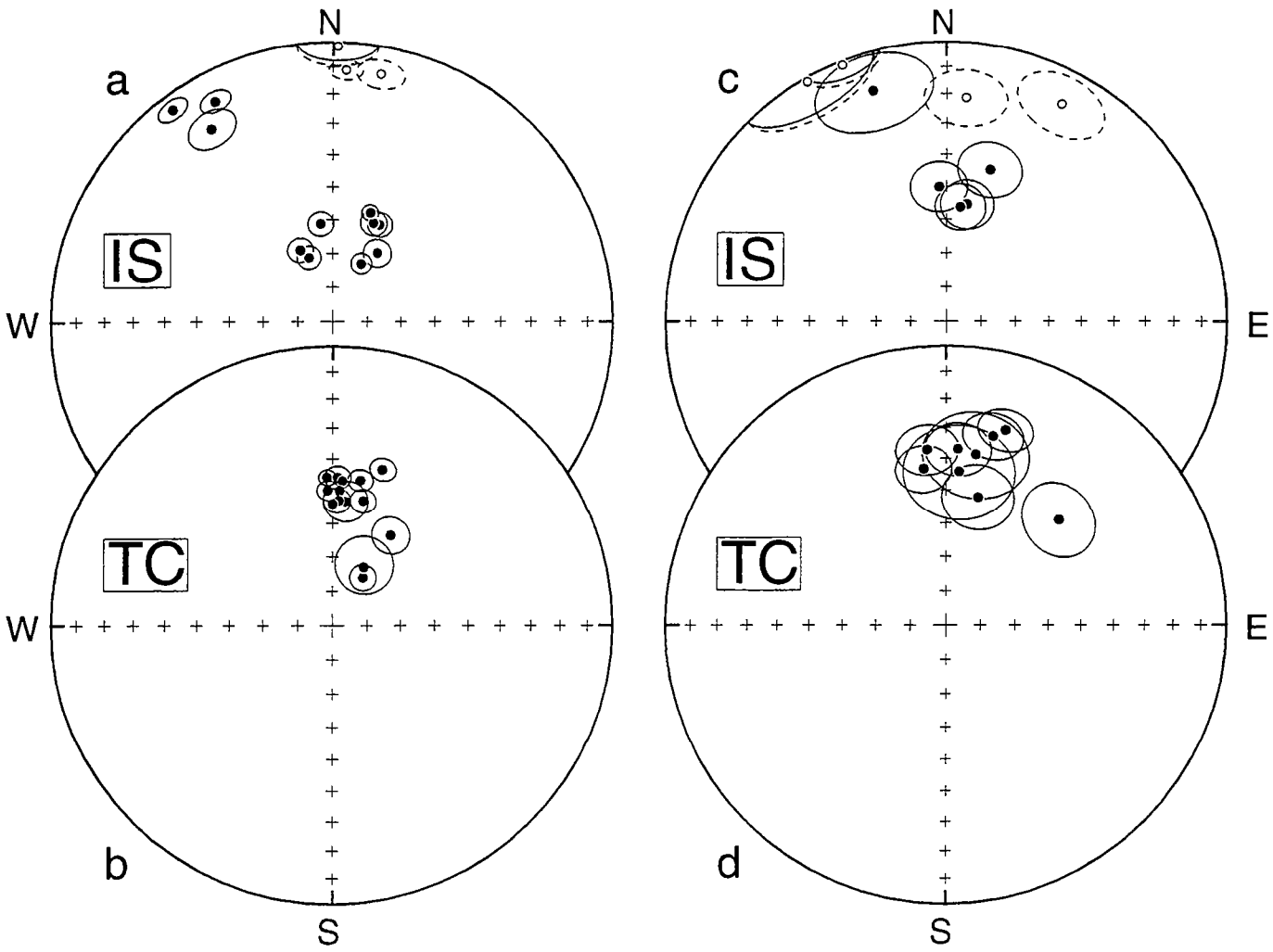

FIGURE 3. Cretaceous paleomagnetism of Tajikistan

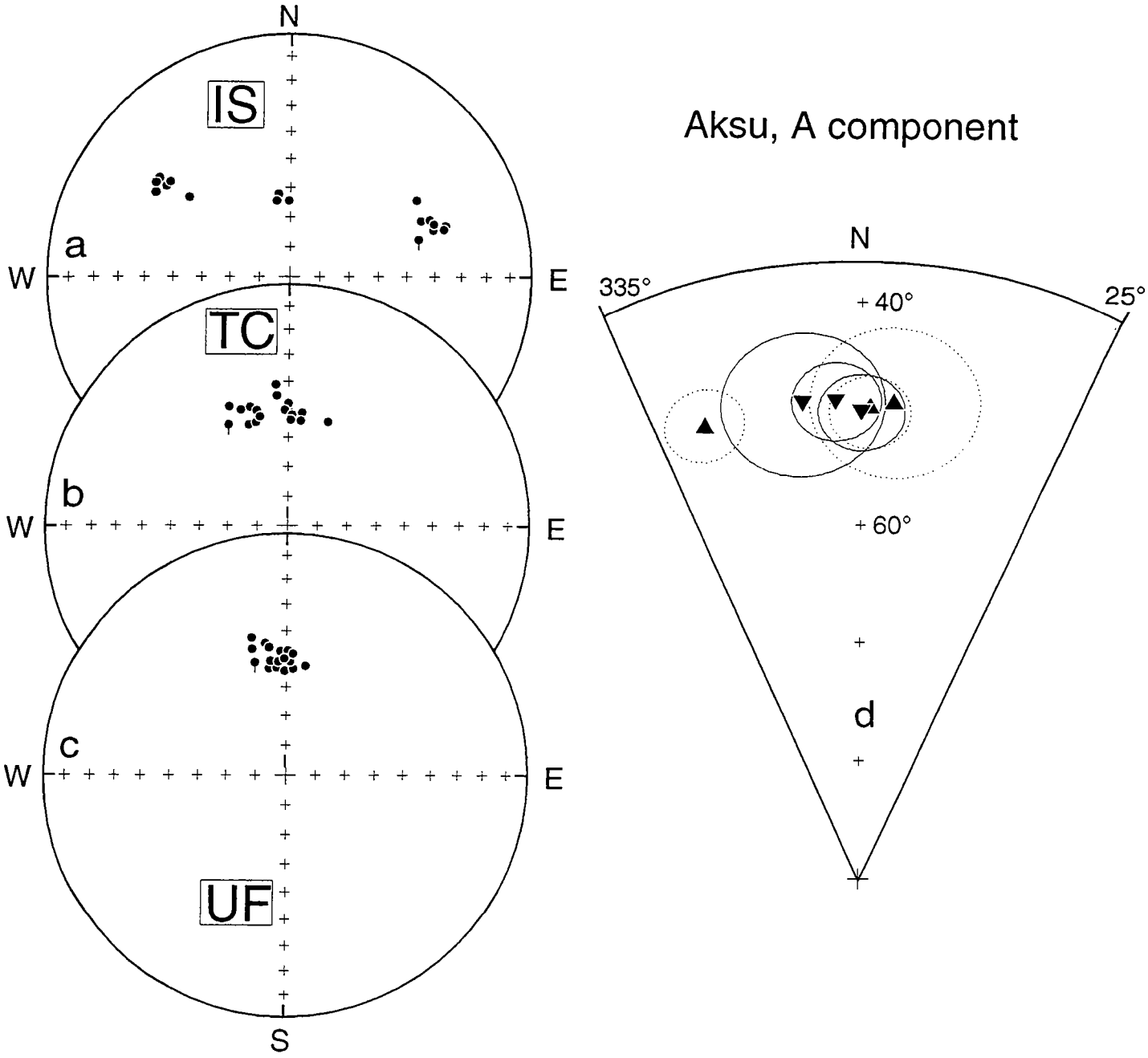

FIGURE 4. Cretaceous paleomagnetism of Tajikistan

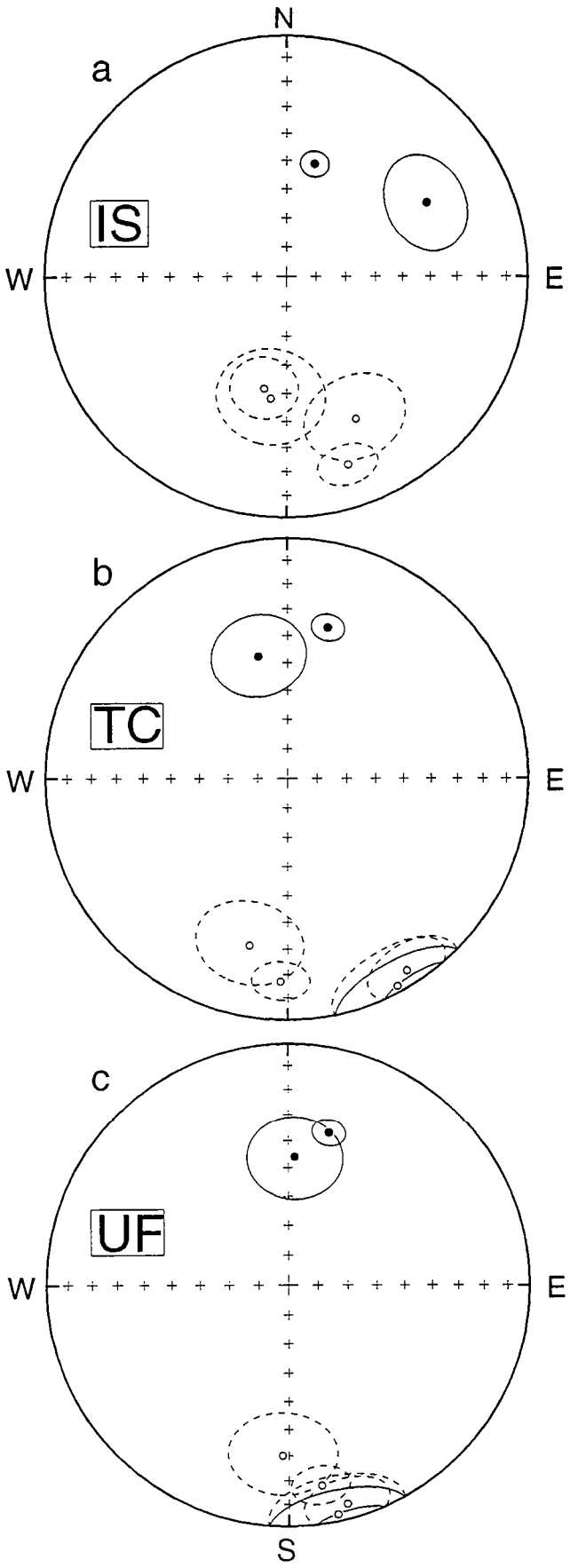

FIGURE 5. Cretaceous paleomagnetism of Tajikistan

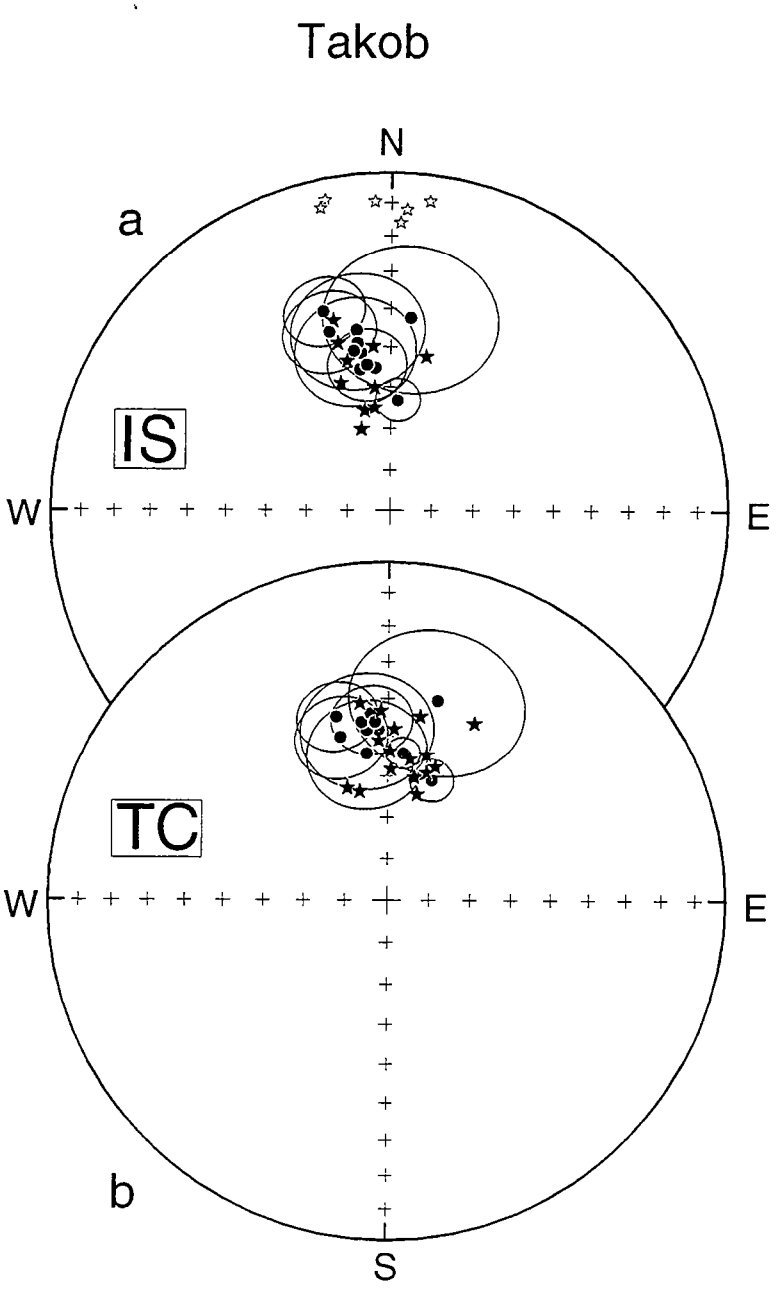

FIGURE 6. Cretaceous paleomagnetism of Tajikistan

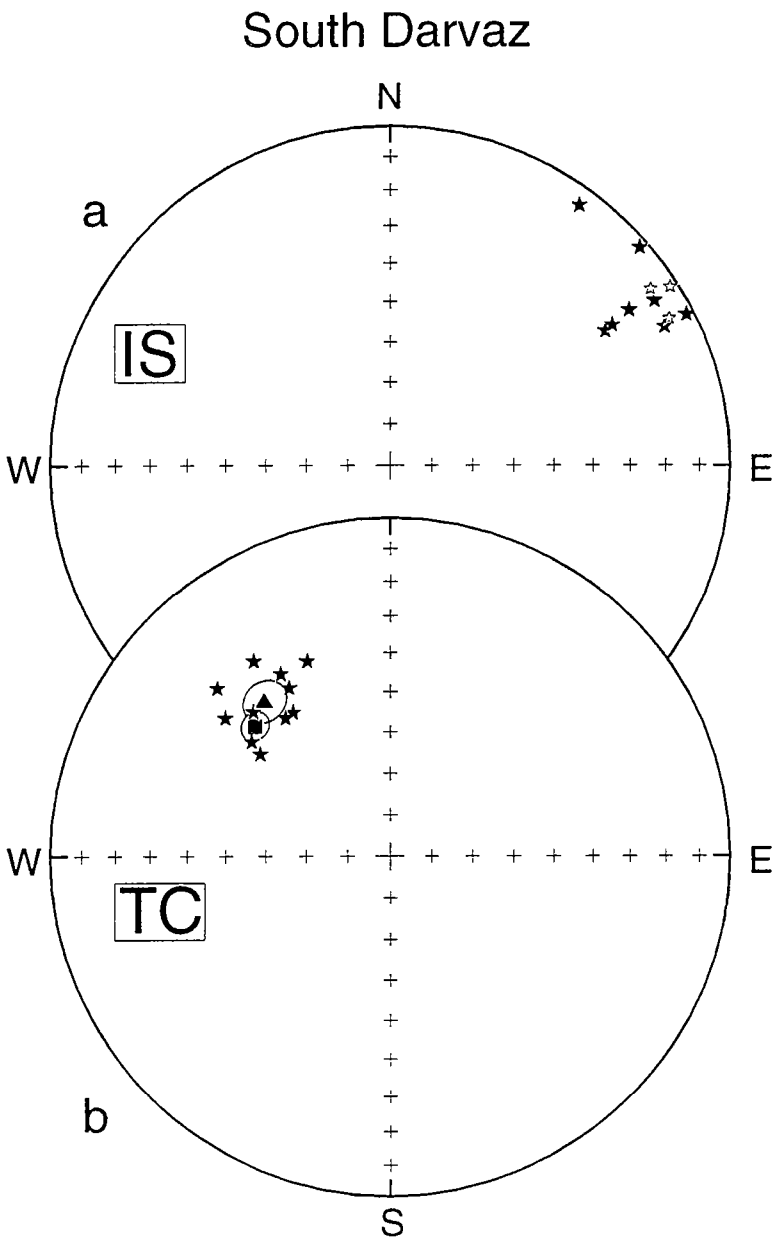

FIGURE 7. Cretaceous paleomagnetism of Tajikistan

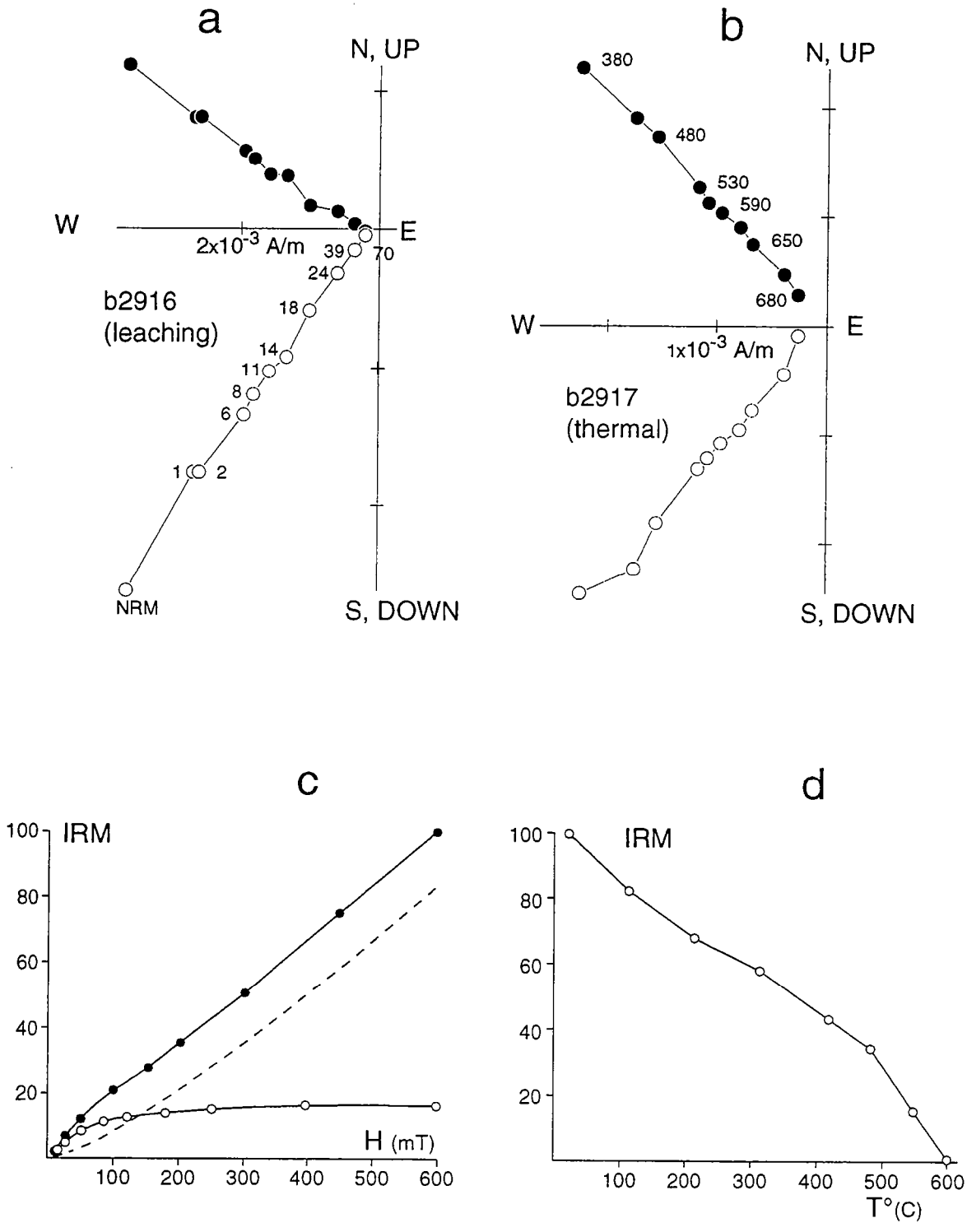

South Darvaz.

FIGURE 8 Cretaceous paleomagnetism of Tajikstan

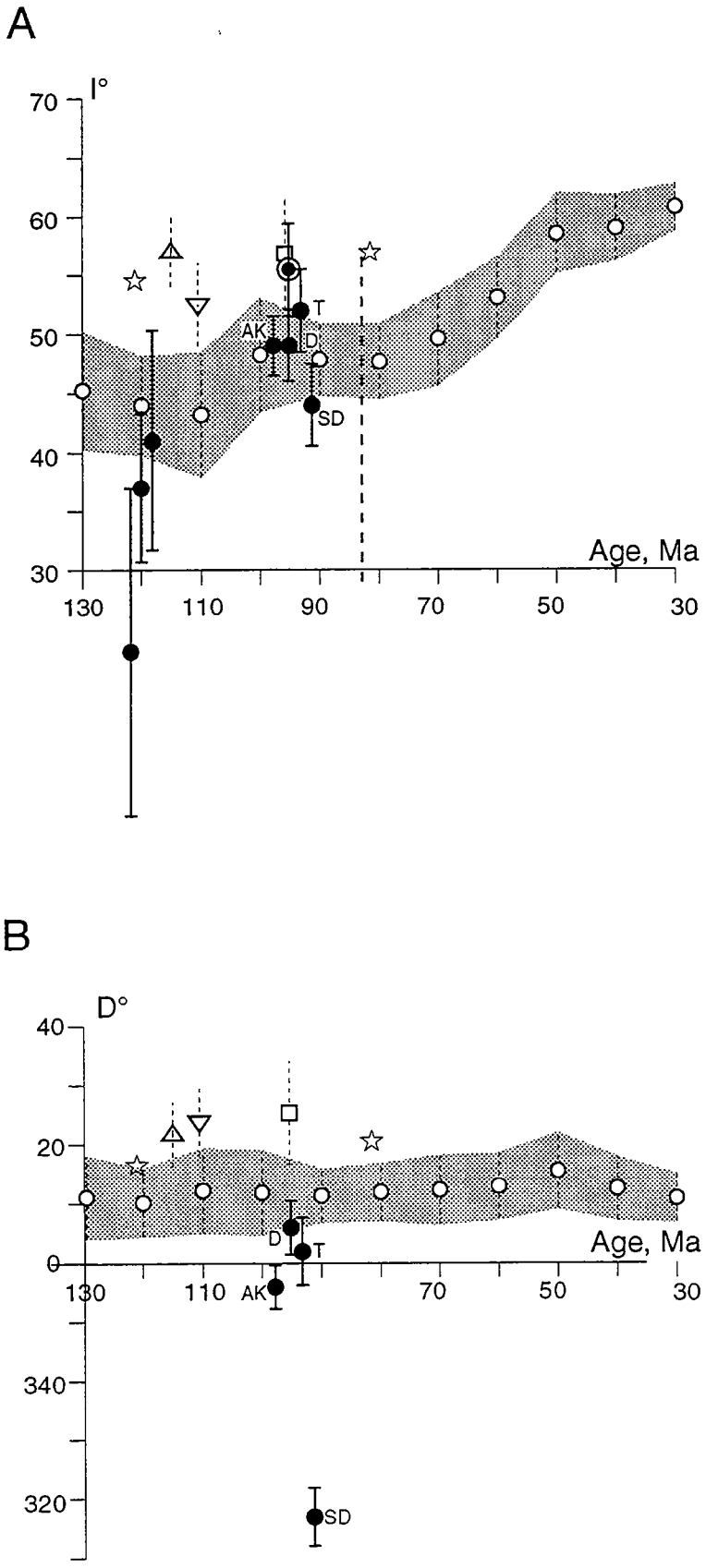

FIGURE 9. Cretaceous paleomagnetism of Tajikistan

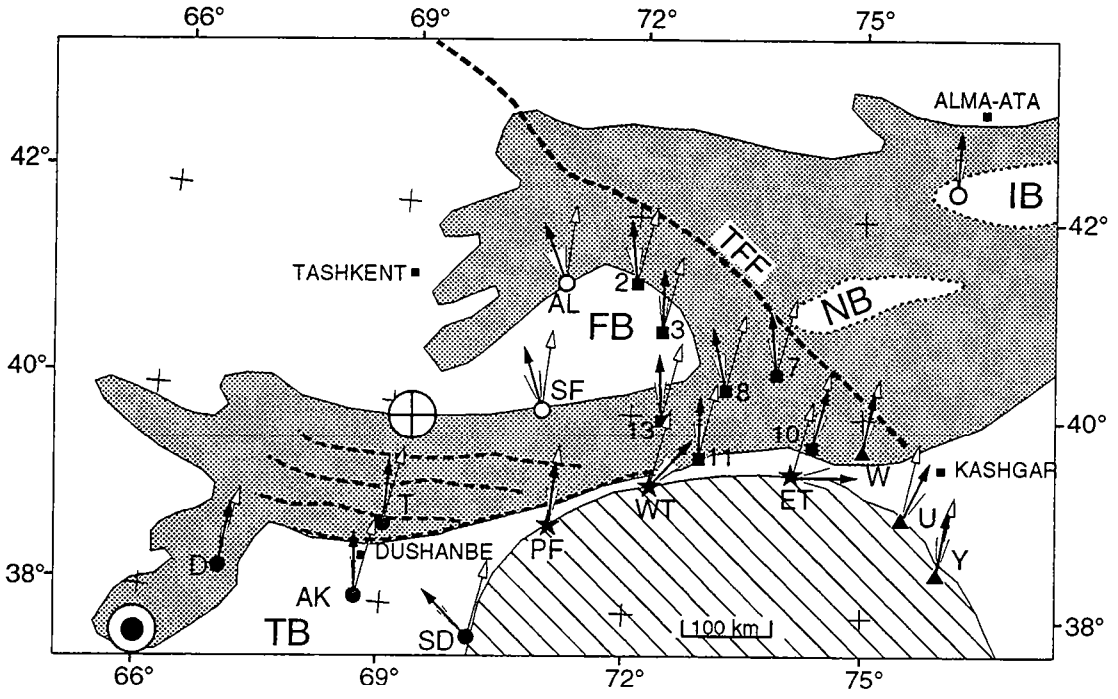

FIGURE 10. Cretaceous paleomagnetism of Tajikistan

ANNEXE III

Sedimentary basins and crustal thickening

Sedimentary Geology, 86 (1993) 77–89
Elsevier Science Publishers B.V., Amsterdam

Sedimentary basins and crustal thickening

P.R. Cobbold *, P. Davy, D. Gapais, E.A. Rossello, E. Sadybakasov, J.C. Thomas, J.J. Tondji Biyo and M. de Urreiztieta

Géosciences (CNRS), Université de Rennes, 35042 RENNES Cedex, France

Accepted April 20, 1993

ABSTRACT

Cobbold, P.R., Davy, P., Gapais, D., Rossello, E.A., Sadybakasov, E., Thomas, J.C., Tondji Biyo, J.C. and de Urreiztieta, M., 1993. Sedimentary basins and crustal thickening. In: S. Cloetingh, W. Sassi, F. Horvath and C. Puigdefabregas (Editors), Basin Analysis and Dynamics of Sedimentary Basin Evolution. Sediment. Geol., 86: 77–89.

We consider the development of sedimentary basins in a tectonic context dominated by horizontal shortening and vertical thickening of the crust. Well-known examples are foreland basins; others are ramp basins and buckle basins.

We have reproduced various styles of compressional basins in experiments, properly scaled for gravity. A multilayered model lithosphere, with brittle and ductile layers, floats on a model asthenosphere. A computer-driven piston provides shortening and thickening, synchronous with erosion and sedimentation. After a first stage of lithospheric buckling, thrust faults appear, mainly at inflection points. Slip on an isolated reverse fault is accompanied by flexure. Footwall flexure results in a foreland basin and becomes accentuated by sedimentation. Hangingwall flexure is less marked, but may become accentuated by erosion. Motion on a fault leads to hangingwall collapse at the surface. Either footwall sedimentation or hangingwall erosion tends to prolong the active life of a reverse fault. Slip on any pair of closely spaced reverse faults of opposite vergence results in a ramp basin. Simultaneous slip produces a symmetric ramp basin, whereas alternating slip results in a butterfly-shaped basin, with superposed foredeeps. Some well-developed ramp basins become pushed down, until bounding faults meet at the surface and the basin disappears from view. At this stage, the basin depth is equivalent to 15 km or more. Slip on any pair of widely spaced reverse faults of opposite vergence results in a pronounced central anticline, between two distinct foredeeps.

In Central Asia and in Western Europe, Cenozoic crustal thickening is due to continental collision. For Central Asia (Western China, Kyrgyzstan, Uzbekistan, Tajikistan), we have compiled a regional structure-contour map on the base of the Tertiary, as well as 4 regional sections. Foreland basins and ramp basins are numerous and associated with Cenozoic thrusts. Large basins (Tarim, Junggar, Fergana, Tajik) occur around and between mountain ranges, but smaller basins (Issyk-Kul, Naryn) occur within them. In Western Europe, the Alps and Pyrenees are surrounded by foreland basins, ramp basins or intermediate styles. In the Andes and its foreland, Neogene thrusts and compressional basins are due to subduction of oceanic lithosphere. In Colombia, they account for much of the Cordillera Oriental; in NW Argentina, for the Altiplano; in West-Central Argentina, for the Sierras Pampeanas. Compressional basins are also common in other areas of older crustal thickening.

Introduction

McKenzie (1978) developed a simple but powerful model for the formation of sedimentary basins, in a context of horizontal stretching and vertical thinning of the lithosphere. If thinning is rapid and vertically uniform, the reduction in fractional thickness of light continental crust, overlying heavier mantle material, results in immediate isostatic readjustment, with subsidence at the free surface and upwelling of deep mantle material. A second phase of subsidence then results from slow cooling of the upwelled material.

Later numerical models allow for realistic complications, such as flexure of the lithosphere (see Watts et al., 1982) and faults in the upper

* Corresponding author.

crust (see Kusznir and Ziegler, 1992). Thus motion on a single normal fault and associated flexure of both hangingwall and footwall result in a half rift (Fig. 1). The width of the half rift is proportional to the effective thickness of the bending layer. Although it is fashionable to speak of elastic behaviour, this is not strictly necessary for flexure. Permanent bending and large strains may follow upon plastic yield. A full rift results from motion on two closely spaced normal faults of opposite vergences (Fig. 1). The footwalls acquire tilted shoulders, whereas flexure is inhibited within the down-dropped hangingwall block, if it is short (Kusznir and Ziegler, 1992). Full rifts are probably better-known than half rifts, yet they may be less common. Recent work on the East African rift system has shown it to be a string of half rifts, with alternating vergences (Rosendahl et al., 1986; Kusznir and Ziegler, 1992).

For many years now it has been recognized that sedimentary basins can also form in a compressional context (horizontal shortening and vertical thickening of the crust), where there is faulting and associated flexure. A foreland basin (or half ramp, Fig. 1) forms by footwall flexure, under a single reverse fault or thrust (Beaumont, 1981; Allen and Homewood, 1986; Letouzey, 1990). Because of its association with a single fault, a foreland basin is analogous to a half rift. In a compressional context, the structure analogous to a full rift valley is a ramp valley (Willis, 1928). It forms by motion on two reverse faults of opposite vergences (Fig. 1). If the faults are closely spaced, footwall flexure is inhibited and the resulting ramp basin has a flat bottom. A few natural examples of ramp basins have been described (Bally, 1982; Mann et al., 1991), but the terminology is little known.

Other compressional basins may perhaps initiate by buckling alone, but the subject is controversial (Martinod, 1991;, Stephenson and Cloetingh, 1991). For elastic buckling, values of compressive stress are unrealistically large. Fluid buckling is inhibited by gravitational forces. Nevertheless buckling does occur in physical models, properly scaled for gravity, where a fluid asthenosphere is overlain by a multilayered lithosphere, containing an uppermost sand layer with Mohr-Coulomb frictional strength (Davy and Cobbold, 1988, 1991; Martinod, 1991; Martinod and Davy, 1992). Buckling is then due to the permanent strength of the sand layer, which increases with depth. If similar strength profiles hold for the upper crust, buckling stresses may be as high as

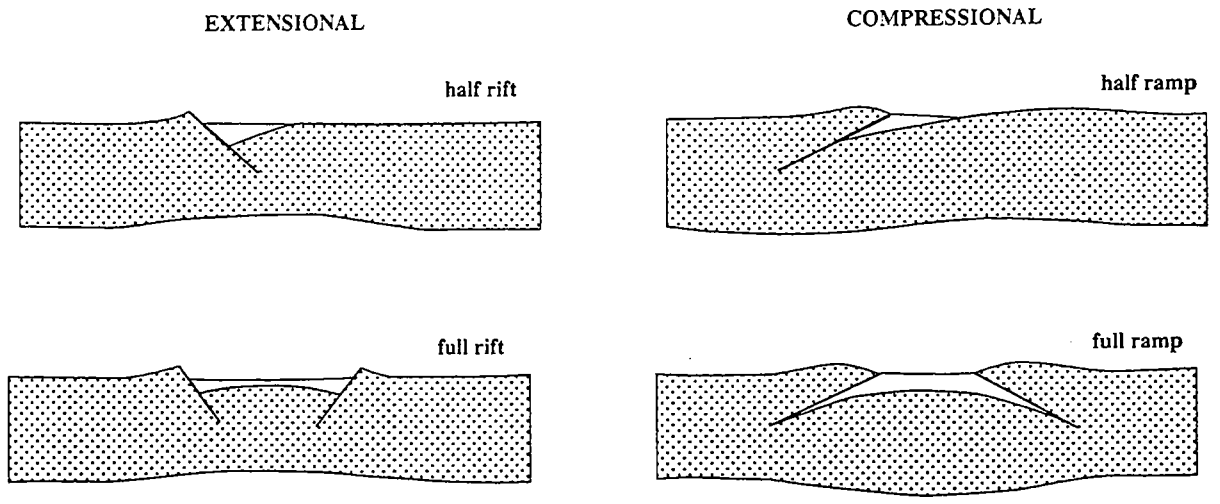

Fig. 1. Shape of sedimentary basins, according to tectonic context and number of bounding faults. Each basin is associated with either a single bounding fault (top), or with paired faults of opposite vergences (bottom). For extensional context (left), cross-sections of half rift or full rift (white) and of crust (stippled) are from the flexural cantilever models of Kusznir and Ziegler (1992, fig. 9). For compressional context (right), cross-sections of half ramp or full ramp and of crust are all schematic. Half ramp is another name for foreland basin.

100 MPa for continental lithosphere and 500 MPa for oceanic lithosphere (Stephenson and Cloetingh, 1991). Linearized theories of buckling then predict wavelengths of about 200 km for the whole lithosphere and about 30 km for the upper crust alone (Martinod, 1991; Martinod and Davy, 1992). Such wavelengths have indeed been observed, not only in physical models, but also in a few areas of oceanic and continental lithosphere (Martinod, 1991; Stephenson and Cloetingh, 1991; Burov et al., 1993a, b).

In early experiments with physical models, where the lithosphere contained both brittle and ductile layers, initial stages of buckling rapidly gave way to faulting. Thrust faults tended to initiate at the inflection points of earlier buckles. Motion on these faults led to the development of topographic lows, including foreland (half ramp) valleys and full ramp valleys (Davy and Cobbold, 1988, 1991; Martinod, 1991; Martinod and Davy, 1992) However, these features were far too small for detailed study and also there was no accompanying sedimentation or erosion.

In this paper, we first describe compressional basins obtained in more recent experiments, where we used larger physical models and incorporated sedimentation and erosion. Under these conditions, basins became much deeper. We then describe natural examples of compressional basins that we have studied in major areas of Cenozoic crustal thickening (Central Asia, Western Europe and the Andes). We compare the basin styles with those obtained in the physical models.

New physical models

We chose a length ratio of 7×10^5, so that a sedimentary basin, 7 km deep in nature, scaled down to 1 cm deep in a model. This was enough for proper observation of internal structures. We made our models 1 m long, to allow for serial formation of structures during progressive shortening (Fig. 2). To limit the volume and cost of model materials, we restricted model width to 30 cm. As a result, we had to pay particular attention to lateral boundary conditions, especially frictional resistance.

For proper scaling in a normal gravity field, the strength ratio must equal the product of the length ratio and the density ratio (Vendeville et al., 1987; Davy and Cobbold, 1988, 1991; Cobbold and Jackson, 1992). We chose a density ratio of 2.5. The strength ratio was therefore 1.8×10^6. Assuming that the upper crust obeys a Mohr-Coulomb yield criterion, where strength increases with depth, we modelled it using dry quartz sand, with a grain size of about 400 μm. This material has a very small cohesive strength and an angle of internal friction of about 40°. Its density of about 1.3 g cm^{-3} can be reduced by admixture of ethyl cellulose powder. Assuming that the lower crust is ductile, with an average effective viscosity of about 10^{20} Pa s, we modelled it using Silbione silicone putty (manufactured by Rhône-Poulenc, France). This material is an almost perfectly Newtonian fluid, with a viscosity of about 10^4 Pa s and a density of 1.16 g cm^{-3}. The viscosity ratio

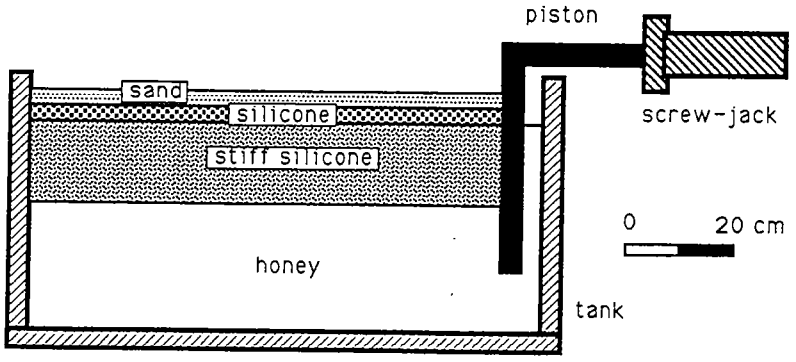

Fig. 2. Experimental apparatus and model in undeformed state. Longitudinal vertical section shows stratified model lithosphere (made of sand, silicone and stiff silicone) floating on model asthenosphere (honey). Lithosphere will shorten and thicken as piston advances (towards left), driven by screw jack.

was therefore 10^{16}. Together with the strength ratio, it set the time ratio at 10^{10}. To model the lithospheric mantle, we used a mixture of Silbione silicone putty and powdered galena, with a viscosity of 10^5 Pa s and a density of 1.3 g cm^{-3}. For the asthenosphere, we assumed linear viscous behaviour and modelled it using natural honey, with a viscosity of about 10^2 Pa s and a density of 1.35 g cm^{-3}. Our models were isothermal, with no allowance for the mechanical effects of thermal readjustments. They thus represented rapid tectonic deformations.

We built our models and deformed them within simple rectangular tanks with transparent plastic walls (Fig. 2). Before deformation, the model lithosphere floated stably upon the asthenosphere. Horizontal shortening was provided by a piston, driven by a computer-controlled screw-jack. Sidewall constraint resulted in thickening of the lithosphere. To render compressive stress as uniform as possible, we reduced friction at the sidewalls, by coating them with petroleum jelly. To prevent the petroleum jelly from percolating into the sand, we inserted between them thin sheets of silicone putty. To model syntectonic erosion, we episodically removed sand from topographic highs, using a vacuum cleaner fitted with a fine nozzle. To model sedimentation, we episodically sprinkled sand, by letting it fall freely from a container, as in an hour-glass. To model closed drainage systems, we deposited in topographic lows as much material as we eroded from topographic highs.

We have done about 30 experiments, for various initial thicknesses of lithospheric layers, rates of shortening and histories of sedimentation and

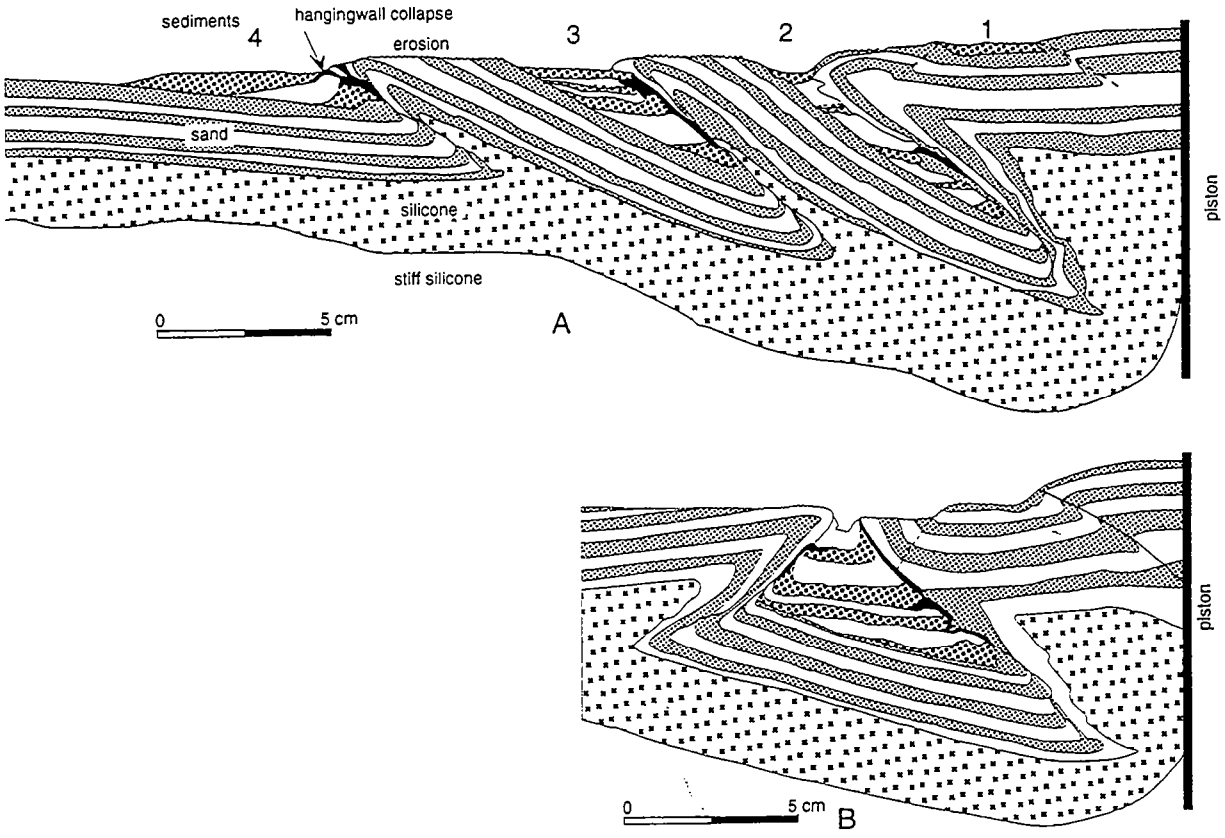

Fig. 3. Two models of compressional basins (final states). Model A shows crustal prism with stacked foreland basins, numbered (*1* to *4*) in order of appearance. Model B shows single ramp basin. Silicone (spaced crosses) represents ductile lower crust. Stratified sand layer (alternating fine stipple and white) represents brittle upper crust. It is offset across major reverse faults and truncated by hangingwall erosion (wavy lines). New sediments (alternating coarse stipple and white) were deposited intermittently within basins. Hangingwall collapse has resulted in footwall deposits (black).

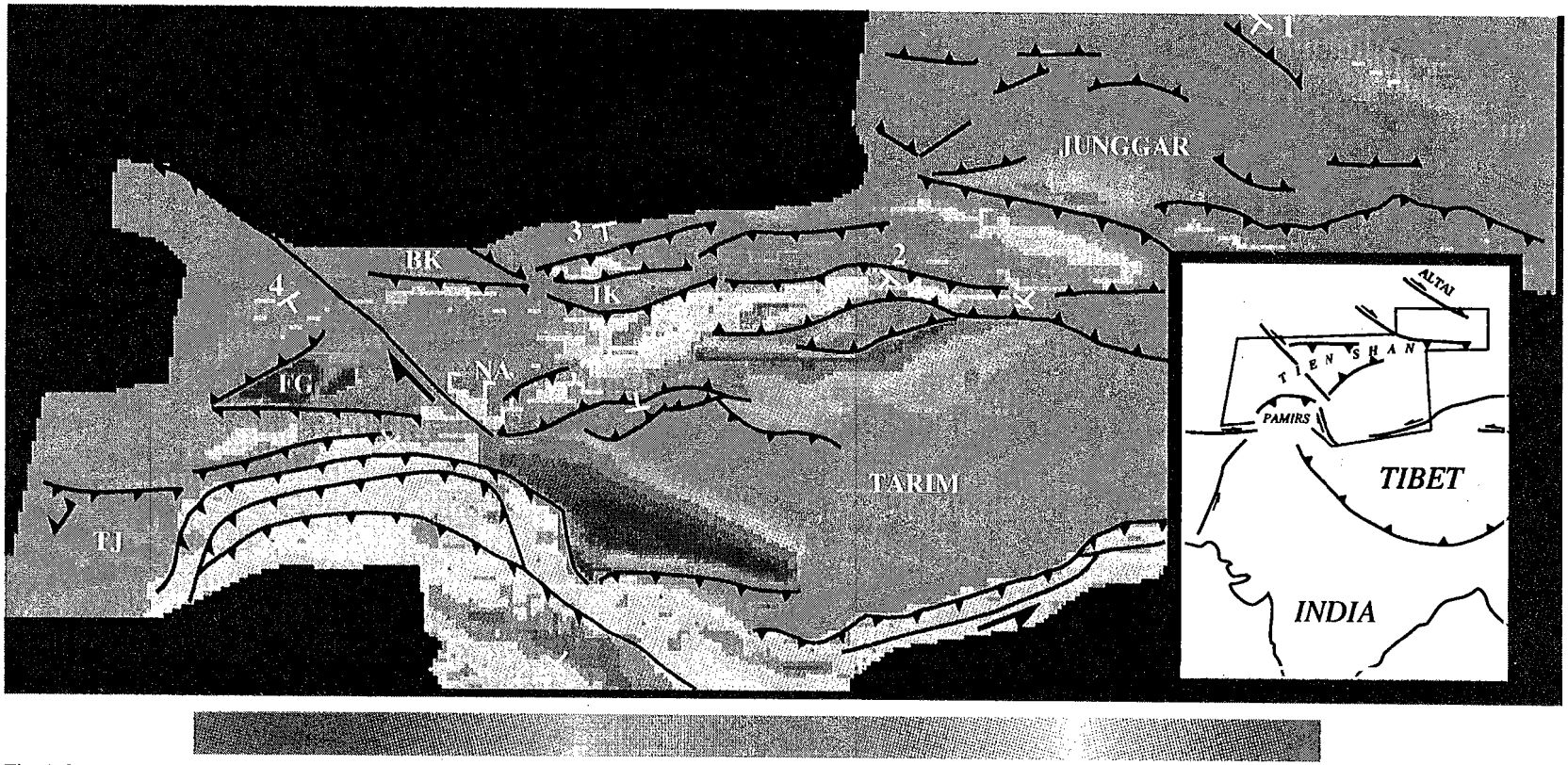

Fig. 4. Structure-contour map on base of Tertiary sequence, Central Asia. Inset map (right) shows general location and areas of high mountains (grey). Coloured map is digital, with pixels of 5′×5′, artificially coded for elevation above sea level (code bar ranges from −8 to +8 km). Projection is Mercator. Map covers most of Western China (Xinjiang), Kyrgyzstan, Uzbekistan and Tajikistan. It is based on published data (see references in text), new data of our own and data from A.B. Hayward (pers. commun., 1992). Major basins (labelled in white) are Tarim, Junggar, Fergana (*FG*), Issyk-Kul (*IK*), Tajik (*TJ*), Bishkeck (*BK*) and Naryn (*NA*). Basin-bounding faults of Cenozoic age (black traces) have reverse and strike-slip components (triangles point in approximate direction of underthrusting). Section lines (ends labelled *1* to *4*, in white) locate regional sections through major basins (Fig. 5).

erosion. Here we summarize our main observations, leaving a detailed description of the experiments to a companion paper (Tondji Biyo and Cobbold, in prep.).

(1) In all experiments, progressive shortening was accommodated by reverse faulting and associated flexure (Fig. 3), but in some experiments, we detected buckling at early stages.

(2) As in earlier experiments (Davy and Cobbold, 1988, 1991; Martinod, 1991; Martinod and Davy, 1992), faults developed serially, often at the inflection points of earlier buckles, but the location, spacing, vergence and timing of faults was also seen to be dependent upon the distribution of heterogeneities. Some of these we induced deliberately, by varying the initial structure; others resulted from involuntary imperfections in layer thicknesses, sand packing or boundary conditions.

(3) Slip on an isolated reverse fault was always accompanied by flexure. The strains were almost entirely anelastic. Footwall flexure resulted in a foreland basin and became accentuated by sedimentation (Fig. 3A). Hangingwall flexure was less marked, but became accentuated by erosion in some instances. Motion on the fault led to hangingwall collapse at the surface.

(4) Either footwall sedimentation or hangingwall erosion tended to prolong the active life of a reverse fault. One possible reason for this is that footwall loading or hangingwall unloading transmits laterally, over a distance dependent on the flexural resistance. Hence in most instances there is a reduction in the normal stress acting upon a fault surface. The frictional resistance then decreases and the fault slips more readily. Another reason is that erosion reduces the thickness of the uppermost brittle layer, which is the strongest layer in any model (Davy and Cobbold, 1991).

(5) In general, the model lithosphere thickened in a non-uniform way. Frequently, it adopted a somewhat tapered profile, with greatest thicknesses next to the piston (Fig. 3A). This we attribute to a longitudinal gradient in compressive stress, balancing a small amount of sidewall friction. In many experiments, crustal prisms grew, by serial formation of thrusts and associated foreland basins, in piggyback sequence. Older thrusts and basins became progressively tilted. Sediments reached depths of burial equivalent to 30 km or more.

(6) In some experiments, slip on any pair of closely spaced reverse faults of opposite vergence resulted in a ramp basin (Fig. 3B). Simultaneous slip produced a symmetric ramp basin, whereas alternating slip resulted in a butterfly-shaped basin, with superposed foredeeps (not illustrated).

(7) Some well-developed ramp basins became pushed down, by horizontal compression and sediment load, until the bounding faults met at the surface and the basin disappeared from surface view. At this stage, the basin depth was equivalent to 15 km or more (Fig. 3B).

(8) Slip on any pair of widely spaced reverse faults of opposite vergence resulted in a pronounced central anticline, between two distinct foredeeps.

(9) Sediment onlap caused many a reverse fault to relocate into a higher position within its hangingwall. Our explanation is that the increase in thickness caused an increase in strength at the first location, inhibiting fault motion.

Cenozoic examples

Central Asia

In Central Asia (Fig. 4), Cenozoic deformation occurs throughout an area of at least 2000 km by 2000 km. It has been attributed to indentation of Asia by India, following continental collision (Argand, 1924; Molnar and Tapponnier, 1975; England and Houseman, 1986; Cobbold and Davy, 1988; Dewey et al., 1989). Deformation includes both crustal thickening and lateral extrusion, but thickening is responsible for much of the current topography, especially the Tibetan plateau and the Pamir and Tien Shan mountains (Argand, 1924; England and Houseman, 1986). Between and around them are large basins, containing Cenozoic sediments.

For Western China (Xinjiang), Kyrgyzstan, Uzbekistan and Tajikistan, we have compiled a regional structure-contour map on the base of the Tertiary (Fig. 4). Across basins, we recorded the depth of Paleocene marine shelf sediments, or

Eocene shales, using seismic and borehole data. Across mountain ranges, we recorded the height of perched erosion surfaces, of Cretaceous to Palaeogene age (Sadybakasov, 1991; Cobbold et al., 1993). We also mapped major basin-bounding faults, finding them to have reverse and strike-slip components. From stratigraphic and structural relationships, we infer that crustal shortening and sedimentation operated together throughout the Cenozoic. The structure-contour map provides an immediate record of vertical motions since the Early Tertiary, when India collided with Asia. Provided the dips of thrust faults are known, the map provides a record of horizontal displacements as well. It can then be used for palinspastic restoration in map view, according to the method of Rouby et al. (1993a, b).

From the map and using the original data, we have also constructed regional sections through the major basins (Fig. 5). These show only the major faults and stratigraphic units (Cenozoic and Mesozoic). No attempts have been made, either to extrapolate major faults at depth, or to show details of thin-skinned detachments.

The largest basin in the region is Tarim (Figs. 4 and 5), with up to 8 km of continental Cenozoic sediments, mainly in marginal foredeeps, associated with reverse faults (Meyerhof and Willums, 1976; Lee, 1985; Tian et al., 1985; Lu, 1987; Watson et al., 1987; Nishidai and Berry, 1990; Windley et al., 1990; Graham et al., 1990; Allen et al., 1991; Wang et al., 1992). Uplift and erosion of the Tibetan plateau and Tien Shan mountains have provided the source material. The eastern Tarim is of symmetrical ramp-basin style. The western Tarim is a double foreland basin: there is a central uplift, where Pre-Cenozoic basement reaches the surface above a major Cenozoic thrust.

Almost as large is the Junggar basin, north of

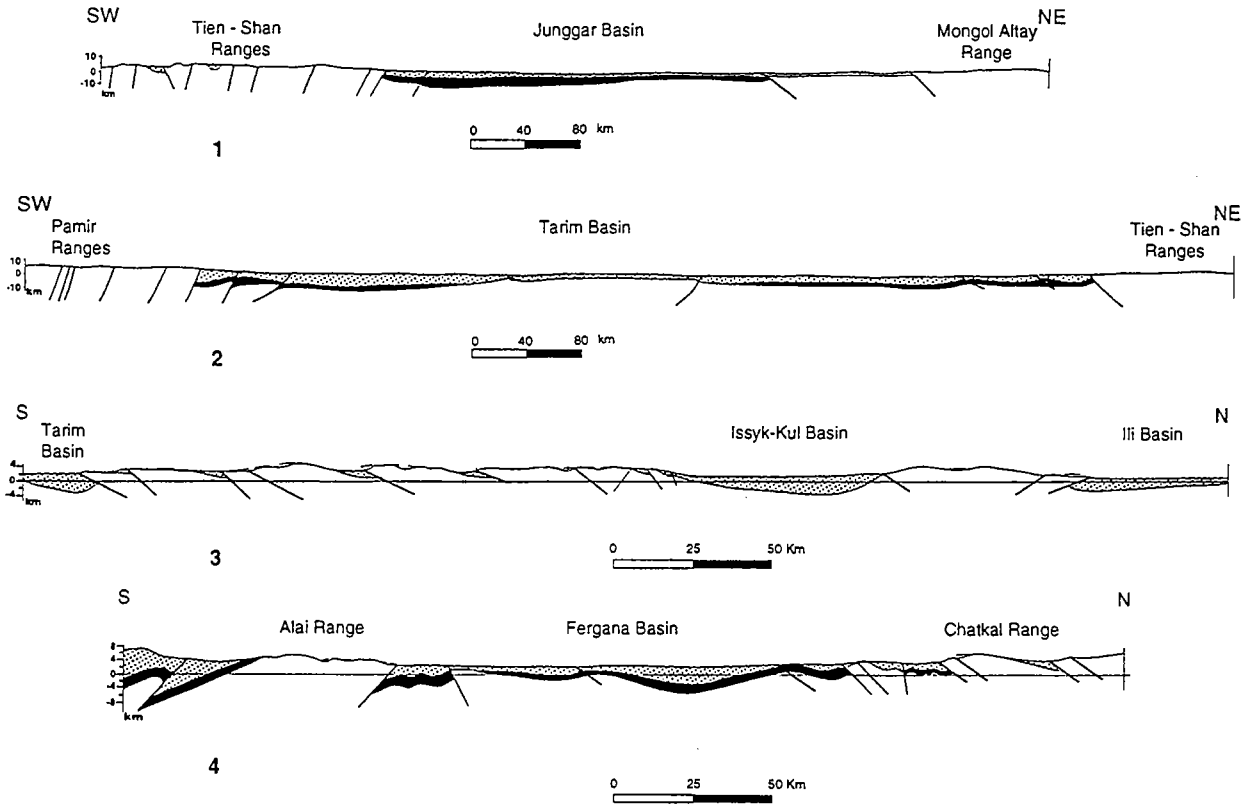

Fig. 5. Regional sections through Cenozoic basins of Central Asia. Sections are through major basins: Junggar (*1*), Tarim (*2*), Issyk-Kul and Ili (*3*) and Fergana (*4*). For section lines, see structure-contour map (Fig. 4). Sections show Cenozoic sediments (stippled), Mesozoic sediments (black), pre-Mesozoic basement (white), major reverse faults (continuous traces) and warped peneplain (dashed lines enveloping mountain ranges in sections *3* and *4*). In each section, vertical scale equals horizontal scale.

the Tien Shan (Figs. 4 and 5). This is mainly a foreland basin, associated with northward-verging boundary thrusts of the Tien Shan; but it is also bounded to the north by smaller faults with reverse and strike-slip components, at the edge of the Altai mountains (Meyerhof and Willums, 1976; Lu, 1987; Watson et al., 1987; Windley et al., 1990; Graham et al., 1990; Allen et al., 1991).

Around and within the western Tien Shan are smaller Cenozoic basins (Figs. 4 and 5), associated with crustal thickening and reverse faulting (Schulz, 1948; Kalvoda et al., 1987; Sadybakasov, 1991; Khain et al., 1991; Cobbold et al., 1993; Thomas et al., 1993). The basin style ranges from simple foreland to full ramp, with many intermediate or composite styles.

Fergana is a composite ramp basin (Figs. 4 and 5). The valley floor is mostly less than 400 m high, whereas the surrounding mountain ranges (Chatkal to the NW, Fergana to the NE, Alai to the S) reach 4000 m or more. On its western side, the basin contains up to 8 km of mainly Neogene sediment. Major reverse faults mark the edges of the basin, whereas minor ones offset the underlying basement (Cobbold et al., 1993). Although the position of the underlying Moho is not accurately known, a map based on detailed gravity measurements (every 5 min) shows a large negative gravity anomaly coinciding with the basin (Beekman et al., 1993). We infer that the Moho is depressed (as in Fig. 3B) and that the basin is not in local isostatic equilibrium, being loaded by surrounding mountain ranges.

Issyk-Kul (Figs. 4 and 5) is a simple, somewhat symmetric ramp basin, between parallel ranges of the Tien Shan (Cobbold et al., 1993). Tajik (Fig. 4) is a complex ramp basin, bounded on 4 sides by mountain ranges (Thomas et al., 1993). Bishkeck (Fig. 4) and Ili (Fig. 5) are foreland basins, next to northward-verging boundary thrusts of the Tien Shan (Cobbold et al., 1993). Naryn (Fig. 4) is a composite basin, spanning several reverse faults, both major and minor (Cobbold et al., 1993). On a smaller scale, all the western Tien Shan ranges contain small Cenozoic basins, associated with thrust faults (Figs. 4 and 5). Some of the ramp basins are partly, if not completely, hidden from surface view. Most boundary thrusts are active today. Late thrusts have usually appeared at the edges of ranges; but early thrusts, instead of being carried passively by new thrusts in piggy-back sequence, have had long active lifespans (Cobbold et al., 1993). Similar histories were observed in physical models (for example, Fig. 3A)

East of our structure-contour map, the entire Tibetan plateau (Fig. 4) appears to have grown northwards, by serial formation of reverse faults (Molnar, 1989). At its current northern edge are the Nan Shan mountains, with active boundary thrusts and an associated foreland basin. Well within the plateau is the Qaidam basin, bounded by conjugate thrusts of opposite vergences (Wang and Coward, 1990). The faults are still active today and Cenozoic sediments within the basin are being folded. Further south, the Tibetan plateau is higher and shortening is probably greater, but the deep crustal structure has not been sufficiently explored. Deep seismic profiling might show whether reverse faults at the surface hide Cenozoic basins at depth.

In conclusion, crustal thickening in Central Asia has involved large displacements on reverse faults, associated with basin development. Basin styles, ranging from foreland to ramp, are very similar to those obtained in physical models (Fig. 3). It is difficult to tell whether or not buckling (without faulting) has occurred in Central Asia. Martinod (1991) and Burov et al. (1993b) have analyzed topographic wavelengths, to see if they compare with those predicted by theory or experiment. We suggest that it would be more appropriate to consider, not current topography, but structure contours on the base of the Tertiary (Fig. 4). Even then, the contributions of reverse faults should be taken into account.

Western Europe

In Western Europe, Palaeogene crustal thickening (the Pyrenean phase) is probably due to collision of Africa with Eurasia, via Iberia, whereas Neogene crustal thickening (the Alpine phase) is probably due to collision of Adria with Eurasia.

All around the Western Alps, there are major

Cenozoic basins, associated with thrusts. The western Piemonte basin, with up to 10 km of Cenozoic sediments, is a major ramp basin, between boundary thrusts of the southern Alps (Roeder, 1990) and of the Apennines (Ricci Lucchi, 1986). At the surface, the Po plain is less than 200 m high; but below it, the seismic Moho sags to a maximal depth of 45 km, generating a negative gravity anomaly (Miletto and Polino, 1992). Apparently the basin is not in isostatic equilibrium, but held down in part by the weights of the hangingwalls (Alps and Apennines). The eastern Po plain and underlying Venetian basin have a similar, but less pronounced structure (Massari et al., 1986). The North Alpine basin of Switzerland contains up to 7 km of Cenozoic deposits. It is primarily a foreland basin, associated with the frontal Helvetic thrusts; but it also abutts against the backthrusted southern limb of the Jura mountains (Homewood et al., 1986; Pfiffner, 1986).

In Spain, the Ebro basin, with up to 3 km of Cenozoic sediments, is primarily a foreland basin, associated with southward-verging thrusts of the Pyrenees, but it is also bounded to the south by reverse faults of the Iberian range and the Catalan coastal range (Puigdefabregas et al., 1986; Casas-Sainz and Simon-Gomez, 1992).

Andes

The Andes lie along a convergent margin, where oceanic plates subduct eastwards beneath continental South America. So far, there is little evidence for continental collision in the Cenozoic, or even in the Mesozoic. The orogenic material has therefore been attributed mainly to plutonism, vulcanism and underplating of material along the subduction zone. Recent studies however have uncovered evidence for east–west shortening and crustal thickening, especially in the Neogene (see, for example, Jordan and Allmendinger, 1986; Baby et al., 1992)

We have compiled three sections (Fig. 6) using published data (Jordan and Allmendinger, 1986; Chebli and Spaletti, 1989; Butler and Schamel, 1988), supplemented by our own observations. The sections show that Cenozoic crustal thickening reaches well into the Andean foreland. Most of the thrusts are still active today.

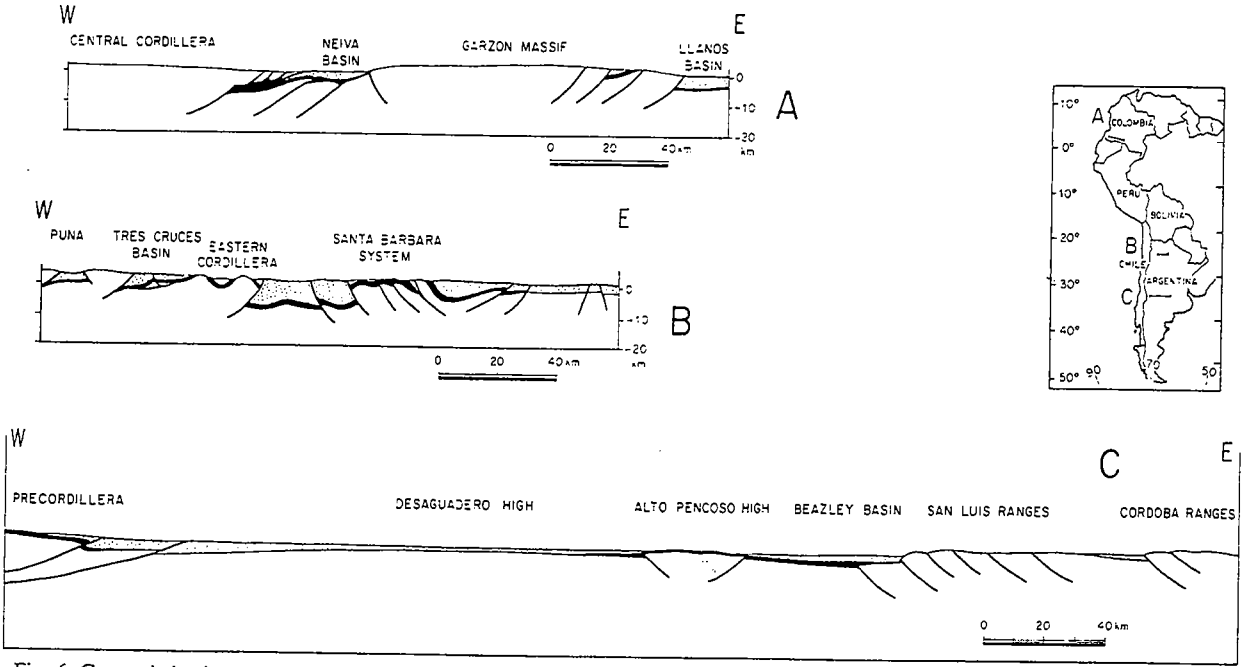

Fig. 6. Cenozoic basins and reverse faults in the Andes and their foreland. Inset map shows general location and lines of section. Sections A, B and C show Cenozoic sediments (stippled), Mesozoic sediments (black), pre-Mesozoic basement (white) and major reverse faults. For sources of data, see text.

In Colombia (Fig. 6A), the Magdalena–Neiva basin contains up to 5 km of Cenozoic sediments, trapped between boundary thrusts of the Cordillera Central and Cordillera Oriental (Butler and Schamel, 1988). Those of the Cordillera Central formed first and the basin is butterfly-shaped, as in analogue models. Towards the south, the boundary thrusts merge at the surface, hiding the basin beneath crystalline basement. This provides a good example of a hidden ramp basin. The Cordillera Oriental itself is a composite structure, spanning several major thrusts and minor Tertiary basins (Colletta et al., 1990). At its eastern edge, a fold-and-thrust belt bounds the Llanos foredeep, with its 4 km or more of continental Cenozoic sediments.

In northwestern Argentina (Fig. 6B), Bolivia and southern Peru, the high plateau (Altiplano) is a composite structure, where Cenozoic reverse faults separate basement ranges from intervening ramp basins, containing up to 10 km of Cenozoic continental sediments. Some of these ramp basins are almost hidden from surface view.

In west-central Argentina (Fig. 6C), the eastern edge of the Andean chain is a thrust belt, with its own foreland basin. Further east, the pre-Mesozoic basement has been uplifted as a series of ranges (Sierras Pampeanas), bounded by reverse faults. The ranges alternate with Cenozoic basins, ranging in style from foreland to ramp. This structural province reaches as far east as Cordoba, half way across the continent.

Pre-Cenozoic examples

Although these are often less amenable to study than Cenozoic ones, notable exceptions do occur.

In western China, continental sediments accumulated in asymmetric foredeeps (Fig. 5), against reverse faults of the Tien Shan ranges, not only during the Cenozoic, as documented above, but also during the Mesozoic (Hendrix et al., 1992). In general, crustal thickening and basin development seem to have occurred synchronously, throughout the entire period, since the Late Palaeozoic, when fragments of Gondwana were colliding and accreting with Eurasia.

Throughout the eastern foreland of the Rocky Mountains (Gries, 1990), thrusts of Laramide (Late Cretaceous) age are associated with well-preserved foreland basins (such as the Wind River) and ramp basins (such as the Big Horn). The structures probably formed in an Andean setting.

In southern Africa, Permo–Triassic sediments accumulated in the Karroo foredeep, next to northward-verging thrusts of the Cape Fold Belt (De Wit and Ransome, 1992). All the way from the Cape to the Zambezi River, basins alternate with basement highs. They may have formed in part by lithospheric buckling (Cobbold et al., 1992). Similar Late Palaeozoic basins are to be found on the other side of the Atlantic, in Brazil, Uruguay and Central Argentina (Cobbold et al., 1992). Once again, the setting was probably of Andean type.

How important are compressional basins?

Our field investigations have shown that sedimentary basins of various kinds have developed in all major areas of Cenozoic crustal thickening and in some areas of older thickening as well. Compressional basins formed in most of our experiments and we inferred that sedimentation and erosion provide mechanical aids to crustal thickening.

If so, why have relatively few examples of compressional basins been described so far? There are several possible reasons. First, the hangingwalls of emerging low-angle thrust faults tend to collapse easily, blurring the structural relationships at basin edges. Second, ongoing sedimentation may onlap and bury the hangingwalls, or scarp erosion may destroy them. Third, seismic images of basin edges may not be sharp, if footwall conglomerates contain few reflecting horizons, or if low-angle thrusts reflect and refract seismic waves, distorting or masking underlying reflectors. Fourth, well-developed ramp basins may become pushed down, out of sight of the surface geologist. Fifth, high plateaux are not the most obvious strategic targets for petroleum exploration. Sixth, Central Asia has long been one of the least accessible areas on Earth.

As these reasons disappear, we believe that more compressional basins will be discovered. They may become more important targets for oil exploration and they may influence the way geologists draw sections across areas of crustal thickening. There is a current tendency to assume a constant vergence for mountain chains, neglecting backthrusts. As deep seismic data accumulate, we believe that backthrusts and ramp basins will be given greater emphasis.

Foreland basins have been well studied and well modelled, numerically. Less is known about ramp basins and intermediate styles. As in our physical models, rates of subsidence for narrow ramp basins are likely to be high, because of additive contributions from paired bounding faults. Other aspects, remaining to be explored for ramp basins and intermediate styles, are thermal histories, migration pathways for hydrocarbons and internal traps, both structural and stratigraphic.

Acknowledgements

Fieldwork in Central Asia was funded by the CNRS (France) and the Academy of Sciences (ex-URSS), in Argentina by the INSU (France). The Institut Français du Pétrole and BP Exploration funded most of our physical modelling. We are grateful to Dr. R.H. Graham, Prof. N.J. Kusznir and Dr. B. Colletta for encouragement and helpful discussions.

References

Allen, M.B., Windley, B.F., Zhang, C., Zhao, Z-Y. and Wang, G-R., 1991. Basin evolution within and adjacent to the Tien Shan Range, NW China. J. Geol. Soc. London, 148: 369–378.

Allen, P.A. and Homewood, P. (Editors), 1986. Foreland basins. Int. Assoc. Sedimentol. Spec. Publ., 8, 453 pp.

Argand, E., 1924. La tectonique de l'Asie. Congrès Géologique International, Comptes Rendus de la XIII Session, Belgique, 1922, Premier fascicule, pp. 1–596.

Baby, P., Sempere, T., Oller, J. and Hérail, G., 1992. Evidence for major shortening on the eastern edge of the Bolivian Altiplano: the Calazaya nappe. In: R.A. Oliver, N. Vatin-Perignon and G. Laubacher (Editors), Andean Geodynamics. Tectonophysics, 205 (1–3): 155–169.

Bally, A.W., 1982. Musings over sedimentary basin evolution. Philos. Trans. R. Soc. London, A305: 325–338.

Beaumont, C., 1981. Foreland basins. Geophys. J.R. Astron. Soc., 65: 291–329.

Beekman, F., Burov, E.B., Cloetingh, S. and Bull, J.M., 1993. Folding of oceanic and continental lithosphere by the Indian–Eurasian collision: constraints from numerical modelling. European Union of Geosciences, 7th Meeting (EUG VII), Strasbourg, Abstr., p. 253.

Burov, E.B., Lobkovsky, L.I., Cloetingh, S. and Nikishin, A.M., 1993a. Continental lithosphere folding in Central Asia: constraints from tectonic modelling. European Union of Geosciences, Seventh Meeting (EUG VII), Strasbourg, Abstr., p. 255.

Burov, E.B., Lobkovsky, L.I., Cloetingh, S. and Nikishin, A.M., 1993b. Continental lithosphere folding in Central Asia (Part 2): constraints from tectonic modelling. Tectonophysics, in press.

Butler, K. and Schamel, S.J., 1988. Structure along the eastern margin of the Central Cordillera, Upper Magdalena Valley, Colombia. J. South Am. Earth Sci., 1: 109–120.

Casas-Sainz, A.M. and Simon-Gomez, J.L., 1992. Stress field and thrust kinematics: a model for the tectonic inversion of the Cameros Massif (Spain). J. Struct. Geol., 14: 521–530.

Chebli, G. and Spaletti, L. (Editors), 1989. Cuencas sedimentarias Argentinas. Univ. Nac. Tucuman, Tucuman, 512 pp.

Cobbold, P.R. and Davy, P., 1988. Indentation tectonics in nature and experiment, 2. Central Asia. Bull. Geol. Inst. Uppsala, N.S., 14: 143–162.

Cobbold, P.R. and Jackson, M.P.A., 1992. Gum rosin (colophony): a suitable material for thermomechanical modelling of the lithosphere. Tectonophysics, 210: 255–271.

Cobbold, P.R., Gapais, D., Rossello, E.R., Milani, E.J. and Szatmari, P., 1992. Permo–Triassic intracontinental deformation in SW Gondwana. In: M.J. de Wit and I.G.D. Ransome (Editors), Inversion Tectonics of the Cape Fold Belt, Karroo and Cretaceous Basins of Southern Africa. Balkema, Rotterdam, pp. 23–26.

Cobbold, P.R., Sadybakasov, E. and Thomas, J.C., 1993. Cenozoic basins and crustal thickening in the Kyrgyz Tien-Shan. In: F. Roure (Editor), Geodynamic Evolution of Sedimentary Basins. Ed. Technip, Paris, in press.

Colletta, B., Hébrard, F., Letouzey, J., Werner, P. and Rudkiewicz, J.-L., 1990. Tectonic style and crustal structure of the Eastern Cordillera (Colombia) from a balanced cross-section. In: J. Letouzey (Editor), Petroleum and Tectonics in Mobile Belts. Ed. Technip, Paris, pp. 81–100.

Davy, P. and Cobbold, P.R., 1988. Indentation tectonics in nature and experiment. 1. Experiments scaled for gravity. Bull. Geol. Inst. Uppsala, N.S., 14: 129–141.

Davy, Ph. and Cobbold, P.R., 1991. Experiments on shortening of a 4-layer model of the continental lithosphere. In: P.R. Cobbold (Editor), Experimental and Numerical Modelling of Continental Deformation. Tectonophysics, 188: 1–25.

Dewey, J.F., Cande, S. and Pitman, W.C., 1989. Tectonic evolution of the India/Eurasia collision zone. Eclogae Geol. Helv., 82: 717–734.

De Wit, M.J. and Ransome, I.G.D (Editors), 1992. Inversion Tectonics of the Cape Fold Belt, Karroo and Cretaceous Basins of Southern Africa. Balkema, Rotterdam, 269 pp.

England, P. and Houseman, G., 1986. Finite strain calculations of continental deformation, 2. Comparison with the India–Asia collision zone. J. Geophys. Res., 91: 3664–3676.

Graham, S.A., Brassell, S., Carroll, A.R., Xiao, X., Demaison, G., McKnight, C.L., Liang, Y., Chu, J. and Hendrix, M.S., 1990. Characteristics of selected petroleum source rocks, Xinjiang Uygur Autonomous Region, Northwest China. Am. Assoc. Pet. Geol. Bull., 74: 493–512.

Gries, R.R., 1990. Rocky Mountain foreland structures: changes in compression direction through time. In: J. Letouzey (Editor), Petroleum and Tectonics in Mobile Belts. Ed. Technip, Paris, pp. 129–148.

Hendrix, M.S., Graham, S.A., Carroll, A.R., Sobel, E.R., McKnight, C.L., Schulein, B.J. and Wang, Z., 1992. Sedimentary record and climatic implications of recurrent deformation in the Tian Shan: evidence from Mesozoic strata of the north Tarim, south Junggar and Turpan basins, northwest China. Geol. Soc. Am. Bull., 104: 53–79.

Homewood, P., Allen, P.A. and Williams, G.D., 1986. Dynamics of the Molasse Basin of western Switzerland. In: P.A. Allen and P. Homewood (Editors), Foreland Basins. Int. Assoc. Sedimentol. Spec. Publ., 8: 199–217.

Jordan, T.E. and Allmendinger, R.W.. 1986. The Sierras Pampeanas of Argentina, a modern analogue of Rocky Mountain foreland deformation. Am. J. Sci., 286: 737–764.

Kalvoda, J., Leonov, Yu.G. and Nikonov, A.A., 1987. Main features of the neotectonic evolution of the Pamirs–Thyan Shan and the Karakoram–Himalayas mountain ranges. Acta Montana, 77: 65–84.

Khain, V.E., Sokolov, B.A., Kleschev, K.A. and Shein, V.S., 1991. Tectonic and geodynamic setting of oil and gas basins in the Soviet Union. Am. Assoc. Pet. Geol. Bull., 75: 313–325.

Kusznir, N.J. and Ziegler, P., 1992. The mechanics of continental extension and sedimentary basin formation: a simple shear/pure shear flexural cantilever model. Tectonophysics, 215: 117–131.

Lee, K.Y., 1985. Geology of the Tarim Basin with special emphasis on petroleum deposits, Xinjiang Uygur Zizhiqu, Northwest China. U.S. Geol. Surv. Open-File Rep., 85–616, 55 pp.

Letouzey, J. (Editor), 1990. Petroleum and Tectonics in Mobile Belts. Ed. Technip, Paris, 209 pp.

Lu Banggan (Chief Editor), 1987. Typical Seismic Section Atlas of China. Petroleum Industry Press, Beijing, 260 pp.

Mann, P., McLaughlin, P.P. and Cooper, C., 1991. Geology of the Azua and Enriquillo basins, Dominican Republic, 2. Structure and tectonics. In: P. Mann, G. Draper and J.F. Lewis (Editors), Geologic and Tectonic Development of the North America–Caribbean Plate Boundary in Hispaniola. Geol. Soc. Am. Spec. Pap., 262: 367–389.

Martinod, J., 1991. Instabilités périodiques de la lithosphère (flambage, boudinage) en compression et en extension. Mémoires et Documents du Centre Armoricain d'Etudes Structurales des Socles, 44, 283 pp.

Martinod, J. and Davy, P., 1992. Periodic instabilities during compression or extension of the lithosphere, 1. Deformation modes from an analytical perturbation method. J. Geophys. Res., 97 (B2): 1999–2014.

Massari, F., Grandesso, P., Stefani, C. and Jobstraibizer, P.G., 1986. A small polyhistory foreland basin evolving in a context of oblique convergence: the Venetian basin (Chattian to Recent, Southern Alps, Italy). In: P.A. Allen and P. Homewood (Editors), Foreland Basins. Int. Assoc. Sedimentol. Spec. Publ., 8: 141–168.

McKenzie, D.P., 1978. Some remarks on the development of sedimentary basins. Earth Planet. Sci. Lett., 40: 25–32.

Meyerhof, A.A. and Willums, J.O., 1976. Petroleum geology and industry of the People's Republic of China. United Nations ESCAP-CCOP Tech. Bull., 10: 103–112.

Miletto, M. and Polino, R., 1992. A gravity model of the crust beneath the Tertiary Piemonte basin (northwestern Italy). Tectonophysics, 212: 243–256.

Molnar, P., 1989. The geological evolution of the Tibetan plateau. Am. Sci., 77: 350–360.

Molnar, P. and Tapponnier, P., 1975. Cenozoic tectonics of Asia: effects of a continental collision. Science, 189: 419–426.

Nishidai, T. and Berry, J.L., 1990. Structure and hydrocarbon potential of the Tarim Basin (NW China) from satellite imagery. J. Pet. Geol., 13: 35–58.

Pfiffner, O.A., 1986. Evolution of the north Alpine foreland basin in the Central Alps. In: P.A. Allen and P. Homewood (Editors), Foreland Basins. Int. Assoc. Sedimentol. Spec. Publ., 8: 219–228.

Puigdefabregas, C., Munoz, J.A. and Marzo, M., 1986. Thrust belt development in the eastern Pyrenees and related depositional sequences in the southern foreland basin. In: P.A. Allen and P. Homewood (Editors), Foreland Basins. Int. Assoc. Sedimentol. Spec. Publ., 8: 229–246.

Ricci Lucchi, F., 1986. The Oligocene to Recent foreland basins of the northern Apennines. In: P.A. Allen and P. Homewood (Editors), Foreland Basins. Int. Assoc. Sedimentol. Spec. Publ., 8: 105–139.

Roeder, D., 1990. Tectonics of South Alpine crust and cover (Italy). In: J. Letouzey (Editor), Petroleum and Tectonics in Mobile Belts. Ed. Technip, Paris, pp. 1–14.

Rosendahl, B.R., Reynolds, P.M., Lorber, P.M., Burgess, C.F., McGill, J.W., Scott, D., Lambiase, J.J. and Derksen, S.J., 1986. Structural expressions of rifting: lessons from Lake Tanganyika, Africa. In: L.E. Frostick, L.W. Renaut, I. Reid and J.J. Tiercelin (Editors), Sedimentation in the African Rifts. Geol. Soc. London Spec. Publ., 25: 27–38.

Rouby, D., Cobbold, P.R., Szatmari, P., Demercian, S., Coelho, D. and Rici, J.A., 1993a. Least-squares palinspastic restoration of regions of normal faulting. Application to the Campos basin (Brazil). Tectonophysics, in press.

Rouby, D., Cobbold, P.R., Szatmari, P., Demercian, S., Coelho, D. and Rici, J.A. 1993b. Restoration in plan view

of faulted Upper Cretaceous and Oligocene horizons and its bearing on the history of salt tectonics in the Campos Basin, Brazil. Tectonophysics, in press.

Sadybakasov, E., 1991. Neotectonics of High Asia. Nauka, Moscow, 181 pp.

Schultz, S.S., 1948. Analysis of the Neotectonics and Relief of the Tien Shan. Geografgiz, Moscow, 222 pp.

Stephenson, R.A. and Cloetingh, S.A.P.L., 1991. Some examples and mechanical aspects of continental lithospheric folding. Tectonophysics, 188: 27–37.

Thomas, J.C., Gapais, D., Cobbold, P.R., Meyer, V. and Burtman, V.S., 1993. Tertiary kinematics of the Tajik depression (Central Asia): inferences from fault and fold patterns. In: F. Roure (Editor), Geodynamic Evolution of Sedimentary Basins. Ed. Technip, Paris, in press.

Tian, Z., Chai, G. and Lin, L., 1985. Tectonic evolution of the Tarim Basin and its hydrocarbon potential. Oil Gas Geol., 6(3): 250–258 (in Chinese).

Vendeville, B., Cobbold, P.R., Davy, P., Brun, J.P. and Choukroune, P., 1987. Physical models of extensional tectonics at various scales. In: M.P. Coward, J.F. Dewey and P.L. Hancock (Editors), Continental Extensional Tectonics. Geol. Soc. London Spec. Publ., 28: 95–107.

Wang, Q. and Coward, M.P., 1990. The Chaidam Basin (NW China): formation and hydrocarbon potential. J. Pet. Geol., 13: 93–112.

Wang, Q.M., Nishidai, T. and Coward, M.P. 1992. The Tarim Basin, NW China. Formation and aspects of petroleum geology. J. Pet. Geol., 15(1): 5–34.

Watson, M.P., Hayward, A.B., Parkinson, D.N. and Zhang, Zh.M., 1987. Plate tectonic history, basin development and petroleum source rock deposition onshore China. Mar. Pet. Geol., 4: 205–225.

Watts, A.B., Karner, G.D. and Steckler, M.S., 1982. Lithospheric flexure and the evolution of sedimentary basins. Philos. Trans. R. Soc. London, A305: 249–281.

Willis, B., 1928. Dead Sea problem: rift valley or ramp valley? Geol. Soc. Am. Bull., 39: 490–542.

Windley, B.F., Allen, M.B., Zhang, C., Zhao, Z-Y. and Wang, G-R., 1990. Paleozoic accretion and Cenozoic redeformation of the Chinese Tien Shan range, central Asia. Geology, 18: 128–131.

ANNEXE IV

Données microtectoniques de la dépression Tadjik et de la Kirghizie

Dans cette annexe sont présentés les données microtectoniques de la dépression Tadjik et de la kirghizie utilisées dans les chapitre II.3 et III.3.

Les données sont présentées par localitée. Les résultats de la méthode inverse d'Etchecopar et al. (1981) sont indiqués lorsque celle ci a été utilisée ($\sigma1$ = direction principale de compression, Inclinaison/Déclinaison; $\sigma3$ = direction principale d'extension; R=Rapport des contraintes principales $\sigma2$-$\sigma3$/$\sigma1$-$\sigma3$).

Autres légendes :
N°: numéro de la faille; **PenF**: pendage du plan de faille; **AzF**: direction du pendage du plan de faille; **PlgS**: plogement de la strie; **DirS**: direction de la strie; **Mvt**: sens de la faille; **Com**: Commentaires (**n**: R.A.S, **M**: direction majeure, **?**: incertitude)

N° PenF AzF PlgS DirS Mvt Com

TUKAYNARON
01,89,090,05,179,S,n
02,35,001,35,001,N,n
03,35,001,35,350,N,n
04,20,110,17,145,I,M
05,89,070,01,160,S,n
06,70,265,62,219,N,n
07,20,235,08,165,D,n
08,85,290,01,020,D,n
09,64,270,52,320,N,n
10,30,160,18,212,I,n
11,62,260,54,302,I,n
12,78,275,78,275,I,n
13,60,090,48,140,I,n

KALINABAD
01,35,137,25,190,I,n
02,18,205,02,290,D,n
03,60,265,24,188,S,n
04,84,001,42,275,S,n
05,56,150,26,224,I,n
06,45,270,41,239,N,n
07,08,290,08,280,N,n
08,45,210,27,270,N,n
09,45,265,45,265,N,n
10,36,210,21,267,N,n
11,82,125,29,039,I,?
12,45,145,44,123,I,n
13,38,125,38,135,I,n
14,38,090,27,135,I,n
15,80,125,72,182,N,n

KAFIRNIGAN
01,40,288,39,270,N,n
02,60,290,59,280,N,n
03,62,265,62,270,N,n
04,75,294,62,352,N,n
05,32,275,29,245,N,n
06,42,290,41,299,N,n
07,45,234,44,240,N,n
08,76,056,71,100,N,?
09,57,096,57,090,I,n
10,60,085,56,115,I,n
11,30,227,29,240,N,n
12,45,120,45,110,I,n
13,89,050,89,050,N,n
14,25,105,24,115,I,n
15,45,115,44,120,I,n
16,70,098,70,100,I,n
17,40,227,40,235,N,n
18,50,090,49,080,I,n
19,60,080,60,080,I,n
20,20,245,20,235,N,n

N° PenF AzF PlgS DirS Mvt Com

AKSU
01,70,290,63,240,I,n
02,80,288,80,288,I,n
03,01,001,01,080,I,n
04,85,285,80,280,I,n
05,65,285,64,275,I,n
06,70,285,68,315,I,n
07,40,255,23,315,I,n
08,30,100,30,095,N,n
09,30,280,28,300,I,n
10,60,010,60,200,N,n
11,70,255,54,193,N,n

PULKHAKIM
01,37,295,35,305,I,n
02,10,245,08,300,I,n
03,75,260,15,347,S,n
04,38,260,24,325,S,n
05,68,230,01,140,S,n
06,30,235,19,290,S,n
07,73,090,19,175,S,n
08,85,217,10,128,S,n
09,75,145,20,058,D,n
10,01,270,01,115,S,n
11,85,145,30,056,D,n
12,89,245,00,155,S,n
13,34,260,32,290,I,n
14,10,315,10,296,I,n
15,25,320,26,300,I,n
16,01,260,01,115,D,n
17,35,090,35,095,N,n

DERBENT
01,40,340,40,328,I,n
02,67,040,38,328,D,n
03,90,350,20,260,D,n
04,90,350,60,260,D,n
05,75,060,74,070,D,n

DEKHANABAD
01,50,326,50,326,I,n
02,20,140,17,166,I,n
03,18,142,18,142,I,n
04,28,148,28,150,I,n
05,35,324,26,014,I,n
06,26,154,26,154,I,n
07,37,126,33,158,I,n
08,42,156,42,160,I,n
09,40,320,40,320,I,n

N° PenF AzF PlgS DirS Mvt Com

GHISSAR CARBONIFERE
01 , 50 , 345 , 33 , 286 , D , n
02 , 60 , 001 , 40 , 300 , D , n
03 , 60 , 180 , 37 , 245 , D , n
04 , 30 , 040 , 04 , 119 , D , n
05 , 75 , 225 , 56 , 162 , I , n
06 , 69 , 032 , 48 , 262 , I , n
07 , 24 , 150 , 23 , 130 , N , n
08 , 70 , 340 , 02 , 252 , D , n
09 , 90 , 225 , 35 , 135 , S , n
10 , 64 , 155 , 63 , 182 , N , n
11 , 20 , 335 , 15 , 296 , I , n
12 , 40 , 164 , 40 , 160 , N , n
13 , 62 , 001 , 30 , 289 , D , n
14 , 80 , 345 , 40 , 264 , D , M
15 , 85 , 350 , 31 , 269 , D , n
16 , 57 , 290 , 22 , 006 , S , n
17 , 48 , 277 , 20 , 347 , S , n
18 , 40 , 260 , 34 , 297 , I , n
19 , 52 , 350 , 52 , 350 , I , n
20 , 55 , 030 , 54 , 015 , I , n
21 , 57 , 340 , 26 , 268 , D , n
22 , 84 , 220 , 83 , 280 , N , n
23 , 28 , 330 , 25 , 304 , I , n
24 , 75 , 140 , 72 , 110 , N , n
25 , 90 , 140 , 40 , 230 , S , n
26 , 60 , 043 , 34 , 336 , D , n
27 , 78 , 005 , 38 , 283 , D , n
28 , 75 , 320 , 11 , 047 , S , n
29 , 52 , 310 , 51 , 320 , I , n
30 , 63 , 215 , 58 , 264 , D , n
31 , 25 , 292 , 25 , 288 , N , n
32 , 75 , 030 , 15 , 116 , D , n
33 , 60 , 290 , 45 , 345 , I , n
34 , 77 , 325 , 76 , 001 , I , n
35 , 69 , 295 , 66 , 330 , I , n
36 , 37 , 310 , 35 , 286 , I , n

GHISSAR CRETACE
01 , 60 , 112 , 60 , 102 , N , n
02 , 90 , 118 , 72 , 028 , S , n
03 , 74 , 194 , 70 , 230 , I , n
04 , 47 , 150 , 42 , 115 , I , n
05 , 75 , 120 , 52 , 050 , I , n
06 , 85 , 128 , 64 , 212 , I , n
07 , 56 , 298 , 54 , 324 , I , n
08 , 53 , 252 , 13 , 330 , S , n
09 , 43 , 304 , 03 , 217 , D , n
10 , 60 , 290 , 38 , 353 , D , n
11 , 58 , 145 , 18 , 074 , D , n
12 , 20 , 090 , 14 , 140 , N , n
13 , 75 , 050 , 34 , 331 , S , n
14 , 22 , 064 , 09 , 125 , N , n
15 , 50 , 350 , 26 , 284 , D , n
16 , 85 , 100 , 50 , 014 , I , n
17 , 61 , 161 , 60 , 184 , I , n

N° PenF AzF PlgS DirS Mvt Com

Donnes microtectoniques pour la Kirghizie

FERGANA
01 , 50 , 002 , 45 , 014 , I , n
02 , 45 , 350 , 45 , 350 , I , n
03 , 84 , 073 , 24 , 335 , D , n
04 , 72 , 136 , 09 , 050 , S , n
05 , 80 , 059 , 22 , 335 , D , n
07 , 82 , 019 , 29 , 286 , D , n
08 , 84 , 056 , 18 , 325 , D , n
09 , 64 , 014 , 52 , 345 , I , n
10 , 89 , 052 , 26 , 322 , D , n
11 , 39 , 341 , 37 , 358 , I , n
12 , 89 , 059 , 29 , 329 , D , n
13 , 78 , 151 , 03 , 061 , S , n
14 , 42 , 338 , 42 , 336 , I , n
15 , 67 , 152 , 13 , 232 , S , n
16 , 68 , 155 , 01 , 065 , S , n
17 , 89 , 255 , 10 , 355 , D , n

$\sigma 1$=345°/16° $\sigma 3$=92°/46° R=0.14
Histogramme des écarts angulaires entre stries théoriques et stries mesurées
0°-6° : 15 12 11 2
6°-11° : 10 4 3
11°-17° : 8
17°-23° : 14 1 917 13
29°-34° : 5 16
52°-57° : 7

CHATKAL OUEST
01 , 50 , 002 , 45 , 032 , I , n
02 , 45 , 350 , 45 , 350 , I , n
03 , 84 , 073 , 24 , 345 , D , n
04 , 72 , 136 , 50 , 068 , S , n
05 , 80 , 059 , 22 , 335 , D , n
06 , 82 , 019 , 29 , 286 , D , n
07 , 84 , 056 , 18 , 328 , D , n
08 , 62 , 014 , 52 , 330 , I , n
09 , 89 , 052 , 26 , 322 , D , n
10 , 39 , 341 , 37 , 358 , I , n
11 , 89 , 059 , 29 , 329 , D , n
12 , 78 , 151 , 03 , 061 , S , n
13 , 42 , 338 , 42 , 336 , I , n
14 , 67 , 152 , 13 , 244 , S , n
15 , 68 , 155 , 01 , 065 , S , n
16 , 89 , 255 , 10 , 345 , D , n

$\sigma 1$=352°/15° $\sigma 3$=85°/10° R=0.1
Histogramme des écarts angulaires entre stries théoriques et stries mesurées
0°-6° : 10 7 2
6°-11° : 8 16 14
11°-17° : 12 11 9 15 3
17°-23° : 5 13

29°-34° : 1
46°-52° : 4
57°-69° : 6

N° PenF AzF PlgS DirS Mvt Com

CHATKAL OUEST-DECROCHEMENTS
01 , 84 , 073 , 24 , 335 , D , n
02 , 72 , 136 , 09 , 050 , S , n
03 , 80 , 059 , 22 , 335 , D , n
04 , 82 , 019 , 29 , 286 , D , n
05 , 84 , 056 , 18 , 325 , D , n
06 , 89 , 059 , 29 , 329 , D , n
07 , 89 , 255 , 10 , 345 , D , n
08 , 78 , 151 , 09 , 061 , S , n
09 , 78 , 155 , 01 , 065 , S , n

σ1=198°/16° σ3=289°/7° R=0,99
Histogramme des écarts angulaires entre stries théoriques et stries mesurées
0°-6° : 4 9 8
6°-11° : 6 7
11°-17° : 5 1
29°-34° : 3 2

CHATKAL OUEST-FAILLES INVERSES
01 , 50 , 002 , 45 , 014 , I , n
02 , 45 , 350 , 45 , 350 , I , n
03 , 62 , 014 , 52 , 345 , I , n
04 , 39 , 341 , 37 , 358 , I , n
05 , 42 , 338 , 42 , 336 , I , n

CHATKAL EST
01 , 84 , 271 , 09 , 184 , D , n
02 , 66 , 313 , 04 , 038 , D , n
03 , 78 , 329 , 07 , 239 , S , n
04 , 88 , 158 , 10 , 068 , S , n
05 , 83 , 274 , 23 , 178 , D , n
06 , 52 , 344 , 01 , 044 , S , n
07 , 65 , 188 , 10 , 274 , S , n
08 , 75 , 250 , 25 , 174 , D , n
09 , 85 , 198 , 08 , 104 , S , n

σ1=54°/7° σ3=145°/7° R=0,12
Histogramme des écarts angulaires entre stries théoriques et stries mesurées
0°-6° : 8 9 2 7 3
6°-11° : 10 4 5
11°-17° : 1

N° PenF AzF PlgS DirS Mvt Com

TALAS
01 , 84 , 024 , 21 , 112 , D , n
02 , 69 , 018 , 04 , 106 , D , n
03 , 81 , 353 , 01 , 083 , D , n
04 , 79 , 041 , 02 , 131 , D , n
05 , 67 , 082 , 08 , 175 , S , n
06 , 65 , 019 , 05 , 291 , D , n
07 , 87 , 150 , 20 , 239 , S , n
08 , 88 , 302 , 03 , 032 , S , n
09 , 90 , 002 , 06 , 272 , D , n
10 , 61 , 016 , 02 , 105 , D , n
11 , 60 , 022 , 02 , 112 , D , n
12 , 61 , 345 , 04 , 256 , D , n

σ1=155°/2° σ3=64°/24° R=0.57
Histogramme des écarts angulaires entre stries théoriques et stries mesurées
0°-6° : 3 10
6°-11° : 7 2
11°-17° : 1 8 9 6
23°-29° : 4
34°-40° : 5
69°-80° : 1 12

TALAS-FAILLES PLIOCENE
01 , 44 , 324 , 20 , 028 , I , n
02 , 17 , 241 , 17 , 241 , I , n
03 , 30 , 245 , 30 , 245 , I , n
04 , 38 , 201 , 31 , 145 , I , n
05 , 19 , 199 , 19 , 199 , I , n

NARYN SUD-OUEST
01 , 58 , 093 , 20 , 172 , D , n
02 , 51 , 119 , 02 , 030 , D , n
03 , 41 , 078 , 01 , 352 , D , n
04 , 79 , 118 , 26 , 204 , D , n
05 , 83 , 152 , 15 , 232 , S , n
06 , 79 , 120 , 01 , 030 , D , n
07 , 52 , 072 , 08 , 349 , D , n

σ1=240°/32° σ3=71°/57° R=0.4
Histogramme des écarts angulaires entre stries théoriques et stries mesurées
0°-6° : 1 5
6°-11° : 1
11°-17° : 2 7
17°-23° : 5 4 3 6
29°-34° : 6 1
40°-46° : 7 2

NARYN NORD-OUEST
01 , 62 , 289 , 09 , 208 , D , n
02 , 71 , 318 , 02 , 048 , D , n
03 , 79 , 340 , 03 , 070 , S , n
04 , 62 , 009 , 05 , 099 , S , n
05 , 65 , 315 , 01 , 045 , D , n

06 , 49 , 298 , 14 , 222 , D , n
07 , 57 , 352 , 21 , 070 , S , n
08 , 40 , 002 , 01 , 092 , S , n

$\sigma 1$=63°/4° $\sigma 3$=154°/15° R=0.15
Histogramme des écarts angulaires entre stries théoriques et stries mesurées
0°-6° : 5 2 3
6°-11° : 6 8
11°-17° : 1 4
17°-23° : 7

MEMOIRES DE GEOSCIENCES-RENNES
Universite de Rennes I - Campus de Beaulieu
35042 - RENNES Cedex tel : 99.28.60.80

Dans la même collection :

N°1 - **H. MARTIN** - Nature, origine et évolution d'un segment de croûte continentale archéenne : contraintes chimiques et isotopiques. Exemple de la Finlande orientale. **392 p., 183 fig., 51 tabl., 4 pl. (1985).** **Epuisé**

N°2 - **G. QUERRE** - Palingénèse de la croûte continentale à l'archéen les granitoïdes tardifs (2,5-2,4 Ga) de Finlande Orientale. Pétrologie et géochimie. **226 p., 74 fig., 41 tabl., 3 pl. (1985).** **85F.**

N°3 - **J. DURAND** - Le Grès Armoricain. Sedimentologie. Traces fossiles. Milieux de depôt. **150 p., 76 fig., 9 tabl., 19 pl. (1985).** **Epuisé**

N°4 - **D. PRIOUR** - Genèse des zones de cisaillement : Application de la méthode des éléments finis à la simulation numérique de la déformation des roches. **157 p., 106 fig., 7 tabl., (1985).** **55F.**

N°5 - **V. NGAKO** - Evolution métamorphique et structurale de la bordure sud-ouest de la "série de Poli". Segment camerounais de la chaîne panafricaine. **185 p., 76 fig., 16 tabl., 12 pl. (1986).** **Epuisé**

N°6 - **J. DE POULPIQUET** - Etude géophysique d'un marqueur magnétique situé sur la marge continentale sud-armoricaine. **159 p., 121 fig., 5 tabl. (1986).** **55F.**

N°7 - **P. BARBEY** - Signification géodynamique des domaines granulitiques. La ceinture des granulites de Laponie : une suture de collision continentale d'âge Protérozoique inférieur (1.9-2.4 Ga). **324 p., 89 fig., 46 tabl., 11 pl. (1986).** **Epuisé**

N°8 - **Ph. DAVY** - Modélisation thermo-mécanique de la collision continentale. **233 p., 72 fig., 2 tabl. (1986).** **Epuisé**

N°9 - **Y. GEORGET** - Nature et origine des granites peralumineux a cordiérite et des roches associées. Exemples des granitoides du Massif Armoricain (France) : Petrologie et geochimie. **250 p., 140 fig., 67 tabl., (1986).** **Epuisé**

N°10 - **D. MARQUER** - Transfert de matière et déformation progressive des granitoides. Exemple des massifs de l'Aar et du Gothard (Alpes centrales Suisses). **287 p., 134 fig., 52 tabl., 5 cartes hors-texte (1987).** **120 F.**

N°11 - J.S. SALIS -Variation séculaire du champ magnétique terrestre. Direction et Paléointensité sur la période 7.000 70.000 BP dans la chaîne des Puys. **190 p., 73 fig., 28 tabl., I carte hors-texte (1987).** **90F.**

N°12 - Y. GERARD - Etude expérimentale des interactions entre déformation et transformation de phase. Exemple de la transition calcite-aragonite. **126 p., 42 fig., 3 tabl., 10 pl. (1987).** **75F.**

N°13 - H. TATTEVIN - Déformation et transformation de phases induites par ondes de choc dans les silicates. Caractérisation par la microscopie électronique en transmission. **150 p., 50 fig., I tabl., 13 pl. (1987).** **95F.**

N°14 - J.L. PAQUETTE - Comportement des systèmes isotopiques U-Pb et Sm-Nd dans le métamorphisme éclogitique. Chaîne Hercynienne et chaîne Alpine. **190 p., 88 fig., 39 tab., 2 pl. (1987).** **95F.**

N°15 - B. VENDEVILLE - Champs de failles et tectonique en extension modélisation experimentale. **392 p., 181 fig., I tabl.,82 pl. (1987).** **Epuisé**

N°16 - E. TAILLEBOIS - Cadre géologique des indices sulfures a Zn, Pb, Cu, Fe du secteur de Gouézec-St-Thois : Dévono-Carbonifère du flanc Sud du Bassin de Châteaulin (Finistere). **195 p., 64 fig., 41 tabl., 8 pl. photo., 8 pl. h.texte. (1987).** **110F**

N°17 - J.P. COGNE - Contribution a l'étude paléomagnétique des roches déformées. **204 p., 86 fig., 17 tabl., (1987).** **90F.**

N°18 - E. DENIS - Les sédiments briovériens (Protérozoïque supérieur) de Bretagne septentrionale et occidentale : Nature, mise en place et évolution. **263 p., 148 fig., 26 tab., 8 pl. (1988).** **140F.**

N°19 - M. BALLEVRE - Collision continentale et chemins P-T : l'unité pennique du Grand Paradis (Alpes Occidentales). **340 p., 146 fig., 10 tabl., (1988).** **Epuisé**

N°20 - J.P. GRATIER - L'équilibrage des coupes géologiques. Buts, méthodes et applications. Atelier du Groupe d'Etudes Tectoniques le 8 Avril 1987 à Rennes. **165 p., 82 fig., 2 tabl. (1988).** **85F.**

N°21 - R.P. MENOT - Magmatismes paléozoïques et structuration carbonifère du Massif de Belledonne (Alpes Francaises). Contraintes nouvelles pour les schémas d'évolution de la chaine varisque ouest-européenne. **465 p., 101 fig., 31 tab., 6 pl., (1988).** **200F**

N°22 - **S. BLAIS** - Les ceintures de roches vertes archéennes de Finlande Orientale : Géologie, pétrologie, géochimie et évolution géodynamique. **312 p., 107 fig., 98 tab., 11pl. photo, I pl. h.texte, (1989).** **160F**

N°23 - **A. CHAUVIN** - Intensité du champ magnétique terrestre en période stable de transition, enregistrée par des séquences de coulées volcaniques du quaternaire. **217 p., 100 fig., 13 tab. (1989).** **100F.**

N°24 - **J.P. VUICHARD** - La marge austroalpine durant la collision alpine évolution tectonométamorphique de la zone de Sesia-Lanzo. **307 p., 143 fig., 26 tab., 6 pl. hors-texte. (1989).** **170F.**

N°25 - **C. GUERROT** - Archéen et Protérozoïque dans la chaîne hercynienne ouest-européenne : géochimie isotopique (Sr-Nd-Pb) et géochronologie U-Pb sur zircons. **180 p., 68 fig., 29 tab., I pl. (1989)** **90F.**

N°26 - **J.L. LAGARDE** - Granites tardi carbonifères et déformation crustale. L'exemple de la Méseta marocaine. **353 p., 244 fig., 15pl. (1989)** **210F.**

N°27 - **Ph. BARDY** - L'orogène cadomien dans le Nord-Est du Massif Armoricain et en Manche Occidentale. Etude tectonométamorphique et géophysique. **395 p., 142 fig., 7 tab., I pl. hors-texte. (1989).** **175F.**

N°28 - **D. GAPAIS** - Les Orthogneiss : Structures, mécanismes de déformation et analyse cinématique. **377 p., 184 fig., 3 tab., (1989).** **275F.**

N°29 - **E. LE GOFF** - Conditions pression-température de la déformation dans les orthogneiss : Modèle thermodynamique et exemples naturels. **321 p., 146 fig., 42 tab. (1989).** **150F.**

N°30 - **D. KHATTACH** - Paléomagnétisme de formations paléozoiques du Maroc. **220 p., 97 fig., 35 tab., (1989).** **100F.**

N°31 - **A. HAIDER** - Géologie de la formation ferrifère précambrienne et du complexe granulitique encaissant de Buur (Sud de la Somalie). Implications sur l'évolution crustale du socle de Buur. **215 p., 18 fig., 42 tab., 7 pl. (1989).** **130 F.**

N°32 - **T. DANIEL** - Traitement numérique d'image appliqué a l'analyse texturale de roches déformées. **186 p., 121 fig., 4 tab., (1989).** **210 F.**

N°33 - **C. LECUYER** - Hydrothermalisme fossile dans une paléocroûte océanique associée a un centre d'expansion lent : Le complexe ophiolitique de Trinity (N. Californie, U.S.A). **342 p., 109 fig., 73 tab., (1989).** **200 F.**

N°34 - P. RICHARD - Champs de failles au dessus d'un décrochement de socle: modélisation expérimentale. 382 p., 137 fig., (1989). 400 F.

N°35 - J. de BREMOND d'ARS - Estimation des propriétés rhéologiques des magmas par l'étude des instabilités gravitaires. Pétrologie du complexe plutonique lité de Guernesey. 370 p., 128 fig., 64 tabl., (1989). 180 F.

N°36 - A. LE CLEAC'H - Contribution a l'étude des propriétés physiques des mineraux à haute pression : Spectroscopie et calcul des grandeurs thermodynamiques de la lawsonite, des épidotes et des polymorphes de SiO_2. 190 p., 72 fig., 37 tabl., (1989). 100 F.

N°37 - 0. MERLE - Cinématique des nappes superficielles et profondes dans une chaîne de collision. 280 p., 165 fig., 3 tabl., (1990). 160F.

N°38 - P. ALLEMAND - Approche expérimentale de la mécanique du rifting continental. 205 p., 106 fig., 13 tabl., (1990). 160F.

N°39 - Ch. BASILE - Analyse structurale et modélisation analogique d'une marge transformante : l'exemple de la marge de Côte-d'Ivoire - Ghana. 230 p., 161 fig., 7 tabl., (1990). 130F .

N°40 - M. AUDIBERT - Déformation discontinue et rotations de blocs. Méthodes numériques de restauration. Application à la Galilée. 250 p., 80 fig., 5 tabl., (1991). 150F.

N°41 - G. RUFFET - Paléomagnétisme et 40Ar/39Ar : étude combinée sur des intrusions Précambriennes et Paléozoïques du Trégor. (Massif Armoricain) . 261 p., 80 fig., 19 tabl., (1991). 120F.

N°42 - P. SUZANNE - Extrusion latérale de l'Anatolie : Géometrie et mécanisme de la fracturation. 262 p., 100 fig., 12 pl., 5 tabl., (1991). 210F.

N°43 - G. FIQUET - Propriétés thermodynamiques de minéraux du manteau superieur. Calorimétrie à haute tempéerature et spectroscopie Raman à haute pression et haute témperature. 274 p., 101 fig., 53 tabl., (1991). 130F.

N°44 - J. MARTINOD - Instabilités périodiques de la lithosphère (Flambage, Boudinage en compression et en extension). 283 p., 117 fig., 3 tabl., 2 pl. couleur., (1991). 170F.

N°45 - M.O. BESLIER - Formation des marges passives et remontée du manteau: Modélisation expérimentale et exemple de la marge de la Galice. 257 p., 86 fig., 5 tab., 2 pl. noir/blanc, 2 Pl. couleur., (1991). 180F.

N°46 - **J.B.L. FRANCOLIN** - Analyse structurale du Bassin du Rio Do Peixe. (Brésil), **250 p., 83 fig., 3 tab., 9 pl. couleur, (1992).** **300F.**

N° 47 - **5. TOURPIN** - Perte des mémoires isotopiques (Nd, Sr, O) et géochimiques (REE) primaires des komatiites au cours du métamorphisme : exemple de la Finlande Orientale **185 p., 53 fig., 23 tabl., (1992).** **100F.**

N° 48 - **J.A. BARRAT** - Genèse des magmas associés à l'ouverture d'un domaine océanique : Géochimie des laves du Nord-Est de l'Afrique (Mer Rouge - Afar) et d'Arabie. **175 p., 47 fig., 23 tab., (1992).** **100F.**

N° 49 - **E. HALLOT** - Injection dans les réservoirs magmatiques Contraintes pétrologiques (Massifs de Fort La Latte et de Saint Brieuc, Bretagne Nord) et modélisation analogique. **331 p., 101 fig., 30 tabl., (1993).** **180F.**

N°50 - **T. SOURIOT** - Cinématique de l'extension post-pliocène en Afar. Imagerie SPOT et modélisation analogique. **225 p., 2 pl. coul., I tabl., 91 fig., 16 pl. photo., I carte H.Texte, (1993).** **I90F.**

N° 51 - **T. EUZEN** - Pétrogenèse des granites de collision post- épaississement. Le cas des granites crustaux et mantelliques du Complexe de Pontivy Rostrenen (Massif Armoricain, France). **350 p., 2 pl. coul., 34 tabl. en annexe, (1993).** **I90F.**

N° 52 - **J. LE GALL** - Reconstitution des dynamismes éruptifs d'une province paléovolcanique : l'exemple du graben cambrien du Maine (Est du Massif Armoricain). Pétrogenèse des magmas andésitiques et ignimbritiques et leur signification dans l'évolution géodynamique cadomienne. **370 p., 30pl. photo., I pl. coul. (1993).** **350 F.**

N° 53 - **J. C. THOMAS** - Cinématique tertiaire et rotations de blocs dans l'ouest de l'Asie Centrale (Tien Shan Kirghiz et dépression Tadjik). Etude structurale et paléomagnétique. **330 p., 107 fig., 2 pl. coul., 18 tabl., 1 carte, annexes. (1993).** **220 F.**

BON DE COMMANDE

à retourner à : Madame Arlette FALAISE
MEMOIRES DE GEOSCIENCES
Université de Rennes I - Campus de Beaulieu
35042 - RENNES Cédex (France)
Tél: 99.28.60.80 Fax : 99.68.67.80

NOM .....

ORGANISME .....

ADRESSE .....

Veuillez me faire parvenir les ouvrages suivants :

N°	Auteur	Nb exemplaires	P.U.	Total

Frais d'envoi : 20,00F par volume	Total	
par volume supplémentaire : 5,00 F	Frais d'envoi	
	Montant total	

Veuillez établir votre chèque au nom de Monsieur l'Agent Comptable de l'Université de Rennes I et le joindre à votre bon de commande.

Résumé

Depuis 45 Ma, le continent asiatique se déforme sous l'effet de la collision continentale de l'Inde. L'épaississement crustal et l'extrusion de blocs le long de grands décrochements sont considérés comme les deux principaux mécanismes accommodant la déformation. Par ailleurs, des observations structurales suggèrent la présence de rotations de blocs autour d'axes verticaux au niveau des syntaxes Est et Ouest-himalayennes et dans une zone allant de l'Afghanistan au Baïkal. L'étude des relations entre épaississement, décrochement et rotations de blocs qui constitue l'objet de ce travail, est un des points importants pour la compréhension de la cinématique Tertiaire de l'Asie.

Les mécanismes de déformation et la cinématique Tertiaires de l'Ouest de l'Asie Centrale ont été abordés par le biais du paléomagnétisme et de la géologie structurale. La présente étude a été réalisée dans la dépression Tadjik et le Tien Shan Kirghiz, situés respectivement au nord-ouest et au nord de la syntaxe Ouest-Himalayenne et du Pamir.

L'étude paléomagnétique permet de mettre en évidence deux domaines distincts de rotations de part et d'autre de la faille décrochante dextre de Talass-Fergana qui traverse le Tien Shan de part en part. A l'Est de cette faille, les bassins Cénozoïques du Tien Shan présentent une rotation faible ou nulle par rapport à l'Asie stable. A l'inverse, à l'Ouest, les rotations antihoraires sont significatives, de l'ordre de 20° dans le bassin de Fergana, de 15 à 50° dans la dépression Tadjik.

L'étude structurale montre que le contexte cinématique régional combine chevauchement et décrochement sénestre. La déformation et la rotation des bassins de type compressifs est principalement localisée dans la couverture sédimentaire, à l'opposé des zones faillées d'échelle crustale qui les limitent.

La cinématique Tertiaire du Tien Shan et de la dépression Tadjik apparaît fortement associée au poinçonnement vers le Nord du Pamir par rapport à l'Asie. La faille de Talass-Fergana est une discontinuité majeure à l'Ouest de laquelle la déformation est accommodée par de l'épaississement, du décrochement et des rotations de blocs.

Mots clés : Asie Centrale, cinématique, rotations de blocs, bassins Tertiaires.

Editions de GEOSCIENCES RENNES
Université de Rennes I
F - 35042 - RENNES Cédex